THE MARINE GEOLOGY OF THE NORTHERN KWAZULU-NATAL CONTINENTAL SHELF, SOUTH AFRICA

by

Andrew Noel Green (MSc)

Submitted in fulfillment of the requirements

For the degree of Doctor of Philosophy

In the

School of Geological Sciences

University of KwaZulu-Natal

Westville

April 2009

PREFACE

The research described in this thesis was undertaken in the School of Geological Sciences, University of KwaZulu-Natal, from April 2004 to March 2008. These studies represent original work by the author and have not been submitted in any form to another university. Where use was made of the work of others, it has been duly acknowledged in the text. The portions of this thesis which have appeared in peer-reviewed publications were the original work of the first author in terms of analysis, writing and diagrammatic content. Secondary authors are acknowledged on the basis of their supervisory roles.

Andrew Greyson 7/4/2009

ABSTRACT

This study proposes that the submarine canyons of the northern KwaZulu-Natal continental margin formed contemporaneously with hinterland uplift, rapid sediment supply and shelf margin progradation during the forced regression of upper Miocene times. These forced regressive systems tract deposits volumetrically dominate the shelf sediments, and comprise part of an incompletely preserved sequence, amongst which six other partially preserved sequences occur. The oldest unit of the shelf corresponds to forced regression systems tract deposits of Late Cretaceous age (seismic unit A), into which a prominent erosive surface, recognized as a sequence boundary, has incised. Fossil submarine canyons are formed within this surface, and underlie at least one large shelf-indenting canyon in the upper continental slope. Smaller shelf indenting canyons exhibit similar morphological arrangements. Late Pliocene deposits are separated from Late Cretaceous lowstand deposits (seismic unit B) by thin veneers of Late Palaeocene (seismic unit C) and mid to early Miocene (seismic unit D) transgressive systems tract deposits. These are often removed by erosive hiatuses of early Oligocene and early to mid Pliocene age. These typically form a combined hiatus surface, except in isolated pockets of the upper slope where late Miocene forced regressive systems tract units are preserved (anomalous progradational seismic unit). These sediments correspond to the regional outbuilding of the bordering Tukhela and Limpopo cones during relative sea level fall. Either dominant late Pliocene sediments (seismic unit E), or transgressive systems tract sediments which formed prior to the mid Pliocene hiatus, overlie these sediments.

Widespread growth faulting, slump structures and prograding clinoforms towards canyon axes indicate that these sediments initiated upper slope failure which served to create proto-canyon rills from which these canyons could evolve. The association of buried fossil canyons with modern day canyons suggests that the rilling and canyon inception process were influenced by palaeo-topographic inheritance, where partially infilled fossil canyons captured downslope eroding flow from an unstable upper slope. Where no underlying canyons occur, modern canyons evolved from a downslope to upslope eroding system as they widened and steepened relative to the surrounding slope. Statistical quantification of canyon forms shows a dominance of upslope erosion. Landslide geomorphology and morphometric analysis indicate that this occurred after downslope erosion, where the canyon axis was catastrophically cleared and incised, leading to headward retreat and lateral excavation of the canyon form. Trigger mechanisms for canyon growth and inception point to an overburdening of the upper slope causing failure, though processes such as freshwater sapping

may emulate this pattern of erosion. It appears that in one instance, Leven Canyon, freshwater exchange with the neighbouring coastal waterbodies has caused canyon growth.

The canyons evolved rapidly to their present day forms, and have been subject to increasingly sediment starved conditions, thus limiting their evolution to true shelf breaching canyon systems. Sedimentological and geomorphological studies show that the shelf has had minor fluvial influences, with only limited shelf-drainage interaction having occurred. This is shown by isolated incised valleys of both Late Cretaceous and Late Pleistocene/Holocene age. These show classic transgressive valley fills of wave dominated estuaries, indicating that the wave climate was similar to that of today. The narrowness of the shelf and the inheritance of antecedent topography may have been a factor in increasing the preservation potential of these fills. Canyons thus appear to have been "headless" since their inception, apart from Leven Canyon, which had a connection to the Last Glacial Maximum (LGM) St Lucia estuary, and Wright Canyon, which had an ephemeral, shallow LGM channel linking it to the Lake Sibaya estuarine complex.

Coastline morphology has been dominated by zeta bays since at least 84 000 BP, thus littoral drift has been limited in the study area since these times. The formation of beachrock and aeolianite sinks during regression from the last interstadial has further reduced sediment supply to the shelf. The prevalence of sea-level notching in canyon heads, associated with sea levels of the LGM indicates that canyon growth via slumping has been limited since that time. Where these are obscured by slumping in the canyon heads (Diepgat Canyon), these slumps have been caused by recent seismic activity. The quiescence of these canyons has resulted in the preservation of the steep upper continental slope as canyon erosion has been insufficient to plane the upper slope to a uniform linear gradient such as that of the heavily incised New Jersey continental margin.
Progressive sediment starvation of the area during the Flandrian transgression has resulted in a small shore attached wedge of unconsolidated sediment (seismic unit H) being preserved. This is underlain by a mid-Holocene ravinement surface. This crops out on the outer shelf as a semi-indurated, bioclastic pavement. Thinly mantling this surface are Holocene sediments which have been reworked by the Agulhas Current into bedforms corresponding to the flow regime and sediment availability to the area. Bedforms are in a state of dis-equilibrium with the contemporary hydrodynamic conditions, and are presently being re-ordered. It appears that sediment is not being entrained into the canyons to the extent that active thalweg downcutting is occurring. Off-slope sediment loss occurs only in localized areas, supported by the dominance of finer grained Early Pleistocene sediments of the outer slope. A sand ridge from the mid shelf between Wright and

White Sands Canyons appears to have been a palaeo-sediment source to White Sands Canyon, but is currently being reworked southwards towards Wright Canyon. The prevalence of bedform fields south of regularly spaced canyon heads is considered a function of hydrodynamic forcing of the Agulhas Current by canyon topography. These bedforms are orientated in a northerly direction into the canyon heads, a result of northerly return eddying at the heads of these canyons.

ACKNOWLEDGEMENTS

This thesis was funded by the African Coelacanth Ecosystem Programme (ACEP) via grants from the National Research Foundation, Department of Science and Technology, and the Department of Environmental Affairs and Tourism. Dr. Tony Ribbink, ACEP programme director, did an admirable job of heading the programme. His encouragement, motivation and inordinate belief in this research is gratefully acknowledged. I also thank my supervisor Ron Uken for not only providing critical reviews of this dissertation, but for wading through huge amounts of red tape in keeping the wheels of the geosciences programme running! My HOS and "line manager" Prof. Steve McCourt is thanked for his understanding and patience in the final write up of this thesis. I promise to not unduly wash *anything* in the tearoom sink again.

To my parents: I love you. Mom and Dad (both saints) have endured a nine year long obsession with Maputaland starting with my first research attempts and culminating in this. In those times, they have provided a place to stay during the odd "failed launch" or two, lunch on Saturdays (far superior to the usual Spar coke and pie), and as much love and support a human could need. I am, and will remain, eternally grateful. I also remain your favourite son, but that is another story (sorry Dave).

The employees of the Council for Geoscience-Marine Geoscience Unit are thanked for their help in the loan of equipment. Chief amongst these is Rio Leuci, a true mafia boss who procured equipment, *ship time* and tea and scones when they were needed most. Without Rio's genuine interest in this project and his altruism, it would never have succeeded. Charl Bosman, Paul Young and Wade Kidwell are also thanked for their various contributions to this study.

Peter Ramsay, director of Marine Geosolutions, has been my mentor and benefactor for several years now, and was instrumental in the initiation and completion of this project. Pete initially recommended me to ACEP, provided equipment, data and frequent employment. I thank Pete for his endless friendly advice, support, and encouragement, for which I am eternally indebted. Warwick Miller, fellow director, is also thanked for the excellent decision to loan the two Andrews much expensive equipment without which this study would have been a complete disaster. Similarly John Goff of the University of Texas Institute for Geophysics provided encouragement, ideas and the impetus to begin this project in earnest. Burg Flemming of the Senckenberg Institute

of Marine Science is also thanked for his helpful advice and interest in several aspects of this project. It would also be fitting here to acknowledge Doug Slogrove's much needed help in the setting up and general maintenance of the geophysical equipment, as well as for his friendliness and support whilst at sea.

In my capacity as Head of School, tea break division, I would like to thank the various postgraduate students of the School of Geological Sciences (in alphabetical order):
William Ansell (Tea drinker, sister hider, inventor of equations)
Matthew Brayshaw (Monday night beer and girl's soccer extravaganzas, fellow hair farmer)
Hayley Cawthra (Fellow marine geologess, boat puker, never wears suntan lotion)
Warwick Hastie (Tomato hater, Babanango conspirator, fellow bear rustler)
Roxanne Jacobs (Joke appreciator, sediment shaker, long-time partner in crime)
Warren Kretzinger (Kobayashi challenger, architect romancer, floor dweller)
Alain Le Vieux (Weird name, fellow marine geologist, Plettenberg Bay holiday home)
I will never forget the fun and laughter we have had these last few years.

To the captain and crew of the FRS Algoa, thank you for the awesome times at sea. To my friends from the programme: Kerry Sink, Tammy Morris and Niel Engelbrecht, thank you for all the good times at conferences and during data collection. The captain and crew of the MV Ocean Mariner and MV TB Davie are especially thanked for their help during the acquisition of seismic data, in addition to side scan sonar data for Innovation Fund no. 24401. Mr. D. Chelin, the captain, poured coke and liberal canes, both in commiseration and celebration, and is thanked for the after effects, both scientifically and behaviourally.

On a personal note, thank you to my "early morning" friends (Ryan Edwards, Hamish Douglas, Warren Burton, Dean Maber, Mark Ryan and Luke Dalton) who I have spent so many amazing hours sharing waves, jokes and marathon car rides searching the coasts of KwaZulu-Natal with. I would also like to thank the Hoyer family for the use of their colour printer, the availability of frequent delicious dinners and access to their television, even if Gray's Anatomy is always on. I especially thank Lauren, for being the kind, patient and loving girlfriend she is. Around you I am eager to please, quick to smile and anxious to love.

Lastly, Andrew Richardson deserves a special place in heaven with the angels. Probably the greatest human being I have ever met, Drew helped in almost every aspect of data collection and

processing. From the murky depths of Tiger Reef and Scottburgh Caravan Park, Drew is the greatest friend a person could ask for. He weathered every storm with me, provided kind words, and when necessary shots of morphine administered directly to the jugular. He was as excited as I when things worked, and never too worried when they didn't. Objective, selfless and kind, nothing in the last six years would have happened without you. Thank you buddy. I love you man.

CONTENTS

PREFACE ii

ABSTRACT iii

ACKNOWLEDGEMENTS vi

CHAPTER 1

Introduction 1

CHAPTER 2

Regional Setting 3

2.1. Locality 3

2.1.1. Climate 3

2.2. Sediment and coastal hydrodynamics 5

2.3. East coast Quaternary sea-levels 8

2.4. Regional geology of the Zululand Basin 8

2.4.1. Mesozoic to Holocene geology 10

CHAPTER 3

Sequence and chronostratigraphic models of shelf development 15

3.1. Introduction 15

3.1.1. Terminology 15

3.2. Methods 15

3.2.1. Data collection and processing 16

3.3. Results 17

3.3.1. Unit A 17

3.3.2. Unit B 17

3.3.3. Units C and D 19

3.3.4. Unit E 19

3.3.5. Unit F 19

3.3.6. Units G and H 25

3.3.7. Anomalous progradational unit 25

3.4. Discussion 25

3.4.1. Sequence stratigraphic interpretation 25

3.4.1.1. Lowstand systems tract deposits 25

3.4.1.2. Transgressive systems tract/highstand systems tract deposits 29

3.4.1.3. Forced regressive systems tract 29

3.4.2. Chronostratigraphic models 31

3.4.3. Deltaic deposits and fluvial-shelf interaction 36

CHAPTER 4

Seismic facies of incised valley fills 38

4.1. Introduction 38

4.2. Methods 39

4.3. Regionally developed sequence boundaries 39

4.4. Palaeo-drainage reconstruction 41

4.5. Seismic facies 42

4.5.1. Cretaceous incised valley fills 41

4.5.2. Late Pleistocene/Holocene incised valley fills 45

4.6. Discussion 48

CHAPTER 5

The seismic structure and development of submarine canyons 60

5.1. Introduction 60

5.2. Regional seismic structure of the continental shelf 60

5.3. Seismic structure of submarine canyons 61

5.3.1. Southern structural domain 61

5.3.1.1. Leven and Chaka Canyons 61

5.3.1.2. Leadsman Canyon and northern environs 63

5.3.2. Northern structural domain 69

5.3.2.1. Diepgat Canyon 69

5.3.2.2. Sodwana Bay block: Jesser, Wright and White Sands Canyons 69

5.3.2.3. Mabibi Block 72

5.4. Discussion 82

5.4.1. Topographic inheritance and downslope driven canyon erosion processes 82

5.4.2. Terracing, axial incision and wall instability 83

5.4.3. Unit E and shelf- edge wedge genesis 84

5.4.4. Tectonic versus sedimentary controls on canyon evolution 87

5.5.5. Aeolianite ridges, surface 3 and relative age constraints on canyon erosion 88

CHAPTER 6

Geomorphological evidence for upslope canyon-forming processes 90

6.1. Introduction 90

6.1.2. Theories of canyon formation 91

6.2. Materials and methods 92

6.3. Results 93

6.3.1. Morphologic observations 93

6.3.2. Quantitative classification 94

6.4. Discussion 100

6.4.1. Dominance of upslope processes 100

6.4.2. Downslope capture of canyons 104

6.4.3. Recent quiescence 106

CHAPTER 7

Submarine landsliding and canyon growth mechanisms 107

7.1. Introduction 107

7.1.1. Regional geomorphological setting 109

7.1.2. Terminology 114

7.2. Methods 115

7.2.1. Slide determination and measurement 115

7.3. Results 118

7.3.1. Landslide location, depth, regional gradient 118

7.3.2. Landslide geomorphology 118

7.3.3. Landslide statistics 120

7.3.4. Area, volume, runout 120

7.3.5. Slope gradients 121

7.3.6. Headscarps 128

7.4. Discussion 128

CHAPTER 8

First observations of sea level indicators related to glacial maxima 135

8.1. Introduction 135

8.2. Indicators of glacial maxima along the South African coastline 135

8.3. New evidence for East coast sea levels 136

CHAPTER 9

Sediment dynamics, surficial geology & coastline configuration models 141

9.1. Introduction 141

9.2. Methods 143

9.3. Shelf morphology and acoustic facies 144

9.3.1. Leven Point 146

9.3.2. Leadsman Shoals 147

9.3.3. Diepgat 147

9.3.4. Sodwana Bay 149

9.3.4.1. 2 Mile Reef and Wright Canyon south 149

9.3.4.2. Wright Canyon north, 7 Mile and 9 Mile Reefs 152

9.3.5. Mabibi 154

9.4. Bedload parting and zones of convergence 154

9.5. Morphometric observations 156

9.5.1. Shallow stratigraphy 157

9.6. Discussion 159

9.6.1. Controls on facies distribution 159

9.6.2. Sediment bypass and loss from the shelf 160

9.6.3. Sediment migration patterns and bedform distribution 161

9.6.4. Aeolianite ridges and palaeo-bay morphology 164

CHAPTER 10

Conclusions 167

REFERENCES 174

APPENDICES 194

Appendix 1 A0 fold out: Palaeocoastline configuration of the northern KwaZulu-Natal continental Leven Point to Island Rock

Appendix 2 A0 fold out: Side scan sonograph mosaic and interpretative sea floor geology of the Sodwana Bay continental shelf

Appendix 3 Additional publications in press or review of overlapping interest to this study

a) Green A.N., Ovechkina M., Uken R., 2008. Nannofossil age constraints for the northern KwaZulu-Natal shelf edge wedge: Implications ofr contiental margin development, South Africa, SW Indian Ocean. Cont. Shelf Res. 28, 2442-2449.

b) Green, A.N., Perritt, S.H., Leuci, R., Uken, R., Ramsay, P.J., 2008. Potential sites for coelacanth habitat using bathymetric data from the western Indian Ocean. S. Afr. J. Sci. (in press)

c) Green, A.N., Uken, R., 2005. First observations of sea-level indicators related to glacial maxima at Sodwana Bay, northern KwaZulu-Natal. S. Afr. J. Sci. 101, 236-238.

d) Green, A.N., Uken., R., 2008. Submarine landsliding and canyon evolution for the northern KwaZulu-Natal continental shelf, South Africa, SW Indian Ocean. Mar. Geol. 254, 152-170.

e) Green, A.N., Goff, J.A., Uken, R., 2007. Geomorphological evidence for upslope canyon-forming processes on the northern KwaZulu-Natal shelf, South Africa. GeoMar. Lett. 27, 399-409.

Appendix 4 Disclaimer concerning raw seismic and sedimentological data presented within this thesis

CHAPTER 1
Introduction

With the recent discovery of the coelacanth, *Latimeria chalumnae* in several submarine canyons of the northern KwaZulu-Natal continental shelf, South Africa (Sink et al., 2006), scientific interest in these submarine canyons has steadily increased. This is because many of these submarine canyons impinge the shelf break (Green et al., 2007) and satisfy the morphological and bathymetric constraints for coelacanth habitation (Fricke and Plante, 1988; Fricke and Hismann, 1994). The African Coelacanth Ecosystem Programme (ACEP) was formed in response to the need to study both the coelacanth and its relationship to the bio-physical and chemical environment of the area (Ribbink and Roberts, 2006). A multidisciplinary scientific programme was thus established, a component of which was a dedicated marine geoscience programme, aimed at investigating the evolution of the coelacanth habitat, or more broadly, the marine geology of the continental shelf and slope in which coelacanths are found. It was under the auspices of this programme that this PhD was undertaken.

Despite several studies of the marine geology of the continental shelf and fringing coastal plain of northern KwaZulu-Natal (Bang, 1969; Dingle et al., 1978; Martin, 1984; Sydow, 1988; Ramsay, 1991; 1994; 1996; Shaw, 1998; Miller, 2001; Wright et al., 2000; Wright, 2002, Ramsay and Miller, 2006) geomorphological, stratigraphic and sedimentological models of the area are relatively poorly advanced in comparison to other continental shelves worldwide. This has been exacerbated by sparse coverage by seismic, and a dearth of borehole data with which lithostratigraphic correlations can be made. The recent acquisition of multibeam bathymetry, side scan sonar and high resolution seismic data in the area, in conjunction with ground truthing investigations by submersible and grab sampling, has provided a means to better understand the evolution of this portion of the continental shelf of South Africa.

The area investigated stretches from Leven Point in the south, to Island Rock in the north, a distance of ~ 100 km (Fig. 2.1). This segment of continental margin is notable for its steep, narrow and heavily incised shelf and upper slope. The numerous submarine canyons which dissect the upper slope have been discussed by several authors (Bang, 1969; Dingle et al., 1978; Flemming, 1980; Botes, 1988; Ramsay, 1991; Sydow, 1988; Shaw, 1998; Ramsay and Miller, 2006), though a

definitive study concerning their morphology, evolution and stratigraphic significance has not been undertaken until now.

The objectives of this thesis are as follows:

1) To assess the role of stratigraphy in the historical development of submarine canyons. Particular attention is given to the development of sequence and chronostratigraphic models for the shelf.
2) To identify the influence of palaeo-drainage during lowstand conditions on shelf geomorphology and sedimentology.
3) To understand the dominant types of erosion contributing to modern submarine canyon geomorphology.
4) To ascertain the triggering mechanisms for submarine canyon inception and growth.
5) To map and identify sea level variations in the study area.
6) To understand the interaction between submarine canyons, surface geology and the present day sediment dynamics of the shelf and slope.
7) To provide a definitive model for the formation of submarine canyons from the northern KwaZulu-Natal shelf by integrating the conclusions drawn from stratigraphic, geomorphological and sedimentological investigations.

This thesis takes the form of a collection of several published (and some unpublished) papers collated as individual chapters. Chapter 2 is an outline of the regional setting of the area. Chapters 3 to 5 are concerned with seismic data collected from the continental shelf and upper slope. Chapter 3 investigates sequence and chronostratigraphic models for the continental shelf, and chapter 4 provides an attempt at reconstructing the palaeo-drainage associated with sequence boundary development in the area. Chapter 5 discusses seismic-structural models for the formation of submarine canyons. Chapters 6 to 8 detail the geomorphological setting of the area. Chapters 6, 7 and 8 comprise publications related to the role of headward erosion in the development of submarine canyons (Green et al., 2007), the role of landsliding in canyon evolution (Green and Uken, 2008) and the significance of sea-level indicators related to glacial maxima in canyon heads (Green and Uken, 2005) respectively. The sediment dynamics and coastal configuration of the study area are investigated in chapter 9 (published as Green, 2009).

CHAPTER 2
Regional setting

2.1. Locality

The northern KwaZulu-Natal continental shelf and coastal plain (Fig. 2.1) comprise the submerged and emergent portions of a continuous feature, the degree of separation dependent upon the relative sea level at any given time (Martin and Flemming, 1988). The continental shelf and coastal plain are underlain by rocks of Mesozoic to Pleistocene/Holocene age which document the rifting and drifting phases of the passive margin development of southeastern Africa (Dingle et al., 1983). The coastal plain is bounded in the west by the Lebombo Mountain chain and in the east by the Indian Ocean. The coastline itself is defined by a series of curved, log-spiral bays that extend for approximately 6 km between each rocky headland.

2.1.1. Climate

According to the Köppen Classification (Boucher, 1975), the northern KwaZulu-Natal coastal belt has a humid sub-tropical climate with a warm summer, the climatic zone being dominated by the southern sub-tropical high pressure belt (Tyson and Preston-Whyte, 2000). Records from Lake Nhlange 80 km north of the study area indicate annual rainfall averages of 900 mm per annum, though this may vary between 1200 mm per annum in the southeast, and 700 mm per annum in the west (Pitman and Hutcheson, 1975). Wright and Mason (1990) state that 43% of the rain falls in the three-month period from January to March. Monthly rainfall data collected at Lake Nhlange, from September 1981 to present, is outlined in figure 2.2.

For the period September 1994 to February 1996, the mean wind speed measured at Mabibi School ~10 km north of Sodwana Bay (27° 19' 43" S 32° 43' 52" E) was 4.6 ms^{-1}, with a maximum gust speed of 23.7 ms^{-1} (Diab and Sokolic, 1996). Diab and Sokolic (1996) point out that ~ 60% of the winds are in excess of 4 ms^{-1} and 30% in excess of 6 ms^{-1} (Fig. 2.3a). The dominant wind directions are bidirectional and coast parallel (NE and SW) (Fig. 2.3b). North of Cape St. Lucia, southerly winds normally have higher velocities, although they tend to blow less frequently than those from the north (Van Heerden and Swart, 1986).

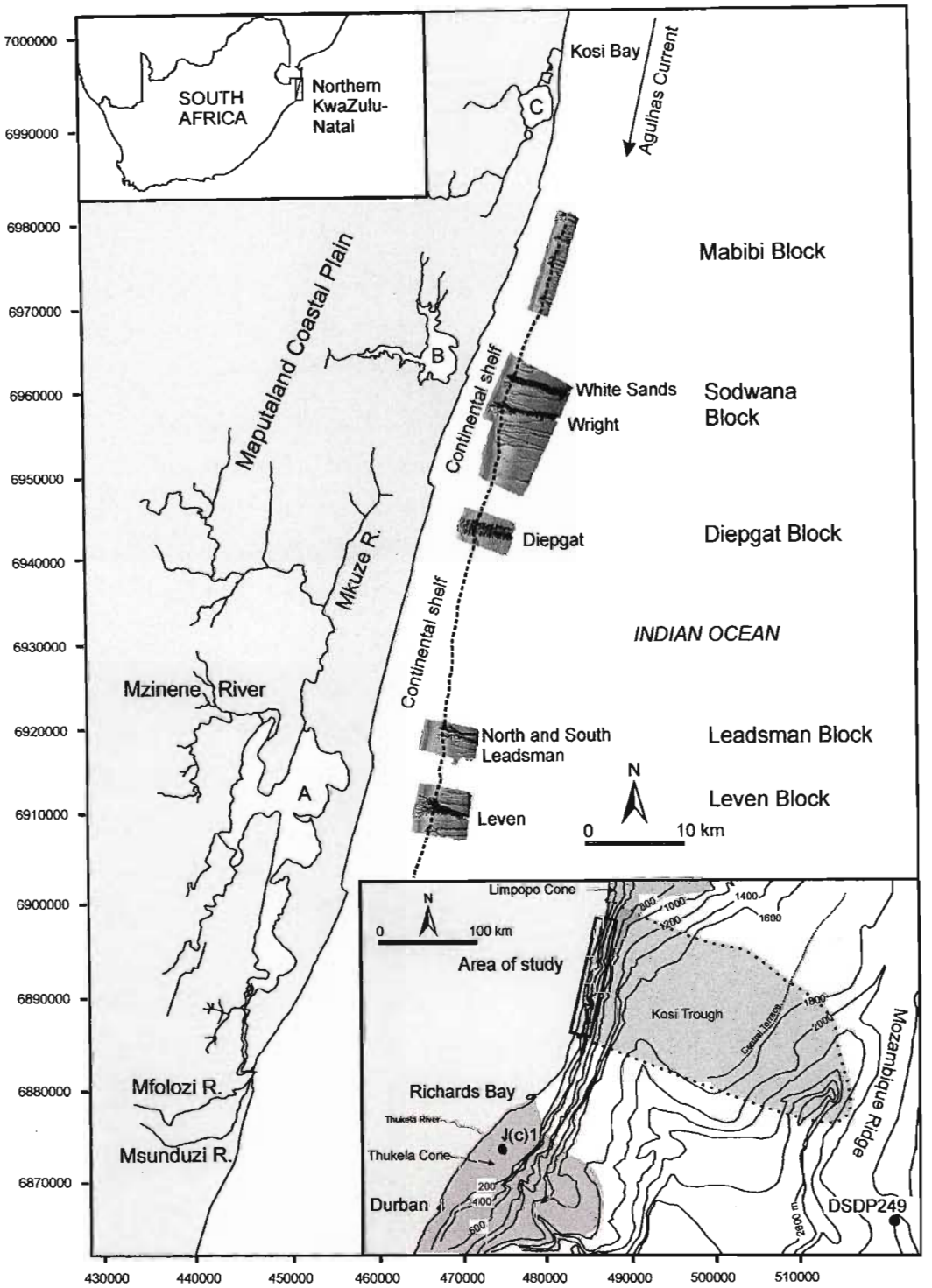

Figure 2.1. Locality map of the study area, outlining the northern KwaZulu-Natal continental shelf and upper slope, in relation to the bathymetry of the Zululand Basin (Natal Valley) (after Martin, 1984), exploration well sites, fringing coastal waterbodies and major drainage patterns of the Maputaland coastal plain. UTM zone 36S, eastings and northings in metres. A = Lake St Lucia, B = Lake Sibaya, C= Kosi Lake System. Sunshaded bathymetric areas denote the original survey blocks of the ACEP programme (see Ramsay and Miller, 2006).

In the St. Lucia Estuary area the potential sand transport direction by wind was calculated by Wright (1995) and Wright and Mason (1993) as having a northward resultant drift potential of 13 × 10^3 m^3km per year. Lindsay et al. (1996) obtain similar values for the Mfolozi River mouth, based on short term wind rose data.

2.2. Sediment and coastal hydrodynamics

Tides on the northern KwaZulu-Natal coast are semi-diurnal. Tidal range for the northern KwaZulu-Natal coastline averages 2 m (SAN, 2007) and may be classed as upper micro-tidal (Davies, 1964) or lower meso-tidal (Hayes, 1979). Persistent high-energy waves (derived from local storms) dominate the coastline, the prevailing large amplitude swells (derived from distant storms) occur out of the southeast 40% of the year (Rossouw, 1984, Van Heerden and Swart, 1986). Ramsay et al. (1989) consider large amplitude northeasterly to easterly swell as atypical, occurring as small amplitude wind swell superimposed on the dominant southerly motion. Only when the northeasterly wind blows for a considerable period does it generate the dominant swell direction (Ramsay et al., 1989).

According to Cooper (1994) littoral drift in the area is limited as a result of the complex log-spiral (zeta) bay morphology of the coast. In addition, the nearest source of sediment is the Mfolozi River mouth some 175 km south of the Kosi system. According to Ramsay (1996), the interception of shelf sediment pathways by submarine canyons accounts for a significant reduction in sediment to the area. Recently acquired side scan sonar investigations of the area spanning Mabibi to Kosi Bay indicate a pattern of sediment starvation, particularly in the mid-outer shelf areas (Ramsay et al., 2006).

The physical and biological processes on the continental shelf are controlled by the Agulhas Current (Ramsay, 1996). Under the influence of Agulhas flow, large-scale subaqueous dunes form in the unconsolidated sediment on the outer-shelf; with a dominant southerly transport direction (Ramsay et al., 1996). However, in isolated areas, bedload parting zones exist where the sediment transport direction is towards the north (Ramsay et al., 1996). According to Cooper et al. (in prep) offshore-onshore sand movement, associated with spring and neap tides, may occasionally be associated with the sediment that is being re-distributed by counter Agulhas Current flows. Return gyres are common within the Agulhas Current systems, and form predominantly in the lee of large coastal offsets (Lutjeharms, 2006).

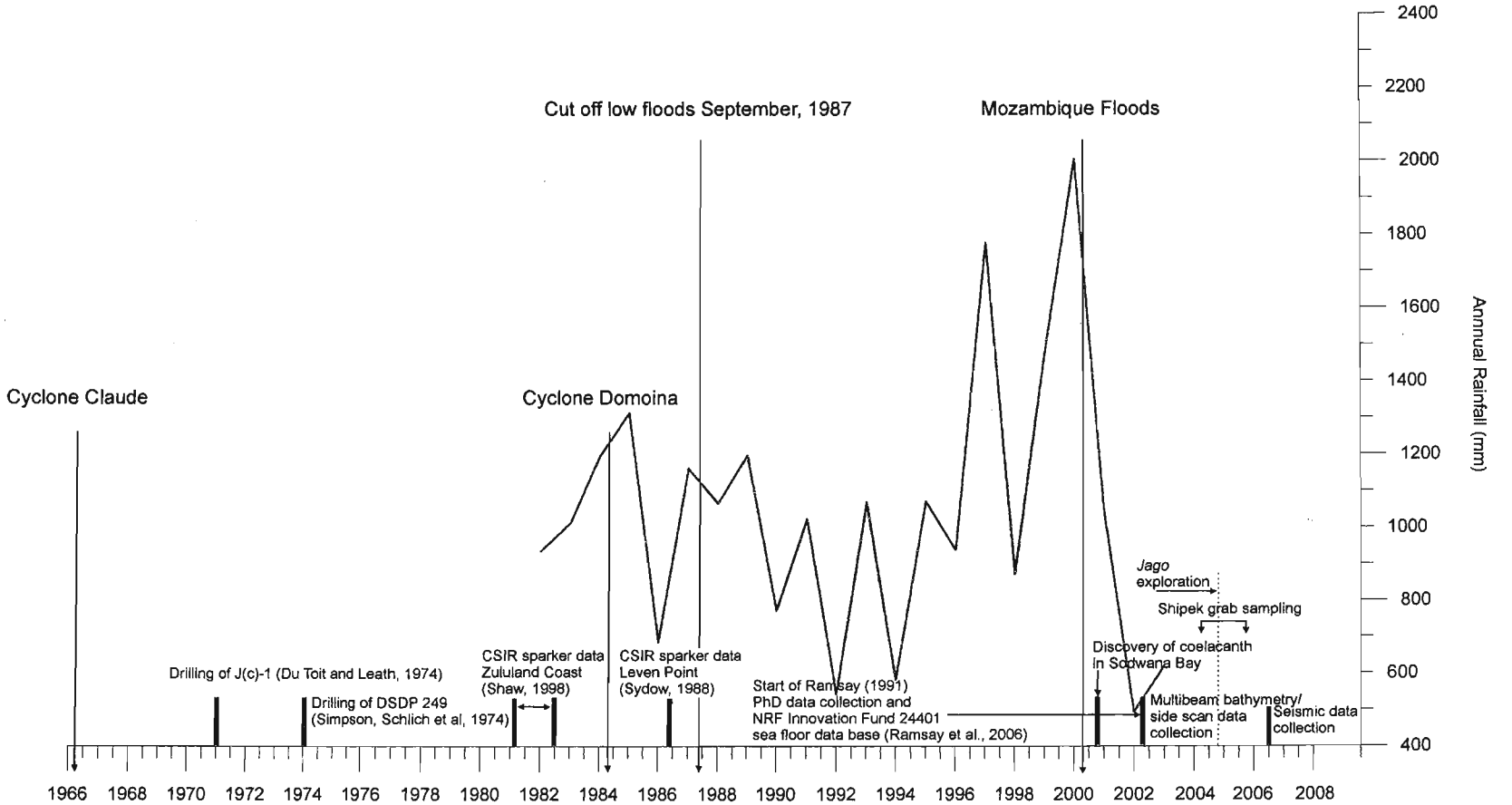

Figure 2.2. Time line displaying rainfall data for the area (as measured from Lake Nhlange, Kosi Bay, ~ 80 km north of Sodwana Bay) and the dates of major floods. Also included are the dates of important research activity, the dates when major exploration boreholes were drilled, and the dates of recent ACEP related activities in the area, as outlined in this thesis.

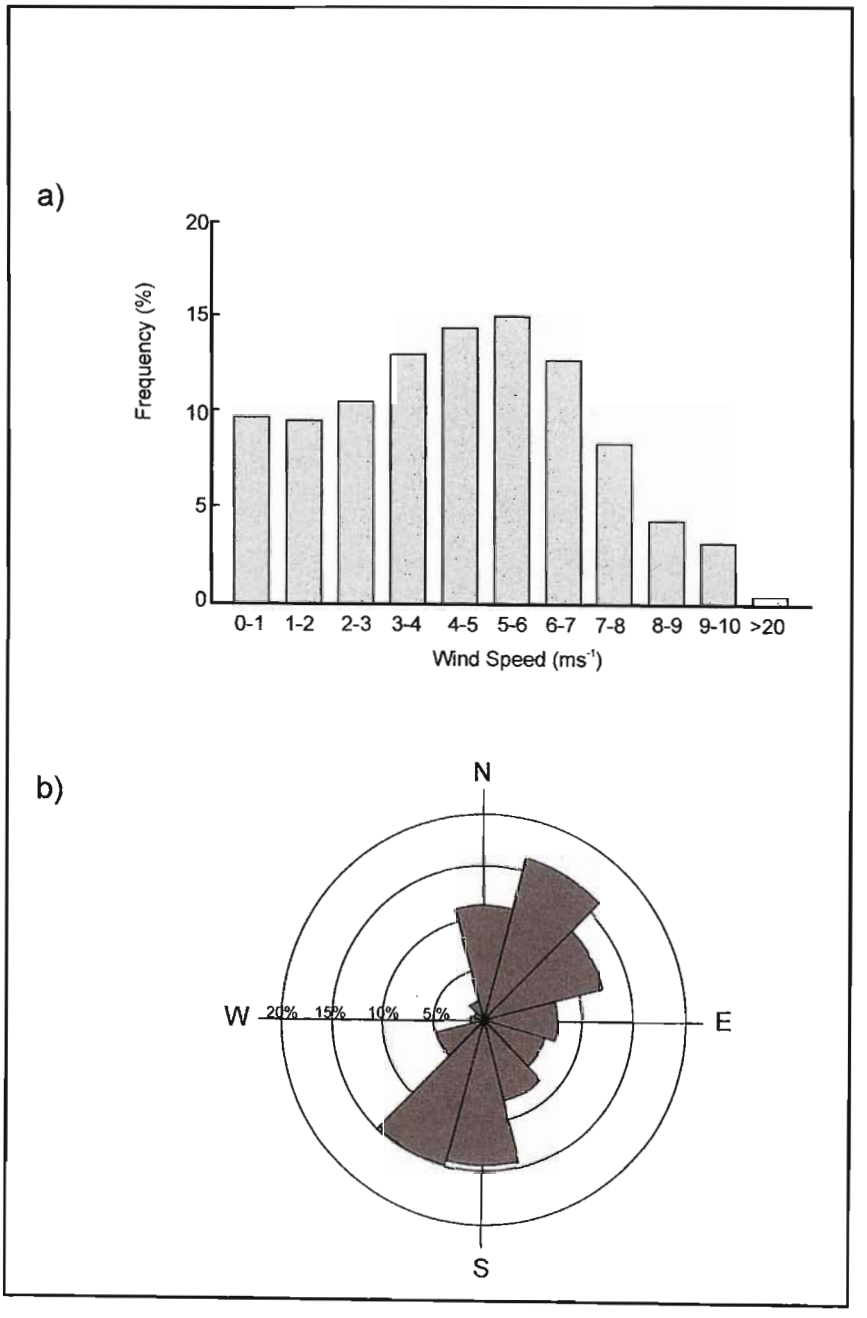

Figure 2.3.a Percentage distribution of wind speed at Mabibi school, 15 km north of Kosi Bay, for the period December 1994 to January 1996 (from Diab and Sokolic, 1996). **b.** Wind rose for the weather station at Mabibi school for the period December 1994 to January 1996 (from Diab and Sokolic, 1996).

As the Agulhas Current follows the shelf edge, shelf width is often the dominant control on rotating bodies of water in the current fringe (Lutjeharms et al., 1989). Where the shelf is narrow, as in northern KwaZulu-Natal, counter Agulhas flows may thus be expected at most rocky fronted headlands, where the shelf break in most cases mirrors the coastline configuration (Ramsay, 1991). This is considered the cause of complex nearshore sedimentation patterns, possibly explaining isolated incidents of erosion or accretion on an otherwise stable coastline (Cooper et al. in prep).

2.3. East coast Quaternary sea levels

The Quaternary sea level of southern Africa has varied considerably over time (Fig 2.4a and b). Maximum Quaternary sea levels of +5 m were attained during the Last Interglacial Maximum oxygen-isotope stage (OIS) 5e, approximately 125 000 BP (Ramsay and Cooper, 2002). According to Ramsay (1996), and Ramsay and Cooper (2002), two schools of thought exist concerning Late Pleistocene sea level curves. One school of thought considers sea levels at 40 to 50 m below present sea level, the other that a high interstadial sea level, prior to the Last Glacial Maximum, 25 000 - 30 000 BP existed. Evidence along the Southern African coastline tends to favour the former view (Ramsay, 1996). Between 90 000 and 21 000 BP, sea level showed a gradual fall to a low stand of -120 m, well past the shelf break. After the eustatic low at 16 000-18 000 BP sea level rose very rapidly.

The ensuing transgression (Flandrian-OIS 2) eroded much of the exposed shelf sands, before stabilising at its present level 7 000 to 6 000 BP (Ramsay and Cooper, 2002). Sea level then rose to +2.75 m which persisted for a period of 2 500 years, before culminating in the Holocene sea level high of +3.5 m, at roughly 4 500 BP (Ramsay, 1995; 1997). Sea level retreated to about –2 m, approximately 2 000 BP, before rising to +1.5 m at 1 610 BP (Ramsay and Cooper, 2002). Sea levels reached their current position at approximately 900 BP and are continuing to rise in accordance with deglaciation and ocean warming.

2.4. Regional geology and evolution of the Zululand Basin

The Zululand Basin, forming the coastal plain and continental shelf, comprises Mesozoic, Tertiary and Quaternary sediments (Dingle et al., 1983; Broad et al., 2007) underlain by volcanic successions extruded during Gondwana break-up (Watkeys et al., 1993). The overlying

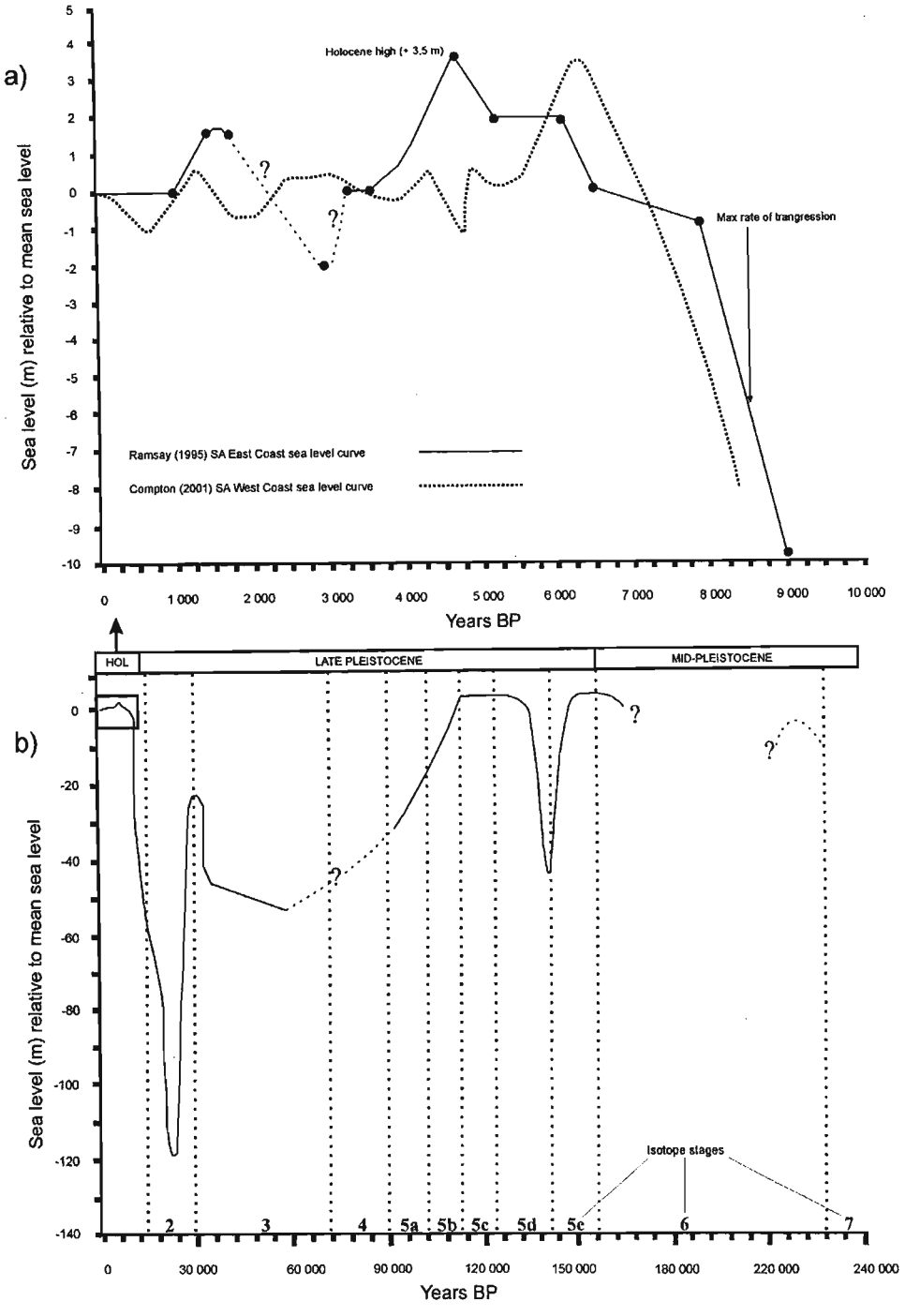

Figure 2.4. Holocene (Ramsay, 1995; Compton, 2001) (a) and Late Pleistocene (Ramsay and Cooper, 2002) (b) sea-level curves for the east coast of South Africa. Note the last interglacial maximum (LGM) sea-level of ~120 m, followed by rapid transgression during OIS 2. Holocene sea-levels have been similar to those of today, interspersed with three highstands of + 2.5, + 3.5 and + 1.5 m respectively. Sea-levels decreased to - 2 m following the + 3.5 m high at 4500 BP. Note Ramsay's (1995) curve is preferred on the basis of his use of significantly more accurate sea level indicators. The argument of the various merits of particular indicators is beyond the scop e of this thesis and the reader is referred to both publications whihc discuss the vertical accuracy of each indicator used.

sedimentary succession comprises thick Cretaceous sediments, which in turn, are thinly overlain by Cenozoic sediments (Roberts et al., 2007) (Table 2.1, Fig. 2.5). The lack of borehole data in the offshore portions of the Zululand Basin allows only an incomplete inference of the offshore stratigraphy to be made, based on onshore well data, limited seismic data and coastal plain outcrop.

2.4.1. Mesozoic to Holocene geology

The Mesozoic to Holocene geology of the study area has been reviewed by Watkeys et al. (1993), the oldest rocks outcropping on the fringing coastal plain are the 179 ± 7 Ma rhyolites of the Jozini Formation, part of the Lebombo Group volcanics. These form the western limit to the Zululand Basin, dipping eastward under the overlying units. Conglomerates of the Msunduze Formation conformably overlie the Jozini Rhyolites, which are in turn overlain by the basalts of the Movene and Mpilo Formations (Watkeys et al., 1993). Pyroclastics, rhyolites and trachytes of the Bumbeni Complex comprise the upper part of the igneous basement (Watkeys, 1997).

A northeast trending basement ridge, the Bumbeni Ridge extends eastwards offshore from the Lebombo Mountains and divides the Zululand Basin into two troughs (Broad et al., 2007). The northern Kosi Trough extends from Kosi Bay and progressively shallows towards Lake St Lucia (Dingle et al., 1983; Broad et al., 2007), thus encompassing the entire area of study. The sedimentary infill of the onland portions of this sub-basin comprises the Zululand Group, a thick succession of sediments of Cretaceous age (Shone, 2007). The lowermost Cretaceous rocks comprise terrestrial sandstones and conglomerates that grade upwards into shallow marine shales (Kennedy and Klinger, 1975; Watkeys et al., 1993). Shone (2007) considers these strata Barremian to Aptian in age. These strata are separated from the overlying Mzinene Formation by a well-indurated, bored concretionary horizon showing evidence of a long period of non-deposition (Shone, 2007). The Mzinene Formation consists of fossiliferous silts and sands, and shallow marine glauconitic silts, the lowermost portions of this formation possibly Barremian in age (Shone, 2007). The Mzinene Formation is capped by a hardground similar to that of the Makatini-Mzinene boundary, believed to be ~ 95 million years old (Dingle et al., 1983).

Rifting along this portion of newly formed coastline is considered to have ceased during deposition of the Mzinene Formation (Watkeys, 2002) which coincides with a regional hiatus, identified offshore as unconformities of Cenomanian and Turonian age (Simpson, Schlich et al., 1972; Dingle et al., 1983). A basin-wide transgression then occurred, marking the onset of deposition of the

Upper Cretaceous St Lucia Formation (Kennedy and Klinger, 1975; Dingle et al, 1983; Shone, 2007). The St Lucia Formation lies unconformably on Lower Cretaceous rocks in the study area, whereas further south, it rests unconformably on basement rocks that pre-date Gondwana break-up (Martin and Flemming, 1988). Sediments of the St Lucia Formation comprise basal conglomerates, overlain by a succession of cross-bedded fine sands and silts. According to Kennedy and Klinger (1975), the upper St. Lucia Formation contains an abundance of calcareous concretions within upward fining glauconitic silts and fine bands of interbedded hardgrounds.

The top of the St. Lucia Formation is marked by a short hiatus recorded in the JC-series boreholes further south of the study area (Figs. 2.1 and 2.5), though borehole DSDP 249 from the Mozambique Ridge (Fig. 2.1) indicates a prolonged hiatus that spanned Mid Maastrichtian to Mid/Late Miocene times. This is recognised as regional reflector Angus of the northern Natal Valley (Dingle et al., 1978; Martin, 1984) which separates Maastrichtian and Miocene open-ocean carbonates (Simpson, Schlich et al., 1974). Late Tertiary deposits are generally not well preserved on the northern KwaZulu-Natal coastal plain, though a coquina of Miocene-Pliocene age occurs throughout northern KwaZulu-Natal (Martin and Flemming, 1988; Kruger and Meyer, 1988, Roberts et al., 2007) and may correspond to regional seismic reflector Jimmy (Martin et al., 1982; Goodlad, 1986) (Fig. 2.5). Offshore, sediments between Angus and Jimmy occur as deposits of mixed offlap/onlap configuration. According to Goodlad (1986), these represent alternating periods of progradation and upper slope/shelf erosion, during complex fan construction of the Thukela River. Reflector Jimmy represents a small hiatus between Miocene and Pliocene times, and is not recognised in the JC series boreholes, but in borehole DSDP 249 (Fig. 2.5). According to Siesser and Dingle (1981), both a short Late Miocene/Early Pliocene and a Pliocene hiatus occurred.

Offshore, post-reflector Jimmy strata occur as a shelf off-lapping wedge of indeterminate composition (Goodlad, 1986). These are unconformably overlain by Pleistocene aeolianites and loosely consolidated barrier type sediments of the Port Durnford Formation (Hobday and Orme, 1974, Roberts et al., 2007), which are in turn overlain by beachrock/aeolianite complexes that correspond to palaeo-sea level positions of the Late Pleistocene (Ramsay, 1994; 1996). These are correlated with sediments of the Isipingo Formation (see Cooper and Flores, 1991; Roberts et al., 2007).

Table 2.2. Stratigraphic table of the regional geology of the study area. Note lithological descriptions, in addition to the relative timing of the development of major offshore geological features and processes.

Offshore	Era	Sub-Era	Period	Epoch	Group	Formation	Lithology
Unconsolidated sediment wedge; Isipingo Fm; Palaeo-shorelines	Cenozoic	Quaternary		Holocene	Maputaland	Sibayi Formation	High coastal dune cordon, calcareous sand, lagoonal sands, lacustrine muds
						Kwambonambi Formation	Inland stabilised dunes and reworked sand, diatomite
				Pleistocene		Kosi Bay Formation	Red sandy soil, cross bedded sand, local calcarenite, lensoid carbonaceous sand
						Port Durnford Formation	Beachrock, coral bearing coquina, lignite, fossiliferous mudrock, calcarenite
Shelf offlapping wedge; Reflector Jimmy; Mixed offlap/onlap configuration seds; Hiatus Angus		Tertiary	Pliocene to Miocene	Early to Late		Umkwelane Formation	Red sandy soil, aeolian cross bedded calcarenite
						Uloa Formation	Coquina (*Pecten* beds), conglomerate
Basin wide transgression (Kennedy&Klinger, 1976; Dingle et al., 1983); DRIFT			Palaeocene	Early	Zululand		Fossiliferous shallow marine silts, thin clay lenses, hard concretionary horizons
				Late		St. Lucia Formation	Fossiliferous shallow marine silts and fine sands, concretionary horizons, cross bedded silts, basal conglomerate
Rifting ceases; RIFT	Mesozoic		Cretaceous			Mzinene Formation	Fossiliferous shallow marine silts and sands
						Makathini Formation	Fossiliferous shallow marine clays
				Early		Bumbeni Complex Mpilo/Movene Formations	Pyroclastics, rhyolites, trachytes; Basalts
						Msunduze Formation	Conglomerate
			Jurassic	Middle	Lebombo	Jozini Formation	Rhyolites

A thin veneer of modern day unconsolidated sediment marks the most recent sedimentation on the continental shelf (Martin and Flemming, 1986; Birch, 1991; Ramsay et al., 1996). Martin and Flemming recognise five depocentres on the KwaZulu-Natal coast (Fig. 2.6), the most northern example occurring ~ 25 km south of the study area, related to the St Lucia-Mfolozi River confluence (Flemming and Hay, 1988). Sydow (1988) in turn recognises a depocentre offshore Leven Point which he relates to a reworked compound ebb-tidal delta which formed at ~ 5000 BP during the Holocene High. This may be linked to depocentre 4 of Martin (1985).

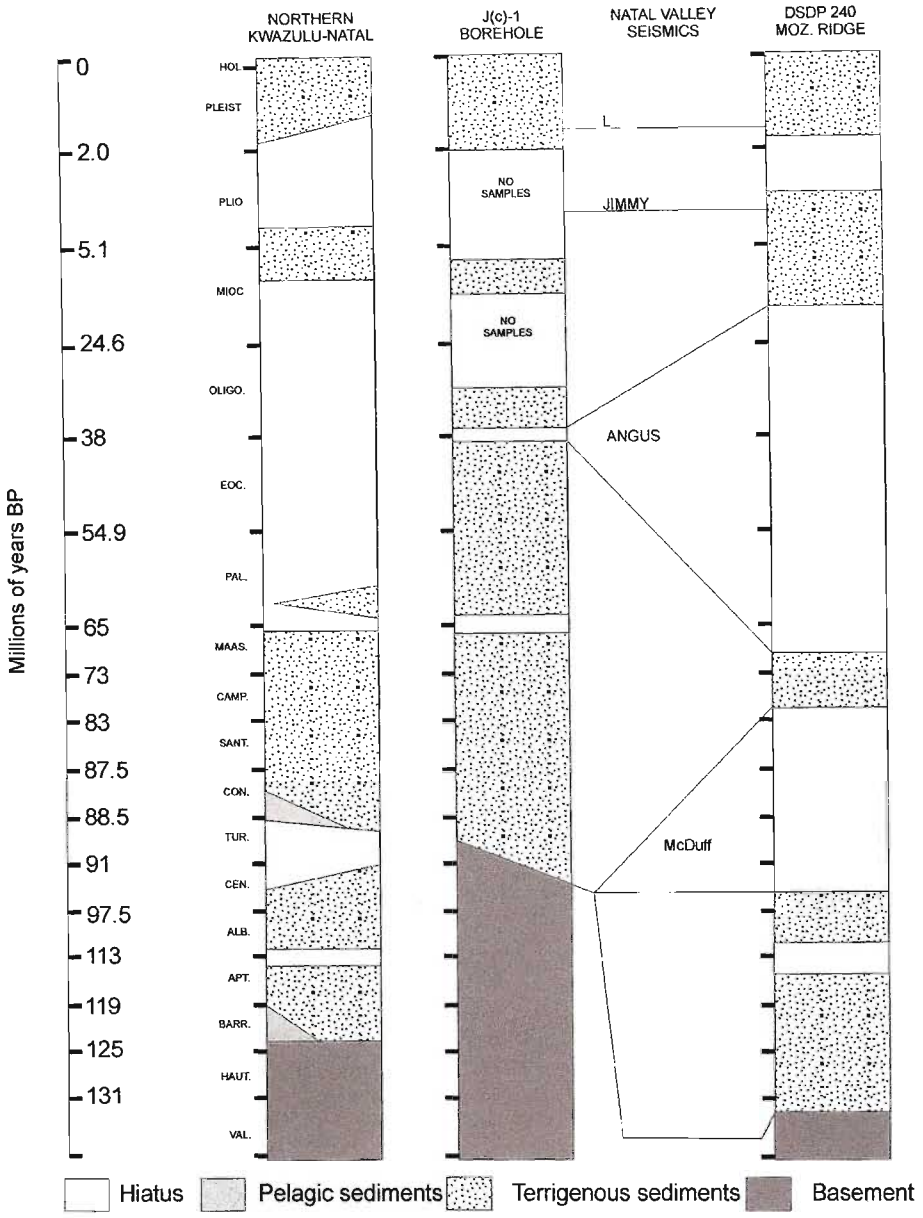

Figure 2.5. Stratigraphic columns for the KwaZulu-Natal continental margin based on the data of Du Toit and Leith (1974), Simpson, Schlich et al. (1974), McLachlan and McMillan (1979), and Martin et al. (1982) (modified from Martin and Flemming, 1988). Borehole localities are provided in figure 3.1.1. Reflectors Angus and Jimmy are discussed in the text. Ful names of eras, epochs and ages: Valenginian, Hauterivian, Barremian, Aptian, Albian, Cenomanian, Turonian, Coniacian, Santonian, Campanian, Maastrichtian, Palaeocene, Eocene, Oligocene, Miocene, Pliocene, Quaternary, Pleistocene, Holocene. Figure modified from Martin and Flemming (1988).

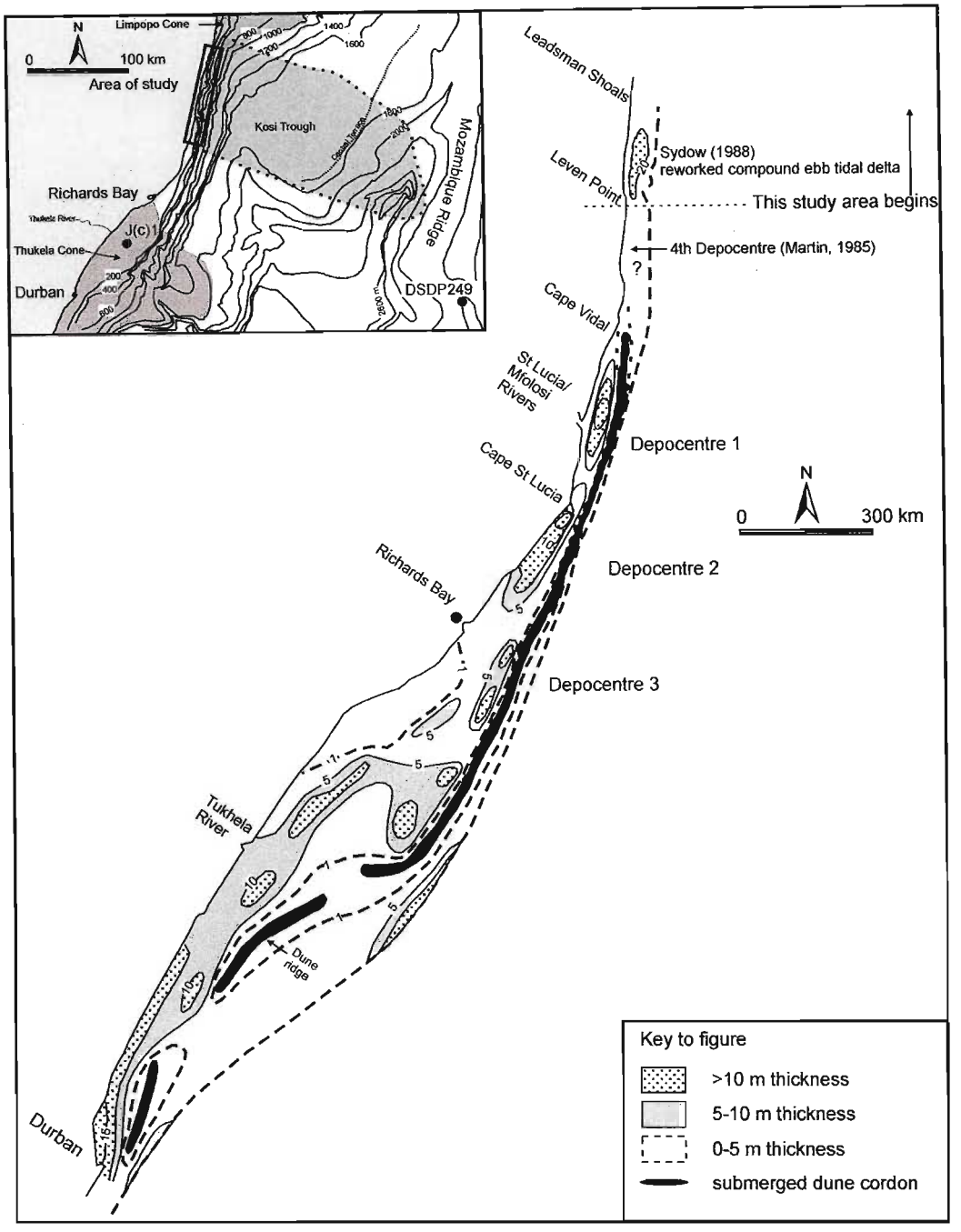

Figure 2.6. Holocene sediment isopach map (thickness in metres) of the continental shelf north of Durban to Leadsman Shoals (after Flemming and Hay, 1988; Sydow, 1988). Note the three recognised depocentres corresponding to 1) the St Lucia/Mfolosi River confluence, 2) offshore Cape Vidal and 3) offshore Richards Bay. A fourth depocentre was recognised by Martin (1985) extending between the St Lucia Estuary to just south of Leven Point, ~ 18 m thick. Sydow (1988) recognises a fifth depocentre offshore Leven Point stretching to Leadsman Shoals, which may possibly be an extension of Martin's (1985) depocentre.

CHAPTER 3

Sequence and chronostratigraphic models of shelf development

3.1 Introduction

Seismic stratigraphic studies of the northern KwaZulu-Natal continental shelf and upper slope (Fig. 3.1) have focused either on low resolution single-channel seismic reflection studies concerned with the basin evolution of the adjoining Natal Valley (Dingle et al., 1978; Martin et al., 1982; Goodlad, 1986) or with high resolution single-channel seismic reflection studies concerned with sediment-current interaction on the continental shelf (Martin and Flemming, 1988; Sydow, 1988; Ramsay, 1994; Shaw, 1998). To date, little agreement exists concerning the seismic stratigraphy of the continental shelf of northern KwaZulu-Natal. Many of the interpretations made in previous studies were based on poor quality analogue records which reduced the data resolution, thus placing serious constraints on the development of a true sequence stratigraphic appraisal of the area. Similarly, age controls on the development of the continental shelf have been hindered by sparse borehole, outcrop and sample data. This chapter is concerned with the evolution of the northern KwaZulu-Natal continental shelf from a sequence stratigraphic perspective, based on newly acquired high resolution single-channel seismic reflection data. In addition, a chronostratigraphic reconstruction of the continental shelf development based on previous borehole and regional seismic data; recent submersible samples; and established sea level curves for the region is made with which the sequence stratigraphy may be compared.

3.1.1. Terminology

All sequence stratigraphic interpretations are based on established procedures in sequence stratigraphy (Mitchum and Vail, 1977; Vail, 1987; Posamantier et al., 1988; Posamantier and Vail, 1988; Coe et al., 2003). Four systems tracts are recognised in each complete sequence: the forced regressive systems tract (FRST); the lowstand systems tract (LST); the transgressive systems tract (TST); and the high stand systems tract (HST) (Fig. 3.2a). The FRST corresponds to periods of sea-level lowering, beginning at the point of maximum sea-level and terminating at minimum sea-level. The LST represents the period of time where sea-level begins to slowly rise from its minimum level to a point where the rate of sea-level rise begins to increase rapidly. Sediment is thus deposited in an aggradational manner, as the rate of increase in accommodation space and the rate of sediment

supply are balanced. The TST occurs once the rate of rate of sea-level rise is stabilised and ends where the rate of sea-level rise begins to decrease. The LST and TST characterise periods of time where topography exposed or eroded during sea-level lowering is subsequently infilled.

This paper considers the sequence boundary to occur at the base of the basinward prograding FRST deposits, and is considered to form by subaerial erosion, normally associated with stream downcutting and basinward shift in facies and onlap of overlying strata (Posamantier et al., 1988). Though much controversy surrounds the relative position of the sequence boundary with respect to FRST deposits, it is assigned this position on the assumption that it forms under periods of sea level fall and occurs contemporaneously, or just prior to, the deposition of progradational sedimentary bodies characteristic of forced regression (Coe et al., 2003; Catuneanu, 2006). In this case, the sequence boundary represents the surface of maximum incision i.e. the valley surface which bounds the subsequent incised valley fill.

3.2. Methods

3.2.1. Data collection and processing

Four hundred line kilometres of single-channel, high resolution seismic reflection data were collected covering an area of 478 km^2 of the northern KwaZulu-Natal continental shelf and upper slope (Fig. 3.1). Positioning was achieved using a differential GPS, with position fixes acquired at 1 second intervals. These were corrected using an MSK beacon correction, providing sub-metre accuracy. Seismic data were collected using a Design Projects boomer system and 20 element array hydrophone, and recorded digitally in raw SEG-Y format via an Octopus 360 seismic acquisition system. Power levels of 500 J were used throughout the study. Raw data was processed, with time-varied gain, bandpass filter (300-1200 Hz), swell filter and manual sea-bed tracking. Data were later stacked during post processing. Streamer layback and antenna offset corrections were applied to all digitised data and constant sound velocities in water (1500 ms^{-1}) and sediment (1650 ms^{-1}) were used to extrapolate all time-depth conversions. All lines are compressed to ~ 25 × vertical exaggeration unless otherwise stated. All seismic data resolve to approximately 6 m in the vertical as a result of source ringing during data acquisition.

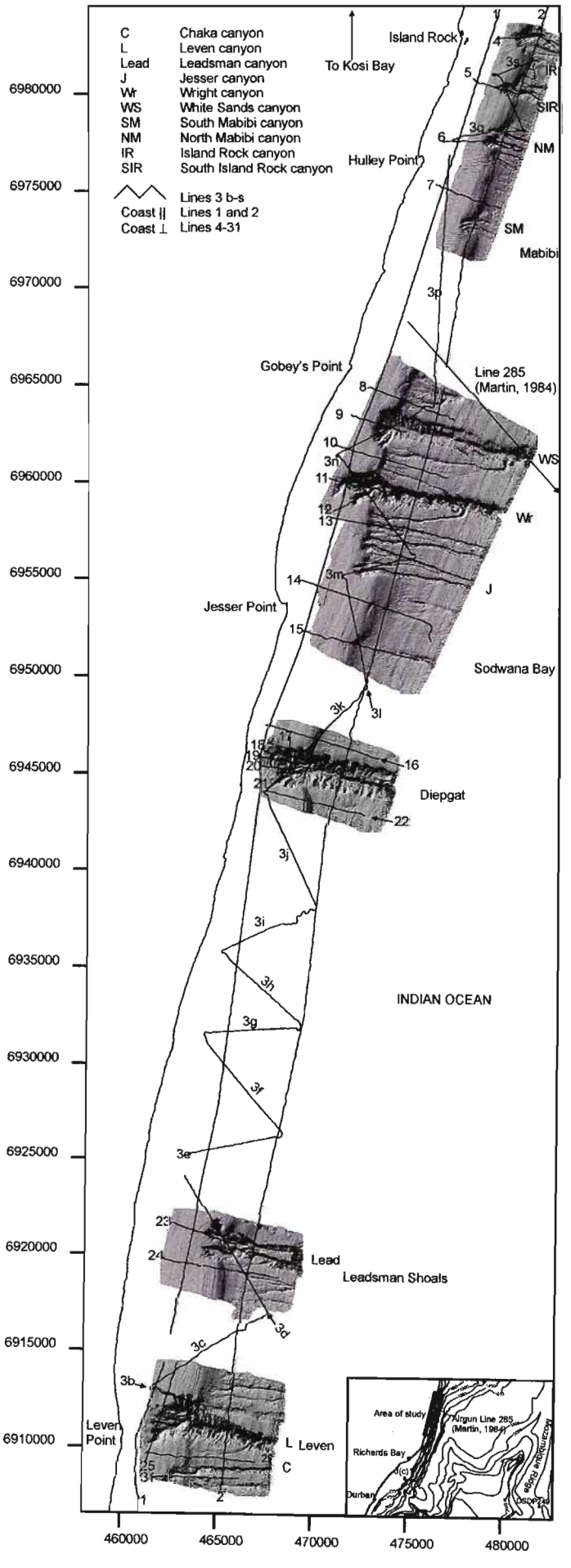

Figure 3.1. Seismic tracklines acquired across the northern KwaZulu-Natal continental shelf, from Leven Point in the south to Island Rock in the north. Lines 1 and 2 were acquired parallel to the shelf strike, lines 4 to 31 parallel to shelf dip. Line 3 b-s are slope oblique. Lines are superimposed over sunshaded multibeam bathymetry. For a comprehensive discussion of the bathymetry, please see chapter 4, sections 1 and 2. Inset depicts the study area relative to the regional bathymetry of (Dingle et al., 1978) and exploration borehole localities DSDP249 and J(c)1.

3.3. Results

Preserved systems tracts of the various sequences are separated by significant erosional hiatuses, particularly the late Palaeocene to Late Miocene (Fig. 3.2b, Fig. 2.5). In addition, sea-level fluctuations during the Quaternary (Fig. 3.2c) have produced erosional hiatuses, resulting in incomplete sequence preservation (Ramsay, 1994; 1996). As such, no full stratigraphic sequences are recognised; however, the systems tracts of known depositional periods are delineated on the basis of parasequence set architecture and bounding surface configuration. Pre-existing sea-level curves (Fig. 3.2) and stratigraphic data (Du Toit and Leith, 1974; McLachlan and McMillan, 1979; Martin et al., 1982) (Fig. 2.5), in conjunction with seismic data of this study indicate at least 5 incompletely preserved sequences having formed since Late Cretaceous times. Figure 3.3 is a schematic representation of the various seismic units of the continental shelf. These comprise eight discrete seismic units (Figures 3.4 to 3.8), identified on the basis of parasequence set architecture and bounding unconformities (Table 3.1).

3.3.1. Unit A

Deposits of Unit A display three unique seismic facies which include the progradational acoustic basement (A1), and onlapping lateral accretion (A2) and draped (A3) channel fills (Table 3.1, Fig. 3.4 a and b: Line 2, 29). The topsets of A1 are erosionally truncated, either by modern erosion processes on the seafloor, or the overlying sequence boundary SB1 (Fig. 3.4b: Line 29). Unit A pinches out northwards towards Diepgat Canyon (Fig. 3.4a: Line 2), where it is truncated by apparently younger sediments.

3.3.2. Unit B

Unit B comprises an aggradational to progradational inner shelf connected sediment wedge that dips shallowly (~1°) towards the southeast (Table 3.1; Fig 3.4a: Line 2). Seismic Facies B1 displays high amplitude low angle reflectors that gradually steepen seaward, and which onlap SB1 landwards and may downlap SB1 below the seismic penetration limit of this study (Fig. 3.4b: Line 29). Seismic Facies B2 occurs as a predominantly draped fill within the incised portions of SB1.

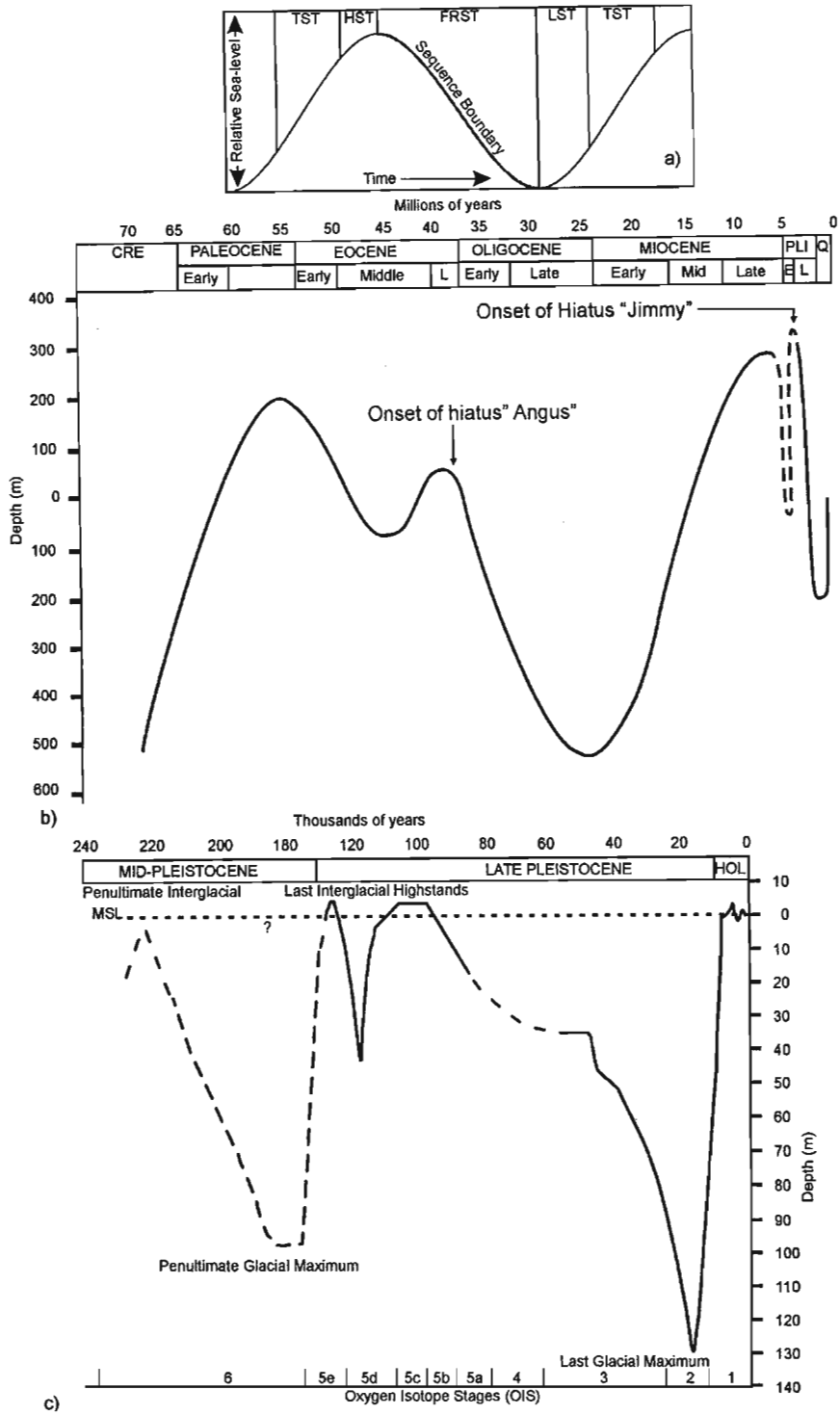

Figure 3.2a. Idealised positions of the various systems tracts over a theoretical cycle of sea-level rise and fall over time. Note the diagram assumes a uniform rate of sediment supply and rate of subsidence. TST = transgressive systems tract, HST = highstand systems tract, FRST = forced regressive systems tract, LST = lowstand systems tract. The sequence boundary here is considered to form between the maximum and minimum sea-level positions. **3.2b.** South African sea level variations since the Late Cretaceous (from Siesser and Dingle, 1981). CRE = Cretaceous, PLI = Pliocene, Q = Quaternary, E = early, L = late. **3.2c.** Late Pleistocene sea-level curve for the East coast of southern Africa (after Ramsay and Cooper, 2002).

3.3.3. Unit C and D

Unit C is characterised by a mid slope attached, thinly developed wedge, with sporadic low continuity reflectors that onlap the underlying transgressive ravinement surface RS1 (Fig. 3.5: Line 14). This unit pinches out landwards on the upper slope, the top of which in most instances forms the modern seafloor erosion surface. Unit D is separated from Unit B by ravinement surface RS2, upon which thin, acoustically transparent sediments are deposited as sheets. Unit D is most prominent south of Diepgat Canyon, and thins towards Leadsman Canyon in the south and Sodwana Bay in the north (Fig. 3.1, appendix 1).

3.3.4. Unit E

Deposits of Unit E volumetrically dominate the observed shelf sequences, forming a landward thinning sediment wedge composed of several seismic facies of variable architecture. Facies E1 comprises low amplitude, high angle (5°-7°), oblique tangential clinoforms that downlap the underlying bounding surface (Fig. 3.5a: Line 7). These may be truncated seawards by several small prograding wedges of steeper orientation, with clinoforms becoming progressively steeper until they become concordant with the modern shelf edge and upper slope (Facies E2) (Fig. 3.6a: Line 7). Alternatively, E1 may be truncated by oblique parallel clinoforms that onlap E1 and downlap onto the flooding surface beneath (Facies E3) (Fig. 3.4b: Line 29). The outer-mid shelf areas exhibit low amplitude, irregular reflectors which onlap RS1 (Facies E4), and which represent the reworked topsets of facies E2 and E3 (Fig. 3.6b: Line 15). These are truncated by fluvial incisions, associated particularly with areas where facies E3 is prominent (Fig 3.7: Line 1). These are filled by draped sediments (facies E5) of conformable age to facies E2-E3 (Fig 3.7: Line 1).

3.3.5. Unit F

Unit F is a thin poorly developed inner-to outer shelf attached wedge that is close to the seismic resolution of this study (Fig. 3.4a and b: Lines 2 and 29). Unit F displays high acoustic impedance, and a channelled internal reflection configuration, separated from unit E by a ravinement surface (RS3) which truncates the topsets of E3/E2. Seaward pinch-out depths of the wedge coincide with the modern shelf edge, where unit F crops out forming seafloor lineations which mirror the modern day coastline configuration (appendix 1).

Table 3.1. Seismic stratigraphic column of the northern KwaZulu-Natal shelf, illustrating underlying horizons, seismic facies, thicknesses, stratal relationships, interpreted depositional environment, systems tract and the sequence to which each belongs.

Underlying horizon	Seismic Unit	Seismic Facies	Modern Description	Thickness	Stratal Relationship	Interpreted Depositional Environment	Systems Tract	Sequence
-	A	A1	Mid-upper slope prograding acoustic basement. Subordinate incision	> 110 m	High amp. parallel to sub parallel clinoforms, high continuity, dip shallowly to SE		FSST (?)	1
		A2	Mid slope incised channel fill	10-20 m	Onlapping lateral accretion fill	Estuarine	Late FSST	
		A3	Mid slope incised channel fill	10-20 m	Onlapping drape fill	Abandoned estuarine/ fluvial channel	Late FSST	
SB1			Mid to upper slope prominent reflector		Erosional truncation of A, incised undulating surface, dip towards SE		Sequence Boundary	
SB1	B	B1	Inner shelf connected progradational wedge	> 110 m	High amp. oblique parallel-sub parallel clinoforms, high continuity, dip shallowly to SE, onlap SB1, may downlap SB1 in deeper sections	Marine deltaic	LST	2
		B2	Mid-upper slope incised channel fill	< 35 m	Onlapping drape fill	Drowned estuarine channel/river valley fill	LST	
RS1	C	C	Mid slope, thinly developed retrogradational unit	< 20 m	Onlapping low amplitude, low continuity reflectors. Not always present	Deeper marine sequence	?	
Major erosional hiatus-spanning ~Late Cretaceous-Miocene "Angus"								
RS2			Upper slope-outer shelf		Erosional truncation B, may be concordant, curvilinear surface			
RS2	D	D	Upper slope-outer shelf thinly developed profile	< 10 m. Close to seismic resolution	Acoustically transparent sheet drape, concordant with RS1	Marine flooding surface. Reworking by transgressive wave base shift	TSST	3
RS3	Anomalous Unit	-	Forms basal wedge beneath shelf edge	< 50 m	Low amp. high continuity oblique tangential clinoforms. Dowlaps Rs3	Shelf margin clinoform	FRST	
Major erosional hiatus-spanning ~ Mid Pliocene "Jimmy"								

MFS	E	E1	Landward unit at base of shelf edge wedge		Low amp. high continuity oblique tangential clinoforms. Downlaps MFS.	Shelf margin clinoform	FRST	4
OS1		E2	Buried mid slope retrograding wedge		Low amp. high continuity oblique parallel clinoforms. Onlap OS1, downlap MFS.	Shelf margin clinoforms proceeding still stand minor transgression	FRST-LST	
OS2		E3	Mid-upper slope retrograding wedge		Low amp. high continuity sigmoid oblique clinoforms, onlap OS2, downlap MFS and/or RS1	Relative SL fall, then shelf edge delta progradation during SL rise	Late LST	
		E4	Outer-mid shelf landward extent of shelf edge wedge	Obscured by multiple	Low amp. low continuity, irregular reflectors. Onlaps SB2/RS1 (?) grades into E1-3. Topsets of E3.	Shelf aggradation and progradation during relative SL fall	FRST	
		E5	Incised channel fill	< 10 m	Onlapping drape fill	Delta top distributary channel abandonment	Late LST	
Major erosional hiatus-spanning Late Pliocene-Early Pleistocene (?)								
RS4	F	F1	Inner-outer shelf attached wedge	< 25 m	Channelled internal reflection config. High acoustic impedance. Truncates topsets of E3 and incises into E4	Shallow marine nearshore facies	?	5
	G	G1	Inner-outer shelf stranded sediment outcrop	< 35 m	High acoustic impedance, rests erosionally on F1/E3-4/B1	Late Pleistocene Aeolianite/beachrock. Palaeoshoreline.	LST-TSST-HST-FSST	?
SB2	H	H1	Shore connected prograding wedge	< 50 m	Acoustically transparent, low amplitude obliquely divergent reflectors, downlaps RS3, SB2/RS1 and E-3-4. May onlap RS3 as fill of drowned topographic low.	Holocene inner shelf wedge	LST-TSST	6
		H2	Incised valley fill (see ch. 3 section 2)	< 80 m	Onlapping drape fill	Transgressive fill of incised river valley.	LST-TSST	

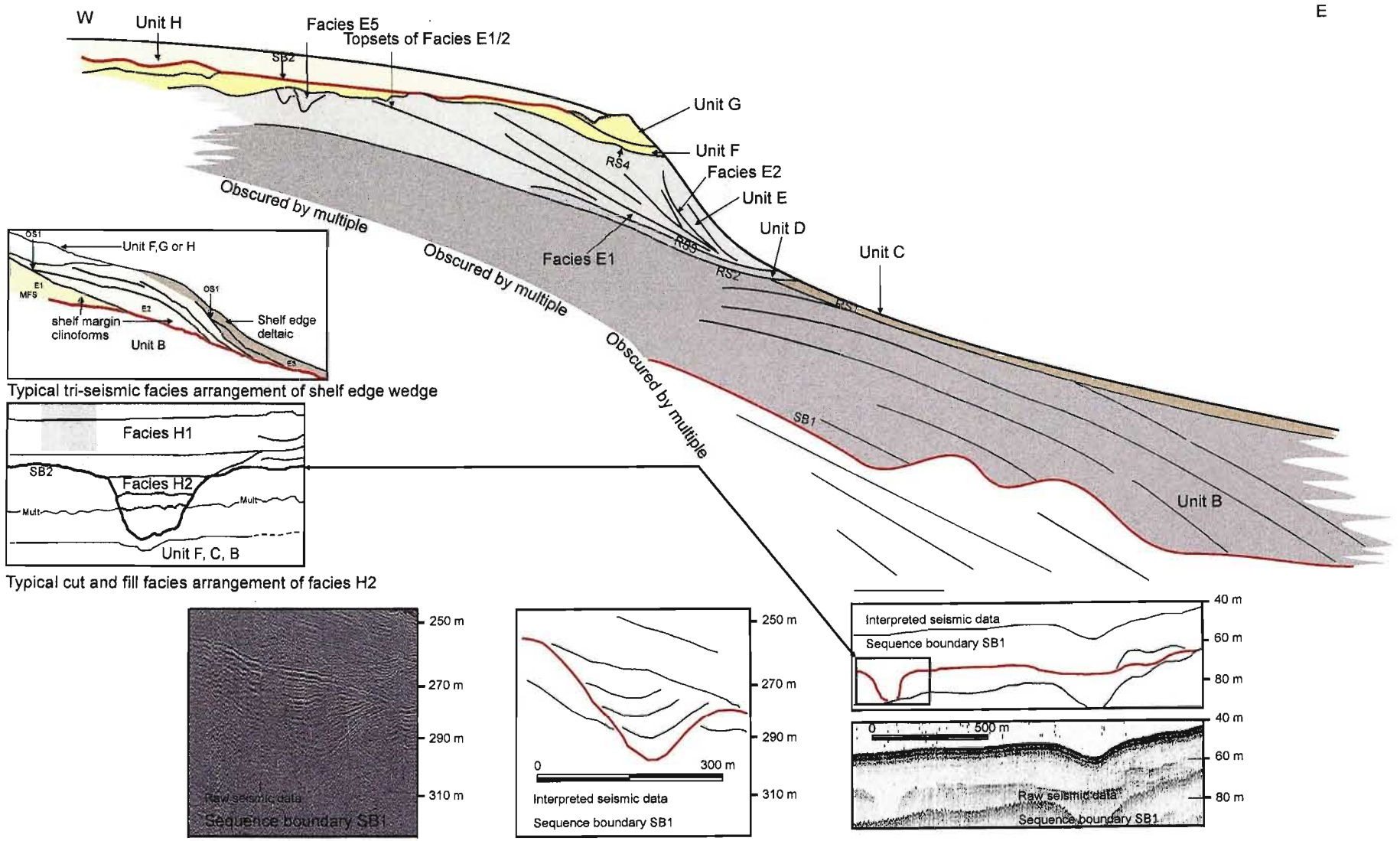

Figure 3.3. Schematic cross section of the Northern KwaZulu-Natal continental shelf revealing typical arrangement of shelf seismic facies and bounding unconformities as discussed in table 3.1. SB = sequence boundary, RS = ravinement surface, MFS = marine flooding surface, OS = onlap surface. Not to scale.

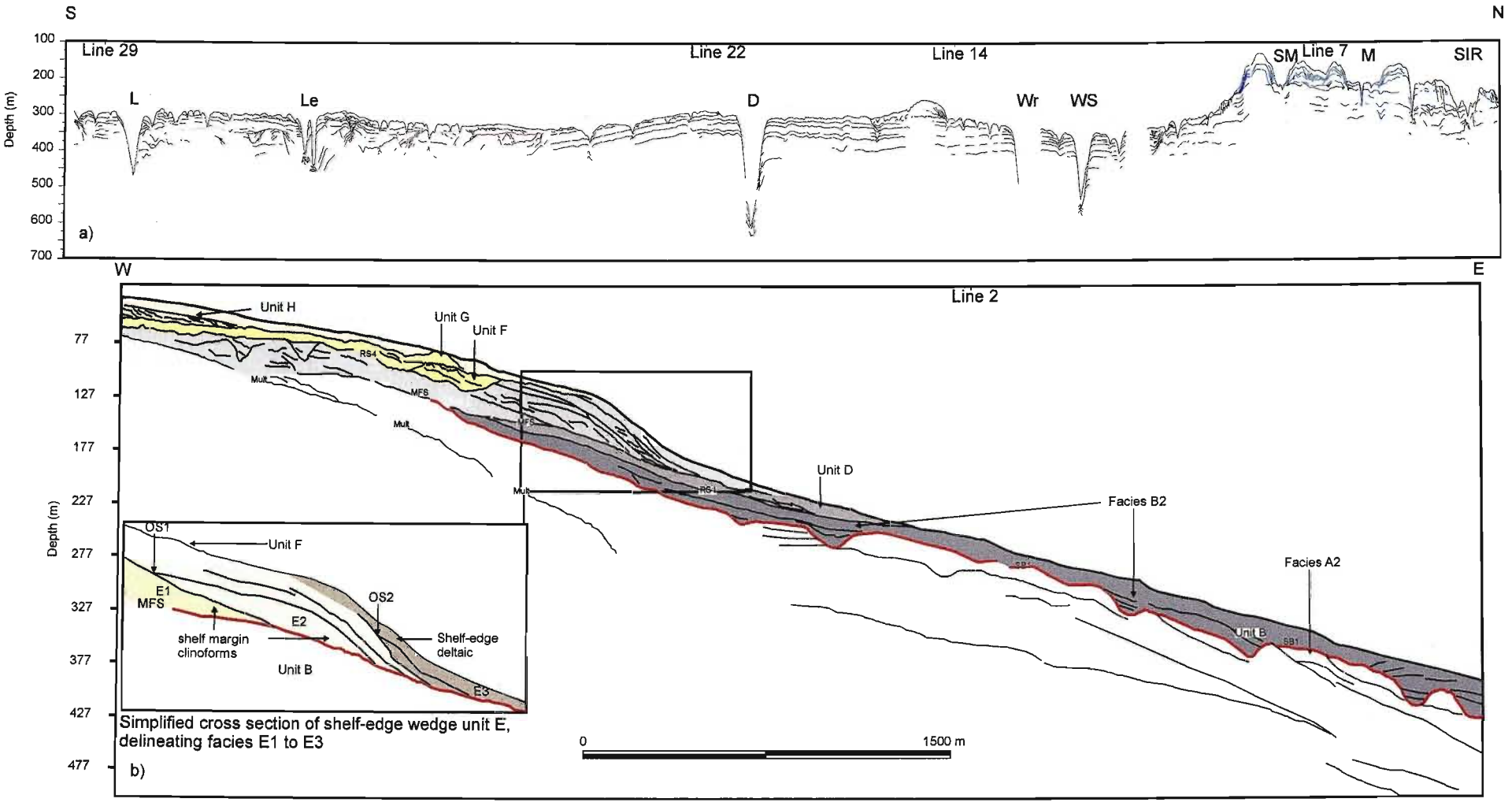

Figure 3.4a. Interpretative line drawing of strike parallel line 2. Red lines represent sequence boundaries. Dashed red lines represent inferred sequence boundary. Lower sequence boundary = SB1, upper sequence boundary = SB2. Blue reflectors represent Unit E sediments. Black reflectors between SB2 and uppermost blue reflectors = units F and G. Black reflectors between lowermost blue reflectors and SB1 = Unit B. Black reflectors beneath SB1 = Unit A. Reflectors of unit A pinch out towards Diepgat Canyon. All canyons, apart from Leven and Leadsman canyons,erosionally truncate both unit B and SB1. Length of section ~100 km. **3.4b.** Strike perpendicular line 29. Note the acoustic basment, unit A, which comprises prograding clinoforms, and small onlapping channel fills (right hand corner). The overlying unit B rests on the erosion SB1, and forms a landward pinching shelf attached wedge. Note the channel fill facies, B2. Mult = multiple, red lines = sequence boundaries

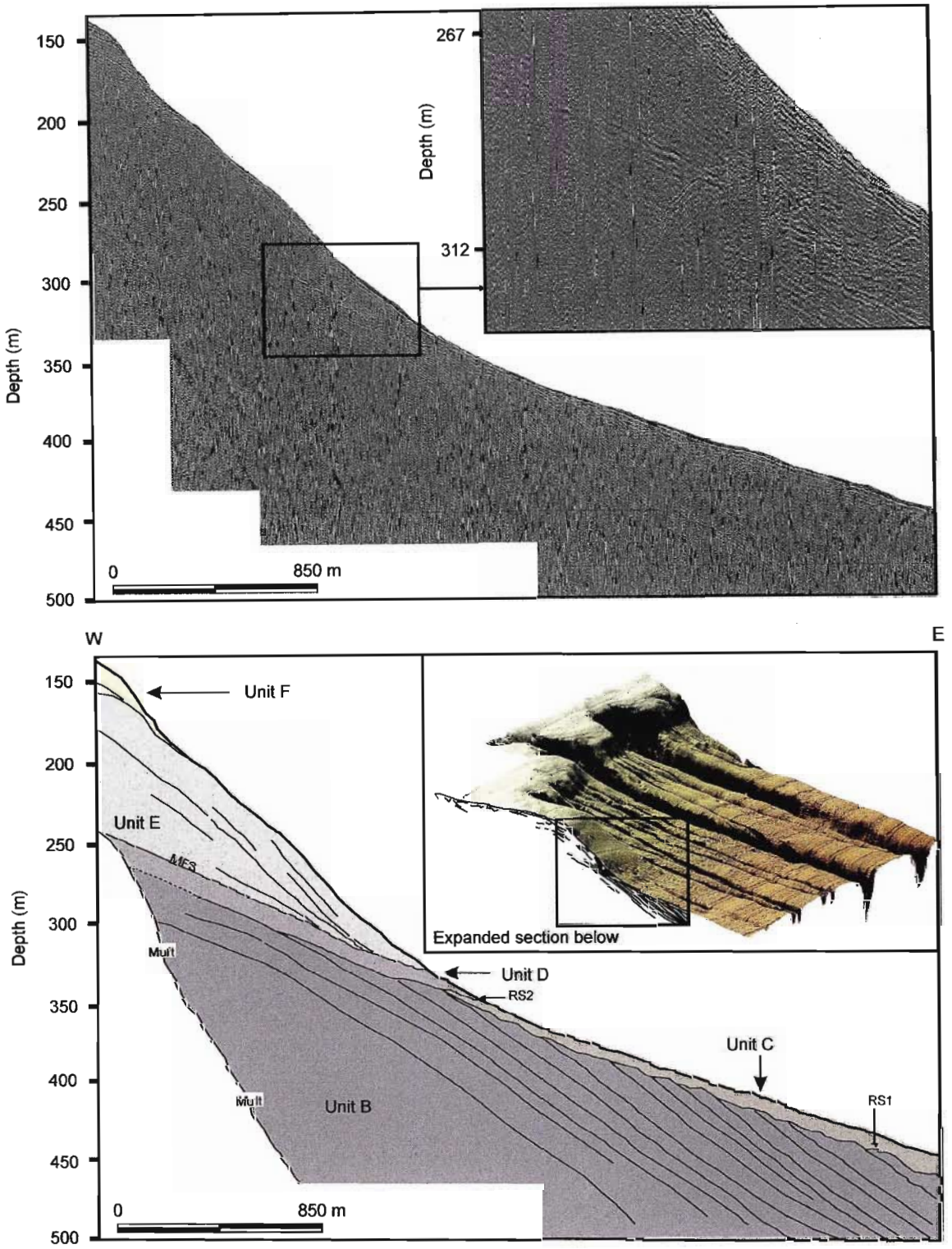

Figure 3.5. Slope perpendicular line 14 offshore of Jesser Point. Note the steep, seaward dipping reflectors of unit B, overlain by the slope attached, thinly developed wedge of unit C. Internal reflectors of unit C onlap the underlying surface ravinement surface RS1. Unit D overlies this thin wedge and unit B, separated by ravinement surface RS2.

3.3.6. Units G and H

Unit G occurs as isolated, acoustically opaque outcrop across the continental shelf, forming ridges of variable height (< 35 m). This unit may be buried by younger units which abut against the seaward flanks of these ridges (Fig. 3.8: Line 22). Unit H occurs as a shore attached prograding wedge, comprised of two distinct seismic facies, H1 and H2. Thin backstepping units within Unit H are evident (facies H1), and abut buried ridges of unit G (Fig. 3.8: Line 22). Unit H is separated from the underlying sequences by sequence boundary 2 (SB2), a south easterly dipping, heavily incised erosive surface that is laterally continuous along strike. Onlapping drape fills within the incised portions of SB2 are typical of seismic facies H2 (Fig. 3.7: Line 1). These comprise the dominant portion of this fill and are examined more thoroughly in chapter 3, section 2.

3.3.7. Anomalous progradational unit

This unit occurs intermittently as a progradational, landward thinning wedge of variable thickness, and is recognised from shore perpendicular seismic sections of the southern Mabibi area (Fig. 3.6a: Line 7). The unit is characterised by low amplitude, high angle, reflectors which downlap RS2 or RS1, or most commonly where Units C and D are absent and it directly overlies unit B. The wedge comprises a series of divergent oblique tangential clinoforms which may have smaller subsidiary lensatic bodies of chaotic reflectors within this arrangement. This unit is very similar to Unit E in its appearance, yet is truncated erosionally by MFS at the base of unit E.

3.4. Discussion

3.4.1 Sequence stratigraphic interpretation

3.4.1.1 Lowstand Systems Tract Deposits

Lowstand system tract deposits of the northern KwaZulu-Natal continental shelf are preserved as the landward pinching wedge of the progradational-aggradational unit facies B1, and the onlapping aggradational wedge of facies E3 (Figs. 3.4, 3.6 and 3.8).

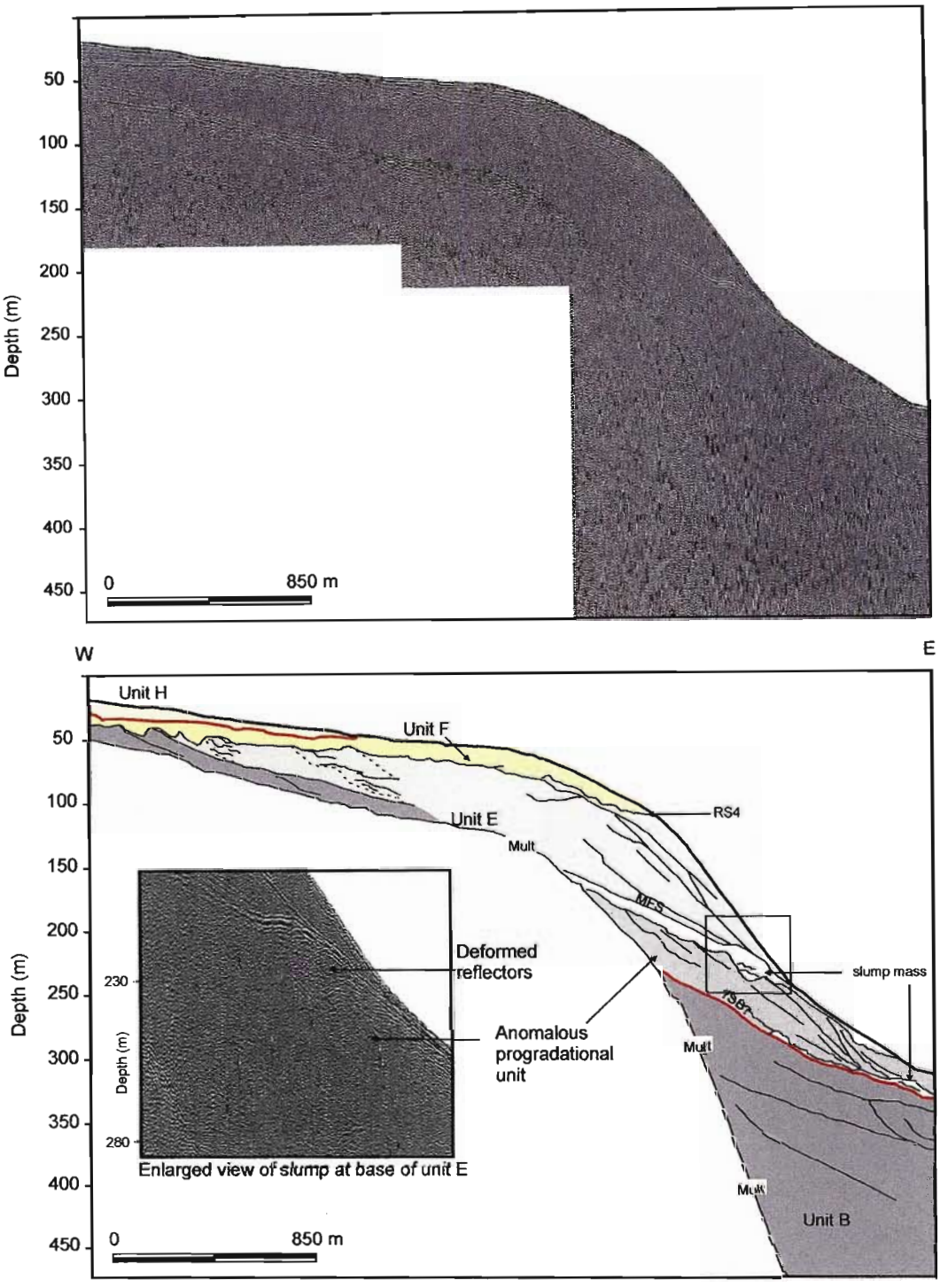

Figure 3.6a. Strike perpendicular line 7. Note the low amplitude, high angle, oblique tangential clinoforms of Unit E, which downlap the underlying bounding surface (interpreted as a slump-mass top). Note the seaward truncation of unit E clinoforms by small prograding wedges of steeper orientation. Dotted lines represent small scale slump deformation in facies E4 and E5.

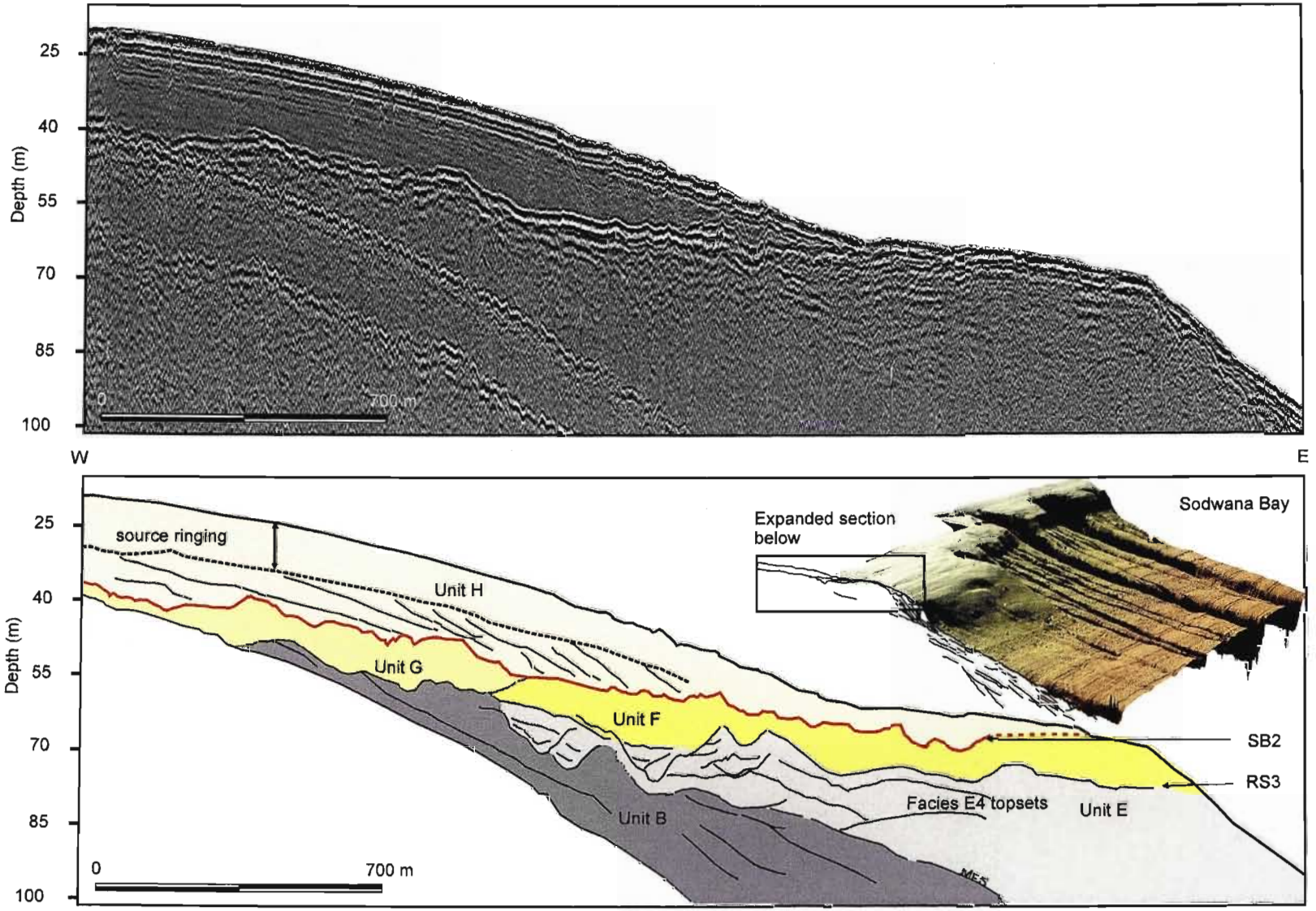

Figure 3.6b. Strike perpendicular line 15. Note the irregular reflectors of unit E in the mid-shelf, and the presence of small incisions which truncate the topsets of unit E, facies E4. The fill of each incision corresponds to facies E5.

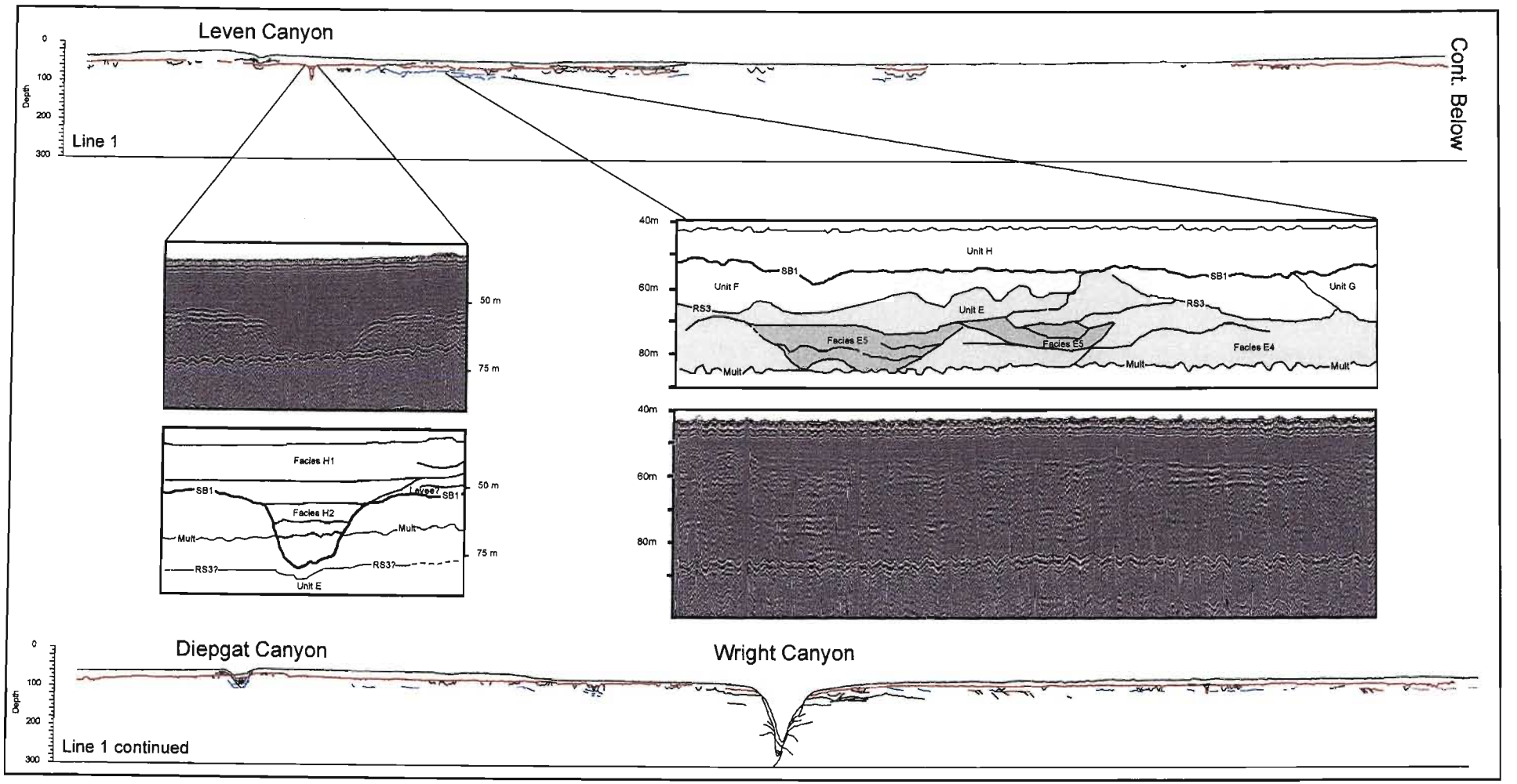

Figure 3.7. Strike parallel line 1. For line drawing: red lines indicate SB2 separating unit H from underlying sediments, blue lines indicate unit E reflectors, black (at depth below blue) indicates unit A and B reflectors. Insets depict areas of incision. Left inset and line drawing shows facies of H2 within an incision of SB2. Right inset and line drawing depicts incisions into facies E4 and the resultant fill facies E5. Note the erosive forms of the lower surfaces of unit G and unit F. Length of line 1 ~ 100 km.

3.4.1.2 Transgressive systems tract/highstand systems tract deposits

Transgressive systems tract deposits include the thinly developed retrogradational unit C (Fig. 3.4), the sheet-like unit D (Fig. 3.4), the shore connected wedge of unit H (Figs. 3.3 and 3.6b), and the incised valley fill of facies H2 (Fig. 3.7). Deepening environmental conditions, indicated by deep marine Mid-Upper Palaeocene clays retrieved from gravity cores off the mid slope (-692 m) south of Leven Canyon (Siesser, 1977), suggest a landward shift in distal facies. Unit C, however, is not laterally continuous along strike; this age is thus tentative, pending more detailed sediment sample analyses. Sediments of unit D are interpreted as more proximal sand sheets that are reworked and deposited by shoreface erosion and wave base shifting during the transgressive systems tract (e.g. Swift et al., 1972; Posamantier and Allen, 1993; Goff et al., 2005). Unit H is characterised by unconsolidated sediments of Holocene age that accumulated as a shore attached prograding wedge during the transgression following the Last Glacial Maximum (LGM) of ~ 18 000 BP (Ramsay and Cooper, 2002). The thin, backstepping facies within unit H are interpreted as either having formed during periods of slower transgression, stillstand or temporary regression during lower order transgression (Hernandez-Molina et al., 2000; Osterberg, 2006). SB2 is interpreted as the lowstand erosional surface formed during the Last Glacial Maximum, within which the onlapping incised valley fill of facies H2 occurs. Facies H2 is strongly associated with the modern day location of fringing coastal waterbodies, suggesting that the infilled portions of H2 represent the LGM open ocean connections of the Lake St Lucia system (Fig. 3.9).

3.4.1.3 Forced regressive systems tract

Deposits that formed under relative sea-level fall consist of unit A, facies E1 and E2 of the shelf-edge wedge (Fig. 3.4) and the anomalous progradational unit of the Mabibi area (Fig. 3.6a). The overall progradational architectures of unit A and E1 are indicative of general basinward advance of the sediment supplier due to sea level lowering. The channel cut and fill features (A2/A3) may possibly indicate the seaward shift of estuarine and fluvial facies belts, accompanied by respective channel incision and abandonment during the late falling stage systems tract and early lowstand systems tract (Plint and Nummedal, 2000; Hannebuth et al. 2003). The prograding shelf-edge margin clinoforms of facies E1 are truncated by a similar progradational wedge of facies E2.

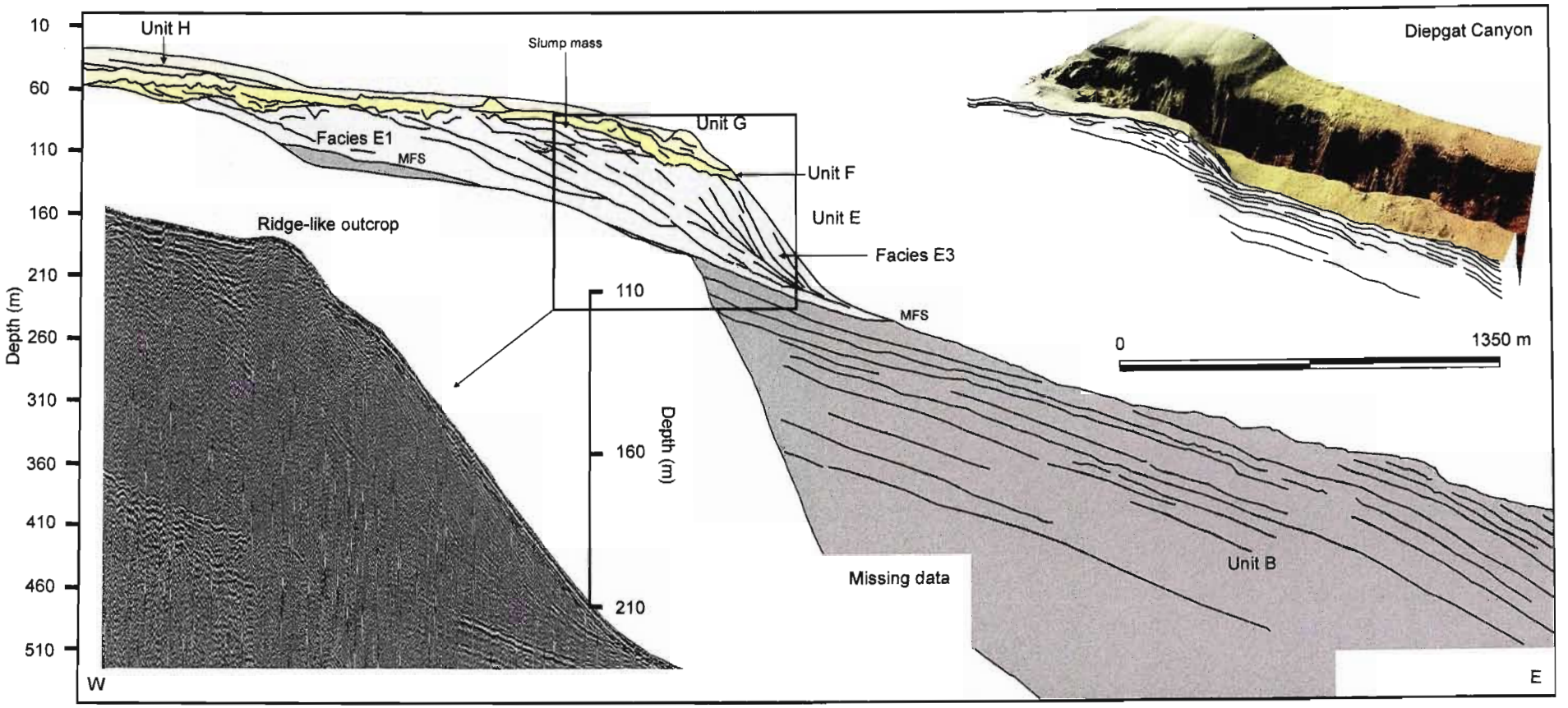

Figure 3.8. Strike perpendicular line 22. Note the isolated ridge-like outcrop of unit G in the mid-shelf and at the shelf break. In the inner shelf portions of the line, unit G is completely buried by younger sediments of unit H which abut these ridges. Unit F typically displays an erosive lower contact with unit E, facies E4 and E5, and overlies a slump body in the mid-outer shelf region. The seaward thickening wedge of divergent, aggradational/progradational unit B reflectors is prominent in this line.

Facies E2 represents a subsequent stage of shelf margin progradation, and rests on an underlying marine flooding surface which has truncated the underlying E1 clinoforms, indicating periods of inactivity or reworking, followed by active shelf margin progradation. The anomalous progradational unit found in the Mabibi Block is interpreted as having formed in a similar manner to the facies E1 and E2, a result of sea-level lowering and the production of large subparallel shelf margin clinoforms. The lenses of chaotic internal reflector configuration within both unit E and the anomalous unit are interpreted as slump bodies which formed contemporaneously with the deposition of these units. This indicates a high rate of sediment supply to the shelf-edge, causing sediment instability and slope failure (c.f. McHugh et al., 2002). Mass wasting conditions and contemporaneous slope progradation have been related to swift falls in relative sea-level (Miller et al., 1996a and b), high sediment supply and tectonic uplift (Poag and Sevon, 1989, Pazzaglia, 1993; Fulthorpe and Austin, 1998) and climatic change (Weaver and Kuijpers, 1993; Weaver et al., 1992). Major uplift during the Miocene and Pliocene has been documented for the hinterland of southern Africa, thus swift falls in sea level and rapid sediment delivery are favoured as the mechanism for shelf-edge wedge genesis of both unit E and the anomalous progradational units.

3.4.2. Chronostratigraphic models

Despite the lack of reliable borehole data from which a chronostratigraphic model for the continental shelf might be constrained; shelf sequences may be correlated with sea-level data for the South African coastline (Siesser and Dingle, 1981, Ramsay and Cooper, 2002). The chronostratigraphy of the shelf is further bolstered using foraminifer assemblages from limited gravity core (Siesser, 1977), grab and submersible samples (appendix 3a, Green et al., in review) taken where the various seismic units crop out. Unit A is the oldest unit in the area, interpreted as forming under forced regressive conditions. This is immediately overlain by unit B which is correlated with the acoustic basement identified by Sydow (1988) in an overlapping area of study which are of Middle Maastrichtian (Upper Cretaceous) age (Siesser, 1977; Martin and Flemming, 1988). Unit B is interpreted as having formed under lowstand conditions, and is assigned to the Late Cretaceous lowstand described by Siesser and Dingle (1981). Unit A must therefore be placed on the falling limb of sea-level preceding this Late Cretaceous lowstand (Fig. 3.10a). Known sea-level curves from South Africa do not recognise a Late Cretaceous forced regression-lowstand, suggesting that the curve should be ammended to accommodate the presence of these two systems tracts of this time period. The absence of a landward pinch out for the LST wedge of unit B precludes the establishment of a palaeo-shoreline depth for this period. This either extends to the

inner shelf where it is obscured by multiples, or under the coastal plain where seismic data are absent.

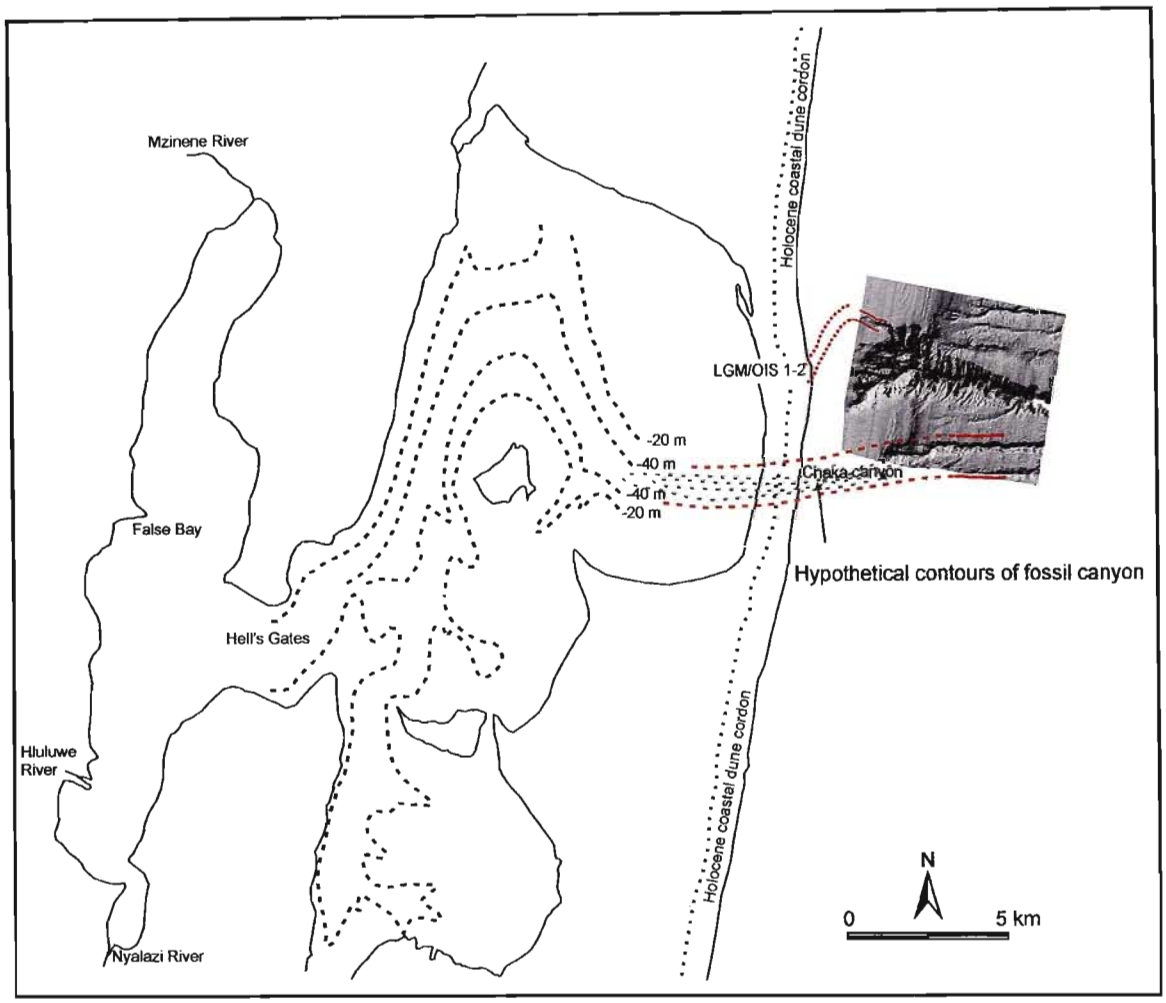

Figure 3.9. Position of unit H, facies H2, on multibeam bathymetry of Leven Canyon, and juxtaposed with onshore palaeo-bathymetry of Lake St Lucia (after Van Heerden, 1987). Solid red lines depict palaeo-topographic lows discovered from seismic data (this study). Dashed red lines indicate inferred continuation of topographic low. Please see chapter 4 for a more detailed examination of unit H, facies H2.

Sydow (1988) recognised similar deposits from the Leven Point area as those of unit C, which Siesser (1977) determined from a fringing gravity core as Mid-Upper Palaeocene in age. These are interpreted as having formed during a basin-wide transgression and agree with established sea level data (Siesser and Dingle, 1981) (Fig. 3.10a). However, the relatively thin unit C appears mismatched when considering the length of time over which transgression occurred. This would theoretically allow for thick TST deposits to accrete as back stepping parasequences which are characteristically absent from the northern KwaZulu-Natal shelf. It is proposed that unit C is a

remnant of these TST deposits which have been subsequently eroded during the pronounced sea-level regression of the Late Oligocene. This is documented by basin wide hiatuses in boreholes J(c)1 (Du Toit and Leith, 1974); DSDP 249 from the Mozambique Ridge (Simpson, Schlich et al., 1974) and seismic reflection studies from the deeper marine portions of the Natal Valley basin, offshore the study area (Martin et al., 1982). It is not uncommon for the more proximal portions of the TST to be removed by subsequent cycles of sea-level lowering and erosion (Posamantier and Allen, 1993; 1999).

The interpretation of unit D as a transgressive wave base-reworked sand sheet overlying a major erosional unconformity at depths of ~ 220 m, suggests the onset of transgressive conditions with a sea level above at least the -180 m (subsidence uncorrected) isobath (Fig. 3.10a). The resumption of deposition (post hiatus Angus) following the Upper Palaeocene-Middle Miocene, as recorded by Martin (1984) and borehole DSDP 249 (Simpson, Schlich et al., 1974) (Fig. 2.5) occurs at a time when suitable transgressive conditions prevailed (Fig. 3.10a). The lack of reliable borehole data in this area unfortunately precludes any meaningful calculation of margin subsidence to date, thus a Miocene age, based on the appropriate transgressive conditions, is tentative without proper depth constraints based on thermal and loading subsidence values. Alternatively, unit D may have formed on the climbing sea level limb of Early Pliocene age, prior to a forced regression of Late Pliocene age, however this appears unlikely based on a Late Miocene age assigned to overlying units (the anomalous progradational unit described in section *3.4.1.3*). The sea level curve of Siesser and Dingle (1981) indicates a maximum sea level of approximately 300 m above mean sea level for the Late Miocene and Early Pliocene. However extensive TST deposits are characteristically absent from the shelf. FRST deposits of unit E, facies E1 unconformably overlie unit D instead. Thus, a major erosional hiatus ensued, which is not recognised from borehole data (Fig. 2.5). This corresponds to regional seismic reflector Jimmy as described by Martin (1984). TST and HST deposits of this phase in the sea level were possibly eroded during the initiation of later sequences comprising post unit D sediments.

Palaeontological dating of a coquina outcrop from unit E2 (appendix 3a, Green et al., in review), acquired during submersible operations from Sodwana Bay, ascribes a Late Pliocene age to this unit. This lies within the falling sea level limb of Late Pliocene times (Siesser and Dingle, 1981), and correlates well with the interpretation of units E1 and E2 as FRST deposits produced by shelf margin accretion during relative sea level fall.

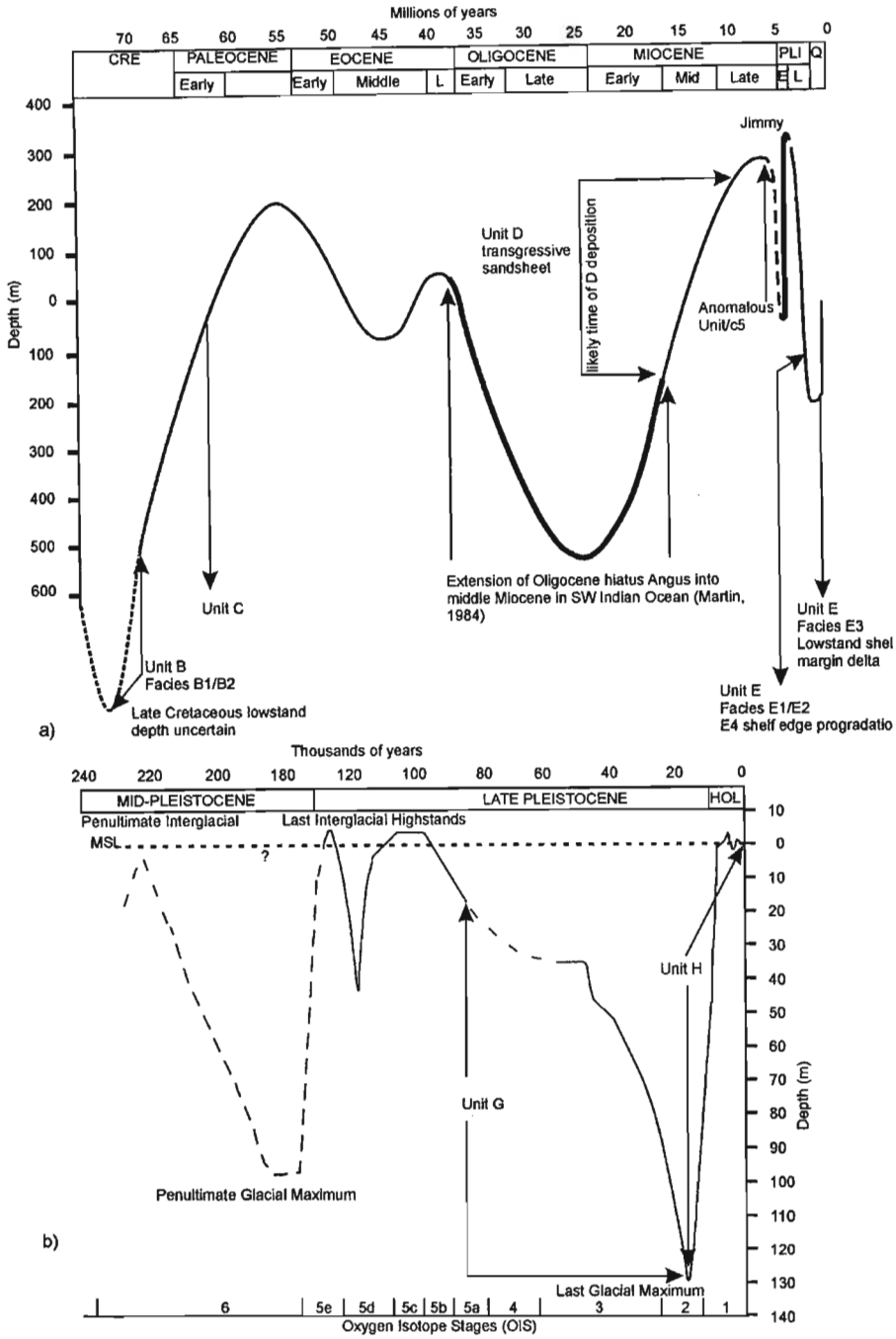

Figure 3.10a. Chronostratigraphic framework for the northern KwaZulu-Natal shelf, based on the sea-level curve of Siesser and Dingle (1981), palaeontological descriptions of gravity cores by Siesser (1977), and palaeontological dating of submersible and grab samples (this study). A lowstand of late Cretaceous age is proposed in order to accommodate the occurrence of unit B lowstand deltaic deposits of similar age. CRE = Cretaceous, PLI = Pliocene, Q = Quaternary, E = Early, L = Late. Grey shading on limbs represents hiatus development. **b.** Sea level curve of Ramsay and Cooper (2002) with chronostratigraphic delineation of units G and H. Unit G is inferred as being similar to the drowned coastline model of Ramsay (1994, 1996), in that outcrop depths of the ridge-like unit G closely correspond to the depths of aeolianite ridges recognised in Ramsay's (1994, 1996) study. Unit H, the transgressive unconsolidated modern sediment wedge post-dates the last glacial maximum, and formed during the ensuing transgressive systems tract (Flandrian Transgression-OIS 2). See chapter 9 for a discussion of the significance of the depth of unit G outcrop.

Additionally, hinterland uplift during the Pliocene (Partridge and Maud, 1987) would have resulted in increased erosion and sediment loading of the shelf, causing the formation of large scale margin clinoforms (< 150 m height) and shelf progradation. Studies from the Durban continental slope indicate that similar shelf-edge wedge sequences overlie slumps of deformed Pliocene strata, Martin and Flemming (1988) thus interpreted these sediments as Late Pliocene or Pleistocene age. This study suggests that these are most likely of the former age and indicate basinwide uplift and shelf-edge progradation along an uplift axis extending along the present coastal plain to offshore of Durban (Partridge and Maud, 1987) (Fig. 3.1).

Facies E3 and E5 of unit E are interpreted as shelf margin deltaic and deltaic distributary channel fill sediments of the late LST respectively. These coincide with the observed -200 m lowstand of the Late Pliocene-Early Quaternary, and the high levels of sediment supply that were available to form shelf margin deltaic sequences at that time. Similar situations of shelf margin delta formation associated with hinterland uplift are provided by Edwards (1981), Galloway (1989; 1990) and Olsson et al. (2002). Shelf margin deltas have in this case spilled over the palaeo-shelf edge, supplementing shelf-margin accretion during this time period (cf. Morton and Suter, 1996). The anomalous progradational unit from the Mabibi upper slope is interpreted as having formed during the Late Miocene forced regression, prior to the onset of hiatus Jimmy. Angus to Jimmy age sediments of the Tugela Cone are described by Goodlad (1986) from the adjoining Natal Valley. The most northern facies of these, C5 with which this anomalous unit is correlated, is described as a mixed onlap-offlap sequence, with alternating cut and fill structures. This implies phases of progradation and upper slope/shelf erosion, the result being sporadic preservation of this unit, such as that seen in Mabibi. Where this unit is absent, a combined Angus-Jimmy hiatus surface occurs, particularly on the continental shelf where these surfaces converge. Where they diverge, as in the deeper adjoining Natal Valley, this unit is preserved along with unit D.

The Quaternary chronology of seismic units is more complex to unravel, in that well constrained sea level curves that span the Quaternary of southern Africa are unavailable. Quaternary sediments (units F-H) are separated from the underlying unit E by a short hiatus, the probable offshore equivalent of that recognised by Siesser and Dingle (1981) as late Pliocene in age. Unit F cannot be assigned an age without borehole data, though previous authors have interpreted it as a Pleistocene shallow marine deposit (Sydow, 1988; Shaw, 1998). The various ridge-like outcrops of unit G have been assigned palaeo-coastline episodes by Ramsay (1994, 1996) and Ramsay and Cooper (2002). These correspond to sea level still stands having formed beachrock/aeolianite complexes at or near

the previous coastline during the regression towards the LGM of ~ 18 000 BP (Fig. 3.10b). These culminate in the youngest, and most offshore ridge, being assigned an age of 23 000-22 000 (Ramsay, 1994).

The final sequence observed on the continental shelf is the one presently being deposited. Unit H, facies H1 and H2 are interpreted as a TST wedge and incised valley fill respectively, which formed after a period of maximum marine incision associated with the sequence boundary of the LGM (SB2). This sequence will be complete once a full cycle of forced regression to lowstand has created the upper sequence boundary.

3.4.3. Deltaic deposits and fluvial-shelf interaction

Deposits of facies 3 of unit E are interpreted as shelf-edge deltaic, based on their stratal architecture. This is supported by the presence of associated incised channels which confirm that either fluvial or deltaic feeder channels meandered across an exposed continental shelf during periods of lowstand. Shelf-edge deltaic facies occur in the Leadsman and Leven Canyon regions, and to a lesser extent in the southern Sodwana Bay region, suggesting an open ocean connection of the palaeo-St Lucia (Mfolozi River?) and palaeo-Lake Sibaya fluvial system during the Late Pliocene lowstand. There is less evidence to the north of deltaic sedimentation at the shelf edge, implying that the northern survey blocks were not as strongly influenced by fluvial systems at these times. SB1 is not as heavily incised in the far northern extremes of the study area implying that fluvial-continental shelf interaction was most pronounced and frequent in the southern portions, strongly influenced by the palaeo-Lake St Lucia drainage. This influence may thus extend as far back as Late Cretaceous times. Palaeo-Lake Sibaya drainage appears to have been equally important in supplying sediment to the shelf edge and deep ocean areas.

Resistivity profiling seaward of Lake Sibaya on the coastal plain reveals a coast-parallel channel of LGM age that is deflected behind the recent barrier complex (Meyer, pers comm., 2006). This may have debouched onto the continental shelf in the southern Kosi Bay area, where seismic profiling interpreted by Shaw (1998) indicates several incised valley fills of Holocene age. Alternatively, it may have been deflected south, breaching the barrier complex in the southernmost portion of Lake Sibaya. Seismic profiling inshore of White Sands and Wright Canyons shows a pronounced topographic low in SB2 which diverts into the head of Wright Canyon (see chapter 4 for a comprehensive explanation), a strong possibility thus exists that both a southern and northern mouth

of Lake Sibaya were open during the LGM. The effects of fluvial-shelf interaction on palaeo-drainage and shelf evolution are discussed more thoroughly in the following section on incised valley fills.

CHAPTER 4

Seismic facies of incised valley fills and transgressive systems tract sedimentation

4.1. Introduction

Since the early documentation of incised valley systems from outcrop studies by Van Wagoner et al. (1990) and Posamantier and Allen (1993), several models concerning the evolution of incised valley fills during transgressive conditions have been forwarded to explain the complicated patterns of sedimentation observed therein (e.g. Dalrymple et al., 1992; Zaitlin et al.; 1994; Allen and Posamantier, 1994; Ashley and Sheridan, 1994). Clearly, the accommodation space these topographic depressions provide for lowstand and transgressive sedimentation (Van Wagoner et al., 1990; Foyle and Oertel, 1997; Nordfjord et al., 2006) offers a unique opportunity to study a relatively uninterrupted stratigraphic history of an area, where in other parts of the shelf system, accommodation space may have been insufficient to preserve small scale (~10 ka) eustatic and sedimentary cycles accurately. Buried incised valley systems are commonly observed on continental shelves worldwide and attempts to reconcile seismo-/sequence stratigraphic and sedimentological observations with the early models of Dalrymple et al. (1992) and Zaitlin et al. (1994) are common (Foyle and Oertel, 1997; Anderson et al., 2004; Weber et al., 2004; Nordfjord et al., 2006). In southern Africa, despite the prevalence of relatively large fluvial-estuarine complexes, scant attention has been given to the sedimentary behaviour of these features since their formation during forced regression to their infilling during transgression. Notable exceptions include studies from the Namibian coastline (Stevenson and McMillan, 2004), the southwest coast of South Africa (Rogers, 1985) and latest transgressive sedimentation in modern estuaries from the east coast of South Africa (Cooper, 1991; Wright et al., 2000). Other authors have previously recognised fluvial incision surfaces in the region (e.g. Shaw, 1998). However little attention has been paid to the exact location of each incision, the nature of the incised surface, and the ensuing transgressive valley fill. This chapter represents the first results of a regional, high-resolution, single-channel seismic survey from which a sequence stratigraphic model for incised valley formation and fill for both late Cretaceous and latest Pleistocene examples is forwarded. A further attempt is made to reconstruct the palaeo-drainage of the continental shelf during lowstand conditions and link this to the evolution of shelf indenting submarine canyons of the adjoining upper continental slope.

4.2. Methods

Owing to the relatively sparse seismic coverage of the study area, sequence boundary surfaces which occur seaward of the shelf break could not be gridded effectively without introducing significant amounts of spurious data. In the mid shelf areas where seismic data are denser, isopach maps of the infilling sediments were created in order to provide an approximation of the coastal drainage during the LGM. In all other areas, each palaeo-valley location was delineated using the thalweg co-ordinates derived from seismic reflection profiles, and then plotted on a map where a schematic drainage pattern was created. In areas of high density, it was possible to delineate drainage features relatively accurately. Where isolated incisions were encountered, only a point marking the valley thalweg is depicted. (Please see chapter 3 for a comprehensive explanation of the seismic profiling methods).

4.3. Regionally developed sequence boundaries

Two sequence boundaries, SB1 and SB2, are recognised on the northern KwaZulu-Natal continental shelf. Each is characterised by its distinctive erosional surface, marked by V-or U-shaped incised valleys, rugged topography and high amplitude acoustic returns (Figs. 4.1 and 4.2). SB1 represents a late Cretaceous sequence boundary and is mantled by progradational-aggradational, landward-pinching lowstand deposits of unit B. SB2 represents a late Pleistocene sequence boundary which formed during regression from the last interglacial of ~ 95700 ± 4200 BP (Ramsay and Cooper, 2002). Palaeo-valleys within these sequence boundaries represent the previous occupation of seaward discharging drainage systems onto the exposed continental shelf where the shoreline lay at ~ 120 m below present day. These were subsequently drowned during the ensuing sea level transgression.

Late Cretaceous palaeo-valleys are up to 650 m wide, have buried thalwegs depths up to -365 m relative to MSL (reference to stratigraphic height), and thalweg-channel margin relief of up to 50 m. SB1 in these sections is characterised by several incisions which trend obliquely to the regional gradient of the upper continental slope and shelf. Several smaller incisions are apparent from coast parallel seismic reflection profiles (thalweg- channel relief 10-15 m). These will not be dealt with further as the corresponding channel fill is too thinly developed for the seismic resolution of the tool employed.

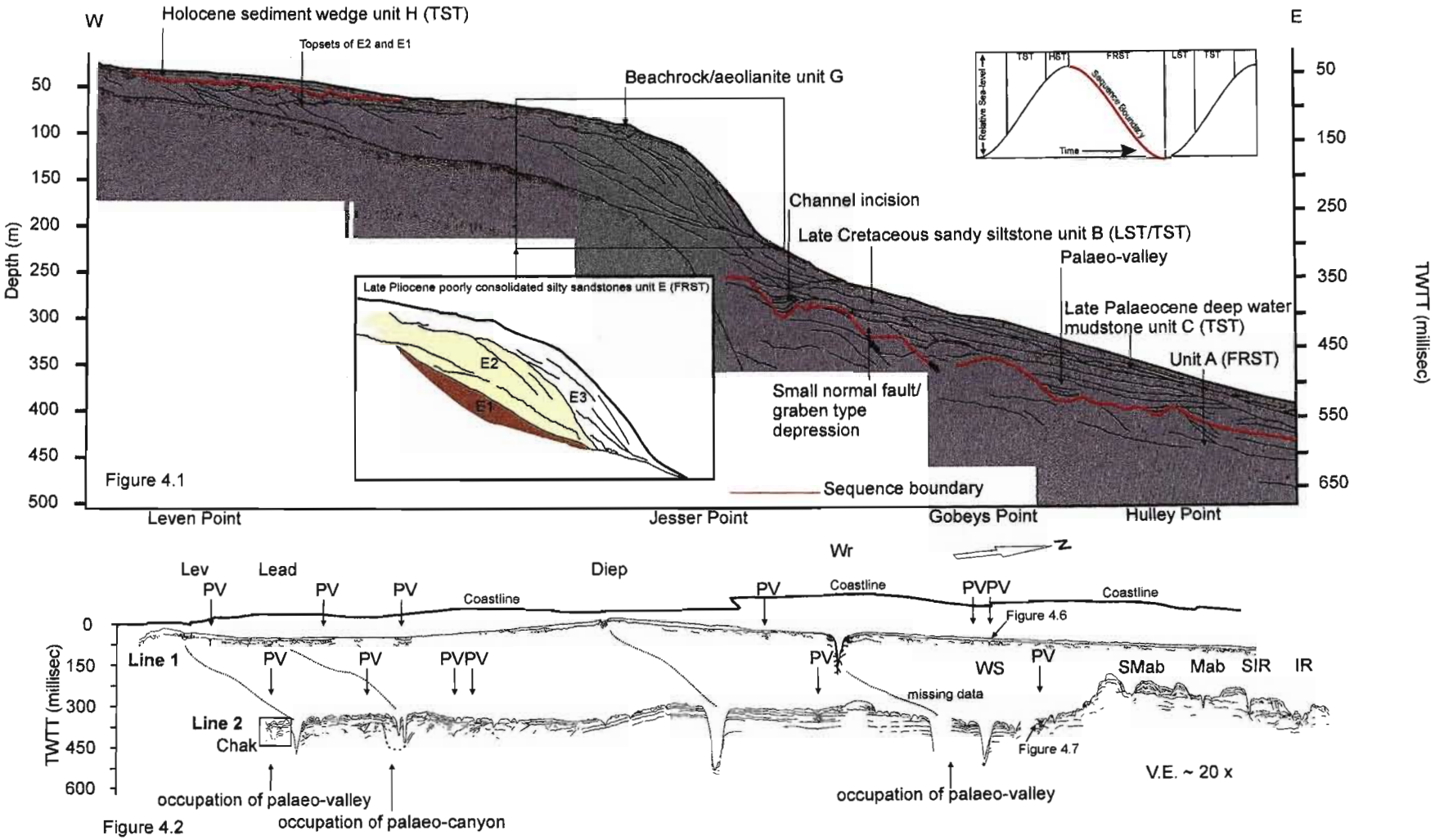

Figure 4.1. Downdip seismic section from the northern KwaZulu-Natal shelf, outlining the two sequence boundaries (shown in red). The lower and upper sequence boundaries are abbreviated to SB1 and SB 2 respectively. Each is characterised by high amplitude acoustic returns and rugged topography, within which small channel cut and fill features are evident. Note the various seismic units (A-H) delineated by bounding unconformity surfaces. Unit D is too thinly developed in this section to be resolved by the seismic tool. **Figure 4.2.** Interpreted fence diagram of strike parallel lines 1 and 2. The position of palaeo-valleys in each line is marked by PV (palaeo-valley). Note, line 1 indicates palaeo-valleys within SB2, and line 2 is restricted to palaeovalleys within SB1. Note that in the south of Leven Canyon, narrow rill-like canyons occupy an old palaeo-valley subsurface depression. Leadsman canyon complex occupies a fossil canyon, incised during SB1 formation. Lev = Leven, Chak = Chaka, Lead = Leadsman, Diep = Diepgat, Wr = Wright, WS = White Sands, SMab = South Mabibi, Mab = Mabibi, SIR = South Island Rock, IR = Island Rock.

Late Pleistocene palaeo-valleys, incised into the SB2 surface, are narrower, V-shaped features up to 180 m wide, and display channel-thalweg margin relief of up to 40 m (Fig. 4.2). The maximum thalweg depth of these features is -92 m MSL. Two major palaeo-valleys are observed in section, a larger incision-fill feature associated with the head of Leven Canyon, and a smaller feature located between White Sands and South Mabibi canyons (Fig. 4.2). These were fed by the Lake St Lucia and Lake Sibaya last glacial maximum (LGM) drainage systems (see previous chapter).

4.4. Palaeo-drainage reconstruction

Schematic representations of the major drainage patterns, derived from the palaeo-thalwegs of corresponding palaeo-valleys, are provided in figures 4.3a and b. The Leven-Leadsman Blocks show evidence of widespread valley formation in SB1, whereas incision in the Diepgat, Sodwana and Mabibi Blocks is less pervasive. A subdued-relief canyon, interpreted as moribund by Green et al. (2007), occupies a previous incised valley in the southern portions of both Sodwana and Leven Blocks (Fig. 4.3a-b). Within SB2, the Leven Point palaeo-valley comprises a similar nested arrangement within which recent submarine erosion has occurred, removing the transgressive fill in the upper reaches of the canyon head (Fig. 4.4). A number of smaller SB2 incisions in the vicinity of Leadsman Canyon are noteworthy (Fig. 4.3b), although mapping of the individual seismic facies of the corresponding valley fills is not possible. An incised valley associated with the upper margin of Leadsman Canyon is apparent, bounded by beachrock/aeolianite complexes of Unit G.

Isopach maps of unit H for the Leven Point and Sodwana Bay areas indicate meandering bodies of significantly thicker sediment which correspond to infilled channels within SB2 (Figs. 4.5 and 4.6). Palaeo-channels of the fringing lake systems, most notably Lake Sibaya, are evident (Miller, 2001) and closely reflect these offshore channel features (Fig. 4.5). The Lake Sibaya SB2 channel truncates portions of the fringing inner-mid shelf reef complex, thus separating 9-Mile and 7-Mile Reefs from each other. The palaeo-channel widens in the mid-inner shelf region in what may possibly have been a palaeo-lagoon. In the case of Lake St Lucia, a palaeo-channel (~ 45 m deep) was recognised by Van Heerden (1987). This is aligned immediately offshore with the fossil Chaka Canyon, incised into SB1 (Fig. 4.6). Isopach data for Unit H reveals a buried, ~ 50 m deep channel which extends landwards from the upper tributary of Leven Canyon. A well developed incised valley fill is preserved within this (Fig. 4.4).

4.5. Seismic facies

4.5.1. Cretaceous incised valley fills

Cretaceous incised valley fills within SB1 may comprise up to 5 seismic facies, though these are not pervasive in all valley fills, and occur in several combinations (Fig. 4.7; Table 4.1).

Seismic Facies 1b (SF1b) comprises high-amplitude chaotic to wavy reflectors which form the basal seismic unit of V-shaped infilled valleys (Fig. 4.7). SF1b is characteristically absent from flatter U-shaped valleys and fault bounded graben style valleys and varies from ~6-20 m. SF1b is separated from overlying seismic facies by Reflector i, a concave upwards, low relief seismic horizon.

Seismic Facies 2b (SF2b) consists of low amplitude, steeply dipping parallel to sigmoidal clinoforms which downlap onto SF1b or the valley floor, and gently onlap the valley flanks (Fig. 4.7). The stacking geometry of SF1b indicates an aggradational to progradational architecture with offlap breaks becoming progressively more distal with respect to the valley thalweg. The upper boundary of SF2b may also occur as a gentle toplap with the overlying reflectors of SF3b. The boundary between SF2b and overlying units is represented by Reflector ii, which is in many cases difficult to discern unless overlying units discordantly onlap this horizon.

Seismic Facies 3b (SF3b) is expressed as low angle, low amplitude, oblique parallel reflectors which downlap onto the valley floor or SF1b, and onlap the valley flanks and SF2b as a drape. SF3b is pervasive in all valley fills of the study area, and attains thicknesses of up to 50 m. Within SF3b, smaller progradational flank attached lenses of ~6 m thickness are apparent, and occur towards the upper margin of the valley feature. Similar thinly developed features are also apparent from the upper valley flanks, forming levee like mounds orientated parallel to the valley axis. This unit is erosionally truncated by Reflector iii, a smooth low amplitude reflector marking an angular unconformity between SF3b and younger seismic facies.

Seismic Facies 4b (SF4b) is characterised by oblique parallel, gently dipping high amplitude reflectors, which downlap onto SF3b and grade into wavy reflectors in the upper limits of the valley fill. The upper boundary is mostly unclear, however figure 4.7 depicts a rugged surface, Reflector iv, upon which clinoforms of Unit E downlap.

Figure 4.3

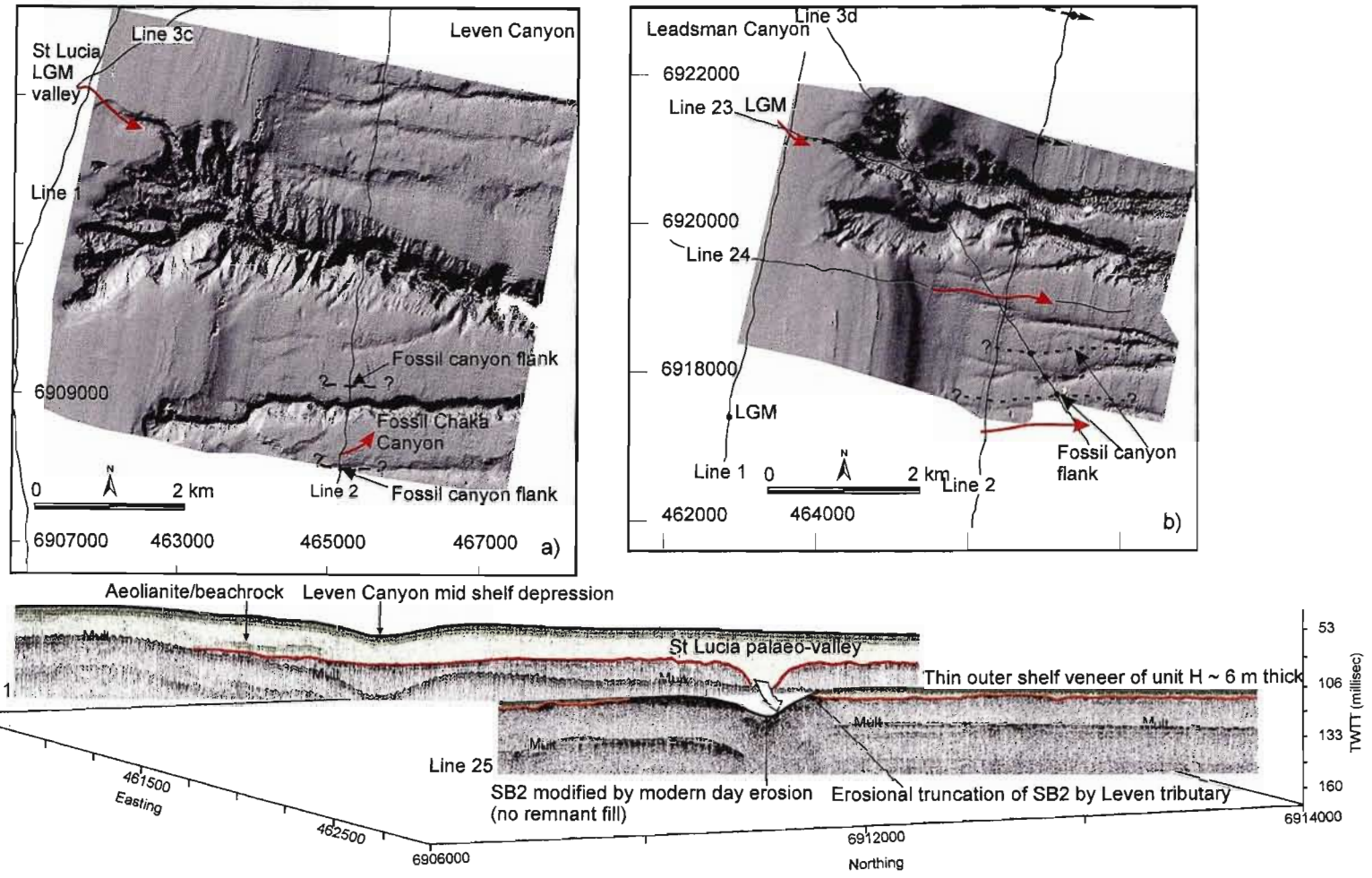

Figure 4.4

Figure 4.3a. Reconstructed drainage pattern for Leven and Chaka Canyons superimposed on multibeam bathymetry. Note the fringing tributary in the head of Leven Canyon, which occupies an older palaeo-drainage line within SB2 (LGM age). The modern smaller, shelf indenting Chaka Canyon forms a nested stacking arrangement within an older fossil canyon within the SB2 surface (boxed portion of Line 2, Fig. 4.2).**4.3b**. Reconstructed drainage pattern for Leadsman canyon superimposed on multibeam bathymetry. The small subdued relief canyon in the southern portion of the survey block is interpreted as moribund (Green et al., 2007), and is bounded on either side by fossil canyon flanks within SB1. Small incisions into SB1 are evident surrounding the survey block. Within SB2, a LGM connection to the northern limb of Leadsman Canyon is observed, but is significantly smaller in comparison to that found in Leven Canyon. **Figure 4.4.**. Interpreted fence diagram overlays of the coast-parallel line 1 and the coast-perpendicular Line 25 across Leven Canyon, showing the position of the LGM palaeo-valley in the inner shelf region, and its relationship to the recently active fringing upper tributary of Leven Canyon head. Note how the transgressive fill has been removed by modern day erosional processes in the upper reaches of the canyon head, where SB2 is truncated by the modern tributary walls.

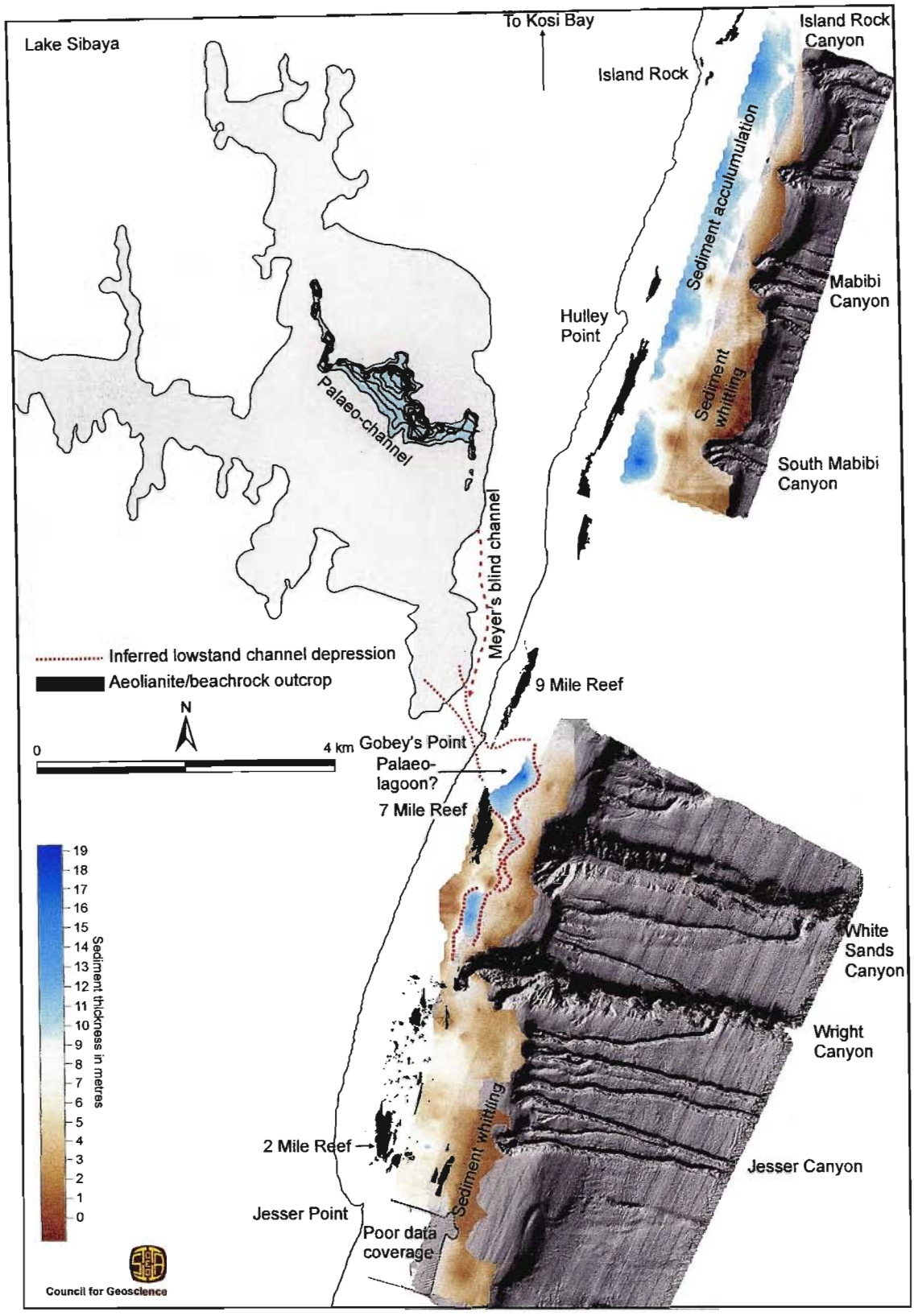

Figure 4.5. Isopach map of Unit H for Sodwana and Mabibi areas, overlaid on multibeam bathymetry and juxtaposed with the onshore palaeo-bathymetry of Lake Sibaya (from Miller, 1998). These data complement the onshore data of Miller (1998). Miller (1998) considers the modern day bathymetry of Lake Sibaya as a relict topography formed during the LGM, when the lake established an open oceanic connection. A channel, indicated by thicker deposits of Unit H, extends in a southerly direction between 7 and 9 Mile Reefs, inshore of White Sands Canyon before entering Wright Canyon's narrow V-shaped upper portions. There appear to be no channel features in Mabibi, but rather a continuous, well developed (~19 m thick) inshore wedge of Unit H which rapidly thins seaward into a zone of sediment whittling by current activity. Meyer's onshore channel position (pers. comm. Meyer, 2006). Interpreted seafloor data (reef shape files) provided by the Marine Geoscience Unit, Council for Geoscience, Copyright Council for Geoscience. Multibeam data UTM zone 36S, eastings and northings in metres.

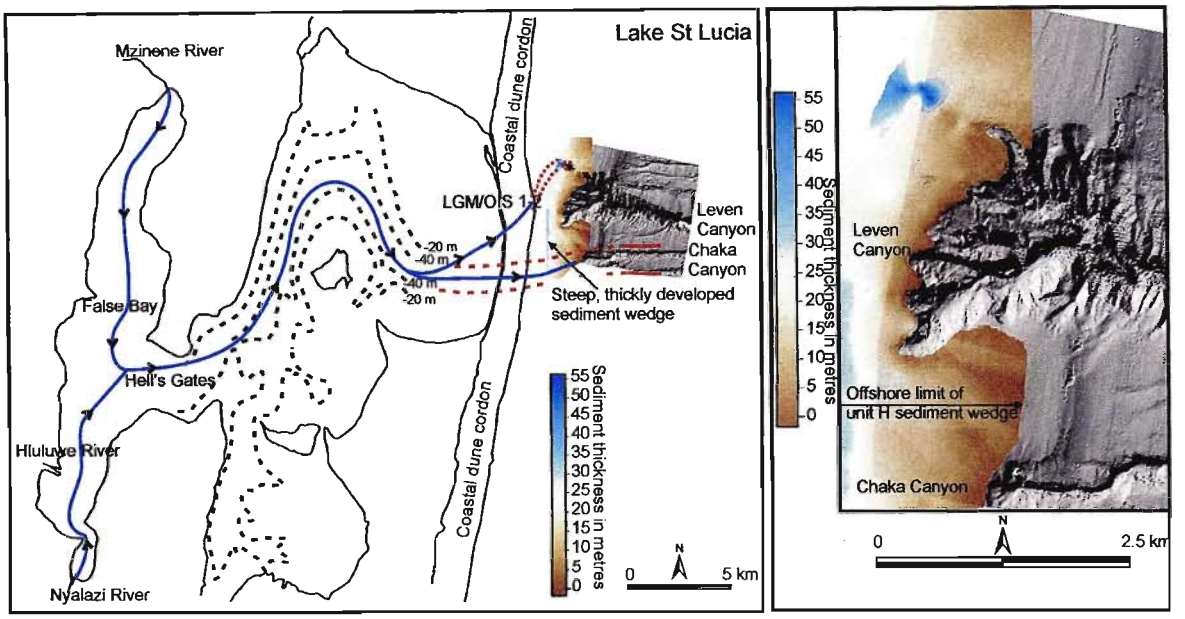

Figure 4.6. Isopach map of Unit H, offshore Leven Point, overlaid on multibeam bathymetry of Leven Canyon, and juxtaposed with onshore palaeo-bathymetry of Lake St Lucia (after Van Heerden, 1987). Solid red lines depict palaeo-topographic lows discovered from seismic data, dashed red lines indicate inferred continuation of topographic low. LGM/OIS2 refers to the ~18 000 BP lowstand connection to Leven Canyon. Note the close relationship between the onshore palaeo-channel of Lake St Lucia and the offshore fossil canyon which underlies Chaka Canyon. Also note the palaeo-channel which extends landwards from the northern upper tributary of Leven Canyon. Multibeam data UTM zone 36S, eastings and northings in metres.

The maximum thickness of SF4b is ~25 m. Facies SF4b is capped by regional reflector MFS onto which reflectors of the late Pliocene Facies E downlap (Table 4.1).

4.5.2. Late Pleistocene-Holocene incised valley fills

Four seismic facies (SF1-4) are identifiable within late Pleistocene-Holocene incised valley fills associated with SB2 (Fig. 4.8; Table 4.1). These may not be present in all incised valleys, but occur in some combination throughout the study area. These are described on the basis of internal reflector configuration and the character of the bounding seismic surfaces.

Seismic Facies 1 (SF1). SF1 is characterised by chaotic to wavy, high amplitude reflectors which form the basal seismic unit of each channel fill. SF1 is best resolved in valleys which are incised more than 20 m vertically into the underlying sediments. SF1 is strongly expressed in the northern Sodwana incised valley, compared to the Leven Point valley which is masked by multiple stacking. SF1 attains a maximum thickness of ~12 m.

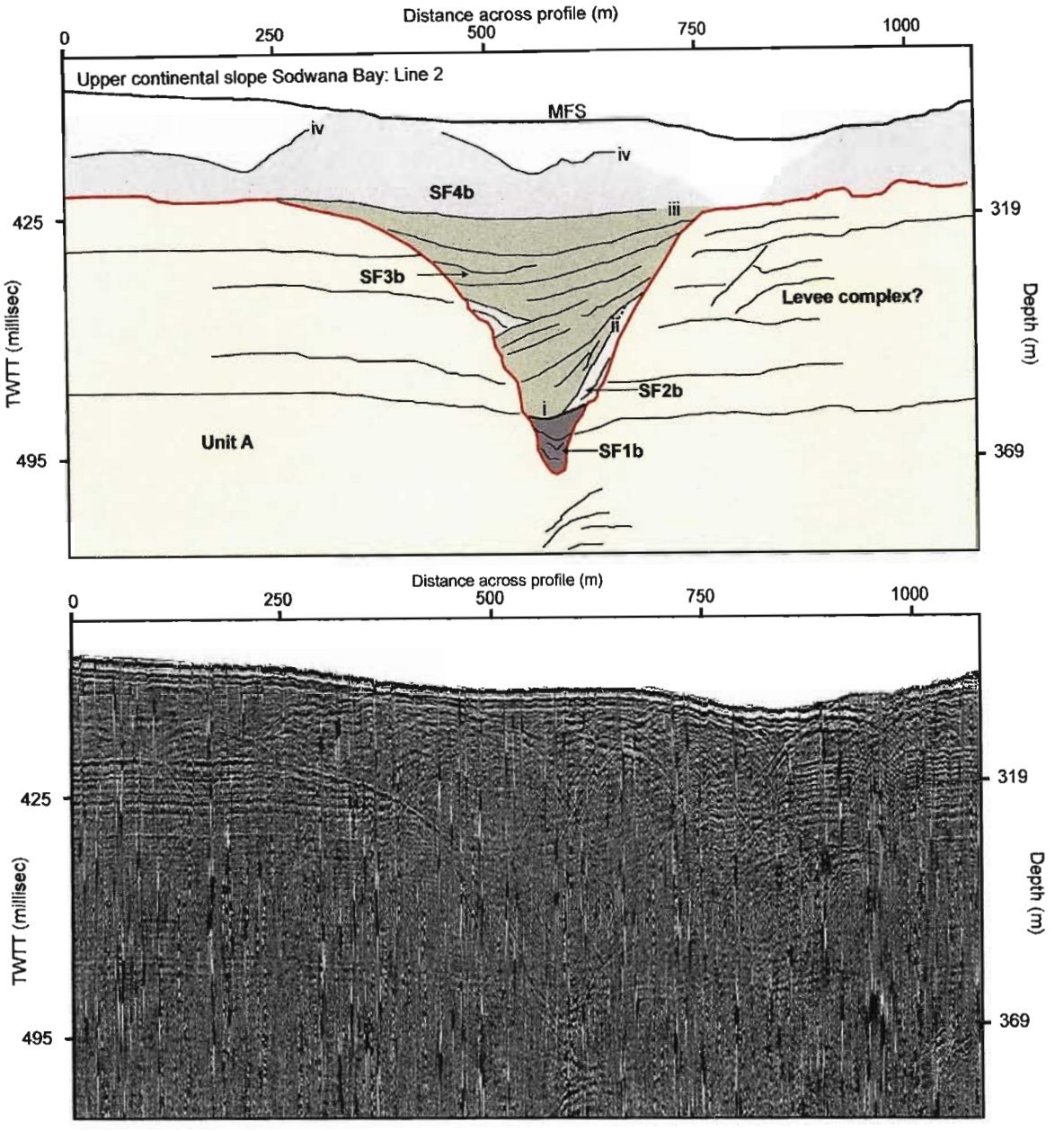

Figure 4.7. Interpreted and raw data from strike-parallel line 2 depicting an incised and filled palaeo-valley of Sequence Boundary (SB1). The deposits of SF3b dominate the transgressive fill sequence of the late Cretaceous palaeo-valleys, and are interspersed with small lenses of wedge shaped material which dips obliquely, downlapping reflectors of SF3b. The fill sequence is capped by deposits of SF4b, which comprise high amplitude oblique parallel to wavy reflectors.

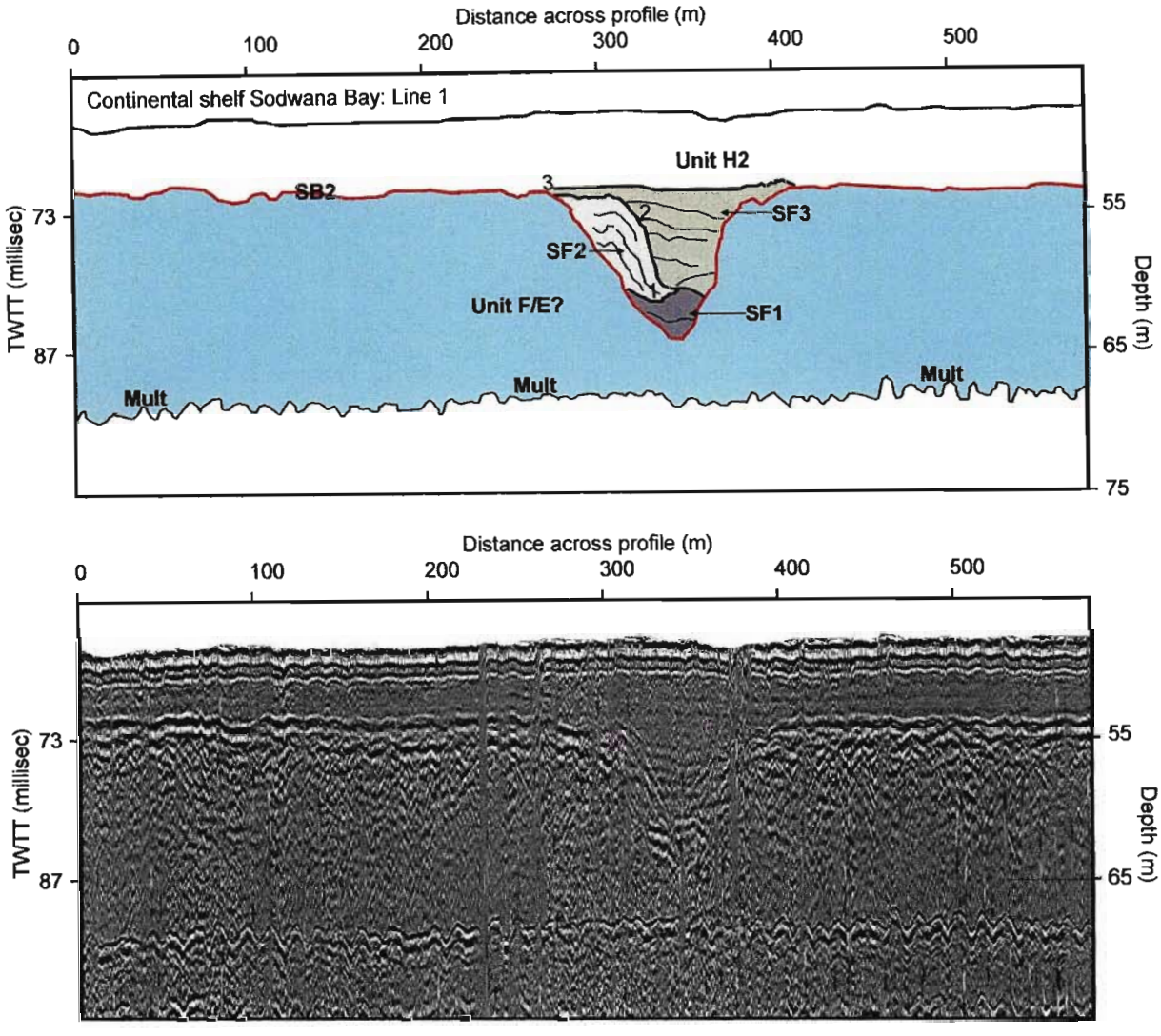

Figure 4.8. Interpreted and raw data from strike parallel line 1, depicting a filled palaeo-valley, north of White Sands Canyon. The various fill facies and reflectors are delineated. The presence of Seismic Facies SF1 is notable. However, the sediments of SF3 volumetrically dominate the fill body. The sedimentary fill body is capped by sediments of Unit H1. Mult = Multiple. These fill facies infill Sequence Boundary 2 (SB2).

Seismic Facies 2 (SF2). SF2 comprises wavy to sub-parallel, variable to high amplitude reflectors which downlap SF1 and onlap the valley flanks. Along the valley flanks, SF2 comprises smaller clinoforms that form aggradational-progradational mounded deposits of up to 14 m thickness. The seismic expression of SF2 becomes less pronounced further south towards Leven Point. SF2 is separated from SF1 by Reflector 1

Seismic Facies 3 (SF3). SF3 consists of weakly layered, parallel to sub-parallel, low amplitude reflectors which drape SF2 and the valley flanks. Alternatively, SF3 may be acoustically

transparent. SF3 may attain thicknesses of up to 20 m and is prominent in all late Pleistocene-Holocene valley fills, separated from SF2 by Reflector 2. This is overlain by Seismic Facies H1 of the mid-late TST, a thinly developed, shore attached sediment wedge comprising backstepping units, the basal units downlapping onto an intermittent, variable amplitude, moderate relief surface (Reflector 3).

4.6. Discussion

Several unique seismic facies are identifiable within incised river valleys of two different ages. These are interpreted on the basis of similar clinoform architecture from seismic facies reported in previous high resolution studies of incised river valley systems (Dalrymple et al., 1992; Zaitlin et al., 1994; Ashley and Sheridan, 1994; Foyle and Oertel, 1997; Nordfjord et al., 2006). Interpreted seismic facies units and stratigraphic boundaries are depicted in two idealised strike sections from the northern KwaZulu-Natal continental margin. Figure 4.9 illustrates idealised sections of both late Cretaceous and late Pleistocene-Holocene valley fills. The delineation of various palaeo-valleys and the interpretations of seismic facies are expanded to illustrate the drainage patterns and influences associated with lowstand conditions of a late Cretaceous and late Pleistocene lowstand (LGM). The chaotic, high amplitude reflectors of basal fill units SF1 and SF1b, suggests deposition of these facies under high energy conditions. In addition, surfaces SB1 and SB2 represent the regional basal incision surfaces on which SF1and SF1b rest. These facies are thus interpreted as fluvial lag deposits having most likely formed during sequence boundary development when these systems were initially incised (e.g. Nordfjord et al., 2006). The facies of SF1 are interpreted as deposits having formed during the sudden drop in sea level from the previous highstand at 24950 ±950 ^{14}C BP to the lowstand of 18 000 BP (Ramsay and Cooper, 2002). Deposits comprising SF1b are associated with a proposed late Cretaceous sequence boundary and may be considered comparable to those of facies SF1, based on their similar seismic expressions. The absence of facies SF1b from U-shaped valleys suggests that modification of these valleys during subsequent transgression, most likely by bay or tidal ravinement processes, removed the lag deposits and resulted in shoreface or estuarine deposition directly onto a modified SB1 during early transgression and base level rise (Dalrymple et al., 1992; Allen and Posamantier, 1993; Zaitlin et al., 1994; Foyle and Oertel, 1997; Nordfjord et al., 2006).

Table 4.1. Seismic facies, bounding unconformity surfaces, strata relationships and interpretative environments of Late Pleistocene/Holocene and Late Cretaceous incised valley fills.

Underlying horizon	Seismic facies	Modern description	Thickness	Stratal relationship	Interpreted environment
Late Pleistocene/Holocene Valleys					
SB2	SF1	Basal unit, best resolved in > 20 m incision	~ 12 m	Chaotic-wavy high amp reflectors	Fluvial lag
Reflector 1	SF2	Flank attached deposits	Up to 14 m	Wavy-sub parallel variable to high amp reflectors downlap surface 2, onlap SB2.	Intertidal flats
Reflector 2/Reflector 1	SF3	Prominent central drape	Up to 20 m	Weakly layered, parallel -sub parallel low amp reflectors/drape surface 2 and SB2. Alternatively, acoustically transparent	Central basin fill
Late Cretaceous Valleys					
SB1	SF1b	Basal unit	6-20 m	Chaotic-wavy high amp reflectors	Fluvial lag
Reflector i	SF2b	Flank attached deposits	<20 m	Low amp, steeply dipping parallel-sigmoidal clinoforms, downlap surface i/SB1	Intertidal flats
Reflector ii	SF3b	Prominent in central valley	Up to 50 m	Low angle, low amp, oblique parallel reflectors, downlap SB1/surface i, onlaps SB1/surface ii	Central basin fill
Reflector iii	SF 4b	Capping of fill	~ 25 m	Oblique parallel, gently dipping-wavy reflectors, capped by surface iv (MFS)	Shoreface/flood tide deltaic sediments

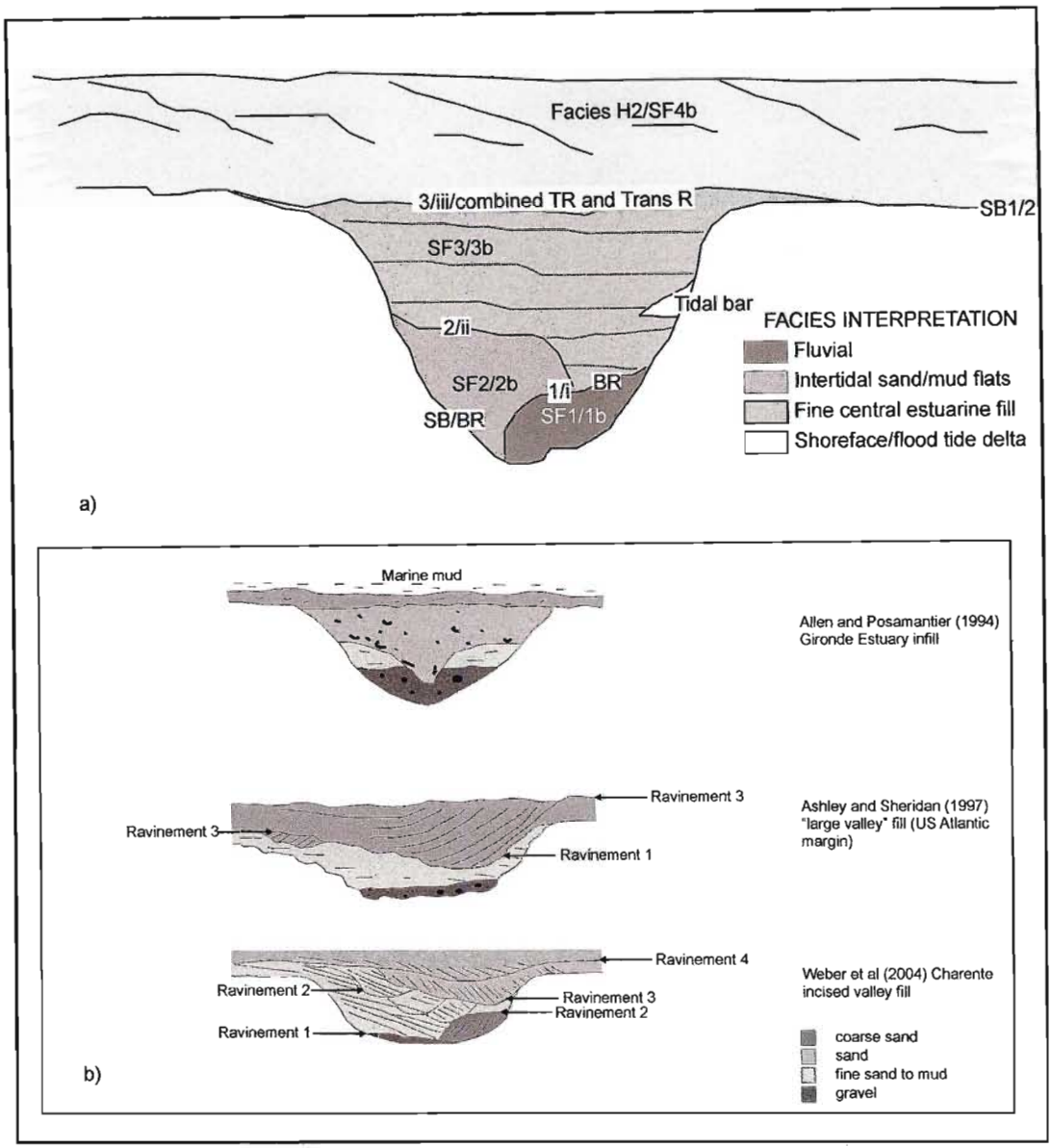

Figure 4.9a. Idealised section showing the relative stratigraphic positions and the sedimentary environmental interpretation of the various facies within palaeo-valley transgressive fills of the northern KwaZulu-Natal continental shelf. The bounding surfaces between each facies are highlighted. SB = sequence boundary, BR = bay ravinement, TR = tidal ravinement, Trans R = transgressive ravinement surface. **4.9b**. Other schematic models from various studies of incised valley fills. Note the similarity in facies fill, with basal coarse material overlain by relatively flat-lying central basin deposits of an idealised wave dominated estuary, when compared to the Gironde Estuary infill model from the Atlantic French coast (Posamantier and Allen, 1994) and the large infill model of Ashley and Sheridan (1994) for the US Atlantic coast. The Charente Estuary's incised valley (fringing the French Atlantic coast) is different in that relatively higher angle reflectors comprise the base of the fill, indicating tidal scour and bar fill. All schematics have approximately equal exaggerations.

The seismic facies SF2 is characteristically attached to the valley flanks in each fill (Fig. 4.8), and forms aggradational-progradational mounded complexes. Similarly, SF2b is associated with the valley flanks. However, there is no mounding of these deposits. The flank association suggests that

these facies represent side attached channel margin deposits such as tidal flat and salt marsh sediments (Masselink and Hughes, 2003). These would occur during the early stage of transgression with the landward migration of the shoreline causing backfilling and fluvial aggradation (Dalrymple et al., 1992; Zaitlin et al., 1994). The typical drape style of the sigmoidal reflectors of SF2b indicates that these sediments are fine grained in nature, possibly the result of a more distal depositional environment, or of finer sediment supply during the late Cretaceous. Foyle and Oertel (1997) describe similar seismic facies from the Virginia continental shelf which they consider as representative of estuary mouth deposits, though these types of deposits are normally sandier in nature, consisting of washover and flood-tide deltaic sediment (Zaitlin et al., 1994).

Mounded facies, may represent smaller point bar or side attached bars that were preserved on the flanks of the main channel such as those found in the modern day wave-dominated Kosi Bay estuary from this portion of coastline (Green, 2004). The low amplitude, shallowly dipping and draped nature of these reflectors suggest a low energy environment characterised by tranquil conditions. Consequently, SF3 and SF3b are interpreted as either fine grained central estuarine basin fill (e.g. Nordfjord et al., 2006), or lagoonal deposits. Transgression would have been at a maximum to drown the valley and facilitate the settling of finer material in tranquil conditions, so deposits of SF3 probably correspond to the mid to late transgressive systems tract (TST) and accelerated sea level rise of the early Holocene (~ 10 000 BP) (see sea level curve of Ramsay, 1995; Ramsay and Cooper, 2002). Small progradational, axis parallel, flank attached lenses within SF3b could represent the preservation of small tidal bars on the seaward side of the palaeo-estuary.

The erosional truncation of Seismic Facies SF3 and SF3b indicates a change in hydrodynamic regime with sea level rise. The landward shift in wave base and tidal influence in this case has resulted in the formation of a regional transgressive ravinement surface (formed by wave base shifting) which caps the valley fills. Overlying Reflector iii of the late Cretaceous incised valley fills is Seismic Facies SF4b. The shift from oblique parallel to wavy reflectors signifies a progressive increase in energy. This mirrors the predicted facies model for a transgressive wave dominated estuarine succession, where the central basin deposits are separated from the overlying transgressive shelf facies by a ravinement surface (Dalrymple et al., 1992; Zaitlin, et al., 1994). Theoretically, transgressive shelf sediments comprise flood-tidal delta/washover/barrier sediments (Dalrymple et al., 1992; Zaitlin et al., 1994) which would account for the observed heterogeneity in seismic reflector configurations of Seismic Facies SF4b. Seismic Facies H1 (Fig. 4.8) of the modern day sediment wedge, which overlies Seismic Facies SF4, exhibits similar characteristics. It

overlies Reflector 3, a moderate relief surface which truncates the underlying seismic facies, and exhibits mounded and thin backstepping units (Fig. 4.1). Nordfjord et al. (2006) consider the flood tidal delta/barrier/washover sediments as part of the valley fill, separated from the overlying transgressive surficial sand sheet by a wave/shoreface ravinement surface. A similar situation is postulated here, except the high wave energy of the northern KwaZulu-Natal coastline removed these "estuary mouth" components (Nordfjord et al., 2006) during shoreface/wavebase ravinement, the transgressive surficial sand sheet thus occurring directly above the central basin fill deposits. These have subsequently been reworked by the modern day Agulhas Current, into very large dune fields (c.f. Flemming, 1978; 1981). Foyle and Oertel (1997) consider mounded, seaward stepping clinoforms of the Virginia continental shelf to be part of the HST, formed as regressive shore face and strand deposits. The absence of aggradational-progradational stacking geometries, and the fact that the northern KwaZulu-Natal continental shelf is still undergoing transgression, precludes H1 from being considered part of the HST.

Where the modern Holocene sediment wedge thins, and the underlying Reflector 3 crops out, side scan sonar investigations reveal this surface to be a high backscatter, bioclastic pavement (Fig. 4.10). Sedimentological observations show that this comprises reworked broken bivalve, echinoid spine and coral detritus which has accumulated as a thick semi-indurated regionally outcropping pavement (Green, 2008; Shaw, 1998). This pavement may be inferred as the surface expression of the transgressive lag underlying the Holocene sediment wedge and capping the transgressive valley fill sequence. Similar examples are documented by Goff et al. (2004) and Goff et al. (2005) for the New Jersey continental shelf, where shell hashes of high acoustic backscatter were identified as the excavated portions of the Holocene transgressive ravinement surface. Based on sea level data from the northern KwaZulu-Natal region (Ramsay, 1995; Ramsay and Cooper, 2002), these lags appear to be mid to late Holocene in age, corresponding to the maximum rate of transgression for the shelf.

Seismic Reflectors i and 1 (Figs. 4.7-4.8) are interpreted as classical bay ravinement surfaces in that they are low relief surfaces which separate underlying alluvial plain/fluvial deposits from overlying draped or side-attached estuarine deposits (cf. Dalrymple et al., 1992; Zaitlin et al., 1994). The bay ravinement surface forms by wave and/or tidal-current scour, is restricted to estuarine settings, and marks the first major marine flooding event in a palaeo-estuary (Allen and Posamantier, 1993). Its development is confined to coastal embayments, and is absent from headland fronted coastal compartments.

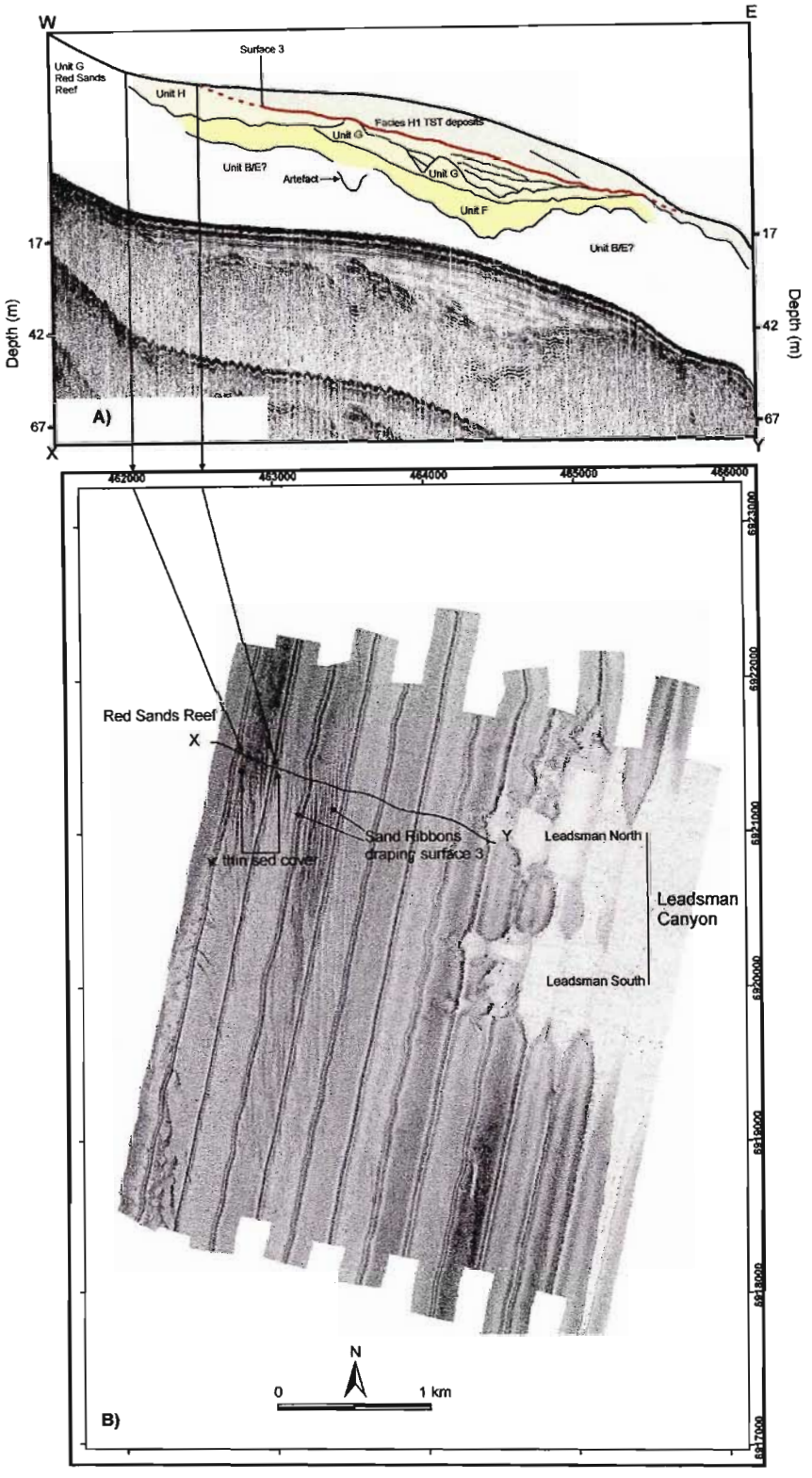

Figure 4.10. Strike-parallel line 23 and line interpretation (a) depicting the relationship of Reflector 3 to the surface expression of carbonate rich gravel in side scan sonar images of Leadsman Block (b). It appears that Reflector 3 crops out to form these gravel deposits which are thinly draped by sand ribbons. A higher resolution seismic tool is required in order to verify the exact relationship between these two features. See figure 1 for location of line.

Seismic reflectors 2 and ii (Figs. 4.7-4.8) are interpreted as conformable depositional surfaces which separate side attached flank deposits from central basin estuarine deposits. These may merge with the Reflectors 1 and i and with localised small-scale incision, indicating local erosion by tidal-creek scour significantly smaller than full scale tidal-ravinement processes. Tidal-ravinement surfaces are formed in bay-mouth settings by tidal-scour which deepens the antecedent fluvial valley during landward and lateral migration of the mouth during transgression (Allen and Posamantier, 1993; Zaitlin et al., 1994). The absence of such features suggests that the coast parallel seismic lines (Fig. 4.2: Lines 1 and 2) crossing both late Cretaceous and late Pleistocene-Holocene incised valley fills respectively, lie close to the palaeo-estuary margins, where the tidal-ravinement surface is truncated or removed by oceanic ravinement processes (Foyle and Oertel, 1997).

The contemporaneous formation of Reflectors 3 and iii (Figs. 4.7-4.8) with an expected tidal-ravinement (cf. Foyle and Oertel, 1997), in addition to the inherent diachroneity of ravinement surfaces, could result in there being little height variance between the two in the vicinity of the palaeo-estuary mouths, and might even result in the two merging, forming a combined tidal/oceanic ravinement which is indistinguishable morphologically from either of the two sub-processes. The depth of Reflector 3 on seismic line 1 thus indicates that a Holocene palaeo-shoreline of~ -40 to -50 m occurred with the onset of the maximum rate of transgression ~ 9 000 BP (Ramsay and Cooper, 2002). A similar calculation is not possible for the late Cretaceous examples as subsidence cannot be ignored when back tracking palaeo-depths on this coastline.

Figure 4.11 depicts the schematic evolution of palaeo-valley fills from both late Cretaceous and late Pleistocene/Holocene examples. Seismic data from this study indicate that these evolved from a traditional fluvial-type setting, evidenced by basal chaotic fills, into an intertidal estuarine setting, the two separated by a bay ravinement formed by bayline migration during transgression (Fig. 4.11b). These were then overlain by central basin deposits separated from side attached facies by a conformable deposition surface. As transgression ensued, these deposits were drowned and truncated by a transgressive ravinement surface which occurs sporadically on a regional scale. This was then overlain by transgressive shelf deposits (heterogeneous internal reflectors, or thin backstepping units).

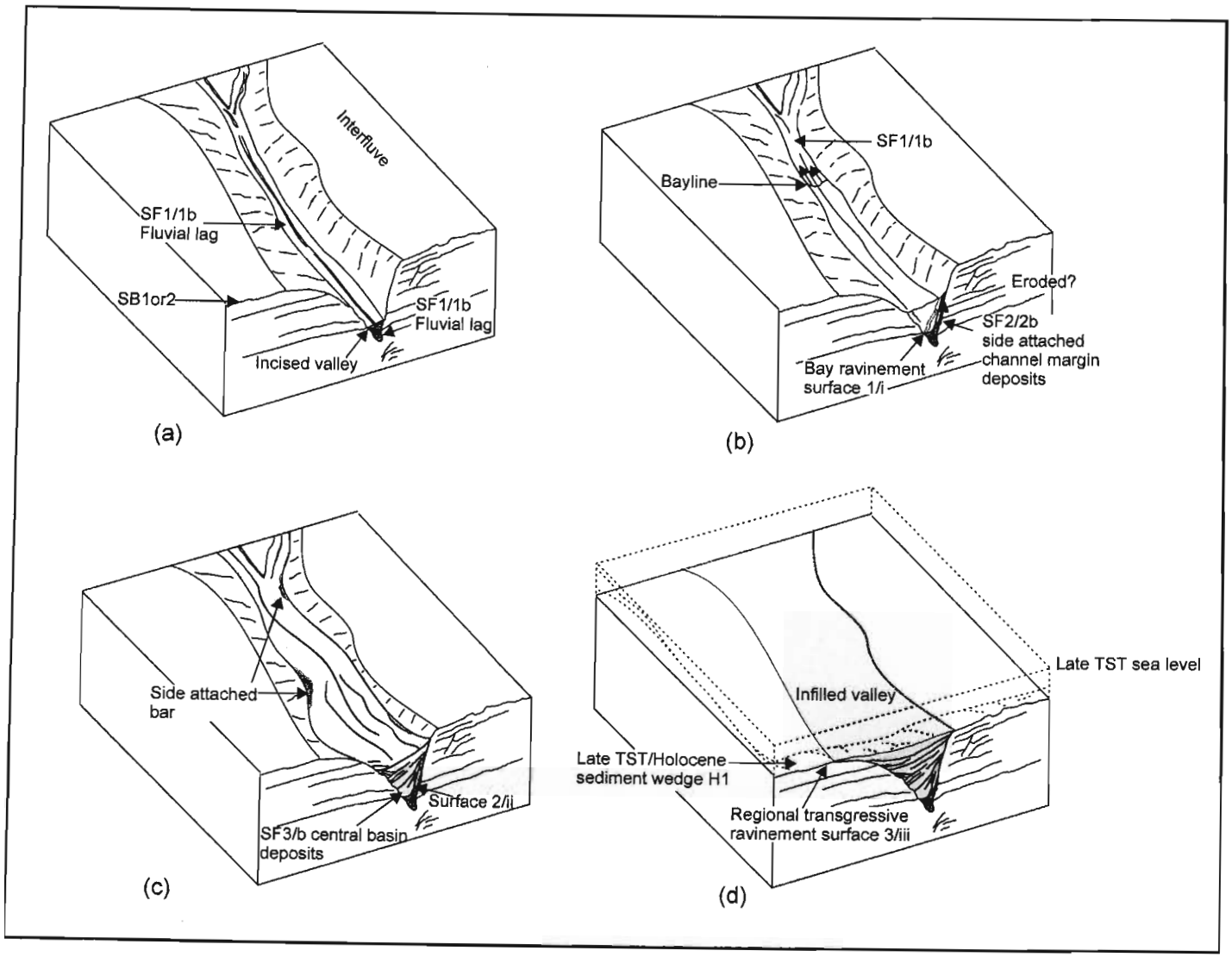

Figure 4.11. Schematic evolution of palaeo-valley fills, based on both Late Pleistocene/Holocene and Late Cretaceous examples. **(a)** Incision of valley during lowering of sea-level and the formation of sequence boundary (SB1/2). A coarse fluvial lag remains at the valley base. **(b)** As sea level rises, the proto-estuarine bayline migrates landwards, causing a bay ravinement surface to form. This separates fluvial lags of SF1/b from the overlying side attached channel margin deposits which form as the upper estuary migrates landwards. **(c)** As transgression ensues and drowning of the valley continues, the deposits grade into central basin estuarine deposits, interspersed by small migrating side attached bar deposits. SF3/b is separated from SF2/b by a depositional surface. **(d)** The fill sequence is capped by the regional transgressive ravinement surface, upon which late TST sediments lie. This is preserved only in the Late Pleistocene/Holocene examples.

This model compares favourably to the sedimentological models of incised valley fills proposed by Allen and Posamantier (1994) for the Gironde Estuary on the coast of western France, and by Ashley and Sheridan (1997) for their large valley fill model of the US Atlantic margin (Fig. 4.9b). Both describe a coarse sand/gravel basal constituent, which is interpreted in the northern KwaZulu-Natal examples as a fluvial lag, of similar material. These are then overlain by mud/fine sand of the central basin deposits, which is predicted for the northern KwaZulu-Natal shelf on the basis of the finely draped acoustic layering within the central fill unit. Lastly these are overlain by possible flood-tide deltaic sand capped by modern day shoreface sands, which are confirmed in the study area by numerous diver and grab observations (Green, 2008). Based on their seismic characteristics, these valleys most closely represent those described by Nordfjord et al. (2006) for the buried systems of the New Jersey shelf. Compared to the 'seismic sandwich' model proposed by Weber et al. (2004) for the Charente River Estuary of the Atlantic French coast, seismic units of the northern KwaZulu-Natal valley fills differ in that Weber et al.'s (2004) 'high to middle-angle' reflectors in the basal and uppermost fill units (Fig. 4.9b) are absent, replaced rather by chaotic reflectors at the base and an absence of higher angle reflectors above the low angle central valley fill, and beneath the confining wave/shoreface ravinement surface. In the northern KZN example, the basal units are fluvial rather than the point bar type deposit envisioned by Weber et al. (2004). The upper high angle unit, interpreted as estuarine mouth deposits cut by tidal inlets (Weber et al., 2004), was probably removed by ravinement during transgression. Despite providing a seismic alternative to sedimentological models of valley fills (Ashley and Sheridan, 1994; Allen and Posamantier, 1994), the seismic expression of these fills may thus not only be limited to the "seismic sandwich" model of Weber et al. (2004). Instead, slightly different seismic expressions may too represent these sedimentological models.

On the whole, the northern KwaZulu-Natal examples conform well to recent models of incised valley fill on a passive margin, which formed during a single sea-level transgression. These fills appear to conform to those predicted for the wave-dominated estuarine models of Dalrymple et al. (1992) and Zaitlin et al. (1994) and as such differ from Nordfjord et al.'s (2006) examples where both tide and wave dominated facies are preserved. The steep and very narrow shelf of northern KwaZulu-Natal may have reduced the tidal prism for each valley and as such promoted a wave dominated setting at the expense of tidal influences. In contrast the New Jersey examples document a wide, shallowly dipping shelf which provided extensive accommodation space and an increased tidal prism (Nordfjord et al., 2006). A steep and narrow shelf into which these features incise may thus increase the preservation potential of wave dominated facies in the ensuing transgressive fill.

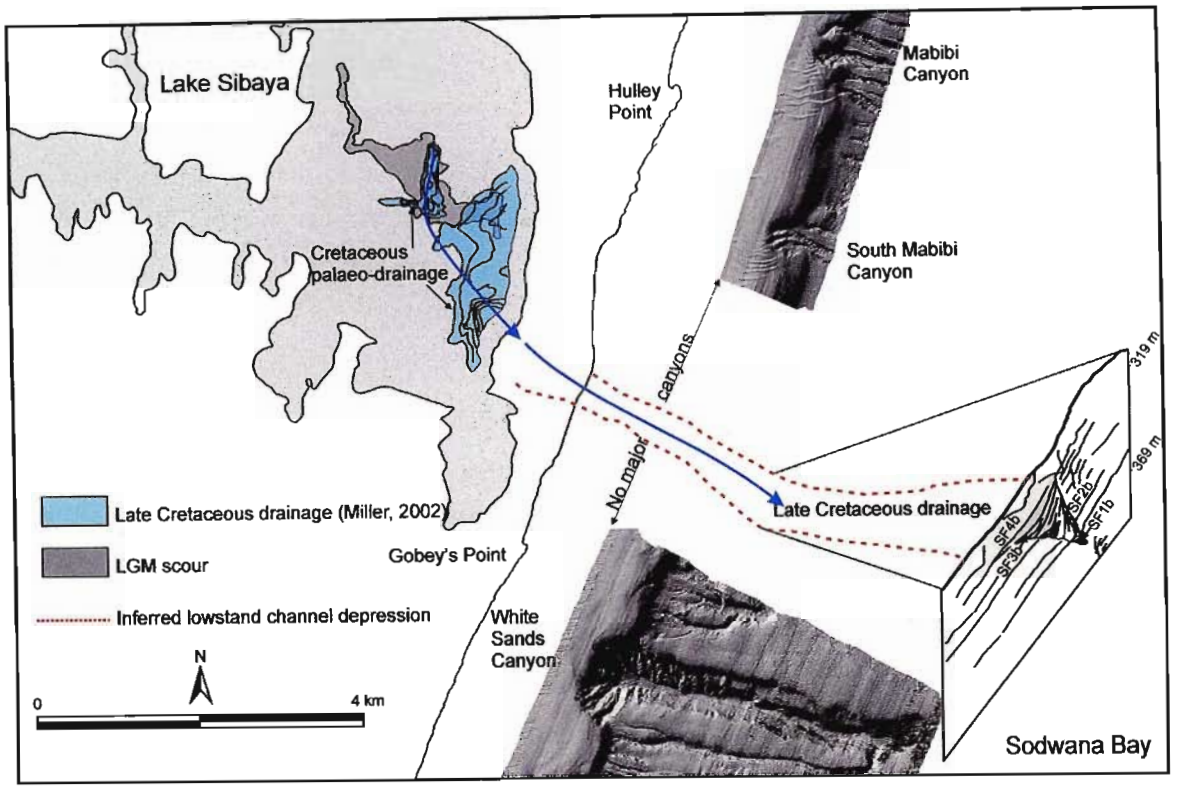

Figure 4.12. Palaeo-drainage of Lake Sibaya and the fringing continental shelf, depicting late Cretaceous drainage patterns (Miller, 2001) adjacent to incised valley fills of late Cretaceous age. Note how the LGM drainage pattern (highlighted in light grey) appears to rest within the space occupied by the Cretaceous drainage of Miller (2001). Interpreted seafloor data (reef shape files) provided by the Marine Geoscience Unit, Council for Geoscience, Copyright Council for Geoscience.

With respect to palaeo-drainage to the shelf, Lake St Lucia appears to have had *at least* two generations of incision, forming a composite palaeo-channel within the present day lake margins (Fig. 4.6). The surface within which the buried channel of Van Heerden (1987) is found occurs at an elevation of ~ -20-30 msl. Onshore borehole data in the vicinity of the lake indicate the depth of the Cretaceous surface at + 9.9 msl (Maud, unpublished data), so it is likely that this channelled surface corresponds to the onshore portions of SB1. In addition, the channel is aligned immediately offshore with the fossil Chaka Canyon within SB1, indicating a genetic relationship between the two. Buried channels of LGM age which extend towards Lake St Lucia occur to the north of Van Heerden's (1987) palaeo-channel. As there is no evidence for other buried channels within the lake, the LGM channels must have exploited the older palaeo-channel, most likely as a partially infilled topographic low, before debouching onto the shelf north of Leven Point where the barrier is less well developed. This implies that Lake St Lucia, prior to the formation of the Holocene sediment prism and the input of aeolian and washover sediment, was underfilled in order to maintain a relict channel feature in its palaeo-bathymetry. When compared with Lake Sibaya's palaeo-drainage, the offshore equivalents are similar. Miller (2001) recognises incisions within an upper Cretaceous

surface of Lake Sibaya, offshore of which a late Cretaceous incised valley occurs (Fig. 4.12). It seems likely that these two features are thus related, having formed when the Sibaya complex was an active fluvio-estuarine system. Pratson et al. (1994) and Bertoni and Cartwright (2005) show how partially infilled submarine canyons on the continental slope may similarly house younger canyon forms. This study documents examples of how antecedent channelled topography on a narrow *continental shelf* may similarly constrain the position, and ultimately the fill, of incised river valleys.

The offshore LGM channel (the incised valley feature in Fig. 4.8) appears to be a southern extension of a channel which was diverted behind the barrier complex, exiting from the southern basin of Lake Sibaya in the vicinity of 7/9 Mile Reef complexes (Fig. 4.5). This channel flows parallel to the coast where it enters Wright Canyon head. The increased influx of LGM sediment to Wright Canyon is the reason why this is the only canyon within the entire study area which exhibits characteristics of a shelf breaching canyon (e.g. Farre et al., 1983; Green et al., 2007). Ramsay (1991; 1994) postulated a similar scenario, considering Wright Canyon to have been an across shelf extension of fluvial drainage during lowstand. The occupation of the sinuous fringing upper tributary of Leven Canyon within the Leven Point Holocene-infilled LGM channel reveals that late Holocene erosion has utilised the topographic low of the LGM channel as a preferential erosional conduit. The sinuous tributary increases in relief downslope, with the base of the tributary coinciding with the base of the palaeo-channel in the outer shelf (Fig. 4.4). Morphometric analyses indicate that this portion of Leven Canyon is characterised by fluidised landsliding, and suggest that the trigger mechanism for these landslides is freshwater exchange from the adjacent Lake St Lucia (Green and Uken, 2008). Mulligan et al. (2007) show that relict fluvial channels infilled with high permeability sediments act as preferred pathways for groundwater flow.

In coastal regions these provide connections between freshwater aquifers and the ocean, and may in some instances facilitate saltwater intrusion into the freshwater body (Barlow, 2003). The sediments of the flank and central basin fill deposits of the Leven palaeo-channel, despite the presence of clays, would be relatively more permeable compared to the surrounding carbonate cemented shallow marine and beachrock/aeolianite facies of Seismic Units F and G and silty finer-grained sediments of Seismic Unit E/Seismic Facies E5 (Green et al., 2008) into which the channel incised. These could provide a preferred route for groundwater flow, as described by Falls et al. (2005) and Mulligan et al. (2007). The measure of relief increases with depth in the sinuous tributary, indicating a downslope erosional regime (c.f. Goff, 2001; Nordfjord et al., 2005). This

would be caused by groundwater exchange and sediment winnowing along the palaeo-channel, confirming speculations made by Green and Uken (2008) (Chapter 7).

CHAPTER 5

The seismic structure and development of submarine canyons

5.1. Introduction

Detailed studies concerning the seismic structure of the northern KwaZulu-Natal continental shelf have been limited as seismic investigations have instead focussed on deep water hydrocarbon exploration, for example studies of SOEKOR (Southern Oil Exploration Company, now Petroleum Agency SA-now the Petroleum Agency of South Africa, and the regional seismic structure of the fringing Natal Valley (Dingle et al., 1978; Martin, 1984; Goodlad, 1986). Sydow (1988) and Shaw (1998) provided brief examinations of the shelf structure, though neither related these fully to the development of submarine canyons in this area. The earliest speculations concerning the formation of submarine canyons on this portion of continental margin considered faulting to be a precursor to canyon inception, as faults provide a point of weakness for large slump induced turbidity currents to exploit (Bang, 1968). Shaw (1998) discounted Late Tertiary faulting as a possible mechanism for canyon development, and considered these canyons to be intrinsically linked to fluvial-shelf interaction during sea level lowstands. Most recently, Ramsay and Miller (2006) stated that the spacing and orientation of these canyons, as evidenced by multibeam bathymetric studies, is defined by an underlying structural control which they related to Tertiary and pre-Tertiary crustal weaknesses. Regular canyon spacing may however be related to hydrological controls such as fluid venting and ground water sapping, rather than an underlying structural influence (Orange et al., 1994). Seismic stratigraphic studies from northern KwaZulu-Natal (chapter 4) indicate that significant palaeo-valley development during a Late Cretaceous forced regressive systems tract; coupled with high rates of Late Pliocene deltaic and shelf margin sedimentation have influenced the controlling factors on continental shelf evolution, particularly in areas which are marked by canyon incision. This chapter thus aims to address the possible structural and sedimentological controls on submarine canyon development on the northern KwaZulu-Natal continental shelf, and provide a more refined model for the development of submarine canyons from this area.

5.2. Regional seismic structure of the continental shelf

The continental margin of northern KwaZulu-Natal, from Leven Point to Island Rock, may be

subdivided into two distinct structural domains:

A southern structural domain comprising marked palaeo-valley development within SB1 and relatively thick deposits of seismic unit A.

A northern structural domain comprising thick deposits of seismic unit B, an absence of seismic unit A, and no SB1. SB1 may occur beyond the maximum depth of penetration of the seismic tool used. Extensional faulting is most prevalent within this domain.

5.3. Seismic structure of submarine canyons

Several representative dip, strike and strike-oblique seismic sections from submarine canyons within each seismic structural domain are presented, and the varying structural features highlighted. The locations of each seismic section are shown in figure 5.1.

5.3.1. Southern structural domain

5.3.1.1. Leven and Chaka Canyons

Line 2 (Fig. 5.2) shot across the upper slope of the Leven Block, reveals relatively flat lying sediments of unit A (>75 m thick) erosionally truncated by Leven Canyon and several other smaller slope confined canyons to the north. Sediments of unit B (~ 50 m thick) are truncated by Leven Canyon, where several reflectors terminate against a sediment glide plane in the upper margins of the southern canyon wall. Beneath Chaka Canyon an erosional depression within SB1 forms a nested pattern with the overlying incised modern topography. Steeply dipping, high amplitude reflectors onlap the southern wall of the Chaka Canyon SB1 incision, which truncates shallow, south-easterly dipping reflectors of unit A. Richardson Canyon, a small slope confined canyon immediately north of Leven Canyon, exhibits a similar nested arrangement, where several palaeo-valleys of varying stratigraphic depth overlie incisional features of similar cross sectional morphology. Apart from the large shelf indenting Leven Canyon, no other canyons within this block erode into sediments of unit B.

Line 1 (Figs. 5.1 and 5.4), shot across the inner continental shelf reveals the upper limits of the shelf indentation of Leven Canyon. The subsurface structure of the upper canyon is characterised by a flat lying SB2 on which a buried aeolianite/beachrock complex of unit G rests (~7 m thick). SB2 and unit G are overlain by sediments of unit H which onlap the southern margin of the unit G

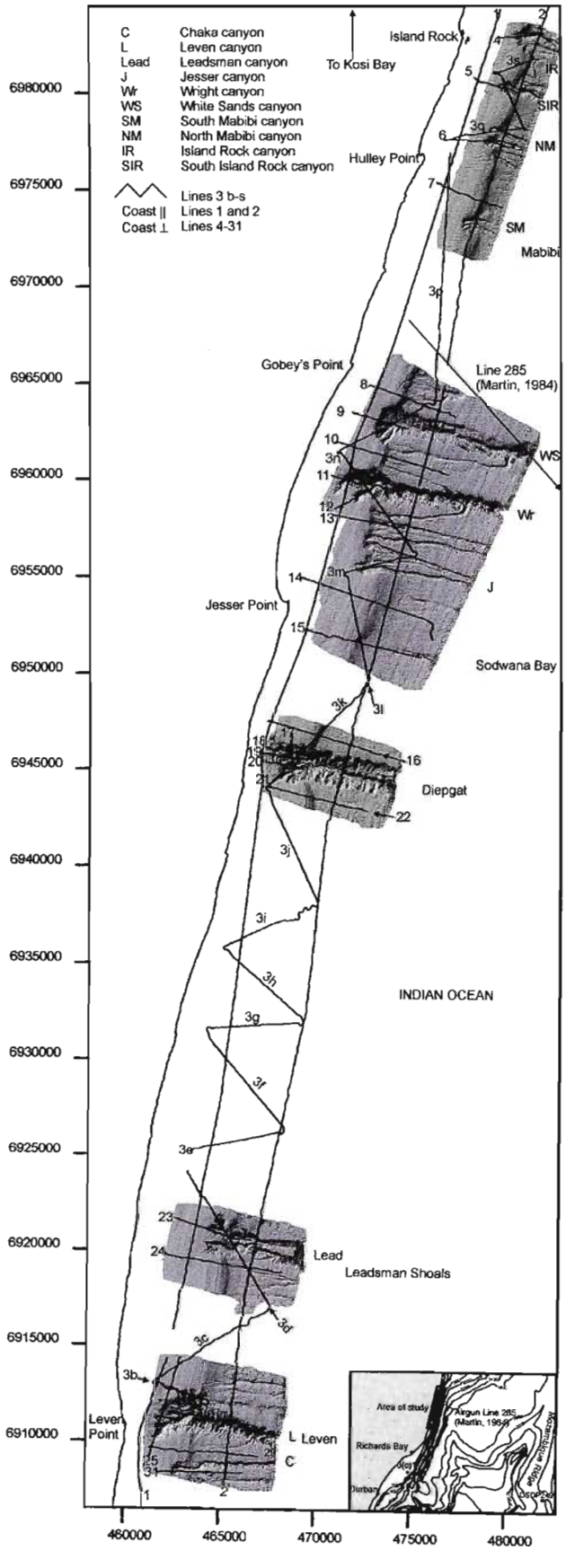

Figure 5.1. Seismic tracklines acquired across the northern KwaZulu-Natal continental shelf, from Leven Point in the south to Island Rock in the north. Lines 1 and 2 were acquired parallel to the shelf strike, lines 4 to 31 parallel to shelf dip. Line 3 b-s are slope oblique. Lines are superimposed over sunshaded multibeam bathymetry. For a comprehensive discussion of the bathymetry, please see chapters 6 and 7. Inset depicts the study area relative to the regional bathymetry of Dingle et al. (1978) and Martin (1984) and exploration borehole localities DSDP249 and J(c)1 . Line 285 of Martin (1984) is shown in full on the regional inset.

complex (basal depth ~ 55 mbsl). Within these sediments, the transgressive ravinement surface 3 (discussed in chapters 4 and 9) forms a north-south concave up depression into which Mid to Late Holocene sediments have progradationally cascaded. Underlying this are chaotic reflectors into which surface 3 incises. Further north, a v-shaped infilled valley is evident (discussed in chapter 4). Strike perpendicular lines 27, 28, 29 and 30 (Figs. 5.5-5.8) indicate that the aeolianite complex forms a buried coast parallel ridge ~ 2 km long, at a depth of 40-50 MBSL. The ridge has been removed by the upper portions of Leven Canyon.

In Line 3b (Fig. 5.9), shot strike perpendicular down the sinuous upper limb of Leven Canyon, the downslope extension of the v-shaped infilled valley in Line 1 is observed. The infilled valley is diverted by buried aeolianite/beachrock of unit G, the subsurface expression of which may be seen in both sidescan and bathymetry data (Fig. 5.9). Unit G mantles sediments of unit E, facies E4, in a small erosional depression. As discussed in chapter 4, the sinuous upper limb of Leven Canyon occupies the sub-surface depression of the underlying infilled valley.

5.3.1.2. Leadsman Canyon and northern environs

The strike parallel line 2 (Figs. 5.2 and 5.10) from the upper slope indicates a major palaeo-incision into SB1, within which the Leadsman Canyon system lies. The maximum depth of this incision extends beyond the penetration capabilities of the seismic tool. High amplitude deformed and chaotic reflectors underlie the modern thalwegs of Leadsman North and South Canyons, and grade into the shallowly dipping high amplitude reflectors of unit B. The upper walls of Leadsman Canyon truncate the reflectors of unit B, except where they terminate against axis-normal orientated sediments of unit E. Unit E forms the upper limit of the North-South Leadsman Canyon interfluve, and rests unconformably on a steeply southward dipping surface. Several smaller canyons with thalweg-margin relief not exceeding 40 m from the upper slope section are evident.

Line 23 (Fig. 5.11) extending from the inner shelf into the northern head of Leadsman Canyon, reveals the Red Sands Reef complex. This comprises unit F, the upper surface of the reef marked by SB2 where these portions of the reef were erosionally planed during LGM regression. In the mid shelf, SB2 is overlain by aeolianite/beachrock of unit G with a base depth of 55-77 mbsl. Unit G forms a submerged reef complex of 16 m maximum thickness.

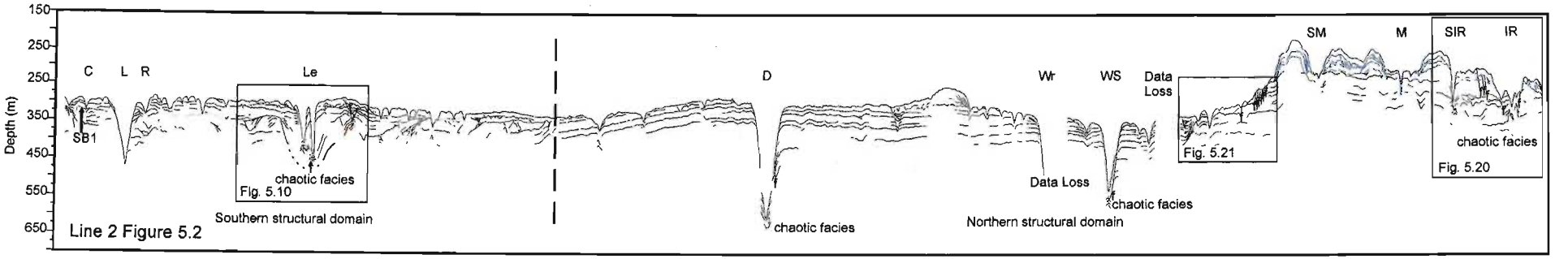

KEY TO FIGURES

	Sequence boundary		
	Interpretative sequence boundary		
	Tertiary strata		
	Late Cretaceous strata		
	Fault		
C	Chaka Canyon	SM	South Mabibi Canyon
L	Leven Canyon	M	Mablbi Canyon
R	Richardson Canyon	SIR	South Island Rock Canyon
Le	Leadsman Canyon	IR	Island Rock Canyon
D	Diepgat Canyon		
J	Jesser Canyon		
Wr	Wright Canyon		
WS	White Sands Canyon		

Figure 5.2. Interpretative line drawing of strike parallel line 2. Red lines represent sequence boundaries. Lower sequence boundary = SB1, upper sequence boundary = SB2. Blue reflectors represent Unit E sediments. Black reflectors between SB2 and uppermost blue reflectors = units F and G. Black reflectors between lowermost blue reflectors and SB1 = Unit B. Black reflectors beneath SB1 = Unit A. Reflectors of unit A pinch out towards Diepgat Canyon. All canyons, apart from Leven and Leadsman Canyons, erosionally truncate both unit B and SB1. Note the differences between the southern structural domain, characterised by palaeo-valley development in the SB1 surface, and the northern domain, where SB1 is not evident. Small scale faulting in the northern domain is prevalent in unit E and anomalous progradational unit sediments, which mantle comparatively thicker deposits of unit B than further south. **Figure 5.3.** Strike parallel line 1. Red lines indicate SB2 separating unit H from underlying sediments, blue lines indicate unit E reflectors, black(at depth below blue) indicates unit A and B reflectors. Note the subsurface structure of SB2 beneath Leven Canyon, which is flat lying compared to the complicated subsurface depressions beneath the modern day Diepgat Canyon. Wright Canyon thalweg is bounded by chaotic reflectors, indicative of slump-infilling.

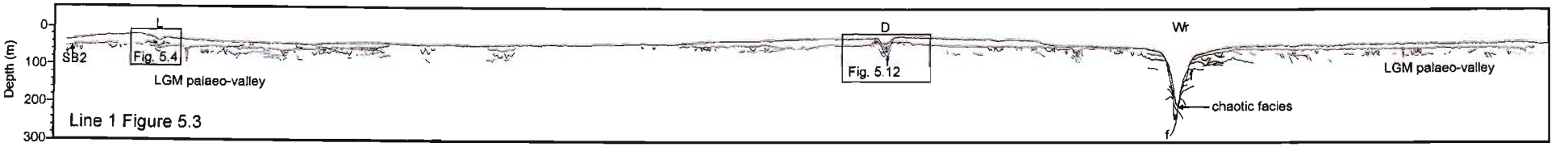

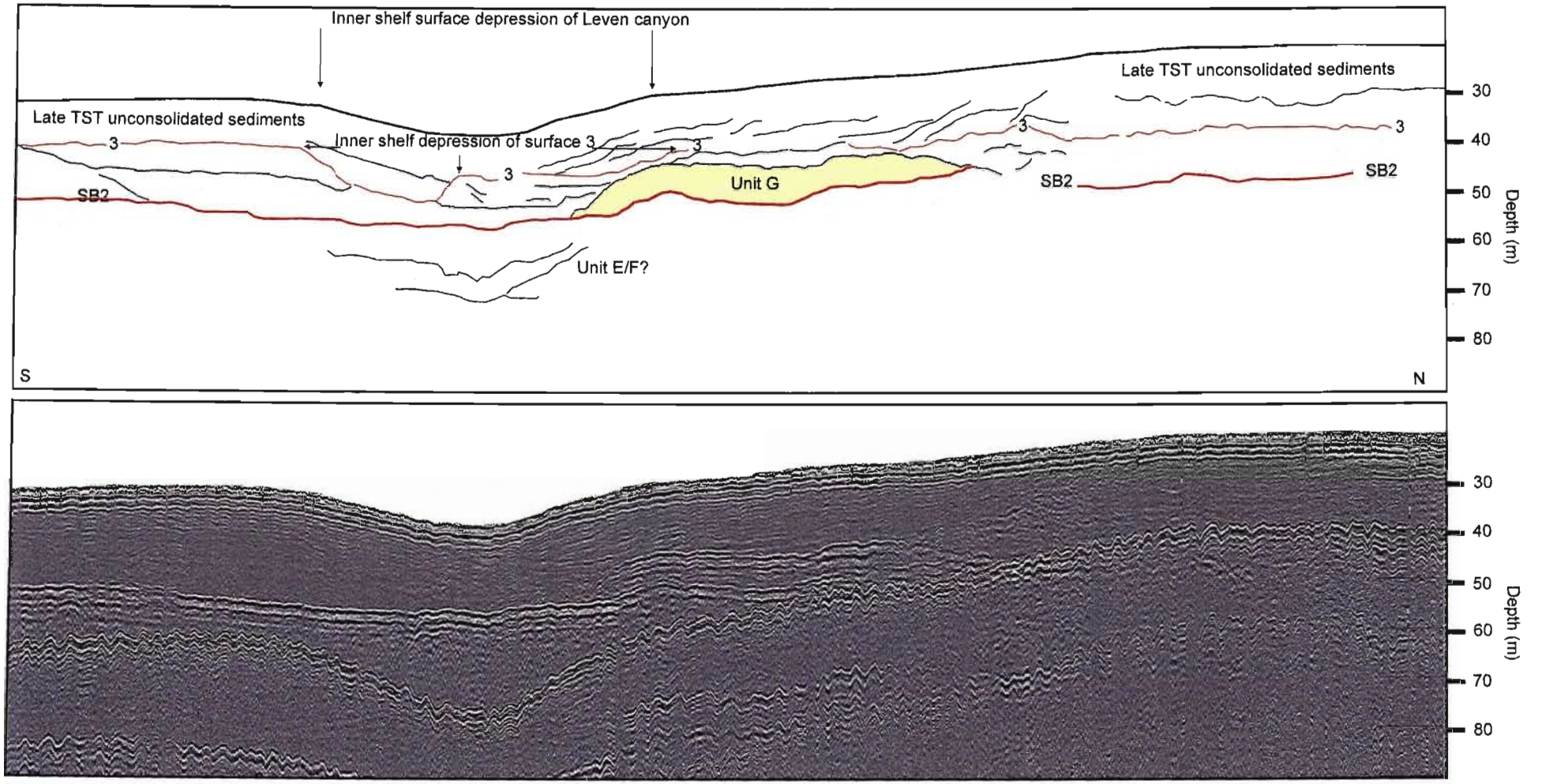

Figure 5.4. Interpreted line drawing and uninterpreted raw data of line 1, inner shelf region of Leven Canyon. The upper limit of Leven Canyon is shown, marked by a slight topographic depression. SB2 is flat-lying in this area, whereas surface 3, representing the Holocene transgressive ravinement surface, occurs as a concave up surface beneath the surface depression. Sediments of the late transgressive systems tract have cascaded progradationally into this micro-depocentre. In certain portions of the head, surface three has incised into underlying chaotic to wavy reflectors. An isolated stub of unit G mantles SB2, which is atypical, as it clearly postdates the SB2 surface, thus having formed on the rising limb of sea level since the LGM, contrary to the models of Ramsay (1991; 1994) discussed later in the etxt..

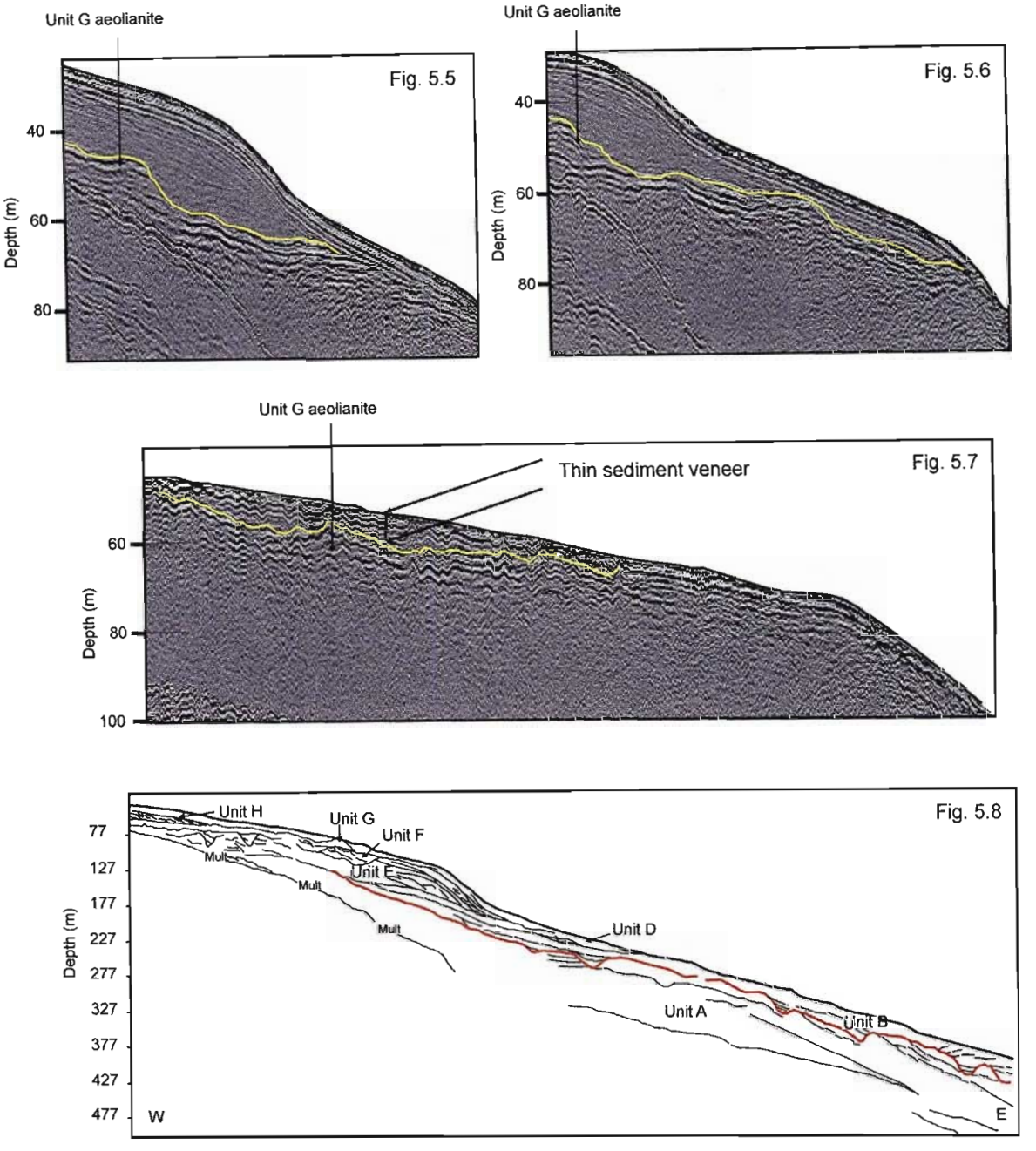

Figure 5.5. Interpretative overlay of strike perpendicular line 27 detailing subsurface aeolianite of unit G. **Figure 5.6.** Interpretative overlay of strike perpendicular line 28 detailing subsurface aeolianite of unit G. **Figure 5.7.** Interpretative overlay of strike perpendicular line 30 detailing subsurface aeolianite of unit G, covered by a thin sediment veneer of thickness just greater than the seismic resolution. **Figure 5.8.** Interpreted line drawing of strike perpendicular line 29. An aeolianite ridge of unit G clearly crops out in the mid-outer shelf region at a depth of 82 m (basal depth of unit = 90 m).

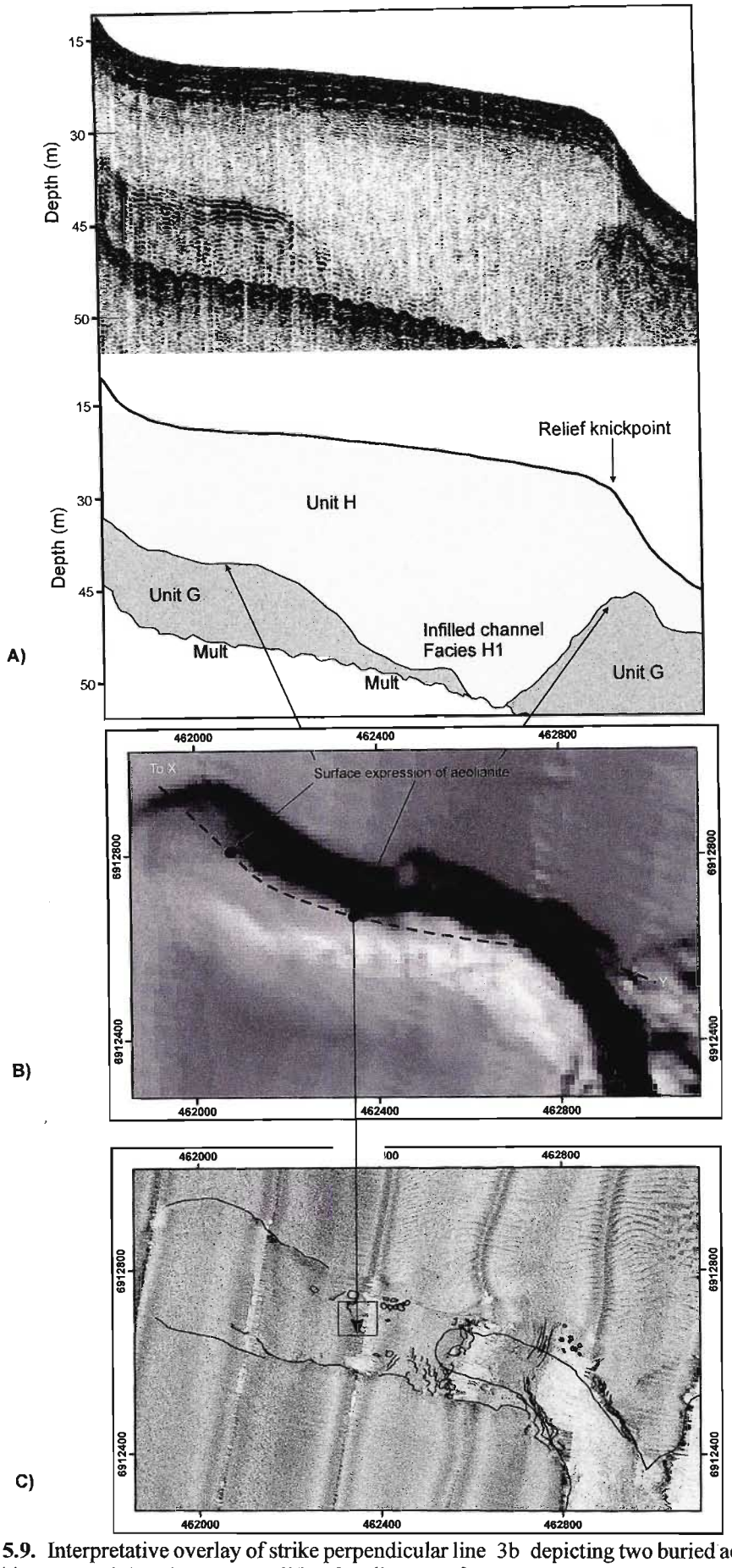

Figure 5.9. Interpretative overlay of strike perpendicular line 3b depicting two buried aeolianite ridges, covered by seaward thinning unconsolidated sediments of unit H. The LGM palaeo-valley is diverted between these features. These manifest themselves as surface gradient knickpoints recognised in both bathymetry data (B) and side scan sonar data (C). Side scan sonar data is discussed comprehensively in chapter 9.

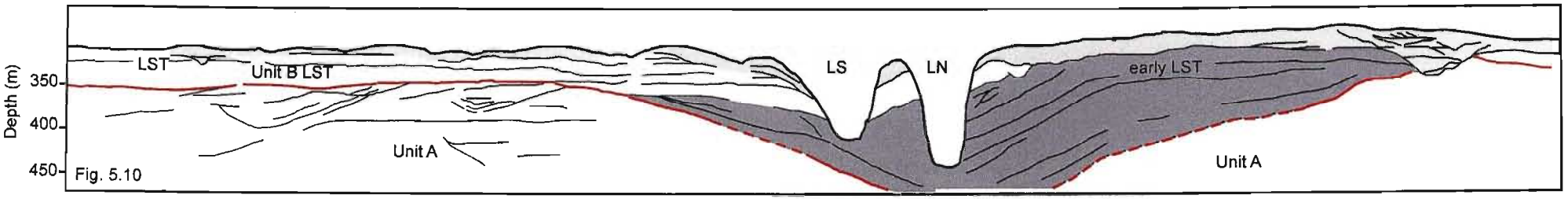

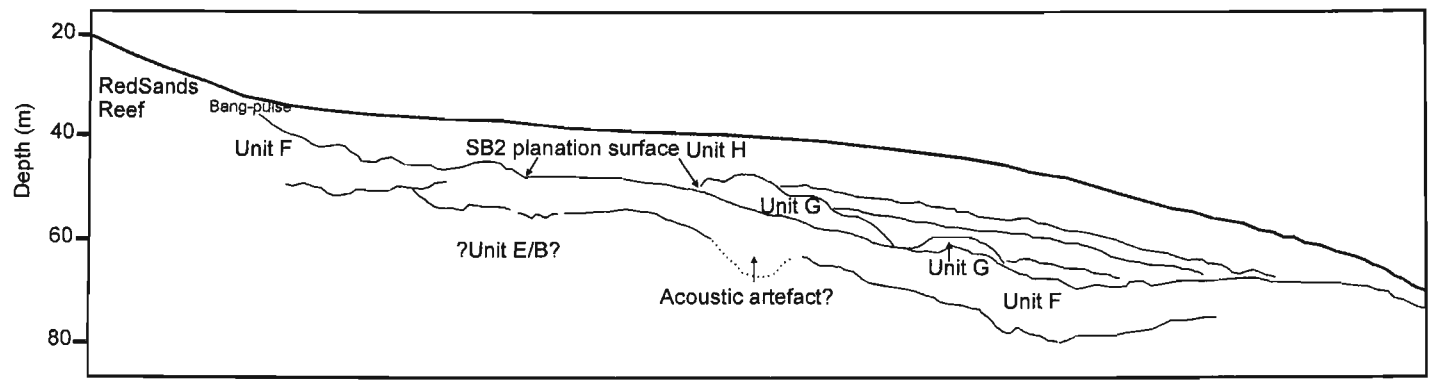

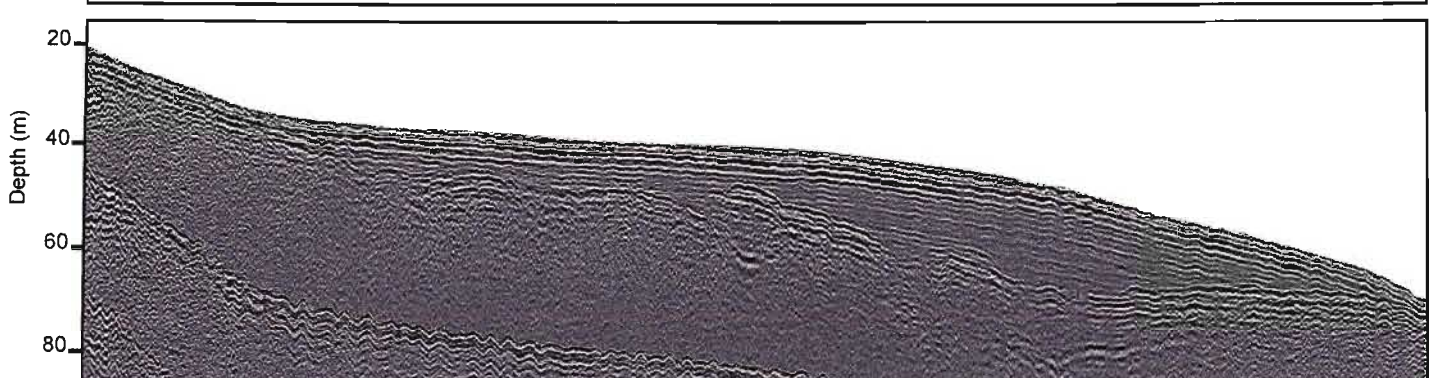

Fig. 5.11

Figure 5.10. Interpretetative line drawing of strike parallel line 2 detailing Leadsman Canyon and surrounds. Note the presence of a broad saucer shaped fossil canyon which underlies the modern day Leadsman thalweg. The fossil canyon fill corresponds to early LST deposition immediately after SB1 incision and pre-dates the TST fill of the SB1 palaeo-valleys. LS = Leadsman South, LN = Leadsman North, red line = SB1, darker grey fill = early LST fill, lighter gray = thin veneer of Late Pliocene unit E. Note the arrangement of unit E reflectors inwards towards the canyon thalweg. **Figure 5.11.** Strike perpendicular line 23 and interpretative line drawing, detailing the Red Sands Reef complex. Unit F comprises the reef core, and exhibits a planation surface in the inner to mid shelf regions which corresponds to SB2. Small ridges of unit G are welded to unit F at a depth of 50-60 m in the mid shelf.

5.3.2. Northern structural domain

5.3.2.1. Diepgat Canyon

Strike parallel line 1 (Figs. 5.3 and 5.12), from the inner continental shelf, indicates subsurface depressions underlying the inner shelf expression of the head of Diepgat Canyon. SB1 and the transgressive ravinement surface 3 form a composite concave upward reflector upon which modern shelf sediments downlap.

The most striking mid shelf features are the semi-circular collapse structures in the head of Diepgat Canyon. Line 20 (Fig. 5.13) reveals a set of up to four fault bounded terraces comprising blocks of unit F and G. The bounding faults comprise diverging splays which bifurcate from a basal listric fault (cf. Ramsay and Huber, 1993). The splays may be rejoining, as inferred from the bathymetry, though this relationship is unclear from seismic data. The bases of the lowermost terraces comprise deformed, high amplitude reflectors and overlie sediments of unit B. Sediments of unit H appear to have infilled the small tensional depressions created by fault block rotation.

Line 2 (Fig. 5.2) from the upper slope reveals that the gently-dipping reflectors of unit B are erosionally truncated by the canyon walls. Two splayed listric faults, which truncate several reflectors of unit B, appear to bind the southern canyon flank. Chaotic high amplitude reflectors comprise the subsurface facies which underlie the canyon thalweg. Strike oblique line 3k (Fig. 5.14), acquired across Diepgat Canyon, reveals sigmoidal clinoforms of the aggradational-progradational unit E orientated progradationally towards the canyon axis where the shelf-edge wedge intersects the canyon edge. Localised slump deformation of the internal reflectors is apparent.

5.3.2.2. Sodwana Bay Block: Jesser, Wright and White Sands Canyons

Line 2 (Fig. 5.2) reveals a subdued-relief shelf-indenting canyon in the southern portion of the Sodwana Block which occupies the subsurface depression of a palaeo-valley incision-fill episode (see chapter 4) (Fig. 4.6). Along-thalweg line 15 indicates a relief knick-point in the upper slope, which is the surface manifestation of several rotational faults underlain by wavy high amplitude reflectors (Fig. 5.15). The base of each rotational fault attaches to the combined RS1 and MFS regional seismic surfaces. Several growth faults in the overlying shelf-edge wedge are also apparent, and have been rotated by slumping of unit E sediments.

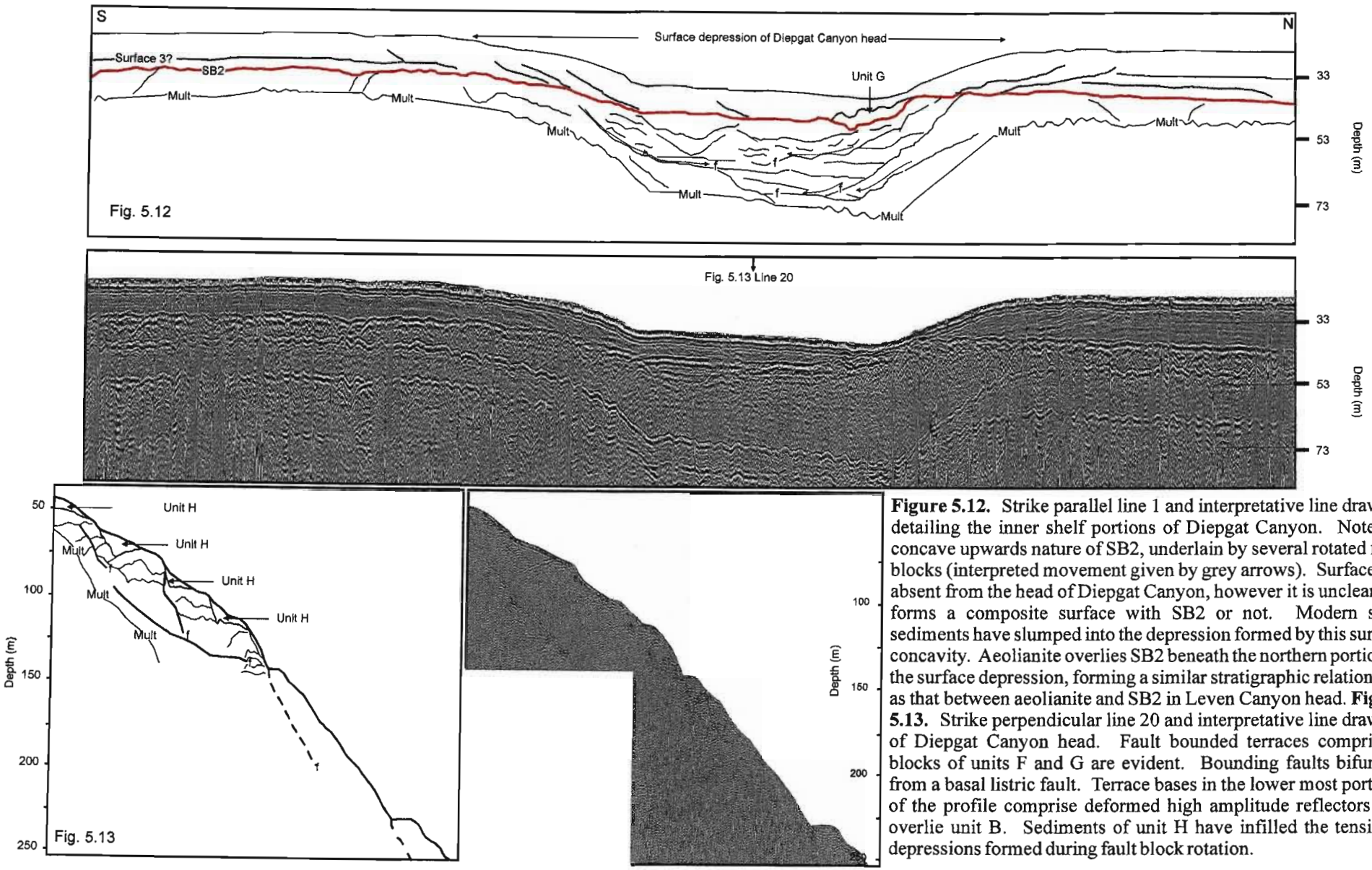

Figure 5.12. Strike parallel line 1 and interpretative line drawing detailing the inner shelf portions of Diepgat Canyon. Note the concave upwards nature of SB2, underlain by several rotated fault blocks (interpreted movement given by grey arrows). Surface 3 is absent from the head of Diepgat Canyon, however it is unclear if it forms a composite surface with SB2 or not. Modern shelf sediments have slumped into the depression formed by this surface concavity. Aeolianite overlies SB2 beneath the northern portion of the surface depression, forming a similar stratigraphic relationship as that between aeolianite and SB2 in Leven Canyon head. **Figure 5.13.** Strike perpendicular line 20 and interpretative line drawing of Diepgat Canyon head. Fault bounded terraces comprising blocks of units F and G are evident. Bounding faults bifurcate from a basal listric fault. Terrace bases in the lower most portions of the profile comprise deformed high amplitude reflectors and overlie unit B. Sediments of unit H have infilled the tensional depressions formed during fault block rotation.

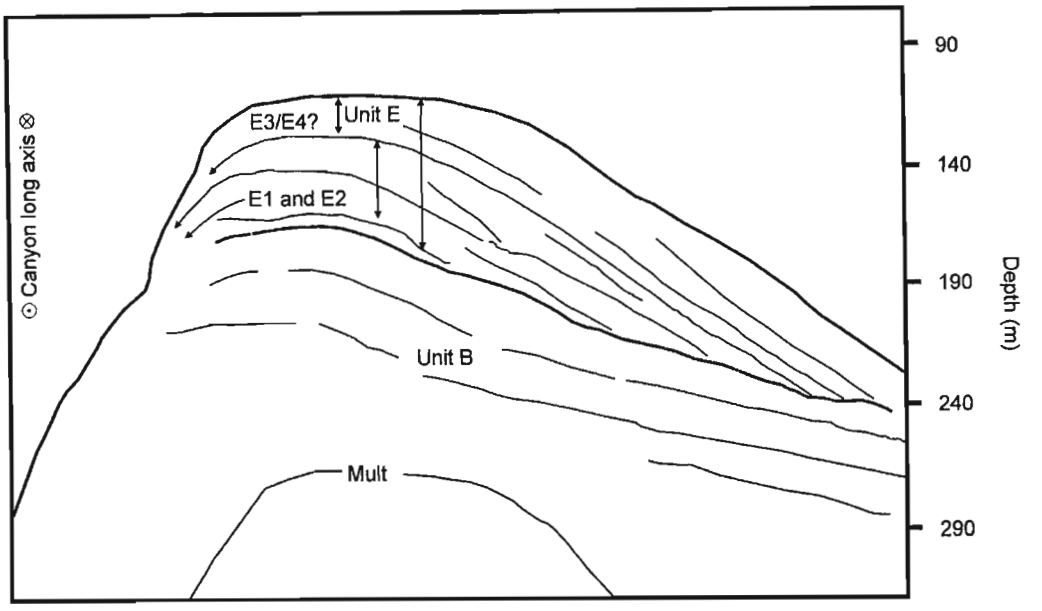

Figure 5.14. Schematic line drawing of line 3k, acquired strike obliquely over the northern wall of Diepgat Canyon. Note the sigmoidal clinoforms of aggradational/progradational unit E which comprises the shelf edge wedge. Facies E1 and E2 form the core, over which facies E3/E4 are deposited as progradational units. An important feature recognised from this profile is the overspilling nature of the clinoforms across the canyon rim and in towards the canyon axis. This typical stacking geometry does not occur in the acoustic basement of the area, the reflectors being erosionally truncated by the canyon margins. Look direction of figure is along the up-canyon axis.

Jesser Canyon, a narrow, straight shelf-indenting canyon; is bordered by aggradational mounded deposits of unit E sediments which form a widened lobe of the shelf-edge wedge, adjacent to the southern canyon wall (Fig. 5.3). This lobe overlies sporadic deposits of unit D, irregular masses of chaotic internal geometry, and unit B- where the sediments of unit E abut directly against the canyon margin in an axis normal progradational arrangement.

Wright Canyon exhibits several large glide planes which truncate reflectors of unit B on the mid-shelf portions of the canyon head (Figs. 5.2 and 5.3). These bind several stages of slump-fill which occupy the canyon thalweg. A single listric fault underpins the northern canyon wall, against which both the modern and palaeo-thalwegs of Wright Canyon abut. Data loss from the upper slope portions of the canyon precludes an understanding of the upper slope canyon seismic structure, though re-interpretation of the slope oblique airgun line 285 (Fig. 5.16) depicted in Martin (1984) indicates limited downcutting of the thalweg into a mid/lower-slope slump facies.

Slope oblique line 3n (Fig. 5.17) indicates that the outer-mid shelf sediments of unit E, facies E4, and the high acoustic impedance unit F have been eroded, which has resulted in a relatively thick

unit H resting directly on sediments of unit B in the inner shelf region. The underlying unit E onlaps unit B, and comprises multiple rotational slumps which have affected the facies E1 and E2 where they are erosionally truncated by the canyon wall. An isolated pocket of unit H has spilled over the canyon rim, and is separated from the landward portions of the shore connected modern sediment wedge by a ridge of outcropping unit G. Sediments of unit H onlap thick (~30 m) unit G sediments, identified as beachrock/aeolianite of the 6/7 Mile Reef complexes (see Fig. 4.12). Internal reflector configuration is obscured by the high surface reflectivity of this unit.

Line 11 (Fig. 5.18), shot through the landwards narrowing valley of upper Wright Canyon, reveals the complete removal of the onlapping wedge of unit E sediments, with reflectors of unit B erosionally truncated by the canyon head. Unit F sediments rest on an erosional surface which caps unit B. Internal reflectors of units B and H, which border the canyon margin, exhibit deformed high amplitude reflectors. Deformation becomes less intense with increasing distance from the canyon rim. White Sands Canyon is similar to Wright Canyon in that erosion of units E and G from the inner shelf has occurred (Fig. 5.19; line 3o). Sediments of unit H downlap onto unit B, and occupy a saucer shaped erosional depression. The broad and flat upper canyon thalweg is underlain by several generations of chaotic slump fill, indicated by chaotic, very high amplitude reflectors which limit penetration to the underlying strata.

Strike parallel line 2 reveals a large slump fill bounded by a listric fault which truncates reflectors of unit B (Fig. 5.2). The fill overlies multiple deformed high amplitude reflectors and conforms exactly to the underlying palaeo-thalweg topography. A reinterpretation of slope oblique airgun line 285 (Fig. 5.16) (Martin, 1984) indicates shallowly sloping canyon edges, which become more v-shaped towards the thalweg. The canyon incises into a mid/lower-slope slump facies. The interfluve separating Wright and White Sands Canyons appears to be aggradational though the poor vertical resolution of the airgun makes it difficult to truly establish this.

5.3.2.3. Mabibi Block

The coast parallel line 2 (Fig. 5.2) shoals slightly in the Mabibi Block, intersecting the upper slope portion of the shelf-edge wedge. Mounded aggradational deposits of unit E characterise the shelf-edge wedge interfluves between canyons (Fig 5.20). These downlap onto sediments of unit B and D, in addition to laterally extensive slump masses, preserved as chaotic to wavy high amplitude internal configuration sediment bodies.

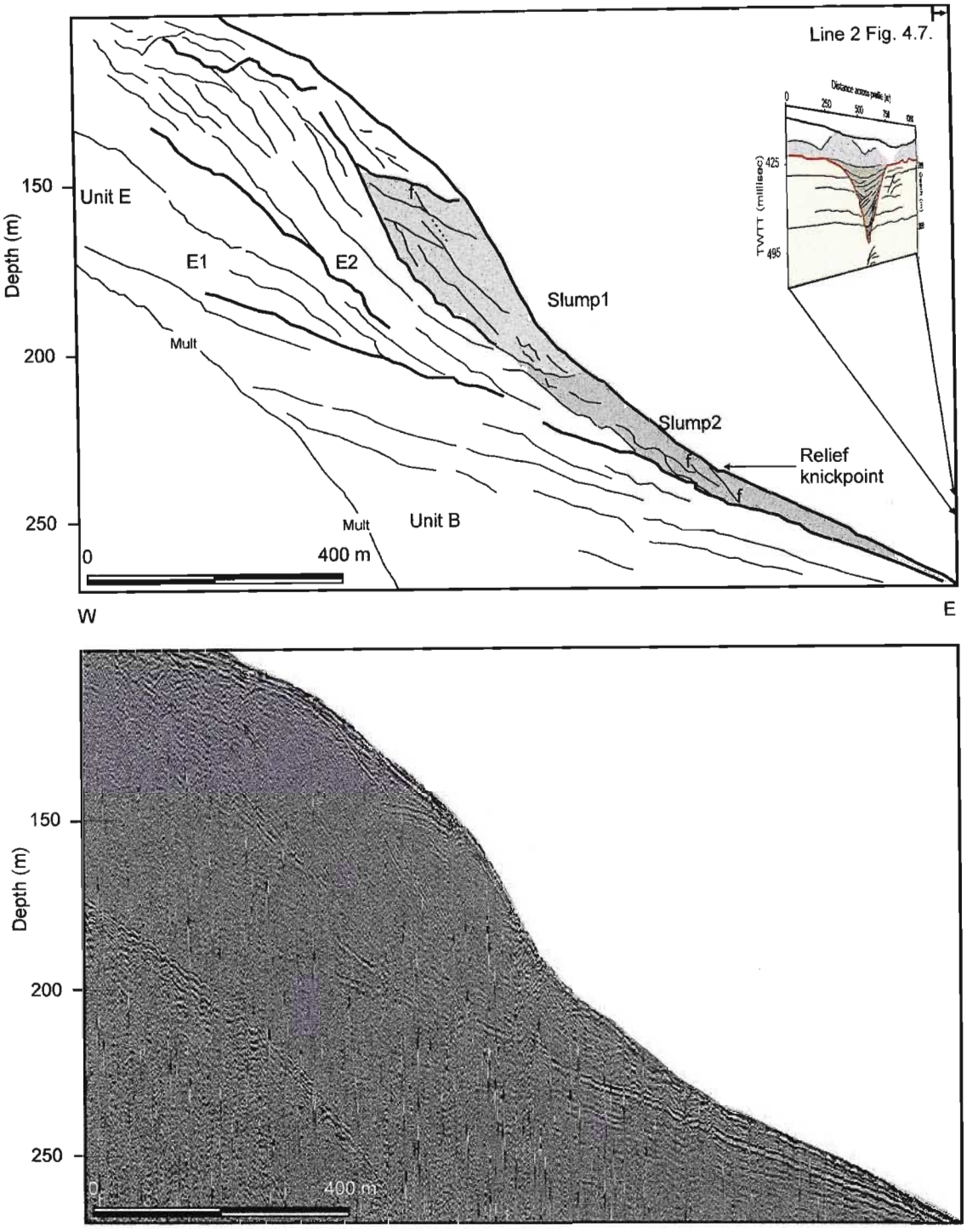

Figure 5.15. Strike perpendicular line 15 and interpretative line drawing indicating a relief knickpoint in the upper continental slope profile. This corresponds to rotational faulting at the base of the shelf edge wedge, each fault attaching to the MFS regional reflector (see table 3.1). In the upper shelf wedge, growth faulting is apparent. Rotational faults correspond to the head position of a subdued relief canyon where it impinges the shelf-edge wedge. This occupies the subsurface expression of an underlying palaeo-valley incision/fill, as depicted in figure 4.7.

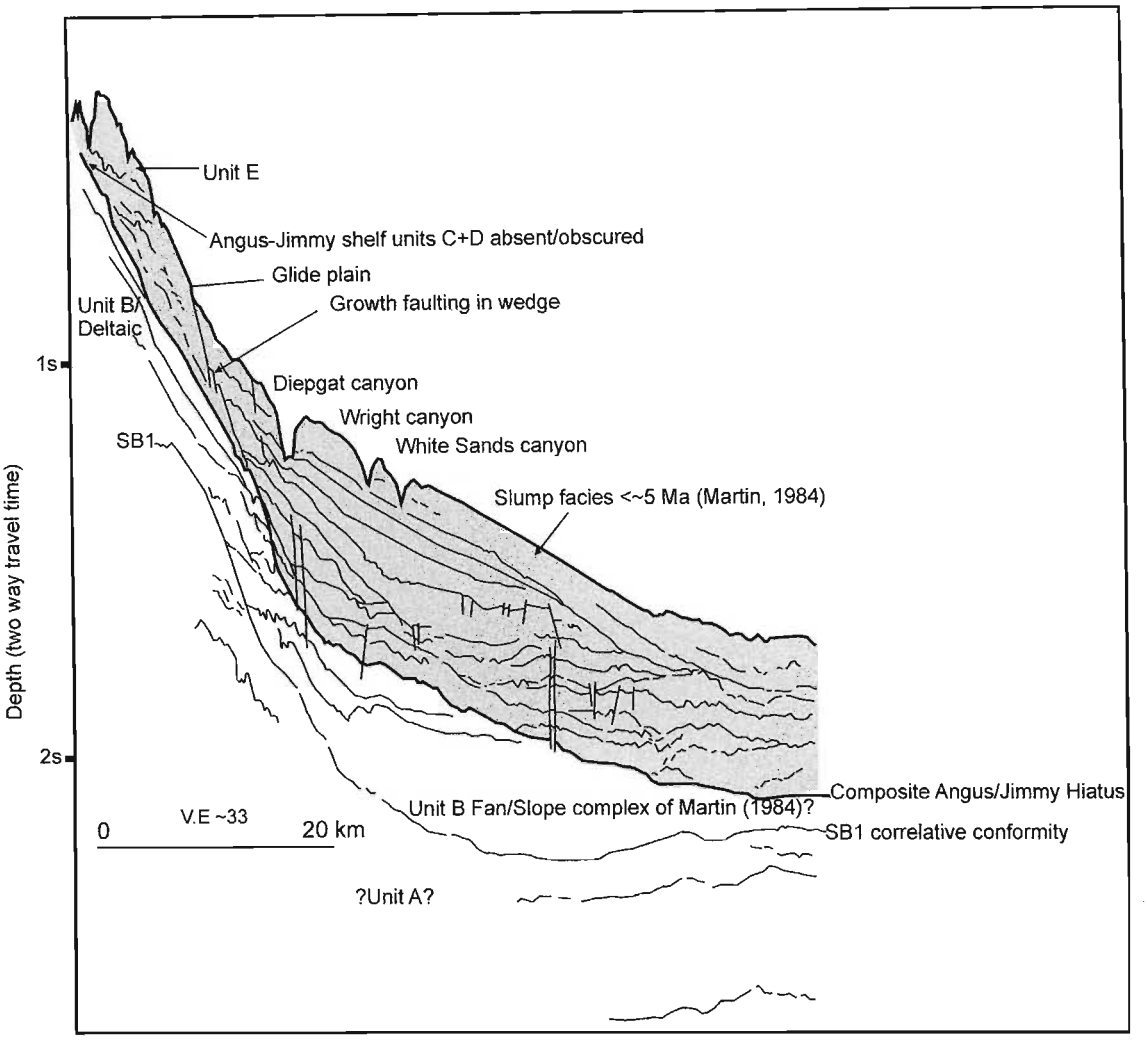

Figure 5.16. Re-interpreted seismic airgun profile 285 (from Martin, 1984) across the outer continental shelf and continental slope. Note the growth faulting of the shelf-edge wedge, and the seaward thickening body of Zululand slump mass (~5 Ma, discussed in chapter 7, see fig 7.1) described by Martin (1984). Diepgat, Wright and White Sands Canyons are clearly imaged (see text for discussion). Note the correlative conformable nature of SB1 in the continental rise portions. Grey shaded area corresponds to deposits of, or those forming contemporaneously with shelf edge wedge development and slump facies <5 Ma (Martin, 1984). V.E. = vertical exaggeration (~ 33×).

Where line 2 shoals from the Sodwana Bay Block, extensive growth faulting at the base of the aggradational shelf-edge wedge occurs (Fig. 5.21). This faulting is widespread within the shelf-edge sediments of unit E, and in most cases may be divorced from localised faulting within canyon walls of this area. Reflector RS1 which caps unit B displays domino style faulted blocks in this region, which have a cumulative downthrow to the south-southwest of 80 m. The apparent dip and strike of these faults is 280°/16° (Fig. 5.22). Isolated growth faults south of Island Rock Canyon are also common (Fig. 5.2). These terminate against RS1, and toplap unit E derived slump masses.

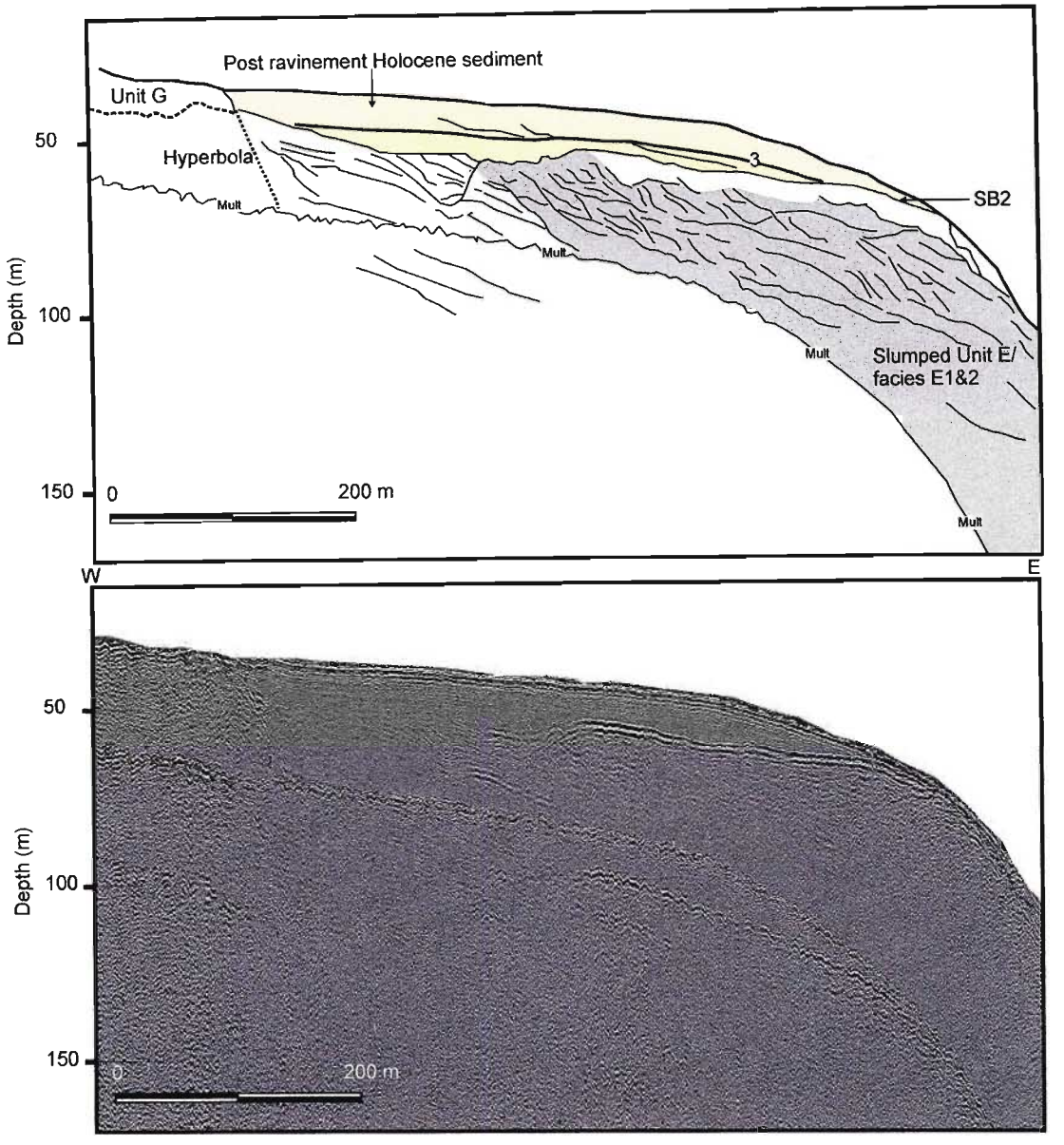

Figure 5.17. Slope oblique line 3n and interpretative line drawing across Wright Canyon head. Mid-shelf sediments of unit E (facies E4) and unit F are eroded, resulting in thick unit H deposits having accumulated in a saucer shaped erosional depression. Unit E onlaps unit B just landwards of the shelf break (~60 m depth), and comprises multiple rotational slumps. Thick unit G sediments crop out in the mid to inner shelf region, identified as the 6/7 Mile Reef complex (see chapter 9).

Island Rock Canyon is the most structurally complex of this area as it appears to comprise several stages of slump infilling and axial canyon incision (Fig. 5.20). Chaotic, high amplitude deformed reflectors underlie a wide infilled thalweg. Chaotic reflectors are truncated by more recent canyon thalweg formation, with up to three distinct incisions evident (Fig. 5.2).

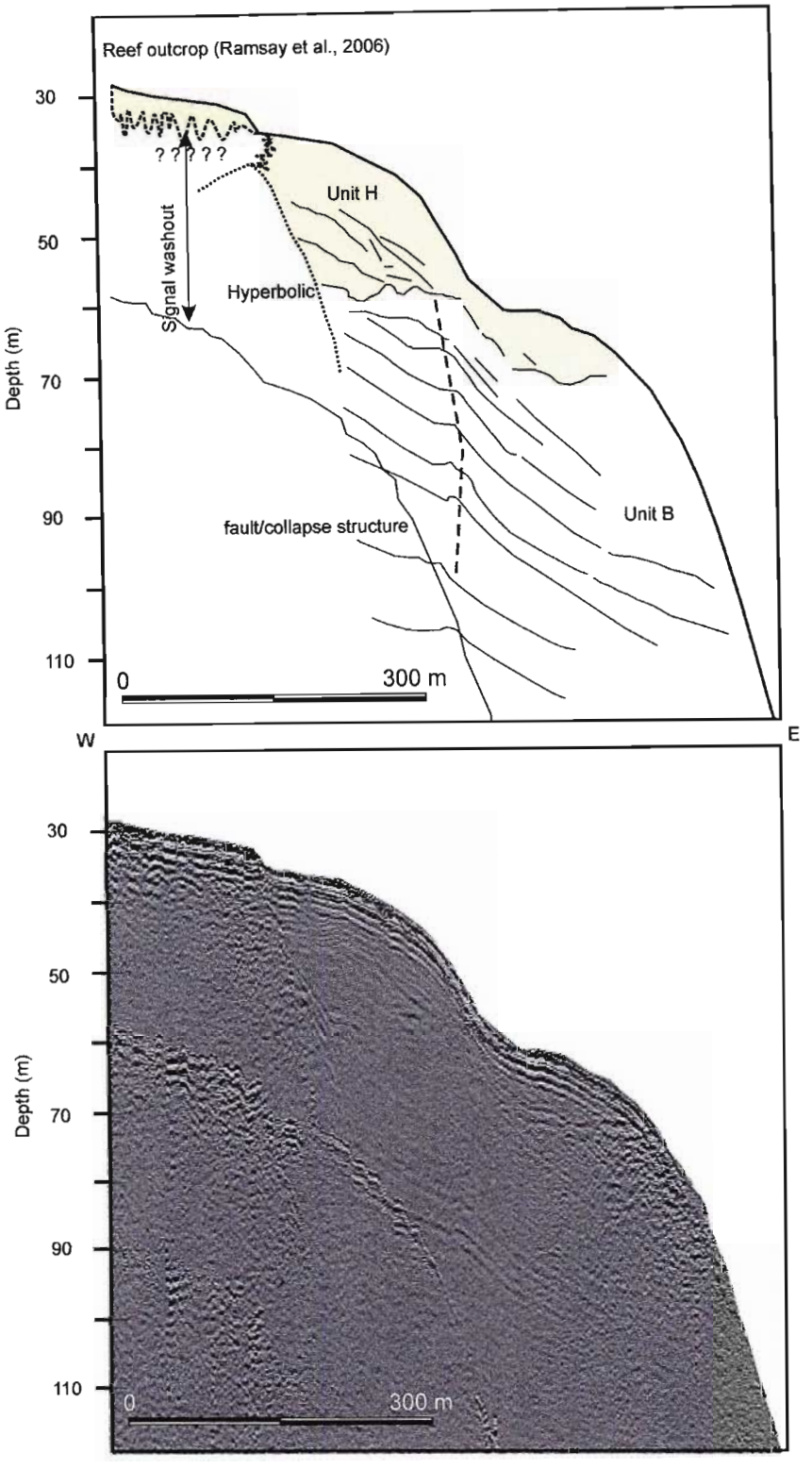

Figure 5.18. Strike perpendicular line 11 and interpretative line drawing across landwards narrowing valley of upper Wright Canyon. A complete removal of unit E sediments is apparent, with unit B cropping out in the canyon head. A fault extends through the sediments of unit B, marked by a line of sediment collapse.

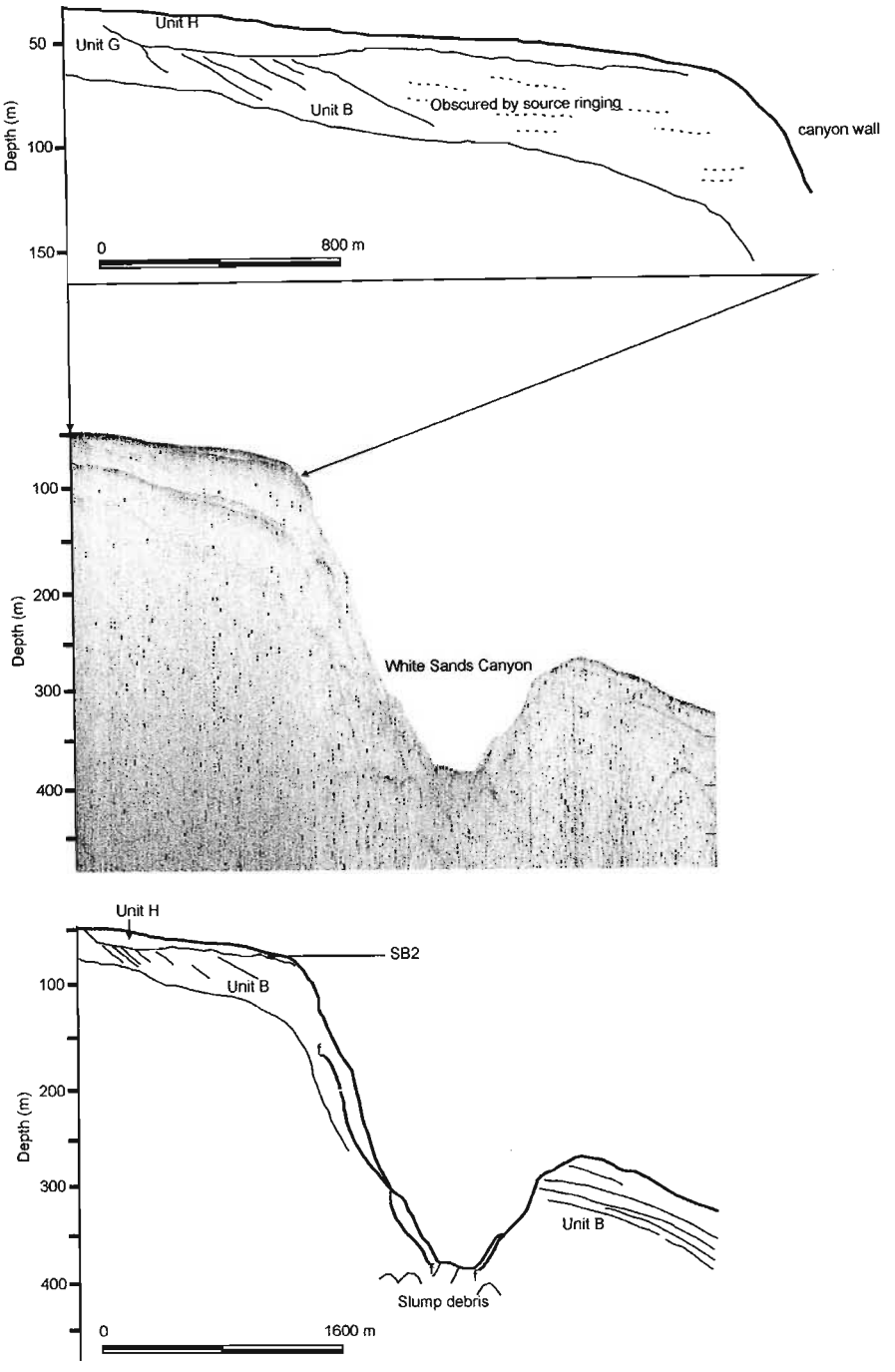

Figure 5.19. Interpretative line drawing and compressed data image of slope oblique line 3o, acquired across the head of White Sands Canyon. Note the absence of units E, F and G on the continental shelf, sediments of Unit H directly onlapping sediments of unit B which have been erosionally truncated by SB2. This has formed a shallow depression in which relatively thick (~16 m) unit H sediments have accumulated. Data in the shallow sections of the line are obscured by source ringing, making interpretation difficult. Note the slump debris and glide plain/fault bounded slump blocks in the canyon walls and thalweg.

Bathymetric analysis of this canyon indicates a slump headwall in the upper slope, which has removed the lower portions of at least two small canyons (Green et al., 2007; chapter 6). This comprises the southern portions of the canyon, forming a large mass wasting feature that joins with the northern flank of the adjacent South Island Rock Canyon (Fig. 5.20). Seismic line 3s (Fig. 5.22), acquired in the upper portions of this feature, indicates a large glide plane which erosionally truncates sediments of unit B, D and anomalous Miocene sediments.

High amplitude wavy reflectors of the slide mass onlap this glide plane, and show evidence of fault drag where reflectors become asymptotic to the plane itself. This feature is then overlain by a thin (~10 m thick) lenticular slump package comprising high amplitude chaotic reflectors upon which reflectors of unit E onlap. The modern day seafloor does not truncate reflectors of the slide mass, despite having what appears to be a localised steepening (glide scar?) in the lower most section of the profile.

South Island Rock Canyon incises to the base of the adjacent infilled thalweg of Island Rock Canyon, and erosionally truncates reflectors of units B. Sigmoidal Unit E reflectors are aggradationally stacked along the interfluves and progradationally spill over into the canyon feature (Fig. 5.20). Island Rock Canyon is relatively less incised, the modern thalweg overlying three distinct packages of high amplitude chaotic reflectors each of which are truncated by an overlying high amplitude erosional palaeo-canyon surface. The canyon rests in a wide, flat indentation between aggradational interfluves comprising unit E and anomalous Miocene sediments (Fig. 5.20). Within unit E, several reflectors downlap onto non-regionally defined surfaces, and represent isolated lenses of the shelf margin progradational facies E2. The reflector truncating the top of the anomalous Miocene sediments surface reflector here has a very hard return, characterised by high-angle parabolics. The indentation itself is underlain by a thin lens containing flat lying reflectors of unit E (~10 m thick), a thin layer of anomalous Miocene sediments (~20 m thick), and thick unit B sediments. These are all truncated by the modern canyon thalweg. The canyon interfluves comprise lobate sediment wedges which curve inwards towards the canyon complex indentation (Fig. 5.23), composed of the progradational unit E and the underlying progradational anomalous Miocene unit (Fig. 3.6a).

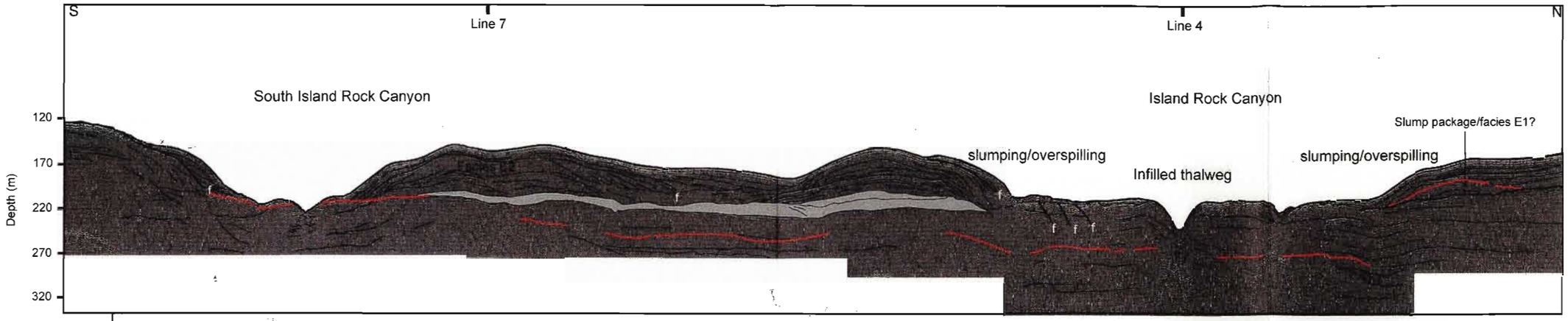

Figure 5.20. Strike parallel line 2 from the Mabibi area. Growth faulting is evident within the shelf-edge wedge unit E (denoted by f). Deposits of unit E are typically mounded-aggradational and characterise the interfluves between canyons. Unit E characteristically overspills, via slumping, into the canyons. Note the modern thalweg of Island Rock Canyon which overlies several packages of distinct high amplitude chaotic reflectors. These are truncated by palaeo-canyon thalweg surfaces. Modern infilling of the recent Island Rock Canyon thalweg is apparent. Upper red line = base of Unit E. Lower red line = base of anomalous Miocene unit. White overlay = lower slump package depicted in figure 3.6a.

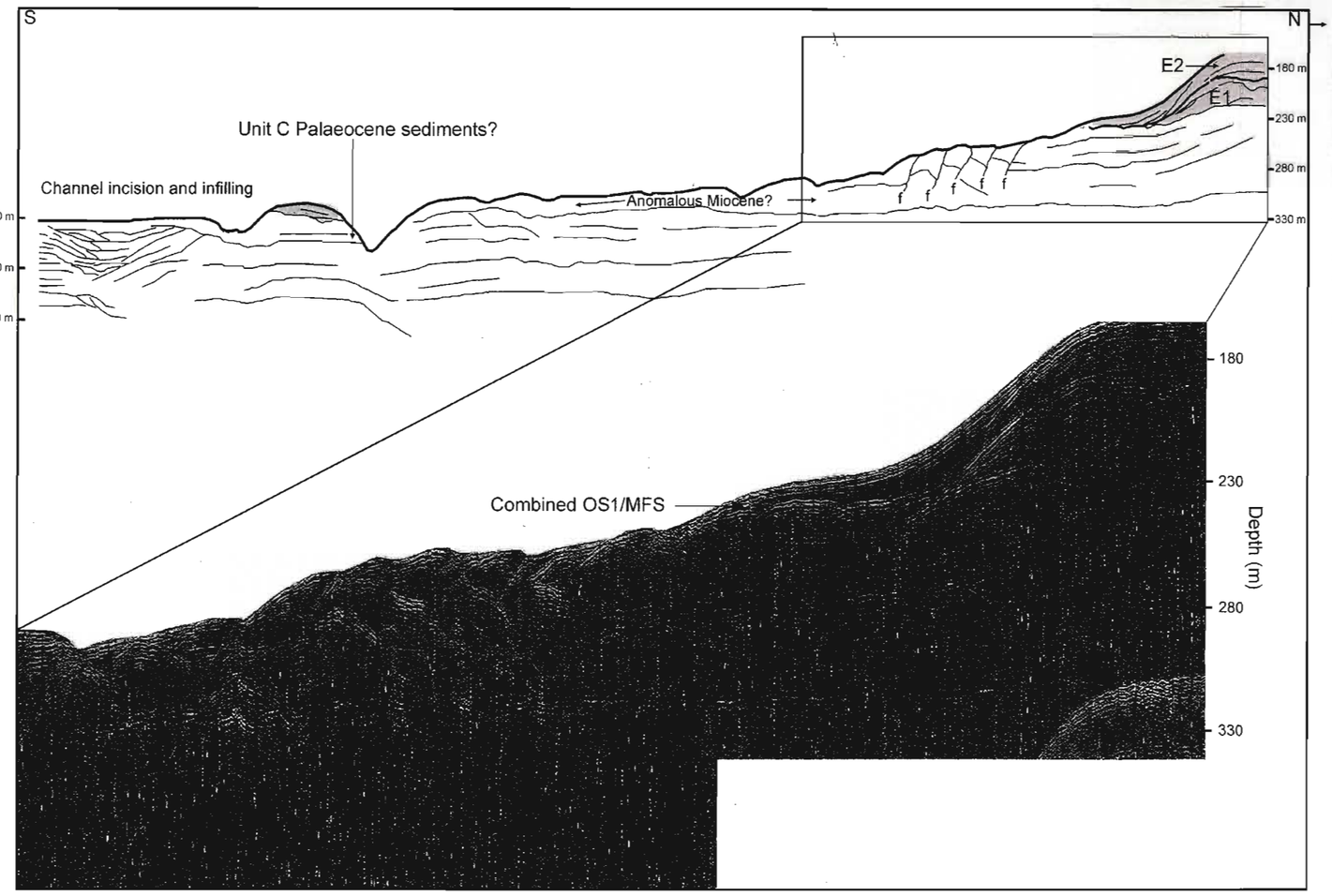

Figure 5.21. Strike parallel line 2 and interpretative line drawing depicting the region where line 2 shoals between the Sodwana and Mabibi Blocks. Note the extensive growth faulting in the shelf edge wedge (denoted by f). apparent dip and strike of the faults is 280°/16°. RS1 appears to be similarly faulted in these portions of the shelf-edge wedge, though this does not occur elsewhere. The cumulative downthrow of these domino style faults is 80 m to the south-southwest.

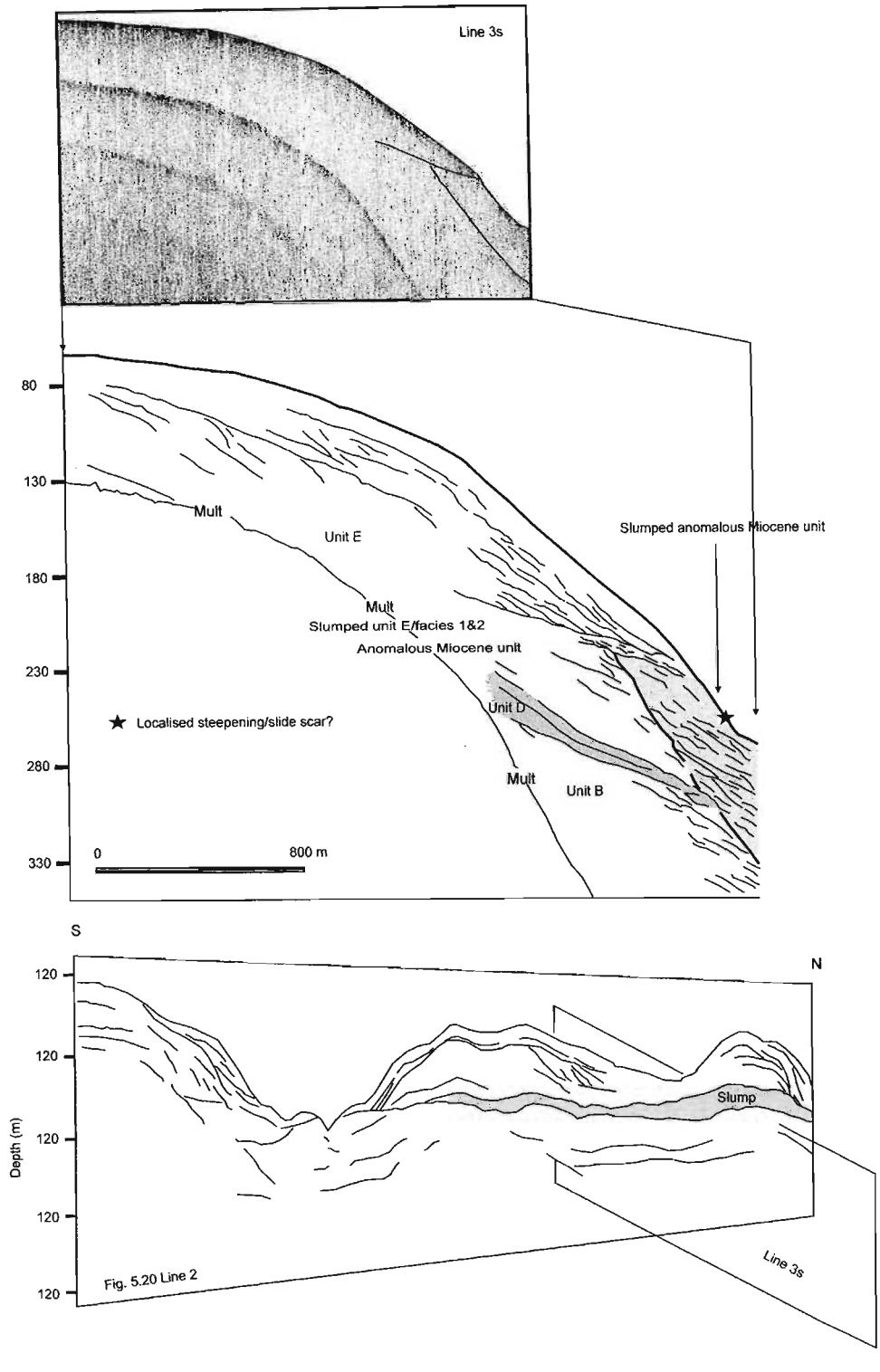

Figure 5.22. Interpreted line drawing of strike-oblique seismic line 3s, from Island Rock Canyon. A prominent glide plain truncates units B, D and the anomalous Miocene unit. Wavy, high amplitude reflectors onlap the glide plain and display evidence of fault drag. A thin slump overlies the slump-affected units over which undisturbed sediments of unit E have been deposited. The fence diagram indicates where line 3s crosses the shelf-edge wedge (depicted by line 2, figure 5.20).

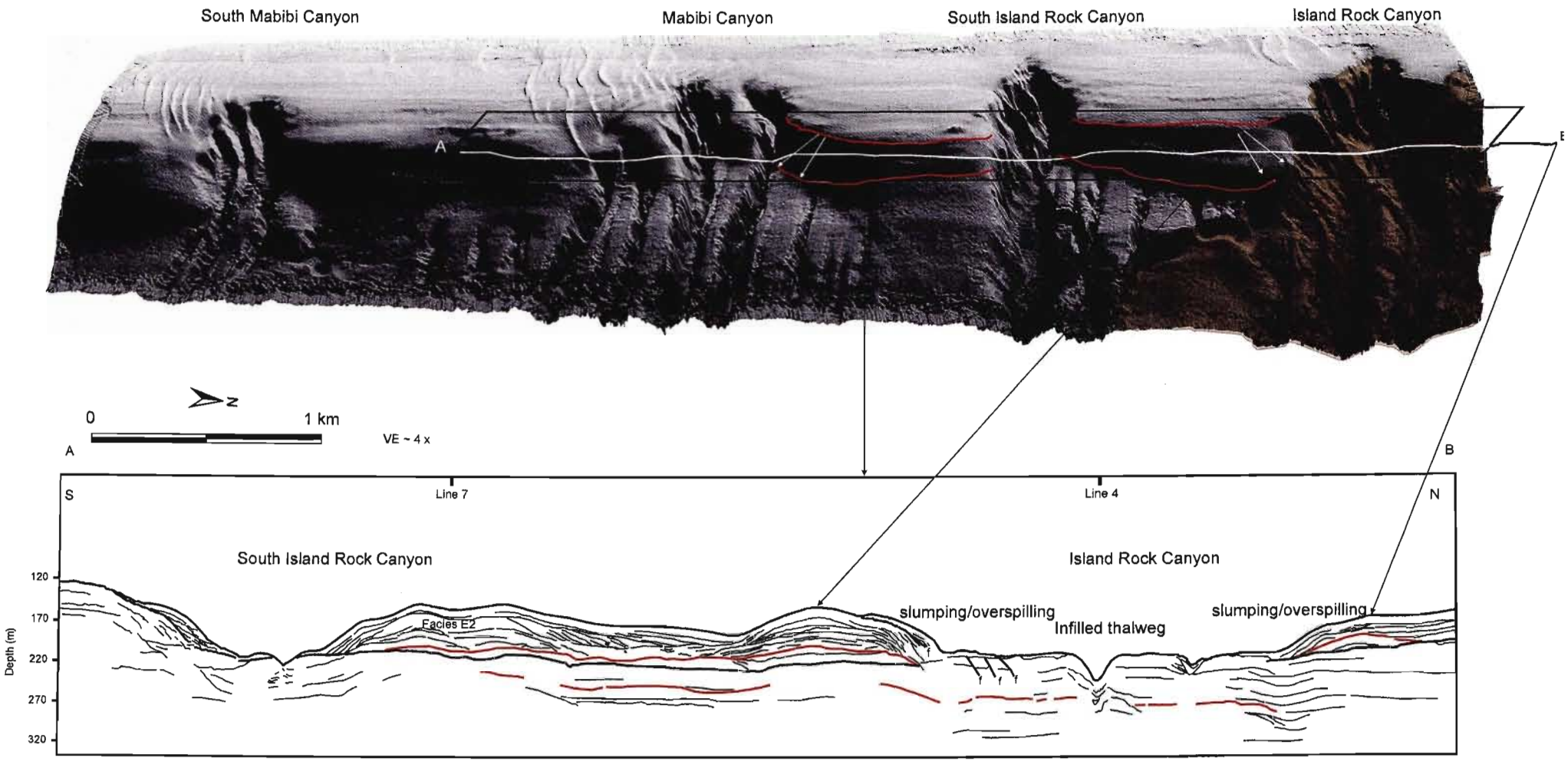

Figure 5.23. Multibeam image of the Island Rock Canyon/slump complex (shaded in brown). The shelf-edge wedge extent, as mapped from the bathymetry and seismic records, is delineated by the red lines. White arrows indicate direction of sediment progradation towards the canyon axis. Note the nature of the canyon interfluves (comprising unit E) which form lobate sediment wedges orientated inwards toward the canyon complex indentation. VE = vertical exaggeration.

The southernmost canyon of the Mabibi area has a w-shaped thalweg which shallowly incises sediments of the anomalous Miocene unit (?). The canyon interfluves consist of aggradationally stacked reflectors of unit E which prograde towards the canyon edges and are asymptotic with the canyon walls. Reflectors of unit B, which underlie this canyon, are typically concave upwards. Throughout the Mabibi area, the mid shelf is underlain by buried aeolianite complexes of unit F/G which occur at depths of 50, 55, 65 and 75 m depth. These do not occur between Island Rock and South Island Rock Canyons, the surface reflector characterised in these portions by very hard returns. In this section of shelf, the Holocene sediment wedge is either completely absent, or thinner than the vertical resolution of the seismic tool.

5.4. Discussion

5.4.1. Topographic inheritance and downslope driven canyon erosion processes

Canyon development models proposed by Pratson et al (1994), Pratson and Coakley (1996) and most recently Green et al (2007) discuss the importance of inheritance by modern shelf and slope erosional systems of older topographic features. Leadsman Canyon, in addition to several smaller slope confined canyons from both the Leven Point and Sodwana Bay areas, are arranged in nested patterns, within older topographic depressions. Leadsman Canyon rests within a fossil canyon, and the presence of well defined interfluves comprising unit E, between the bifurcating canyon head, indicates that the fossil Leadsman Canyon was infilled to a critical point during the development of the shelf-edge wedge, before the modern day Leadsman Canyon was eroded. Similarly the slope confined canyons reside in small palaeo-slope gullies, formed by the incision of SB1 during forced regression, most notably the prominent palaeo-valley cut and fill feature which underlies the southernmost slope confined canyon in Sodwana Bay. These features provide compelling evidence for the upper and mid slope capture of downward eroding sediment flows by older topographic constraints. These would not have been completely infilled by post SB1 sedimentation in these portions of the slope, and may have been exacerbated during hiatus periods, providing a preferable route for gravity driven sediment flows that would have arisen during the Late Pliocene FSST/LST shelf-edge wedge development. Essentially, during subsequent stages of axial incision by downslope sediment flows, the buried axial incision's topography would be re-utilised and portions partially (but never fully) re-excavated (Fig. 5.24). This would preserve underlying thalweg cut and fill episodes, creating a nested arrangement of palaeo-thalweg and associated fill facies, resting beneath a modern thalweg.

Examples from the ancient record are provided in the completely buried headless canyons of Plio-Pleistocene age from the Ebro continental margin of the western Mediterranean. These display a characteristic nested stacking pattern of alternating incision and infilling (Bertoni and Cartwright, 2005), but are dissimilar to the KwaZulu-Natal canyons in that they are completely slope confined, as defined by their occurrence downslope of the offlap break of the topsets of the progradational system within which they formed. In addition, several regional phases of large scale canyon incision and fill have occurred in the Ebro example, compared to two localised phases in northern KwaZulu-Natal (as seen in the Leadsman example). This suggests that limited sediment supply and frequent hiatus development off northern KwaZulu-Natal stunted the development of more elaborate incision-fill episodes. These are limited in most instances to the inheritance of Late Cretaceous sequence boundary topography, which then remained significantly dominant to influence sedimentation and erosion to this day, manifested by the surface expression of canyon features. Modern day exploitation of palaeo-topographic lows is most evident in the sinuous limb of Leven Canyon, which occupies the LGM incised valley.

5.4.2. Terracing, axial incision and wall instability

Baztan et al (2005) document similar axial incision morphologies from canyon valleys in the Gulf of Lion, when compared to Island Rock Canyon (Fig 5.20), the mid slope portions of White Sands Canyon (Fig 5.16), and Mabibi Canyon. This canyon morphology suggests several periods of incision and subsequent fill during quiescence, ascribed to fluvial interaction with the terrestrial portions of a submarine canyon (see also Mulder and Syvetski, 1995; Berné et al, 2002). No evidence of an inner shelf extension of the northern KwaZulu-Natal canyons, apart from Leven and Wright Canyons, exists. These canyons are thus different in that slump derived flows, rather than hyperpycnal plumes, cause initial axial incision, which would later be filled by axially-directed wall slumps as the canyon widened by wall oversteepening, as growth faulting in the rapidly deposited aggradational-progradational unit E sediments became pronounced (Fig. 5.24). Failure of the canyon walls would occur, forming glide-plane bounded slump blocks (see also figures of other failures) overlying a base comprising high amplitude chaotic reflectors formed by the toe of the failure (Fig. 5.25). This type of terracing process is documented by Antobreh and Krastel (2006) for the upper slope segments of the Cap Timiris Canyon, offshore Mauritiana, though it appears to be controlled more by pre-existing fault structures than the axial incision driven model envisioned here. Similar slump-fill episodes are evident in the head portions of White Sands Canyon (Figs. 5.2 and 5.3; line 2 and 1) however terraces are either not well preserved (inner shelf) or are replaced in

the upper slope by a v-shaped canyon valley instead. This suggests that slump material was more efficiently removed in the upper slope portions (by strong turbidity flows?), whereas in the shelf portions, slump blocks were not removed and could form terraces. These type of v-shaped, glide-plane bounded canyon valleys are also common in both the upper slope portions of Leven and Wright Canyons. The end result of this slump/terracing process is envisioned as forming a planation surface by lateral shelf-edge retreat away from the instability source (axial incision) as headwall slumps occur, which overlies several stages of deformed slumped material. The morphology of the complex mega-slump bound Island Rock Canyon (Green et al., 2007) is explained by these processes (Fig. 5.24).

5.4.3. Unit E and shelf- edge wedge genesis

Slope failure, and the initiation of the critical slope rilling phase of submarine canyon evolution (Pratson et al., 1994; Pratson and Coakley, 1996; Green et al., 2007), has been ascribed to various regional factors such as sea-level changes and tectonic regime (Wonham et al., 2000) and local controls such as fluid venting (see chapter 7) and rapid upper slope progradation (Poag and Sevon, 1989; Pazzaglia, 1993; McHugh and Olson, 2002; McHugh et al., 2002; Bertoni and Cartwright, 2005; Green et al., 2007). Unit E, in the shelf-edge region occurs as a rapidly deposited, aggradational-progradational sediment body, resting on lens-like bodies of chaotic internal configuration. These are interpreted as contemporaneous slump bodies formed during shelf-edge wedge development, over which unit E subsequently prograded. The most notable characteristics of the shelf-edge wedge are:

1) associated growth faulting, and the rotation or deformation of those faults which border canyon heads.
2) associated canyon incision into deeper reflectors. Sediments of unit E abut against, and sigmoidally prograde into, these features (Fig 5.14).
3) the partial infill of canyons in this region by unit E sediments which overlie older stratigraphic units.

These suggest that the development of the shelf-edge wedge (unit E) was characterised by widespread instability (prominent slumping, development of growth faults, rotation of faults), and that canyon topography in these areas grew by both incision and interfluve aggradation (c.f. Mitchell, 2005). Canyon growth is thus intrinsically linked to shelf-edge instability as the resulting slope failure would provide the genesis for the downslope sediment flows needed to initiate slope rills (e.g. Pratson and Coakley, 1996) (Fig 5.24).

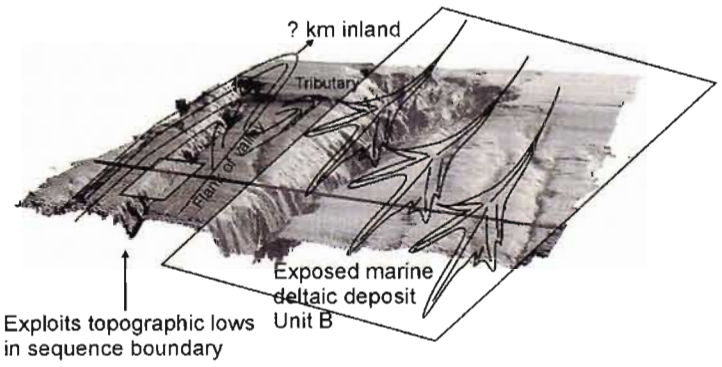

(1) Deposition of unit A during forced regression, followed by formation of sequence boundary, valley incision and sediment bypass. Lowstand deltaic sedimentation follows, forming unit B, which is entrained into these topographic lows and may incise them further by downslope erosion.

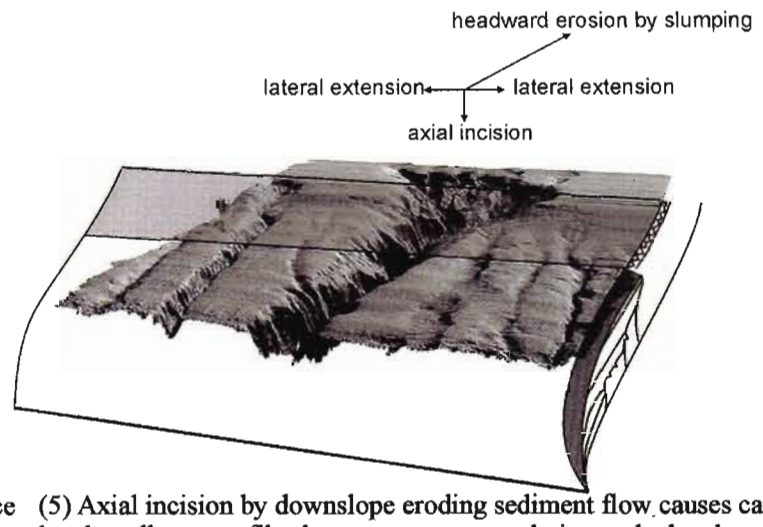

(5) Axial incision by downslope eroding sediment flow causes canyons to erode headwardly, as profiles become oversteep relative to the headward portions of the thalweg. Slumping occurs, which prompts further downslope incision of the axis by turbidity flow. As the axis incises further, the side walls become oversteep relative to the canyon floor and fail laterally, thus widening the system.

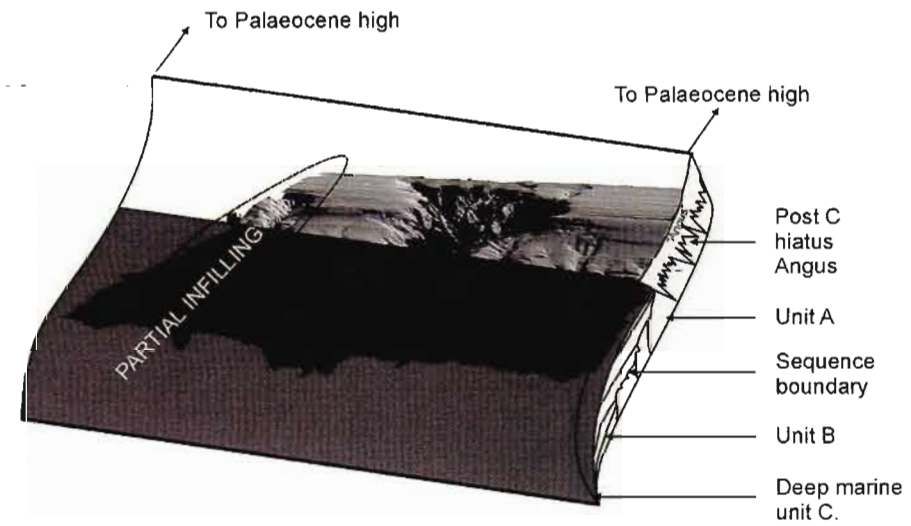

(2) Transgression ensues during Palaeocene, causing widespread marine deepening. This partially infills the topographic depression as a draped deposit of unit C. Unit C deposition is either terminated, or post unit C sediments are removed during hiatus "Angus". This results in no record of unit C sediment inshore of the upper slope.

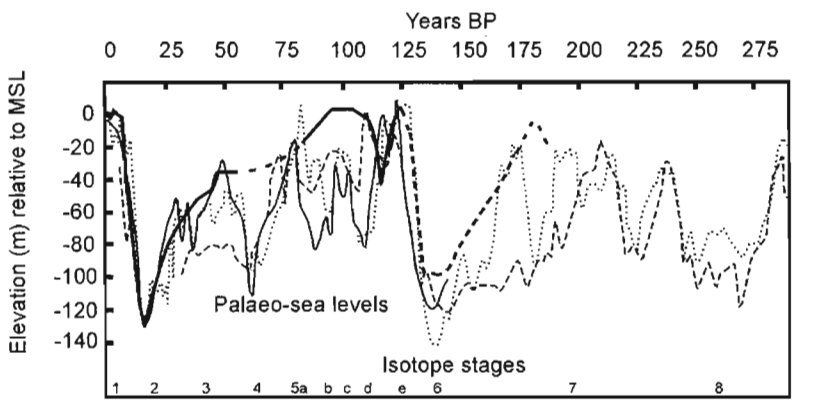

(6) The process of burial and exhumation of the canyons is exacerbated by intense glaciations, followed by sea-level rise and system quiescence during the TST/HST periods of the Pleistocene. Few to no Mid or Early Pleistocene sediments are found on this shelf, though some Early Pleistocene sediments are preserved as thin veneers on the upper slope (appendix 3a, Green et al., in review). The figure, and sources of data shown above are discussed further in chapter 8. Bold black line = South African east coast sea level curve (Ramsay and Cooper, 2002).

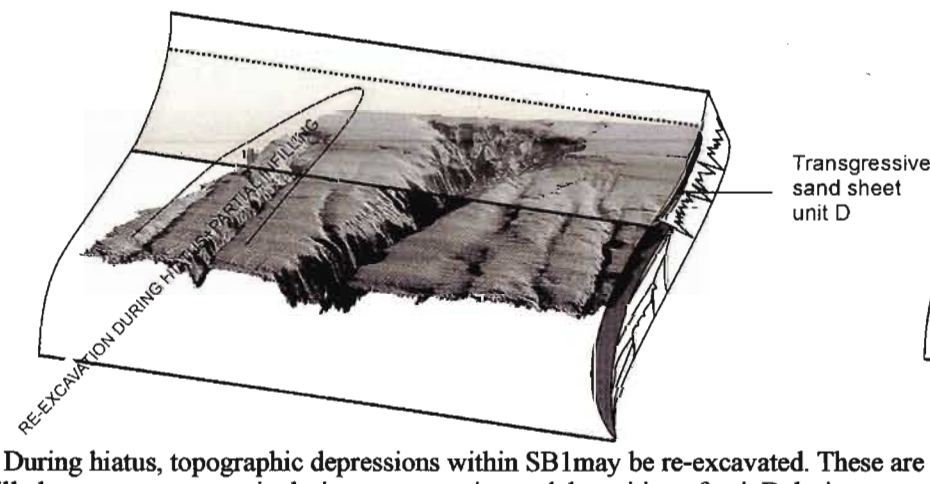

(3) During hiatus, topographic depressions within SB1may be re-excavated. These are infilled to some extent again during transgression and deposition of unit D during wave base shifting and reworking.

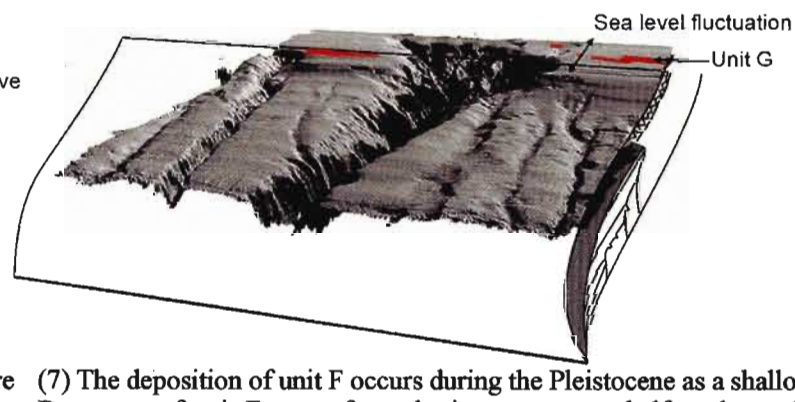

(7) The deposition of unit F occurs during the Pleistocene as a shallow marine deposit. Remnants of unit F occur from the inner to outer-shelf, and may have been altered considerably during the Pleistocene glaciations. Unit G, was deposited during the Late Pleistocene, as sea level fell towards the last glacial maximum (LGM). The formation of small incised valleys during the FSST created fluvial links to some of the canyons. Compared to the sediment flowdriven model envisioned here, these would play a negligible role in the sculpting and evolution of canyons. Formation of (LGM) sea level notches in canyon heads occurs, indicating that most canyons have not experienced headwall failure since the LGM (chapter 8).

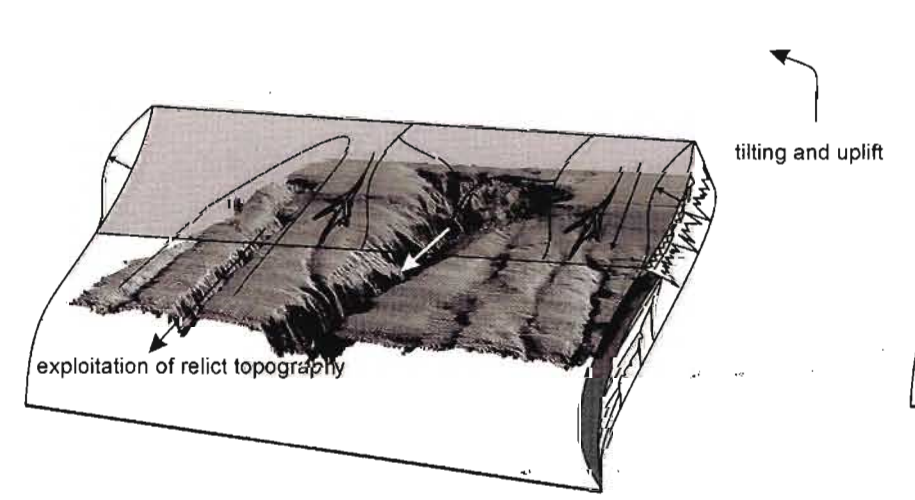

(4) TST deposits of unit D are not fully preserved or are removed during hiatus "Jimmy". Tilting and uplift of the hinterland during the Pliocene caused an extensive lowstand shelf-edge wedge to rapidly form. This was supplemented by shelf-edge deltas. The wedge is unstable, marked by growth faults, and feeds several downslope eroding sediment flows. These are constrained to relict topography which has not been completely infilled in the mid-slope sections. Canyons, as are found today, begin to form by this rilling process. Where no relict pathway may be associated with modern canyons, these began by random downslope erosion patterns during wedge oversteepening and failure.

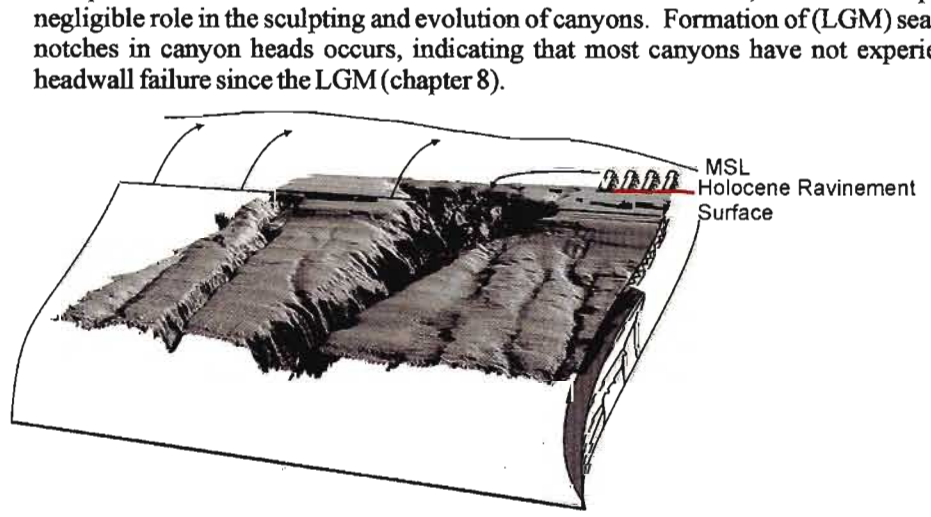

(8) Post LGM. The incision of palaeo-valleys ceased, and these were infilled by TST sediments. These currently provide a role in the exchange of fresh water between the fringing coastal lakes and the shelf. Landsliding within Leven and Leadsman Canyons is influenced by this (chapter 7). TST fills are capped by a Holocene ravinement surface, over which unconsolidated sediment has accumulated and been reworked into dunes (chapter 9). These may spill into the canyons. Sediment starvation of the areas is too great however, to spur large-scale debris avalanching within these canyons, these systems have thus remained quiescent since LGM times.

Figure 5.24. Schematic evolutionary model of the submarine canyons of northern KwaZulu-Natal.

1) Axial incision by downslope eroding gravity flows, channeled by subsurface, relict topography preserved in sequence boundary. Flows are caused by the progressive development and steepening of the regional shelf-edge wedge.

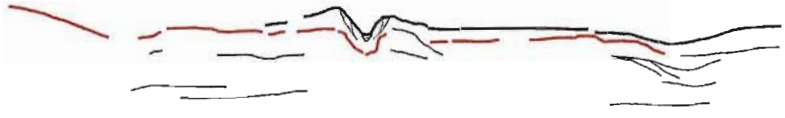

2) Axial incision leads to oversteepening of the rill/proto-canyon walls, and slumping which contributes further material to downslope eroding flows. During periods of quiescence, the thalweg will infill by pelagic means. Dotted lines show zones prone to failure as wall instability increases by thalweg downcutting.

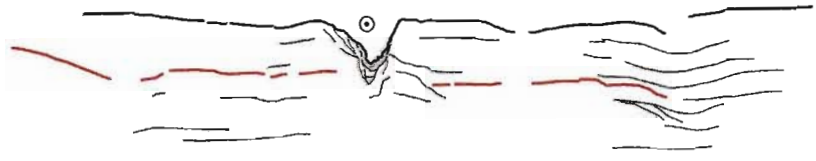

3) This process is repeated, causing a stacked pattern of alternating cut and fill episodes. As slumping becomes larger and more catastrophic, the resultant mass wasting causes increasing axial incision.

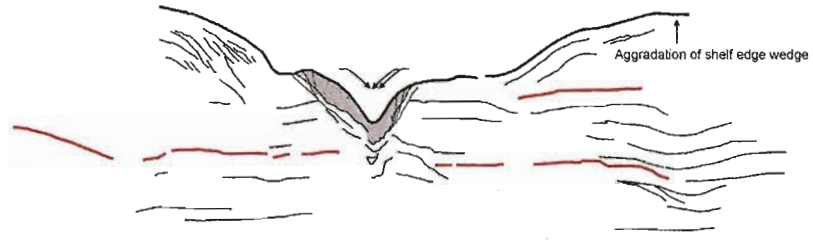

4) As the shelf-edge wedge aggrades, bolstered by lowstand deltaic sedimentation, growth faulting, and glide plain bounded slumps become increasingly pronounced in the canyon system. Sediment exchange from the shelf edge to the canyon floor and eventually the abyssal plain/slope basin occurs.

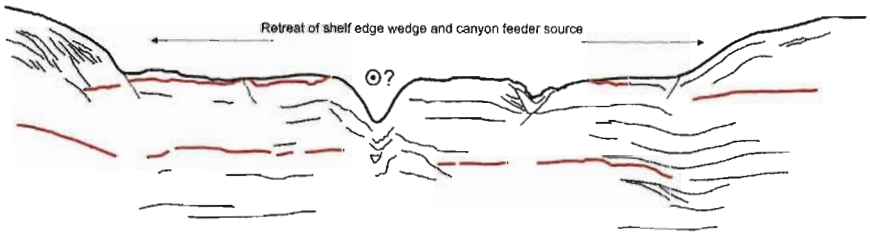

5) Eventually, the shelf-edge erodes back, away from the incision point where undercutting occurs, leaving a planation surface derived by axial incision, related to slope oversteepening.

Figure 5.25. Schematic evolution of slump/terracing in submarine canyons, using data from line 2, Island Rock Canyon.

As the shelf-edge became more established, supplemented by high sediment supply rates (Partridge and Maud, 1987; Partridge et al., 2007) together with the formation of lowstand shelf margin deltas, the walls of these rills would be critically oversteepened relative to the failure-prone silty sediments of unit E (chapter 9). Downslope erosion would thus now be supplemented by retrogressive slump-derived material, initiating the headward phase of excavation proposed by Pratson and Coakley (1996) and Green et al (2007) (Fig. 5.24). Both Sydow (1988) and Shaw (1998) allude to the role of the accretion of the shelf-edge wedge unit as important in supplying sediment to the system, though neither provide an appropriate explanation as to how these sediments were deposited, and or the role they played in sculpting the Late Pliocene landscape. The presence of unit E as canyon fill, particularly in the Leadsman Canyon (Fig 5.10) which has been re-excavated from its filled (partially filled?) fossil state to create an upper slope inter-canyon spur, suggests that these sediments were provided via slumping during the canyon's lateral extension phase, and that it was the direct result of shelf-edge wedge aggradation-progradation. Similar canyon fills are documented by McHugh et al (2002) from a buried middle Miocene canyon on the New Jersey slope, the fill correlated to a rapid glacio-eustatic lowering. Likewise, mass transport deposits within a Miocene canyon-fill of the modern Berkeley Canyon, New Jersey, are interpreted as being autochthonous, derived from the canyon walls. McHugh et al. (2002) thus envision a similar process of rapid loading by high sediment delivery, slope failure during initial excavation of the canyon, and exacerbation of this process by relative sea-level fall and high sediment transport to the slope.

As the northern KwaZulu-Natal shelf-edge evolved during rapid relative sea-level lowering, it is thus probable that canyon incision-fill processes, similar to that documented by McHugh et al (2002) from the New Jersey slope, would have occurred in a comparable manner. Differences exist in that the fossil Leadsman Canyon was re-excavated in Late Pliocene/Early Pleistocene times, most likely the result of continued high sediment delivery to the shelf-edge during hinterland uplift (Partridge and Maud, 1987) and the re-initiation of sediment flows constrained to an incompletely infilled fossil Leadsman Canyon.

5.4.4. Tectonic versus sedimentary controls on canyon evolution

Morphometric analyses of a large landslide within the head of Diepgat Canyon revealed that the dimensions of this landslide are anomalous when compared to landslides within other canyons

(chapter 7). The large area of the failed mass, despite the small headscarp height and low angle of the adjacent local unfailed slope, indicate that rheology and slope angle were not the dominant controls on slide formation. A tectonic trigger is proposed as the cause of the resulting landslide morphology. The deep seated listric fault underlying these portions, accompanied by smaller attached splays provides compelling evidence for a deeper structural impetus for landsliding in the head of Diepgat Canyon (Fig 5.13). This would undoubtedly be controlled by seismic triggering. The absence of any erosional terracing by sea-levels at -125 m (Green and Uken, 2005), the removal of portions of aeolianite/beachrock from this area, the slumping of late TST shoreface sediments of unit H, and the absence of the transgressive ravinement surface 3 constrains the age of this failure to a minimum of ~ Mid Holocene. Modern unconsolidated sediments slump into the surface depression, indicating that these sediments too have been influenced by the most recent stage of canyon growth. A seismic trigger, associated with the most recent St Lucia earthquake (31st December, 1932) as described by Krige andVenter (1933), is thus postulated. This earthquake was assigned a surface wave magnitude of 6.8, the epicentre lying directly on the Nubia-Lwandle plate boundary, just south of the Nubia-Somali rotation pole (Hartnady, 2002) (and depicted in figure 7.1). It seems logical that future motion along this boundary will undoubtedly be responsible for further canyon growth in northern KwaZulu-Natal, possibly becoming the dominant mode of landslide initiation in light of the continued sediment starvation of the area. This shelf starvation would be exacerbated by the trapping of sediment in increasingly proximal areas as transgression ensues.

5.5.5. Aeolianite ridges, surface 3 and relative age constraints on canyon erosion

The erosion of aeolianite ridges by the headwards advance of canyon heads provides a means to constrain the minimum age of the most recent phase of canyon growth. Drowned aeolianite/beachrock complexes which are considered reliable palaeocoastline indicators (Ramsay, 1991; 1994), extend throughout the northern KwaZulu-Natal continental margin, occurring at similar depths from Leven Point in the south to Kosi Bay in the north (Ramsay et al., 2006) (see chapter 9 and fold out map: Marine geology of northern KwaZulu-Natal continental shelf: Leven Point to Island Rock). These correspond to:

Palaeo-coastline 1 between -15 and -25 m on the mid shelf (OIS 2)

Palaeo-coastline 2 between -13 and -45 m on the shelf, dated at 84 000 ± 3000 BP (OIS 5a)

Palaeo-coastline 3 between -50 and -60 m on the outer shelf (OIS 2)

Palaeo-coastline 4 between -70 and -95 m on the outer shelf (OIS 2)

Palaeo-coastline LGM between -120 and -130 m on the outer shelf (~18 000 BP)

The palaeo-coastline models of Ramsay (1991; 1994) can thus be extended to similar outcrops of comparable depths, and the ages constrained for the more recent phases of canyon growth. The removal of the 40-50 mbsl ridge by the Leven sinuous tributary indicates that the growth of this portion of the canyon post dates ridge formation. Ramsay (1991; 1994) considers this cordon to have formed during the regression of OIS 2. It appears the underlying palaeo-valley was incised either contemporaneously with this dune cordon development, causing a zone of erosion where subaerial dunes could not form, or it may postdate cordon development, thus eroding unit G post formation. This latter argument seems unlikely, as incised valley fills show evidence for regressive conditions in the form of SB2 incision, and fluvial lag facies at the channel base, this feature thus having evolved during the forced regression of OIS 2. The former argument is thus preferred.

The upper portion of Leven Canyon, as evidenced from line 1 (Fig. 5.3), shows that the canyon rim has been subject to shallow, post ravinement phase infilling, where the overlying modern sediment has cascaded into a small slump depression in surface 3. Incipient slumping of the head of the canyon may thus be either contemporaneous with, or older than the formation of the transgressive ravinement surface 3. This has exerted an influence on the modern day seafloor by virtue of incomplete sedimentary filling of the surface micro-depocenter. The onlapping nature of this surface onto unit G, which has a basal depth of ~55 m, signifies that it post-dates Ramsay's (1991; 1994) palaeo-coastline 3.

The erosion of unit G from the head of Wright Canyon indicates that the head was active at least until the LGM (contemporaneous and post OIS 2 slumping). This agrees with palaeo-drainage reconstructions which indicate that Wright Canyon had a LGM connection to Lake Sibaya (Fig. 4.12), allowing the system to headwardly enlarge itself, removing, or precluding the development of unit G. The presence of unit G inshore of White Sands Canyon is a result of the LGM channel being diverted coast parallel towards Wright Canyon head.

CHAPTER 6

Geomorphological evidence for upslope canyon-forming processes

Green, A.N., Goff, J.A., Uken, R., 2007. Geomorphological evidence for upslope canyon-forming processes on the northern KwaZulu-Natal shelf, South Africa. GeoMar. Lett. 27, 399-409.

6.1. Introduction

Recent acquisition of high-resolution multibeam bathymetric data from the upper slope and continental shelf of northern KwaZulu-Natal, South Africa has provided the basis for a detailed investigation of the geomorphology of continental slope canyons in this region. These data were collected for the African Coelacanth Ecosystem Programme, as part of an initiative to map the south-eastern Indian Ocean coelacanth habitat. Submarine canyons which impinge the continental shelf break in this region satisfy the morphological and bathymetric constraints of this "fossil fish" habitat (Fricke and Plante, 1988; Fricke and Hissmann, 1994); i.e. shelter requirements, in the form of caves and overhangs, associated with lower than present-day sea levels of between 100 and 130 m depth (Green et al., in press). To date, bathymetric studies from this area have concentrated either on small portions of the continental shelf (Ramsay 1994), or have favoured regional interpretations of the lower rise and abyssal plain, making use of low resolution bathymetric data (Dingle et al., 1978; Goodlad, 1986). This survey, employing a 100 kHz Reson Seabat 8111 ER multibeam echosounder, covered 392 km^2 over depths ranging from ~30 to 850 m, with a spatial resolution of ~10 m^2. Submarine canyons and gullies are prevalent throughout this area, indicating that periods of erosion have occurred, or are still actively operating as major morphologic influences on the upper continental margin. Studies by Goodlad (1986), Sydow (1988), Ramsay (1996) and Shaw (1998) have attempted to address the origins of these systems; however a comprehensive geomorphological study of these systems has previously been impossible due to the non-availability of high resolution bathymetric mapping systems.

Work by Adams and Schlager (2000), O'Grady et al. (2000) and Goff (2001) has aimed to quantitatively classify the shape of continental slopes as a means to infer the depositional and erosional processes. Goff (2001) focused in particular on the downslope progression of canyon relief in relation to the slope profile, and inferred from these quantities either "upslope" or "downslope" physical processes (e.g. Pratson and Coakley 1996) of canyon growth. This methodology was applied to the northern KwaZulu-Natal upper continental margin canyon systems,

comparing these with previous analyses on the Atlantic margin of the USA, to provide a geomorphological model for the formation of these canyons.

6.1.2. Theories of canyon formation

The earliest hypotheses for the formation of slope-canyon systems considered these to be the products of downslope eroding turbidity flows (Daly, 1936). Later evidence gathered by more comprehensive echosounding surveys (Chamberlain, 1964), dives (Shepard et al., 1964) and oceanographic surveys (Drake et al., 1978) indicated that processes such as creep, slumping and internal waves (Carlson and Karl, 1988) were also important factors. Since the early 1980s, substantial improvements in sonar technology resulted in a better understanding of the morphology of canyon systems. Twichell and Roberts (1982), using side scan sonar images of the New Jersey continental slope, documented canyons and gullies existing which were evidently in several different stages of evolution. Canyons and gullies which had not yet breached the shelf break ("headless canyons") provided evidence of canyon-forming processes which were not necessarily related to river systems and the supply of sands to the shelf edge. Farre et al. (1983) associated the presence of slump deposits with headless canyons, and proposed a model of canyon formation based on retrogressive headward slumping of the canyon head and walls. Once these canyon heads had breached the shelf break by progressive upslope slumping, a constant supply of sediment from the shelf would be entrained within the canyon and the system would then erode downwards via turbidity currents. Slope-confined canyons are thus considered by Farre et al. (1983) as immature stages in canyon development, which eventually evolve headwards into mature canyons which breach the shelf break. This "upslope" erosion theory of canyon formation has been supported by a number of authors investigating southern African slope canyons (e.g. Dingle and Robson, 1985; Sydow, 1988; Ramsay, 1996; Shaw, 1998).

More recently, evidence for a combined upslope and downslope eroding model of canyon formation was provided by Pratson et al. (1994) and Pratson and Coakley (1996), based on multibeam bathymetry, single-channel seismic reflection profiles and computer modelling of the New Jersey continental slope. These studies revealed a cyclic process of canyon cut and fill as shelf-edge depocenters shift and bury areas of active canyon incision. The subdued topography of filled canyons is then exploited during subsequent depocenter shifts where buried channels have created bathymetric lows in the middle portions of the slope, thereby constraining sediment flows which are ignited from a theoretically oversteepened upper slope. This downslope sediment flow is today

considered to be the major impetus of modern canyon initiation. As these flows erode the floor of the older canyon, they oversteepen the walls and head, causing a series of large retrogressive slumps which advance headwards along this chute, and excavate much of the canyon profile (Pratson and Coakley, 1996). Where canyons have not existed previously, rilling induced by the downward flow of sediment acts as the topographic constraint from which the canyon develops. Canyons are thus viewed as erosional systems evolving from slope-confined, through shelf-breaching to defunct existence, driven primarily by sediment flows and relative sediment supply.

In his quantitative analysis of slope-canyon systems on the USA Atlantic margin, Goff (2001) examined variations in slope gradient and canyon relief with depth. He identified what he considered to be two canonical ways in which canyon relief progresses along the slope. Along the New Jersey margin, canyon relief increases upslope, terminating in large, amphitheatre-shaped indentations in the shelf edge. Further south, along the Virginia margin, canyons are narrow and small at the top but increase in relief and breadth while converging downslope to the slope/rise break. Goff (2001) hypothesized that these two patterns correspond to a predominance of "upslope" and "downslope" processes respectively, the former exhibiting similarities to spring sapping systems, the latter to subaerial fluvial systems.

The slope gradients documented by Goff (2001) also revealed important differences between the two sites, with the New Jersey slope exhibiting a nearly constant gradient from shelf break to rise, and the Virginia slope a general decrease in gradient with depth (i.e. concave). Goff (2001) attributed the lack of steepening towards the top of the New Jersey slope to the extensive grading of the upper slope by the headward-growing canyons. This could explain the lack of oversteepening which would otherwise have been predicted by the Pratson and Coakley (1996) model. Goff (2001) argued that the concave profiles on the Virginia slope are also consistent with a downslope, fluvial-style erosion process which might be caused by turbidity flows.

6.2. Materials and methods

Submarine canyons systems are geomorphically complex, often with narrow and steep features. Adequate characterization of such canyons requires the dense coverage of high quality bathymetry which is available only with multibeam technology. The continental shelf and upper slope was surveyed between depths of ~30 and 850 m within five survey blocks (Figs. 3.1 and 5.1) using a 100 kHz Reson Seabat 8111 ER multibeam echosounder (cf. Ramsay and Miller 2006). These data

resolve vertically to within 30 cm, with the final sounding data output as a 10 m matrix. The survey area comprised five regions, identified here as the Leven, Leadsman, Diepgat, Sodwana and Mabibi Blocks (Fig. 3.1 and 5.1). Six large canyons were surveyed in the study area: the Leven Canyon (Leven Block); Leadsman South and Leadsman North Canyons (Leadsman Block); Diepgat Canyon (Diepgat Block); and Wright and White Sands Canyons (Sodwana Block), as well as a number of smaller canyons.

The quantitative analysis presented here follows the statistical characterization techniques developed by Goff (2001). From a stochastic viewpoint, canyon systems are considered as ensembles, rather than discrete morphological features. As such, canyons are included within a bulk assemblage of features which comprise the upper slope and continental shelf. A series of shelf-parallel profiles were initially extracted from the bathymetric datasets along a series of slope-parallel, low-order (degree four or less) polynomial curves fit to selected isobaths. Isobath intervals of 50 m were chosen. However, in areas of particular interest, these were increased to 25 m intervals. Each profile was then analyzed based on the parameters outlined by Goff (2001). The slope gradient for each profile depth is calculated from the downslope spacing between adjacent profiles, and the difference in mean depth between these profiles. The root mean square (RMS) relief is a measure of the departure from the mean depth, and is calculated by taking the square root of the profile variance. Profiles typically extend for 3-4 km along slope, and were extracted to water depths up to 550 m.

In addition, several slope-perpendicular cross sections were constructed for each canyon thalweg and the adjacent uneroded slope, in order to give a better visualization of the downslope progression in canyon incision compared to unaffected slope profiles.

6.3. Results

6.3.1. Morphologic observations

Throughout the study area the largest canyons terminate in amphitheatre-shaped indentations at, or just past, the shelf edge. Some canyons, such as Leven (Fig. 6.1), North and South Leadsman (Fig. 6.2) and Diepgat (Fig. 6.3) possess large arcuate slumps which extend into the outer shelf regions. Aside from Wright and White Sands Canyons of the Sodwana Block (Fig. 6.4), the largest canyons are relatively isolated, interspersed by smaller, shelf-indenting, subdued or slope-confined canyons. The Mabibi Block (Fig. 6.5) comprises smaller, narrow and straight shelf indenting features, some of which coalesce into apron shaped indentations.

In all survey blocks a contrasting morphology is observed, some canyons are sharply defined in their relief whereas others are more subdued (Figs. 6.1-6.5). In accordance with the interpretations of Pratson et al. (1994) for similarly contrasting canyon morphology on the New Jersey slope, this is identified these as evidence of recently active and moribund canyons, respectively.

6.3.2. Quantitative classification

The plot of slope gradient as a function of water depth in the five survey blocks (Fig. 6.6) reflects a consistent behaviour: (1) a sharp increase in average slope gradient denoting the shelf break, (2) a strong peak in gradient, with a maximum slope in the ~150-200 m depth range, corresponding to the shelf-edge wedge, and (3) a gradual decrease in gradient with depth below the shelf-edge wedge. The generally concave trend of decreasing gradient with depth is similar to that of the Virginia slope examined by Goff (2001); however, the Virginia slope does not exhibit a sharp peak in slope gradient at the upper slope, rather maintaining slopes of 7-8° from the shelf edge to ~750 m water depth before substantially declining. Peak slope gradients are highest in the Mabibi, Leadsman and Diepgat areas, reaching values of ~8-12°. The Sodwana Bay and Leven Blocks are more subdued, with peak gradients of ~5-7°. Apart from Mabibi, survey areas attain a minimum slope gradient of between 2° and 3° near depths of approx. 400 m. Diepgat has the shallowest slope gradient of 2° at a depth of 425 m.

Although the overall relief varies by as much as a factor of 4 among the five blocks, the plot of RMS relief (Fig. 6.7) indicates a general pattern (with minor exceptions) of decreasing relief with water depth below the shelf break. Peak RMS values are at depths slightly shallower than for the peak slope values, i.e. where the canyon heads indent into the shelf edge. The statistical analysis of these canyon systems is complemented visually by dip-direction bathymetric profiles (Fig. 6.8). Here, the convex nature of the continental slope and the oversteepened shelf edge are readily apparent in all survey blocks. Diepgat has the widest continental shelf of the study area, with Sodwana and Mabibi having the narrowest widths. These profiles also demonstrate the decreasing progression of canyon relief with water depth: the difference between thalweg and interfluve is largest at, or near the shelf edge and then decreases steadily with depth.

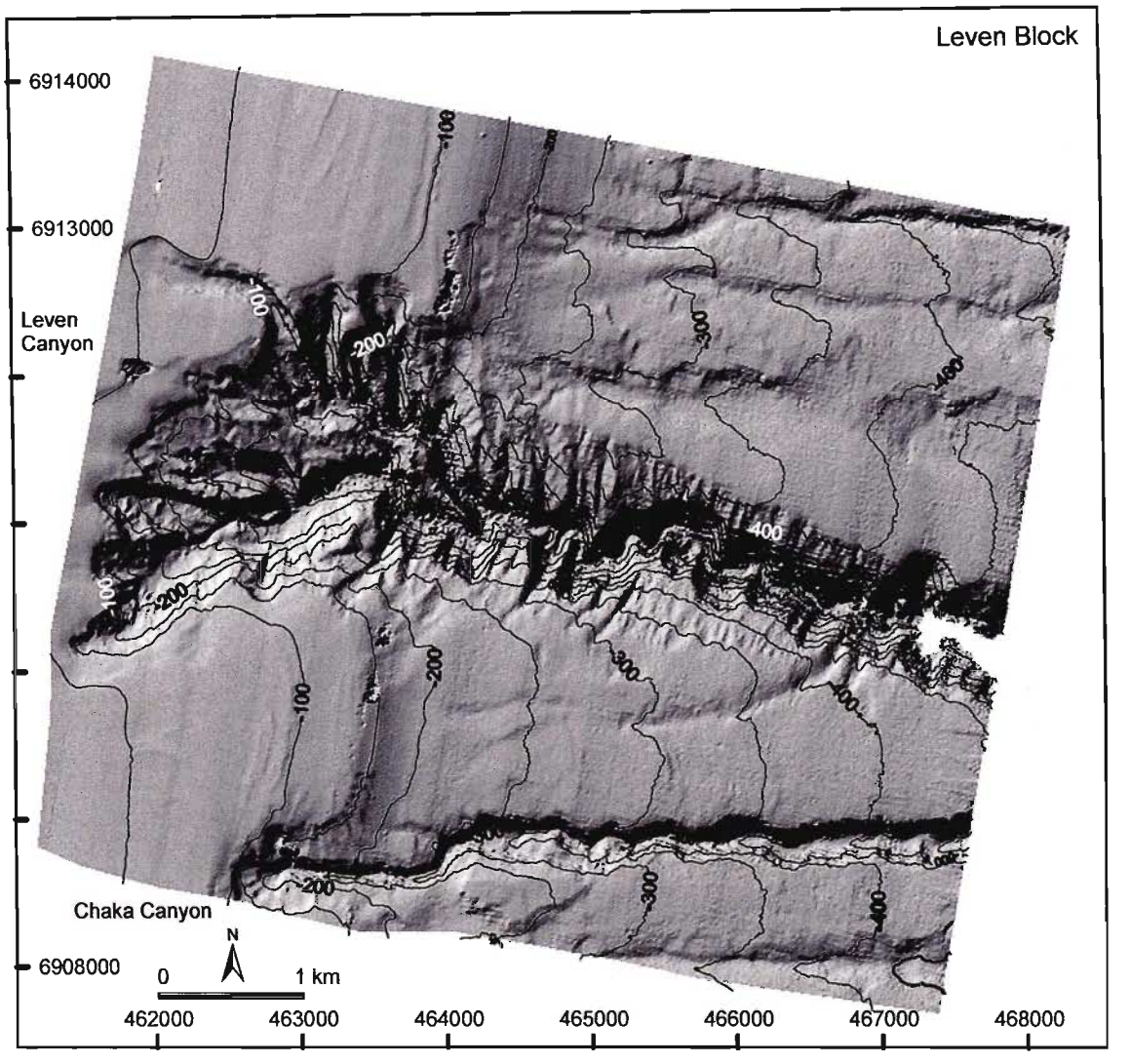

Figure 6.1. Bathymetric data in the Leven survey block, artificially illuminated from the northeast. Contours are in meters. Northing and easting coordinates are in meters, UTM projection Zone 36. Highly subdued, and thus presumably older rill-like canyon morphologies are present both north and south of the large, shelf-indenting Leven Canyon. Chaka Canyon, further to the south, also indents the shelf edge, but with a much smaller headwall area.

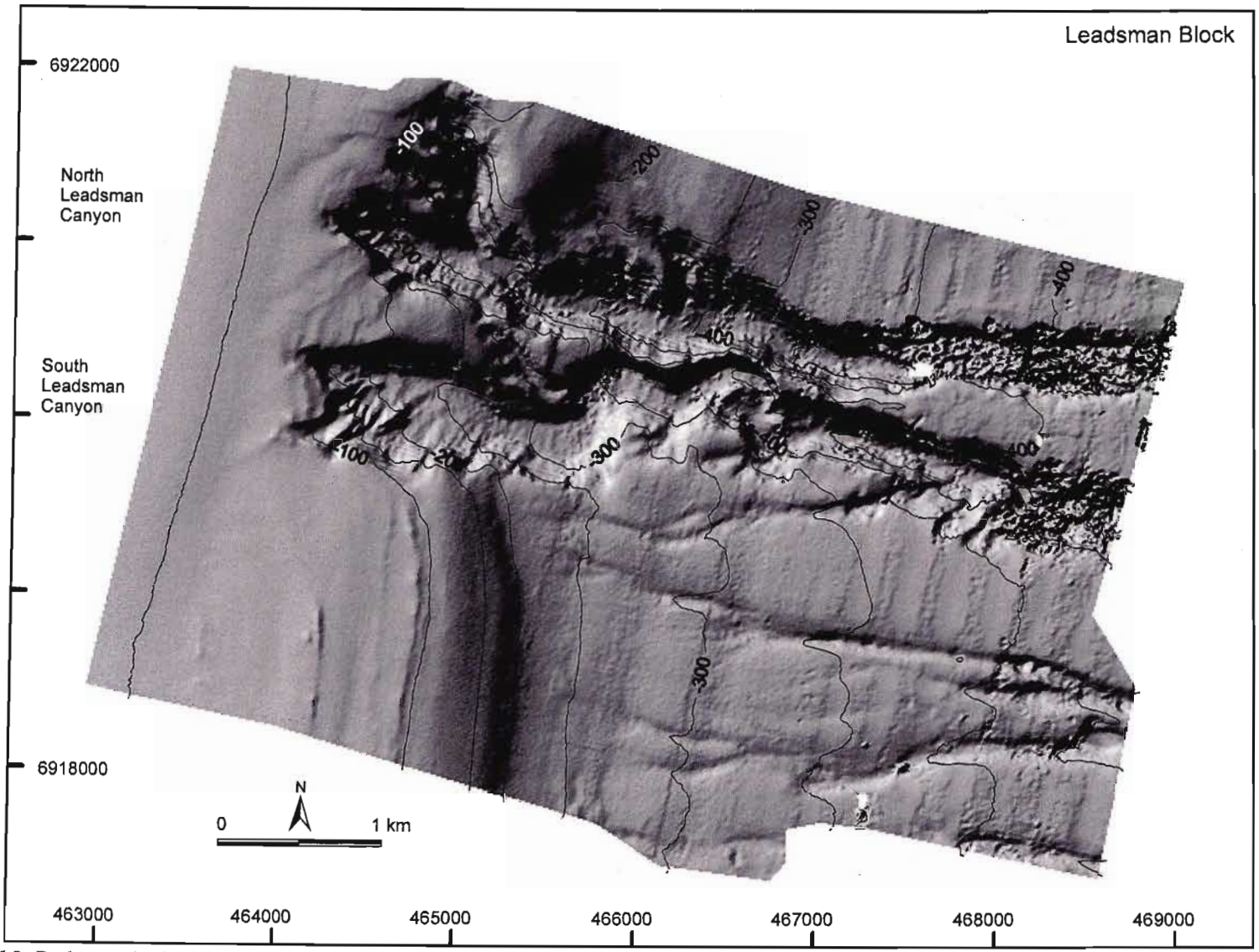

Figure 6.2. Bathymetric data from the Leadsman survey block, artificially illuminated from the northeast. Contours in meters. Northing and easting coordinates are in meters, UTM projection Zone 36. As with the Leven Block (Figure 4.1.2), subdued/older rill-like morphologies are seen in proximity to the larger North and South Leadsman Canyons.

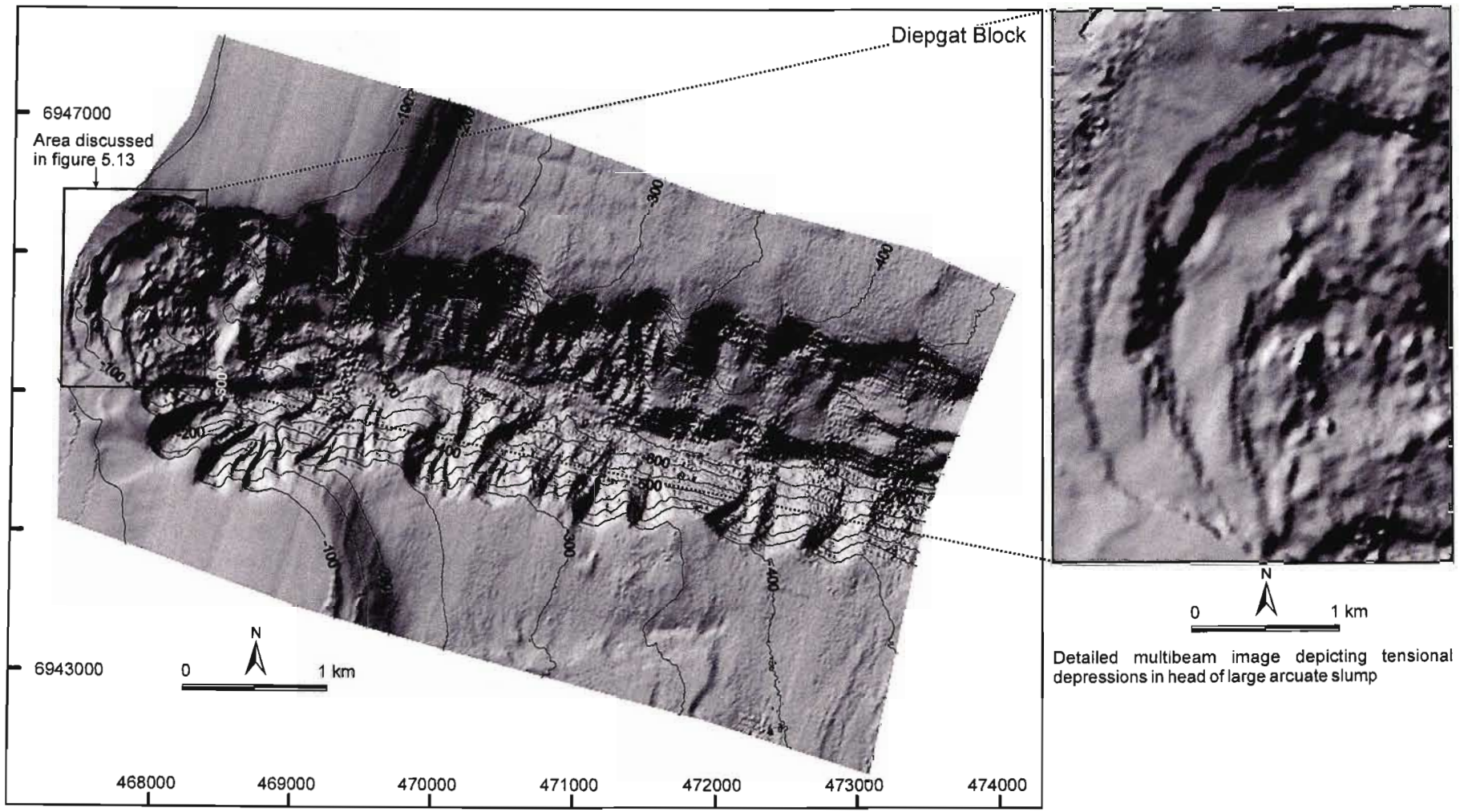

Figure 6.3. Bathymetric data from the Diepgat Block, artificially illuminated from the northeast. Contours in meters. Northing and easting coordinates are in meters, UTM projection Zone 36. Diepgat Canyon exhibits a deeply excavated thalweg and prominent semi-circular landslides in the head. These features are characteristic of headward growth in the upper canyon regions by retrogressive failure

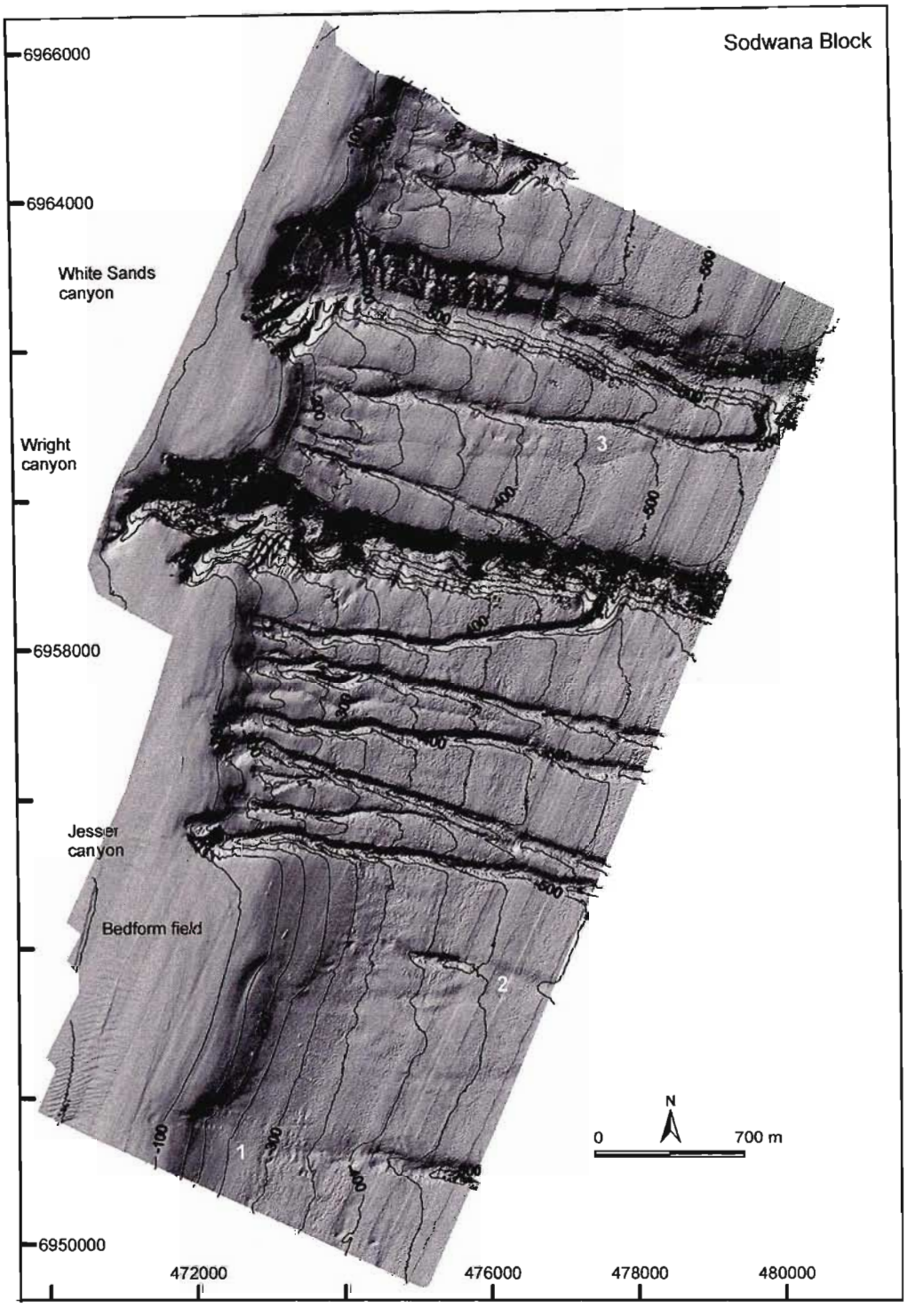

Figure 6.4. Bathymetric data from the Sodwana Bay Block, artificially illuminated from the northeast. Contours in meters. Northing and easting coordinates are in meters, UTM projection Zone 36. Two large shelf indenting canyons are present (White Sands and Wright Canyons), with smaller shelf indenting canyons occupying to the south. As with the Leven and Leadsman Blocks (Figures 2 and 3), subdued-relief rill-like features are present (denoted by white numerals 1-3). The southernmost of these (1) appears to be almost completely filled by sediment in the middle portions . Seismic data (see chapter 5) reveal this feature to be underlain by an incised valley feature, also discussed in chapter 4, Fig. 4.7.

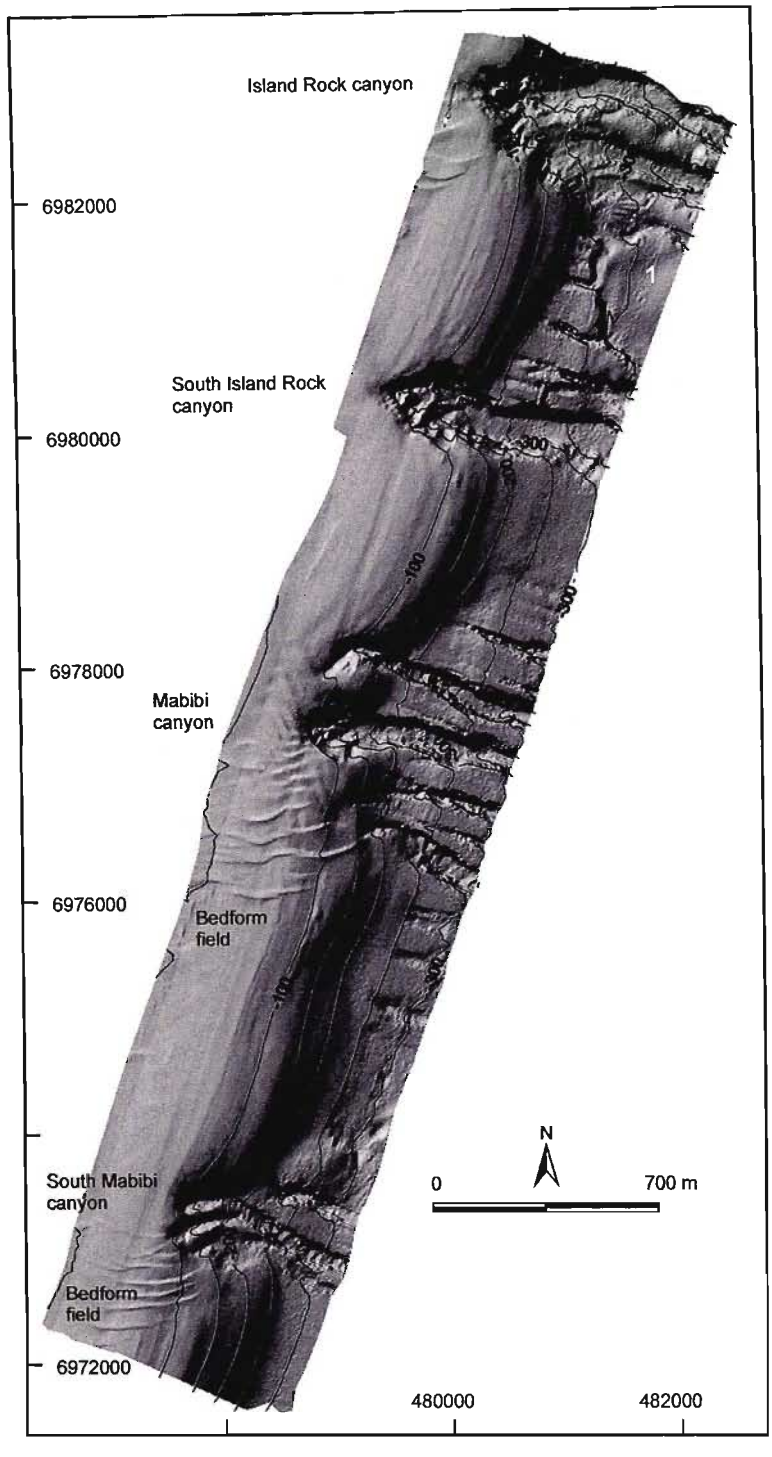

Figure 6.5. Bathymetric data from the Mabibi Block, artificially illuminated from the northeast. Contours in meters. Northing and easting coordinates are in meters, UTM projection Zone 36. Five shelf-indenting canyons are mapped, many with semi-circular collapse morphologies at their heads, along with numerous smaller canyons that head below ~200 m water depth. In the northern part of the survey area, what appears to be the headwall (denoted by 1) of a large slide which removed the lower portions of at least two small canyons is mapped.

6.4. Discussion

With the possible exception of Wright Canyon (Fig. 6.3), none of the canyons mapped are morphologically similar to the mature, shelf-breaching canyons characterized by Farre et al. (1983) on the US Atlantic margin. Rather than terminating in amphitheatre-shaped heads, shelf breaching canyons extend landwards across the shelf in a narrowing valley. Wright Canyon does exhibit a small narrowing valley protruding landwards from a semi-circular shelf indentation, and may thus be indicative of evolving towards a shelf-breaching system. Its thalweg exhibits a pronounced sinuosity, which was cited by Farre et al. (1983) as evidence of maturity. The remaining shelf-indenting canyons appear to conform to the "immature" phase described by Farre et al. (1983), with amphitheatre-shaped heads and generally straight thalwegs. Some of these channels show evidence of retrogressive failure, semi-circular collapse structures occurring most notably in the Diepgat (Fig. 6.3) and, to a lesser extent, Mabibi Block canyons (Fig. 6.5). Farre et al. (1983) and Pratson and Coakley (1996) suggest these as the primary mechanisms of youthful canyon formation. Unpublished seismic data discussed by Shaw (1998) indicate that these features are the result of large retrogressive slumping on the outer continental shelf, also confirmed by seismic investigations of this study (chapter 5). In the case of Diepgat, slope-parallel seismic profiles reveal preserved glide-plain scars of buried landslides within the canyon walls (Shaw, 1998), suggesting that processes of canyon growth must have been active prior to a stage of burial, followed by later canyon re-excavation.

6.4.1. Dominance of upslope processes

The five areas presented here exhibit similar trends in slope gradient and relief with increasing depth, despite variation in the size and depth of incision of the various canyons encountered. The gradient profiles (Fig. 6.6) indicate a concave shape relative to the continental slope, similarly to Goff's (2001) observations for the Virginia slope. Mitchell (2005) identifies concave gradients as evidence of downslope eroding processes such as turbidity flows. However, the decreasing canyon relief with depth observed in this region (Fig. 6.7) is the reverse of the trend for the Virginia canyons. Rather it exhibits strong similarities to the New Jersey canyons, which are inferred by Goff (2001) to be formed primarily by "upslope" (e.g. retrograde failures, sapping) processes.

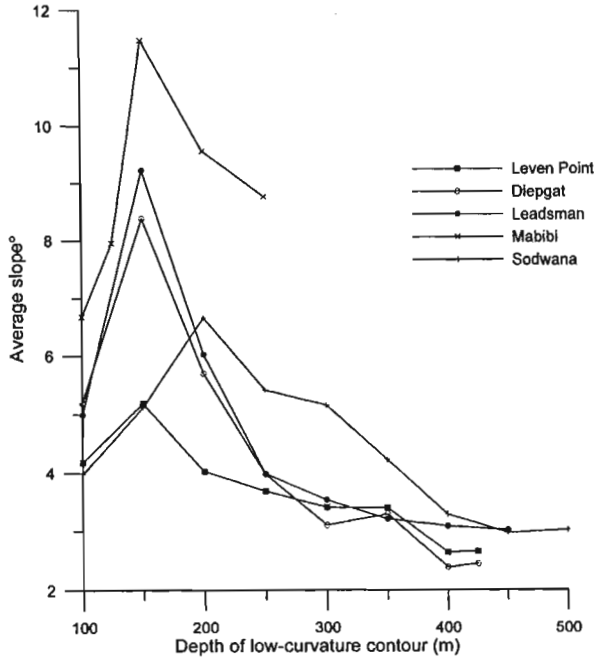

Figure 6.6. Average downslope gradient derived from slope parallel, low curvature bathymetric profiles for the five survey blocks, plotted versus profile depth. Peaks correspond to steepening of the Late Pliocene shelf-edge wedge

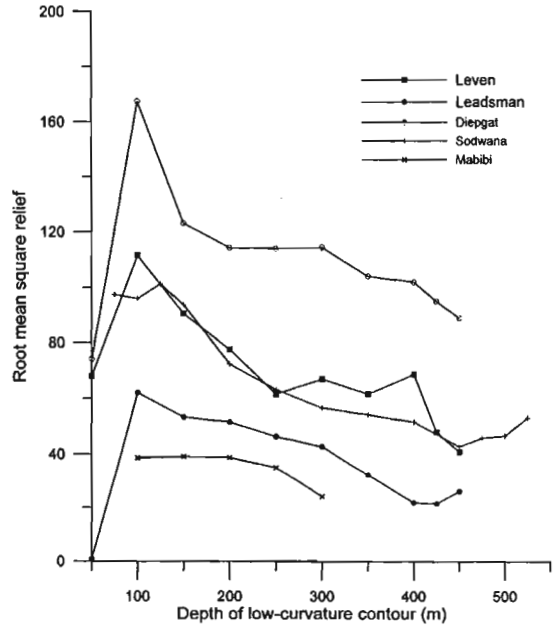

Figure 6.7. Root Mean Square relief values, derived from slope parallel, low-curvature bathymetric profiles for the five survey blocks plotted versus profile depth. RMS values typically decrease downslope of the shelf-edge wedge (of approx. 100-150 m depth)

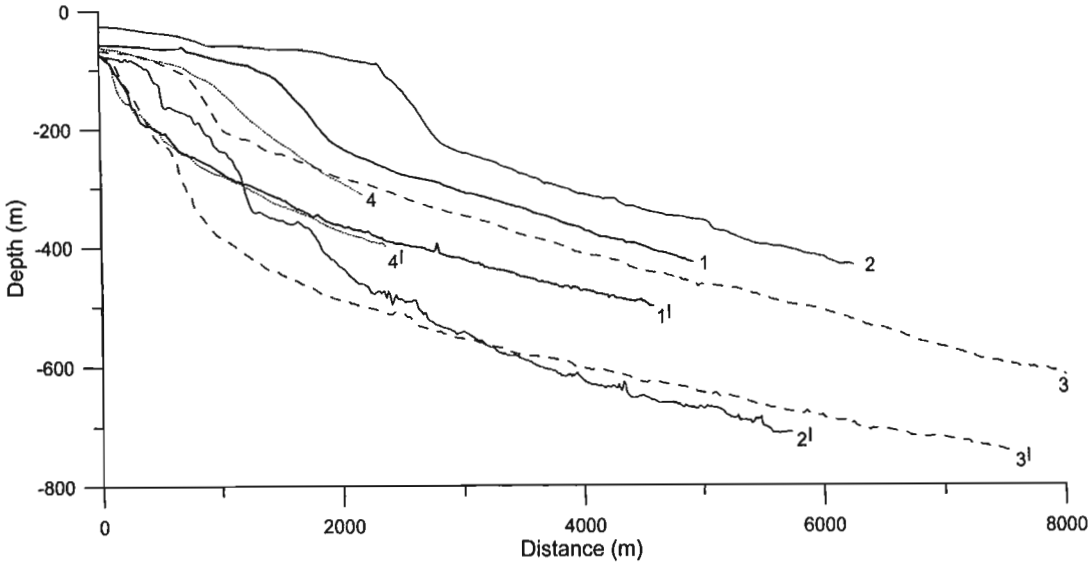

Figure 6.8. Representative dip profiles for canyon thalwegs (*primed numbers*) and adjacent, uneroded slopes (*unprimed numbers*) for South Leadsman (*1*), Diepgat (*2*), White Sands (*3*) and South Island Rock Canyons (*4*). The upper slope is steepest at ~150 m depth, corresponding to the shelf-edge wedge. These shelf-indenting canyons have maximum relief (seen here as the difference between the two profiles) typically at, or just landwards of the shelf edge

Goff (2001) also raised the possibility that the outcropping of more resistant strata on the lower New Jersey slope could be inhibiting erosion, but this study's observations are confined to the upper slope, and borehole data of Du Toit and Leith (1974) as well as seismic studies (cf. Sydow 1988; Shaw 1998, chapter 3 this study) suggest that the KwaZulu-Natal canyons have largely eroded into uniform Late Cretaceous mudstones, siltstones and sandstones of greater than 1 km in thickness. Additional similarities between the KwaZulu Natal and New Jersey slope-canyon systems include the shared presence of inter-canyon rills, interspersed with larger shelf-indenting canyons, the amphitheatre-shaped heads of the larger canyons, and the presence of multiple generations of canyon formation.

Neither the New Jersey nor Virginia continental slopes of the eastern United States exhibit the characteristic upper-slope gradient peak observed in slope gradient profiles, which is created by a preserved Late Pliocene outer shelf wedge which is only partly dissected by the canyons. This part of the upper continental slope may be oversteepened and may thus represent a potential source of retrogressive failure, as envisioned by the modelling work of Pratson and Coakley (1996). Additional differences are likewise notable. These include (1) the relative isolation of the northern KwaZulu-Natal canyons from each other, compared to the densely eroded nature of the New Jersey margin, and (2) the absence of strongly shelf-breaching canyons, such as the Hudson Canyon, on

the KwaZulu-Natal shelf. Of the largest canyons in the study area, only Wright Canyon exhibits the beginnings of a landward-narrowing valley (Fig. 6.4), characteristic of shelf breaching canyons (Farre et al. 1983).

To explain this mix of morphological similarities and differences, the KwaZulu-Natal canyon systems are considered essentially similar to the New Jersey canyons in their upslope formative processes, but are in a far more youthful stage of evolution, either because they are younger, or because the canyon-forming processes have not been as active as on the New Jersey margin. The morphology of these canyons is strikingly similar to that predicted by the numerical model of Pratson and Coakley (1996), even more so than the New Jersey slope canyons which formed the basis for this model. Their model hypothesizes that preferential sedimentation on the upper slope leads to oversteepening. As a result, retrogressive failures develop, which work upslope and eventually broaden into amphitheatre-shaped heads at the shelf edge. Failures also lead to turbidity flows, and thus a combination of upslope- and downslope-forming processes. The Pratson and Coakley (1996) modelling effort was limited in the number of canyons considered, and the time span of the run, and so never reached a point where the resulting synthetic morphology was as dissected by canyons as was the New Jersey slope. The greater extent of retrograde failure on the New Jersey shelf has most likely substantially graded the upper slope there, and is the principal reason that the slope-gradient profiles are differ substantially between the two regions.

As noted above, the Virginia canyon systems differ from the New Jersey and KwaZulu-Natal canyon systems primarily in that the Virginia canyons increase, rather than decrease in relief and breadth down-slope. Gradient analysis by Mitchell (2005) suggests that the canyons of the Virginia slope have been eroded by many small sedimentary flows, analogous to that of tributary flows in a subaerial fluvial setting of which the frequency increases with the up-stream/canyon-contributing area. The similarities in steepness of the upper slope of the Virginia and northern KwaZulu-Natal margins, and thus dissimilarity in canyon morphology suggest that, although steep, the KwaZulu-Natal slope is not oversteepened to the extent that slope overburdening is the sole driving force behind headward canyon growth. Fluid sapping in the mid- to outer shelf may be partly responsible in part for the formation of a headward eroding headless canyon system (Robb, 1984; Orange and Breen, 1992; Orange et al., 1994), which might emulate the predicted headward pattern in the Pratson and Coakley (1996) model. Diver (P.J. Ramsay, personal communication 2004) and submersible observations, in addition to geohydrological studies (Meyer et al., 2001), indicate that artesian conditions do exist in the heads of some of the canyons of northern KwaZulu-Natal.

However the extent to which artesian conditions on the shelf may influence the geomorphology of this area is unclear. Alternatively, the KwaZulu-Natal upper slope may be oversteepened if the sediments of the outer shelf wedge are more readily mobilized than those sediments of the upper Virginia slope, in which case the Pratson and Coakley (1996) model would be fully applicable for this region.

6.4.2. Downslope capture of canyons

Three generations of canyon cutting are evident in figure 6.9. The shelf-indenting White Sands Canyon, for example, is a sharply-defined feature, and is therefore inferred to be of the most recent generation (third-generation). It truncates a canyon with a more subdued-morphology canyon just to its south (second-generation), which in turn truncates an even more subdued canyon to its south (first-generation). Slumping is noted at the base of the second-generation canyon, near where it enters the White Sands Canyon (Figs. 6.4 and 6.9). This is the result of entrenchment of the third-generation canyon thalweg, undercutting the fill of the second-generation.

In explaining the contrasting morphology of recently active and moribund canyons, Pratson et al. (1994) and Pratson and Coakley (1996) describe the evolution of submarine canyons as resulting from the exploitation of the downslope reaches of older buried or defunct canyons by downslope-eroding sediment flows. The prevalence of multiple generations of canyon incision throughout the study area, particularly in the White Sands Canyon (Fig. 6.4) supports their hypothesis. As envisioned by Pratson et al. (1994), each subsequent canyon generation has shared the downslope reaches of a common bathymetric low, and then diverged towards the shelf break where upper-slope sedimentation has reduced the constraining effect of older canyon incision. The first-generation canyon is then sheltered from the prevailing sediment input by the Agulhas Current on the shelf by the larger second-generation canyon, thus precluding the further growth or re-establishment of the older canyon by sediment starvation. It appears that the more subdued canyons occupying the lee side of each larger second-generation or third-generation slope-indenting canyon have ceased eroding towards the shelf break as a result of this up-current sediment capture.

The straight, narrow, slope-confined canyons with no discernible retrogressive failures present throughout the study area are analogous to the slope rills of Pratson and Coakley (1996). Data presented in chapters 4 and 5 indicate several of these are underlain by older canyon systems.

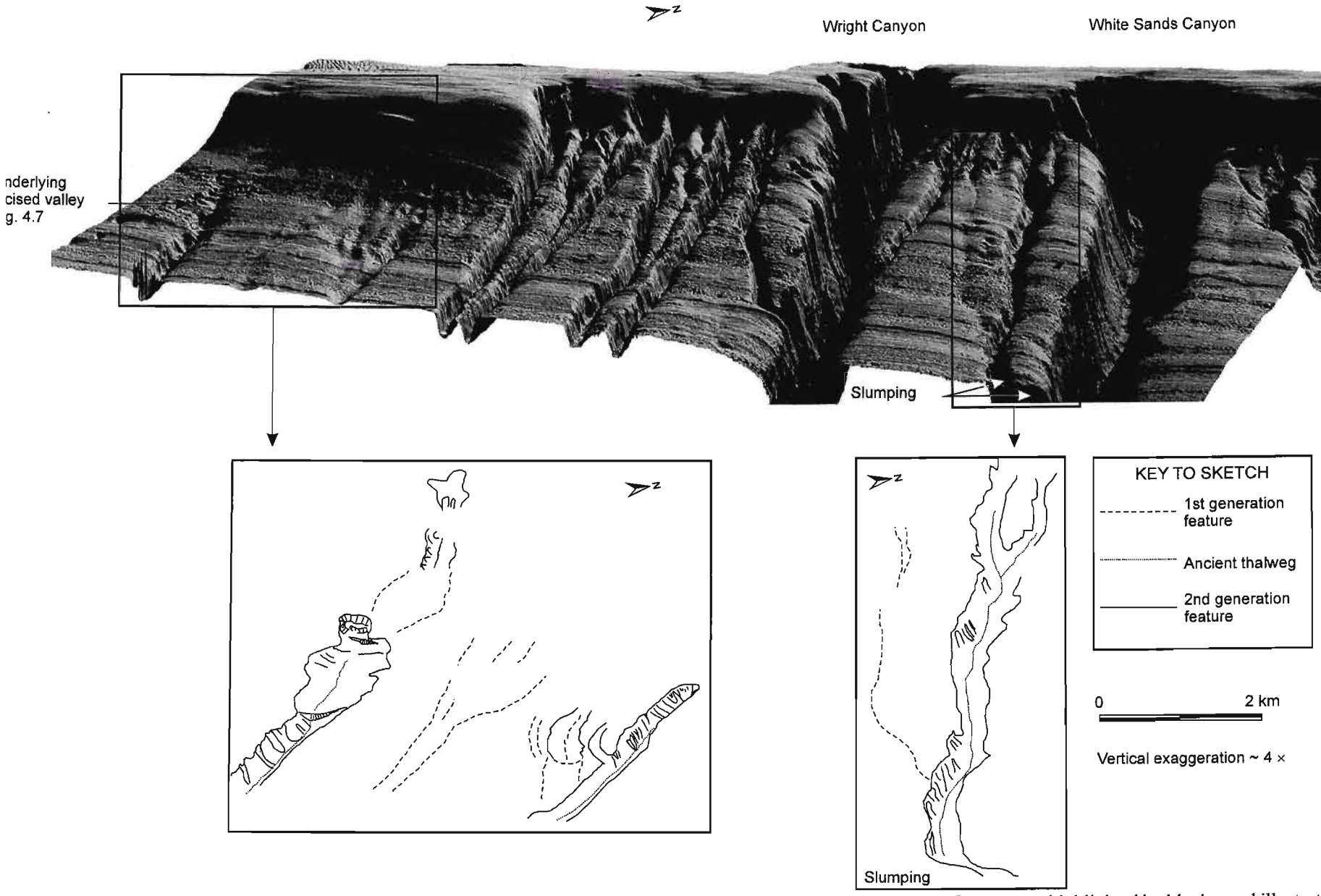

Figure 6.9. Three-dimensional view (*top*) of the Sodwana Bay survey block. The older-generation rill-like features are highlighted by blocks, and illustrated by interpretative sketch diagrams (*bottom*) depicting the different stages of erosion. See text for discussion. Note coast parallel lineations are data artefacts of the vessel track.

The presence of localized subdued downslope relief in some cases suggests that these features may be older buried systems that have not been re-activated by further exploitative sediment flows that would have been constrained to these topographic lows.

6.4.3. Recent quiescence

Prevalent notching within the canyon heads of the northern KwaZulu-Natal canyons associated with the previous lowstand at ~18,000 years BP (Green and Uken 2005, chapter 5) suggests that head slumping, and the consequent headward growth of these canyons, has been inactive since at least this time. The lack of fluvial sedimentary inputs, in conjunction with the denudation of slope sediments by the Agulhas Current core, has resulted in the sediment starvation of the shelf and upper slope (Cooper 1994; Ramsay 1996). This starvation is envisioned as a major limiting factor in the initiation of further upslope erosion by retrogressive failure, and downslope erosion by turbidity flows. Quiescent conditions during high sea-level stands such as that currently being experienced, and the prevailing sediment starvation have resulted in the preservation of both the shelf-edge wedge and the canyon morphology before more complex processes of burial and erosion would take place.

CHAPTER 7

Submarine landsliding and canyon growth mechanisms

Green, A.N., Uken., R., 2008. Submarine landsliding and canyon evolution for the northern KwaZulu-Natal continental shelf, South Africa, SW Indian Ocean. Mar. Geol. 254, 152-170.

7.1. Introduction

Submarine landslides are key features in the exchange of sediment between the continental shelf and abyssal plain and the ensuing geomorphological evolution of continental margins. Where submarine canyons erode the continental slope and shelf, landsliding along the walls of these features is common. These result in the headward incision and lateral extension of the canyon walls into the upper slope and shelf (Farre et al., 1983; Pratson et al., 1994; Pratson and Coakley, 1996). Landsliding within submarine canyons has been documented in various tectonic and physiographic settings (Dingle and Robson, 1985; Hampton et al., 1996; McAdoo et al., 2000; Greene et al., 2002; Arzola et al., 2008), but owing to their small size relative to non-canyon specific landslides and the inherent difficulties in data collection in these challenging environments, relatively little is known concerning landslide geomorphology within submarine canyons.

This chapter describes the morphometric and geomorphological analysis of 117 landslides found within 23 canyons of varying size and degree of incision along the Northern KwaZulu-Natal continental slope (Fig. 7.1). Multibeam bathymetric data are used to map each landslide locality and are interpreted to provide initial insights into pre-conditioning factors and potential trigger mechanisms for each. By isolating commonalities and differences in intra-canyon landslide morphology, observations of the processes responsible for the various landslides can be made. This aids in the establishment of simple hypotheses regarding landslide rheology and triggering mechanisms which can be validated in later, more focussed sedimentological, seismic and geotechnical surveys. Ultimately, this yields a relatively quick insight into the sub-processes that interact to cause submarine canyon initiation and growth, and present day canyon geomorphology on the KwaZulu-Natal continental margin.

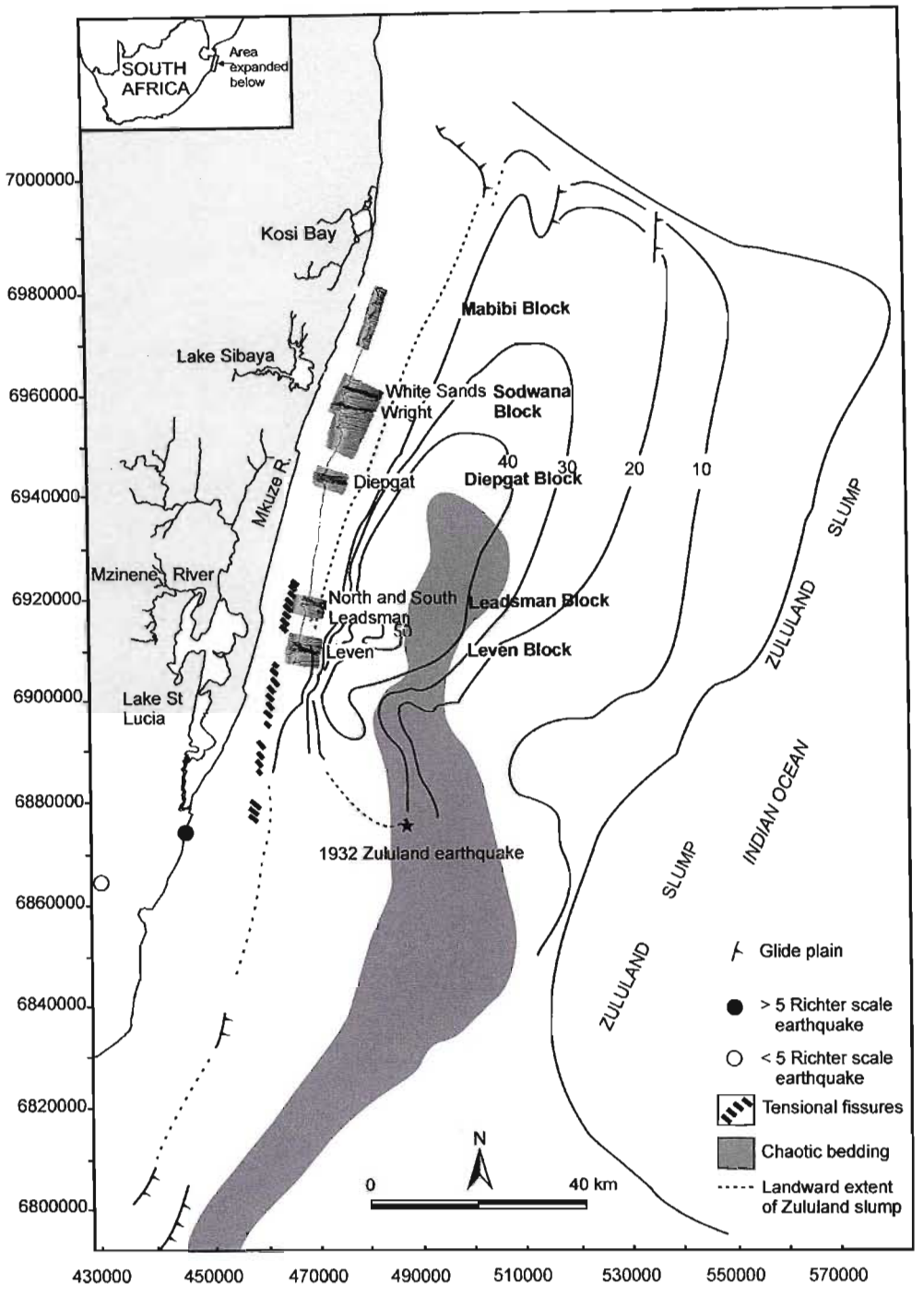

Figure 7.1. Location map of the study area, detailing the multibeam survey blocks and major submarine canyons, superimposed with the 125 m isobath corresponding to the Last Glacial Maximum shoreline. Northing and easting co-ordinates in metres, Universal Trans-Mercator (UTM) projection. Note the presence of two large freshwater coastal waterbodies fringing the study area, the southernmost is Lake St Lucia, followed to the north by Lake Sibaya. The Zululand Slump is depicted as isopleths of thickness in two-way travel time. The 1932 Zululand earthquake is the highest magnitude earthquake experienced in recent times (Hartnady, 2002).

7.1.1. Regional geomorphological setting

The northern KwaZulu-Natal continental slope and shelf (Fig. 7.1) is characterised by a set of incised submarine canyons of varying size and depth. These are confined to five distinct blocks, stretching from Leven Point in the south, to Mabibi, in the north (Fig. 7. 1). In light of the scale of true shelf breaching canyons such as the Hudson Canyon on the Atlantic coast of USA (Twichell and Roberts, 1982; Farre et al., 1983), even the largest canyons encountered here may only be considered as shelf indenting. Shelf indenting canyons typically terminate in amphitheatre-shaped heads, whereas shelf breaching canyons extend landwards across the shelf in a landwards narrowing valley which may be associated with an adjacent incised valley onshore (Farre et al., 1983). The shelf break in the study area occurs at approximately 120 m water depth, the shelf divided into an inner- (depths > 15m), mid-(depths between 15m and 65 m) and an outer shelf zone (Ramsay, 1994). Six prominent shelf indenting canyons exist in the study area (Fig. 7.1). These are Leven (Leven Block), North and South Leadsman (Leadsman Block), Diepgat, Wright and White Sands (Sodwana Block) Canyons (Figs. 7.2-7.5). Smaller shelf indenting canyons occur in the Mabibi area. The largest canyons of the various blocks are relatively isolated and interspersed with narrow, shelf indenting or upper-slope confined canyons (Fig. 7.6).

Large submarine landslides along the South African coastline have been recognised by other authors (e.g. Emery et al., 1975; Dingle, 1980; Dingle and Robson, 1985). Dingle (1977) described one of the largest recorded landslides, the Agulhas Slump, having shifted 20 000 km^3 of sediment seaward off the southern African margin. Martin (1984) recorded an even larger slump off the northern KwaZulu-Natal margin, of ~34 000 km^2 in aerial extent. Goodlad (1986) and Sydow (1988) both recorded similar, though much smaller, slumps occurring on the unconfined shelf for that area. Sydow (1988), Ramsay (1994; 1996) and Shaw (1998) in turn described landsliding confined to submarine canyons for the northern KwaZulu-Natal margin.

The earliest reference to the submarine canyons of the area by Bang (1968), postulates that these features formed by several means, the most important being the undermining of the canyon walls by fluid sapping and the subsequent triggering of landslides associated with canyon development. Seismic profiling through Chaka Canyon (Leven Block), a smaller canyon which indents the shelf, revealed that rotational slumping had affected the entire profile of the canyon (Fig. 7.7).

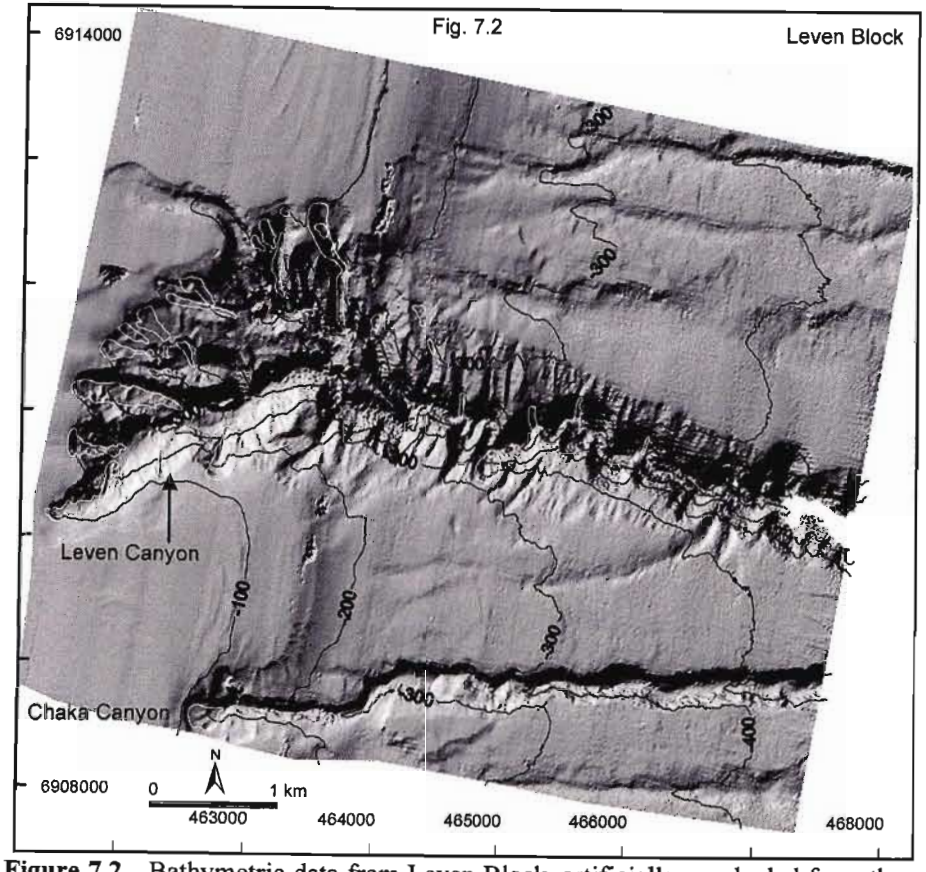

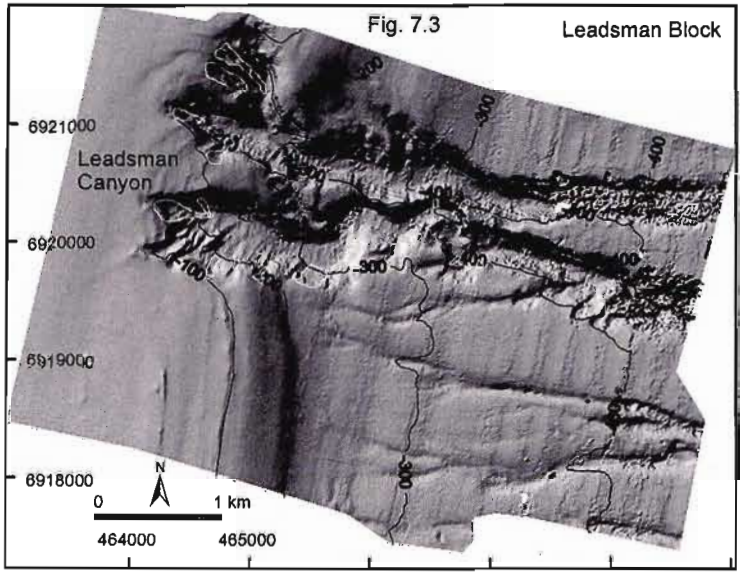

Figure 7.2. Bathymetric data from Leven Block, artificially sunshaded from the northeast. Contour interval is 100 m, northing and easting co-ordinates in metres, UTM projection zone. Leven Canyon occurs as the larger shelf indenting canyon, Chaka Canyon is the smaller shelf indenting feature in the southern most portion of the figure. Identifiable landslides are depicted with white borders. Note the higher number of landslides in Leven Canyon, as compared to the narrow Chaka Canyon with a single identifiable retrogressive failure at the canyon head. **Figure 7.3.** Bathymetric data from Leadsman Block, artificially sunshaded from the northeast. Contour interval is 100 m, northing and easting co-ordinates in metres, UTM projection zone. North and South Leadsman Canyon appear to be a bifurcated head complex of a single canyon which coalesces in the mid slope section. Note the presence of slope confined rills in the southern portion of the block.

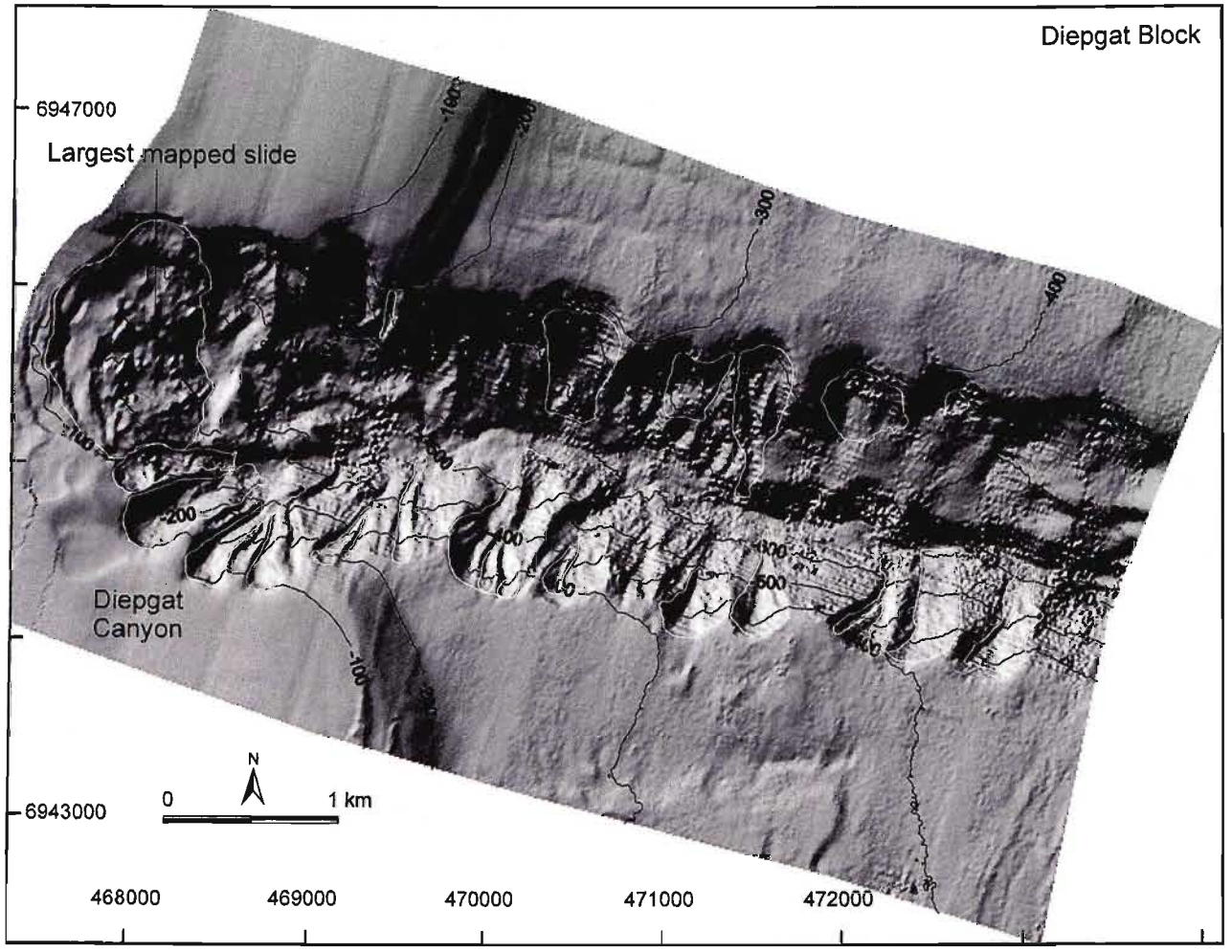

Figure 7.4. Bathymetric data from Diepgat Block, artificially sunshaded from the northeast. Contour interval is 100 m, northing and easting co-ordinates in metres, UTM projection zone. Diepgat Canyon exhibits a deeply excavated thalweg and prominent semi-circular collapse structures in the head, one of which comprises the largest landslide mapped in this study. Note the strong axis perpendicular alignment of landslides along the canyon margins.

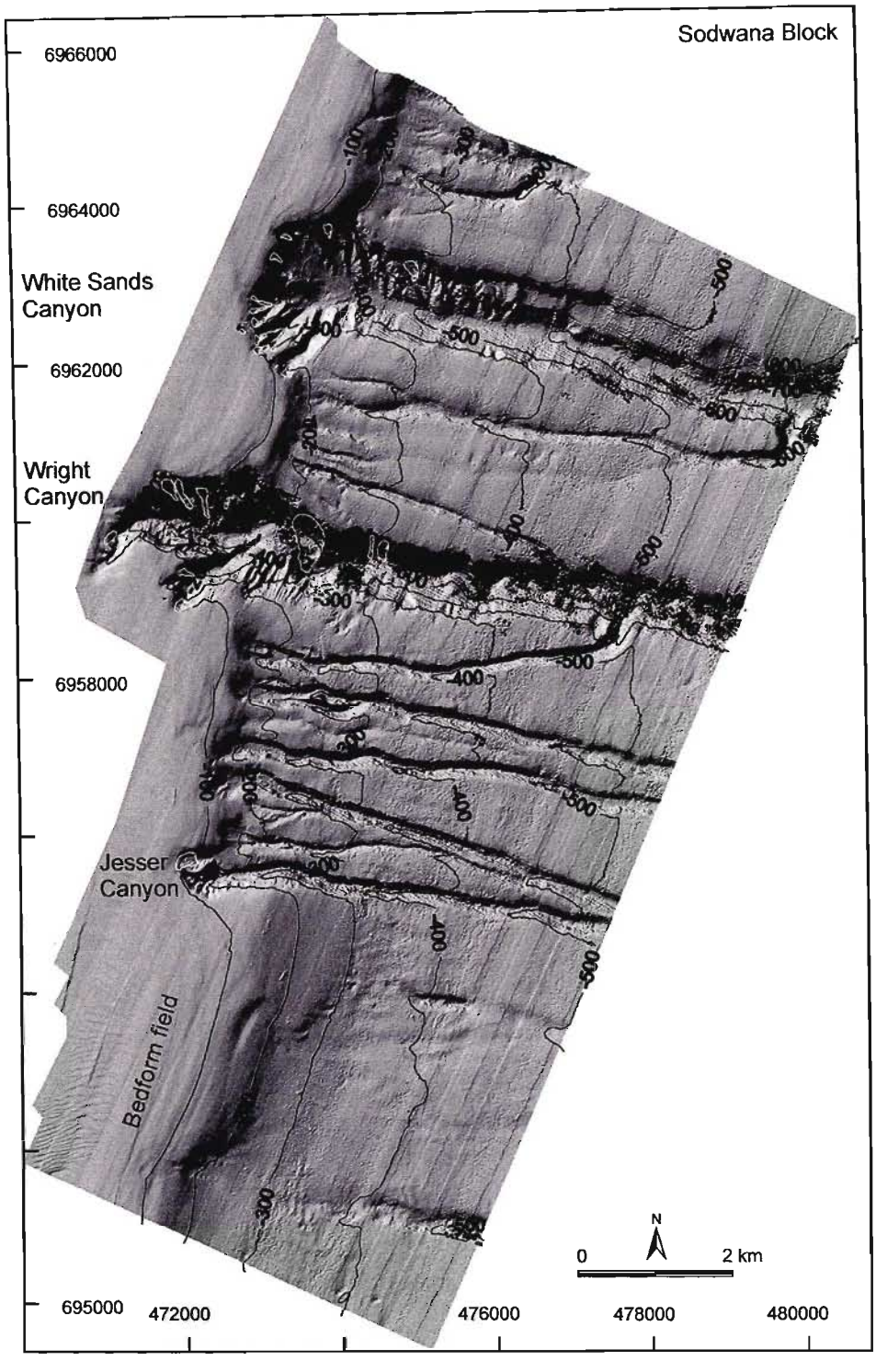

Figure 7.5. Bathymetric data from Sodwana Block, artificially sunshaded from the northeast. Contour interval is 100 m, northing and easting co-ordinates in metres, UTM projection zone. Two large shelf indenting canyons are evident (Wright and White Sands Canyons), and are interspersed with smaller narrow, shelf indenting canyons and slope confined rills. Note the development of a prominent bedforms field in the southern portions of the block.

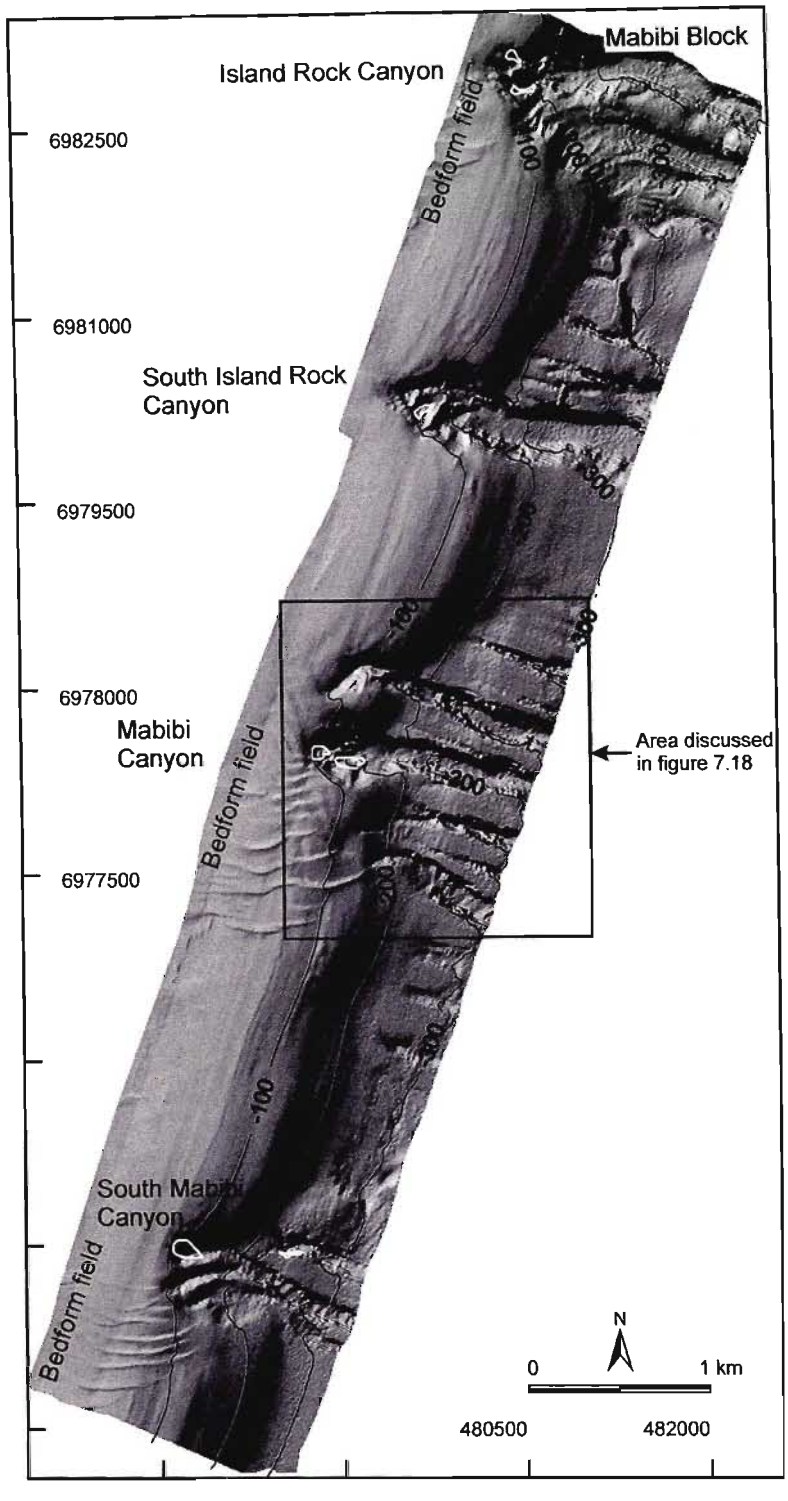

Figure 7.6. Bathymetric data from Mabibi Block, artificially sunshaded from the northeast. Contour interval is 100 m, northing and easting co-ordinates in metres, UTM projection zone. The largest canyon of the Mabibi area (South Island Rock Canyon) occurs in the northernmost extent of the study area. Canyons of the Mabibi area are narrow features which are comparatively smaller and less shelf indenting than canyons of the other blocks studied. Note the well developed bedform fields on the comparatively wider continental shelf, compared to the blocks further south.

The valley was assumed to have propagated shorewards by retrogressive rotational slumping along the head scarp and side walls, inducing debris flows and channel turbidites which eroded previous slump fills within the thalweg (Sydow, 1988). Shaw (1998) recognised characteristic slump morphologies within submarine canyon walls from single channel seismic data. Slumping in Wright Canyon (Sodwana block) and Diepgat Canyon was described from the headwalls of the canyons and attributed to an increase in the sediment input to the rim of the canyon head. Shaw (1998) also recognised several buried landslides, occurring in semi-consolidated sediments of a speculative Miocene/Pliocene age that formed as a result of slope instability during the Late Tertiary. Ramsay (1994) recognised that larger landslides occurred on the southern walls of Wright and White Sands Canyons, based on observations from single beam echosounding.

7.1.2. Terminology

The nomenclature used in describing submarine mass movements is a complex one (Canals et al., 2004; Masson et al., 2006) with various terms used to describe submarine mass movements e.g. slumps, slides, debris flows etc. Each term implies a genetic relationship to some mass transport process (e.g. Tripsanas et al., 2008), which may be difficult to interpret based solely on the surficial characteristics of slope failure products resting on the sea floor. Slides and slumps are traditionally considered translational or rotational movements of material, bounded by distinct scarps with relief ranging from a few to several hundred metres (Coleman and Prior, 1988; Hünerbach and Masson, 2004). No distinction is made between the two and any slope failure, which has resulted in the preservation of the material as a coherent deposit, is considered a slide or *cohesive* slide.

Debris flows, which form by the plastic deformation of coherent slide blocks (Tripsanas et al., 2008) are considered as a form of *disintegrative* slope failure where the mass wasting deposit is still observed at the base of the failure, yet is no longer intact. *Fluidised* type failures, where there is no apparent deposit, yet an unmistakable scarp in the upper regions of the slope failure are considered as turbidity flows, the material either being derived from partial disintegration of a slide mass, or during transition from a debris flow via the erosion and entrainment of canyon floor sands (e.g. Piper et al., 1999). Boyd et al. (2008) provide an alternate view of shallow to deep water sediment transport, whereby active turbidity currents are not associated with landsliding, but rather the interaction between local hydrodynamic conditions and margin orientation which causes cascading over the shelf edge and gravity transport of sediments downslope.

7.2. Methods

Until now, landslide analysis along this section of shelf has been restricted to discrete cross sections through a single failure. With dense, high resolution multibeam data, slumps may be imaged in three dimensions and their geomorphology intensively studied. Multibeam bathymetric data, acquired for the African Coelacanth Ecosystem Programme (ACEP), is used to identify failures within the study area. These data form the first detailed swath bathymetric data set for the east coast of South Africa, and expose a number of undiscovered canyons and landslides. Data were acquired at 100 kHz using a Reson 8111 SeaBat system and covered 392 km^2 over depths ranging from 29 to 838 m, with a spatial resolution of ~1 m given navigational uncertainties. Acquisition was over a 150° swath with a beam separation of 1.5°. All data were tidally corrected using Admiralty (South African Navy) charts to Mean Sea Level (MSL) datum. Bathymetric data were binned at 5 m, the data thus capable of resolving discrete landslides greater than ~ 25 m^2. The vertical accuracy of the data is considered to be approximately 30 cm.

7.2.1. Slide determination and measurement

The bathymetric data were incorporated into the GIS software packages ER Mapper 6.1 and Surfer 7 and sunshaded digital terrain models (DTMs) for each survey block were created. These were used to identify landslide localities. Sunshading serves to illuminate bathymetric features such as head scarps, side walls and failed masses at the base of a slide. In order to ascertain slope angles of failed and unfailed sediments, a grid calculus was performed on the bathymetry and the slope angle extracted. These were subsequently gridded at 5 m resolution, and contoured to give an indication of the stability of the available sediment to the canyon margin.

Measurements of the head scarp height; runout length; gradient of failed slope (failure scar); gradient of the unfailed adjacent slope; gradient of runout slope; scar angle; failure scar area; and total failure area were made from the multibeam bathymetric data for each individual failure (Fig. 7.8). Where no failure deposit was encountered, the slide runout was considered to terminate where the side walls opened out into unconfined space, thus giving a minimum possible distance for the failure mass. Measurements were made from slices of the bathymetric data that were then used to create depth vs. absolute distance cross sectional data. Absolute distance in this case refers to cross sections that are not directionally specific along a principal axial plane, but instead are calculated on the basis of distance from start to finish.

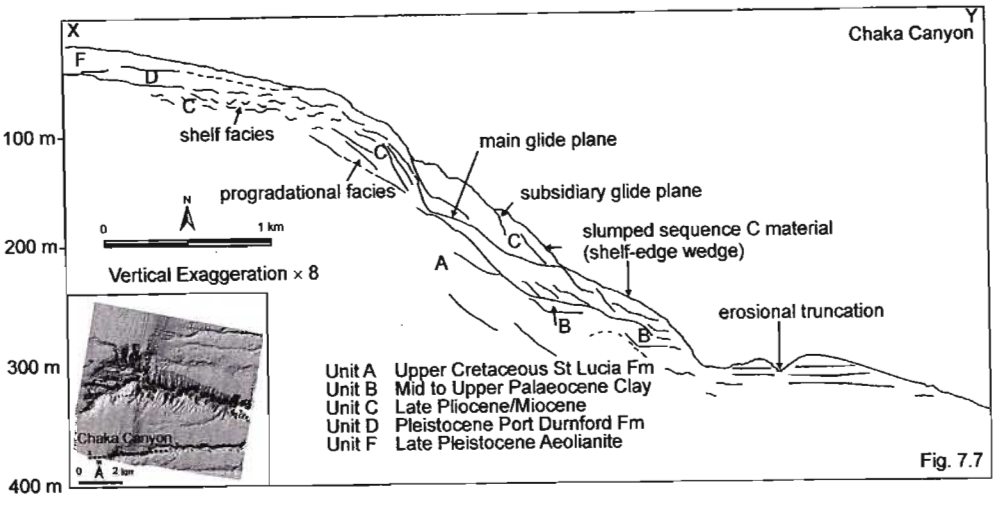

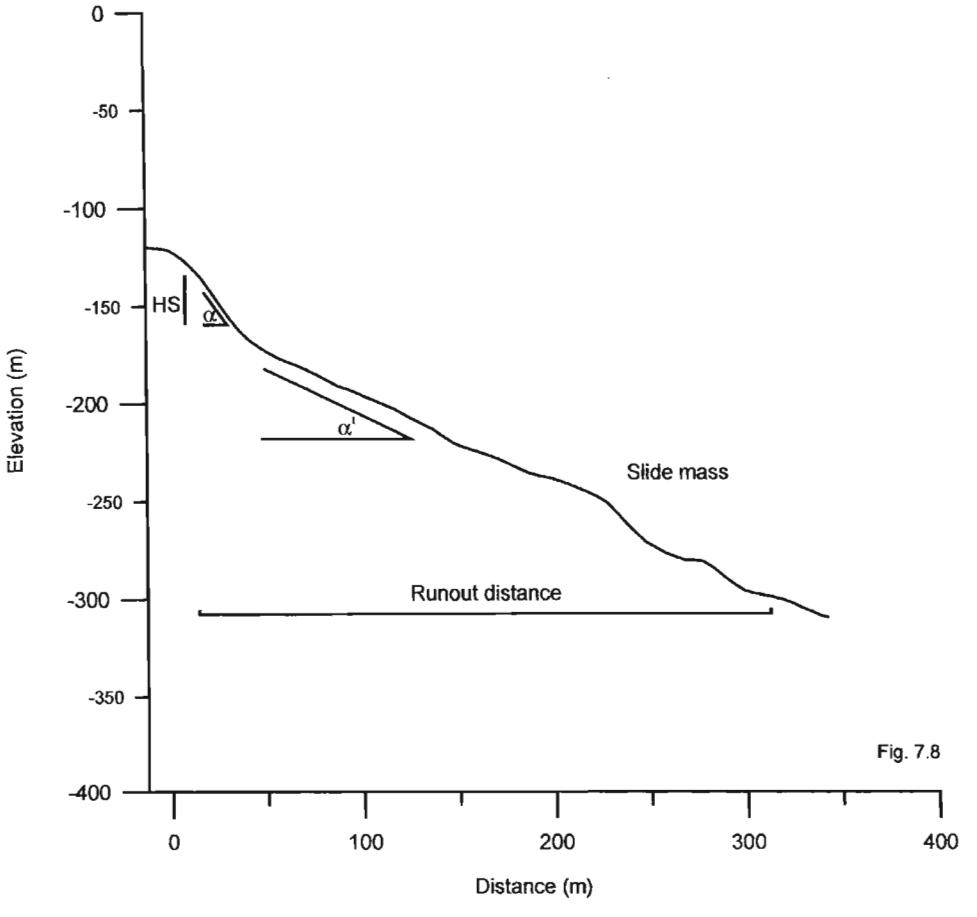

Figure 7.7. Interpreted line drawing of single channel sparker seismic reflection line through Chaka Canyon (after Sydow, 1988). Shoreward propagation of the canyon by retrogressive failure has resulted in a hummocky canyon profile, with previous slump fills subsequently excavated by debris flows and channel turbidites (Sydow, 1988). Note that slumping has not extended landwards of the shelf edge wedge. **Figure 7.8.** Measured features of landslides from this study, depicted on an idealised profile through a canyon margin landslide. HS = headscarp height; α = headscarp slope; α^1 = scar slope; runout distance = distance from headscarp to most distal point of failed mass accumulation.

Any bias that obliquity of the bathymetric slices would introduce to the study is thus eliminated. As a result of the natural variation across each landslide feature, several measurements were made from several adjacent cross sections in order to present a mean value of these features. As with McAdoo et al. (2000), less angular features such as slumps, or older more subdued failure expressions give rise to less prominent scarp features, the scarp height is thus measured as the steepest possible section from the slump scar. Unlike McAdoo et al. (2000) slope gradients are not measured from GIS constructed slope maps, but rather from slope cross sections made from the grid slices used in creating the bathymetric cross sections. Gradients were then digitised from a number of depth vs. gradient plots that overlie the bathymetric cross sections, in order to pick the appropriate corresponding gradients for slump scar, runout slope and headscarp slope. These values are presented as the mean value derived from several cross sections. Similarly, for the local unfailed adjacent slope, several cross sections were constructed and the mean value for unfailed adjacent slope acquired.

Landslide volume is calculated based on the thickness ($T = h \cos \alpha$, where h is the headscarp height, and α the scar slope angle). A basic wedge geometry is used where:

Slide volume $(V) = \frac{1}{2} (A)(T)$

A is the area derived from the sunshaded bathymetry GIS, corrected for dip aberration based on an average slope angle for the landslide feature.

Limitations to these methods exist. Firstly, by using bathymetric data without the aid of seismic reflection data, the results are biased towards more recent failures that have stronger topographic expressions. As such, features that may be older and lack the consequent bathymetric signature used in this methodology are ignored altogether. Secondly, it is unclear to which stratigraphic depth these failures extend, and the exact volumes of the failed mass accumulating at the base of each slide. This method is useful in that it allows a comparative view of certain "type" landslides that are occurring based on the various features described, and allows a preliminary interpretation of the mechanism (either rheological or mechanical) responsible for canyon enlargement and proliferation.

7.3. Results

7.3.1. Landslide location, depth, regional gradient

The majority of landslides from the study area occur in Leven (n = 30) and Diepgat Canyons (n = 27), with the other significant locations occurring in the White Sands (n = 14), Wright (n = 16) and Leadsman Canyons (n = 19) (Figs. 7.2-7.6). The Mabibi Block, despite having numerous small canyons, has significantly fewer landslides in comparison, with only six recognisable features being measurable based on this study's requisites for failure identification. The remainder of the landslides in the study area occur in the heads of smaller shelf indenting or slope confined canyons that reside between the larger shelf indenting canyons. These are typically narrow, shallow features with linear thalwegs and subdued downslope topography (Fig. 7.6). Canyons with heads that occur deeper than 120 meters below sea level (mbsl) have typically fewer than three failures per canyon, compared to no failures found in the small inter-canyon rills (Fig. 7.6). Studies by Green et al. (2007) indicate that the Mabibi shelf, despite having fewer failures, has the steepest average gradient of 6° before the shelf edge wedge, followed by Leadsman (5°), Diepgat (5°), Sodwana Bay (4°) and Leven Point (4°) respectively. Average gradients of the shelf edge and upper slope are highest at Mabibi (11.5°), proceeded by Leadsman (9°), Diepgat (8°), Sodwana (6.5°) and Leven (5°).

Landsliding occurs most frequently in the southern flanks of Diepgat, South Leadsman and White Sands Canyons compared to the northern flanks (Figs. 7.2-7.6). Conversely, landsliding is most prominent in the northern flanks of Wright, Leven and North Leadsman Canyons (Figs. 7.2-7.6). Landslides occur most commonly in the canyon heads of the study area, apart from Diepgat, where a series of semi-circular collapse structures, ~ 1.5 km across, dominate the upper portions and obscure any older failures (Fig. 7.4). The headscarps of landslides in the canyon heads occur parallel to sub-parallel to the canyon axis, whereas those along the canyon walls are orientated parallel to the thalweg. Failures in the lower portions of Leven Canyon occur at strongly sinuous meanders in the thalweg.

7.3.2. Landslide geomorphology

Landslides occur as cohesive slides with smaller runout distances compared to disintegrative slides (debris or turbiditic flows) where little or no failure rubble is discernible at the base of the failure. Several landslide associated morphologies are common (Fig. 7.9).

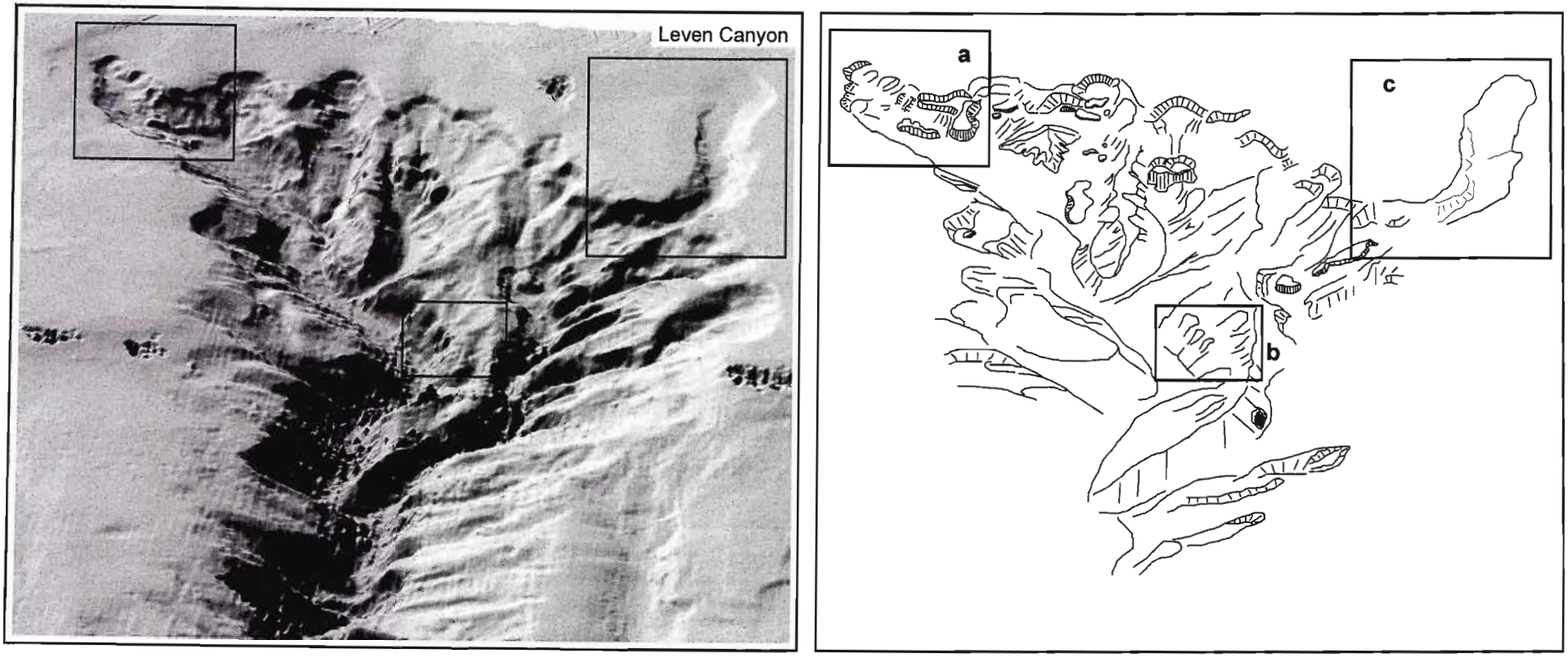

Figure 7.9. Three dimensional view and interpretative sketch of the head of Leven Canyon, exhibiting several landslide morphologies. View is from the south-south east, V.E ~ 2 ×. Inset **a** depicts an incised inner gorge at the base of a slide on the southern portion of Leven Canyon head. Inset **b** indicates a series of stranded hanging slides on a small interfluve. Inset **c** depicts a fluidised landslide extending onto the mid continental shelf. Note the sinuous morphology and lack of appreciable headscarp of this landslide.

These include: 1) incised inner gorges; 2) hanging or perched slides in the canyon headwalls; 3) terraced slides; and 4) benches in the slide material. These occur prominently in several slope failures of Diepgat, Leven, Wright and White Sands Canyons, with exceptions in Leadsman Canyon and the Mabibi canyons. Inner gorges form where the slide terminates close to the thalweg or is truncated by a gully or larger axis-oblique slide leaving a steeply cliffed section at the base of the failure deposit (c.f. Densmore et al., 1997; McAdoo et al., 2000). Several failures, particularly in Leven Canyon have sinuously channelled features, synonymous with fluidised slope failures (Figure 7.9, box c).

7.3.3. Landslide statistics

Tables 7.1a-f summarise the landslide morphometry from each individual survey block and presents the correlation coefficients for the various attributes. A statistical comparison is made of all landslides encountered in the study area (Table 7.1g), and the morphometric differences between cohesional and non-cohesional failures are also provided (Table 7.1h-i). These are referred to as cohesive and disintegrative slides respectively. Landslide area, volume, headscarp height, local unfailed slope and headscarp slope are presented as histograms for the various survey blocks (Figs. 7.10-7.14).

7.3.4. Area, volume, runout

The largest failures occur in Diepgat Canyon. The aerial extents of 13 of the 27 failures exceed 80 000m^2 (Fig. 7.10). The largest failure (so large as to not fit to the scale of figure 7.10) in Diepgat Canyon covers an area of sea floor 928 024 m^2 in extent. Leven Canyon and Wright Canyon are the only other canyons to possess failures exceeding 80 000 m^2, the largest failures disturbing 105 519 m^2, 90 577m^2 (Leven) and 199 129 m^2 (Wright) of sea floor respectively (Fig. 7.10). The mean areas encompassed by landslides are calculated at 107 703 m^2 (Diepgat), 23 023 m^2 (Leven), 19 457 m^2 (Sodwana), 10 666 m^2 (Mabibi) and 10 467 m^2 (Leadsman).

Figure 7.15 is a plot depicting landslide area vs. headscarp depth for the study area. Landslide area correlates poorly with headscarp depth for all canyons except Mabibi and Leadsman Canyons, which have a moderate negative correlation indicating a reduction in slide area with depth. The

largest failures are distributed at random depths throughout the study area. Conversely, the smaller isolated landslides in the heads of the Mabibi Canyons tend to occur at ~ 100 mbsl.

Volume relationships exhibit similar trends across each canyon (Fig. 7.11). Volume correlates well with landslide runout for all canyons, excluding Wright Canyon (Table 7.1). Landslide area similarly has a poor correlation with runout in both Wright Canyon, and the Mabibi area, yet has a strong correlation with runout for the other survey blocks. The mean runout values of 413 ± 48 m (Diepgat), 165 ± 28 m (Leadsman), 404 ± 66 m (Leven), 157 ± 14 m (Mabibi), 168 ± 19 m (White Sands) and 229 ± 25 m (Wright) show a strong variability in runout within the study area. Overall, cohesive slides have significantly lower runout values of 190 m, compared to 439 m of disintegrative slides and turbidity flows. Leven Canyon, and to a lesser extent, Leadsman Canyon, tend to have landslides with larger runouts at shallower depths, whereas Diepgat, the Sodwana Bay, and Mabibi Canyons have a random spread of runout distance with depth (Figure 7.16, Table 7.1).

7.3.5. Slope gradients

The highest mean local unfailed slope (LUS) gradients occur in Mabibi at 15.6° ± 2.6°, compared to Leadsman's 14.7° ± 1.8°, Wright Canyon's 13.5° ± 1.9°, White Sands Canyon's 12.4° ± 1.3° and 11.81° ± 1° for Leven Canyon (Fig. 7.14). Despite having the largest failure areas, Diepgat Canyon has the lowest mean LUS gradients at 9° ± 0.7°. The adjacent unfailed slope gradient increases with depth in Wright, Leven and Leadsman Canyons. Conversely, the LUS gradient decreases with depth in Diepgat canyon, and remains variable in White Sands Canyon and the canyons of Mabibi. Mean scar slope gradients are steepest in the landslides of Diepgat Canyon (40.7° ± 1.2°), followed by those of Wright (33.3° ± 2°), Leadsman (33.2° ± 1.9°), Leven (32° ± 1.8°), and White Sands (27.5° ± 1.9°) Canyons. Mabibi Block has the gentlest mean scar slopes at 26° ± 1°. Scar slopes in all cases are steeper than the LUS; however, those areas with the highest LUS do not necessarily have the steepest scar slopes as confirmed by the Mabibi area (Table 7.1f). Scar slope is unaffected by depth, the values fluctuating randomly across depth profiles for all the canyons, apart from the Leadsman Canyon system, which has a good correlation between increasing depth and increasing scar angle (Fig. 7.17; Table 7.1b).

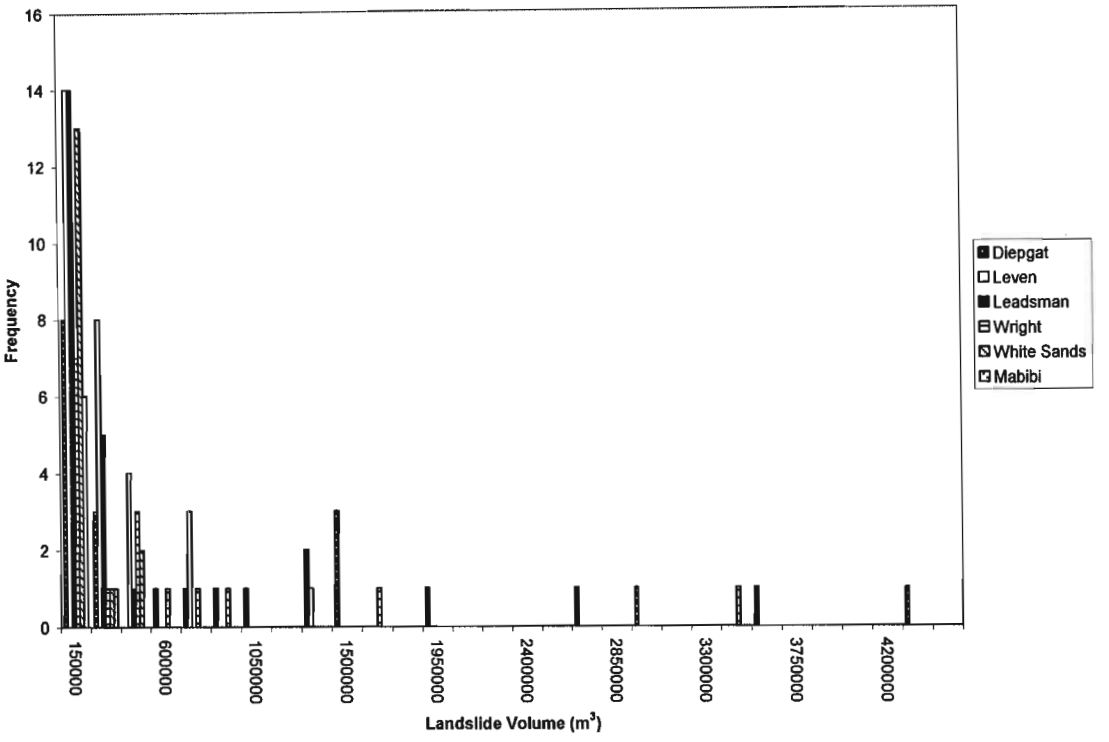
Frequency
Landslide Volume (m^3)
150000
600000
1050000
1500000
1950000
2400000
2850000
3300000
3750000
4200000
Diepgat
Leven
Leadsman
Wright
White Sands
Mabibi

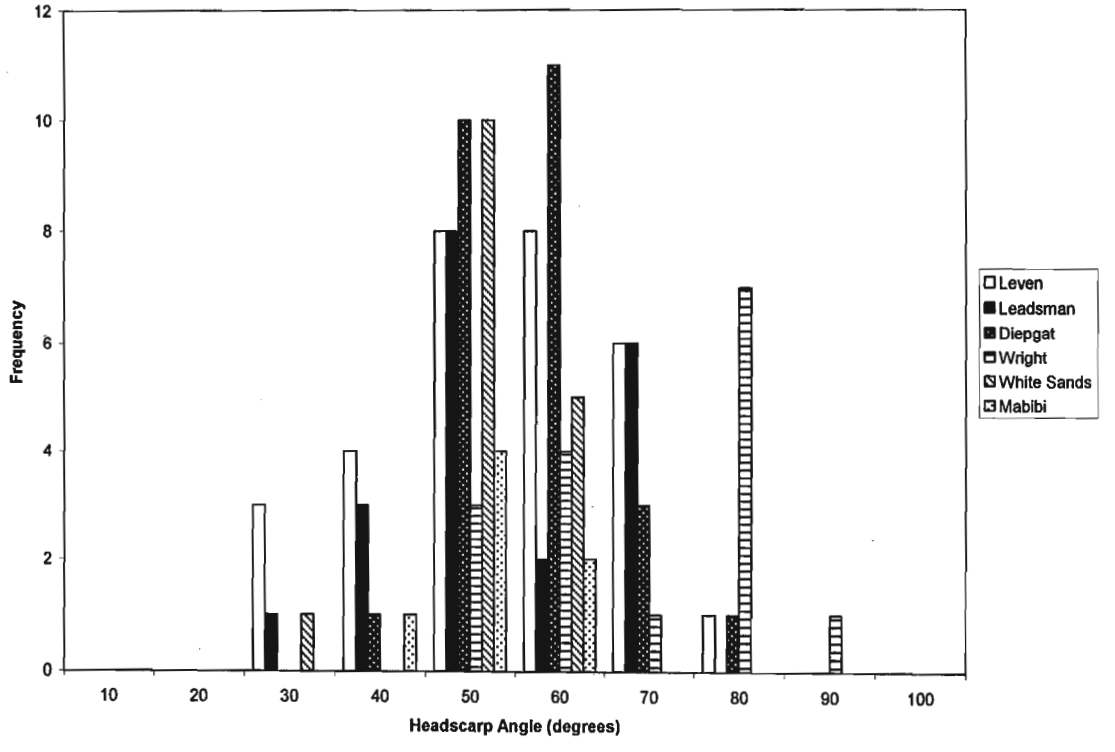
Frequency
Headscarp Angle (degrees)
Leven
Leadsman
Diepgat
Wright
White Sands
Mabibi

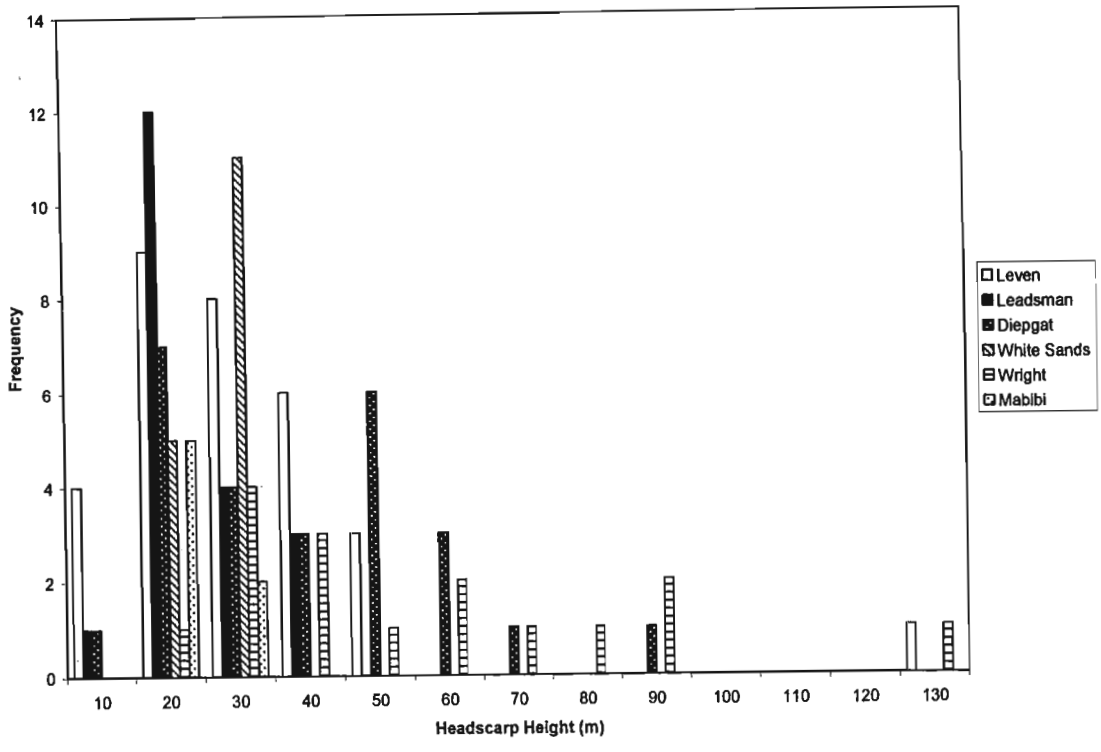

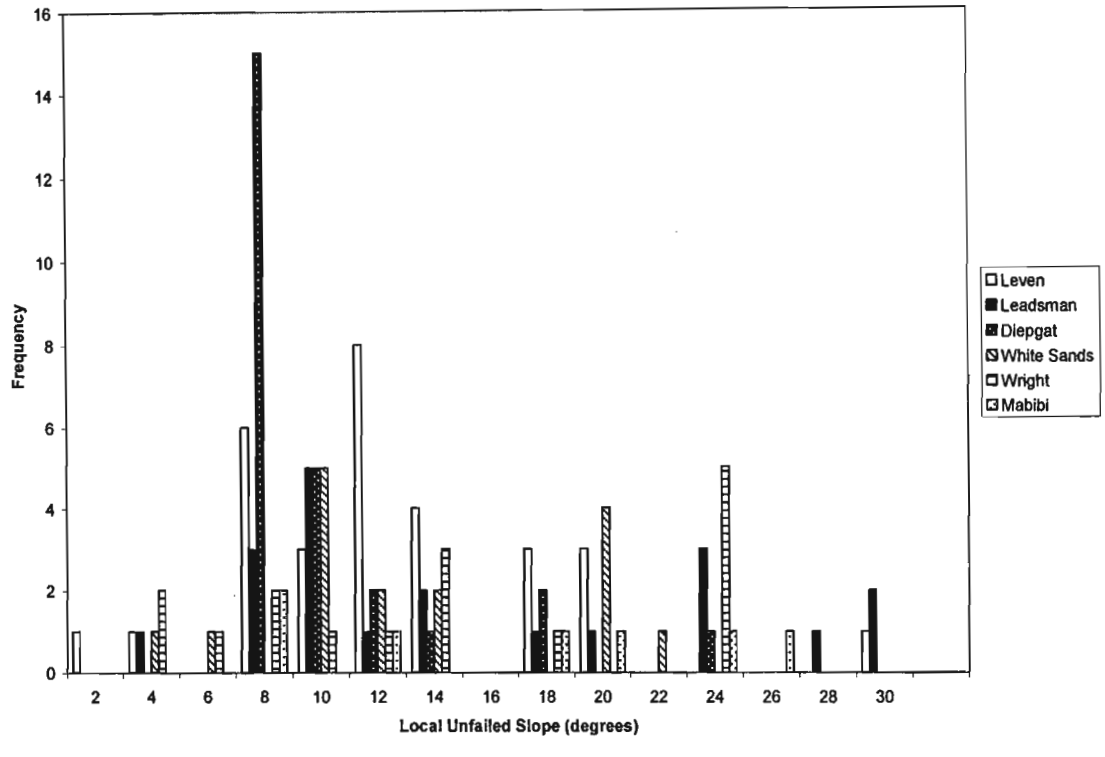

Figures 7.10-7.14. Histograms separated by shelf indenting submarine canyon. These depict area; volume; headscarp slope; headscarp height; and local unfailed slope respectively. The submarine canyons of Mabibi are included as a single entry owing to their uniform size and morphology. North and South Leadsman Canyons are similarly included as a single entity (Leadsman).

Table 7.1. Summary of statistical comparison between various landslide attributes for each survey block. HS = head scarp; LUS = local unfailed slope; *D/L* = ratio between runout distance and headscarp height. Correlation coefficients greater than 0.5 are highlighted in bold.

	Area	Volume	Runout	Runout slope	HS slope	HS height	Scar slope	LUS	HS depth	*D/L*
a)										
Leven Point (n = 31)										
Area	1.00									
Volume	**0.95**	1.00								
Runout	**0.88**	**0.55**	1.00							
Runout slope	-0.15	-0.04	-0.38	1.00						
HS slope	-0.16	0.00	-0.45	0.16	1.00					
HS height	0.07	0.29	-0.05	-0.02	**0.52**	1.00				
Scar slope	-0.24	-0.09	-0.37	0.15	**0.61**	0.36	1.00			
LUS	-0.42	-0.33	**-0.55**	0.10	0.36	0.01	0.28	1.00		
HS depth	-0.44	-0.30	**-0.52**	-0.20	**0.56**	0.22	0.31	**0.67**	1.00	
D/L	**-0.51**	-0.36	**-0.64**	0.13	**0.60**	**0.53**	0.36	0.38	**0.64**	1.00
b)										
Leadsman (n = 20)										
Area	1.00									
Volume	**0.94**	1.00								
Runout	**0.86**	**0.93**	1.00							
Runout slope	0.05	0.08	0.10	1.00						
HS slope	**-0.62**	**-0.62**	**-0.54**	-0.23	1.00					
HS height	0.17	0.34	0.29	0.12	0.11	1.00				
Scar slope	**-0.50**	**-0.54**	**-0.53**	-0.16	**0.80**	0.16	1.00			
LUS	**-0.54**	**-0.57**	**-0.57**	-0.04	0.31	-0.26	0.23	1.00		
HS depth	**-0.59**	**-0.68**	**-0.70**	-0.29	**0.71**	-0.31	**0.67**	**0.50**	1.00	
D/L	**-0.61**	**-0.61**	**-0.67**	-0.41	**0.68**	0.10	**0.59**	0.41	**0.76**	1.00
c)										
Diepgat (n = 26)										
Area	1.00									
Volume	**0.88**	1.00								
Runout	**0.80**	**0.77**	1.00							
Runout slope	-0.29	-0.32	-0.47	1.00						
HS slope	0.10	0.04	0.13	-0.26	1.00					
HS height	0.44	**0.69**	**0.67**	**-0.50**	0.18	1.00				
Scar slope	-0.03	-0.13	0.02	-0.09	**0.70**	0.01	1.00			
LUS	-0.33	-0.30	-0.29	0.30	0.08	0.29	0.20	1.00		
HS depth	0.06	0.06	-0.21	-0.08	-0.13	-0.12	-0.14	-0.38	1.00	
D/L	-0.49	-0.30	**-0.60**	0.48	-0.06	-0.14	-0.07	-0.49	-0.12	1.00

d)

Wright Canyon (n = 16)										
Area	1.00									
Volume	**0.93**	1.00								
Runout	-0.01	0.16	1.00							
Runout slope	-0.03	-0.09	-0.20	1.00						
HS slope	0.04	-0.04	-0.19	0.17	1.00					
HS height	-0.02	0.32	0.42	-0.17	0.09	1.00				
Scar slope	-0.04	-0.18	**-0.65**	0.10	**0.58**	-0.25	1.00			
LUS	-0.35	-0.35	0.10	-0.04	**0.70**	0.21	0.42	1.00		
HS depth	0.12	0.09	-0.02	-0.15	**0.78**	0.21	0.41	**0.69**	1.00	
D/L	-0.01	0.20	-0.23	0.06	0.33	**0.73**	0.17	0.23	0.24	1.00

e)

White Sands (n = 16)										
Area	1.00									
Volume	**0.85**	1.00								
Runout	**0.74**	**0.86**	1.00							
Runout slope	**0.57**	**-0.57**	**-0.73**	1.00						
HS slope	**-0.6**	-0.19	-0.18	0.16	1.00					
HS height	-0.09	0.30	0.28	0.04	0.48	1.00				
Scar slope	**-0.61**	-0.45	-0.39	**0.63**	0.39	0.35	1.00			
LUS	-0.45	-0.36	-0.33	0.24	0.48	-0.02	0.23	1.00		
HS depth	0.03	0.18	0.01	0.01	0.14	-0.34	-0.06	-0.12	1.00	
D/L	**-0.59**	-0.47	**-0.65**	**0.67**	0.47	0.42	**0.64**	0.32	-0.19	1.00

f)

Mabibi (n = 7)										
Area	1.00									
Volume	**0.72**	1.00								
Runout	-0.05	**0.63**	1.00							
Runout slope	**0.68**	0.10	**-0.63**	1.00						
HS slope	-0.43	0.18	**0.74**	**-0.68**	1.00					
HS height	0.03	**0.65**	**0.87**	**-0.55**	**0.83**	1.00				
Scar slope	0.35	-0.12	**-0.6**	0.29	**-0.61**	-0.36	1.00			
LUS	0.48	0.09	**0.50**	**0.79**	-0.19	-0.17	0.21	1.00		
HS depth	**-0.52**	-0.44	-0.20	-0.44	-0.21	-0.22	0.39	**-0.50**	1.00	
D/L	0.07	0.45	0.49	-0.34	**0.71**	**0.86**	-0.04	0.19	-0.19	1.00

g)

All areas (n = 116)

Area	1.00									
Volume	**0.91**	1.00								
Runout	**0.68**	**0.60**	1.00							
Runout slope	-0.07	-0.09	-0.25	1.00						
HS slope	-0.01	0.04	-0.22	0.05	1.00					
HS height	0.29	**0.50**	0.36	-0.08	0.39	1.00				
Scar slope	0.17	0.14	-0.09	0.16	**0.57**	0.17	1.00			
LUS	-0.37	-0.31	-0.4	0.04	0.32	-0.03	0.08	1.00		
HS depth	0.11	0.14	-0.18	-0.06	0.38	0.05	0.39	0.17	1.00	
D/L	-0.32	-0.15	**-0.50**	0.15	**0.50**	0.31	0.24	0.38	0.26	1.00

h)

Cohesive (n = 116)

Area	1.00									
Volume	**0.91**	1.00								
Runout	**0.68**	**0.60**	1.00							
Runout slope	-0.07	-0.09	-0.25	1.00						
HS slope	-0.01	0.04	-0.22	0.05	1.00					
HS height	0.29	**0.50**	0.36	-0.08	0.39	1.00				
Scar slope	0.17	0.14	-0.09	0.16	**0.57**	0.17	1.00			
LUS	-0.37	-0.31	-0.4	0.04	0.32	-0.03	0.08	1.00		
HS depth	0.11	0.14	-0.18	-0.06	0.38	0.05	0.39	0.17	1.00	
D/L	-0.32	-0.15	**-0.50**	0.15	**0.50**	0.31	0.24	0.38	0.26	1.00

i)

Disintegrative (n = 116)

Area	1.00									
Volume	**0.91**	1.00								
Runout	**0.68**	**0.60**	1.00							
Runout slope	-0.07	-0.09	-0.25	1.00						
HS slope	-0.01	0.04	-0.22	0.05	1.00					
HS height	0.29	**0.50**	0.36	-0.08	0.39	1.00				
Scar slope	0.17	0.14	-0.09	0.16	**0.57**	0.17	1.00			
LUS	-0.37	-0.31	-0.4	0.04	0.32	-0.03	0.08	1.00		
HS depth	0.11	0.14	-0.18	-0.06	0.38	0.05	0.39	0.17	1.00	
D/L	-0.32	-0.15	**-0.50**	0.15	**0.50**	0.31	0.24	0.38	0.26	1.00

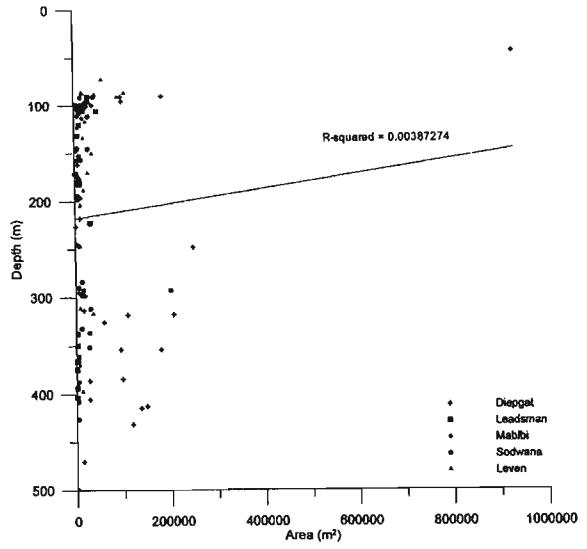

Figure 7.15. Plot of landslide depth against landslide area. Area correlates poorly with depth ($R^2 = 0.0039$).

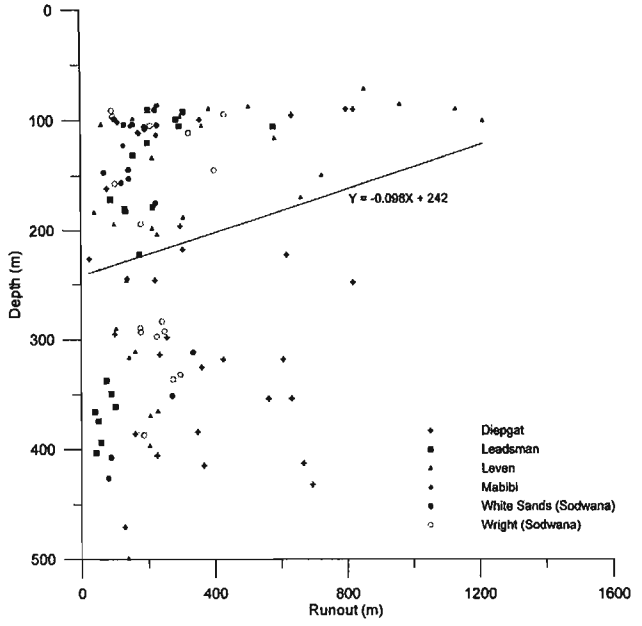

Figure 7.16. Plot of landslide depth against runout distance. Note that Leadsman and Leven Canyons have comparatively larger runout distances at ~ 100 m depth compared to those of deeper landslides, both in Leven/Leadsman Canyons and other canyons studies throughout the depth range of landslide occurrences.

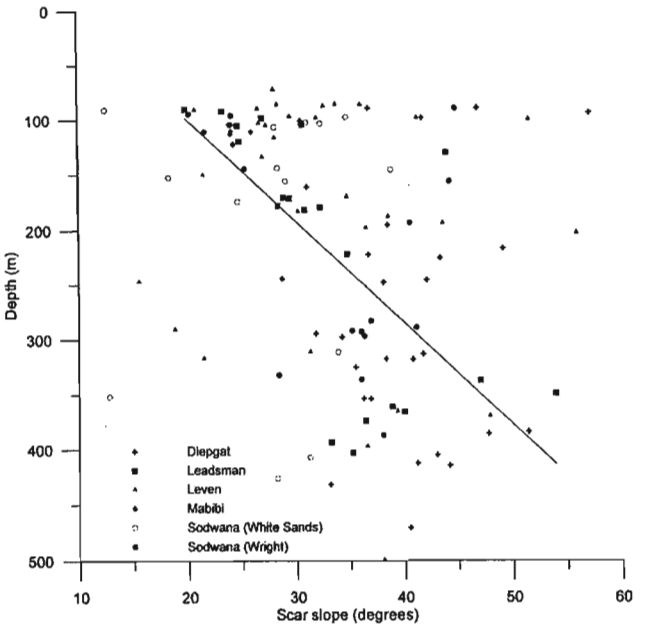

Figure 7.17. Plot of landslide depth against scar slope. A very poor correlation between depth and scar slope is evident (R^2 = 0.139). Note that the regression line is for the Leadsman Canyon system, showing a moderate correlation between the two variables (R^2 = 0.446).

7.3.6. Headscarps

Headscarp heights and angle vary considerably throughout the study area, the tallest and steepest headscarps occur in Wright Canyon (50.9 ± 7.3 m; 63.6 ± 3.3) (Figs. 7.12 and 7.13). The mean headscarp height of failures in Diepgat Canyon is 35 ± 3.8 m, with a mean slope of 50.7° ± 1.6°. The headscarps of Leven (27.6 ± 3.9 m; 49.6° ± 2.4°), White Sands (21.8 ± 1.7 m; 46.3° ± 2°), Leadsman (19.6 ± 1.7 m; 49.8° ± 2.7°) and Mabibi (17.6 ± 2.7 m; 45.6° ± 2.5°) are comparatively smaller and gentler. Diepgat and Wright Canyons have the largest degree of variability in headscarps, compared to the comparative uniformity in height of the headscarps of the Mabibi, Leadsman and White Sands Canyons (Fig. 7.13).

7.4. Discussion

The five areas presented here have a marked degree of spatial variation in their morphometric characteristics, which suggests that different controls are being exerted on the submarine canyon evolution. Here the correlative relationships of the variables measured (Table 7.1) are discussed

and an attempt to define the possible mechanical or rheological influences imposed on the geomorphology of the study area, in relation to each canyon system is made.

The strongest correlations exist between headscarp slope and headscarp depth (Table 7.1) indicating that for Leven, Leadsman, and White Sands Canyons, headscarp slope increases with depth. McAdoo et al (2000) show that headscarp height and slope may be used as a proxy for sediment strength, steeper scarps indicating sediment overconsolidation and higher dynamic strengths, in comparison to gentler scarp slopes that indicate normally consolidated and weaker material. Similar trends are evident from the scar slope vs. depth relationships. This suggests that sediment strength increases with depth within these three canyons, a trend observed from borehole data (Du Toit and Leith, 1974) and seismic data (Sydow, 1988; Shaw, 1998) which indicate that canyons most likely incise loosely consolidated (inferred by Sydow (1988) as Palaeocene age) silty sandstones, as observed from submersible dive observations (Green, 2004) before meeting more consolidated silty sandstones (Green, 2004). These are aged by virtue of their microfossil assemblages from gravity cores (Siesser, 1977) which sampled the acoustic basement of the area, assigning it a late Cretaceous (Maastrichtian) age. These rocks are typically of higher strength than the Palaeocene silty sandstones of the area (R. Maud pers.comm). Puzzlingly, this trend is not reflected in any of the depth-headscarp height relationships (Table 7.1) and suggests that the headscarp height may be significantly altered by subsequent re-failure along the scarp, reducing its height, but maintaining the angle of repose of the failing sediment. The coalescence of headscarps confirms that these failures are subject to re-failure, which would influence the headscarp height to some extent.

Crozier (1973) and McAdoo et al. (2000) consider runout a good prediction of rheology during failure (i.e. rotational slides, viscous or fluid flows etc.). Increasing runout values indicate increasingly higher mobility within the failure mass (Norem et al., 1990). Runout values compared to depth of failure indicate that 1) sediment in the upper portions of Leadsman and Leven Canyons is weaker or fluidised during failure and 2) sediment strength in Diepgat, Wright, White Sands and the Mabibi Canyons does not vary with depth (Fig. 7.16). Submersible dives indicate that the upper portions of Leadsman and Leven Canyons comprise carbonate cemented beachrock and aeolianite, which mantle partially consolidated Tertiary mud-rich silts and sands. A reduction in strength in the overlying materials is thus unlikely. Rather, the large runouts and small headscarps may be the result of the partial fluidisation of the failed mass (Mohrig et al., 1998) due to fluid sapping in the canyon heads. Subduction derived fluid seeps from convergent margins produce similar canyon

slope failure via seepage (Orange and Breen, 1992; Orange et al., 1994; Orange et al., 1997, McAdoo et al., 1997), though the fluid source is incompatible with a passive margin such as that of Northern KwaZulu-Natal. Fluid escape and slope failure via slope overburdening, is recognised from passive margin settings (Robb, 1984; Dugan and Flemings, 2000), but is irreconcilable with the absence of an offshore aquifer along the KwaZulu-Natal margin (c.f Martin, 1984). Fresh water seeps in the northern KwaZulu-Natal region appear to be driven rather by an established hydraulic head from the fringing groundwater table (Meyer et al., 2001) than by any means of overpressuring on an underlying offshore acquirer.

Artesian conditions on the Florida Escarpment are documented by Paull et al. (1990) who consider this to be the dominant driving force in canyon formation and slope failure. A similar system of headless canyons is produced, but differs in that dissolution is the dominant process in comparison to the KwaZulu-Natal canyons where few dissolution features are evident (Green, 2004). Fluid introduction is most likely the product of fresh water exchange between the perched water table of the fringing coastal waterbodies and the lower continental shelf along the unconformity between Cretaceous and Tertiary sediments (Meyer et al., 2001; Ramsay and Miller, 2006). In the case of Wright Canyon, despite the moderately large mean runout distance of the landslides, the poor correlation between area and runout indicates that the failed material is particularly cohesive, precluding the dissipation of the slide masses over wider areas. In the case of Leven Canyon's sinuous upper tributary (Fig. 7.9, box c), this landslide morphology could possibly be the result of alongshelf-transported sediments being intercepted by this canyon limb, forming fluid turbidity currents (e.g. Boyd et al., 2008) which exploit a pre-existing scar (e.g. Pratson et al., 1996). This appears unlikely as along-shelf sediment transport in this region is limited by the sediment starved nature of the region (Cooper, 1994; Ramsay et al., 2006). We thus consider this morphology, again, a product of fluid exchange with the coastal aquifer and the continental shelf.

Hampton et al. (1996) provide a review of several submarine landslide studies and indicate that a range of headscarp height to runout ratios (*D/L*) occurs, varying from 0.1 for slumps, to 0.002 for flows. This is several times lower than the average *D/L* values for sub-aerial landslides as described by Ritter et al. (1995). McAdoo et al. (2000) indicate that for the both the eastern and western U.S continental slope, slumps have a *D/L* ratio of 0.02, compared to 0.015 for blocky slides and 0.002 for disintegrative slides. In the case of the northern KwaZulu-Natal continental margin, cohesive slides such as slumps have average *D/L* ratios of 0.14, compared to a ratio of 0.05 for disintegrative slides (including fluid flows which have *D/L* ratios < 0.01). This indicates that slide masses are

moving seven to twenty five times the distance in open slope settings, such as those measured from the U.S continental slope, compared to intra-canyon slides. Failure runout within a canyon setting is thus constrained by: 1) proximity of the thalweg to the failure, particularly if the failure is occurring perpendicular to the thalweg; 2) the thalweg width, narrower thalwegs will cause a damming effect of sediment against the facing canyon wall; and 3) the efficiency of catastrophic along-thalweg sediment flows to remove slide deposits.

The canyons of Mabibi are the least incised of the area (Green et al., 2007), yet occur on the steepest section of continental slope and shelf and have the least and smallest landslides. Those landslides measured are retrogressive slumps in the heads of shelf indenting canyons. The nature of these landslides is related to the relative shallowness of the canyon thalwegs, which are under-incised, compared to the larger shelf indenting canyons studied (Green et al., 2007). Studies by Pratson and Coakley (1996) indicate that failures will only occur in the flanking walls of the thalweg once critical oversteepening of the walls is achieved via downcutting of the thalweg. Prior to this, failures will be restricted to headward retrogressive slumping as the canyon excavates towards the shelf before capturing the shelf sediments and incising to the point of wall failure and widening of the system. This explains the rill-like appearance of the strongly linear, slope confined and shelf indenting canyons, which have failures restricted to the upper canyon limits. The Mabibi regional slope gradient (as described by Green et al., 2007) is the steepest studied as a result of this relative under-incision.

The largest landslides (e.g. 928 024 m^2) occurring on relatively shallow average slope gradients (~ 4°) of the Diepgat outer-shelf (Fig. 7.4), are cohesive, and have headscarps heights and slopes (e.g. 62 m; 36°) in the lower range of distribution. This indicates that the material is unlikely to have a fluid rheology during failure, despite the failure size. It appears that these failures could be deep seated landslide features initiated by earthquake activity, which would account for the size of the failure and the intact slide mass. Landslide pre-conditioning factors such as underlying weak layers (Kvalstad et al, 2005) along which progressive deformation may occur provide an equally plausible hypothesis for landslide generation, causing failure in a bedding plane parallel style (Masson et al., 2006). However, it seems most likely on the basis of work by Bryn et al. (2005) and Kvalstad et al. (2005) that pre-conditioning factors such as high sediment availability during lowstand and underlying weak layers (in the partially consolidated Tertiary strata) must be met with an accompanying trigger, in this case possibly an earthquake. The most recent seismic activity to have

occurred in the area is the 1932 Zululand Earthquake of a surface wave magnitude of 6.8 (Hartnady, 2003). This may have been the possible trigger for the largest landslide in Diepgat Canyon head.

The deep seated nature of this type of failure would expose more consolidated material that would be less likely to fail, steepening the continental shelf (McAdoo et al., 2000). A similar type of failure occurs in the mid-slope portions of Wright Canyon; however the failure area is significantly smaller. The next largest failures, apart from those of Diepgat Canyon, occur in the mid continental slope regions of Leven Canyon (Fig. 7.3), on the shallowest regional slope, with low headscarp angles and small head scarp height modes. These are disintegrative, and indicate that rheology was significantly weaker during failure compared to the failures of Diepgat and Wright Canyons of comparative size.

Overall, the most well defined landslides occur in the heads of the large shelf indenting canyons, which reside in the Mio/Pliocene shelf edge wedge (Green et al., 2007). The presence of hanging slides, benches, and incised gorges attest to periods of thalweg downcutting, where the slide extended to a palaeo-thalweg floor, and was subsequently stranded once downcutting of the canyon continued. Incised gorges would be preserved when material at the toe of the slide was removed by this incision (Densmore et al., 1997), which would also leave pronounced erosional benches in the slide material. Periods of periodic slope clearing thus occurred, interspersed with periods of thalweg excavation. Benches possibly represent periods of increased thalweg erosion at the base of the failure (Nelson et al., 1970). Similar examples are documented by McAdoo et al. (2000) for the New Jersey continental slope and Arzola et al. (2008) for the western Iberian continental slope. Models presented by Pratson et al. (1994) and Pratson and Coakley (1996) for the continental margin of the US Atlantic, indicate that canyon incision by sediment flow is followed by several episodes of along-thalweg retrogressive failure, interspersed with side wall failure. Arzola et al. (2008) ascribe this type of canyon response to instability processes preconditioned by the resultant steep topography. These models also explain the complex failure morphology of the canyons of northern KwaZulu-Natal. The smaller narrow canyons with failures restricted to the canyon heads represent a change in erosional regime from a downward eroding sediment flow phase responsible for the formation of intercanyon rills with no failures (Fig. 7.18) such as those commonly seen in the Mabibi Block, to a headward eroding phase once oversteepening relative to the downslope portions of the intercanyon rill is sufficient to cause headward slumping (Fig. 7.19), such as Diepgat Canyon. The larger canyons exhibit evidence for catastrophic headwall failure due to oversteepening by downward eroding sediment flow, periodic catastrophic slope clearances and

active canyon enlargement by retrogressive failure, as envisioned by these modelling attempts. The role of axial incision is similarly documented by both Baztan et al. (2005) and Arzola et al. (2008), where stages of axial incision and oversteepening are shown to be the key preconditioning factor in the establishment of mass wasting processes that affect the canyon head and flanks. The fact that hanging slides, benches and incised gorges are preserved, suggests that the canyons of northern KwaZulu-Natal are currently in a period of quiescence following a period of axial incision, where the walls are not currently subject to catastrophic slope clearances. The low sediment availability of the area (Cooper, 1994), particularly during highstand of the Holocene, has reduced the impetus for sediment loading of the shelf and the means to incise the thalweg, which has resulted in canyon quiescence (Green et al., 2007).

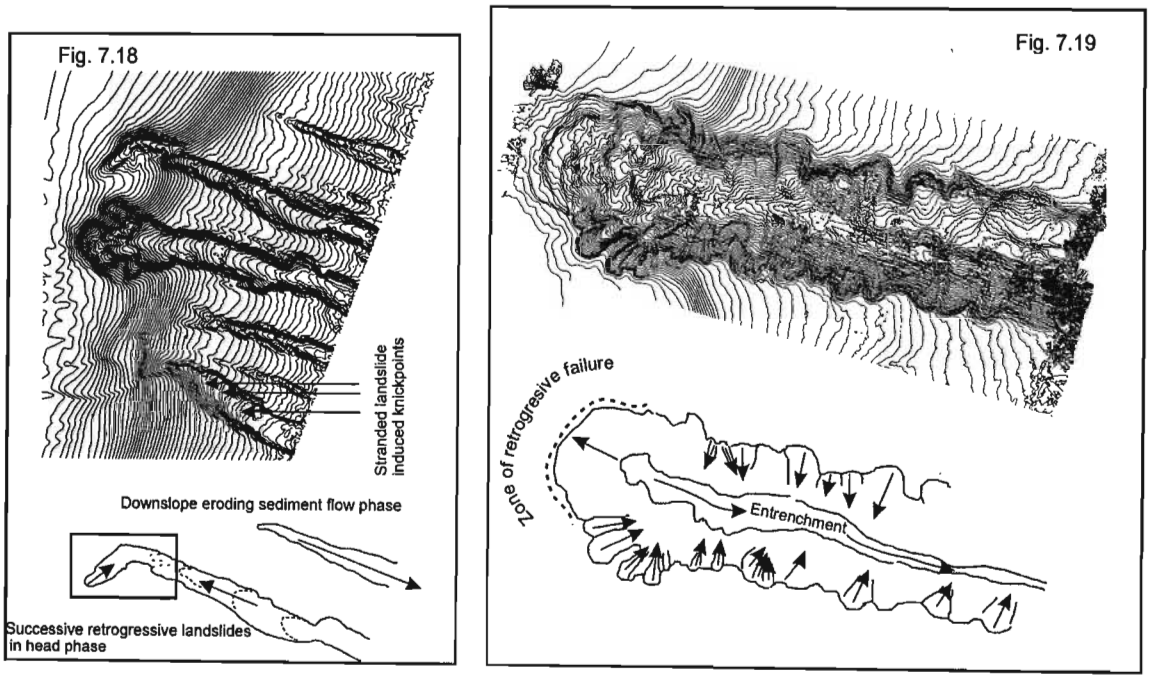

Figure 7.18. Bathymetric contours and interpretative schematic depicting the evolution from slope rills, commonly observed between larger erosive features, to narrow shelf indenting canyons with a single retrogressive failure in the head portions. Note the evidence in the contour data for older scar morphology preserved successively downslope in the small canyon as the head advances landwards, stranding older landslide scarps. It is postulated that critical oversteepening of the rill walls and head occurs due to erosion by sediment flow, which causes headwall failure and eventual canyon excavation headwardly. **Figure 7.19.** Bathymetric contours and interpretative schematic of the large shelf indenting Diepgat Canyon. Retrogressive failure, coupled with the entrenchment of the axis by failure-derived sediment flows, oversteepen the canyon form relative to the flanks. This prompts lateral extension by retrogressive, axis perpendicular landsliding which further entrenches the canyon axis.

The random distribution of failures with depth in all canyons implies that there is no dominating influence on the depth zonation of failure. In particular, the largest failures are spread at random and are not restricted to depths of the previous lowstand of ~ 18 000 BP at -125 m (Green and Uken, 2005) or the penultimate lowstand of ~ 180 000 BP at -130 m (Ramsay and Cooper, 2002; Green and Uken, 2005). Posamentier and Vail (1988) and Posamantier et al. (1988) indicate that the maximum degree of erosion will occur during the maximum rate of sea-level fall (i.e. towards the lowstand systems tract). Thus, despite lowstand conditions (which provide favourable pre-conditioning factors) having prevailed, failures appear to be unrelated to the sea levels of the last and penultimate glacial periods, suggesting that sediment starved conditions were operating since at least these times. The presence of sea level notches throughout the failures of the heads of the canyons at the LGM level indicates that these failures pre-date this time period (Green and Uken, 2005). The notable exception is Diepgat Canyon head, the landslides within which post-date the LGM (Green and Uken, 2005).

CHAPTER 8

First observations of sea level indicators related to glacial maxima

Green, A.N., Uken, R., 2005. First observations of sea level indicators related to glacial maxima at Sodwana Bay, northern KwaZulu-Natal. S. Afr. J. Sci. 101, 236-238.

8.1. Introduction

Relative sea level fluctuations during the late Pleistocene–Holocene period have been described by a number of authors for the South African coast and continental shelf. Well-constrained sea level curves have been presented for the west coast (Miller, 1990; Compton, 2001), the last 50 000 yr (Cooper, 1991) and the late Holocene (Ramsay, 1995). The recent work of Ramsay and Cooper (2002) has provided an amalgamation of existing sea level indicators along the entire South African coast spanning the penultimate interglacial period (182 000 BP) to modern-day sea levels (Fig. 8.1). There is a lack of evidence constraining sea levels that span the Penultimate Glaciation and the Last Interglacial periods of between 182 000 ± 18 000 (Ramsay and Cooper, 2002) and 112 000 ± 23 000 BP (Ramsay et al., 1993). Evidence for a penultimate Glacial Maximum has not been described for the South African coast. Similarly, records for the Last Glacial Maximum (16 000–18 000 BP) are scarce, limited only to those indicators discovered on the west coast (Siesser, 1972; Dingle and Rogers, 1972; Rogers and Li, 2002). Recently, observations made from the German submersible *Jago* within a series of incised submarine canyons off the Sodwana bay continental shelf, northern KwaZulu-Natal, have unearthed a number of lower than present sea level indicators at depths that have been either little explored, or completely unexplored, by traditional methods. In particular, strong evidence can be presented for sea levels that have occurred at depths greater than the LGM. This chapter thus aims to substantiate previous evidence for sea levels that occur within the proposed Last Glacial Maximum depth bracket.

8.2. Indicators of glacial maxima along the South African coastline

Several dates exist around the Last Glacial Maximum, the maximum depth of 130 m being derived from relict wave rolled rhodolites of 16 990 ± 100 yr BP (Vogel and Marais, 1971; Siesser, 1972). The probable vertical accuracy is considered to be within 5 m of mean sea level (Ramsay and Cooper, 2002). Seismic profiling off the Orange River revealed preliminary evidence for a lowstand shoreline at 120 m depth (De Decker and Van Heerden, 1987). The sequence was not dated, but assigned to the Last Glacial Maximum. Similarly, coarse-grained sands with "typical

littoral grain surfaces" were recorded at comparable depths offshore of the Orange (Rogers, 1977). No data exist for an east coast LGM. Evidence for a penultimate Glacial Maximum is not described for the South African coast, though isotope evidence from the Huon Peninsula, New Guinea, suggest sea levels of between –130 m and –145 m at 135 000 BP (Chappell and Shackleton, 1986). No physical observations have been made regarding sea levels lower than the LGM or corresponding to a glacial period prior to the Oxygen Isotope Stage 5e high stand (125 000 BP).

8.3. New evidence for east coast sea levels

The recent introduction of the German submersible *Jago* to the area has allowed observations to be made at depths greater than those attainable by traditional SCUBA methods. Dives using compressed air are limited to depths of 50 m by law in South Africa, though deeper dives using mixed gases have been described from the study area (Sink et al., 2006). These dives focused almost solely on the biological habitat of these regions, so evidence from video footage and dedicated geological dives of the *Jago* is particularly valuable as a preliminary eye-witness account of the geomorphology of the canyon habitats. First observations of these features suggest that the canyons have cut into older rocks of Tertiary and late Cretaceous age, which may be tentatively correlated with previous seismic stratigraphic interpretations of the continental shelf (Sydow, 1988; Shaw, 1998).

Within the canyons, a number of deeply notched caves with erosional features typical of sub-aerial intertidal environments are found. In addition, overhangs, planed terraces and notches indicating palaeo-shorelines (Miller and Mason, 1994) are found at various depths along the exposed sections of the canyon walls. As these features are not contemporaneous with deposition, they may be considered to post-date the deposition of the Tertiary rocks in the study area during the Early to Late Pliocene transgression (Siesser and Dingle, 1981, chapters 3and 5). Sea levels indicated by these features thus span the time period from Early Pliocene to Late Pleistocene. Submarine cave localities across six mature canyons can thus be analysed in terms of their cluster relationships, based on depth and location. This implies that only genetically related caves formed by massive events such as glacial maxima be targeted as possible sea level indicators. The Jesser, Diepgat, Wright, White Sands, South Island Rock and Mabibi Canyons have so far been explored for caves and their suitability as habitats for coelacanths. Forty-two caves were recorded as depth versus canyon locality plots (Fig. 8.2). From these, three clusters are recognisable at depths of approximately 106 m, 125 m, and 130 m.

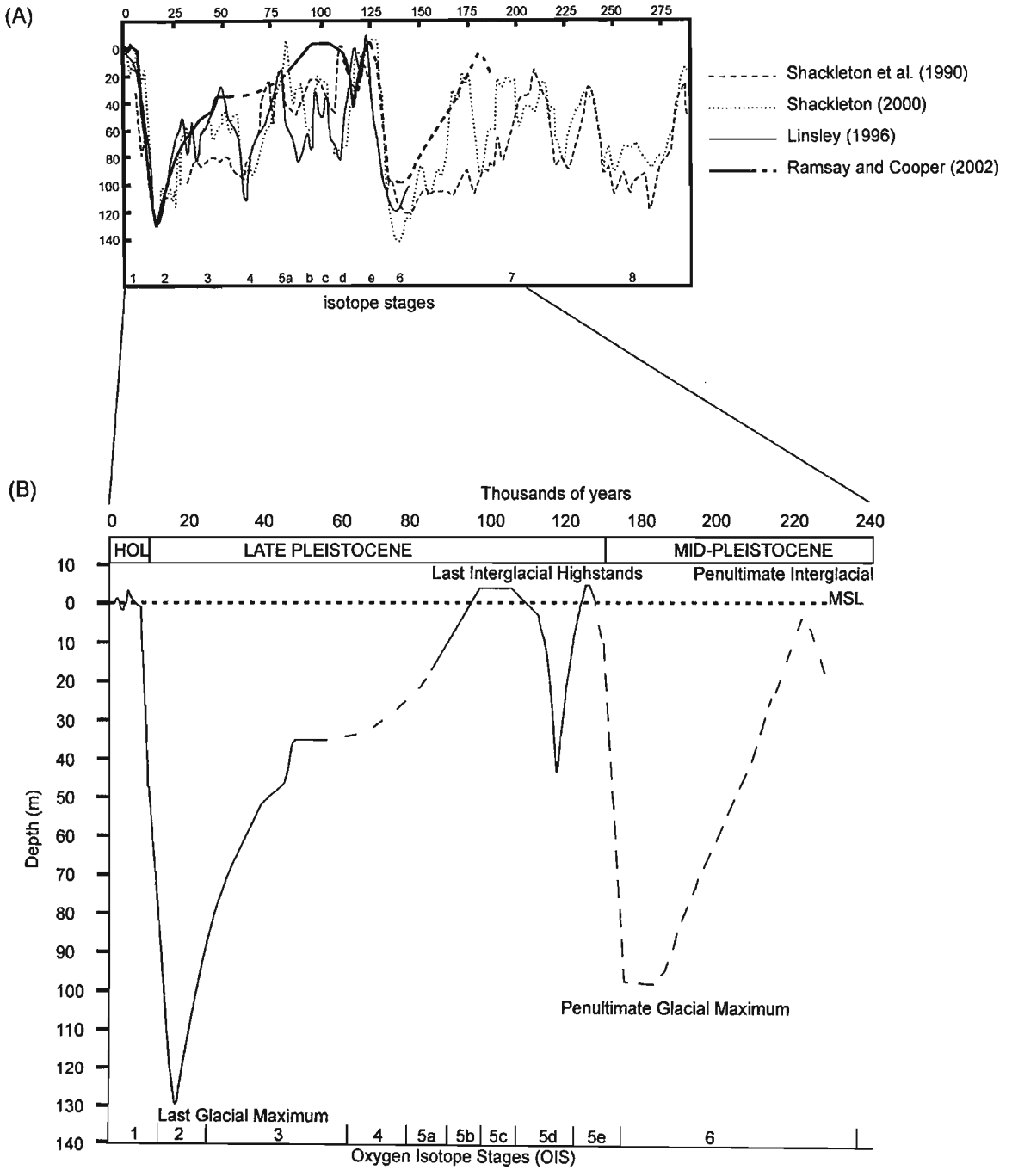

Figure 8.1. A: global sea level curves for the past 275 000 years with Ramsay and Cooper (2002) sea level curve superimposed. B: sea level curve based on available sea level indicators from the South African coastline (Ramsay and Cooper, 2002). Inferred sea level data is defined by the dashed curve, and the lowstands indicate previous glacial maxima.

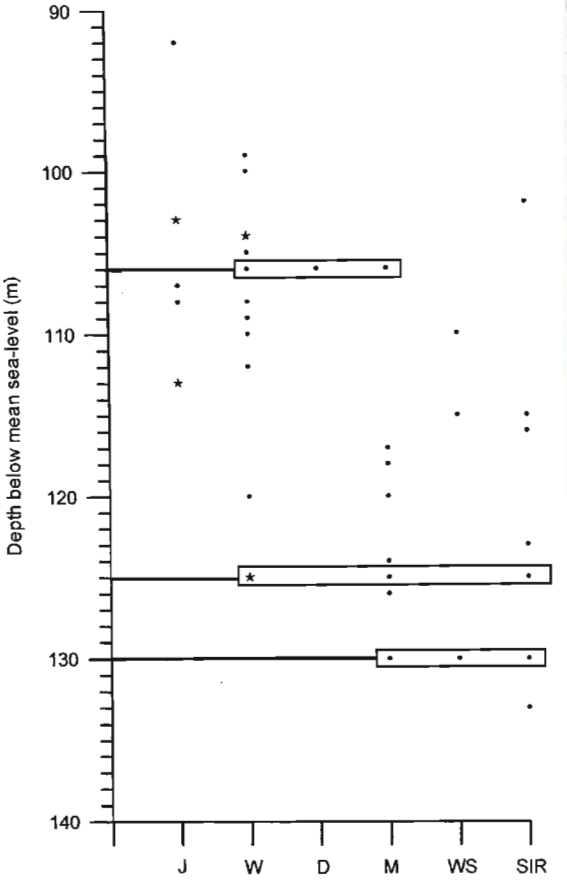

Fig. 8.2

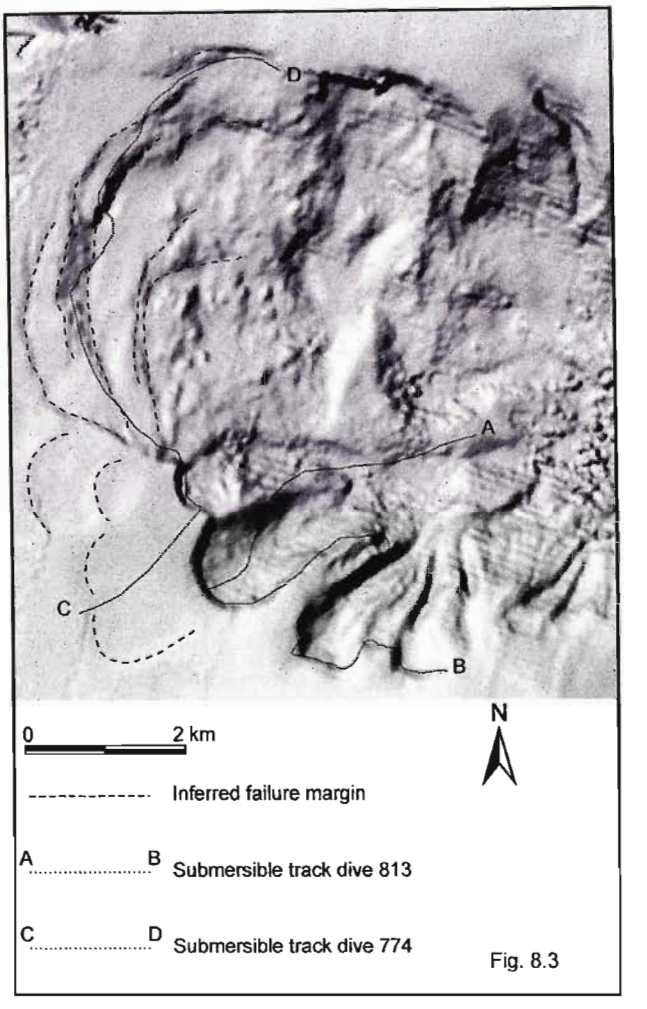

Fig. 8.3

Figure 8.2. Cave clusters relative to the various canyon localities found in the study area. J = Jesser, W = White Sands, D = Diepgat, M = Mabibi, WS = White Sands, SIR = South Island Rock. Stars denote cave with resident coelacanth. **Figure 8.3.** Sunshaded digital terrain model of Diepgat Canyon showing inferred failure margins in the canyon head. The sedimentary log detailed in figure 8.5 is derived from transect A-B.

Though caves at these depths do not occur uniformly throughout the various canyons, they appear to be good indicators of lower past than present sea levels. The two deepest sea level indicators are characteristically absent from Jesser Canyon, which is the youngest and least incised of the sample group. This indicates that the two lowest sea levels prevailed before Jesser Canyon was cut to a depth of ~125 m (± 1 m) and confirms that the 105 m depth indicators are younger than both the -130 m and -125 m sea levels. The absence of the deeper indicators from Diepgat is attributed to scarp slumping within the canyon head, features recognised from the bathymetry of the canyon margins (Fig. 8.3).

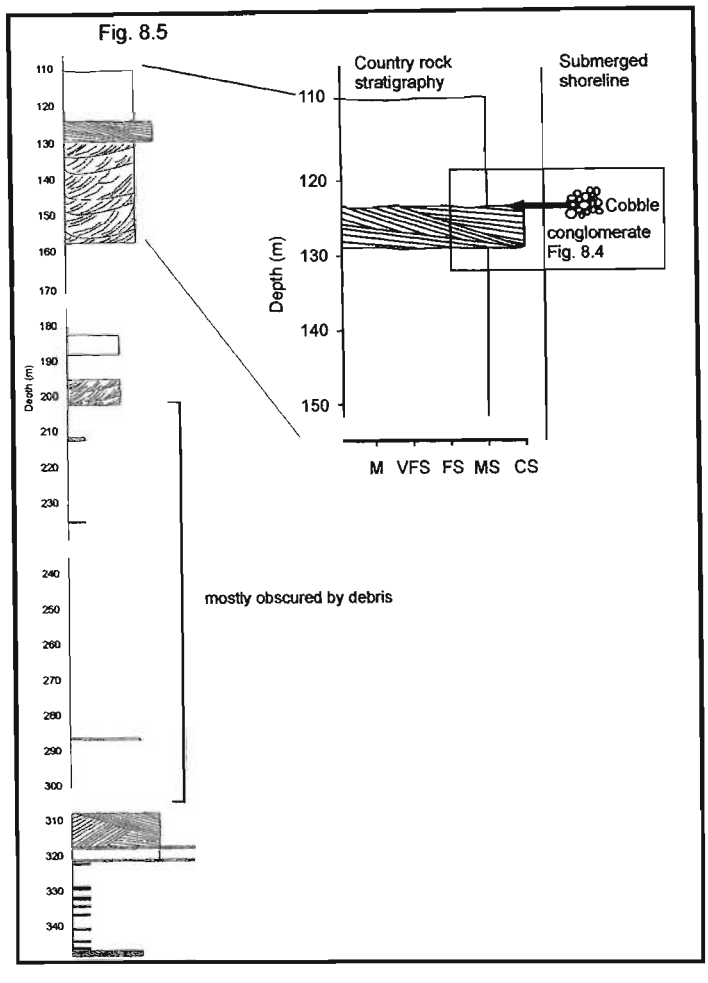

Figure 8.4. A cobble conglomerate found within a cave at 124 m water depth in South Island Rock Canyon, deposited during a sea-level lowstand under storm conditions. **Figure 8.5.** A sedimentary log detailing the country rock upon which the conglomeritic deposit has been superimposed. Note the absence of coarse material from the upper levels, thus precluding deposition of the cobble conglomerate as a product of gravity flow. Sedimentary log created from *Jago* dive 813 (track depicted in figure 8.3).

Within Island Rock Canyon, a partially cemented cobble conglomerate was discovered within a cave at a depth of 125 m (Fig. 8.4). The overlying stratigraphy comprises trough cross-bedded beachrocks and planar bedded aeolianites, with grain size restricted to those between the fine sand and gravel fractions (Fig. 8.5), suggesting that this deposit, without appreciable transport and smoothing, could not have been derived from the upper canyon margins as a weathering product. This indicates that this deposit is *in situ* and was emplaced either contemporaneously with, or just after, cave formation at 125 m depth. Further observations are needed to ascertain whether this deposit is the product of a re-cemented gravity flow or if it was formed by storm action in the intertidal zone. Initial observations suggest that the conglomerate is clast supported, typical of beach deposits emplaced during storm events. Newly interpreted sea levels at -125 m and -130 m are thus considered as being correlative with established sea level curves. The 125 m depth event can possibly be assigned to the Last Glacial Maximum lowstand of 16 000-18 000 BP. Depths of 130 m are likely the expression of sea level oscillations during the LGM. Shallower sea level indicators at 105 m depth can possibly be assigned a much younger age, and can be correlated with *in situ* estuarine molluscan material from the southwest coast inferred as a palaeo-sea level of between 90 m and 102 m below MSL and related to the onset of sea level rise during the Flandrian (OIS 1) transgression (Pether, 1994). As these sea levels were situated below the modern day shelf break, and show evidence for notching in canyon heads, it is reasonable to assume a situation where a sandy coastal plain existed, fronted by a cliffed and rocky shoreline. This is similar to the modern day shoreline of the Eastern Cape of South Africa, which comprises rocky headland and cliff fronted coastal compartments.

CHAPTER 9

Sediment dynamics, surficial geology and coastline configuration models

Green, A.N., 2009. Sediment dynamics on the narrow, canyon-incised and current swept shelf of northern KwaZulu-Natal continental shelf, South Africa. GeoMar. Lett. DOI 10.1007/s00367-009-0135-9.

9.1. Introduction

Over past decades, a considerable amount of work has been undertaken on the delineation of varying acoustic and sedimentary facies of continental shelves, though research has tended in recent times to focus more on the identification of various bedform features, relating these either to the shallow stratigraphic record (Faugères et al., 2002; Le Bot and Trentesaux, 2004; Goff et al., 2005a, 2005b) or to strongly process-driven sedimentary responses to regional controls such as sea level and sediment supply (Snedden and Bergman, 1999; Snedden and Dalrymple, 1999), and (mostly) hydrodynamics (e.g. Swift and Field, 1981; Goff et al., 1999a; van Lancker et al., 2004; Zi and King, 2007). Significant progress has been made in the establishment of numerical and stochastic modelling on the geomorphological evolution of non-deterministic elements in the continental shelf environment (Goff et al., 1999a, 1999b, 2005a; Murray and Thieler, 2004). Surprisingly, relatively little attention has been paid to shelves such as the northern KwaZulu-Natal example, which are dominated by strong geostrophic currents (Viana et al., 1998). Scattered examples exist in the literature regarding such settings (e.g. Kenyon, 1986); the majority, however, focus on contouritic drift accumulation in deeper ocean basin environs (Stoker et al., 1998; Stow et al., 1998, 2002; Hernández-Molina et al., 2006.

In the case of the SE-African continental margin, Martin and Flemming (1986) and Birch (1996) observed several Holocene sediment depocentres on the northern KwaZulu-Natal coastline, the closest to the study area being a submerged spit complex offshore the St. Lucia/Mfolozi River, the largest and closest fluvial source to the study area (Fig. 9.1a). It is the reorganisation of Holocene sediment by strong western boundary flow of the Agulhas Current which most research has focused on (Flemming, 1980). Flemming (1978, 1980) described the southeast African inner shelf as an active zone of terrigenous deposition and transport, reorganised into subaqueous dunes, and the outer shelf as a zone of relict carbonate–rich and terrigenous gravels, with subordinate sediment drapes, reorganised into sediment-starved dunes, ribbons and comet marks.

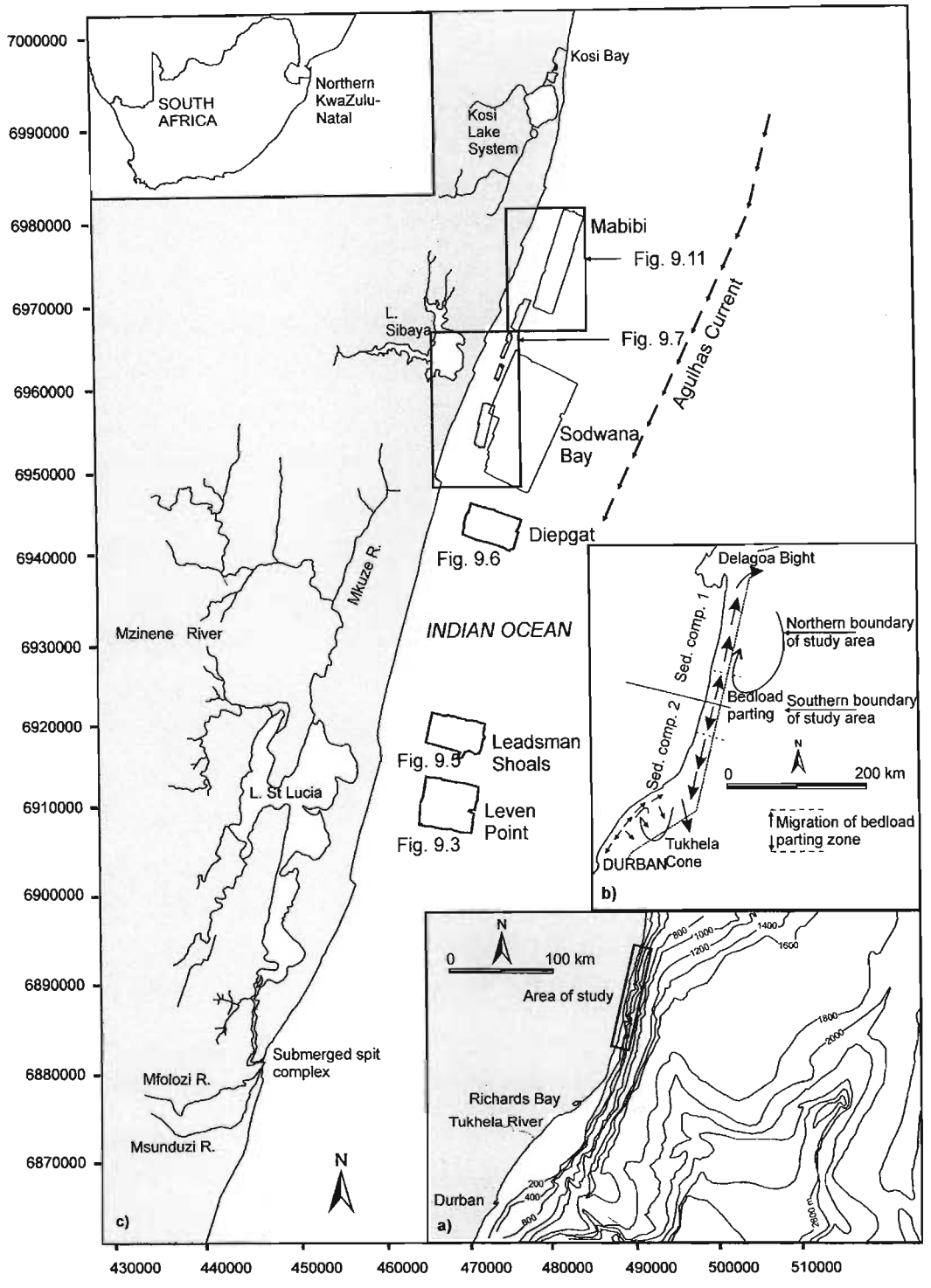

Figure 9.1. Locality map detailing **a** the regional context of the study (after Martin 1984), **b** recognised bedload parting zones from the east coast of KwaZulu-Natal (after Flemming and Hay 1988), and **c** the various areas investigated by co-registered multibeam bathymetry and side-scan sonar data denoted by offshore blocks. The survey areas inshore of the Sodwana and Mabibi blocks comprise side-scan sonar data only (copyright the Council for Geoscience). UTM zone 36S, eastings and northings in metres.

Zones of bedload parting occur, particularly where coastal offsets have resulted in the formation of return flows in leeside gyres, thereby moving sediment counter to the prevailing poleward (north to south) Agulhas flow (Fig. 9.1b). On the northern KwaZulu-Natal shelf, the bedload parting has been postulated to shift over a certain distance along the coast, depending on where the Agulhas Current meets the shelf at any particular time (Flemming, 1980).

Flemming (1978, 1980, 1981), Ramsay (1994) and Ramsay et al. (1996) described large (>150 m wavelength) subaqueous dunes from the inner to outer continental shelf of the northern KwaZulu-Natal continental margin. These vary in size, morphology and composition, with the apparent amalgamation of several large dunes giving rise to the formation of shore-detached sand ridges (L=1.2 km, H=12 m; *L* dune wavelength, *H* dune height) in the Sodwana Bay area (Ramsay et al. 1996). Side-scan sonar observations made by Ramsay et al. (2006) indicate several similar morphogenic features having formed further north in the Kosi Bay area which correspond to changes in coastal orientation relative to the Agulhas Current. According to Ramsay et al. (1996), the Sodwana Bay shelf is characterised by smaller subaqueous dunes on the inner shelf, which grade into large "sand wave" fields on the mid–outer shelf.

Side-scan sonar, multibeam bathymetry, Shipek™ grab samples and limited sub-bottom data, collected across the mid and outer northern KwaZulu-Natal continental shelf (Fig. 9.1), form the basis for an examination of the sediment dynamics of this part of the geostrophic current-dominated southeast African coastline. This part of the continental margin is the best understood example of sediment dynamics in an ocean current-swept shelf setting (e.g. Flemming, 1978, 1980, 1981; Ramsay, 1991, 1994, 1996; Flemming and Bartholomä, 2009). The northern section of this area is particularly unique in that several submarine canyons indent a very narrow (<5 km) shelf break (Green et al., 2007) which was exposed sub-aerially during the last glacial maximum (LGM) ~18 ka B.P. The construction of the modern shelf sediment wedge, and its associated bedforms, has thus been influenced by submarine canyon forms since the ensuing post-LGM transgression. This paper seeks to investigate the dynamics of the continental shelf in the light of newly collected data. Have changes in hydrodynamic regime occurred since the inception of the unconsolidated sediment wedge? Is sediment entrainment and bedform migration quasi-stationary and, in particular, what are the effects of submarine canyon incision on sediment dispersal patterns? A broad-scale model of the sediment dynamics of the shelf is thus proposed in the light of the above questions.

9.2. Methods

Apart from Mabibi, the mid–outer shelf and upper slope areas were imaged by a Klein 2000 side-scan sonar at 500 kHz with a 150 m scan range in order to visualise the seafloor sedimentary characteristics. Acoustic mapping of the inner shelf areas was supplemented by higher-resolution 500-kHz data acquired by a Klein 3000 system using a scan range of 75 m (NRF Innovation fund data courtesy of the Council for Geoscience). Only the 100-kHz frequency port and starboard channels were used in this study, owing to the regional scale of the mapping. The selected channels were then extracted to QMIPs format, and assigned navigational fixes acquired using a differential GPS system. Slant range distortion, antennae sway, and anomalous navigational points caused by DGPS drift were subsequently edited out of each line prior to the correction of tow-fish layback behind the DGPS antennae. The corrections were then reintegrated into the sonar QMIPs data for pre-mosaic visualisation. Corrected lines were processed with 25% overlap at a scan range of 150 m, the image quality enhanced, and the data exported as GeoTiff files used to generate mosaics in ARCGis 9. Multibeam bathymetry (see Green et al., 2007; Chapter 6) were used additionally to delineate topographic features such as depressions, scours, and bedform characteristics. Unfortunately, side-scan sonar data for the Mabibi area were faulty; thus, all interpretations of bedform dynamics for this section of the shelf are based solely on multibeam data. Morphometric measurement of bedforms were made from the multibeam data, capable of resolving targets spaced ~10 m apart and >30 cm in height. Where targets were more closely spaced, side-scan sonar data were used to resolve these features (~0.5–1 m horizontal resolution), though no height estimate could be made.

In addition four hundred line kilometres of single-channel, high resolution sub-bottom profile data were collected covering an area of 478 km^2 of the northern KwaZulu-Natal continental shelf and upper slope, some of which intersect the various bedform features discussed in this study (Fig. 9.1). Positioning was achieved using a differential GPS, with position fixes acquired at 1-s intervals. These were corrected using an MSK beacon correction, providing sub-metre accuracy. Sub-bottom data were collected using a Design Projects boomer system and 20 element array hydrophone, and recorded digitally in raw SEG-Y format via an Octopus 360 seismic acquisition system. Power levels of 500 J were used throughout the study with a median frequency of 600 Hz. Raw data was processed, with time-varied gain, bandpass filter (300-1200 Hz), swell filter and manual sea-bed tracking. Streamer layback and antenna offset corrections were applied to all digitised data. Higher resolution 3.5-kHz pinger sub-bottom profiler data of Shaw (1998) were used where large bedforms

were intersected by these profiles. For groundtruthing purposes a total of 170 grab samples were collected from the shelf and upper slope, and were analysed using a standard set of stacked sieves (see Green et al., 2008). Several SCUBA dives were also made in order to visually inspect various remotely sensed facies.

9.3. Shelf morphology and acoustic facies

The northern KwaZulu-Natal continental shelf may be subdivided into several distinct zones based on the average gradient, shelf width and position of the shelf break. The shelf break occurs at depths of ~100 m for all surveyed areas, average shelf gradients reaching between 4° (Leven Point and Sodwana), 5° (Leadsman and Diepgat) and 7° (Mabibi). The shelf width varies considerably from one area to another. On this basis four morphological provinces have been identified:

1. A narrow shelf with a steep gradient, e.g. Mabibi
2. A wide shelf with a low gradient, e.g. Leven Point
3. A shelf of intermediate width and gradient, e.g. Jesser Point and Wright canyon
4. A shelf of intermediate width and low gradient, e.g. Diepgat and Leadsman.

Within these morphological provinces, a number of acoustic facies have been distinguished on the basis of the acoustic backscatter characteristics of the seabed. These can be summarised as follows (Fig. 9.2):

1. Acoustic facies A: irregular, mottled to rippled high backscatter with subordinate patches of low backscatter;
2. Acoustic facies B: smooth, even-toned low-backscatter seafloor, punctuated by small, randomly orientated high-backscatter patches;
3. Acoustic facies C: high-backscatter, blocky to rugged linear seafloor features;
4. Acoustic facies D: smooth, even-toned moderate backscatter, punctuated by small pockets of higher-backscatter seafloor. This facies is restricted mainly to the upper continental slope.

Acoustic facies A typically comprises bioclastic-rich sediments of variable grain size, ranging from medium sand to pebbles, with typically high carbonate contents (80–100%). Bioclasts comprise whole/broken molluscan shells, echinoderm spicules, fragments of soft coral, bryozoan fragments and foraminifer tests.

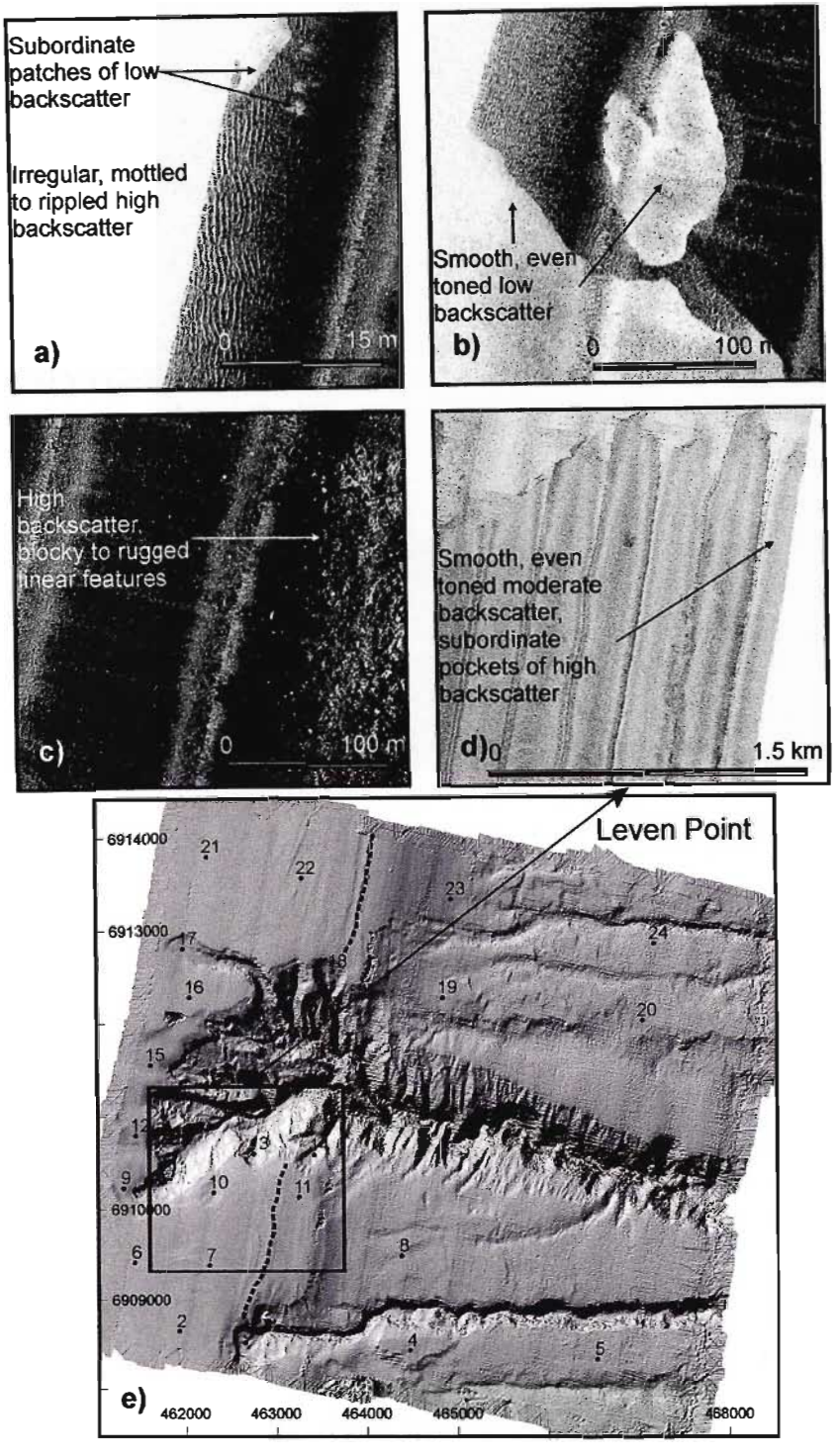

Figure 9.2. Examples of the various acoustic facies identified in the study area. **a.** Irregular, mottled to rippled high backscatter of facies A. **B.** Smooth even-toned low backscatter of facies B. Note the distinct facies boundary between facies A and B. **c.** High-backscatter, blocky to linear rugged seafloor of facies C. **d.** Smooth even-toned moderate backscatter with small pockets of higher backscatter of facies D. **e.** Multibeam bathymetry and Shipek™ grab sites for the Leven Point area. The *dotted line* denotes the shelf break at ~120 m depth.

Acoustic facies B corresponds to a fine to coarse-grained (0.125–1 mm), mixed quartz–carbonate sand. The carbonate content of these sediments is less than 25%. Shipek™ grab samples and Scuba observations reveal acoustic facies C to be comprised of rugged, variable topography beachrock/aeolianite outcrop. The term reef is used as a blanket term for facies C throughout this paper. No distinction is made between coralline/algal/bedrock varieties unless explicitly stated. Finer-grained sands of moderate carbonate content (30–50%) correspond to acoustic facies D of the upper slope (Fig. 9.2d, e). These form pockets of relict early Pleistocene sediments (see Green et al., 2008) which thinly drape the upper slope at depths greater than 140 m.

9.3.1. Leven Point

The inner continental shelf south of Leven Canyon is dominated by quartzose unconsolidated Holocene sediment. Isolated patches of reef occur mainly in the head of the canyon, where boulders of 10–25 m diameter have accumulated as blocky landslide rubble (Fig. 9.3). Two- and three-dimensional shoreface-detached dunes, orientated at 300/120° (L=100 m, H=~0.5 m), terminate against the nearshore Leven Reef complex, behind which quartzose clastic sediments have accumulated. The landward edges of these dunes become near-asymptotic towards the seaward-facing ridge of the aeolianites of Leven Reef and less prominent northwards towards the Leven Canyon southern margin (Fig. 9.3). Featureless quartzose shelf sands dominate the inner shelf flanking the rim of the Leven Canyon head. Sediments are typically medium- to coarse-grained sand, with minor gravel constituents. Where the Leven Canyon's sinuous upper tributary intersects the inner shelf, widespread two-dimensional (2D) dunes (L>15 m, H<0.3 m) orientated at 250/060° migrate towards the topographic depression. The upper limits of this depression are bounded by sandy margins, and the most landward extent is filled by unconsolidated sand which thins seawards. Shipek™ grab samples retrieved from the upper parts of the tributary comprise medium to very coarse sand, are moderately well sorted, and have a slight negative skew (Fig. 9.4). The gravel fraction (0.5%) comprises broken molluscan fragments, sclerites of soft coral, bryozoan fragments and small amounts of broken echinoderm spines. 2D dunes abut against gravel ribbons in the northern extent of the survey block, and become increasingly bioclastic-rich in the mid-shelf region.

Subdued relief reef crops out in isolated patches towards the mid–outer shelf, separating these isolated sand patches from an outer-shelf bioclastic pavement. Where bedforms abut against the steeper and deeper mid-shelf parts of the inner shelf extension of Leven Canyon, they become increasingly sinuous, merging into arcuate isolated sand patches mantling extensive carbonate

sediments. In the mid–outer shelf region between the Leven and Chaka canyons, sinuous 2D dunes (L=75–150 m, H=0.6–5 m) orientated at 100/280° abut at least three reef complexes which are orientated at 010/190° and curve north-westward towards the Leven Canyon margin.

9.3.2. Leadsman Shoals

The inner shelf of the Leadsman Shoals area is dominated by Red Sands Reef, a prominent northeast-southwest-trending reef complex comprising beachrock/aeolianite, which rests within erosional depressions of older beachrock/aeolianites. The southernmost part of the inner shelf comprises extensive carbonate gravels and isolated quartzose sand patches, which abut against the seaward flank of Red Sands Reef (Fig. 9.5). These merge with lobate, sediment-starved dunes (L=70–100 m, H=~0.5 m) orientated at 320/140° and which abut a prominent sand ribbon field.

Sand ribbons extend from the seaward flank of Red Sands Reef into the mid-shelf region and have a relief of ~1 m relative to the surrounding seafloor. Sand ribbons become progressively sediment-starved northwards, exposing extensive sections of carbonate pavement. Small 2D dunes (L=5–10 m, H<resolution of echosounder) orientated at 090/270° extend across much of the northern section of the mid shelf of the Leadsman area. These abut isolated patches of subdued reef, and both the northern and southern sections of the Leadsman Canyon head complex.

9.3.3. Diepgat

A set of large 2D dunes (L=50–150 m, H=1–1.5 m) occurs north of the Diepgat Canyon head on the inner continental shelf (Fig. 9.6). Bedform crests become increasingly flattened with distance away from the canyon head. South of Diepgat Canyon, large 2D dunes (L=40–70 m, H=0.3–0.5 m) are orientated at 010° towards the canyon head (Fig. 9.6). An extensive train of medium-sized 2D dunes with bifurcating crests occurs north of Diepgat Canyon in water depths of 100–120 m. These abut scattered reef outcrops at the shelf break at a depth of 120 m, which exhibit subdued backscatter and a flattened morphology. Similarly, reef crops out south of the canyon at comparable depths with identical morphology and acoustic characteristics.

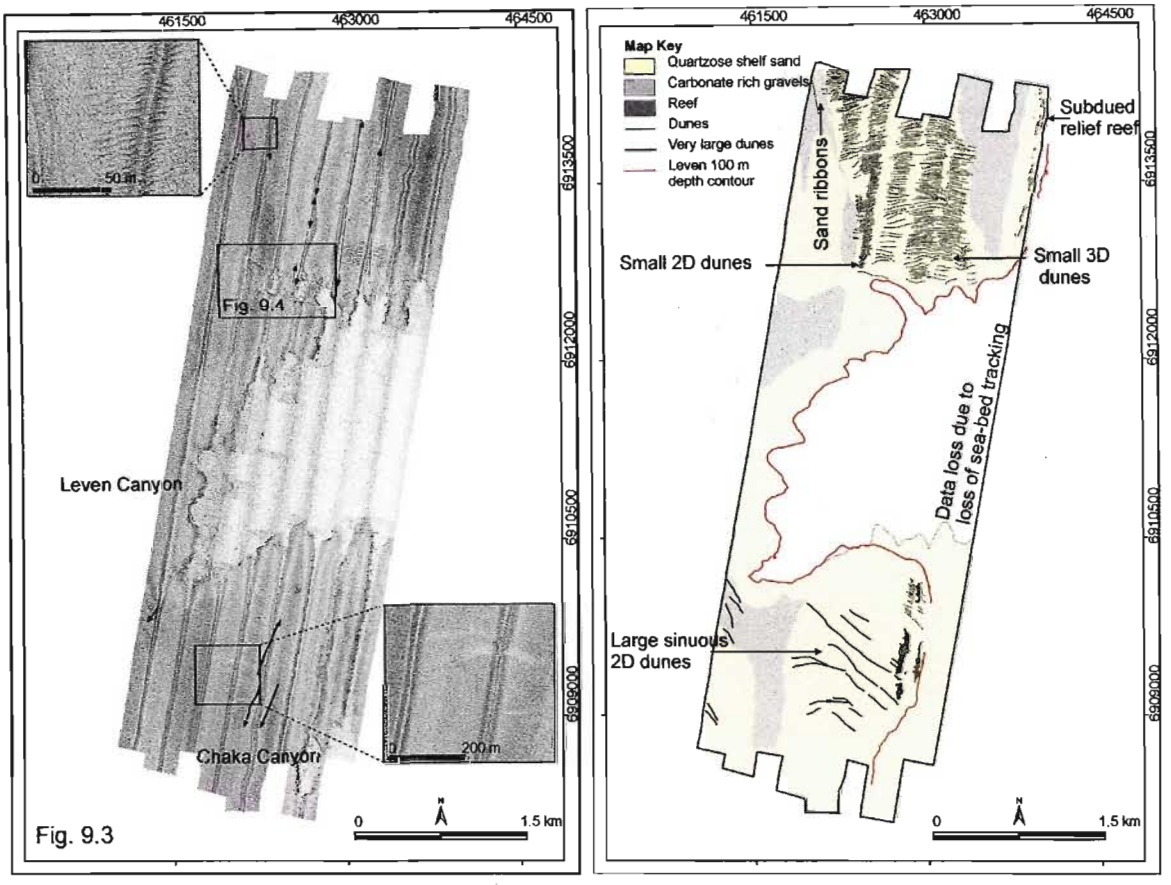

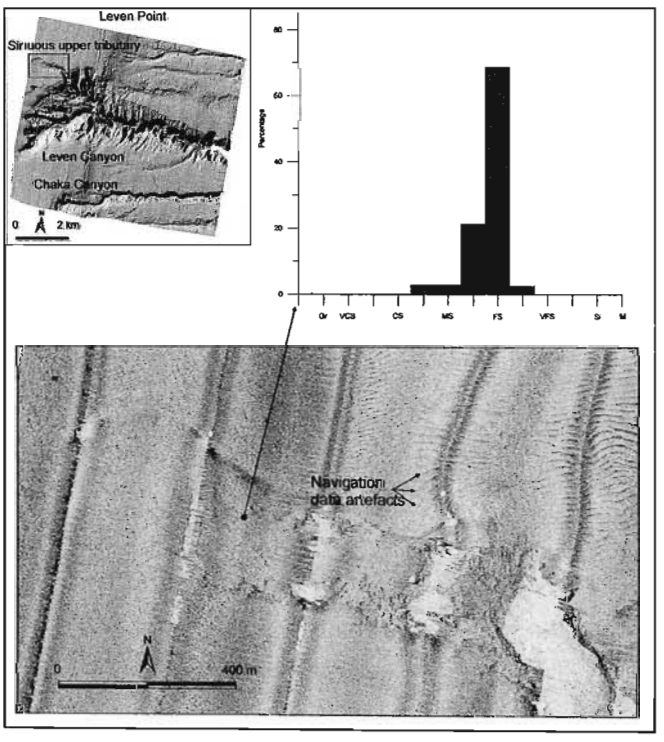

Figure 9.3. Side-scan sonar mosaic of the mid–inner shelf offshore Leven Point and interpretative seafloor geology map. UTM zone 36S, easting and northings in metres. Note the abundance of dunes north of the canyon head, the crests becoming increasingly sinuous towards the canyon rim. **Figure 9.4.** Grain size distribution of a grab sample taken from the upper portions of Leven Canyon's sinuous tributary. The sample is moderately well sorted, and comprises predominantly fine sand. Note, however, the surrounding boulder debris within the tributary, suggesting that this is a fine veneer of shelf sediment which rests on or within debris derived from landslides during tributary extension.

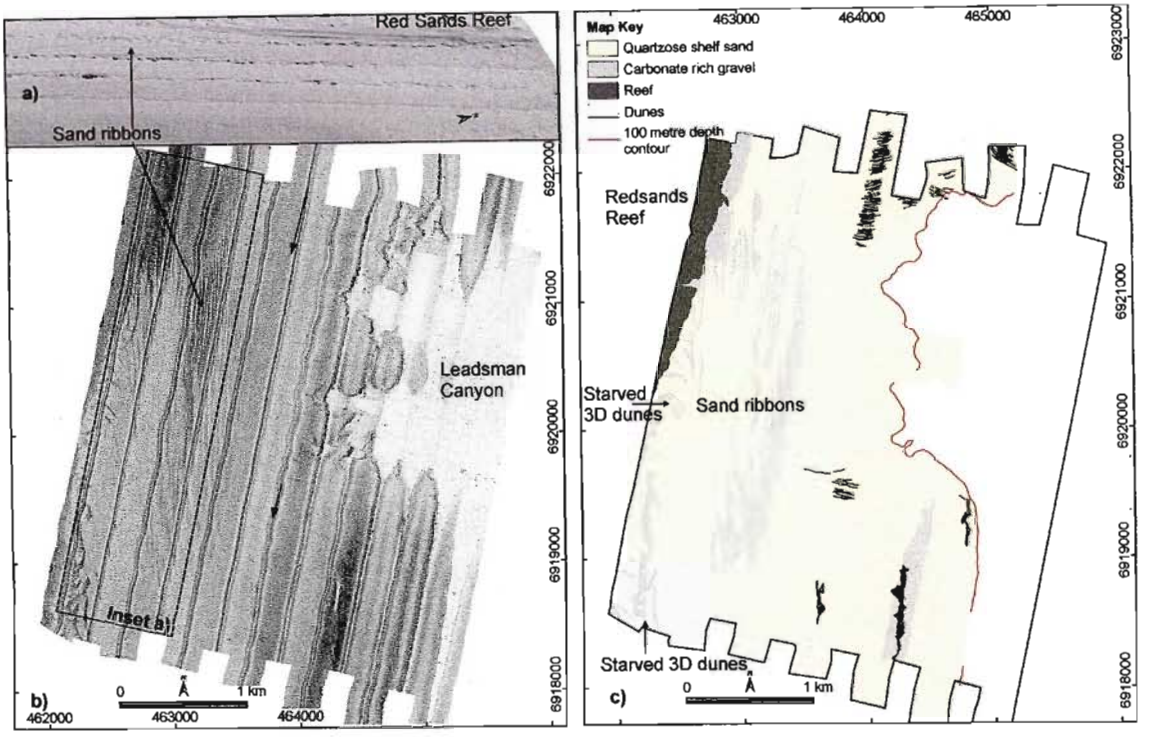

Figure 9.5. Side-scan sonar mosaic and interpretative seafloor geology map of the mid–inner shelf of Leadsman Shoals, detailing the Leadsman Canyon head. UTM zone 36S, eastings and northings in metres. Note the prominence of sediment-starved areas, with abundant sand ribbons covering most of the continental shelf mapped to date. *Arrows* depict the direction of bedform movement.

9.3.4. Sodwana Bay

9.3.4.1. 2 Mile Reef and Wright Canyon South

Side-scan observations reveal extensive reef outcrops from the inner shelf, spanning the area from Jesser Point to Wright Canyon (Fig. 9.7). The largest of these, 2 Mile Reef, comprises beachrocks and aeolianites (Ramsay 1994). Scuba observations reveal that bedforms within the reef complex comprise carbonate-rich gravels reworked into large, sharp-crested wave ripples (L=0.6–1.5 m, H=10 cm; Fig. 9.8c), which rest within gullies in the reef or abut against the most landward part of the reef complex. Gully-confined bedforms occur perpendicular to the confining gullies, which represent a dominant fracture set within 2 Mile Reef, orientated at 100/280°. Smaller isolated patches of carbonate-rich gravels are widespread within the 2 Mile Reef complex, and possess bedforms of orientations and dimensions similar to those mentioned above.

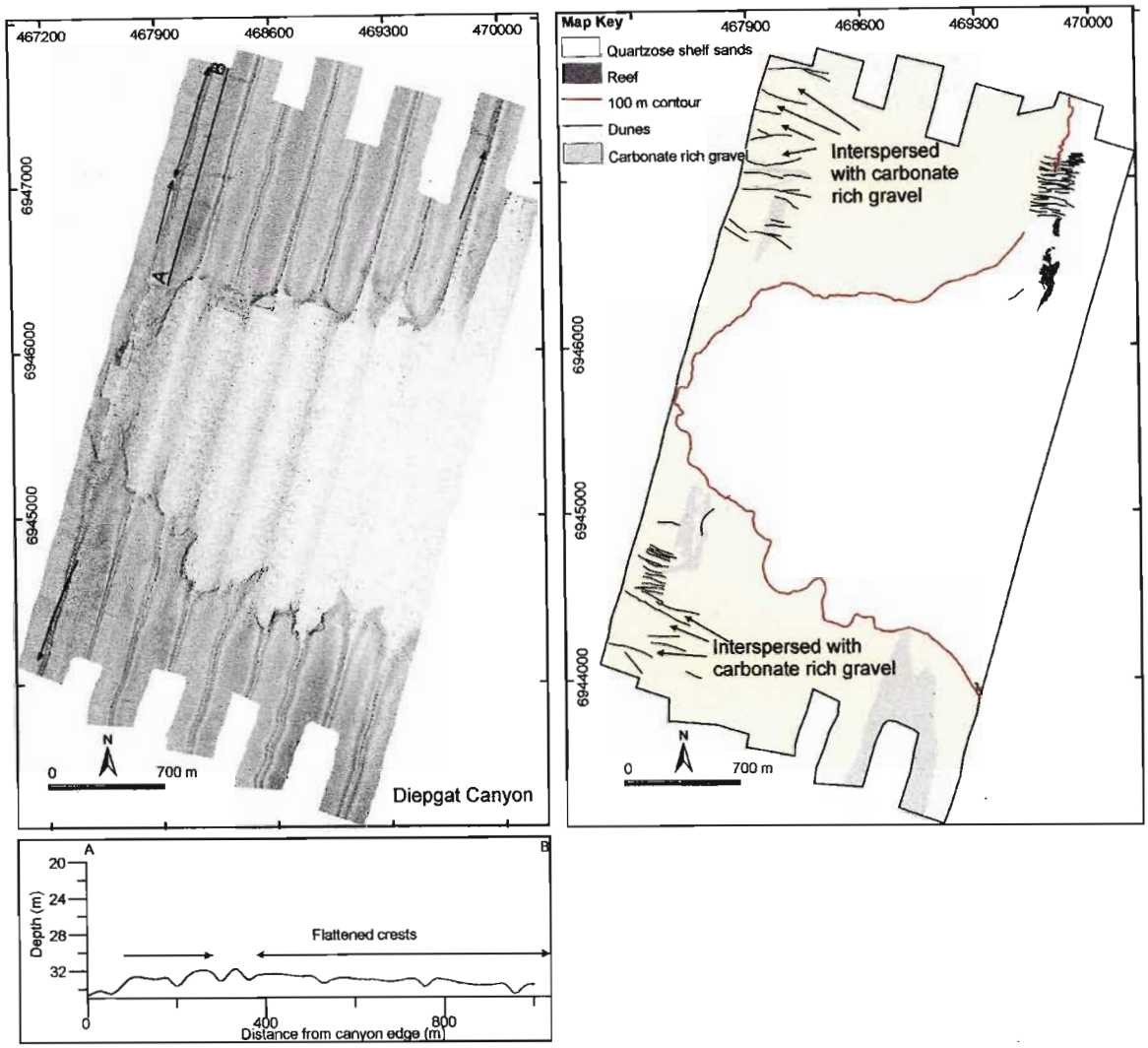

Figure 9.6. Side-scan sonar mosaic and interpretative seafloor geology map of the inner–mid shelf of the Diepgat Block. The bedform field to the south of the canyon head comprises a high proportion of carbonate-rich gravel, occurring mainly within the troughs of each very large dune. *Arrows* depict the direction of bedform movement. Note the progressive flattening of bedform crests northwards from the canyon. UTM zone 36S, eastings and northings in metres

Subordinate interference ripples are common (L=15–20 cm, H=3–5 cm; Fig. 9.8c). Very distinctive facies boundaries occur between the coarse-grained carbonate facies of the inner-shelf rippled scour motes and the adjacent finer-grained quartzose sands. The mid- to outer-shelf sections surrounding Wright Canyon are dominated by large 2D dunes (L=75–150 m, H=0.5 m; Fig. 9.7). Elongate sediment bodies of high backscatter occur within the troughs. These consist of coarse, gravel- to pebble-sized clasts of coral, mollusc valves and other bioclastic material (Fig. 9).

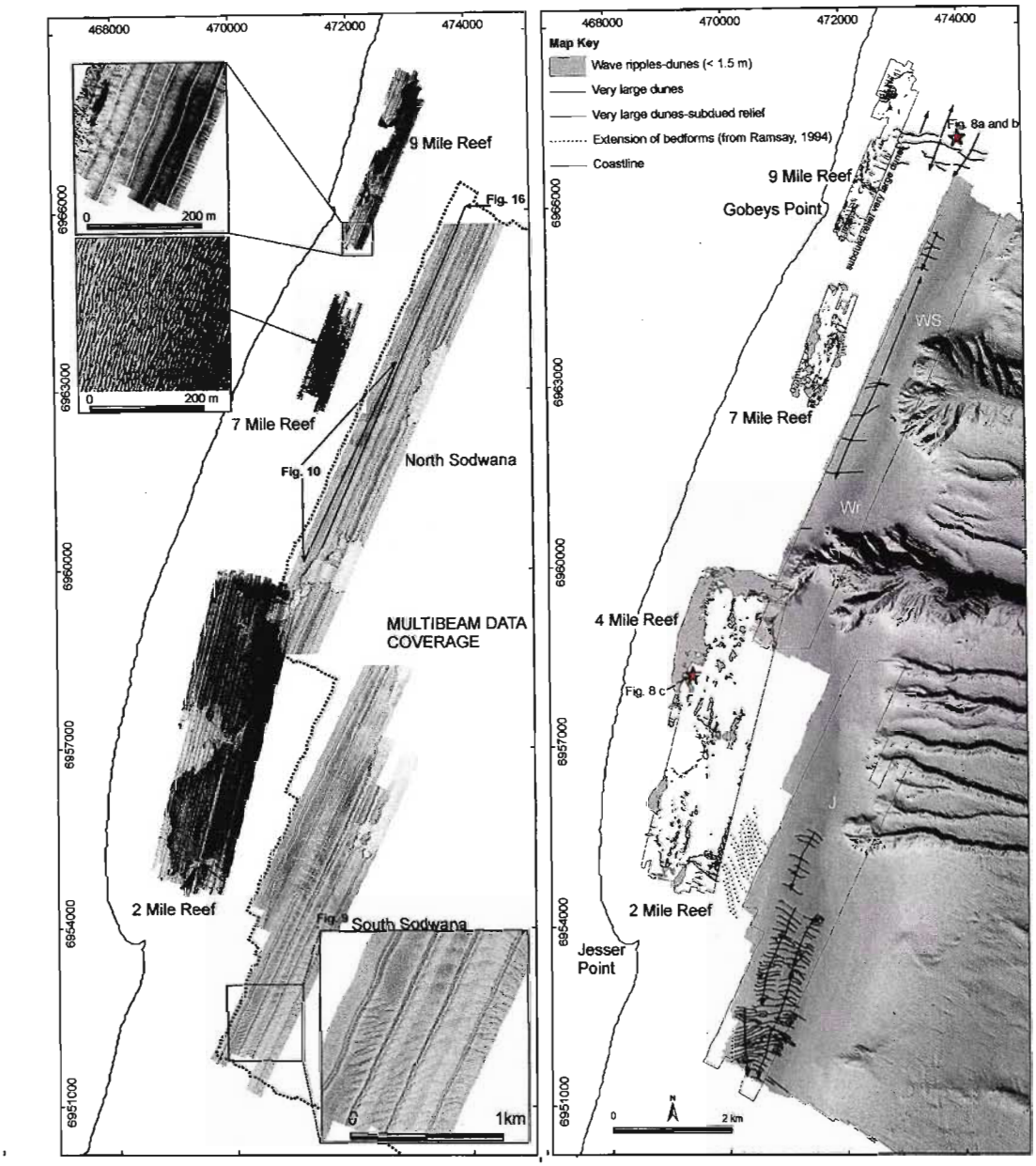

Figure 9.7. Side-scan sonar mosaics for the Two-Mile–Nine-Mile Reef complexes, together with side-scan sonar mosaics and multibeam bathymetry from the mid continental shelf of Sodwana Bay. UTM zone 36S, eastings and northings in metres. *Arrows* depict the direction of bedform movement. *J* Jesser Canyon, *WS* White Sands Canyon, *Wr* Wright Canyon. Note the presence of bedload partings adjacent to the head of White Sands Canyon, and in the Jesser Point bedform field. Similar fringing zones of convergence are apparent, the White Sands convergence coinciding with the sand ridge crest identified in Fig. 9.16. Inshore mosaics of 2 Mile, 7 Mile and 9 Mile Reef copyright Council for Geoscience

The large 2D dunes extend into the mid–inner shelf where they abut the outer margin of 2 Mile Reef. In areas where the sediment cover is very thin, subdued reef outcrops separate the inner extensions of the dune field from the mid-shelf dune field.

9.3.4.2. Wright Canyon North, 7 Mile and 9 Mile Reefs

The middle to outer shelf north of Wright Canyon (Fig. 9.7) displays a poorly defined dune field comprising a sand ridge (L=1,300 m, H=5 m; Fig. 9a, b) superimposed by 2D–3D bedforms with very large wavelengths and heights (L=500 m, H=3–5 m), and climbing, very large 2D dunes (L=100 m, H=0.6 m). These bedforms have a subdued bathymetric expression, display little backscatter variation across troughs and crests, and are best discerned in cross-sectional form derived from the multibeam data (Fig. 9.10). North of White Sands Canyon, an area of thinly developed Holocene sediment occurs, with few to no bedforms. Isolated very large 2D dunes (L=150 m, H=2 m) occur in the northernmost region of the mid-shelf, offshore Gobeys Point (Fig. 9.7). 7 Mile Reef displays few bedforms, apart from locally developed patches of bioclastic gravel reworked into large symmetrical wave ripples. North of this, large 2D dunes with subdued relief occur within quartzose sand patches surrounding 9 Mile Reef. These dunes have heights of less than 0.5 m, spacings of between 10 and 20 m, and grade into very large, sinuous 2D dunes offshore of the reef complex (see Mabibi section below). Inshore of this, on the landward side of the aeolianite/beachrock outcrop of 9 Mile Reef, a well-developed train of large 2D dunes occurs. Throughout the 9 Mile Reef complex, isolated patches of bioclastic sediment are reorganised by wave action into large symmetrical wave ripples (Fig. 9.8a).

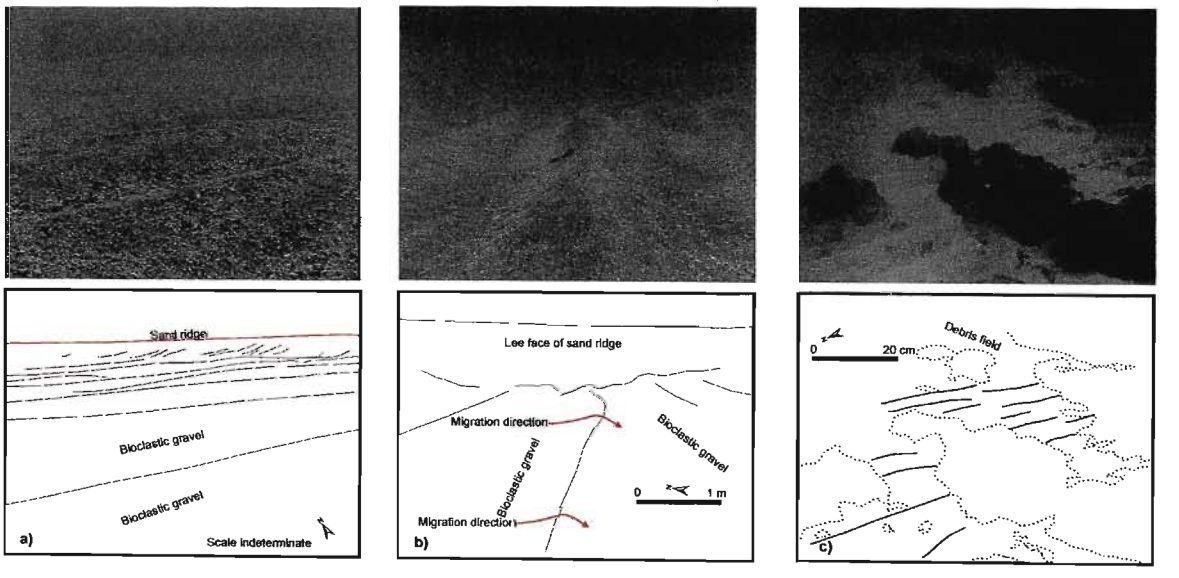

Figure 9.8a. Wave ripples consisting of bioclastic gravel on the mid shelf, 9 Mile Reef area. Note the sand ridge crest in the distance, with secondary ripples aligned shore parallel along the lee face. **b.** Wave ripples of bioclastic gravel in dune troughs. Note how the ripples abut the lee face of the Nine-Mile sand ridge. **c.** Shore-parallel gullies within 2 Mile Reef displaying wave-generated ripples. Photographs courtesy Mr. W. Kidwell

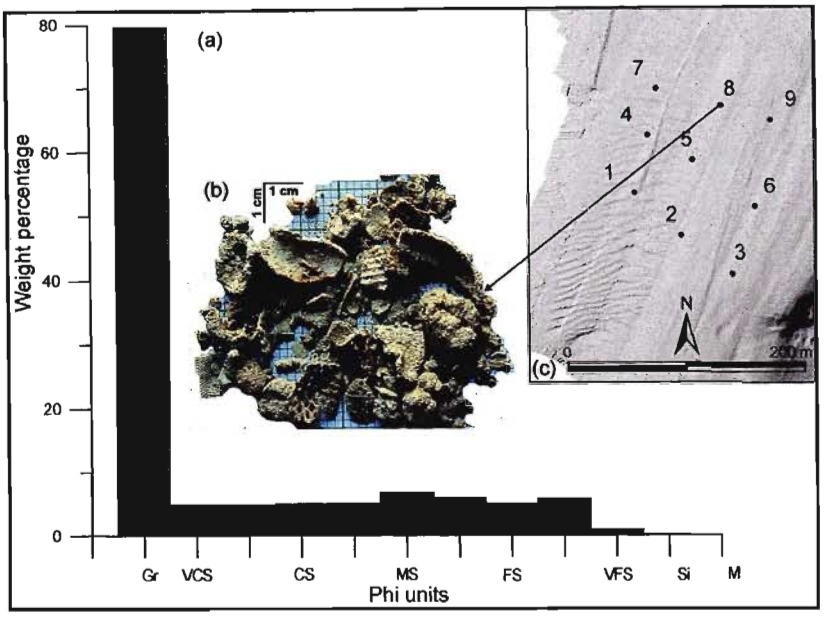

Figure 9.9a Grain size distribution of a typical sample (sample 8) retrieved from high-backscatter areas between very large dunes offshore Jesser Point. Note the skew towards the very coarse sand/gravel fraction. **b.** Photograph of >2 mm (gravel) fraction of sample 8, showing clasts almost entirely of carbonate composition. Bivalve and coral (predominantly *Porites* sp. and *Flavites* sp.) fragments are especially prevalent. Note that the small squares on background=1×1 mm. **c.** Shipek grab sample positions, Sodwana Block. Note the location of sample 8 within the trough between two very large dunes. Grab samples are discussed more thoroughly in Green et al. (2008)

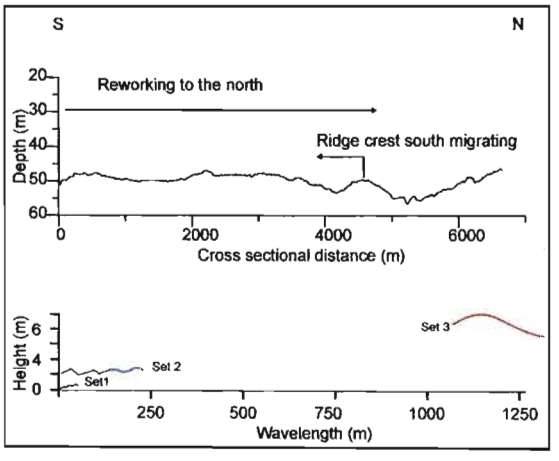

Figure 9.10. Bathymetric cross section across the mid–outer shelf, north of Wright Canyon. Note three generations of bedform, a large sand ridge, upon which very large-wavelength (~500 m) dunes are superimposed (lower graph). Superimposed on these, in turn, are climbing 2D very large dunes (~100 m wavelength). The younger superimposed dunes are moving towards the north, whereas the sand ridge is north to south asymmetrical, indicating southerly migration.

9.3.5. Mabibi

The Mabibi area has several large dune fields, associated with the southern parts of the heads of several submarine canyons (Fig. 9.11). Dunes become progressively better organised towards the southern boundary of the area where extensive dune fields occur (2,000–4,500 m long) before terminating in the mid-shelf seaward of 9 Mile Reef. The mid-shelf parts of these are characterised by very large sinuous dunes (L=>100 m, H=0.5–1 m), which grade into smaller dunes (L=5–10 m, H<resolution of echosounder) on the mid–outer shelf. These smaller dunes become increasingly sediment-starved towards the outer shelf, where they merge into relict bioclastic gravels with thin, subordinate sand ribbons. Interspersed throughout this area are poorly developed small dunes which are surrounded by patchy or pockmarked carbonate gravels. These are concentrated in the troughs of larger dunes, offshore of Beacon 13 and 9 Mile Reef. Lee faces of the larger mid-shelf dunes are orientated at 220/020°, whereas the smaller mid–outer shelf dunes are orientated around the larger dune bodies and the patches of poorly developed small dunes (Fig. 9.11).

9.4. Bedload parting and zones of convergence

Several bedload partings are evident in the area (Figs. 9.3, 9.5, 9.6, 9.7, 9.11), indicating sediment transport directions in a northerly direction, i.e. in the opposite direction to the predominantly south-flowing Agulhas Current. Major parting zones are evident adjacent to the heads of larger shelf-indenting canyons where bedforms migrate in a northerly direction, counter to the flanking southerly migrating dunes. These are most prominent in the Mabibi area, particularly in the heads of South Mabibi and Mabibi canyons which appear to have sediment cascading into the canyon heads from the southern margins (Fig. 9.11). In the mid-shelf region, inshore of the canyon heads, the flow is aligned to the south. A major bedload convergence zone can be observed on the mid-shelf off Hulley Point (–50 m). Here, bedload transport is towards the north until it meets the lee face of a single, southerly migrating sand ridge. South of this, opposite Beacon 13, another bedload parting occurs at a depth of 50 m where an area of laterally extensive bioclastic gravel pavement is mantled by poorly developed small dunes. A localised, inner to mid-shelf bedload parting is situated at the southern limit of the Mabibi bedform field. Less prominent bedload partings occur inshore of the White Sands Canyon head (55 mbsl) and in the mid–outer shelf region of the prominent Jesser Point dune field (corresponding to the coastal offset at Jesser Point; Fig. 9.7). At the Jesser Point bedload parting, the dune field bifurcates sharply. Climbing dunes south of this bifurcation point are characterised by a classic stacking pattern.

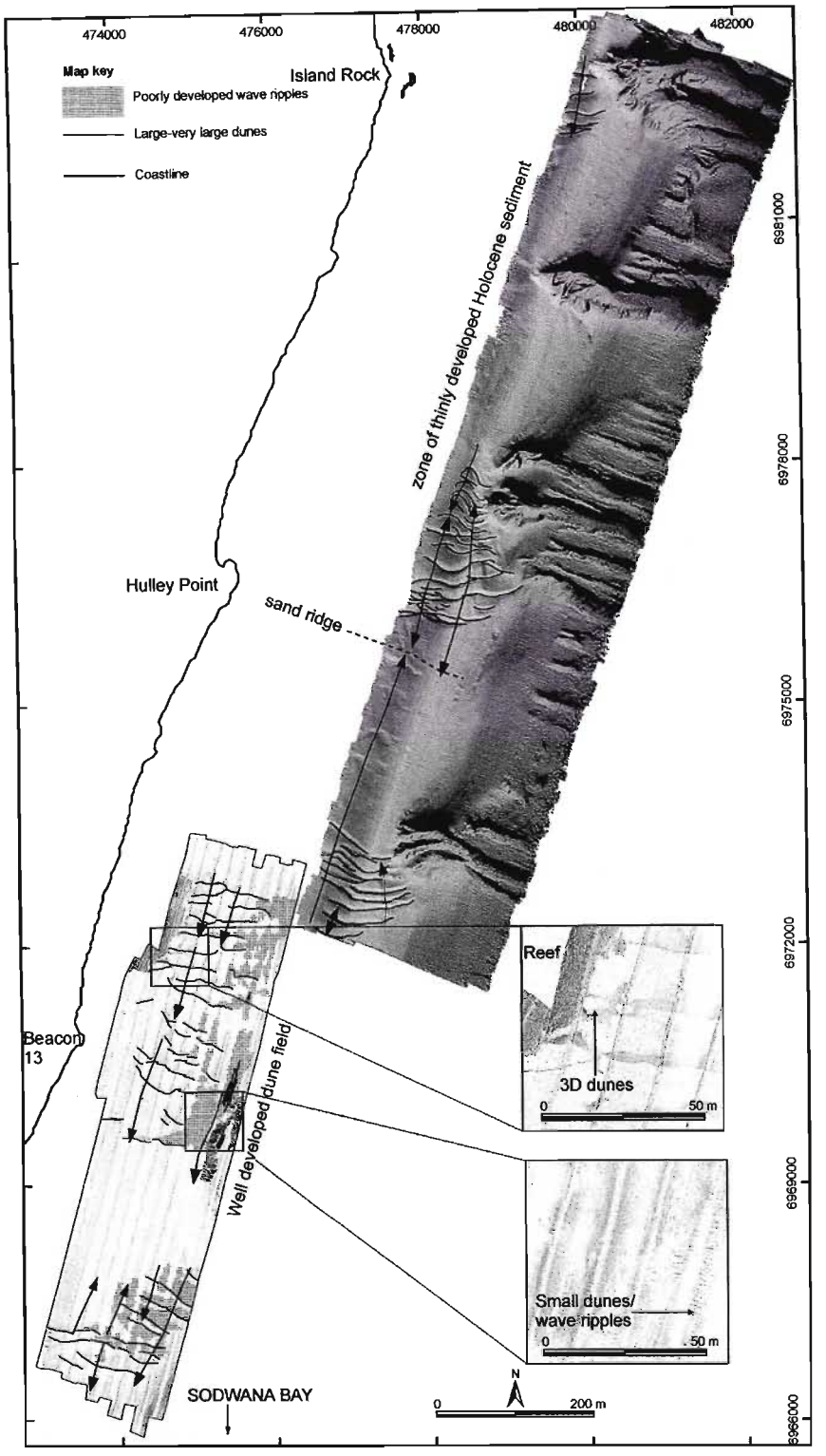

Figure 9.11. Side-scan sonar and multibeam bathymetric data for the Mabibi area, indicating the direction of bedform migration. Zones of bedload parting and convergence are indicated by *arrows* parting and converging respectively. UTM projection zone 36S, eastings and northings in metres. Inshore side-scan sonar mosaic copyright the Council for Geoscience.

In this region, dunes with long axes aligned at 265/085° start to overstack more east-west-aligned dunes and terminate at the lee face of a southerly oriented sand ridge. Overspilling of faster migrating, southerly moving 2D dunes has resulted in dune superimposition down the lee face and into the trough of this ridge. Where bedload transport converges in this region, the convergence zone is marked by flattened, north-oriented dunes within the trough of a sand ridge (H=~3 m). This feature has been heavily reworked, and is superimposed by both northward- and southward-moving 2D dunes. Despite this reworking, the sand ridge is still crudely oriented in a southerly direction (Fig. 9.10).

Notwithstanding the lack of well-developed dune fields, Leven Point has several small-scale bedload partings and convergences (Fig. 9.3). The mid-shelf dunes north of Leven Canyon display micro-partings and -convergence, together with areas of flattened dune crests. Bedload partings become better developed towards the outer-shelf carbonate gravel pavement in this area. Here, sediment is entrained away from the canyon head towards the north whereas, further inshore, 3D dunes and sediment-starved dunes migrate towards the sinuous tributary of the Leven Canyon head. South of Leven Canyon, inshore of the Chaka Canyon head, an isolated bedload parting is located within an arcuate dune field. Southerly bedload migration resumes at the deepest end of this small dune field, and it appears that these dunes bypass the shelf-indenting head of Chaka Canyon.

Bedload reversal against the prevailing Agulhas Current occurs inshore of Diepgat Canyon, where dunes are orientated towards the north (Fig. 9.6). These merge into dunes which become progressively flattened. In the mid–outer shelf region, north of the canyon, smaller dunes are oriented towards the north and abut the outer-shelf gravel pavement.

9.5. Morphometric observations

The dimensionless wave form index L/H (the ratio of wavelength to height) varies considerably between the various morphological provinces (Fig. 9.12). Zone 1 type areas exhibit L/H ratios of between 17 and 421. The outer shelf has smaller L/H values; thus, bedforms become increasingly larger, and increase in relief with depth. The wide shelf and low gradient of the Leven Point shelf is associated with a mixed distribution of L/H values ranging between 47.5 and 984. The mid-shelf area north of Leven Canyon is characterised by very large dunes with subdued relief, whereas south of Leven Canyon a wider spread of values is observed, indicating greater variability in relief and size, most likely a product of the wide shelf accommodating several flow regimes which would

result in spatial heterogeneity of bedforms. Areas of intermediate width and slope such as that of Sodwana Bay area possess a wide array of wave form indices, indicating significant variability in dune morphology in this region. Lastly, areas of intermediate width and low gradients have few well developed bedform fields and show marked variance between height and a relatively constant wavelength of ~90 m (Fig. 9.12). Wave form indices for the Diepgat and Leadsman blocks vary from 73–395 and 272–1,841 respectively, these values indicating that dunes in the Leadsman area have very low relief, relative to their spacing.

Bedform spacing throughout the mapped areas varies considerably and is very poorly correlated with depth (Fig. 9.13). The largest bedforms, sand ridges of subdued relief, occur in the Mabibi mid-shelf and the inner shelf inshore of the Wright Canyon head at ~50 mbsl. Apart from these bedforms, wavelength groupings appear randomly distributed throughout the inner, mid and outer shelf environments. Spacing values are randomly distributed in terms of distance from the canyon thalweg (Fig. 9.14).

9.5.1. Shallow stratigraphy

High-resolution sub-bottom profiling across the dunes of Sodwana Bay reveals little about the internal structure of these features which, on the whole, appear acoustically transparent. They also do not trace the topography of the underlying erosional LGM sequence boundary (SB). 3.5-kHz profiles from the Jesser Point area, as interpreted by Shaw (1998), yield similar results. However, the surface over which these dunes migrate is more clearly visible where it crops out in the dune troughs (Fig. 9.15). This reflector corresponds to reflector 3 which caps the transgressive systems tract found within buried incised valleys along this section of the continental shelf (Chapter 4). It underlies all bedforms in areas associated with high current velocities such as sand ribbons and isolated lobate dunes. Sand ridges on the Mabibi shelf typically form where subsurface depressions mark this sequence boundary (Fig. 9.16). However, their apparent angle of climb (as defined by Allen, 1982) cannot be recognised.

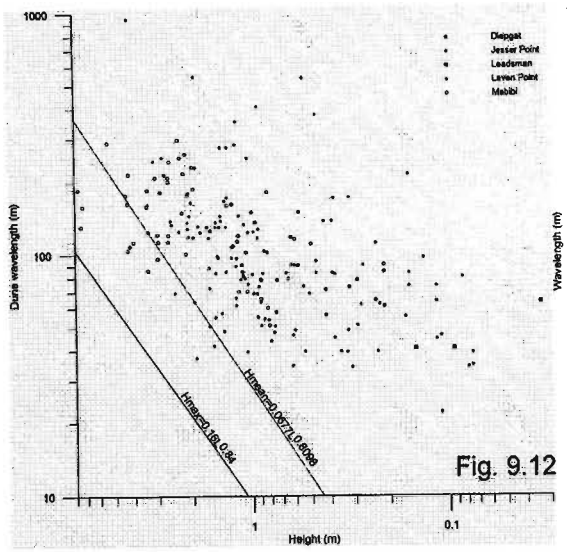

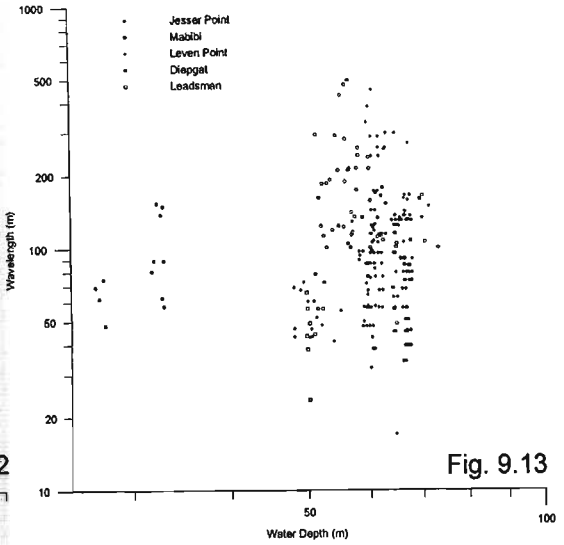

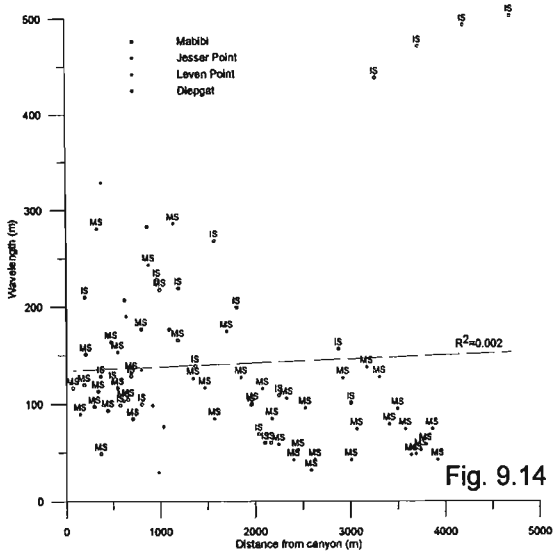

Figure 9.12. Morphometric plot of wave form indices (wavelength vs. height) for the major bedform fields of the study area. Type 2 areas, such as Leven Point, have bedforms which have highly variable L/H values, compared to type 3 areas (e.g. Sodwana dune fields). Type 4 areas, such as Diepgat and Leadsman, appear to have L/H values with very low relief relative to dune spacing. Lines representing global $Hmean=0.067L^{0.8098}$ and global $Hmax=0.16L^{0.84}$ are shown for reference purposes (Flemming and Bartholomä 2009). Axes are on a logarithmic scale, base 10. **Figure 9.13.** Morphometric plot of wavelength–water depth relationships. Spacing varies considerably with depth, and cannot be correlated. The largest bedforms occur in the mid shelf of Mabibi and the mid–inner shelf inshore of the Wright Canyon head. Axes are on a logarithmic scale, base 10. **Figure 9.14.** Plot of wavelength vs. distance from canyon thalweg for the major bedform fields of the study area, showing an absence of relationship between these two parameters. Values for the Mabibi shelf are denoted by text, as this comprises the widest field and an investigation into shelf zonation (e.g. inner–mid shelf) was additionally undertaken. *IS* Inner shelf, *MS* mid shelf.

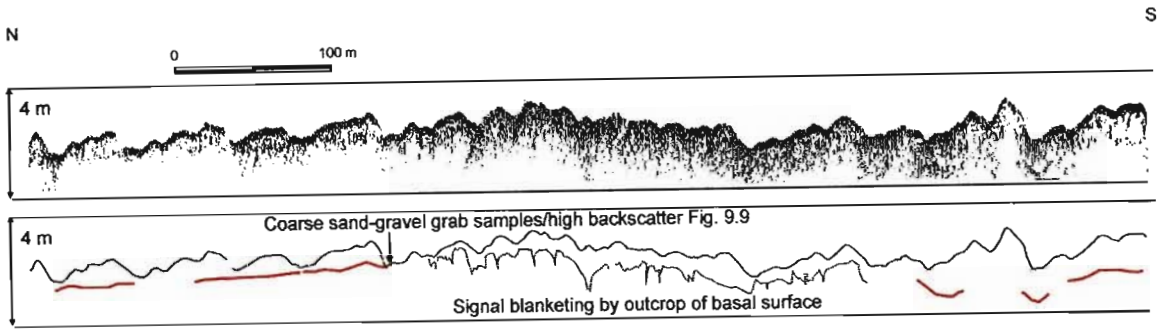

Figure 9.15. 3.5-kHz echosounder profile across very large dunes in the Jesser Point area, and interpretative line drawing of subsurface structure (modified from Shaw 1998). A prominent subsurface reflector crops out within dune troughs of the bedform field. This outcrop coincides with high-backscatter areas within the dune troughs, comprising a coarse shelly hash (see Fig. 9) of predominantly gravel to pebble clast size. This surface is also recognised in boomer profiles (Green 2009) and corresponds to surface 3, or the regional Holocene ravinement surface.

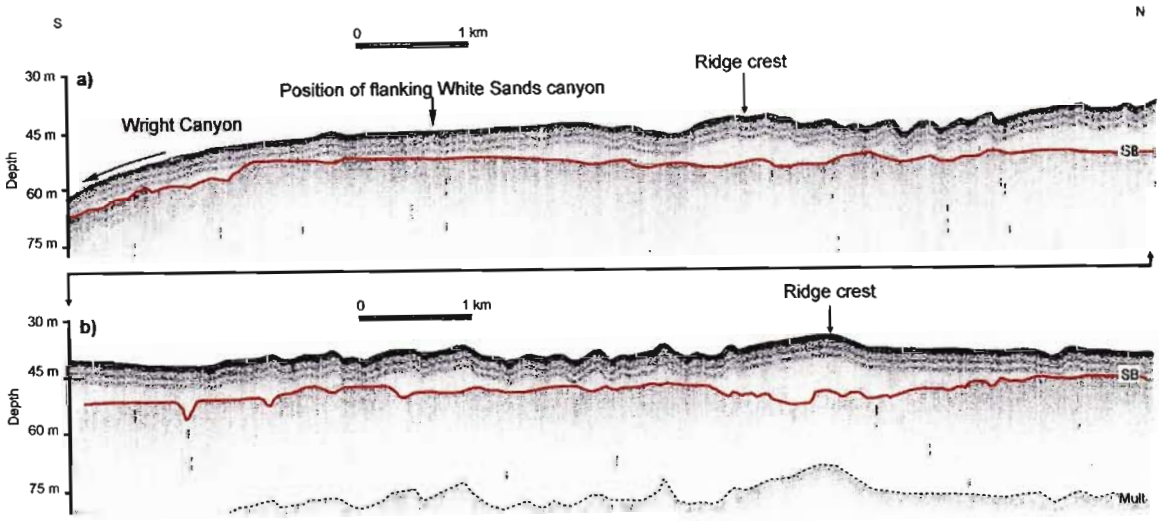

Figure 9.16a. Boomer sub-bottom profile across bedform fields in Sodwana Bay, inner–mid shelf, between Wright Canyon and Mabibi. Note the depression in SB2 beneath the sand ridge crest north of the White Sands canyon head. **b.** Boomer sub-bottom profile through the Mabibi bedform fields. Again, note the subsurface depression within SB2 beneath the sand ridge crest. Images are vertically exaggerated. *SB* sequence boundary.

9.6. Discussion

9.6.1. Controls on acoustic facies distribution

The narrow northern KwaZulu-Natal continental shelf is dominated by the strong geostrophic Agulhas Current, which has exerted a strong influence on the distribution and zonation of the various sedimentary facies of the shelf. Quartz-rich shelf sands occur predominantly on the inner to mid shelf of all areas mapped to date, and comprise the sediments of the modern transgressive sediment wedge. The transition zone between the outer-shelf bioclastic pavements and the inshore

sediment wedge is particularly distinctive, suggesting an erosional contact between these. This relationship is apparent as far north as Kosi Bay (Ramsay et al., 2006) and suggests that a regional control exists on the zonation of these two acoustic facies types. These mirror the inner terrigenous and outer relict carbonate acoustic facies on the southeast African continental margin recognised by Flemming (1978) south of Cape Vidal. Moored ADCP data of Morris et al. (2007) indicate that, on this part of the shelf, the southerly flowing Agulhas Current exceeds the critical bed shear velocity required to move medium sand (the dominant mean sand size) and, as such, has denuded the mid–outer shelf of much of its sediment. The observed extension of this facies into the shallow mid-shelf areas of the Leadsman Shoals sector indicates that inshore meandering of the Agulhas Current, as described by Pivechin et al. (1999) and Lutjeharms (2006) must occur here. In this instance, the bioclastic gravel surfaces underlie scattered sand ribbons. Similar examples occur in the Leven Point area where isolated, lobate patches of quartzose sand mantle extensive carbonate gravels. Shipboard ADCP data are consistent with this observation (Roberts pers. comm.), indicating an area of relatively high current velocities. Flemming (1978) and Flemming and Hay (1988) considered these carbonate gravels to be relict lag deposits. On the basis of the semi-consolidated coralline and beachrock pebble to gravel grain sizes, the large amounts of shelly detritus, and the regional nature of the outcrop of this material, this surface is considered the ravinement surface of the rapid mid Holocene transgression.

9.6.2. Sediment bypass and loss from the shelf

Holocene sediment is concentrated mainly on the inner to middle shelf where they abut late Pleistocene palaeo-dune cordons which separate the active Holocene sediment reservoir from the relict outer gravel pavement. This has reduced to some extent the coast-normal losses of sediment over the shelf break. Similar reservoir effects of a relict mid-shelf coastal dune ridge have been recognised along the south coast of KwaZulu-Natal (Flemming, 1981; Flemming and Hay, 1988). The presence of Lower Pleistocene sediments on the upper slope (Green et al., 2008) suggests that there is no widespread off-shelf sediment transport, very local exceptions being precluded. Ramsay (1994) and Ramsay et al. (1996) consider sediment dispersal via entrainment into submarine canyons as being one of the major factors in exporting sediment to the adjacent abyssal areas. Studies from the Bay of Biscay indicate similar processes, whereby dune trains are intercepted by canyon heads on the outer shelf (Cunningham et al., 2005). Submersible studies in the canyons of the northern KwaZulu-Natal continental margin, particularly deeper submersible dives along the canyon thalwegs (e.g. Green, 2004), show that the dominant material in the canyon floor is a Lower

Pleistocene muddy silt (Green et al., 2008). In addition, grab samples from canyon wall failure deposits comprise terminal Pliocene/lowermost Pleistocene muddy silts (Green et al., 2008). This suggests that very little fine- to medium-grained Holocene sediment is being transported through these canyons, and it is thus unlikely that they play as significant a role in shelf to abyssal plain sediment dispersal as debated, for example, by Ramsay (1994) and Ramsay et al. (1996).

9.6.3. Sediment migration patterns and bedform distribution

Despite there being little evidence of significant quantities of fine- to medium-grained Holocene sand within the submarine canyons of the area, bedform orientation is predominantly aligned orthogonal to the submarine canyon long axes suggesting transport either into or away from the canyons. Bifurcated dunes superimposed on a single sand ridge inshore of White Sands Canyon show modern reworking of this feature to the north away from the canyon axis, though the palaeo-flow direction, given by the southerly ridge orientation, is towards the canyon. If this ridge conforms to the Swift and Field (1981) and Swift et al. (1984) model of ridge evolution, whereby ridges migrate alongshore downcurrent whilst detaching from the shoreface, then during the last transgression in the mid Holocene it would perhaps have been an active sediment source for White Sands Canyon. Conversely, if this ridge is a relict feature, slightly modified by modern oceanographic processes (Stubblefield et al., 1984; Snedden et al., 1994; Berné et al., 1998), then the ridge would not have been a source of sediment to the White Sands Canyon head. Sub-bottom profiles do not reveal a sequence boundary or a transgressive ravinement surface (Figs. 9.15 and 9.16) beneath these features. These observations contrast with studies which have consistently recognised ridges resting on a flat Holocene ravinement surface (Snedden et al., 1994; Harrison, 1996; Twichell et al., 2003. Although this could be the case here (see Fig. 9.15), the vertical resolution of the 3.5-kHz profiles from Mabibi is not good enough to image the ravinement surface properly. The former argument is preferred here, i.e. the ridge actively fed the White Sands Canyon during the Holocene transgression but is now cut off, the sediment being diverted to the north by northerly directed counter Agulhas Current flows.

The prevalence of bedload partings along the Mabibi continental shelf appears to be a function of topographic forcing of the Agulhas Current by the regularly spaced submarine canyons of the area. Immediately south of each canyon head, large dunes are oriented northward towards the canyon, whereas only ~1 km further south they migrate in a southerly direction. This northward entrainment of sediment is a topographically forced bedload parting in response to turbulent counter-current

flows forming off the southern edge of the canyon wall (Fig. 9.17). Fluid modelling of MacCready and Pawlak (2001) over undulations of similar topographic scale shows that sub-inertial (geostrophic) flow, similar to that of the Agulhas Current, produces internal waves which break and cause turbulent mixing in the lee of each corrugation. This could result in return or counter flows moving bedload towards the canyon on the southern side. This arrangement of bedforms counter to the prevailing current at the southern canyon walls indicates that bedload partings along this coast are not solely controlled by the coastal offset and the large return gyre in its lee (e.g. Flemming, 1981; Ramsay, 1994).

The consistent occurrences of dune fields south of the Mabibi Block canyon heads could be a result of successive perturbation in the flow across these canyon features. As flow lines in the fluid column undulate, these undulations may become progressively larger over evenly spaced topographic perturbations, causing areas of flow line convergence to be strong enough to mobilise large dune fields. The regular spacing of the canyons would cause flow line convergence, hence flow acceleration, in the areas immediately south of the canyons where flow reattachment (and compression) would most likely occur, explaining the location of the dune fields (Fig. 9.18).

The presence of rounded crests in many of the bedform fields, the variation in wave form indices, and non-existent depth–wavelength relationships indicate an appreciable amount of reworking of the dune forms in these areas. These mostly appear to be sediment starved to the point where only crest caps are permitted to form, surrounded by outcrop of the Holocene shoreface ravinement surface. In addition, the random distribution of wavelength compared to distance from canyon thalweg in all areas points to these features being out of equilibrium with the surrounding oceanographic regime. The departure of the largest inner shelf bedforms of Mabibi from this non-trend (Fig. 9.12) may be explained by the repeated (~200 m) north –south shifting in the bedload parting zones adjacent to the Mabibi canyon heads, causing the localised amalgamation of dunes in the upper limit of the study area's very large dune category. The temporary shift in current would delay the removal of sediment in any preferred direction, also providing a mechanism by which even larger features on this region of shelf, such as sand ridges, may develop. On the whole, there is little logical order in any of the morphometric parameters measured, as would be expected in a steady-state flow situation (as provided by an "unhindered" Agulhas Current). The use of bedform orientation as a major determinant of net bedload transport direction may thus not be as reliable in this area as previously thought (e.g. Ramsay, 1994).

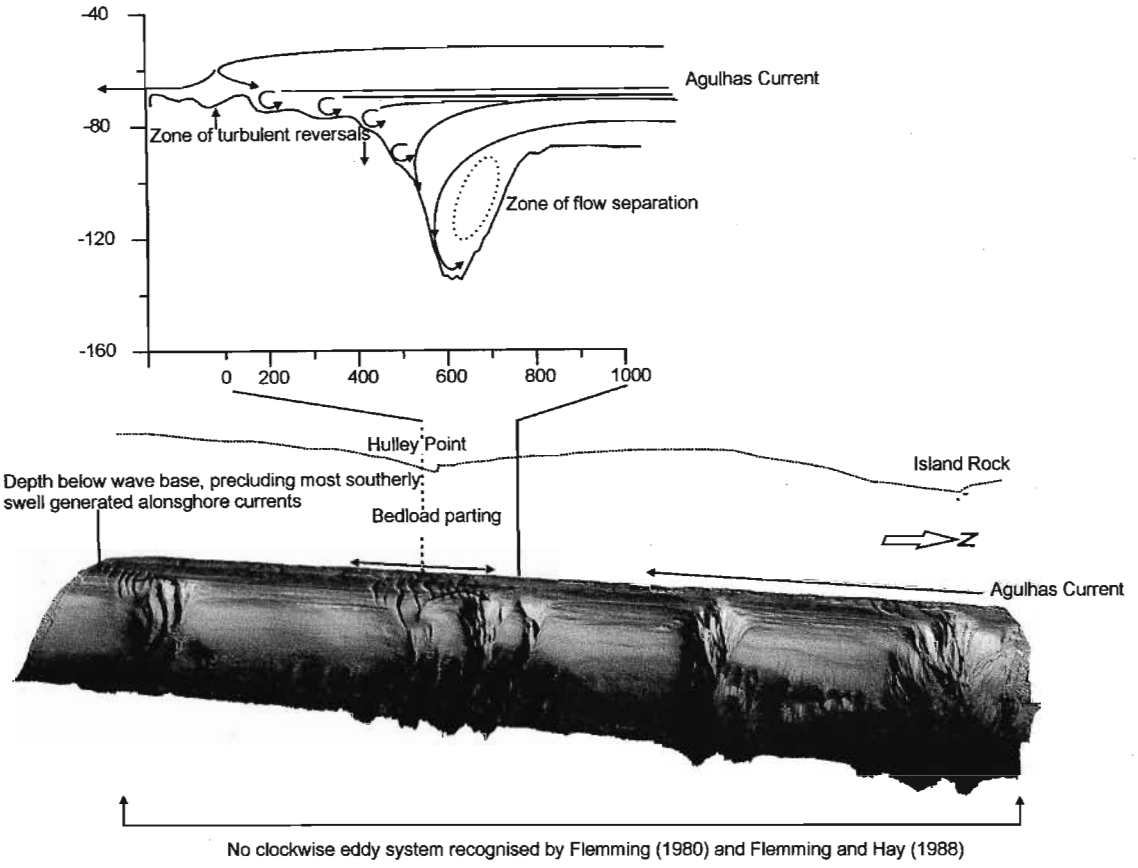

Figure 9.17. Schematic model indicating topographic canyon-induced bedform parting in the mid shelf of Mabibi.

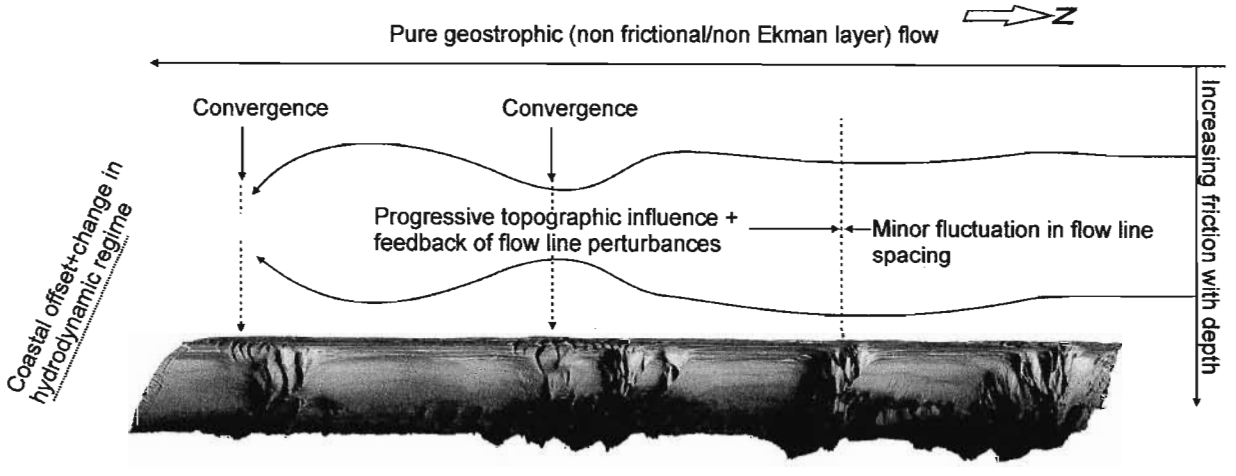

Figure 9.18. Schematic model of the formation of bedform fields in the southerly sections of the canyon heads of Mabibi.

9.6.4. Aeolianite ridges and palaeo-bay morphology

The presence of several laterally continuous, depth specific reef complexes mapped in the study area permits a reconstruction of the coastline which spans the oxygen isotope stages 5a to 1. Four palaeo-coastline development episodes, corresponding to beachrock/aeolianite complexes, were documented by Ramsay (1991; 1994) for the Sodwana Bay continental shelf. These correspond to:
Palaeo-coastline 1 between -15 and -25 m on the mid shelf (OIS 2)
Palaeo-coastline 2 between -13 and -45 m on the shelf, dated at 84 000 ± 3000 BP (OIS 5a)
Palaeo-coastline 3 between -50 and -60 m on the outer shelf (OIS 2)
Palaeo-coastline 4 between -70 and -95 m on the outer shelf (OIS 2)

On the basis of these coastline models, a historical coastal configuration model for the northern KwaZulu-Natal coastline is proposed here, taking into account additional beachrock/aeolianite complexes dated by Ramsay and Cooper (2002) and recognised on a regional scale in this study (appendix 1).

Beachrocks from -10 m at Kosi Bay, ~ 40 km north of Mabibi, yield an age of 8950 ± 80 BP (OIS 1) (Ramsay and Cooper, 2002), and this reef crops out nearly continuously to the southern limit of the study area at Leven Point (Ramsay et al., 2006; appendix 1). Red Sands Reef, and the inner portions of Leven Reef comprise this palaeo-coastline (PCA), and mirror much of the present day coastline configuration. PCA is absent from north of Leadsman Shoals, to Gobey's Point thereafter it comprises a series of zeta bays which reflect the modern day bay morphology. PC1, considered as forming ~22 000 BP (Ramsay, 1991) occurs as a scattered outcrop along the northern KwaZulu-Natal shelf, most prominent in the inshore portions of 2 Mile Reef, and the Leven and Red Sands reefs. PC1, 3 and 4 are considered as having formed during the OIS 2 regression, and young seaward as shelf sediment was exposed and re-ordered into these strandline sinks (Ramsay, 1994). Cooper (1991b) considers this a major factor in reducing littoral sediment transport during the Holocene, and was a factor in the rapid landward migration of the shoreline during OIS 1 (Ramsay and Cooper, 2002). The fact that these shorelines consistently reflect zeta bay morphologies suggest that littoral drift was limited not only by beachrock and aeolianite formation at the shore line, but also by localised impediments to longshore drift, in the form of these bays (Cooper, 1994). As such, sediment starvation was initiated during regression, contrary to traditional sequence stratigraphic models which consider forced regression as a period of instability, sediment mobilisation and redistribution. This undoubtedly exacerbated post-LGM transgressive sediment

starvation of the outer shelf, a factor which has been ascribed as key in maintaining canyon stability since the Flandrian deglaciation (Green and Uken, 2005; Green et al., 2007).

Post-LGM sedimentation has been limited on a regional scale to a single thick wedge which extends from Leadsman Shoals to south of Leven Point (Fig. 4.6, appendix 1), though thinner deposits occur throughout the study area. This appears to be the northernmost reworked fringe of the St Lucia-Mfolozi River confluence depocentre (Martin and Flemming 1985; Flemming and Hay, 1988; Birch, 1996). Unconsolidated sediment exceeding a thickness of 30 m occurs as incised valley fills (chapter 4). Between Wright and White Sands Canyons, a relatively thick (15-18 m) fill occurs in a shallow kidney shaped depression which extends between 7 and 9 Mile Reefs and trends shore parallel before entering Wright Canyon (Fig 4.12). This represents a topographically subdued ephemeral mouth of the LGM Sibaya Estuary which may have been open on a seasonal basis similar to modern lagoon systems on this portion of coastline (Cooper, 2001). As mentioned in chapter 4, it seems probable that this would have been secondary to a major channel which was diverted behind the coastal dune cordon and debouched north of Mabibi in the Kosi Bay area.

CHAPTER 10
Conclusions

The evolution of the submarine canyons offshore of northern KwaZulu-Natal cannot be understood without investigating the surrounding geology of the continental shelf and upper slope. Intrinsically related to canyon development are the responses of these systems to both historical changes in relative sea-level and sediment supply to the actively subsiding passive margin. Linked to this are changes in coastal physiography, geomorphological setting and sedimentation which may foster complex forms of erosion, canyon preservation, or infilling.

Seismic stratigraphic and chronostratigraphic models for the development of the northern KwaZulu-Natal continental margin are proposed through the use of high resolution seismic profiles and established sea-level curves from this area. Age control is supplemented by borehole, submersible and grab samples. These models indicate at least six partially preserved sequences, interrupted by unconformities, which are correlated with sedimentary hiatuses from the boreholes and other regional seismic studies. Forced regressive, lowstand and transgressive/highstand deposits are apparent, forced regressive conditions prevailing during hinterland uplift and high sediment supply. These resulted in FRST deposits volumetrically dominating the stratigraphy of the continental shelf. LST deposits are associated with shelf edge deltaic sedimentation during the Late Pliocene, and are considered to be strongly influenced by the palaeo-drainage of the Lake St Lucia complex at these times. Older lowstand deposits do not fit the regional sea level curve for southern Africa, despite good age control on these features. A re-fit of the sea level curve to accommodate a Late Cretaceous (Mid Maastrichtian) lowstand is thus proposed. Post Pliocene sedimentation is sparse, preserved as Pleistocene shallow marine facies, and Late Pleistocene beachrock/aeolianite complexes. These are overlain by recent sediments which mark the onset of deposition of the most recent stratigraphic sequence. Fluvial –shelf interaction is preserved in the underlying sequence boundary, which is heavily influenced by drainage of the palaeo-Lake St Lucia fluvio-estuarine complex during the last glacial maximum of OIS 2.

Cretaceous and Late Pleistocene/Holocene age palaeo-valley fills are similar in their observed seismic facies, and correspond closely to the predicted fill facies of wave dominated incised valleys. Each valley fill comprises basal chaotic facies, interpreted as fluvial lags, side attached flank facies, interpreted as intertidal deposits, and volumetrically dominant low energy facies, interpreted as

finer grained, central basin deposits. These are separated by a bay ravinement surface and a conformable deposition surface respectively. The predicted flood-tide deltaic facies of Dalrymple et al. (1992) is absent from Holocene examples, yet preserved in Late Cretaceous valleys. In Holocene valley fills, these are replaced by mounded or thin, backstepping facies interpreted as shoreface deposits which downlap onto a moderate relief surface which truncates the underlying central basin fill. This surface is identified as a transgressive ravinement surface which occurs sporadically throughout the study area. Late Cretaceous valley fills also possess a similar ravinement surface which underlies deposits of unit E.

The incised valley fill sequences from this portion of coastline provide valuable evidence to further strengthen seismic models of transgressive systems tract preservation on passive margins. The difference between pre-existing models of valley fills (especially those of New Jersey) and those of northern KwaZulu-Natal may indicate that shelf width and narrowness at the time of valley incision and fill plays a role in limiting the estuarine tidal prism, thus accounting for higher preservation potential of wave dominated estuarine facies in these situations. In addition, it appears that seismic expression may take several forms and yet still satisfy the sedimentological models of Ashley and Sheridan (1994) and Allen and Posamantier (1994). In terms of palaeo-drainage, Lake St Lucia has had at least two generations of palaeo-channel incision into the shelf, corresponding to a Late Cretaceous and a last glacial maximum episode. The palaeo-channel is considered a composite feature re-exploited by the younger LGM oceanic connection. Lake St Lucia's palaeo-bathymetry was probably underfilled prior to the OIS 1 transgression in order for the LGM channel to exploit the palaeo-topography. Lake Sibaya shows two distinct palaeo-channels, a Late Cretaceous channel which fed an incised valley system within which a small canyon is nested, and an LGM channel, which is directed towards the head of Wright Canyon. It appears that underfilling of older topographic features on narrow continental shelves plays a prominent role in the development and preservation potential of incised valleys and their ensuing fills.

The occupation of the Leven Point Late Pleistocene/ Holocene valley by a canyon-connected erosional feature indicates that erosion occurred along a preferred conduit (namely the palaeo-channel). It can be concluded, based on modelling attempts by others, that fresh water exchange between Lake St Lucia has occurred. This has prompted downslope erosion by freshwater sapping and sediment denudation, and the formation of the sinuous, fluvial-like erosional feature. It is recommended that more detailed, higher-resolution seismic and electro-magnetic surveying be undertaken in the inshore portions of Leven Canyon to ascertain the extent to which fresh water

sapping and erosion has utilised palaeo-channels of the LGM St Lucia system. It is also recommended that additional seismic data be acquired over the areas identified as drainage conduits in order to create a denser seismic grid from which a more accurate palaeo-drainage pattern, similar to that of Nordfjord et al. (2006) may be constructed.

The subdivision of the study area into two distinct structural domains based on the presence and incision of a Late Cretaceous sequence boundary reveals that several fossil canyons underlie modern day canyon features. The topographic inheritance of older canyon forms by younger canyons is evident from this nested stacking pattern and indicates that post SB1 sedimentation was either insufficient to completely infill fossil canyon features, or these features were continually re-excavated. Limited sediment supply (prior to Tertiary times) and frequent hiatuses stunted more elaborate incision-fill episodes, giving rise to only localised instances of fossil canyon exploitation. The topographic inheritance of incised valley fills is also observed, where smaller slope confined canyons occupy previously infilled palaeo-valleys.

Geomorphological studies of the northern KwaZulu-Natal continental slope canyon systems indicate the dominance of upslope erosional processes in the formation of canyons from this region. Discounting the slope-gradient profile, canyon morphology is strikingly similar to that of the features predicted for a primarily upslope-eroding paradigm by the numerical modelling of Pratson and Coakley (1996). The presence of a steepened shelf-edge wedge could be a potential source for such retrogressive failure, despite being of similar steepness to that found in areas where downslope-eroding canyon systems have developed. If the northern KwaZulu-Natal upper slopes cannot be considered oversteepened, it is suggested that freshwater sapping may be the fundamental factor differentiating the two styles of canyon formation. Several generations of canyon incision in the study area indicate that downslope turbidity erosion is also an important factor in the evolution of the KwaZulu-Natal canyons.

Despite the strong similarities between the northern KwaZulu-Natal and New Jersey slope-canyon systems noted above, important differences are also documented: (1) the northern KwaZulu-Natal slope is concave whereas the New Jersey slope is essentially linear; (2) the larger northern KwaZulu-Natal canyons are relatively isolated from each other whereas the New Jersey canyons are clustered; and (3) strongly shelf-breaching canyons are absent from the northern KwaZulu-Natal margin. The hypothesis is put forward that these differences indicate that the northern KwaZulu-Natal slope canyons are geomorphologically in a more youthful stage of evolution than is the New

Jersey margin, a result either of the canyons themselves being younger or of the formative processes being less active. Recent quiescence of the KwaZulu-Natal margin, coupled with sediment-starved conditions, has resulted in less complicated patterns of erosion having developed compared to the New Jersey and Virginia continental margins. Intensive headward erosion on the New Jersey margin strongly graded the upper slope, is considered as the key in reducing any concavity that might have existed.

It is postulated that the various relationships between the measured characteristics of landslide area, volume, depth, headscarp height, headscarp slope, runout distance, runout slope, scar slope and local unfailed slope give a good indication of dynamic rheology in the absence of core data for the area. Furthermore, particular differences in these relationships between the various canyons are apparent, and indicate different processes responsible for the growth and evolution of these systems. Diepgat, and to a lesser extent Wright Canyon have relatively large failures (compared to the others measured) despite indications that the failure rheology was competent. Conversely, Leven and Leadsman Canyons have failures with large areas and fluid rheologies. A possible seismic trigger, accompanied by favourable pre-conditioning factors is considered for the Diepgat and Wright landslides, whereas the failures, particularly those in the head, of Leven Canyon may be a product of fresh water sapping on the mid shelf alluded to in the morphometric analysis. This is confirmed in the case of Diepgat Canyon, which displays deep seated listric faults in its head portions, corresponding to the large failures identified from multibeam data. This faulting is considered to be older than the LGM, and may be as recent as the last century, related to the St Lucia earthquake of 1932.

The presence of distinct groupings of failure morphologies indicates the importance of both upslope and downslope erosion in canyon evolution. These two processes are emphasized by the change in landslide type, size and number as the system evolves from an initial downslope eroding sediment flow phase to the headward eroding excavation phase. Early growth in the canyon form conforms to landslide free rills, followed by simple retrogressive slumping in the canyon head, culminating in the widening of the canyon by numerous axis-normal wall failures. The preservation of erosional benchmarks, hanging slumps and inner gorges attests to periods of catastrophic slope clearance during the excavation phase. The random pattern of landslide depth relative to the sea-level expressions of the previous two lowstands suggests a period of quiescence from at least the last glaciation. Canyon systems are thus unlikely to be actively enlarging, barring: 1) the pre-conditioning factors which future lowstand episodes can provide i.e. sufficient sediment to the outer

shelf to increase overburdening, cyclic loading or downward incision by axially constrained sediment flows; and 2) a suitable trigger.

Despite Wright and Leven Canyons, no inner shelf extension of submarine canyons is evident in the study area. Hyperpycnal plumes and continual downslope erosion can be discounted for the genesis of the submarine canyons of the study area. Slump derived flows are thus envisioned as the major source of axial incision, resulting in the glide plain bounded sediment masses in the walls of the canyons and the terracing of submarine canyons in the outer shelf and upper slope. The initiation of a critical phase of slope failure and rilling is attributed to the oversteepening of the rapidly deposited and unstable shelf edge wedge of unit E. Canyon topography has thus grown by both incision, as well as interfluve aggradation during the deposition of this unit. Where this unit forms canyon fills, it indicates slumping of the canyon walls via the lateral widening stage, directly related to aggradation-progradation.

The erosion of dune cordons PC 3 by portions of the heads of Wright and Leven Canyons, as well as shallow slumping and infilling by unit H which directly onlaps this dune cordon, indicates that canyon growth in these cases postdates OIS 2. The presence of LGM connections to Lake Sibaya and Lake St Lucia respectively indicates that these canyons were last active at least until LGM times. Wright Canyon, considered as having the closest resemblance to a shelf breaching canyon, achieved this form via this connection to the LGM Lake Sibaya.

New evidence for lower than present sea levels is described from submarine caves, and *in situ* deposits that suggest intertidal weathering and sedimentation at depths unexplored along the east coast of South Africa. Interpretations suggest an east coast LGM depth of between 125 m and 130m. To date, these data are the most solid observable evidence for glacial maxima on the South African coastline and can contribute significantly to the global understanding of sea-level variability. Close matches in LGM sea level between the east and west coast indicate negligible tectonic activity during the last 18 000 years. The presence of these sea level indicators within canyon heads further allows the age bracketing of canyon growth and instability centred around the previous lowstand, where maximum canyon growth is predicted. It is recommended that further ROV or submersible studies be undertaken to investigate the minimum age of each failure mapped within the canyon walls of the study area.

The modern sediment dynamics of the shelf are heavily influenced by the progressive sediment starvation of the area, which is currently exacerbated by continued transgression. The presence of an outcropping Mid-Holocene ravinement surface on the outer shelf, in the form of a relict gravel pavement attests to this. Where this encroaches closer inshore, these sites pose potential erosion hazards during sea level rise and concomitant wave base shifting. Where Holocene sediment is concentrated inshore, it is dammed behind drowned dune cordons, reducing coast-normal sediment losses. There appears to be less net loss of sediment by canyon entrainment than has been previously thought, with little fine-to medium-grained sand transported through these systems. The topographic forcing of the Agulhas Current by canyon topography does cause sediment entrainment into the system, but from the southern side of the canyon heads, a result of turbulent counter-Agulhas flows back into the canyon form. These dunefields may form as a result of Markovian inheritance and positive feedback of flows over the canyon forms, though fluid modelling via a flume tank is required to test this hypothesis. Cyclical migrations in bedload parting zones are theorised as the key factor in causing these large dunefields to remain in these positions, thus increasing their preservation potential. Sand ridge genesis in the Wright Canyon-White Sands Canyon area may be the result of this. Overall, there appears to be no logical ordering of bedforms within these dunefields. It thus appears that bedforms are in the process of being reworked from a previous equilibrium profile to a new one, based on slowly rising sea-level, coastal orientation and canyon topographic controls.

Coastline models for the study area, based on palaeo-dune cordons (PCA, PC1-PC4), indicate that the coastline had a logarithmic spiral bay configuration since OIS 2. This reduced sediment availability to the area in the form of littoral drift, as well as by sediment retention in beachrock/aeolianite reservoirs. Sediment starvation was thus initiated during the regression of OIS and contradicts traditional sequence stratigraphic models which consider this a period of terrestrial sediment mobility towards the coast. Further dating, by Optical Stimulated Luminescence means, of dune cordons outlined by Ramsay et al. (2006) would enhance our understanding of palaeo-coastline configuration dramatically. In terms of Post-LGM sedimentation, sediment accumulation has been limited to small scale microdepocentres on the inner shelf, most of which relate to the infilling of incised valleys during the consequent transgression to modern day sea levels.

It is strongly recommended that further investigations into the more distal parts of these canyons systems be carried out, as this will facilitate a better understanding of the role of these systems in sediment exchange between shelf, slope and abyssal plain. Comprehensive multibeam mapping of

these lower canyon portions would allow one to further quantify the slope with the techniques outlined in chapter 6 and allow the identification of the dominant processes influencing slope and abyssal plain sedimentation or erosion. Further high resolution seismics, preferably using a deep towed sparker or boomer system, acquired in the deeper portions of these canyons would indicate whether these systems conform to traditional models of submarine canyon-fan development, and would test the validity of traditional sequence stratigraphic models of submarine fan evolution. Lastly, coring of the fans would provide an exact history of upper slope failures, allowing one to constrain the sedimentary evolution of the system in conjunction with palaeontological dating of mass wasting deposits. The continental slope models of McHugh et al. (2002) concerning mass wasting would thus be fully tested on steeper passive margin slopes which may depart from traditional models which consider sequence boundary formation the origin of continental slope mass wasting.

REFERENCES

Adams, E.W., Schlager, W., 2000. Basic types of submarine slope curvature. J. Sediment. Res. 70, 814-828.

Allen, G.P. and Posamentier, H.W., 1993. Sequence stratigraphy and facies model of an incised valley fill: the Gironde estuary, France, J. Sed. Petrol. 63, 378-391.

Allen, G.P., Posamentier, H.W., 1994. Transgressive facies and sequence architecture in mixed tide and wave-dominated incised valleys: example from the Gironde estuary, France. In: Dalrymple, R.W., Boyd, R.J., Zaitlin, B.A. (Eds.), Incised Valley Systems: Origin and Sedimentary Sequences. Soc. Sediment. Geol. Spec. Publ. 51. SEPM, Tulsa, 226-240.

Allen, J.R.L., 1982. Sedimentary structures: their character and physical basis. Development in Sedimentology 30, Elsevier, Amsterdam, Part II, pp 643.

Anderson, J.B., Rodriguez, A., Abdulah, K., Fillon, R.H., Banfield, L., McKeowan, H., Wellner, J., 2004. Late Quaternary stratigraphic evolution of the northern Gulf of Mexico margin: A synthesis. In: Anderson, J.B., Fillon, R.H. (Eds.), Late Quaternary Stratigraphic Evolution of the Northern Gulf of Mexico. Soc. Sediment. Geol. Spec. Publ. SEPM, vol. 79. pp 226-240.

Antobreh, A.A., Krastel, S., 2006. Morphology, seismic characteristics and development of Cape Timris Canyon, offshore Mauritania: A newly discovered canyon preserved-off a major aridclimatic region. Mar. Petrol. Geol. 23, 37-59.

Arzola, R.G., Wynn, R.B., Lastras, G., Masson, D.G., Weaver, P.P.E., 2008. Sedimentary features and processes in submarine canyons: a case study from the Nazaré and Setúbal Canyons, west Iberian margin. Mar. Geol. 250, 64-88.

Ashley, G.M., Sheridan, R.E., 1994. Depositional model for valley fills on a passive continental margin. In: Dalrymple, R.W., Boyd, R.J., Zaitlin, B.A. (Eds.), Incised Valley Systems: Origin and Sedimentary Sequences. Soc. Sediment. Geol. Spec. Publ. 51. SEPM, Tulsa, 285- 301.

Barlow, P.M., 2003. Groundwater in freshwater-saltwater environments of the Atlantic coast. US Geological Survey Circular, 1262.

Bang, N.D., 1968. Submarine canyons off the Natal coast. S. Afr. Geogr. J. 50, 45-54.

Bang, N.D., Pierce, A.F., 1978. Physical Oceanography. In: Heydorn, A.E.F (Ed.), Ecology of the Agulhas Current Region. Trans. R. Soc. S. Afr. 43, 156-162.

Baztan, J., Berné, S., Olivet, J-L., Rabineau, M., Aslanian, D., Gaudin, M., Réhault, J-P., Canals, M., 2005. Axial incision: the key to understand submarine canyon evolution (in the western Gulf of Lion). Mar. Petr. Geol. 22, 805-826.

Berryhill Jr., H.L., Suter, J.R., Hardin, N.S., 1986. Late Quaternary facies and structure, northern Gulf of Mexico; interpretations from seismic data. AAPG Stud. Geol. 23.

Berné, S., Lericolais, G., Marsset, T., Bourillet, J.F., De Batist, M., 1998. Erosional shelf sand ridges and lowstand shorefaces: examples from wave and tide dominated environments of France. J. Sed. Res. 68, 540-555.

Berné, S., Aloïsi, J.C., Baztan, J., Dennielou, B., Droz, L., Dos Reis, T., Lofi, J., Mear, H., Rabineau, M., Satra, C., 2002. Notice de la carte morpho-bathymémtrique du Gulf du Lion. IFREMER et Région Languedoc Rousillon, Brest.

Bertoni,C., Cartwright, J., 2005. 3D seismic analysis of slope-confined canyons from the Plio-Pleistocene of the Ebro continental margin (western Mediterranean). Basin Analysis. 17, 43-62.

Birch, G.F., 1996. Unconsolidated sediments on the eastern margin of South Africa (Cape Padrone to Cape Vidal). Bulletin of the Geological Survey of South Africa 118, pp 55.

Botes, Z.A., 1988. A short note on Diepgat, a submarine canyon south of Sodwana Bay, Natal. S. Afr. Geograph. J. 70: 150 - 154.

Boucher, K., 1975. Global Climate, English Universities Press Ltd., London, pp 323.

Boyd, R., Ruming, K., Goodwin, I., Sandstrom, M, Schröder-Adams, C., 2008. Highstand transport of coastal sand to the deep ocean: A case study from Fraser Island, southeast Australia. Geology 36, 15-18.

Broad, D.S., Jungslanger, E.H.A., McLachlan, I.R., Roux, J., 2007. Offshore Mesozoic basins. In: Johnson, M.R., Anheuser, C.R., Thomas, R.J. (Eds.), The geology of South Africa. The Geological Society of South Africa, Johannesburg/Council for Geoscience, Pretoria, 553-573.

Bryn, P., Berg, K., Lien, R., Forsberg, C.F., Solheim, A., Kvalstad, T.J., 2005. Explaining the Storegga slide. Mar. Petr. Geol. 22, 11-19.

Canals, M., Lastras, G., Urgeles, R., Casamor, J.L., Minert, J., Cattaneo, A., De Batist, M., Halfidason, H., Imbo, Y., Laberg, J.S., Locat, J., Long, D., Longva, O., Masson, D.G., Sultan, N., Trincardi, F., Bryn, P., 2004. Slope failure dynamics and impacts from sea floor and shallow sub-sea floor geophysical data: case studies from the COSTA project. Mar. Geol. 213, 9-72.

Carlson, P.R., Karl H.A., 1988. Development of large submarine canyons in the Bering Sea, indicated by morphologic, seismic and sedimentologic characteristics. Geol. Soc. Am. Bull. 100, 1594-1615.

Catuneanu, O, 2006. Principles of sequence stratigraphy. Elsevier, Amsterdam, pp 375.

Chamberlain, T.K., 1964. Mass transport of sediment in the heads of Scripps Submarine Canyon, California. In: Miller, R. (Ed.), Papers in marine geology, Shepard commemorative volume. MacMillan, New York, 42-64.

Chappell, J., Shackleton, N.J., 1986. Oxygen isotopes and sea level. Nature 324, 137-140.

Coe, A.L., Bosence, D.W.J., Church, K.D., Flint, S.S., Howell, J.A., Wilson, R.C.L., 2003. The sedimentary record of sea level change. Cambridge University Press, Cambridge, pp 288.

Coleman, J.M., Prior, D.B., 1988. Mass wasting on continental margins. Annu. Rev. Earth Plant. Sci. 16, 101-119.

Cooper, J.A.G., 1991a. Sedimentary models and geomorphological classification of river mouths on a subtropical, wave-dominated coast, Natal, South Africa. PhD Thesis, University of Natal, Durban, pp 401.

Cooper, J.A.G., 1991b. Beachrock formation in low latitudes: implications for coastal evolutionary models. Mar. Geol. 98, 145-154.

Cooper, J.A.G., 1994. Lagoons and microtidal coasts. In: Carter, R.W.G., Woodruffe, C.D. (Eds.), Coastal Evolution: Late Quaternary shoreline morphodynamics. Cambridge University Press, Cambridge, pp 219-265.

Cooper, J.A.G., 2001. Geomorphological variability among microtidal estuaries from the wave-dominated south African coast. Geomorph. 40, 99-122.

Cooper, J.A.G., Flores, R.M., 1991. Shoreline deposits and diagenesis resulting from two Late Pleistocene highstands near + 5 and + 6 metres, Durban, South Africa. Mar. Geol. 97, 325-343.

Cooper, J.A.G., Green, A.N., Wright, C.I., in prep. Evolution of an incised river valley under low sedimentation rates, Kosi Bay, South Africa.

Compton, J.S., 2001. Holocene sea-level fluctuations inferred from the evolution of depositional environments of the southern Langebaan Lagoon salt marsh, South Africa. The Holocene 11, 395-405.

Crozier, M.J., 1973. Techniques for the morphometric analysis of landslips. Zeit. Fur Geomorph. 17, 78-101.

Cunningham, M.J., Hodgson, S., Masson, D.G., Parson, L.M., 2005. An evaluation of along-and downslope sediment transport processes between Goban Spur and Benot Spur on the Celtic Margin of the Bay of Biscay. Sed. Geol. 179, 99-116.

Dalrymple, R.W., Zaitlin, R.A., and Boyd, R., 1992. A conceptual model of estuarine sedimentation, J. Sediment Petrol. 62, 1130-1146.

Daly, R.A., 1936. The origin of submarine canyons. Am. J. Sci. 5 31, 401 - 420.

Davies, J.L. (1964). A morphogenic approach to world shorelines. Zeitschr. Fur Geomorph. 8, 27-42.

De Decker R.H., Van Heerden I.L., 1987. The seismic stratigraphy of the Orange delta. In Proc. 6th National Oceanographic Symposium, Stellenbosch, paper C21.

Diab, R. D., Sokolic F., 1996. Report on wind and wind turbine monitoring at Mabibi-period September 1994 to February 1996, Department of Mineral and Energy Affairs Report, pp 8.

Densmore, A.L., Anderson, R.S., McAdoo, B.G., Ellis, M.A., 1997. Hillslope evolution by bedrock landslides. Science 275, 369-372.

Dingle, R.V., 1977. The anatomy of a large submarine slump on a sheared continental margin (SE Africa). J. Geol. Soc. London 134, 293-310.

Dingle, R.V., 1980. Large allochthonous sediment masses and their role in the construction of the continental slope and rise of southwestern Africa. Mar. Geol. 37, 33-354.

Dingle, R.V., Goodlad, S.W., Martin, A.K., 1978. Bathymetry and stratigraphy of the northern Natal Valley (SW Indian Ocean). A preliminary report. Mar. Geol. 28, 89-106.

Dingle, R.V., Robson, S., 1985. Slumps, canyons and related features on the continental margin off East London, SE Africa (southwest Indian Ocean). Mar. Geol. 67, 37-54.

Dingle, R.V., Siesser, W.G., Newton, A.R., 1983. Mesozoic and Tertiary geology of southern Africa. AA Balkema, Rotterdam, pp 375.

Drake, D.E, Hatcher, P.G, Keller, G.M., 1978. Suspended particulate matter and mud deposition in upper Hudson Submarine Canyon. In: Stanley, D.J., Kelling, G.E. (Eds.), Sedimentation in submarine canyons, fans and trenches. Dowden, Hutchinson and Ross, Pennsylvania, 33-41.

Dugan, B., Flemings, P.B., 2000. Overpressure and fluid flow in the New Jersey continental slope: implications for slope failure and cold seeps. Science 289, 288-292.

Du Toit, S.R., Leith, M.J., 1974. The J(c)-1 bore-hole on the continental shelf near Stanger, Natal. Trans. Geol. Soc. S. Afr. 77, 247-252.

Edwards, M.B., 1981. Upper Wilcox Rosita delta system of South Texas. Growth-faulted shelf-edge deltas. AAPG Bull. 65, 54-73.

Emery, K.O., Uchupi, E., Bowin, C.O., Phillips, J. Simpson, E.S.W., 1975. Continental margin off western Africa: Cape St Francis (South Africa) to Walvis Ridge (South West Africa). Am. Assoc. Pet. Geol. Bull. 59, 3-59.

Falls, W.F., Ransom, C., Landmeyer, J.E., Reuber, E.J., Edwards, L.E., 2005. Hydrogeology, water quality and saltwater intrusion in the upper Floridan aquifer in the offshore area near Hilton Head Island, South Carolina and Tybee Island, Georgia 1999-2002. US Geological Survey, Scientific Investigations Report, 2005-5134.

Farre, J.A., McGregor, B.A., Ryan, W.B.F., Robb, J.M., 1983. Breaching the shelfbreak; Passage from youthful to mature phase in submarine canyon evolution. In: Stanley D.J., Moore, G.T. (Eds.), The shelfbreak: critical interface on continental margins. Soc. Econ. Palaeontol. Mineral. Spec. Pub. 33, 25-39.

Faugères, J-C., Gonthier, E., Mulder, T., Kenyon, N., Cirac, P., Griboulard, R., Berné, S., Lesuavé, R., 2002. Multi-process generated sediment waves on the Landes Plateau (Bay of Biscay, North Atlantic). Mar. Geol. 182, 279-302.

Flemming, B.W., 1978. Underwater sand dunes along the southeast African continental margin-observations and implications. Mar. Geol. 26, 177-198.

Flemming, B.W., 1980. Sand transport and bedform patterns on the continental shelf between Durban and Port Elizabeth (southeast African continental margin). Sed. Geol. 26, 179-205.

Flemming, B.W., 1981. Factors controlling shelf sediment dispersal along the southeast African continental margin. Mar. Geol. 42, 259-277.

Flemming, B.W., Bartholomä, A., 2009. Temporal variability, migration rates and preservation potential of subaqueous dune fields generated in the Agulhas Current on the southeast African continental margin. In: Li MZ, Sherwood CR, Hill PER (Eds.), Sediments, morphology and sedimentary processes on continental shelves. Blackwell, Oxford, IAS Spec Publ (in press).

Flemming, B.W., Hay, E.R., 1988. Sediment distribution and dynamics on the Natal continental shelf. In: Schumann, E.H. (Ed.), Lecture notes on coastal and estuarine studies, 26, Springer Verlag, New York, 47-80.

Foyle, A.M., Oertel, G.F., 1997. Transgressibe systems tract development and incised-valley fills within a Quaternary estuary-shelf system: Virginia inner shelf, USA. Mar. Geol. 137, 227-249.

Fricke, H., Hissmann, K., 1994. Home range and migrations of the living coelacanth *Latimeria chlaumnae*. Mar. Biol. 120, 171-180.

Fricke, H., Plante, R., 1988. Habitat requirements of the living coelacanth *Latimeria chalumnae* at Grande Comore, Indian Ocean. Naturwissenschaften 15, 149-151.

Fulthorpe, C.S, Austin, J.A., 1998. Anatomy of rapid margin progradation: three-dimensional geometry of Miocene clinoforms, New Jersey margin. Am. Assoc. Petrol. Geologists Bull., 82, 251-273.

Galloway, W.E., 1989. Genetic stratigraphic sequences in Basin Analysis II: application to northwest Gulf of Mexico Cenozoic Basin. AAPG Bull. 73, 143-154.

Galloway, W.E., 1990. Paleogene depositional episodes, genetic stratigraphic sequences, sediment accumulation rates NW Gulf of Mexico Basin. In: Armentrout, J.M., Perkins, B.F. (Eds.), Sequence Stratigraphy as an Exploration Tool: Concepts and Practices in the Gulf Coast. Soc. Econ. Paleontol. Mineral., Gulf Coast Section. 11th Annual Research Conference Program and Abstracts, 165- 176.

Goff, J.A., 2001. Quantitative classification of canyon systems on continental slopes and a possible relationship to slope curvature. Geophys. Res. Lett. 28, 4359-4362.

Goff, J.A., Kraft, B.J., Mayer, L.A., Schock, S.G., Sommerfield, C.K., Olson, H.C., Gulick, S.P.S., Nordfjord, S., 2004. Seabed characterization on the New Jersey middle and outer shelf: correlatability and spatial variability of seafloor properties. Mar. Geol. 209, 147– 172.

Goff, J.A., Orange, D.L., Mayer, L.A., Hughes-Clark, J.E., 1999a. Detailed investigation of continental shelf morphology using high resolution swath sonar data: the Eel margin, northern California. Mar. Geol. 154, 255-269.

Goff, J.A., Swift, D.J.P., Duncan, C.S., Mayer, L.A., Hughes-Clarke, J., 1999b. High-resolution swath sonar investigation of sand ridge, dune and ribbon morphology in the offshore environment of the New Jersey margin. Mar. Geol. 161, 307-337.

Goff, J.A., Austin Jr., J.A., Gulick, S., Nordfjord, S., Christensen, B., Sommerfield, C., Olson, H., Alexander, C., 2005. Recent and modern marine erosion on the New Jersey shelf. Mar. Geol. 216, 275-296.

Goff, J.A., Mayer, L.A., Traykovski, P., Buynevich, I., Wilkens, R., Raymond, R., Glang, G., Evans, R.L., Olson, H., Jenkins, C., 2005. Detailed investigation of sorted bedforms, or "rippled scour depressions," within the Martha's Vineyard Coastal Observatory, Massachusetts. Cont. Shelf. Res. 25, 461-484.

Goodlad, S.W., 1986. Tectonic and sedimentary history of the mid-Natal Valley (SW Indian Ocean). Joint Geological Survey/University of Cape Town, Marine Geoscience Unit Bull. 15, pp 415.

Green, A.N., 2004. The fish traps and sedimentary dynamics of the Kosi Bay Estuary, northern KwaZulu-Natal. MSc Thesis, University of KwaZulu-Natal, pp 149.

Green, A.N., 2004. Cruise report FRS Algoa cruise April, 2004, Marine Geoscience programme. *African Coelacanth Ecosystem Programme report*, pp 3.

Green, A.N., Ovechkina, M., Uken, R., 2008. Nannofossil age constraints on shelf-edge wedge development: implications for continental margin dynamics, northern KwaZulu-Natal, South Africa. Cont. Shelf. Res. 28, 2442-2449.

Green, A.N., Uken, R., 2005. First observations of sea level indicators related to glacial maxima at Sodwana Bay, Northern KwaZulu-Natal. S. Afr. J. Sci. 101, 236-238.

Green, A.N., Uken., R., 2008. Submarine landsliding and canyon evolution for the northern KwaZulu-Natal continental shelf, South Africa, SW Indian Ocean. Mar. Geol. 254, 152-170.

Green, A.N., Goff, J.A., Uken, R., 2007. Geomorphological evidence for upslope canyon-forming processes on the northern KwaZulu-Natal shelf, South Africa. GeoMar. Lett. 27, 399-409.

Green, A.N., Perritt, S.H., Leuci, R., Uken, R., Ramsay, P.J., 2008. Potential sites for coelacanth habitat using bathymetric data from the western Indian Ocean. S. Afr. J. Sci. (in press)

Greene, G., Maher, N.M., Paull, C.K., 2002. Physiography of the Monterey Bay National Marine Sanctuary and implications about continental margin development. Mar. Geol. 181, 55-82.

Harrison, S.E., 1996. Morphology and Evolution of a Holocene Carbonate/Siliciclastic Sand Ridge Field, West-Central Florida Inner Shelf. MSc Thesis. University of South Florida, St. Petersburg, FL, pp 211.

Hartnady, C.J.H., 2002. Earthquake hazard in Africa: perspectives on the Nubia-Somalia plate boundary. S. Afr. J. Sci. 98, 425-428.

Hampton, M.A., Lee, H.J., Locat, J., 1996. Submarine Landslides. Rev. Geophys. 34, 33-59.

Hannebuth, T.J.J., Stattegger, K., Schimanski, A., Lüdmann, T., Wong, H.K., 2003. Late Pleistocene forced-regressive deposits on the Sunda Shelf (Southeast Asia). Mar. Geol. 199, 139-157.

Hayes, M.O., 1979. Barrier island morphology as a function of tidal and wave regime. In: Leatherman, S.P. (Ed.), Barrier Islands. Academic Press, New York, 2-21.

Hernandez-Molina, F.J., Somoza, L., Lobo, F., 2000. Seismic stratigraphy of the Gulf of Cadiz continental shelf: a model for Late Quaternary very high-resolution sequence stratigraphy and response to sea-level fall. In: Hunt, D., Gawthorpe, R.L. (Eds.), Sedimentary Responses to Forced Regression. Geol. Soc., London, Spec. Pubs. 172, 329-362.

Hernández-Molina, F.J., Llave, E., Stow, D.A.V., García, M., Somoza, L., Vázquez, J.T., Lobo, F.J., Maestro, A., Díaz del Río, V., León, R., Medialdea, T., Gardner, J., 2006. The contourite depositional system of the Gulf of Cádiz: A sedimentary model related to the bottom current activity of the Mediterranean outflow water and its interaction with the continental margin. Deep Sea Research Part II: Topical studies in Oceanography 53, 1420-1463.

Hiscott, R.N., 2001. Depositional sequences controlled by high rates of sediment supply, sea-level variations, and growth faulting: the Quaternary Baram Delta of northwestern Borneo. Mar. Geol. 175, 67-102.

Hobday, D.K., Orme, A.R., 1974. The Port Durnford Formation: a major Pleistocene barrier-lagoon complex along the Zululand coast. Trans. Geol. Soc. S. Afr. 77, 141-149.

Hünerbach, V., Masson, D.G., partners C.P., 2004. Landslides in the North Atlantic and its adjacent seas: an analysis of their morphology, setting and behaviour. Mar. Geol. 213, 343-362.

Kennedy, W.J., Klinger, H.C., 1975. Cretaceous fauna from Zululand and Natal, South Africa. Bulletin of the British Museum of Natural History, 25, 265-315.

Kenyon, N.H., 1986. Evidence from bedforms for a strong poleward current along the upper continental slope of Europe. Mar. Geol. 72, 187-198.

Kolla, V., 1993. Lowstand deep-water siliciclastic depositional systems: characteristics and terminologies in sequence stratigraphy and sedimentology. BCREDP 17, 67-78.

Kruger, G.P., Meyer, R., 1988. A sedimentological model for the Zululand coastal plain. Abstract, 22nd Earth Science Congress of the Geological Society of South Africa, University of Natal, Durban, 423-425.

Kvalstad, T.J., Andresen, L., Forsberg, C.F., Berg, K., Bryn, P., Wangen, M., 2005. The Storegga slide: evaluation of triggering sources and slide mechanics. Mar. Petr. Geol. 22, 245-256.

Le Bot, S., Trentesaux, A., 2004. Types of internal structure and external morphology of submarine dunes under the influence of tide-and wind-driven processes (Dover Strait, northern France). Mar. Geol. 211, 143-168.

Lindsay, P., Mason, T.R.M., Pillay, S., Wright, C.I., 1996. Sedimentology and dynamics of the Umfolozi Estuary, North KwaZulu-Natal, South Africa, S. Afr. J. Geol. 99, 327-336.

Linsley, B.K., 1996. Oxygen-isotope record of sea level and climate variations in the Sulu Sea over the past 150,000 years. Nature 380, 234-237.

Lutjeharms, J.R.E., Grundlingh, M.L., Carter, R.A., 1989. Topographically induced upwelling in the Natal Bight. S. Afr. J. Sci. 310-317.

Lutjeharms, J.R.E., 2006. The ocean environment off south-eastern Africa: a review. S.Afr. J. Sci. 102, 419-425.

MacCready, P., Pawlak, G., 2001. Stratified flow along a rough slope: Separation drag and wave drag. J. Phys. Oceanogr. 31, 2824-2839.

Martin, A.K., 1984. Plate tectonic status and sedimentary basin in-fill of the Natal Valley (SW Indian Ocean). Bulletin of the Joint Geological Survey/University of Cape Town, Marine Geoscience Unit 14, pp 209.

Martin, A.K., Flemming, B.W., 1986. The Holocene shelf sediment wedge off the south and east coast of South Africa. Canadian Society of Petroleum Geologists Memoir 2, 27-44.

Martin, A.K., Flemming, B.W., 1988. Physiography, structure and evolution of the Natal continental shelf. In: Schumann, E.H. (Ed.), Lecture notes on coastal and estuarine studies, 26, Springer Verlag, New York, 11-46.

Martin, A.K., Goodlad, S.W., Salmon, D.A., 1982. Sedimentary basin in-fill in the northernmost Natal Valley, hiatus development and Agulhas Current palaeo-oceanography. J. Geol. Soc. Lond. 139, 183-201.

Masselink, G., Hughes, M.G., 2003. Introduction to Coastal Processes and Geomorphology. Oxford University Press, New York, pp 354.

Masson, D.G., Harbitz, C.B., Wynn, R.B., Pederson, G., Løvholt, F., 2006. Submarine landslides – process, triggers and hazard prediction. Phil. Trans. Royal Soc. A. 364, 2009-2039.

McAdoo, B.G., Orange, D.L., Screaton, E., Lee, H., Kayen, R., 1997. Slope basins, headless canyons, and submarine palaeoseismology of the Cascadia accretionary complex. Basin Res. 9, 313-324.

McAdoo, B.M., Pratson, L.F., Orange, D.L, 2000. Submarine landslide geomorphology, US continental slope. Mar. Geol. 169, 103-136.

McHugh, C.M.G., Damuth, J.E., Mountain, G.S., 2002. Cenozoic mass transport facies and their correlation with relative sea-level change, New Jersey continental margin. Mar. Geol. 184, 295-334.

McHugh, C.M.G., Olson, H.C., 2002. Pleistocene chronology of continental margin sedimentation: new insights into traditional models, New Jersey Continental Margin. Mar. Geol. 186, 295-334.

McLachlan, I.R, McMillan, I.K., 1979. Stratigraphical and sedimentological evidence from the Durban Region of major sea-level movements since the Late Tertiary. Trans. Geol. Soc. S. Afr. Spec. Pub. 6, 161-181.

Meyer, R., Talma, A.S., Duvenhage, A.W.A., Eglington, B.M., Taljaard, J., Botha, J.F., Verwey, J., Van der Voort, I., 2001. Geohydrological investigation and evaluation of the Zululand coastal aquifer. Pretoria, Water Research Commission Report 221/1/01

Miller, D.E., 1990. A southern African Late Quaternary sea level curve. S. Afr. J. Sci. 86, 457-459.

Miller, K.G., Mountain, G.S., Leg 150 Shipboard Party, Members of the New Jersey Coastal Plain Drilling Project, 1996a. Drilling and dating New Jersey Oligocene-Miocene sequences : Ice volume, global sea level, and Exxon records. Science 271, 1092-1095.

Miller, K.G., Liu, C., Feigenson, M.D., 1996b. Oligocene to middle Miocene Sr-isotopic stratigraphy of the New Jersey continental slope. In: Mountain, G.S., Miller, K.G., Blum, P.B., Poag, C.W., Twichell, D.C. (Eds.), Proc. ODP Sci. Results 150, 97-114.

Miller, W.R., 1998. The bathymetry, sedimentology and seismic stratigraphy of Lake Sibaya-Northern KwaZulu-Natal. MSc Thesis, University of Natal, Durban, pp 146.

Miller, W.R., 2001. The Bathymetry, sedimentology and seismic stratigraphy of Lake Sibaya - Northern KwaZulu-Natal. Council for Geoscience Bull. 131, pp 86.

Miller, W.R., Mason T.R., 1994. Erosional features of coastal beachrock and aeolianite outcrops in Natal and Zululand, South Africa. J. Coastal Res. 10, 374-394.

Mitchell, M.C., 2005. Interpreting long-profiles of canyons in the USA Atlantic continental slope. Mar. Geol. 214, 75-99.

Mitchum, R.M., Vail, P.R., 1977. Seismic stratigraphy and global changes of sea level, part 7: Seismic stratigraphy interpretation procedure. In: Payton C.E. (Ed.), Seismic Stratigraphy – Applications to Hydrocarbon Exploration. AAPG Memoir 26, 135-143.

Mohrig, D., Whipple, K.X., Hondzo, M., Ellis, C., Parker, G., 1998. Hydroplaning of subaqueous debris flows. GSA Bull. 11, 387-394.

Morris, T., Roberts, M.J., Schleyer, M.H., 2007. The current on the Sodwana Bay shelf (South Africa): Characteristics, driving forces and implications. 5th WIOMSA Scientific Symposium, Symposium Guide and Book of Abstracts pp 137.

Morton, R.A., Suter J.R., 1996. Sequence stratigraphy and composition of Late Quaternary shelf-margin deltas, northern Gulf of Mexico. AAPG Bull. 80, 505-530.

Murray, A.B., Thieler, E.R., 2004. A new hypothesis for the formation of large-scale inner shelf sediment sorting and "ripple scour depressions". Cont. Shelf. Res. 24, 295-315.

Mulder, T., Syvetski, J.P.M., 1995. Turbidity currents generated at river mouths during exceptional discharges to the world's oceans. Journal of Geology 103, 285-299.

Mulligan, A.E., Evans, R., Lizzaralde, D., 2007. The role of palaeochannels in groundwater/seawater exchange. J. Hydrol. 335, 313-329.

Nelson, C.H., Carlson, P.R., Byrne, J.V., Alpha, T.R., 1970. Development of the Astoria Canyon-Fan physiography and comparison with similar systems. Mar. Geol. 8, 259-291.

Njordford, S., Goff, J.A., Austin, J.A., Sommerfield, C.K., 2004. Seismic geomorphology of buried channel systems on the New Jersey outer shelf: assessing past environmental conditions. Mar. Geol. 214, 339-364.

Nordfjord, S., Goff, J.A., Austin, J.A., Gulick, S.P.S., 2006. Seismic facies of incised valley fills, New Jersey continental shelf: implications for erosion and preservation processes acting during latest Pleistocene-Holocene transgression. J. Sed. Res. 76, 1284-1303.

Norem, H., Locat, J., Schieldrop, B., 1990. An approach to the physics and the modelling of submarine flowslides. Mar. Geotechnol. 9, 93-111.

Normark, W.R., Posamantier, H., Mutti, E., 1993. Turbidite systems: state of the art and future. Rev. Geophys. 31, 91-116.

O'Grady, D.B., Syvitski, J.P.M., Pratson, L.F., Sarg, J.F., 2000. Categorizing the morphologic variability of siliciclastic passive continental margins. Geology 28, 207-210.

Olsson, R.K., Miller, K.G., Browning, J.V., Wright, J.D., Cramer, B.S., 2002. Sequence stratigraphy and sea-level change across the Cretaceous-Tertiary boundary on the New Jersey passive margin. In: Koeberl, C., MacLeod, K.G. (Eds.), Catastrophic Events and Mass Extinctions: Impacts and Beyond. Geol. Soc. Am. Spec. Pap. 356, 97- 108.

Orange, D.L., Breen, N.A., 1992. The effects of fluid escape on accretionary wedges 2. Seepage force, slope failure, headless submarine canyons and vents. J. Geophys. Res. 97, 9277-9295.

Orange, D.L., Anderson, R.S., Breen, N.A. 1994. Regular canyon spacing in the submarine environment: the link between hydrology and geomorphology. GSA Today 4, 29-39.

Orange, D.L., McAdoo, B., Moore, C.J., Tobin, H., Screaton, E., Chezar, H., Lee, H., Reid, M., Vail, R.,1997. Headless submarine canyons and fluid flow on the toe of the Cascadia accretionary complex. Basin Res. 9, 303-312.

Osterberg, E.C., 2006. Late Quaternay (marine isotope stages 6-1) seismic sequence stratigraphic evolution of the Otago continental shelf, New Zealand. Mar. Geo. 229, 159-178.

Pazzaglia, F.J., 1993. Stratigraphy, petrography, and correlation of late Cenozoic middle Atlantic Coastal Plain deposits: Implications for late-stage passive-margin geologic evolution. Geol. Soc. Am. Bull. 105, 1617-1634.

Partridge, T.C., Maud, R.R., 1987. Geomorphic evolution of southern Africa since the Mesozoic. S. Afr.. J. Geol. 90, 179-208.

Partridge, T.C., Botha, G.A., Haddon, I.G., 2006. Cenozoic deposits of the interior. In: Johnson, M.R., Anheuser, C.R., Thomas, R.J. (Eds.), The geology of South Africa. The Geological Society of South Africa, Johannesburg/Council for Geoscience, Pretoria, 585-605.

Paull, C.K., Spiess, F.N., Curray, J.R., Twichell, D.C., 1990. Origin of Florida Canyon and the role of spring sapping on the formation of submarine box canyons. GSA Bull. 102, 502 - 515.

Pether J., 1994. Molluscan evidence for enhanced deglacial advection of Agulhas water in the Benguela Current, off southwestern Africa. Palaeogeog., Palaeoclimatol., Palaeoecol. 111, 99-117.

Piper, D.J.W., Cochonat, P., Morrison, M.L., 1999. The sequence of events around the epicenter of the Grand Banks earthquake: initiation of debris flow and turbidity current inferred from sidescan sonar. Sedimentology 46, 79-97.

Pitman, W.V., Hutcheson, I.P.G., 1975. A preliminary hydrological study of Lake Sibaya, Hydrological Research Unit Report, 4/75, pp 35.

Pivechin, T., Nof, D., Lutjeharms, J.R.E., 1999. Why are there Agulhas Rings? J. Phys. Oceanogr. 29, 693-707.

Plint, A.G., Nummedal, D., 2000. The falling stage systems tract: recognition and importance in sequence stratigraphic analysis. In: Hunt, D., Gawthorpe, R.L. (Eds.), Sedimentary Responses to Forced Regression. Geol. Soc., London, Spec. Pubs. 172, 1-17.

Poag, C.W., Sevon, W.D., 1989. A record of Appalachian denudation in postrift Mesozoic and Cenozoic sedimentary deposits of the U.S. middle Atlantic margin. Geomorph. 2, 119-157.

Porebsky, S.J., Steel, R.N., 2003. Shelf-margin deltas: their stratigraphic significance and relation to deepwater sands. Earth. Sci. Rev. 62, 283-326.

Posamantier, H.W., 2001. Lowstand alluvial bypass systems: incised vs unincised. AAPG Bull. 85, 1771-1793.

Posamantier, H.W., Jervey, M.T., Vail, P.R., 1988. Eustatic controls on clastic deposition, I. Conceptual framework. In: Wilgus, C.K., Hastings, B.S., Kendall, C.G.St.C., Posamentier, H.W., Ross, C.A., Van Wagoner, J.C. (Eds.), Sea-Level Changes: An Integrated Approach. Spec. Publ. SEPM. 42, 125-154.

Posamentier, H.W., Vail, P.R., 1988. Eustatic controls on clastic deposition, II. Sequence and systems tracts models. In: Wilgus, C.K., Hastings, B.S., Kendall, C.G.St.C., Posamentier, H.W., Ross, C.A., Van Wagoner, J.C. (Eds.), Sea-Level Changes: An Integrated Approach. Spec. Publ. SEPM. 42, 125-154.

Posamantier, H.W., and Allen, G.P., 1993. Variability of the sequence stratigraphic model: effects of local basin factors. Sed. Geol. 86, 91-109.

Posamantier, H.W., and Allen, G.P., 1999. Siliciclastic sequence stratigraphy: concepts and applications. SEPM Concepts in Sedimentology and Palaeontology 9, pp 210.

Pratson, L.F., Coakley, B.J. 1996. A model for the headward erosion of submarine canyons induced by downslope eroding sediment flows. Geol. Soc. Am. Bull. 108, 225-234.

Pratson, L.F., Ryan, W.B.F., Mountain, G.S., Twitchell, D.C., 1994. Submarine canyon initiation by downslope-eroding sediment flows: evidence in late Cenozoic strata on the New Jersey continental slope. Geol. Soc. Am. Bull. 106, 395-412.

Ramsay, J.G., Huber, M.I. The techniques of modern structural geology. Volume 2: folds and fractures. Academic Press, London, pp 501.

Ramsay, P.J., 1991. Sedimentology, coral reef zonation and late Pleistocene coastline models of the Sodwana Bay continental shelf, northern Zululand. PhD thesis, University of Natal, Durban, pp 202.

Ramsay, P.J., 1994. Marine geology of the Sodwana Bay shelf, Southeast Africa. Mar. Geol. 120, 225-247.

Ramsay, P.J., 1995. 9000 years of sea-level change along the southern African coastline. Quat. Int. 31, 71-75.

Ramsay, P.J., 1996. Quaternary marine geology of the Sodwana Bay shelf, northern KwaZulu-Natal. Bulletin of the Geological Survey of South Africa 117, pp 154.

Ramsay, P.J., 1997. Holocene sea-level changes. In: Botha, G.A. (Ed.), Maputaland focus on the Quaternary evolution of the south-east African coastal plain. International Union for Quaternary Research Workshop Abstracts. Council for Geoscience, Private Bag X112, Pretoria, South Africa, 56-57.

Ramsay, P.J., Cooper, J.A.G., Wright, C.I., Mason, T.R., 1989. The occurrence and formation of ladderback ripples in subtidal, shallow marine sands, Zululand, South Africa. Mar. Geol. 120, 224-247.

Ramsay P.J., Smith A.M., Lee-Thorp J.C., Vogel J.C., Tyldsey M. and Kidwell W., 1993. 130 000 year-old fossil elephant found near Durban: Preliminary report. S. Afr. J. Sci. 89, 165.

Ramsay, P.J., Cooper, J.A.G., 2002. Late Quaternary sea-level change in South Africa. Quat. Res. 57, 82-90.

Ramsay, P.J., Smith, A.M., Mason, T.R., 1996. Geostrophic sand ridge, dune fields and associated bedforms from the northern KwaZulu-Natal continental shelf, south-east Africa. Sedimentology 43, 407-419.

Ramsay, P.J., Miller, W.R., 2006. Marine geophysical technology used to define coelacanth habitats on the KwaZulu-Natal shelf, South Africa. S. Afr. J. Sci. 102, 427-434.

Ramsay, P.J., Schleyer, M.H., Leuci, R., Muller, G.A., Celliers, L., Harris, J.M., Green, A.N., 2006. The development of an expert marine geographic information system to provide an environmental and economic decision support system for proposed tourism developments within and around the Greater St Lucia Wetland Park world heritage site. Innovation Fund Project 24401, pp 92.

Ritter, D.F., Kochel, R.C., Miller, J.R., 1995. Process Geomorphology, 3rd ed. W.C. Brown Publishers, Boston, 225.

Ribbink, A.J., Roberts, M., 2006. African Coelacanth Ecosystem Programme: An overview of the conference contributions. S. Afr. J. Sci. 102, 409-416.

Robb, J.M., 1984. Spring sapping on the lower continental slope, offshore New Jersey. Geology 12, 278-282.

Roberts, D.L, Botha, G.A., Maud, R.R., Pether, J., 2007. Coastal Cenozoic deposits. In: Johnson, M.R., Anheuser, C.R., Thomas, R.J. (Eds.), The geology of South Africa. The Geological Society of South Africa, Johannesburg/Council for Geoscience, Pretoria, 605-629.

Rogers, J., 1977. Sedimentation on the continental margin off the Orange River and the Namib Desert. Bulletin of the Geological Survey of South Africa/University of Cape Town Marine Geoscience Unit 7, pp 162.

Rogers, J., 1985. Geomorphology, offshore bathymetry and Quaternary lithostratigraphy around the Bot River Estuary. Trans. Royal. Soc. S. Afr. 45, 211-237.

Rogers, J., Li, X.C., 2002.Environmental impact of diamond mining on the continental shelf off southern Namibia. Quat. Int. 92, 101-112.

Rossouw, J., 1984. Review of existing wave data, wave climate and design waves for South African and South West African (Namibian) coastal waters. CSIR Report T/SEA 8401, Stellenbosch, pp 66.

Shackleton, N.J., 2000. The 100 000-year ice-age cycle identified and found to lag temperature, carbon dioxide, and orbital eccentricity. Science 289, 1897-1902.

Shackleton, N.J., Berger, A., Peltier, W.A., 1990. An alternative astronomical calibration of the Lower Pleistocene timescale based on ODP site 677. Trans. R. Soc. (Edinburgh) Earth Sci. 81, 251-261.

Shaw, M.J., 1998. Seismic stratigraphy of the northern KwaZulu-Natal upper continental margin. MSc Thesis, University of Natal, Durban, pp 190.

Shepard, F.P., 1963. Submarine Geology. Harper and Row, New York, 557 pp.

Shepard, F.P., Curray, J.R., Innan, D.L., Murray, E.A., Winterer, E.L., Dill, R.F., 1964. Submarine Geology by Diving Saucer: Bottom currents and precipitous submarine canyon walls continue to a depth of at least 300 meters. Science 145, 1042.

Shone, R.W., 2007. Onshore post-Karoo Mesozoic deposits. In: Johnson, M.R., Anheuser, C.R., Thomas, R.J. (Eds.), The geology of South Africa. The Geological Society of South Africa, Johannesburg/Council for Geoscience, Pretoria, 541-553.

Siesser, W.G., 1977. Biostratigraphy and micropalaeontology of continental margin samples. Technical report, Joint Geological Survey/University of Cape Town Marine Geoscience Unit, 9, 108-117.

Siesser, W.G., Dingle, R.V., 1981. Tertiary sea-level movements around southern Africa. J. Geol. 89, 83-96.

Simpson, E.S.W., Schlich, R., et al., 1974. Initial reports of the deep-sea drilling project 25. Washington D.C., U.S Government Printing Office, pp 884.

Sink, K.J., Boshoff, W., Samaai, T., Timm, P.G., Kerwath, S.E., 2006. Observations of the habitats and biodiversity of the submarine canyons at Sodwana Bay. S. Afr. J. Sci. 102, 491-501.

Snedden, J.W., Tillman, R.D., Kreisa, R.D., Schweller, W.J., Culver, S.J., Winn, R.D., 1994. Stratigraphy and genesis of a modern shoreface attached sand ridge, Peahala Ridge, New Jersey. J. Sed. Res. 64, 560-581.

Snedden, J W and Bergman, K M 1999. Isolated Shallow Marine Sand Bodies: Deposits for all Interpretations. In: Bergman, K M, and Snedden, J (Eds.), Shallow Marine Sandbodies, Spec. Publ. SEPM. 64, 1-12.

Snedden, J.W., Dalrymple, R.W., 1999. Modern shelf sand ridges: from historical perspective to a unified hydrodynamic and evolutionary model. In: Bergman, K.M., Snedden, J.W. (Eds.), Isolated Shallow Marine

Sand Bodies: Sequence Stratigraphic Analysis and Sedimentologic Interpretation, Spec. Pub. SEPM. 64, 13-28.

Steel, R.J., Crabaugh, J., Schellpeper, M., Mellere, D., Plink-Björklund, P., Deibert, J., Loeseth, T., 2000. Deltas versus rivers on the shelf edge: their relative contributions to the growth of shelf margins and basin-floor fans (Barremian and Eocene, Spitsbergen). Proc. GCSSEPM Foundation 20th Ann. Res. Conf., Deepwater Reservoirs of the World, Houston, Dec. 2000., pp. 981-1000.

Stevenson, I.R., McMillan, I.K., 2004. Incised valley fill stratigraphy of the Upper Cretaceous succession, proximal Orange Basin, Atlantic margin of southern Africa. J. Geol. Soc. 161, 184-208.

Stoker, M.S., Akhurst, C., Howe, J.A., Stow, D.A.V., 1998. Sediment drifts and contourites on the continental margin, off Northwest Britain. Sed. Geol. 11, 33-52.

Stow, D.A.V., Taira, A., Ogawa, Y., Soh, W., Taniguchi, H., Pickering, K.T., 1998. Volcaniclastic sediments, process interaction and depositional setting of the Mio-Pliocene Miura Group, SE Japan. Sed. Geol. 115, 351-381.

Stow, D.A.V., Pudsey, C.J., Howe, J.A., Faugères, J.C., Viana, A.R., 2002. Deep-water Contourite Systems: Modern Drifts and Ancient Series, Seismic and Sedimentary Characteristics, Memoirs 22, Geological Society of London, London, pp 464.

Stubblefield, W.L., McGrail, D.W., Kersey, D.G., 1984. Recognition of transgressive and post-transgressive sand ridges on the New Jersey continental shelf. In: Tillman, R.W., Siemers, C.T. (Eds.), Siliciclastic shelf sediments. Soc. Econ. Palaeontol. Mineral., Tulsa, 1-23.

Suter, J.R., Berryhill, H.L., Penland, S., 1987. Late Quaternary sea-level fluctuations and depositional sequences, southwest Louisiana continental shelf. In: Nummedal, D., Pilkey, O.H., Howard, J.D. (Eds.), Sea-Level Fluctuation and Coastal Evolution. Spec. Pub.-Soc. Econom. Paleontol. Mineral. 41, 199-219.

Swift, D.J.P., Kofoed, J.W., Saulsbury, F.P., Sears, P., 1972. Holocene evolution of the shelf surface, central and southern Atlantic shelf of north america. In: Swift, D.J.P, Duane, D.B., Pilkey, O.H. (Eds.), Shelf Sediment Transport: Process and Pattern, Dowden, Hutchinson & Ross, Stroudsburg, Penn, pp 499- 574.

Swift, D.J.P., Field, M.E., 1981. Evolution of a classic sand ridge field: Maryland sector, North America inner shelf. Sedimentology 28, 461-482.

Swift, D.J.P., McKinney, T.F., Stahl L., 1984. Recognition of transgressive and post-transgressive sand ridges on the New Jersey continental shelf: discussion. In: Tillman, R.W., Siemers, C.T. (Eds.), Siliciclastic shelf sediments. Soc. Econ. Palaeontol. Mineral., Tulsa, 25-36.

Sydow, C.J., 1988. Stratigraphic control of slumping and canyon development on the continental margin, east coast, South Africa. BSc Hons Thesis, University of Cape Town, pp 55.

Sydow, C.J., Roberts, H.H., 1994. Stratigraphic framework of a Late Pleistocene shelf-edge delta, northeast Gulf of Mexico. AAPG Bull. 78, 1276-1312.

Tesson, M., Posamentier, H.W., Gensous, B., 2000. Stratigraphic organization of Late Pleistocene deposits of the western part of the Golfe du Lion shelf (Languedoc shelf), western Mediterranean Sea, using high-resolution seismic and core data. Am. Assoc.Petrol. Geol. Bull. 84, 119-150.

Tripsanas, E.K., Piper, D.J.W., Jenner, K.A., Bryant, W.R., 2008. Submarine mass-transport facies: new perspectives on flow processes from cores on the eastern North American margin. Sedimentology 55, 97-136.

Twichell, D.C., Roberts, D.G., 1982. Morphology, distribution and development of submarine canyons on the United States Atlantic continental slope between Hudson and Baltimore Canyons. Geology 10, 408-412.

Twichell, D.C., Brooks, G., Gelfenbaum, G., Paskevich, V., Donahue, B., 2003. Sand ridges off Sarasota, Florida: a complex facies boundary on a low energy inner shelf environment. Mar. Geol. 200, 243-262.

Tyson, P.D., Preston-Whyte, R.A., 2000. The Atmosphere and Weather of Southern Africa, Oxford University Press, Cape Town, pp 375.

Vail, P.R., 1987. Seismic stratigraphy interpretation using sequence stratigraphy, Part 1: Seismic stratigraphy interpretation procedure. In: Bally A.W. (Ed.), Atlas of Seismic Stratigraphy. AAPG, Studies in Geology 27, 1-10.

Van Heerden, I.L., 1987. Sedimentation in the greater St Lucia complex as related to palaeo-sea levels. Abstract, 6th National Oceanographic Symposium, Stellenbosch. Paper 157, B-106.

Van Heerden, I.L., Swart, D.H., 1986. An assessment of past and previous geomorphological and sedimentary processes operative in the St. Lucia Estuary and environs. Marine Geoscience and Sediment Dynamics Division Unit, NRIO, CSIR Research Report, 569, pp 120.

Van Lancker, V., Lanckneus, J., Moerkerke, G., Hearn, S., Hoekstra, P., Levoy, F., Miles, J., Whitehouse, R., 2004. Coastal and nearshore morphology, bedforms and sediment transport pathways at Teignmouth (UK). Cont. Shelf Res. 24, 1171-1202.

Van Wagoner, J.C., Mitchum, R.M., Campion, K.M., Rahmanian, V.D., 1990. Siliciclastic sequence stratigraphy in well logs, cores and outcrops. AAPG Meth. Explor. Ser. 7, 55 pp.

Viana, A.R., Faugères, Stow, D.A.V., 1998. Bottom-current-controlled sand deposits -a review of modern shallow-to deep-water environments. Sed. Geol. 115, 53-80.

Vogel, J.C., Marais, M., 1971. Pretoria radiocarbon dates. Radiocarbon 23, 43-80.

Watkeys, M.K., 1997. The Mkuze River from the Lebombo to the Lower Mkuze bridge. In: Botha, G.A. (Ed.), Maputaland focus on the Quaternary evolution of the south-east African coastal plain. International Union for Quaternary Research Workshop Abstracts. Council for Geoscience, Private Bag X112, Pretoria, South Africa, 42-47.

Watkeys, M.K., 2002. Development of the Lebombo rifted volcanic margin of southeast Africa. In: Menzies, M.A., Klemperer, S.L., Ebinger, C.J., Baker, J. (Eds.), Volcanic Rifted Margins, Geol. Soc. Am. Spec. Pap. 362, 27-46.

Watkeys, M.K., Mason, T.R., Goodman, P.S., 1993. The role of geology in the development of Maputaland, South Africa. J. Afr. Earth Sci. 16, 205-221.

Weaver, P.P.E., Kuijpers, A., 1993. Climatic control of turbidite deposition on the Madeira Abyssal Plain. Nature 306, 360-363.

Weaver, P.P.E., Rothwell, R.G., Ebbing, J., Gunn, D., Hunter, P.M., 1992. Correlation, frequency of emplacement and source directions of megaturbidites on the Madeira Abyssal Plain. Mar. Geol. 109, 1-20.

Weber, N., Chaumillon, E., Tesson, M., Garlan, T., 2004. Architecture and morphology of the outer segment of a mixed tide and wave-dominated-incised valley, revealed by HR seismic reflection profiling: the palaeo-Charente River, France. Mar. Geol. 207, 17-38.

Wonham, J.P., Jayr, S., Mougamba, R., Chuilon, P., 2000. 3D sedimentary evolution of a canyon fill (Lower Miocene-age) from the Mandarove formation, offshore Gabon. Mar. Petrol. Geol. 17, 175-197.

Wright, C.I., 1995. The sediment dynamics of St. Lucia and Mfolozi Estuary mouths, Zululand, South Africa. Report No. 1995-0132, Council for Geoscience, Private Bag X112, Pretoria, 0001, pp 12.

Wright, C.I., Mason, T.R., 1990. The sedimentary environments and facies of St. Lucia estuary mouth, Zululand, South Africa. J. Afr. Earth Sci. 11, 411-420.

Wright, C.I., Mason, T.R., 1993. Management and sediment dynamics of the St. Lucia Estuary mouth, Zululand, South Africa. Env. Geol. 22, 227-241.

Wright, C.I., Miller, W.R., Cooper, J.A.G., 2000. The late Cenozoic evolution of coastal water bodies in Northern KwaZulu-Natal, South Africa. Mar. Geol. 167, 207-229.

Wright, C.I., 2002. Aspects of the Cenozoic evolution of the northern KwaZulu-Natal coastal plain, South Africa. Council for Geoscience Bull. 132, pp 120.

Zaitlin, B.A., Dalrymple, R.W., Boyd, R., 1994. The stratigraphic organisation of incised valley systems associated with relative sea-level change. In: Dalrymple, R.W., Boyd, R.J., Zaitlin, B.A. (Eds.), Incised Valley Systems: Origin and Sedimentary Sequences. Soc. Sediment. Geol. Spec. Publ., 51. SEPM, Tulsa, 45-60.

Zi, M.Z., King, E.L., 2007. Multibeam bathymetric investigations of the morphology of sand ridges and associated bedforms and their relations to storm processes, Sable Island Bank. Scotian Shelf. Mar. Geol. 243, 200-228.

APPENDIX 3

Additional publications of overlapping interest to this study

Continental Shelf Research 28 (2008) 2442–2449

Contents lists available at ScienceDirect

Continental Shelf Research

journal homepage: www.elsevier.com/locate/csr

Nannofossil age constraints for the northern KwaZulu-Natal shelf-edge wedge: Implications for continental margin dynamics, South Africa, SW Indian Ocean

A.N. Green [a,*], M. Ovechkina [a,b], R. Uken [a]

[a] Joint Council for Geoscience-University of KwaZulu-Natal, Marine Geoscience Unit, School of Geological Sciences Westville Campus, PBag X54001, Durban 4000, South Africa
[b] Palaeontological Institute, Russian Academy of Sciences, Moscow, Russia

ARTICLE INFO

Article history:
Received 11 March 2008
Received in revised form
9 June 2008
Accepted 11 June 2008
Available online 26 June 2008

Keywords:
Shelf-edge wedge
Nannofossils
Submarine canyons

ABSTRACT

Samples collected from the shelf-edge wedge using surface grab samples and the *Jago* submersible constrain the KwaZulu-Natal shelf-edge wedge to a late Pliocene age on the basis of the absence of *Gephyrocapsa oceanica* s.l. and *Discoaster brouweri*, and the presence of *Calcidiscus macintyrei*. This correlates with proposed Tertiary sea-level curves for southern Africa and indicates relative sea-level fall during the late Pliocene coupled with hinterland uplift. Exposed failure scarps in the upper portions of submarine canyons yield sediment samples of early Pleistocene ages, indicating the uppermost age of deposition of clinoform topsets exposed in the scarp walls. Partially consolidated, interbedded silty and sandy deposits of similar age outcrop in the thalweg of Leven canyon at a depth of 150 m. These sediments provide an upper age limit of the shelf-edge wedge of early Pleistocene, giving a sedimentation rate of this wedge of 162–309 m/Ma. The distribution of widespread basal-most Pleistocene sediments on the upper slope indicates that these sediments escaped major reworking during sea-level falls associated with Pleistocene glaciations and remain as relict upper slope veneers. The absence of more recent sediments suggests that this area has been a zone of sediment bypass or starvation since the early Pleistocene. Areas where younger sediments mantle deposits of early Pleistocene ages represent areas of offshore bedload parting, re-distributing younger Holocene sediment offshore and downslope.

1. Introduction

With the recent discovery of the coelacanth, *Latimeria chalumnae* in Jesser canyon, northern KwaZulu-Natal, South Africa (Sink et al., 2007), scientific interest in these canyon environments has increased dramatically. This is because many of these submarine canyons impinge the shelf break (Green et al., 2007) and satisfy the morphological and bathymetric constraints for coelacanth habitation (Fricke and Plante, 1988; Fricke and Hissmann, 1994). Multibeam bathymetric, side scan sonar, and high-resolution seismic data were thus acquired by the African Coelacanth Ecosystem Programme in order to unravel the complex evolution of these canyon systems. The aim of this, in part, was to establish a stratigraphic framework within which canyon evolution may be assessed, and, in particular, the chronostratigraphic evolution of the continental shelf and its canyon features (Green, unpublished data). Very little is known regarding the age constraints on the evolution of this portion of the South African continental margin, much of the ages assigned to various units being merely speculative (Shaw, 1998) in light of the dearth of outcrop and core samples. This paper thus aims to assess the biostratographic zonation of several samples collected for seismic groundtruthing, with the intent of constraining the ages of major continental slope and shelf sedimentation episodes, relevant to canyon formation in this area.

2. Regional setting

The northern KwaZulu-Natal continental shelf (Fig. 1) forms part of a linear clastic coastline (Cooper, 1994), bounded by a narrow continental shelf (Martin and Flemming, 1988; Ramsay, 1994; Green et al., 2007). The shelf is considered particularly narrow (~2 km) when compared to the global average of ~50 km (Shepard, 1963). The shelf break occurs at approximately 100 m water depth, and marks the transition from flat shelf to very steep, seaward dipping sediments of the upper slope (Sydow, 1988; Shaw, 1998; Green et al., 2007). These sediments are dissected by

* Corresponding author. Tel.: +27 312602516.
E-mail address: greena@ukzn.ac.za (A.N. Green).

0278-4343/$ - see front matter © 2008 Elsevier Ltd. All rights reserved.
doi:10.1016/j.csr.2008.06.007

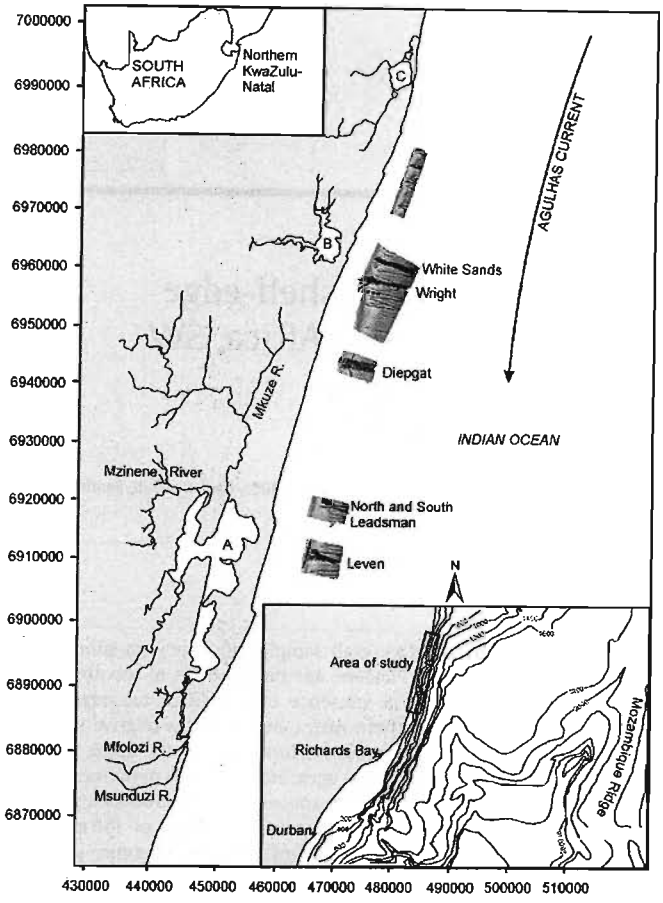

Fig. 1. Locality map of the northern KwaZulu-Natal continental shelf. The lowermost inset shows the area relevant to this study. Note the narrow continental shelf and steep upper continental slope of this region (after Dingle et al., 1978). Main figure details sunshaded multibeam bathymetric survey areas with several submarine canyons, which indent the continental shelf break (WGS 84 projection, UTM zone 36S, eastings and northings in metres). Block capitals A–C denote fringing freshwater lake systems; A = St Lucia Lake, B = Lake Sibaya, C = Kosi Lakes system.

several submarine canyons of varying size, which extend from Leven Point in the south of the study area, to Island Rock in the north (Ramsay and Miller, 2006) (Fig. 1). These systems today lack distinct shelf breaching canyon heads, instead they are slope confined without connection to any modern fluvial sources. Recent evidence suggests that the northern KwaZulu-Natal continental shelf is sediment starved (Cooper, 1994; Ramsay et al., 2006), resulting in submarine canyons becoming moribund features, active in part only prior to the Last Glacial Maximum ~18,000 BP (Green and Uken, 2005). Strong north to south geostrophic flows, associated with the Agulhas Current (Lutjeharms, 2006), have denuded much of the sediment from the outer shelf regions, resulting in a thin veneer of sediment, which mantles relict outer shelf gravels (Flemming, 1978, 1981; Ramsay et al., 2006). The inshore sediment prism is reworked into sub-aqueous bedforms that migrate from north to south, except where northward flowing return gyres of the Agulhas Current occur (Flemming, 1978; Ramsay, 1994).

The Holocene wedge extends from the present shoreline to a depth of 90 m and overlies emergent shelf sediments of Tertiary and Late Cretaceous ages (Dingle et al., 1983). Late Cretaceous (Maastrichtian) strata comprise silty sandstones of the St Lucia Formation (Siesser, 1977; McLachlan and McMillan, 1979; Dingle et al., 1983). Late Tertiary deposits are generally not well preserved on the northern KwaZulu-Natal coastal plain, though a coquina of Miocene–Pliocene age occurs throughout northern KwaZulu-Natal (Martin and Flemming, 1988; Kruger and Meyer, 1988, Roberts et al., 2007) and may correspond to a regional seismic reflector Jimmy (Martin et al., 1982; Goodlad, 1986). Jimmy is thought to represent a small hiatus between Miocene and Pliocene times, according to Siesser and Dingle (1981), both a short late Miocene/early Pliocene and a Pliocene hiatus occurred. Early- to mid-Pleistocene-age sediments are uncommon on this shelf, with only thin exposures of late Pleistocene sediments remaining on the east coast of southern Africa (McLachlan and McMillan, 1979; Dingle et al., 1983; Ramsay, 1991). These sediments comprise thin aeolianite/beachrock reef complexes that occur as discrete lineaments on the shelf, at the shelf edge and in canyon heads (Ramsay, 1994). The lack of borehole data in the offshore portions of the Zululand Basin allows only an incomplete inference of the offshore stratigraphy to be made, based on onshore well data, limited seismic data and coastal plain outcrop.

3. Materials and methods

A total of 170 sediment samples were collected using a Shipek grab or a submersible within the submarine canyon heads (Fig. 2). Submersible sampling from the German submersible *Jago* was particularly successful in that visual observations of the substrate could be undertaken thus increasing the accuracy of the sampling process. Of the total collected samples, nine representative samples associated with particular seismic or acoustic facies were analysed for nannofossils. These samples corresponded to the following:

(1) Weakly reflective sediment veneers of the upper slope (Leadsman 4 and Leven 5).
(2) Semi-consolidated samples of interbedded silt and sand at the base of the canyon walls (Leven canyon; −150 m).
(3) Exposed slump scarps within the canyon walls ~150 m deep (Leven 18 and Leven 13).
(4) Non-sandy thalweg material sampled at the maximum depth range of the *JAGO* submersible (Fig. 3) (Diepgat Dive 813; −369 m).
(5) A semi-consolidated, regionally-outcropping, strongly reflective coquina which occurs at the base of a strongly developed shelf-edge wedge (Dive 809 outcrop; −184 m).

Calcareous nannofossils were investigated using standard techniques (Bown and Young, 1998). Smear slides were systematically examined in phase-contrast and cross-polarized light at 1200× magnification on a Zeiss Axioskop light microscope. Scanning electron microscopy (SEM) was employed to confirm identifications and for photographing biostratigraphically important species.

An average state of preservation was assigned to each sample according to the following criteria: G—good (slight overgrowth and dissolution, but all specimens are easily identifiable); M—moderate (oblivious signs of dissolution and overgrowth, but most specimens are readily identifiable). Reworked nannofossils were noted in some samples. Bibliographic references for most taxa are provided by various authors (Perch-Nielsen, 1985; Sato and Takayama, 1992; Young and Bown, 1997; Bown, 2005). It should be noted here that an informal classification of the stratigraphically important genus *Gephyrocapsa* has been proposed (Rio, 1982), subdividing this complex into

(1) small *Gephyrocapsa*, lumping all forms less than 3.5 μm in size;

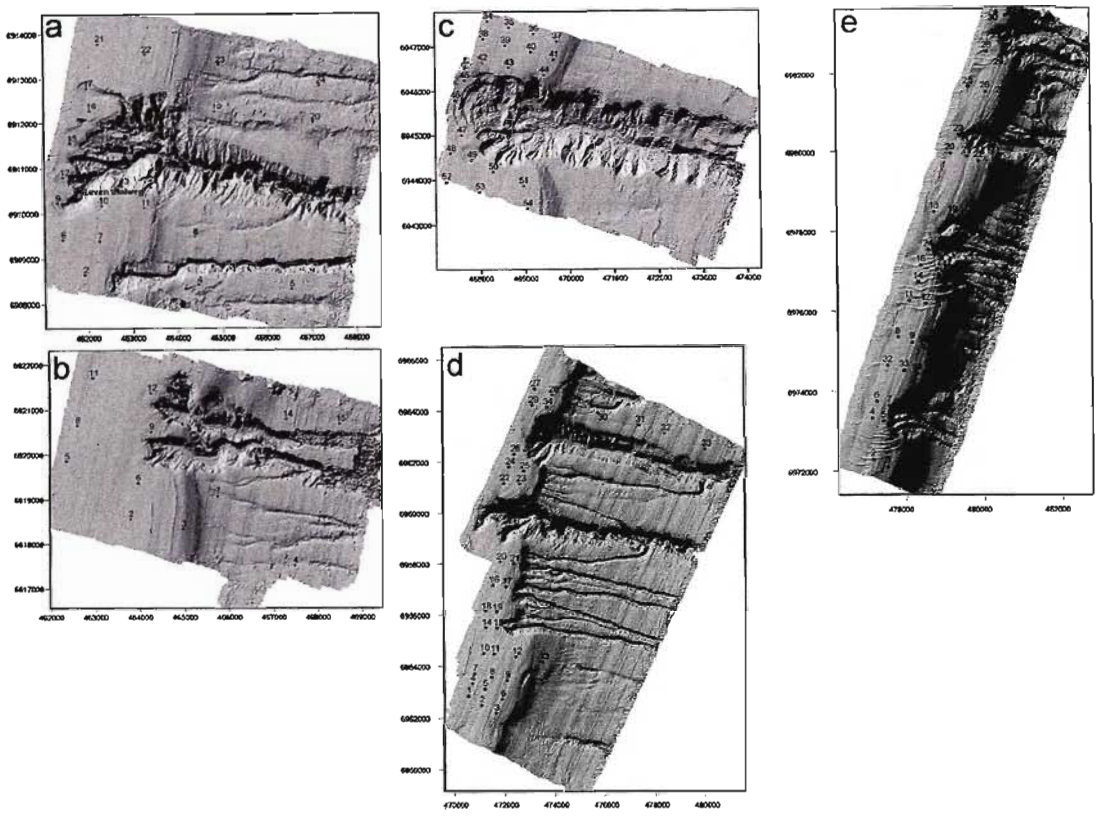

Fig. 2. Grab sample sites from the continental shelf and upper slope for the various multibeam mapped areas: (a) Leven Point, (b) Leadsman Shoals, (c) Diepgat canyon, (d) Sodwana Bay, (e) Mabibi. All maps are in WGS 84 projection, UTM zone 36S, units are in metres. Where prominent shelf-indenting canyons occur, several grab samples were acquired targeting the landslide scarps of the upper canyon walls. Note samples referred to in text for example Leven 4 or Leadsman 12 are from the mapped areas of Leven Point or Leadsman Shoals, respectively.

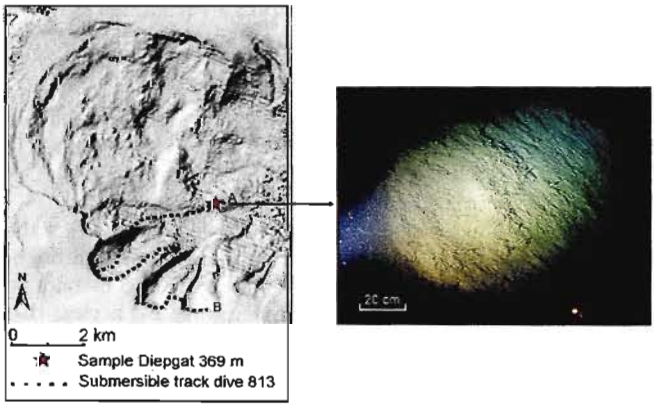

Fig. 3. Submersible track Dive 813 in Diepgat canyon, superimposed on sunshaded multibeam bathymetry. Note the star that denotes the sample position taken for the canyon thalweg. The accompanying photograph, taken from the *JAGO*, whilst sampling depicts the physical location of the sample site. Note the soupy, mud rich nature of the substrate, and the tranquil, low-energy conditions of the locality. Approximate scale is given by the scale bar in the bottom of the picture (~5 m).

(2) *Gephyrocapsa oceanica* s.l., lumping all forms between 3.5 and 5.5 μm, with a distinct and open central area; and
(3) large *Gephyrocapsae*, lumping all forms >6 μm.

4. Results

The shelf-edge wedge is a composite feature consisting of up to three different seismic facies (Fig. 4). Facies E1 and E2 are identified as forced regressive systems tract deposits, possibly formed by shelf margin clinoform advance during sea-level lowering (Green, unpublished data). Facies E3 is considered a lowstand deltaic unit, based on its onlapping progradational–aggradational wedge geometry, and its association with landward points of incision within the topsets of facies E1 and E2. These have been recognised by similar studies elsewhere as small deltaic feeder channels which incised into the delta top during lowstand (e.g. Osterberg, 2006).

4.1. Biostratigraphic results

The relative abundance of individual taxa as well as overall abundance is represented by letter codes and is recorded in Table 1 according to the following definitions:

A—abundant (1–10 specimens per one field of view).
C—common (1 specimen per 2–10 fields of view).
F—few (1 specimen per 11–50 fields of view).
R—rare (1 specimen per 51–100 field of view).
RR—very rare (specimen per 101–200 field of view).

All nine samples contained scarce although representative assemblages of nannofossil, which include 50 species, with 14 species being reworked (Table 1). The preservation of nannofossils is good to moderate, with the best preserved nannofossils presented in Fig. 5. Species of calcareous nannofossils considered in this study are listed in Fig. 6, where they are arranged alphabetically by genus name.

Sample Dive 809 contains *Gephyrocapsa carribbeanica*, with *Discoaster brouweri* and *G. oceanica* s.l. being absent, which places

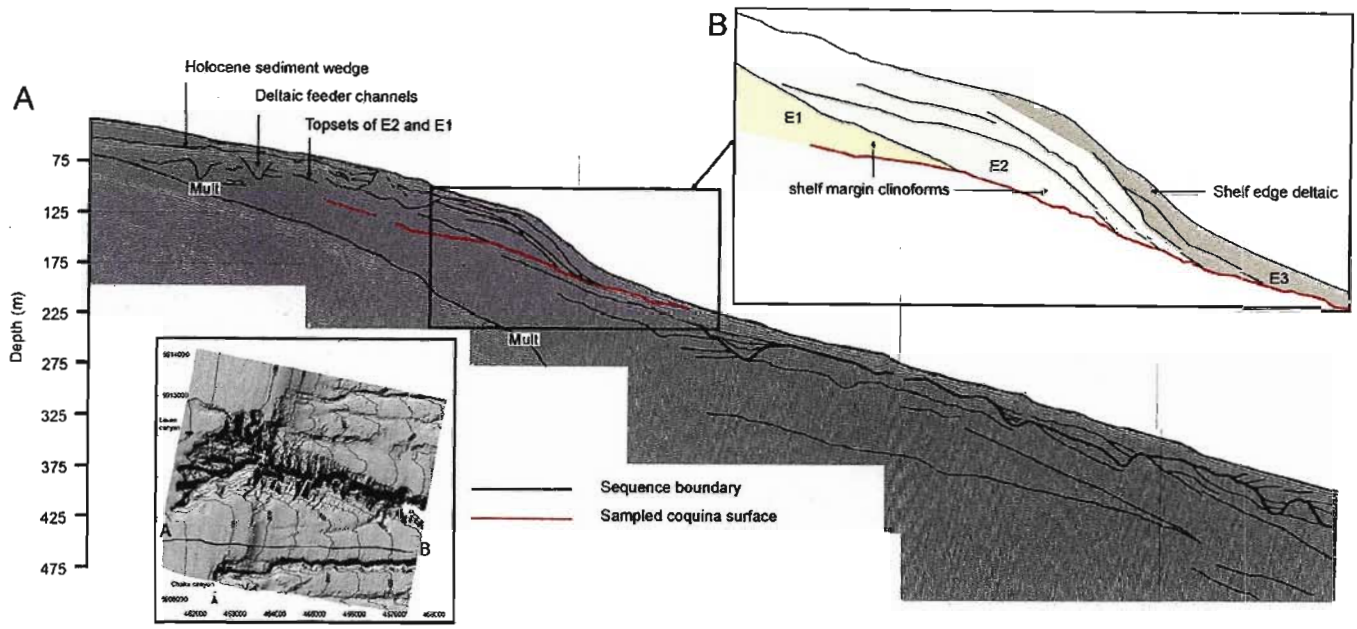

Fig. 4. Line drawing overlay of strike perpendicular seismic section 29, acquired across the continental shelf and upper slope of Leven Point (locality depicting inset). Note the three distinct seismic facies within the shelf-edge wedge, in addition to the small incision/fill features occurring within the topsets of Facies E1 and E2. These facies comprises loosely consolidated, interbedded sandstones and siltstones. The red line onto which the wedge clinoforms downlap is the same as that sampled in dive 813; however, here it is not exposed within the walls of a canyon feature. We consider this wedge to be indicative of forced regressive systems tract sedimentation.

this sample in Subzone MNN19a (NN19a) (terminal Pliocene) (Fig. 6). Dominant species are *G. carribbeanica* and *Calcidiscus leptoporus*; *Reticulofenestra* sp. (<4 μm) and *Coccolithus pelagicus* are subdominant; *Calcidiscus macintyrei*, *Dictyococcites* sp., *Helicosphaera carteri*, *Helicosphaera sellii*, *Pontosphaera japonica*, *Pseudoemiliania lacunosa*, *P. ovata*, *Reticulofenestra* sp., *Thoracosphaera operculata*, *Thoracosphaera saxea* are rare.

Subzone MNN19b (NN19b) (basal-most Pleistocene) accommodates samples Leadman 10, Leadsman 4, Leven 5, and Diepgat 369 m (cf. Table 1), based on the presence of both *G. oceanica* s.l. and *C. macintyrei*; the LO of the latter delineates the upper boundary of this subzone. Dominating are *G. oceanica* s.l., *G. carribbeanica*, *C. leptoporus*, and *T. saxea*. *C. macintyrei*, *D. productus*, *Gephyrocapsa* sp. (3.5–5.5 μm), *H. carteri*, *Helicosphaera wallichii*, *Umbilicosphaera sibogae*, and *Reticulofenestra* sp. (<4 μm) are subdominant. *Gephyrocapsa* sp. (small), *Helicosphaera kamptneri*, *H. sellii*, *P. japonica*, and *T. operculata* are rare.

Subzone MNN19c (NN19b) (lower Lower Pleistocene) embraces samples Leven Thalweg 150 m, Leven 18, Leven 13, and Leven 4 (cf. Table 1), based on the presence of *H. sellii* and the absence of *C. macintyrei* and large *Gephyrocapsa*, the FO of the latter defines the upper boundary of this subzone. Dominating are *G. oceanica* s.l., *G.* sp. (3.5–5.5 μm), and *C. leptoporus*; the species *D. productus*, *H. carteri*, and *T. saxea* are subdominant. *Gephyrocapsa* sp. (small), *H. kamptneri*, *H. sellii*, *P. lacunosa*, and *Reticulofenestra* sp. (<4 μm) are rare.

5. Discussion and conclusions

The majority of works on calcareous nannofossils rely on zonal schemes of various authors (Martini, 1971; Gartner, 1977; Okada and Bukry, 1980), which use the last occurrence (LO) of *D. brouweri* Tan, 1927, emend. Bramlette et Riedel, 1954 to mark the Pliocene/Pleistocene boundary. However, the INQUA and ICS working group (IGCP Project 41) suggested to draw this boundary above the LO of *D. brouweri* and at the first occurrence (FO) of *G. oceanica* s.l., as it had been established in the stratotypic section of the Pliocene/Pleistocene boundary (Vrica section, Calabria, southern Italy) (Aguirre and Pasini, 1985). The top of the laminated level "e" in the Vrica section was selected as the marker horizon for the boundary (Aguirre and Pasini, 1985). This level is just above the top of the Chron C2N (Olduvai) (Lourens et al., 2004), yielding an age of approximately 1.6 Ma for the Pliocene/Pleistocene boundary (Rio et al., 1990a). The FO of *G. oceanica* s.l. has been used for delimiting this boundary in Mediterranean region, Atlantic and western equatorian Indian Ocean (Raffi and Rio, 1979; Rio et al., 1990a, b; Liu et al., 1996). In the present work, we recognise the Pliocene/Pleistocene boundary by the FO of *G. oceanica* s.l.

Ground truthing by several submersible dives shows that the coquina surface, assigned an age of late Pliocene, occurs throughout the study area, and as such provides an excellent constraint on the time of development of the shelf-edge wedge. It is clear that the age assigned using palaeontological data, together with seismic evidence for a forced regression, correlate strongly with the Tertiary sea-level curves for South Africa (Siesser and Dingle, 1981). These indicate relative sea-level falls occurring during the late Pliocene (Fig. 7). In addition, hinterland uplift and relative sea-level fall during the Miocene/Pliocene has been described for the area (Partridge and Maud, 1987). We thus confidently consider these shelf-edge wedge deposits late Pliocene in age based on this evidence. Exposed failure scarps in the upper portions of the heads of these canyons yield sediment samples of early Pleistocene ages, indicating the uppermost age of deposition of facies E2, where the clinoforms topsets are exposed in the scarp walls (Fig. 8). Partially consolidated, interbedded silty and sandy deposits of similar age outcrop in the thalweg of Leven canyon at a depth of 150 m. These sediments confirm that the upper limits of the shelf-edge wedge have a minimum age of early Pleistocene. The age difference between the lower boundary of Subzone MNN19a and the upper boundary of Subzone MNN19c is estimated as 110–210 Ka. The shelf-edge wedge thus had a sedimentation rate of between 162 and 309 m/Ma. This correlates

Table 1
Taxonomic list of nannofossils from the samples of the northern KwaZulu-Natal shelf-edge wedge with abundance and preservation observations

Late Pliocene						Early Pleistocene						Age
NN19a						NN19b						Gartner (1977)
MNN19a	MNN19b					MNN19c						Rio et al. (1990b)
Dive 809	Leadsman 10	Leadsman 4	Leven 5	DiepGat 369 m	Leven Thalweg	Leven 18	Leven 13	Leven 4				Sample
M	G	M	G	G	G	M	G	G				Preservation
			RR									*Braarudosphaera bigelowii*
C	R	R	F	F	F	F	F	F				*Calcidiscus leptoporus*
R	R	RR	R	R								*Calcidiscus macintyrei*
						RR						*Ceratolithus cristatus*
								r				*Chiasmolithus* sp. (reworked)
F			R									*Coccolithus pelagicus*
					r							*Cribrosphaerella ehrenbergii* (reworked)
			R					F				*Dictyococcites perplexa*
	F	R	R	R	R	R	R	R				*Dictyococcites productus*
R												*Dictyococcites* sp.
			r	r		r						*Discoaster* sp. (reworked)
								r				*Eiffellithus eximius* (reworked)
			r									*Eiffellithus turriseiffelii* (reworked)
A	F	R	R	F								*Gephyrocapsa caribbeanica*
	F	F	A	F	F	F	F	A				*Gephyrocapsa oceanica* s.l.
		R	R	F	F	F	F	F				*Gephyrocapsa* sp. (3,5-5,5 μm)
RR		R	R	RR		R	RR	R				*Gephyrocapsa* sp. (small)
RR												*Hayaster perplexus*
R	R	R	R	F	R	R	R	F				*Helicosphaera carteri*
	R		R	RR	R		R	R				*Helicosphaera kamptneri*
R	R		R	R	R		R	R				*Helicosphaera sellii*
	R	F	F	RR			R	RR				*Helicosphaera wallichii*
			r	r								*Micula decussata* (reworked)
			r									*Neochiastozygus perfectus* (reworked)
				r								*Neochiastozygus* sp. (reworked)
		R	R		R							*Pontosphaera discopora*
			R									*Pontosphaera indooceanica*
R		RR	R	R			R	R				*Pontosphaera japonica*
			R	R	R							*Pontosphaera* sp.
			r									*Prediscosphaera cretacea* (reworked)
R			R	R	R	RR		R				*Pseudoemiliania lacunosa*
R				R		R						*Pseudoemiliania ovata*
R					R	R						*Reticulofenestra* sp.
F	R	R	R	R	R		RR	R				*Reticulofenestra* sp. (<4 μm)
			r									*Reticulofenestra umbilica* (reworked)
	RR		R			RR						*Rhabdosphaera claviger*
		RR	RR	RR			RR					*Scapholithus fossilis*
			r					r				*Sphenolithus moriformis* (reworked)
			r			r						*Sphenolithus* sp. (reworked)
				r								*Staurolithites angustus* (reworked)
			R	R	RR							*Syracosphaera pulchra*
	RR		RR									*Syracosphaera* sp.
R	R		F	R		R	F	R				*Thoracosphaera operculata*
R	F	F	F	R	R	F	F	R				*Thoracosphaera saxea*
				RR								*Thoracosphaera tuberosa*
								RR				*Thoracosphaera* sp.
RR												*Umbilicosphaera maceria*
				RR								*Umbilicosphaera rotula*
	R	R	R	R	R	R						*Umbilicosphaera sibogae*
			r									*Zeugrhabdotus sigmoides* (reworked)

A—abundant, C—common, F—few, R—rare, RR—very rare; G—good, M—moderate, r—reworked.

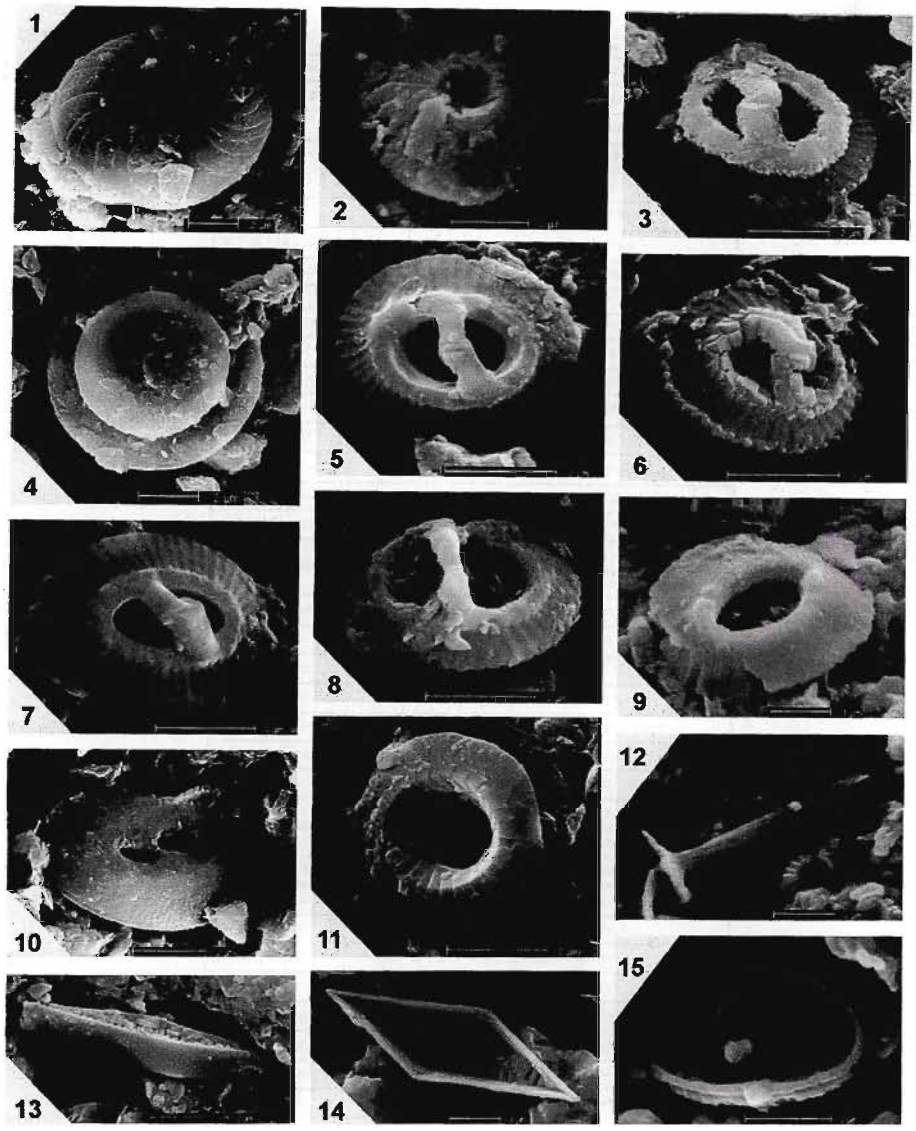

Fig. 5. SEM of calcareous nannofossils from the samples of the northern KwaZulu-Natal shelf-edge wedge. (1) *Calcidiscus macintyrei*, distal view, Leven 5; (2) *Calcidiscus leptoporus*, distal view, Dive 809; (3) *Gephyrocapsa carribbeanica*, distal view, Dive 809; (4) *Calcidiscus* sp., proximal view, Leven 5; (5) *Gephyrocapsa oceanica*, distal view, Leadman 4; (6) *Gephyrocapsa carribbeanica*, distal view, Leven 5; (7) *Gephyrocapsa oceanica*, distal view, Leven 5; (8) *Gephyrocapsa oceanica*, distal view, Leven 5; (9) *Reticulofenestra* sp. (<4 μm), distal view, Leven 5; (10) *Helicosphaera wallichii*, distal view, Leven 5; (11) *Umbilicosphaera sibogae*, distal view, Leadman 4; (12) *Rhabdosphaera claviger*, general appearance, Leven 5; (13) *Scafolithus fossilis*, lateral view, Leadman 4; (14) *Scapholithus fossilis*, general appearance, Leven 5; (15) *Syracosphaera pulchra*, distal view, Leven 5.

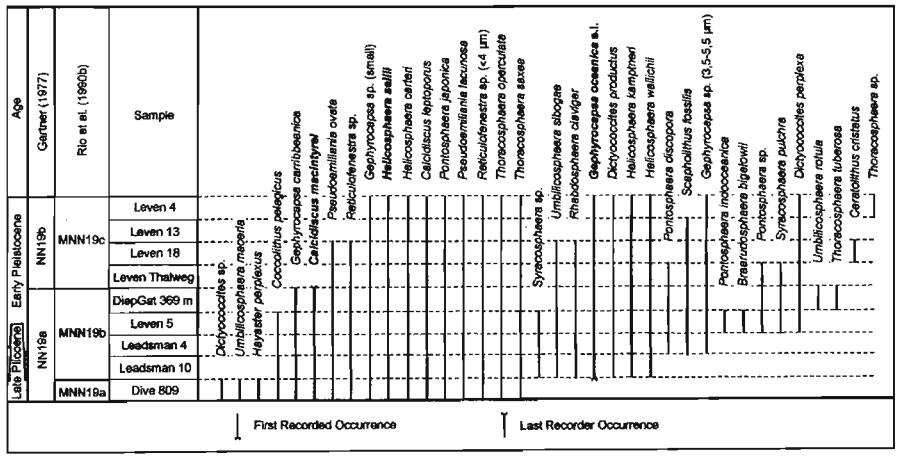

Fig. 6. Distribution of calcareous nannofossils from the samples of the northern KwaZulu-Natal shelf-edge wedge.

well with older data, which assigns a sedimentation rate of 234 m/Ma to post reflector Jimmy (our sampled coquina) sediments (Martin, 1984).

The presence of widespread basal-most Pleistocene sediments on the upper slope as a thin veneer of relict sediment suggests these sediments escaped major reworking in this portion of the continental margin. We postulate that these areas were not exposed to wave base shifting and reworking during sea-level falls associated with later Pleistocene glaciations, it thus seems unlikely that lowstand sea levels fell below the level of these deposits (~200 m), mirrored by global sea-level curves showing some of the early Pleistocene (Haq et al., 1987). Additional evidence regarding the magnitude and extent of regressive episodes of this age for the east coast of southern Africa is needed to clarify this, as deposits of this age are considered as part of a Terminal Pleistocene forced regressive systems tract (McMillan, 1993). Deposits of this type and age have not been recognised from the northern KwaZulu-Natal continental shelf until now.

The absence of more recent sediments (lower to middle Pleistocene) from the upper slope suggests that this area may have later been a zone of sediment bypass or starvation since early Pleistocene times. This hypothesis is supported by an increasingly seaward starved outer shelf, which terminates in relict gravel deposits at the shelf break (Flemming, 1978, 1981; Ramsay, 1994). Areas where younger sediments do mantle these early Pleistocene deposits could possibly be zones of offshore bedload parting, re-distributing younger Holocene sediment offshore and downslope (e.g. Flemming, 1978).

Sediments within Diepgat canyon, as evidenced by muddy deposits of basal-most Pleistocene age, appear to be either relict features formed as drapes within the canyon thalweg, or as mass wasting deposits derived from the upper canyon walls. Submersible dive 813 revealed thick muddy deposits interspersed with partially exposed boulder-cobble-sized debris. We interpret these as debris flows from the upper canyon, comparable to cored debris flow deposits found within Berkeley canyon of the New Jersey continental margin (McHugh et al., 2002). This supports findings by Green and Uken (2008), which allude to recent seismic activity in the area having triggered mass wasting in the head of Diepgat canyon. This is strengthened by eye witness accounts of the first author, during dive 813, of modern pelagic sedimentation occurring within this canyon, precluding these sediments from being relict.

These samples, to date, provide the most rigorous age constraint on the upper slope and continental shelf stratigraphy of the northern KwaZulu-Natal shelf. Additional samples collected, some as far south as Durban (Bosman et al., 2007), will form part of a more comprehensive nannofossil zonation scheme for the east coast of South Africa. These will make chronostratigraphic reconstructions of this coastline, previously unavailable, possible.

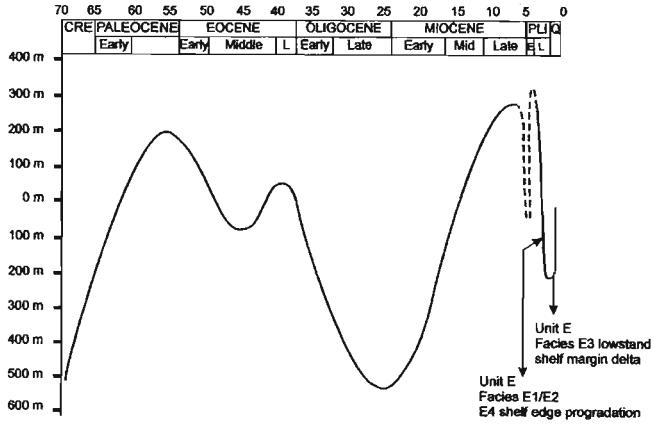

Fig. 7. Sea-level curve for the southeast African coastline (after Siesser and Dingle, 1981). Note the ~500-m drop in sea-level at the Pliocene/Pleistocene boundary. This corresponds to hinterland uplift during the Mio/Pliocene (Partridge and Maud, 1987). We consider the shelf-edge wedge, on the basis of dating, seismic architecture, and onland geomorphological evidence to have formed on this limb of the sea-level curve.

Acknowledgements

We wish to thank the African Coelacanth Ecosystem Programme, funded by the National Research Foundation, the Department of Environmental Affairs and Tourism, the Department of Science and Technology, and the German government for the opportunity to explore this fascinating area. Many thanks to J. Schauer and K. Hissmann of the *Jago* team who made dive time in the submersible available. The captain and crew of the FRS Algoa are also gratefully acknowledged. We would also like to acknowledge the support of the Council for Geoscience-Marine Geoscience Unit, as well as Marine GeoSolutions (Pty Ltd) for their help in the acquisition of seismic data used in this study. In this regard A. Richardson is profusely thanked. We would also like to thank the editor and two anonymous reviewers for their helpful comments. This publication comprises part of A.G.'s PhD thesis at UKZN.

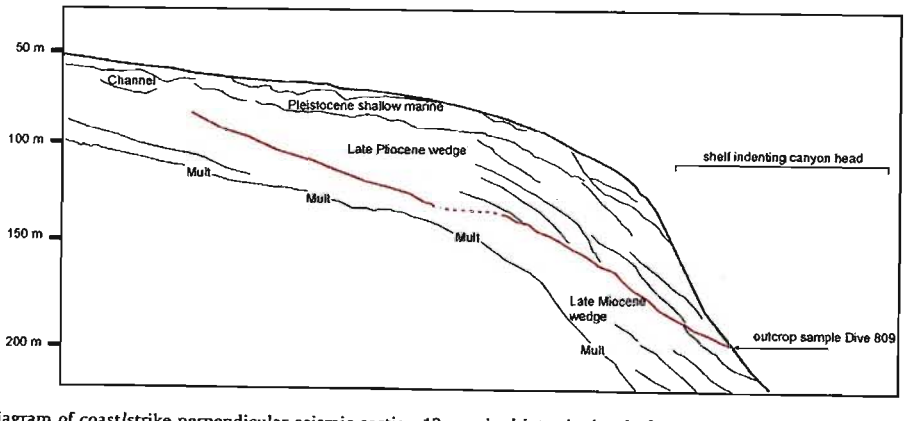

Fig. 8. Interpretative line diagram of coast/strike perpendicular seismic section 12 acquired into the head of a minor shelf indenting canyon in the Sodwana Bay block (locality depicted in inset). A sample collected during *JAGO* dive 809 was taken from a unit cropping out at −184 m, which corresponds to the base of a strongly developed shelf-edge wedge. The lithological unit sampled is shown by the red line onto which clinforms of the shelf-edge wedge downlap, thus providing a maximum age for the genesis of the shelf-edge wedge.

References

Aguirre, E., Pasini, G., 1985. The Pliocene/Pleistocene boundary. Episodes 8, 11–120.

Bosman, C., Ovechkina, M., Uken, R., 2007. The Aliwal Shoal revisited: new age constraints from nannofossil assemblages. South African Journal of Geology 110, 647–653.

Bown, P.R., 2005. Cenozoic calcareous nannofossil biostratigraphy, ODP Leg 198 Site 1208 (Shatsky Rise, northwest Pacific Ocean). In: Bralower, T.J., et al. (Eds.), Proceedings of the Ocean Drilling Program, Scientific Results, vol. 198 (Online). Available from World Wide Web: 〈http://www.dp.tamu.edu/publications/198_SR/VOLUME/CHPTERS/104.PDF〉 (Cited 2006-05-19), pp. 1–44.

Bown, P.R., Young, J.R., 1998. Techniques. In: Bown, P.R. (Ed.), Calcareous Nannofossil Biostratigraphy. British Micropaleontology Society Series. Chapman & Hall, London, pp. 16–28.

Cooper, J.A.G., 1994. Lagoons and microtidal coasts. In: Carter, R.W.G., Woodruffe, C.D. (Eds.), Coastal Evolution: Late Quaternary Shoreline Morphodynamics. Cambridge University Press, Cambridge, pp. 219–265.

Dingle, R.V., Goodlad, S.W., Martin, A.K., 1978. Bathymetry and stratigraphy of the northern Natal Valley (SW Indian Ocean). A preliminary report. Marine Geology 28, 89–106.

Dingle, R.V., Siesser, W.G., Newton, A.R., 1983. Mesozoic and Tertiary Geology of Southern Africa. AA Balkema, Rotterdam.

Flemming, B.W., 1978. Underwater sand dunes along the southeast African continental margin-observations and implications. Marine Geology 26, 177–198.

Flemming, B.W., 1981. Factors controlling shelf sediment dispersal along the southeast African continental margin. Marine Geology 42, 259–277.

Fricke, H., Hissmann, K., 1994. Home range and migrations of the living coelacanth *Latimeria chlaumnae*. Marine Biology 120, 171–180.

Fricke, H., Plante, R., 1988. Habitat requirements of the living coelacanth *Latimeria chalumnae* at Grande Comore, Indian Ocean. Naturwissenschaften 15, 149–151.

Gartner Jr., S., 1977. Calcareous nannofossil biostratigraphy and revised zonation of the Pleistocene. Marine Micropaleontology 2, 1–25.

Goodlad, S.W., 1986. Tectonic and sedimentary history of the mid-Natal valley (SW Indian Ocean). Joint Geological Survey/University of Cape Town, Marine Geoscience Unit Bull. vol. 15, 415pp.

Green, A.N., Uken, R., 2005. First observations of sea level indicators related to glacial maxima at Sodwana Bay, Northern KwaZulu-Natal. South African Journal of Science 101, 236–238.

Green, A.N., Uken, R., 2008. Submarine landsliding and canyon evolution on the northern KwaZulu-Natal continental shelf, South Africa, SW Indian Ocean. Marine Geology, doi:10.1016/j.margeo.2008.06.001.

Green, A.N., Goff, J.A., Uken, R., 2007. Geomorphological evidence for upslope canyon-forming processes on the northern KwaZulu-Natal shelf, South Africa. GeoMarine Letters 27, 399–409.

Haq, B.U., Hardenbol, J., Vail, P.R., 1987. Chronology of fluctuating sea levels since the Triassic. Science 235, 1156–1166.

Kruger, G.P., Meyer, R., 1988. A sedimentological model for the zululand coastal plain. In: Abstract of the 22nd Earth Science Congress of the Geological Society of South Africa, University of Natal, Durban, pp. 423–425.

Liu, L., Maiorano, P., Zhao, X., 1996. Pliocene–Pleistocene calcareous nannofossils from the Iberia abyssal plain. In: Whitemarsh, R.B., et al. (Eds.), Proceedings of the Ocean Drilling Program, Scientific Results, Vol. 149. College Station, TX, pp. 147–164 (Ocean Drilling Programme).

Lourens, L., Hilgen, F., Shackleton, J., Laskar, J., Wilson, J., 2004. Appendix 2. Orbital tuning calibrations and conversions for the Neogene period. In: Gradstein, F.M., Ogg, J.G., Smith, A.G. (Eds.), A Geologic Time Scale. University Press, Cambridge, pp. 469–484.

Lutjeharms, J.R.E., 2006. The Agulhas Current. Springer, Berlin, p. 330.

Martin, A.K., 1984. Plate tectonic status and sedimentary basin in-fill of the Natal Valley (SW Indian Ocean). Bulletin of the Joint Geological Survey, University of Cape Town, Marine Geoscience Unit, vol. 14, 209pp.

Martin, A.K., Flemming, B.W., 1988. Physiography, structure and evolution of the Natal continental shelf. In: Schumann, E.H. (Ed.), Lecture Notes on Coastal and Estuarine Studies, Vol. 26. Springer, New York, pp. 11–46.

Martin, A.K., Goodlad, S.W., Salmon, D.A., 1982. Sedimentary basin in-fill in the northernmost Natal Valley, hiatus development and Agulhas Current palaeo-oceanography. Journal of the Geological Society of London 139, 183–201.

Martini, E., 1971. Standard tertiary and Quaternary calcareous nannoplankton zonation. In: Farinacci, A. (Ed.), Proceedings II Planktonic Conference. Roma, Rome, pp. 739–785.

McHugh, C.M.G., Damuth, J.E., Mountain, G.S., 2002. Cenozoic mass transport facies and their correlation with relative sea-level change, New Jersey continental margin. Marine Geology 184, 295–334.

McLachlan, I.R., McMillan, I.K., 1979. Microfaunal biostratigraphy, chronostratigraphy and history of Mesozoic and Cenozoic deposits of the coastal margin of South Africa. Geological Society of South Africa Special Publication 6, 161–181.

McMillan, I.K., 1993. Foraminiferal biostratigraphy, sequence stratigraphy and interpreted chronostratigraphy of marine Quaternary sedimentation on the South African continental shelf. South African Journal of Science 89, 83–89.

Okada, H., Bukry, D., 1980. Supplementary modification and introduction of code numbers to the low-latitude coccolith biostratigraphic zonation (Bukry, 1973, 1975). Marine Micropaleontology 5, 321–325.

Osterberg, E.C., 2006. Late Quaternay (marine isotope stages 6-1) seismic sequence stratigraphic evolution of the Otago continental shelf, New Zealand. Marine Geology 229, 159–178.

Partridge, T.C., Maud, R.R., 1987. Geomorphic evolution of southern Africa since the Mesozoic. South African Journal of Geology 90, 179–208.

Perch-Nielsen, K., 1985. Cenozoic calcareous nannofossils. In: Bolli, H.M., Saunders, J.B., Perch-Neilsen, K. (Eds.), Plankton Stratigraphy. Cambridge University Press, Cambridge, pp. 427–554.

Raffi, I., Rio, D., 1979. Calcareous nannofossil biostratigraphy of DSDP Site 132—Leg 13 (Tyrrhenian Sea—Western Mediterranean). Rivide Italiana Paleontologica Stratigripha 85, 127–172.

Ramsay, P.J., 1991. Sedimentology, coral reef zonation and late Pleistocene coastline models of the Sodwana Bay continental shelf, northern Zululand. Ph.D. Thesis, University of Natal, Durban, unpublished.

Ramsay, P.J., 1994. Marine geology of the Sodwana Bay shelf, Southeast Africa. Marine Geology 120, 225–247.

Ramsay, P.J., Miller, W.R., 2006. Marine geophysical technology used to define coelacanth habitats on the KwaZulu-Natal shelf, South Africa. South African Journal of Science 102, 427–435.

Ramsay, P.J., Schleyer, M.H., Leuci, R., Muller, G.A., Celliers, L., Harris, J.M., Green, A.N., 2006. The development of an expert marine geographic information system to provide an environmental and economic decision support system for proposed tourism developments within and around the Greater St Lucia Wetland Park world heritage site. NRF InnovationFund Project Report no. 24401.

Rio, D., 1982. The fossil distribution of coccolithophore genus *Gephyrocapsa* Kamptner and related Plio-Pleistocene chronostratigraphic problems. In: Prell, W.L., Gardner, J.V., et al. (Eds.), Initial Reports DSDP, Vol. 68. US Govt. Printing Office, Washington, pp. 325–343.

Rio, D., Fornaciari, E., Raffi, I., 1990a. Late Oligocene through early Pleistocene calcareous nannofossils from western equatorial Indian Ocean (Leg 115). In: Duncan, R.A., et al. (Eds.), Proceedings of the Ocean Drilling Program, Scientific Results, Vol. 115. College Station, TX, pp. 175–235 (Ocean Drilling Programme).

Rio, D., Raffi, I., Villa, G., 1990b. Pliocene–Pleistocene distribution patterns in the Western Mediterranean. In: Kastens, K.A., et al. (Eds.), Proceedings of the Ocean Drilling Program, Scientific Results, Vol. 107. College Station, TX, pp. 513–533 (Ocean Drilling Programme).

Roberts, D.L., Botha, G.A., Maud, R.R., Pether, J., 2007. Coastal cenozoic deposits. In: Johnson, M.R., Anheuser, C.R., Thomas, R.J. (Eds.), The Geology of South Africa. The Geological Society of South Africa, Johannesburg/Council for Geoscience, Pretoria, pp. 605–629.

Sato, T., Takayama, T., 1992. A stratigraphically significant new species of the calcareous nannofossil Reticulofenestra asanoi. In: Ishikazi, K., Sato, T. (Eds.), Centenary of Japanese Micropaleontology. Terra Scientific Publishing Company, Tokyo, pp. 457–460.

Shaw, M.J., 1998. Seismic stratigraphy of the northern KwaZulu-Natal upper continental margin. M.Sc. Thesis, University of Natal, Durban, unpublished.

Shepard, F.P., 1963. Submarine Geology. Harper and Row, New York, p. 557.

Siesser, W.G., 1977. Biostratigraphy and micropalaeontology of continental margin samples. Technical Report, Joint Geological Survey, University of Cape Town Marine Geoscience Unit, vol. 9, pp. 108–117.

Siesser, W.G., Dingle, R.V., 1981. Tertiary sea-level movements around southern Africa. Journal of Geology 89, 83–96.

Sink, K.J., Boshoff, W., Samaai, T., Timm, P.G., Kerwath, S.E., 2007. Observations of the habitats and biodiversity of the submarine canyons at Sodwana Bay. South African Journal of Science 102, 466–474.

Sydow, C.J., 1988. Stratigraphic control of slumping and canyon development on the continental margin, east coast, South Africa. B.Sc. Hons Thesis, University of Cape Town, Cape Town, unpublished.

Young, J.R., Bown, P.R., 1997. Cenozoic calcareous nannoplankton classification. Journal of Nannoplankton Research 19, 36–47.

First observations of sea-level indicators related to glacial maxima at Sodwana Bay, northern KwaZulu-Natal

Andrew N. Green*† and Ron Uken*

RECENT OBSERVATIONS MADE FROM THE submersible *Jago* have shed new light on palaeo-sea levels found off the continental margins of southeastern Africa. The discovery of deep-water caves within the northern KwaZulu-Natal submarine canyon system, and their corresponding intertidal erosional features, indicates three deeper than present sea levels at depths of 106 m, 124 m and 130 m. A clast-supported, cobble conglomerate is associated with caves of 124 m depth. This is interpreted as a beach deposit that formed during the Last Glacial Maximum (LGM) at 18 000 BP. This is the first evidence of the LGM for the east coast, and suggests tectonic stability throughout southern Africa since that time.

Introduction

Relative sea-level fluctuations during the Late Pleistocene–Holocene period have been described by a number of authors for the South African coast and continental shelf. Well-constrained sea-level curves have been presented for the west coast,[1] the last 50 000 yr[2] and the late Holocene.[3] Recent work[4] has provided an amalgamation of existing sea-level indicators along the entire South African coast spanning the penultimate interglacial period (around 182 000 BP) to modern-day sea levels (Fig. 1). There is a lack of evidence constraining sea levels that span the Penultimate Glaciation and the Last Interglacial periods of between 182 000 ± 18 000[4] and 112 000 ± 23 000 BP.[5] Evidence for a penultimate Glacial Maximum has not been described for the South African coast. Similarly, records for the Last Glacial Maximum (LGM, 16 000–18 000 BP) are scarce, limited only to those indicators discovered on the west coast. Recently,

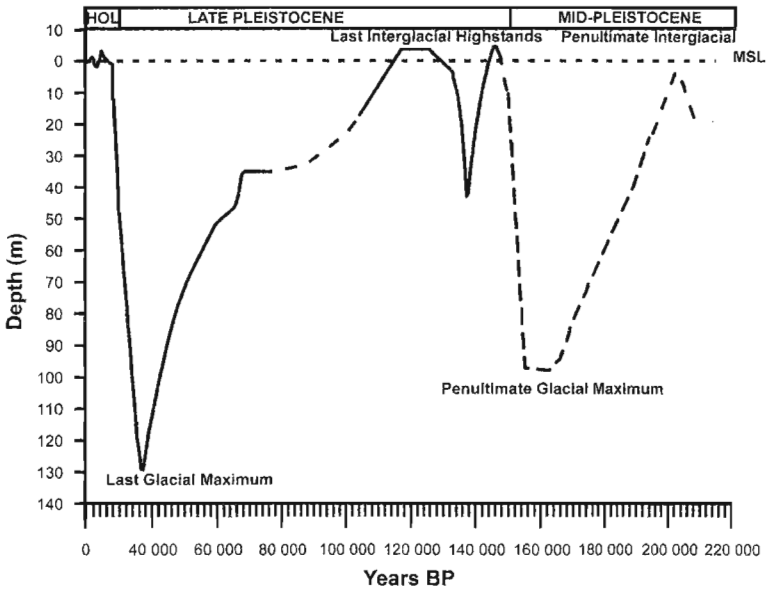

Fig. 1. Sea-level curve for the past 220 000 years, based on indicators from the South African coastline.[4] Inferred sea-level data are defined by the dashed curve. Lowstands indicate previous glacial maxima. MSL, present mean sea level.

*Marine Geoscience Unit, School of Geological Sciences, University of KwaZulu-Natal, Durban 4041, South Africa.
†Author for correspondence.
E-mail: greena1@ukzn.ac.za

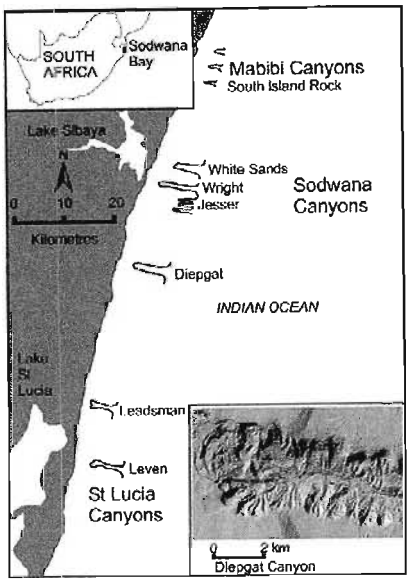

Fig. 2. Locality map of the Sodwana Bay area, detailing canyon localities with respect to major coastal waterbodies. The inset shows a sunshaded bathymetric map of Diepgat Canyon, where the most recent geological exploration took place.

observations made from the German submersible *Jago* within a series of incised submarine canyons off the Sodwana Bay continental shelf, northern KwaZulu-Natal (Fig. 2), have revealed a number of lower than present sea-level indicators at depths that have been either little explored, or completely unexplored, by traditional methods. In particular, we can present strong evidence for sea levels at depths greater than that corresponding to the LGM. This article thus aims to substantiate previous evidence for sea levels that occurred within the depth bracket proposed for the Last Glacial Maximum.

Indicators of glacial maxima along the South African coastline

Several dates circumscribe the Last Glacial Maximum, the maximum depth of 130 m of the corresponding sea level being derived from relict rhodolites of 16 990 ± 100 yr BP.[6] The probable vertical accuracy is considered to be within 5 m of mean sea level.[4] Seismic profiling off the Orange River revealed preliminary evidence for a lowstand shoreline at 120 m depth.[7] The sequence was not dated, but assigned to the Last Glacial Maximum. Similarly, coarse-grained sands with 'typical littoral grain surfaces' were recorded at comparable depths offshore of the Orange.[8] No data exist for an east coast LGM. Evidence for a penultimate Glacial Maximum is not described for the South African coast, though isotope evidence from the Huon Peninsula, New Guinea, suggests sea levels of between –130 m and –145 m at 135 000 BP.[9] No physical observations have been made regarding sea levels lower than that at the LGM or corresponding to a glacial period prior to the Oxygen Isotope Stage 5e high stand (125 000 BP).

New evidence for east coast sea levels

The continental shelf of northern KwaZulu-Natal is characterized by a Holocene sediment wedge mantling late Pleistocene hardgrounds that extend from a depth of 90 m to the present shoreline.[10] The shelf comprises a trailing edge margin, with a narrow shelf and relatively gently inclined (2–3°) continental slope. Multi-beam bathymetry surveys indicate that a number of submarine canyons in varying stages of growth have cut into the continental shelf from Leven Point in the south to South Island Rock in the north of the study area (P.J. Ramsay and W.R. Miller, in prep.).

The recent introduction of the German submersible *Jago* to the area has allowed observations to be made at depths greater than those attainable by traditional SCUBA methods. First observations suggest that the canyons have cut into older rocks of Tertiary and late Cretaceous age, which can be correlated with the recognized seismic stratigraphy of the continental shelf.[11,12]

Within the canyons, a number of deeply notched caves with erosional features typical of sub-aerial intertidal environments are found. In addition, overhangs, planed terraces and notches indicating palaeoshorelines[13] are found at various depths along the exposed sections of the canyon walls. As these features are not contemporaneous with deposition, they may be considered to post-date the deposition of the Tertiary rocks in the study area during the Early to Late Miocene transgression.[14] Sea levels indicated by these features thus span the time period from Early Pliocene to Late Pleistocene.

Submarine cave localities across six mature canyons can thus be analysed in terms of their cluster relationships, based on depth and location. This implies that only genetically related caves, formed by massive events such as glacial maxima, should be targeted as possible sea-level indicators. The Jesser, Diepgat, Wright, White Sands, South Island Rock and Mabibi canyons have so far been explored for caves and their suitability as habitats for coelacanths.

Forty-two caves were recorded as depth versus canyon locality plots (Fig. 3). From these, three distinct clusters are recognizable at depths of 106 m, 125 m, and 130 m. Though caves at these depths do not occur uniformly throughout the various canyons, they appear to be good indicators of lower sea levels in the past than at present. The two deepest sea-level indicators are characteristically absent from Jesser Canyon, which is the youngest and least incised of the sample group. This indicates that the two lowest sea levels prevailed before Jesser Canyon was cut to a depth of 125 m and confirms that the 105 m depth indicators are younger than both the –130 m and –125 m sea levels. The absence of the deeper indicators from Diepgat is attributed to scarp slumping within the canyon head, features recognized from the bathymetry of the canyon margins (Fig. 4).

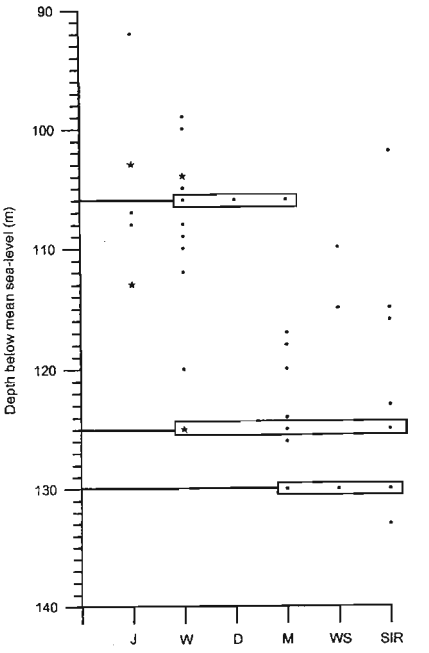

Fig. 3. Cave clusters relative to the various canyon localities found in the study area. Abbreviations: J, Jesser; W, Wright; D, Diepgat; M, Mabibi; WS, White Sands; SIR, South Island Rock.

Within South Island Rock Canyon, a partially cemented cobble conglomerate was discovered within a cave at a depth of 125 m (Fig. 5). The overlying stratigraphy comprises trough cross-bedded beachrocks and planar bedded aeolianites, with grain size restricted to that between the fine sand and gravel fractions (Fig. 6), suggesting that this deposit, without appreciable transport and smoothing, could not have been derived from the upper canyon margins as a weathering product. We therefore suggest that this deposit is *in situ* and was emplaced either contemporaneously with or just after cave formation at 125 m depth. Further observations are needed to ascertain whether this deposit is the product of a

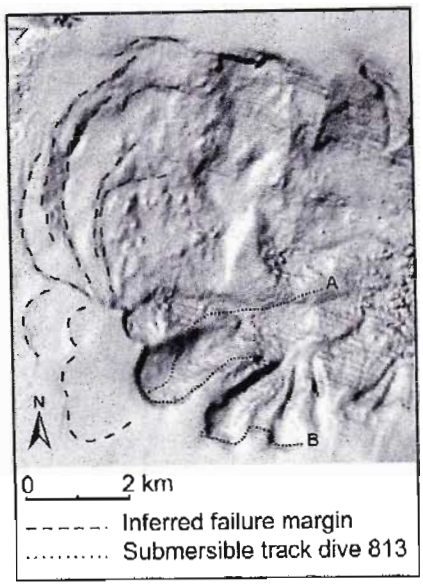

Fig. 4. Sunshaded digital terrain model of Diepgat Canyon, showing inferred failure margins in the canyon head. The sedimentary log outlined in Fig. 6 is derived from transect A–B.

re-cemented gravity flow or if it was formed by storm action in the intertidal zone. Initial observations suggest that the conglomerate is clast supported, typical of beach deposits emplaced during storm events.

We consider that newly interpreted sea levels at –125 m and –130 m can be correlated with established sea-level curves. The event at a depth of 125 m can possibly be assigned to the Last Glacial Maximum lowstand of 16 000–18 000 BP. Depths of 130 m are probably the expression of sea-level oscillations during the LGM. Shallower sea-level indicators at 105 m depth can possibly be assigned a much younger age, and can be correlated with *in situ* estuarine molluscan material from the southwest coast inferred as a palaeo-sea level of between 90 m and 102 m below mean sea level and related to the onset of sea-level rise during the Flandrian transgression.[15]

Conclusions

The submarine canyons off Sodwana Bay provide an ideal window onto the Quaternary history of the continental shelf. New evidence for lower than present sea levels is described from submarine caves, and *in situ* deposits that suggest intertidal weathering and sedimentation at depths unexplored along the east coast of South Africa. Preliminary interpretations indicate a depth at the time of the LGM of between 125 m and 130 m along the coast. These data are the most solid observable evidence for glacial maxima along the South African coastline and can contribute significantly to the understanding of global sea-level variability. Close matches in LGM sea level between the east and west coasts indicate negligible tectonic activity during the last 18 000 years.

Fig. 5. A cobble conglomerate found within a cave at a depth of 124 m in South Island Rock Canyon deposited during a sea-level lowstand under storm conditions.

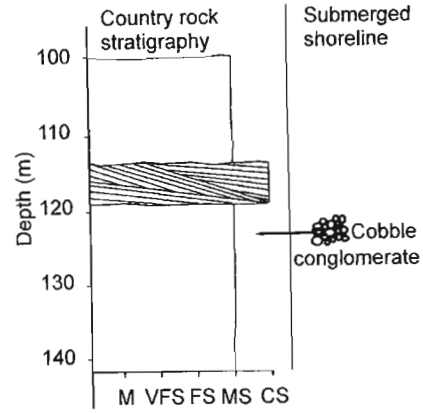

Fig. 6. A sedimentary log detailing the country rock sedimentology upon which the conglomeritic deposit has been superimposed. Note the absence of coarse material from the upper levels, precluding the deposition of the cobble conglomerate as a product of gravity flow.

We gratefully acknowledge P.J. Ramsay and W. Miller of Marine GeoSolutions for the collection and processing of the multibeam bathymetric data used in this study. We also wish to thank both the crew of the *Jago* and the crew and scientists of the FRS *Algoa*. This work was funded through the African Coelacanth Ecosystem Programme by the Department of Science and Technology, the National Research Foundation, the Department of Environmental Affairs and Tourism, and the German government

1. Miller D.E. (1990). A southern African Late Quaternary sea-level curve. *S. Afr. J. Sci.* **86**, 457–459.
2. Cooper J.A.G. (1991). *Sedimentary models and geomorphological classification of river mouths on a subtropical, wave-dominated coast, Natal, South Africa.* Ph.D. thesis, University of Natal, Durban.
3. Ramsay P.J. (1995). 9000 years of sea-level change along the southern African coastline. *Quat. Int.* **31**, 71–75.
4. Ramsay P.J. and Cooper J.A.G. (2002). Late Quaternary sea-level change in South Africa. *Quat. Res.* **57**, 82–90.
5. Ramsay P.J., Smith A.M., Lee-Thorp J.C., Vogel J.C., Tyldsey M. and Kidwell W. (1993). 130 000-year-old fossil elephant found near Durban: Preliminary report. *S. Afr. J. Sci.* **89**, 165.
6. Vogel J.C. and Marais M. (1971). Pretoria radiocarbon dates. *Radiocarbon* **23**, 43–80.
7. De Decker R.H. and Van Heerden I.L. (1987). The seismic stratigraphy of the Orange delta. In *Proc. 6th National Oceanographic Symposium*, Stellenbosch, paper C21.
8. Rogers J. (1977). Sedimentation on the continental margin off the Orange River and the Namib Desert. *Bulletin of the Geological Survey of South Africa/University of Cape Town Marine Geoscience Unit 7*, 162 pp.
9. Chappell J. and Shackleton N.J. (1986). Oxygen isotopes and sea level. *Nature* **324**, 137–140.
10. Ramsay P.J. (1994). Marine geology of the Sodwana Bay shelf, southeast Africa. *Mar. Geol.* **120**, 225–247.
11. Sydow C.J. (1988). *Stratigraphic control of slumping and canyon development on the continental margin, east coast, South Africa.* Hons thesis, University of Cape Town.
12. Shaw M.J. (1998). *Seismic stratigraphy of the northern KwaZulu-Natal upper continental margin.* M.Sc. thesis, University of Natal, Durban.
13. Miller W.R. and Mason T.R. (1994). Erosional features of coastal beachrock and aeolianite outcrops in Natal and Zululand, South Africa. *J. Coastal Res.* **10**, 374–394.
14. Siesser W.G. and Dingle R.V. (1981). Tertiary sea-level movements around southern Africa. *J. Geol.* **89**, 83–96.
15. Pether J. (1994). Molluscan evidence for enhanced deglacial advection of Agulhas water in the Benguela Current, off southwestern Africa. *Palaeogeog., Palaeoclimatol., Palaeoecol.* **111**, 99–117.

In forthcoming issues

Global warming and developing countries • Induced defence responses in sunflower • Robert Broom in retrospect • Newton's chemical laboratory in Cambridge • The latest plant pathology research in southern Africa • Indicators of botanical studies in South Africa • Monitoring the quality of water for human consumption • The achievements of the Royal Society-National Research Foundation bilateral research support programme • Palaeoecology during the Early Pliocene at Langebaanweg • Drought over southern Africa • Recent contributions of South African research in the atmospheric sciences and physical oceanography • Isotope fingerprinting as an indicator of diet selection in herbivores, and as a guide to ore selection in archaeological investigations in Namibia • Astronomy and the inauguration of SALT.

Potential sites for suitable coelacanth habitat using bathymetric data from the western Indian Ocean

Andrew Green[1]*, Ron Uken[1], Peter Ramsay[2], Rio Leuci[1], and Samantha Perritt[1]

[1]Joint Council for Geoscience-University of KwaZulu-Natal, Marine Geoscience Unit, School of Geological Sciences, University of KwaZulu-Natal, Durban, 4041

[2]Marine GeoSolutions, 106 Clark Road Glenwood, Durban, 4001

*Author for correspondence. E-mail greena1@ukzn.ac.za

Bathymetry as a discriminatory tool for targeting suitable coelacanth habitats is explored. A regional bathymetry, garnered from pre-existing data sets, and geo-referenced bathymetric charts for the Western Indian Ocean is collated and incorporated into a GIS. This allows the suitability of coelacanth habitation, based on criteria concerning depth and shelf morphology from known coelacanth habitats, to be interrogated. A best guess for further detailed exploration is provided, targeting Northern Mozambique, between Olumbe and Port Amelia, and the Port St. Johns-Port Shepstone stretch of coastline in South Africa. Sparse data prevents the identification of Tanzanian and Madagascan target sites, though these should not be ignored. Ultimately, the GIS is envisioned as a flexible tool within which other spatial data collected in these areas concerning coelacanths may be incorporated.

Introduction

Geographical Information Systems (GIS) as an interrogative tool for the analysis of spatially related variables is not a new application to the natural sciences. It has

formed the basis for many studies in the fields of bio-geography, ecology and applied geo-sciences. Recent studies in the marine and coastal environment have begun using GIS modelling to understand and explain physical factors that shape and influence these habitats.

It has long been noted that coelacanth habitats are dependent on both the habitat morphology, and the depth of habitation.[1-5] This is due to a) the coelacanths requirement for shelter from predators, b) water temperature-depth constraints which allow for cooler waters required by the coelacanth and c) shelter from direct sunlight. Submarine canyons that indent the continental shelf break and satisfy the morphological and bathymetric constraints on coelacanth habitation are particularly promising habitats for coelacanth exploration. We thus discuss the bathymetric constraints on coelacanth habitation in light of known habitats from the Sodwana Bay submarine canyons, namely caves, overhangs and notches in water depths of ~100 m to 130 m, most often exclusive to heavily incised canyons that extend beyond the -100 m isobath. Though the Comoros is home to a considerable coelacanth population, coelacanths found in this area do not inhabit submarine canyons, but rather caves formed in the irregular basaltic morphology of the islands.[1,3] The East coast of southern Africa provides an alternative habitat in the form of the caves and overhangs within submarine canyons. The relationship between habitat and specific morphological and bathymetric (spatial) criteria thus embraces the use of a geophysically based GIS for the targeting of new coelacanth habitats along the East coast of South Africa, Mozambique, Tanzania, Kenya, Madagascar and the Comoros. In addition, this GIS would form a framework within which other spatially dependant data acquired by the African Coelacanth Exploration Programme (ACEP) (i.e. oceanographic and ecological data) could be investigated.

Previous bathymetric studies

Few, if any, geophysical surveys have been conducted along the passive continental margins of the East coast of Southern Africa. The majority of offshore geophysical work is limited to South Africa and Southern Mozambique.[6-8] Mozambique's geophysical data set has been collected primarily for hydrocarbon exploration purposes and has traditionally targeted depths beyond the continental shelf and slope. As such, little geophysical data concerning the shelf and continental slope exist. With respect to Tanzania and Madagascar, there is a complete lack of accessible bathymetric data. In these areas, admiralty charts used for navigation provide the most reliable and comprehensive bathymetric data set for these areas.

Methods used

The extent of the coelacanth distribution in the western Indian Ocean covers a considerable area, making the search for further elusive coelacanth populations a daunting task. The area of interest extends northwards along the eastern coast of South Africa from East London to Mozambique and Tanzania - as far north as the Tanzanian-Kenyan border, and the entire coastline of Madagascar (Fig. 1).

Initially, the collation of all existing hydrographic data for the study area was undertaken. This included archived bathymetric data acquired by the Marine Geoscience Unit of the Council for Geoscience (formerly the South African Geological Survey) as part of a statutory mapping programme of the continental shelf. This data is limited to the shallow continental margin (Fig. 1), and comprises single frequency data acquired by either an Odom Echotrac Model 3100 echosounder operating at 200 kHz frequency, or a Reson Navisound 2111 echosounder with an operating frequency of 210 kHz. In addition

to digital bathymetry, 5 hydrographic charts were used for the South African East coast to supplement the areas not covered by pre-existing digital data. A further 30 charts were used for Mozambique, 2 charts used for Tanzania and 21 charts for Madagascar to complete the data set (Fig. 1). These data sources are listed in the online addendum to this article (Tables 1-4). Problems arose in that older charts had inherent positioning inaccuracies, and many were projected from obsolete or mismatching spheroids, making mosaics of the bathymetric data difficult. To counter this, all paper charts were scanned on an A0 scanner and the digital images polynomially rectified and re-projected to decimal degrees on the WGS 84 Spheroid using ER Mapper 6.3. This allowed the chart contours to be digitised as vector data and incorporated into the GIS, together with coastline data and geological information. The final digitised products were exported as ESRI shapefiles and finalised as a keyable GIS project in ArcView 3.2. Areas of particular interest were identified where the following criteria could be recognised:

1) Contour lines were arranged in such a way as to either indicate the presence of a submarine canyon (Fig. 2), or steep shelf break and slope relief, analogous to the physical habitat of the Grand Comoros coelacanth.[3]

2) The canyon heads indent the shelf break (~100 m isobath) and in so doing satisfy the known depth criteria for canyon specific coelacanths such as those of Sodwana Bay (Fig. 2). [9]

Owing to the issue of chart scale and resolution, a certain amount of bias is directed towards canyons that are large enough to be identified from the chart data. Based on previous work[10-12] smaller slope confined canyons co-exist with these larger features, the smaller canyons acting as localised conduits for sediment gravity flows that

are actively eroding and thus evolving into larger shelf indenting features. This study does not preclude smaller canyons as target sites, but rather targets broad areas associated with large canyon systems (and most likely including slope confined canyons undetectable due to the data resolution) that may prove fruitful for further detailed investigation as outlined by others.[13] It is still most likely that large canyons, where the canyon head extends beyond the -100 m isobath, would possess cave features suitable for habitation, as these caves are considered to have formed during the Last Glacial Maximum (18 000 BP) when sea levels were at -125 m.[14]

Results

Image geo-referencing accuracy of within a 100 m root mean square error was achieved using the above methods. The resolution of the South African and Mozambique data sets were found to be sufficiently dense to identify some of the major canyons similar and in many instances, greater in size to the Sodwana canyons that most recently yielded coelacanth discoveries. The Tanzanian and Madagascan data however, are sparser and canyons of similar size to the Sodwana canyons are only identifiable in isolated areas of better data coverage.

An analysis of the southeast African continental shelf and slope shows great variation in the presence and abundance of submarine canyons. The highest density of submarine canyons occurs between Olumbe and Porto Amelia in northern Mozambique, a distance of 222 km (Online Fig. 1). Other localised areas, in Mozambique, which have good submarine canyon development include Pemba, Nacala, Mossuril and Vilanculos (Fig. 4). Additional well-developed canyons on the South African East coast shelf, between Port Shepstone and Port St Johns, are indicated in the bathymetric data set (Online Fig. 2). These canyons indent the shelf to the -100 m isobath and good cave

development in the canyon head is expected based on the regional geological setting. Sea-level notching during lowstand episodes and the susceptibility of carbonate rich sand stones to cave development during these periods would provide environmental conditions similar to those found in Jesser Canyon[14], where the most abundant South African coelacanth populations have been documented.

The poor quality of available bathymetric data for Tanzania and Madagascar makes defining areas of submarine canyon prevalence quite difficult. Submarine canyons seem to be less well developed in Tanzania, compared to Mozambique, with the best Tanzanian examples occurring offshore of Mtwara, Lindi and Mchingo (Fig. 4). On the West coast shelf of Madagascar submarine canyons occur at Toliara (where a coelacanth was found) and to the north of Morondava (Fig. 5). Submarine canyons are more prevalent on the Madagascan East coast with examples occurring at Antsiranana and Ankerika, between Ambohitralanana and Masoala and between Fenerive and Mahatsora (south of Toamasina) (Online Fig. 3).

Discussion

The highest density of submarine canyons and most likely habitat area is the outer shelf area between Olumbe and Porto Amelia in northern Mozambique, only 280 km west of Grand Comoros, which supports the only known substantial coelacanth population[3]. Submarine canyons between Port Shepstone and Port St. Johns are also considered to be likely target sites, as the oceanographic conditions of the areas appear suitable for habitation (*pers comm.* M. Roberts).

This data set provides a useful "best guess" approach to identifying and then investigating potential coelacanth habitats based purely on the bathymetric constraints of habitat as encountered in Sodwana Bay and the Grand Comoros.[1] As such it is a useful

guide to establishing areas where coelacanth habitation occurs, but other parameters such as temperature and dissolved oxygen content must also be considered. Furthermore this study has significant value in providing a basal layer for any other GIS projects that are to be developed by ACEP. Where areas of submarine canyon formation have been coarsely targeted by this project, higher resolution geophysical data acquired by multibeam echosounding should then be undertaken and this information re-invested into the GIS, thus constantly updating the system. This GIS thus has the potential to be constantly updated and supplied with new scientific knowledge, broadening not only knowledge concerning potential coelacanth habitats, but also other knowledge of those areas based on biological and oceanographic data.

Conclusion

Specific target sites for coelacanth habitation using geophysical data have been identified for the continental shelf off the Port St. Johns-Port Shepstone stretch of coastline. Northern Mozambique, between Olumbe and Port Amelia, is considered another potential target site, based on the similarity of the submarine canyons to those of Sodwana Bay. Canyon size, depth of incision and the position of the canyon heads relative to the shelf break mirror that of the Sodwana Bay Canyons. As this is a preliminary study it is recommended that higher resolution multibeam echosounding be undertaken in these areas in order to more accurately identify the features considered most likely to support a coelacanth population. These would be based on the presence of caves, overhangs and notches where coelacanths are known to inhabit. It must also be stressed that despite poor coverage of areas such as Tanzania and Madagascar, these should not be excluded as potential sites for further, more detailed exploration.

References

1. Fricke H. and Plante R. (1988). Habitat requirements of the living coelacanth *Latimeria chalumnae* at Grande Comore, Indian Ocean. *Naturwissenschaften* **15**, 149-151.

2. Bruton M.N. and Stobbs, R.E. (1991). The ecology and conservation of the coelacanth *Latimeria chalumnae*. *Environ. Biol. Fishes* **32**, 313-339.

3. Fricke H., Hissmann K., Schauer J., Reinicke O., Kasang L. and Plante R. (1991). Habitat and population size of the coelacanth *Latimeria chalumnae* at Grande Comoro. *Environ. Biol. Fishes* **32**, 287-300.

4. Fricke H. and Hissmann K. (1994). Home range and migrations of the living coelacanth *Latimeria chlaumnae*. *Mar. Biol.* **120**, 171-180.

5. Fricke H., Hissmann K., Schauer J., Erdmann M., Moosa M.K. and Plante R. (2000). Biogeography of the Indonesian coelacanths. *Nature*, **403**, 38.

6. Kolla V., Eittreim S., Sullivan L., Kostecki J.A. and Burckle L.H. (1980). Current-controlled microtopography and sedimentation in Mozambique basin, Southwest Indian Ocean. *Mar. Geol.* **34**, 171-206.

7. Martin A.K. (1984). Plate tectonic status and sedimentary basin infill of the Natal Valley (SW Indian Ocean). *Bulletin Joint Geological Survey/University of Cape Town Marine Geoscience Unit*, **14**, 208 pp.

8. Salman G. and Abdulla I. (1996). Development of the Mozambique and Ruvuma sedimentary basins, offshore Mozambique. *Sed. Geol.* **96**, 7-41.

9. Hissmann K., Fricke, H., Schauer, J., Ribbink, A.J., Roberts, M., Sink, K. and Heemstra, P. (2006). The South African coelacanths –an account of what is known after three submersible expeditions. *S. Afr. J. Sci.* **102**, 491-501.

10. Farre J.A., McGregor B.A., Ryan W.B.F. and Robb J.M. (1983). Breaching the shelfbreak; passage from youthful to mature phase in submarine canyon evolution. In Stanley D.J, and Moore, G.T. (eds). *The shelfbreak: Critical interface on continental margins*, Society of Economic Palaeontologists and Mineralogists Special Publication, **33**, 25-39.

11. Pratson L.F. and Coakley B.J. (1996). A model for the headward erosion of submarine canyons induced by downslope-eroding sediment flows. *Geol. Soc. Am. Bull.* **108**, 225-234.

12. Green A.N., Goff J.A. and Uken R. (2007). Geomorphological evidence for upslope canyon-forming processes on the northern KwaZulu-Natal shelf, South Africa. *GeoMar. Lett.* **27**, 399-409.

13. Ramsay P.J. and Miller W.R. (2006). Marine geophysical technology used to define coelacanth habitats. *S. Afr. J. Sci.* **102**, 427-435.

14. Green A.N. and Uken R. (2005). First observations of sea-level indicators related to glacial maxima at Sodwana Bay, northern KwaZulu-Natal. *S. Afr. J. Sci.***101**, 236-238.

Figure captions

Figure 1. The targeted areas of upper continental margin in the Western Indian Ocean. These include the South African, Mozambican, Tanzanian and Madagascan continental shelf, and span the known range for coelacanth distribution in the Western Indian Ocean. Chart data coverage of this study is depicted by translucent rectangles, digital echosounding data coverage is indicated by shaded rectangles.

Figure 2. Contour lines indicating the presence of submarine canyons, derived from multibeam bathymetry of the Sodwana Bay area. Note the steep walls, relatively flat canyon thalweg, and the incision of the head into the shelf edge wedge. Contour interval 10 m.

Figure 3. Bathymetric plot of the Pemba-Mossuril area, exhibiting the characteristic bathymetric signature for prominent submarine canyon incision into the continental shelf.

Figure 4. Suspected submarine canyons of the Tanzanian coastline, most evident from Mtwara, Lindi and Mchingo areas. Note that poor bathymetric coverage precludes a confident interpretation of the bathymetry of this area. The single contour corresponds to the 50 m isobath.

Figure 5. Submarine canyons of the west coast of Madagascar. Toliara, where the chart coverage indicates a large submarine canyon breaching the shelf break, is another site of recent coelacanth discovery.

Online captions

Figure 1. Bathymetric plot of the Porto Amelia-Olumbe stretch of coastline, northern Mozambique. Note the pronounced inshore extension and steep clustering of the contours, indicating the extension of numerous canyon features, most evident from the Porto Amelia continental shelf.

Figure 2. Suspected submarine canyons off the Durban-Port St Johns coastline. Note the indentation of the 100 m isobaths by submarine canyons. This is similar in its depth incursion to those canyons documented from the northern KwaZulu-Natal continental shelf[13].

Figure 3. Prevalent submarine canyons from the east coast of Madagascar. Examples include occurrences at Antsiranana, Ankerika, the areas between Ambohitralanana and Masoala, and the Toamasina area.

Online material:

Table 1: Data sources used in the creation of the GIS.

Map name	Chart No.	Geological comments
East London to Mbashe River	59	Shelf narrows southwards, overall relatively narrow and with a steep gradient. Evidence of four canyons in the south.
Great Fish Point to Port St John	60	Shelf relatively narrow and widening southwards. No evidence of any major canyons.
Mbashe River to Port St Johns	128	Shelf widens to the south, evidence of one canyon, probably other minor canyons.

Port Shepstone to Cooper Light	129	Shelf width narrow in the north, widens off the Thukela (Thukela sedimentary cone), and narrows again south of Durban. About seven canyons in the southern region.
Port St Johns to Cape St Lucia	131	Two canyons. Shelf narrow with fairly steep gradient.

Table 2

Map name	Chart No.	Geological comments
Rovuma ao Cabo Pequeve	408	Fourteen canyons. Canyons extend very close to the coast.
Northern Entrance to Mocambique Channel	2110	Regional overview. Only for coastline digitising.
Mocambique Channel	1810	Regional overview. Only for coastline digitising.
Mocambique a Angoche	412	Seven canyons. Canyons extend close to the coast.
Rio Zambeze to Ilha Chiloane	61140	No canyons. Wide shelf dominated by the Zambeze sedimentary wedge.
Quelimane as Bocas do Zambeze	416	One canyon. Shelf widens south due to proximity of Zambeze sedimentary wedge.
Ponta da Barra to Rio Limpopo	61120	No canyons. Dominated by Limpopo sedimentary wedge.
Moebase a Quelimane	415	Five canyons. Shelf widening to the south.
Mchinga Bay to Porto do Ibo	61180	At least eighteen canyons which extend close to the coast. Extremely narrow shelf with a very steep slope.
Luiro a Mocambique	410	Five canyons. Canyons extend close to the coast.
Jesser Point to Boa Paz	2930	No canyons. Shelf widens northwards due to presence of Limpopo sedimentary wedge.
Ilha Chiloane to Ponta da Barra	61130	One canyon south of Bazaruto. Shelf widening to the north towards Zambeze sedimentary wedge.
Dar es Salaam to Mombasa Harbour	61200	Extremely narrow shelf, basically starts at coastline. Data sparse. Shelf very shear.
Dar es Salaam to Mchinga Bay	61190	Five canyons, potential for more as data is sparse. Shelf very narrow. Steep shelf.
Cabo Pequeve ao Lurio	409	Six canyons. Canyons extend close to the coast.

Table 3

Map name	Chart No.	Geological comments
Ambavalato to Faraony	61520	Data extremely sparse. Indicates shelf is narrow and with a steep slope.
Cap des Karimboly to Tolanaro	61510	Data very sparse. Does indicate that the shelf is narrow and the shelf is steep.
Toliara to Tanjon Andriamanao	61470	Very narrow shelf and very steep. One canyon off Toliara. Data sparse.
Tolanaro to Ambalavato	61520	Data extremely sparse. Indicates shelf is narrow and with a steep slope.
Toamasina to Tanjon Antsirakosy	61540	Seven canyons. Narrow shelf and steep slope.
Toamasina and Approaches 2	61538	Shelf is narrow, slope is steep. One large canyon.
Toamasina and Approaches 1	61538	Shelf is narrow, slope is steep. One large canyon.
Tanjona Bobaomby to Nosy Be	61410	Potential canyon north of Nosy-Be, shelf is narrow.
Tanjon Antsirakosy to Iharana	61560	Data sparse in the north. Five canyons in the south. Shelf break very close to the coast.
Tanjon Andriamanano Cap des Karimboly	61510	Shelf very narrow in the north, widens to the south. Very steep slope but data too sparse to indicate canyons.
Nosy Lava to Toliara	61470	Very narrow shelf, very steep slope, two canyons. Data sparse in areas. Coelacanths recorded in this area
Nosy Be to Helandro Bometoka	61420	Very narrow shelf, data too sparse to indicate canyons.
Mahanoro to Toamasina	61530	Shelf is narrow, slope is steep. Three canyons. Two quite major. Data in the south is sparse.
Ile Aux Nattes to Tamatave	678	Three canyons, narrow to moderate shelf width.
Iharana_to Tanjona Bobaomby	61560	Narrow shelf, quite sparse data. Four canyons positioned close to shore. Potential for more canyons.
Helodrano Bombetoka to Tamjona Vilanandro	61430	Very narrow shelf incised by at least six minor canyons.
Farnaoy to Mahanoro	61530	Data extremely sparse.
Tanjona Kimby to Nosy Lava	61460	Narrow shelf and very steep slope, data to sparse to indicate canyons.
Tanjona Vilanandro to Tanjona Kimby	61440	Shelf is narrow and slope is steep data is very sparse indicating only one canyon

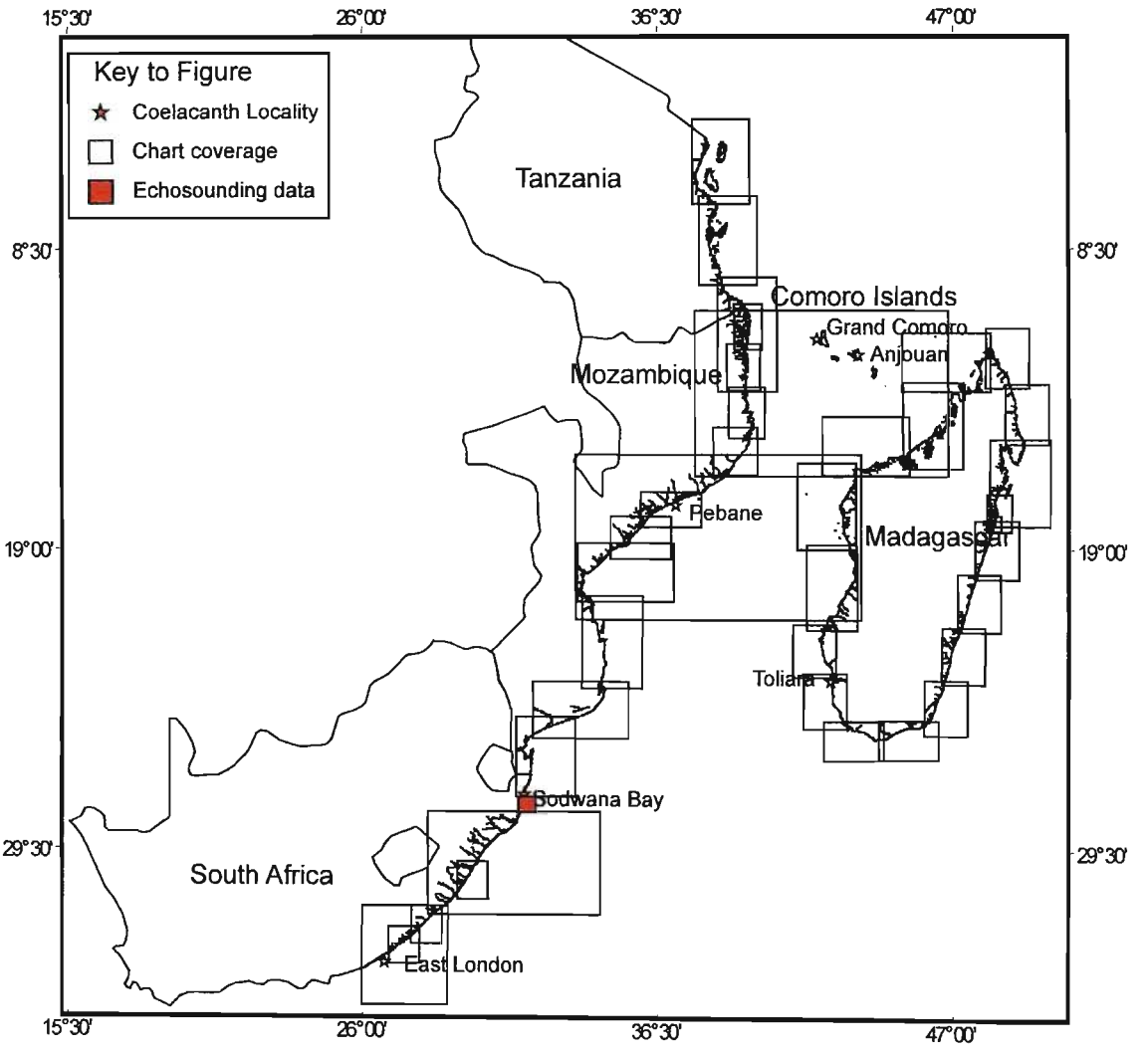
Key to Figure
Coelacanth Locality
Chart coverage
Echosounding data
15°30'
26°00'
36°30'
47°00'
8°30'
19°00'
29°30'
Tanzania
Comoro Islands
Grand Comoro
Anjouan
Mozambique
Bebane
Madagascar
Toliara
Sodwana Bay
South Africa
East London

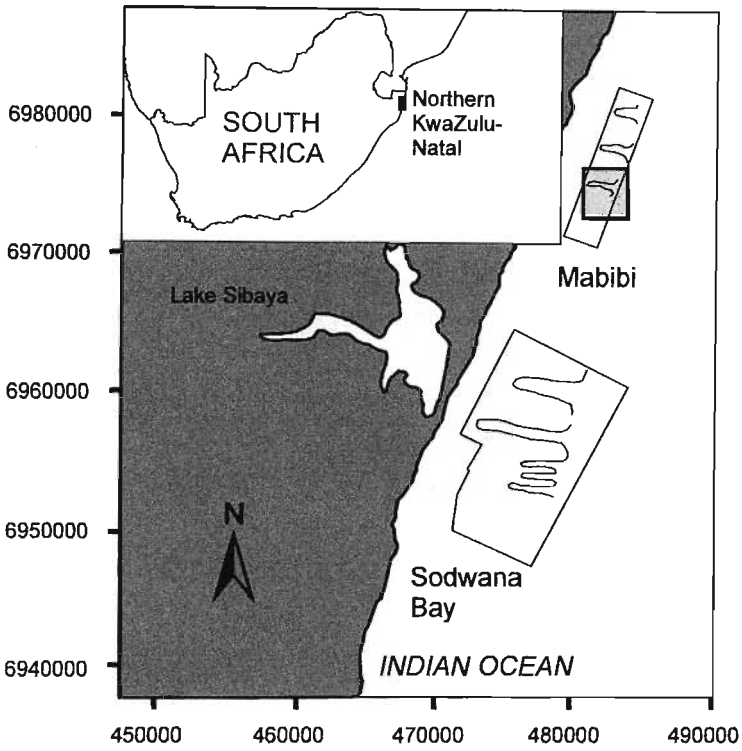
SOUTH AFRICA
Northern KwaZulu-Natal
Mabibi
Lake Sibaya
N
Sodwana Bay
INDIAN OCEAN
6980000
6970000
6960000
6950000
6940000
450000
460000
470000
480000
490000

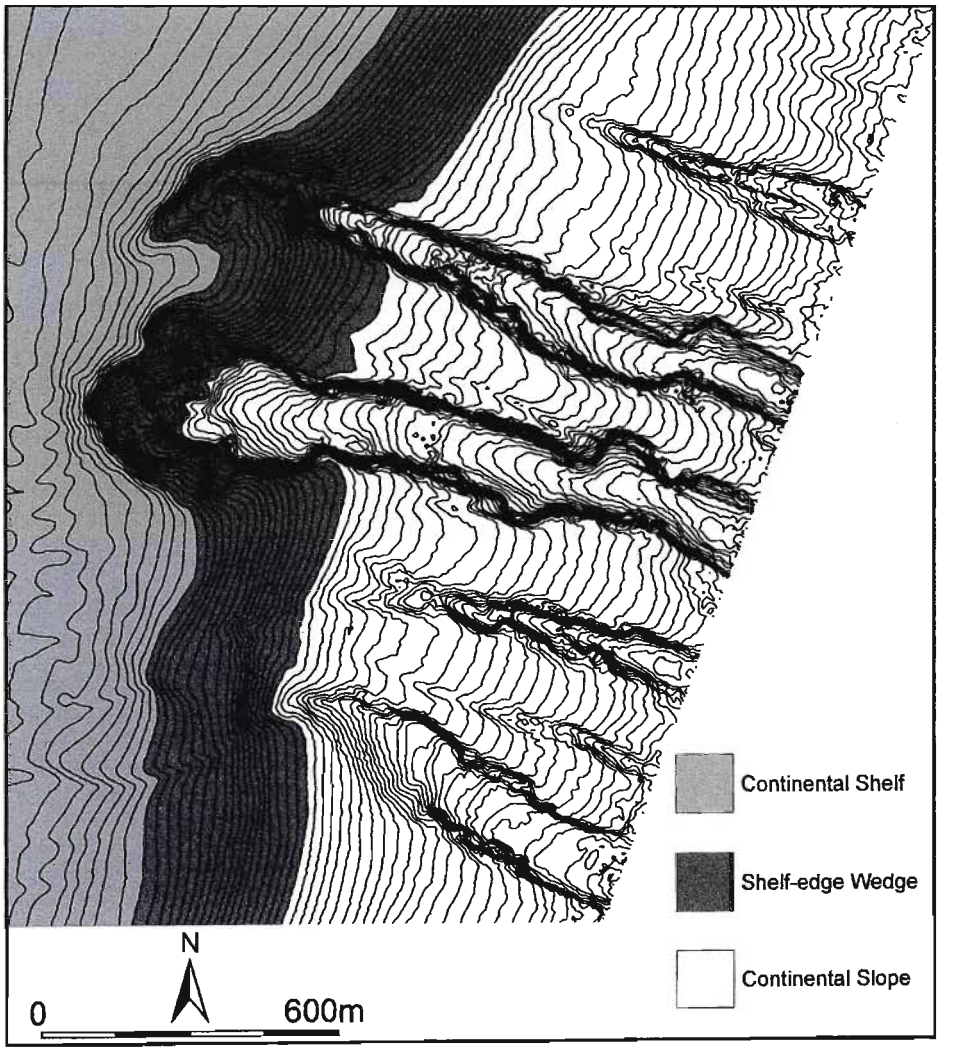
Continental Shelf
Shelf-edge Wedge
Continental Slope
N
0
600m

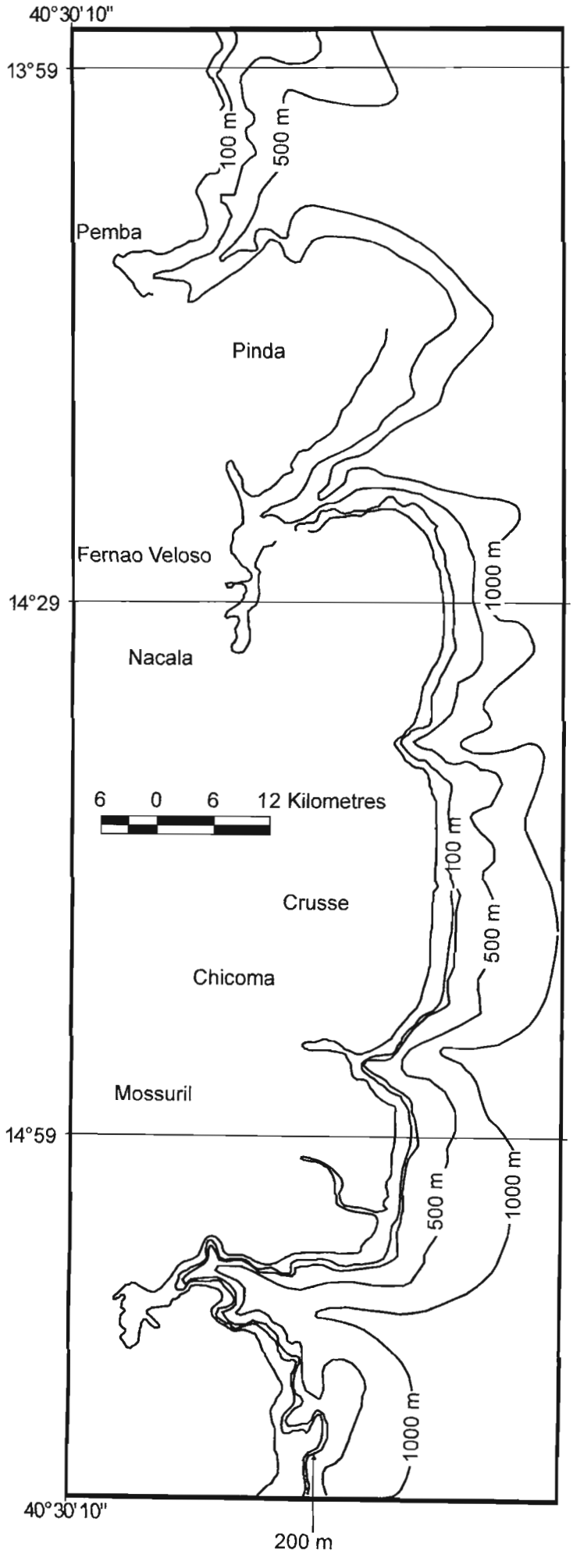
40°30'10"
13°59
100 m
500 m
Pemba
Pinda
Fernao Veloso
1000 m
14°29
Nacala
6 0 6 12 Kilometres
100 m
Crusse
500 m
Chicoma
Mossuril
14°59
500 m
1000 m
1000 m
40°30'10"
200 m

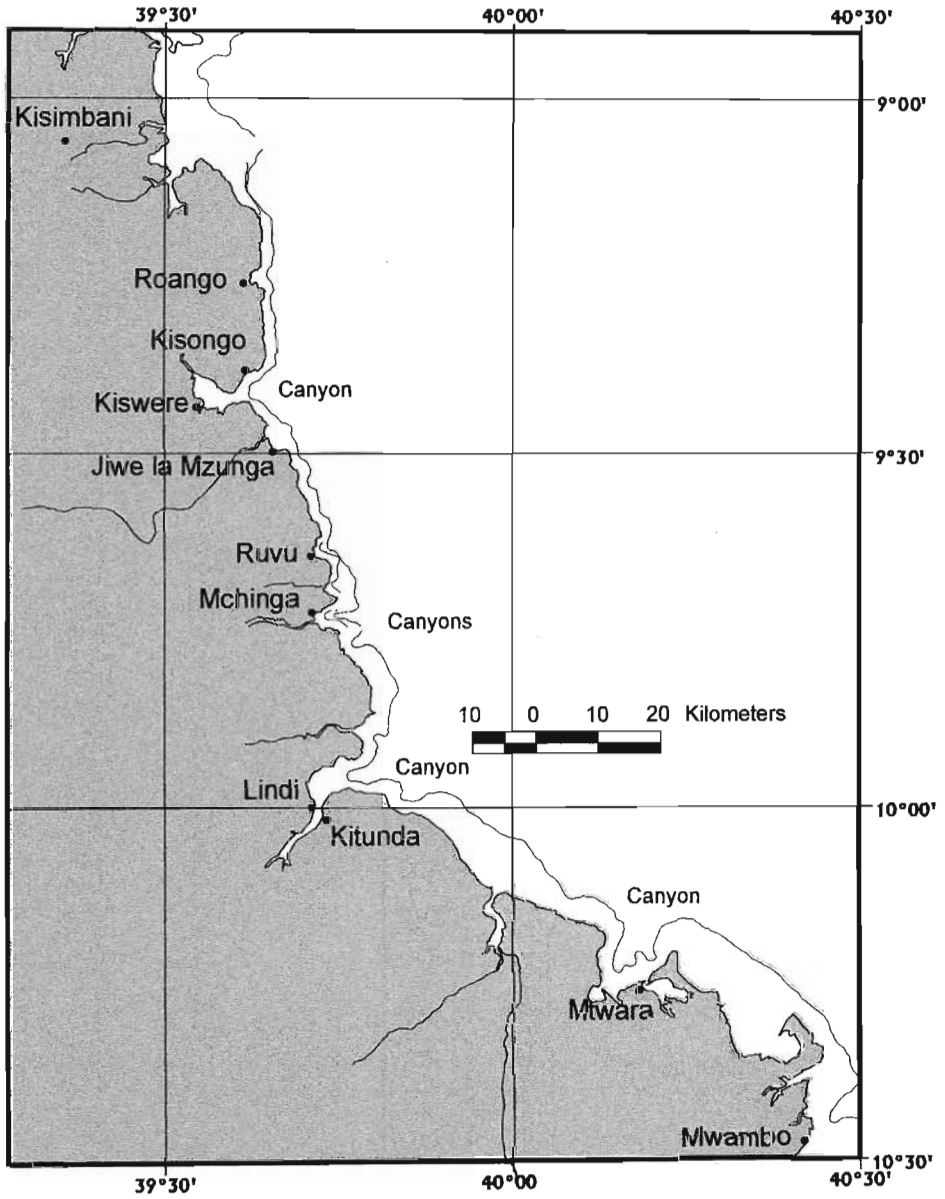
39°30'
40°00'
40°30'
9°00'
9°30'
10°00'
10°30'
Kisimbani
Roango
Kisongo
Kiswere
Canyon
Jiwe la Mzunga
Ruvu
Mchinga
Canyons
10 0 10 20 Kilometers
Canyon
Lindi
Kitunda
Canyon
Mtwara
Mwambo

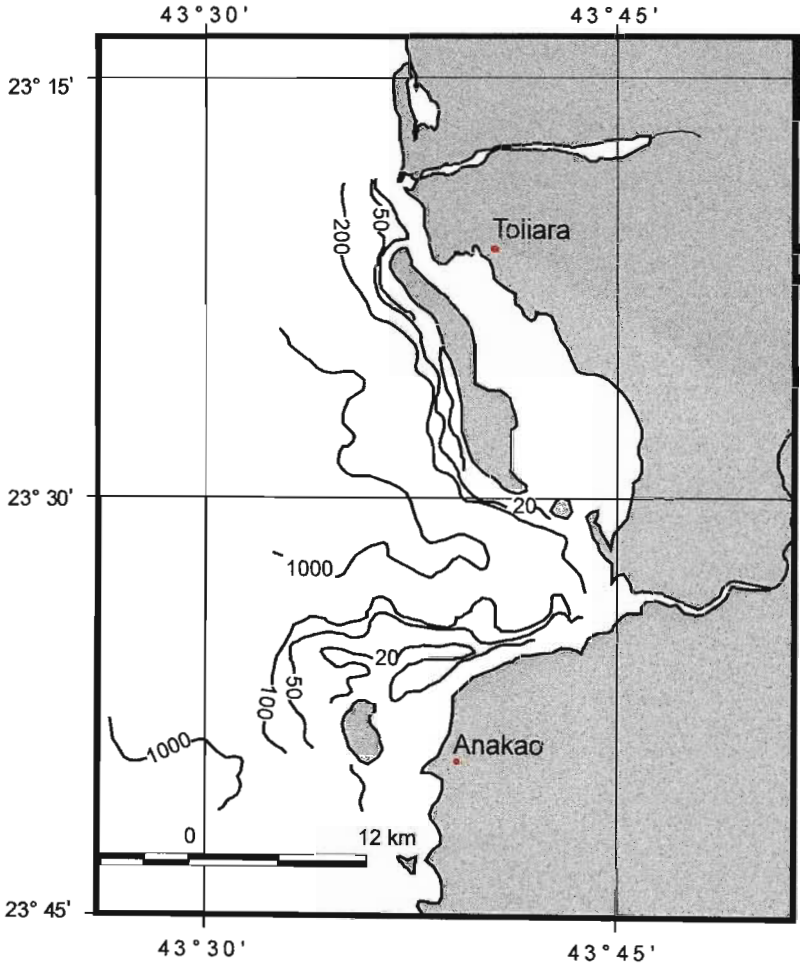
43°30'
43°45'
23° 15'
23° 30'
23° 45'
Toliara
Anakao
200
50
20
1000
20
50
100
1000
0
12 km

Marine Geology 254 (2008) 152–170

Contents lists available at ScienceDirect

Marine Geology

journal homepage: www.elsevier.com/locate/margeo

Submarine landsliding and canyon evolution on the northern KwaZulu-Natal continental shelf, South Africa, SW Indian Ocean

Andrew Green *, Ron Uken

Joint Council for Geoscience-University of KwaZulu-Natal, Marine Geoscience Unit, School of Geological Sciences, University of KwaZulu-Natal, Westville, Private Bag, X54001, South Africa

ARTICLE INFO

Article history:
Received 5 February 2008
Received in revised form 3 June 2008
Accepted 4 June 2008

Keywords:
landslides
submarine canyons
GIS
South Africa

ABSTRACT

The morphometric and geomorphological analysis of landslides found within several submarine canyons of varying sizes and morphologies from the northern KwaZulu-Natal continental shelf, South Africa, provides insight into submarine canyon evolution. Six large shelf indenting canyons are recognised (Leven, North and South Leadsman, Diepgat, Wright, and White Sands) interspersed with smaller canyons that occur prominently in the northernmost Mabibi area. Landslides and their surficial attributes were determined from high resolution multibeam bathymetry data. Landslide area, volume, runout length, the slope of the runout, the headscarp slope and height, scar slope, adjacent local unfailed slope gradient, and the depth of each failure are measured and the relationships statistically analysed for each individual submarine canyon. Landslide position and the type of landslide are also documented. The ratio between headscarp height to runout length (D/L) is assumed as a good proxy for the dynamic rheology of each failure. The largest failures occur in Diepgat, Wright, Leven and Leadsman Canyons. The presence of steeper and larger failure headscarps indicates that the failure rheology was competent in Diepgat and Wright Canyons, whereas failures, particularly in the heads of Leven and Leadsman Canyons are assumed to possess fluidised rheologies based on their small D/L values. A landslide vs. a fluid sapping trigger is postulated for the Diepgat/Wright and Leven/Leadsman landslide sets respectively.

The smallest landslides are found in the Mabibi area, and are limited to single retrogressive slumps in the heads of each small canyon. This style of failure is also evident in other smaller canyons that occur between the larger shelf indenting varieties. Headward erosion by small retrogressive failure is assumed to occur, before the canyon thalwegs become oversteepened relative to their walls. Once oversteepened, lateral canyon extension may occur, coupled with increased downslope erosion by sediment flow. The presence of 1) incised inner gorges; 2) hanging or perched slides in the canyon headwalls; 3) terraced slides; and 4) benches in the slide material indicate that axial incision and catastrophic slope clearances during this phase of submarine canyon evolution were prominent. The presence of sea-level notches within the failure scarps indicates that canyons are currently inactive and are unlikely to enlarge further pending relative sea-level fall during the next hypothermal (glacial) period.

1. Introduction

Submarine landslides are key features in the exchange of sediment between the continental shelf and abyssal plain and the ensuing geomorphological evolution of continental margins. Where submarine canyons erode the continental slope and shelf, landsliding along the walls of these features is common. These result in the headward incision and lateral extension of the canyon walls into the upper slope and shelf (Farre et al., 1983; Pratson et al., 1994; Pratson and Coakley, 1996). Landsliding within submarine canyons has been documented in various tectonic and physiographic settings (Dingle and Robson, 1985; Hampton et al., 1996; McAdoo et al., 2000; Greene et al., 2002; Arzola et al., 2008), but owing to their small size relative to non-canyon specific landslides and the inherent difficulties in data collection in these challenging environments, relatively little is known concerning landslide geomorphology within submarine canyons.

This paper describes the morphometric and geomorphological analysis of 117 landslides found within 23 canyons of varying size and degree of incision along the Northern KwaZulu-Natal continental slope. Multibeam bathymetric data are used to map each landslide locality and are interpreted to provide initial insights into pre-conditioning factors and potential trigger mechanisms for each. By isolating commonalities and differences in intra-canyon landslide morphology, observations of the processes responsible for the various landslides can be made. This aids in the establishment of simple hypotheses regarding landslide rheology and triggering mechanisms which can be validated in later, more focussed sedimentological, seismic and geotechnical surveys. Ultimately, this yields a relatively quick insight into the sub-processes that interact to cause submarine

* Corresponding author.
E-mail address: greena1@ukzn.ac.za (A. Green).

0025-3227/$ – see front matter © 2008 Elsevier B.V. All rights reserved.
doi:10.1016/j.margeo.2008.06.001

canyon initiation and growth, and present day canyon geomorphology on the KwaZulu-Natal continental margin.

1.1. Regional setting

The northern KwaZulu-Natal continental slope and shelf (Fig. 1) is characterised by a set of incised submarine canyons of varying size and depth. These are confined to five distinct blocks, stretching from Leven Point in the south, to Mabibi, in the north (Fig. 1). In light of the scale of true shelf breaching canyons such as the Hudson Canyon on the Atlantic coast of USA (Twichell and Roberts, 1982; Farre et al., 1983), even the largest canyons encountered here may only be considered as shelf indenting. Shelf indenting canyons typically terminate in amphitheatre-shaped heads, whereas shelf breaching canyons extend landwards across the shelf in a landwards narrowing valley which may be associated with an adjacent incised valley onshore (Farre et al., 1983). The shelf break in the study area occurs at approximately 120 m water depth, the shelf divided into an inner- (depths <15 m), mid- (depths between 15 m and 65 m) and an outer shelf zone (Ramsay, 1994). Six prominent shelf indenting canyons exist in the study area (Fig. 1). These are Leven (Leven Block), North and South Leadsman (Leadsman Block), Diepgat, Wright and White Sands (Sodwana Block)

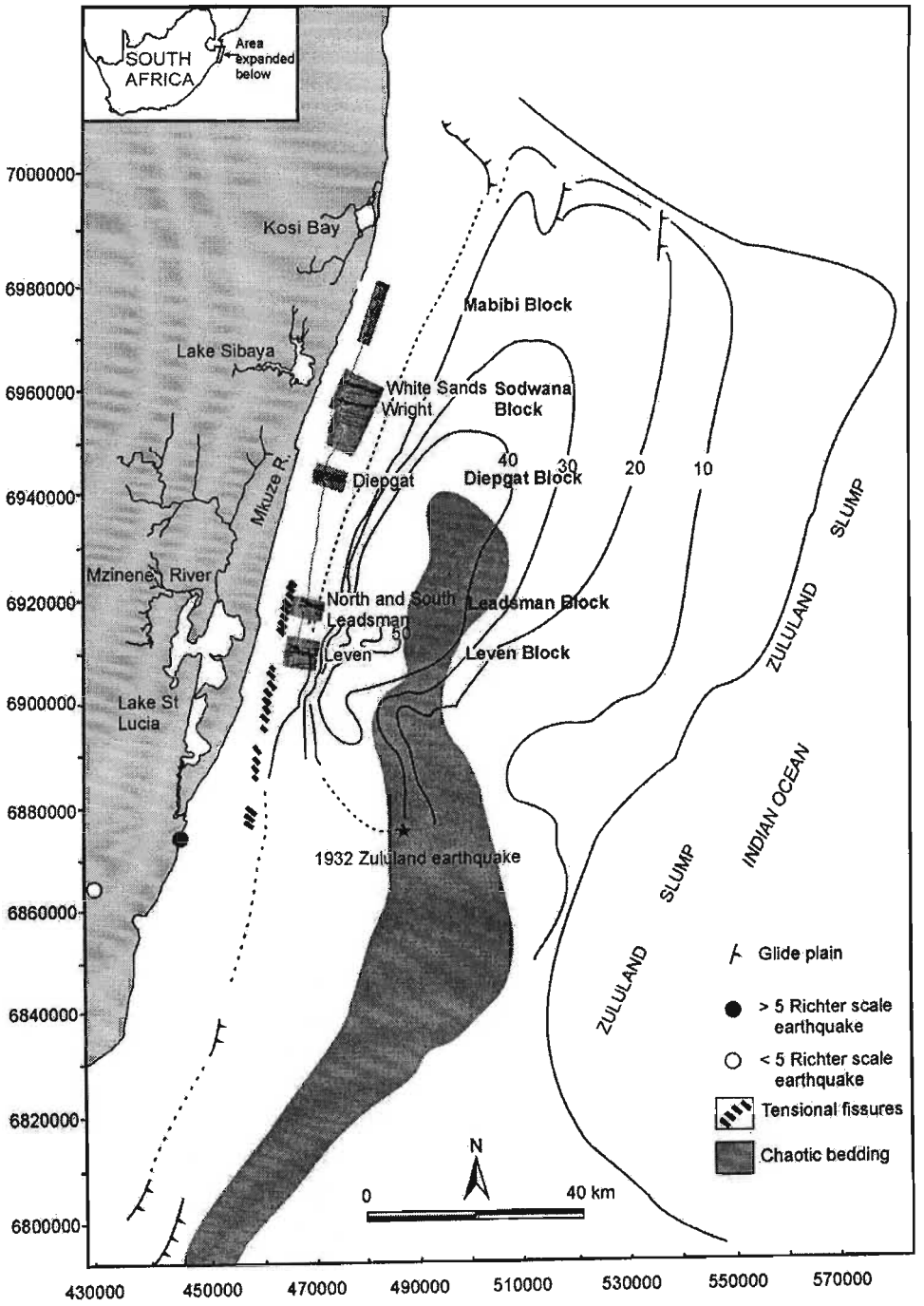

Fig. 1. Location map of the study area, detailing the multibeam survey blocks and major submarine canyons, superimposed with the 125 m isobath corresponding to the Last Glacial Maximum shoreline. Northing and easting co-ordinates in metres, Universal Trans-Mercator (UTM) projection. Note the presence of two large freshwater coastal waterbodies fringing the study area, the southernmost is Lake St Lucia, followed to the north by Lake Sibaya. The Zululand Slump is depicted as isopleths of thickness in two-way travel time. The 1932 Zululand earthquake is the highest magnitude earthquake experienced in recent times (Hartnady, 2002).

Canyons (Figs. 2–5). Smaller shelf indenting canyons occur in the Mabibi area. The largest canyons of the various blocks are relatively isolated and interspersed with narrow, shelf indenting or upper-slope confined canyons (Fig. 6).

The continental shelf of Northern KwaZulu-Natal is characterised by a Holocene sediment wedge of less than 40 m thick (Martin and Flemming, 1986) which mantles hardgrounds of variable thickness (2–25 m) of Late Pleistocene age (Ramsay, 1996). The Holocene wedge extends from the present shoreline to a depth of 90 m and overlies emergent shelf sediments of Tertiary and Late Cretaceous ages (Dingle et al., 1983). Early- to mid-Pleistocene-age sediments are uncommon on this shelf, with only thin exposures of late Pleistocene sediments remaining on the east coast of southern Africa (Dingle et al., 1983; Ramsay, 1994; Miller, 2001). These sediments comprise thin aeolianite/beachrock reef complexes that occur as discrete lineaments on the shelf, at the shelf edge and in canyon heads (Ramsay, 1994).

The shelf break and upper continental slope is dominated by an oversteepened shelf edge wedge of Mio/Pliocene age (Sydow, 1988). This comprises a series of prograding clinoforms formed during times of high sediment supply derived from an uplift of the hinterland (Partridge and Maud, 1987). A number of coastal waterbodies associated with the fringing coastal plain occur in the area (Fig. 1). These systems have, during hypothermal lowstands e.g. the ±18000 BP Last Glacial Maximum (LGM), been associated with palaeo-drainage directly onto the continental shelf and slope (Van Heerden, 1987; Sydow, 1988; Wright et al., 2000). Oceanographically, this portion of coastline is dominated by the strong, poleward-flowing Agulhas Current, which can attain velocities of 3 ms^{-1} (Lutjeharms, 2006). Flemming (1978, 1981) and Cooper (1994) indicate that the strong Agulhas Current, coupled with a lack of fluvially derived terrigenous sediment on the outer shelf has resulted in sediment starvation along this portion of shelf.

Large submarine landslides along the South African coastline have been recognised by other authors (e.g. Emery et al., 1975; Dingle, 1980; Dingle and Robson, 1985). Dingle (1977) described one of the largest recorded landslides, the Agulhas Slump, having shifted 20000 km^3 of sediment seaward off the southern African margin. Martin (1984) recorded an even larger slump off the northern KwaZulu-Natal margin, of ~34000 km^2 in aerial extent. Goodlad (1986) and Sydow (1988) both recorded similar, though much smaller, slumps occurring on the unconfined shelf for that area. Sydow (1988), Ramsay (1994, 1996) and Shaw (1998) in turn described landsliding confined to submarine canyons for the northern KwaZulu-Natal margin.

The earliest reference to the submarine canyons of the area by Bang (1968), postulates that these features formed by several means,

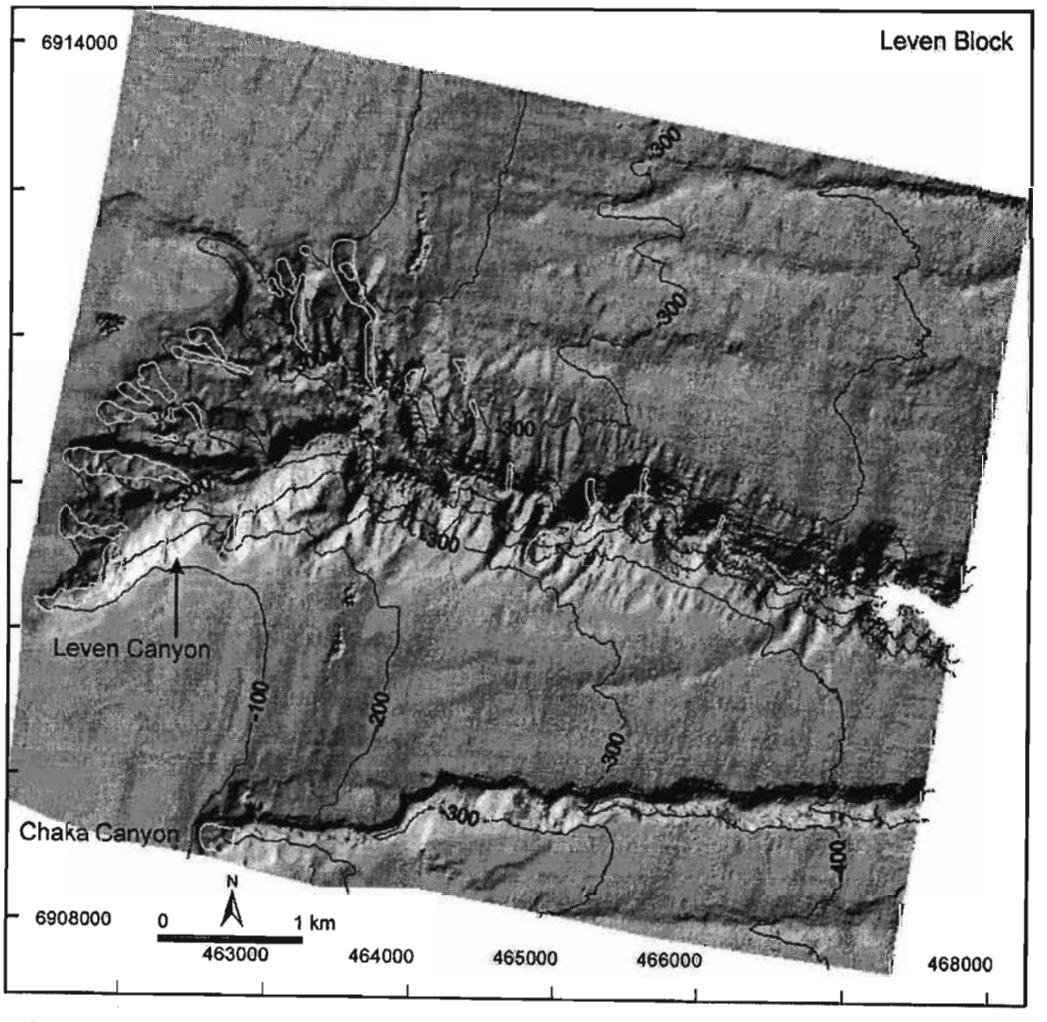

Fig. 2. Bathymetric data from Leven Block, artificially sunshaded from the northeast. Contour interval is 100 m, northing and easting co-ordinates in metres, UTM projection zone. Leven Canyon occurs as the larger shelf indenting canyon, Chaka Canyon is the smaller shelf indenting feature in the southern most portion of the figure. Identifiable landslides are depicted with white borders. Note the higher number of landslides in Leven Canyon, as compared to the narrow Chaka Canyon with a single identifiable retrogressive failure at the canyon head.

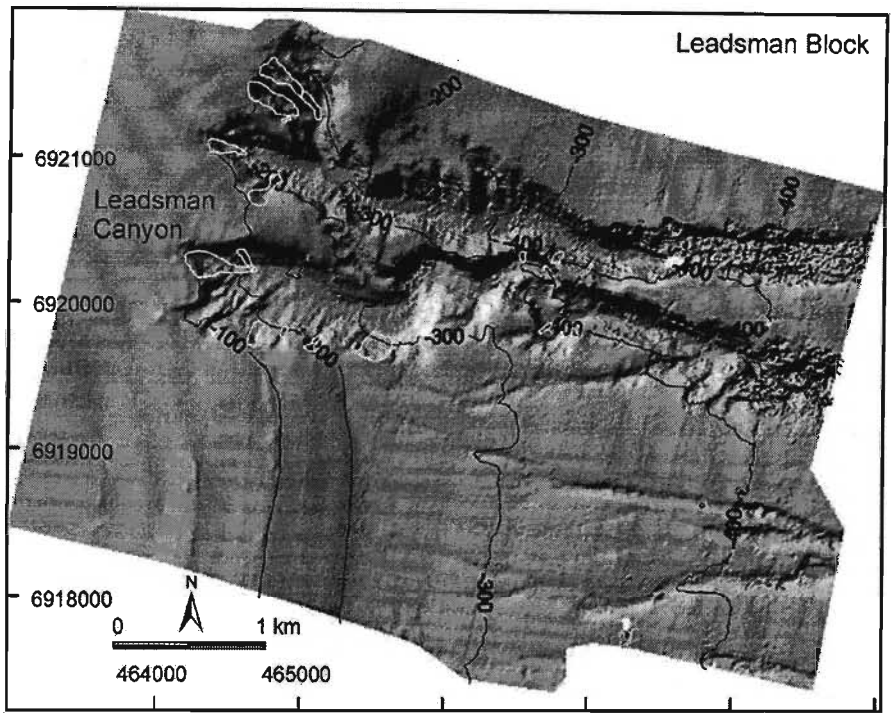

Fig. 3. Bathymetric data from Leadsman Block, artificially sunshaded from the northeast. Contour interval is 100 m, northing and easting co-ordinates in metres, UTM projection zone. North and South Leadsman Canyon appear to be a bifurcated head complex of a single canyon which coalesces in the mid-slope section. Note the presence of slope confined rills in the southern portion of the block.

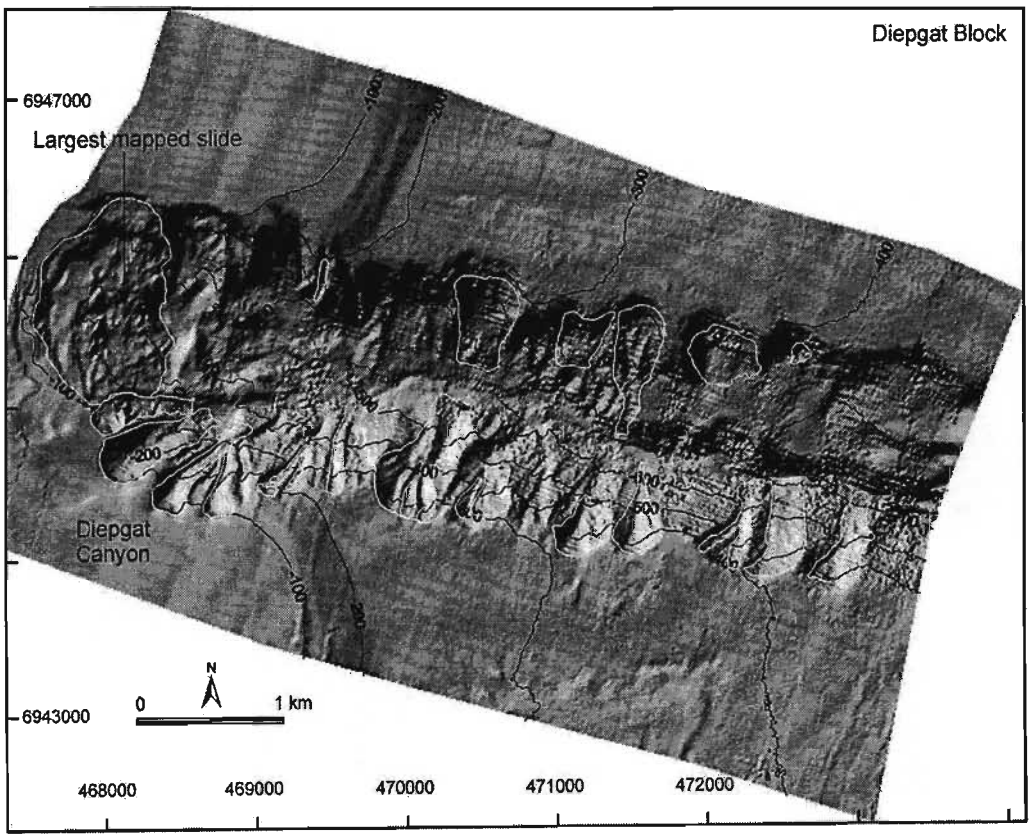

Fig. 4. Bathymetric data from Diepgat Block, artificially sunshaded from the northeast. Contour interval is 100 m, northing and easting co-ordinates in metres, UTM projection zone. Diepgat Canyon exhibits a deeply excavated thalweg and prominent semi-circular collapse structures in the head, one of which comprises the largest landslide mapped in this study. Note the strong axis perpendicular alignment of landslides along the canyon margins.

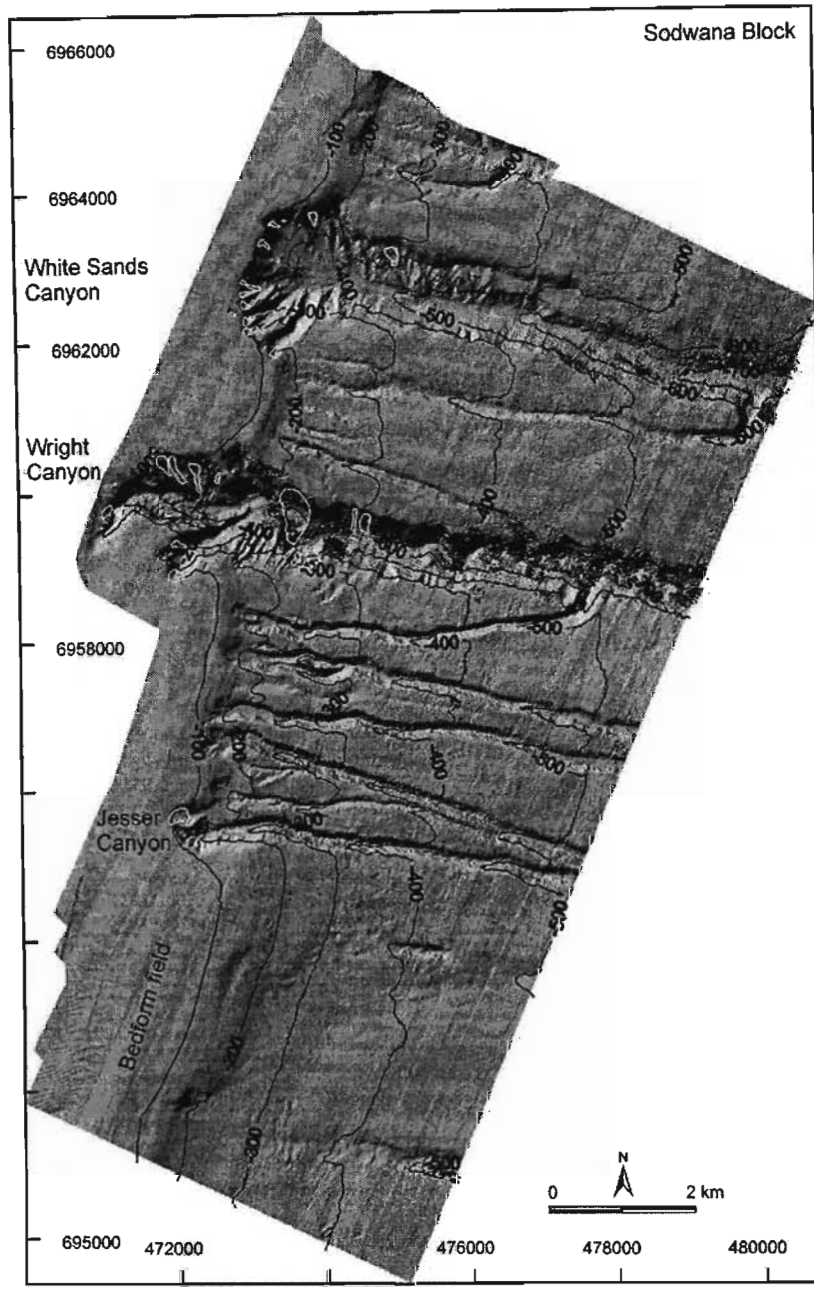

Fig. 5. Bathymetric data from Sodwana Block, artificially sunshaded from the northeast. Contour interval is 100 m, northing and easting co-ordinates in metres, UTM projection zone. Two large shelf indenting canyons are evident (Wright and White Sands Canyons), and are interspersed with smaller narrow, shelf indenting canyons and slope confined rills. Note the development of a prominent bedforms field in the southern portions of the block.

the most important being the undermining of the canyon walls by fluid sapping and the subsequent triggering of landslides associated with canyon development. Seismic profiling through Chaka Canyon (Leven Block), a smaller canyon which indents the shelf, revealed that rotational slumping had affected the entire profile of the canyon (Fig. 7). The valley was assumed to have propagated shorewards by retrogressive rotational slumping along the head scarp and side walls, inducing debris flows and channel turbidites which eroded previous slump fills within the thalweg (Sydow, 1988). Shaw (1998) recognised characteristic slump morphologies within submarine canyon walls from single channel seismic data. Slumping in Wright Canyon (Sodwana block) and Diepgat Canyon was described from the headwalls of the canyons and attributed to an increase in the sediment input to the rim of the canyon head. Shaw (1998) also recognised several buried landslides, occurring in semi-consolidated sediments of a speculative Miocene/Pliocene age that formed as a result of slope instability during the Late Tertiary. Ramsay (1994) recognised that larger landslides occurred on the southern walls of Wright and White Sands Canyons, based on observations from single beam echosounding.

1.2. Terminology

The nomenclature used in describing submarine mass movements is a complex one (Canals et al., 2004; Masson et al., 2006) with various terms used to describe submarine mass movements e.g. slumps, slides, debris flows etc. Each term implies a genetic relationship to some mass transport process (e.g. Tripsanas et al., 2008), which may be difficult to interpret based solely on the surficial characteristics of

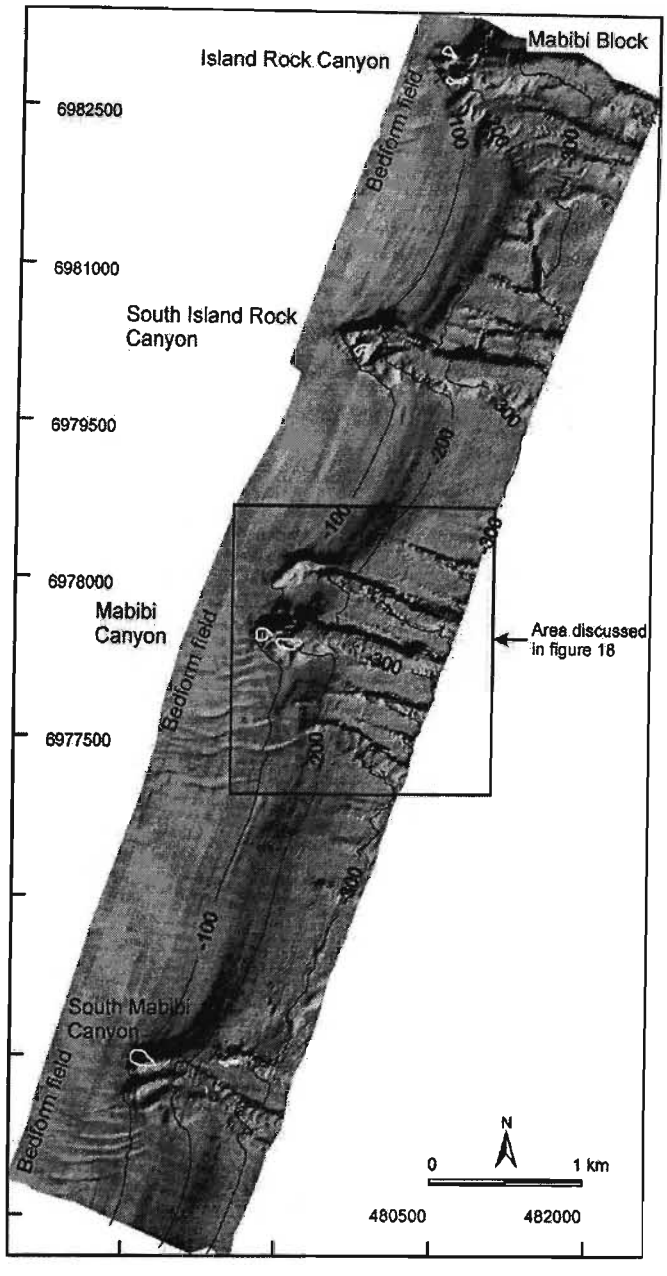

Fig. 6. Bathymetric data from Mabibi Block, artificially sunshaded from the northeast. Contour interval is 100 m, northing and easting co-ordinates in metres, UTM projection zone. The largest canyon of the Mabibi area (South Island Rock Canyon) occurs in the northernmost extent of the study area. Canyons of the Mabibi area are narrow features which are comparatively smaller and less shelf indenting than canyons of the other blocks studied. Note the well developed bedform fields on the comparatively wider continental shelf, compared to the blocks further south.

slope failure products resting on the sea floor. Slides and slumps are traditionally considered translational or rotational movements of material, bounded by distinct scarps with relief ranging from a few to several hundred metres (Coleman and Prior, 1988; Hünerbach and Masson, 2004). We make no distinction between the two and consider any slope failure, which has resulted in the preservation of the material as a coherent deposit, a slide or *cohesive* slide.

Debris flows, which form by the plastic deformation of coherent slide blocks (Tripsanas et al., 2008) are considered as a form of *disintegrative* slope failure where the mass wasting deposit is still observed at the base of the failure, yet is no longer intact. *Fluidised* type failures, where there is no apparent deposit, yet an unmistakable scarp in the upper regions of the slope failure are considered as turbidity flows, the material either being derived from partial disintegration of a slide mass, or during transition from a debris flow via the erosion and entrainment of canyon floor sands (e.g. Piper et al., 1999). Boyd et al. (2008) provide an alternate view of shallow to deep water sediment transport, whereby active turbidity currents are not associated with landsliding, but rather the interaction between local hydrodynamic conditions and margin orientation which causes cascading over the shelf edge and gravity transport of sediments downslope.

2. Methods

Until now, landslide analysis along this section of shelf has been restricted to discrete cross sections through a single failure. With dense, high resolution multibeam data, slumps may be imaged in three dimensions and their geomorphology intensively studied. Multibeam bathymetric data, acquired for the African Coelacanth Ecosystem Programme (ACEP), is used to identify failures within the study area. These data form the first detailed swath bathymetric data set for the east coast of South Africa, and expose a number of undiscovered canyons and landslides. Data were acquired at 100 kHz using a Reson 8111 SeaBat system and covered 392 km^2 over depths ranging from 29 to 838 m, with a spatial resolution of ~1 m given navigational uncertainties. Acquisition was over a 150° swath with a beam separation of 1.5°. All data were tidally corrected using Admiralty (South African Navy) charts to Mean Sea-Level (MSL) datum. Bathymetric data were binned at 5 m, the data thus capable of resolving discrete landslides greater than ~25 m^2. The vertical accuracy of the data is considered to be approximately 30 cm.

2.1. Slide determination and measurement

The bathymetric data were incorporated into the GIS software packages ER Mapper 6.1 and Surfer 7 and sunshaded digital terrain models (DTMs) for each survey block were created. These were used to identify landslide localities. Sunshading serves to illuminate bathymetric features such as head scarps, side walls and failed masses at the base of a slide. In order to ascertain slope angles of failed and unfailed sediments, a grid calculus was performed on the bathymetry and the slope angle extracted. These were subsequently gridded at 5 m resolution, and contoured to give an indication of the stability of the available sediment to the canyon margin.

Measurements of the head scarp height; runout length; gradient of failed slope (failure scar); gradient of the unfailed adjacent slope; gradient of runout slope; scar angle; failure scar area; and total failure area were made from the multibeam bathymetric data for each individual failure (Fig. 8). Where no failure deposit was encountered, the slide runout was considered to terminate where the side walls opened out into unconfined space, thus giving a minimum possible distance for the failure mass. Measurements were made from slices of the bathymetric data that were then used to create depth vs. absolute distance cross sectional data. Absolute distance in this case refers to cross sections that are not directionally specific along a principal axial plane, but instead are calculated on the basis of distance from start to finish. Any bias that obliquity of the bathymetric slices would introduce to the study is thus eliminated. As a result of the natural variation across each landslide feature, several measurements were made from several adjacent cross sections in order to present a mean value of these features. As with McAdoo et al. (2000), less angular features such as slumps, or older more subdued failure expressions give rise to less prominent scarp features, the scarp height is thus measured as the steepest possible section from the slump scar.

Unlike McAdoo et al. (2000) slope gradients are not measured from GIS constructed slope maps, but rather from slope cross sections made from the grid slices used in creating the bathymetric cross sections. Gradients were then digitised from a number of depth vs. gradient

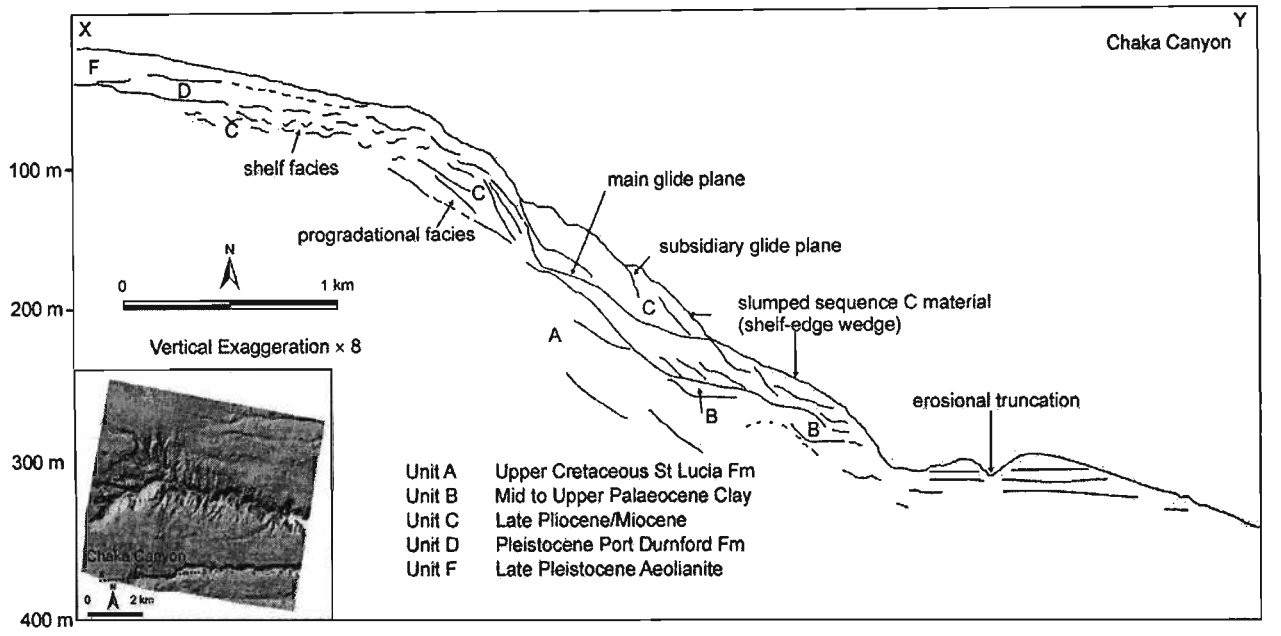

Fig. 7. Interpreted line drawing of single channel sparker seismic reflection line through Chaka Canyon (after Sydow, 1988). Shoreward propagation of the canyon by retrogressive failure has resulted in a hummocky canyon profile, with previous slump fills subsequently excavated by debris flows and channel turbidites (Sydow, 1988). Note that slumping has not extended landwards of the shelf edge wedge.

plots that overlie the bathymetric cross sections, in order to pick the appropriate corresponding gradients for slump scar, runout slope and headscarp slope. These values are presented as the mean value derived from several cross sections. Similarly, for the local unfailed adjacent slope, several cross sections were constructed and the mean value for unfailed adjacent slope acquired.

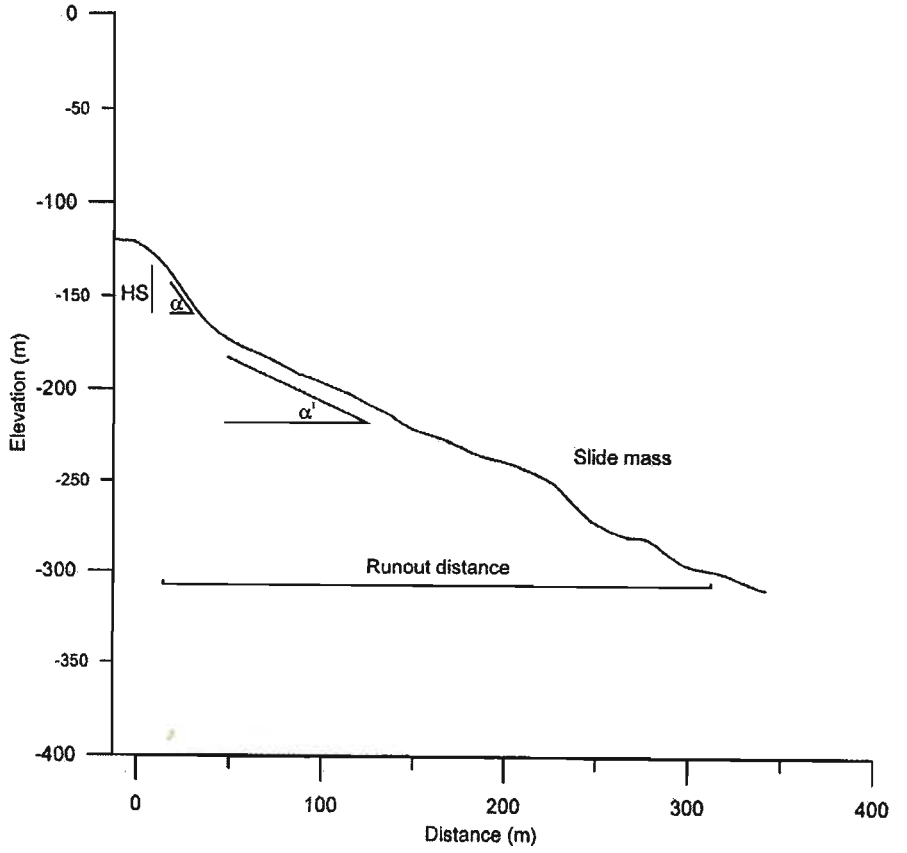

Fig. 8. Measured features of landslides from this study, depicted on an idealised profile through a canyon margin landslide. HS = headscarp height; α = headscarp slope; α^1 = scar slope; runout distance = distance from headscarp to most distal point of failed mass accumulation.

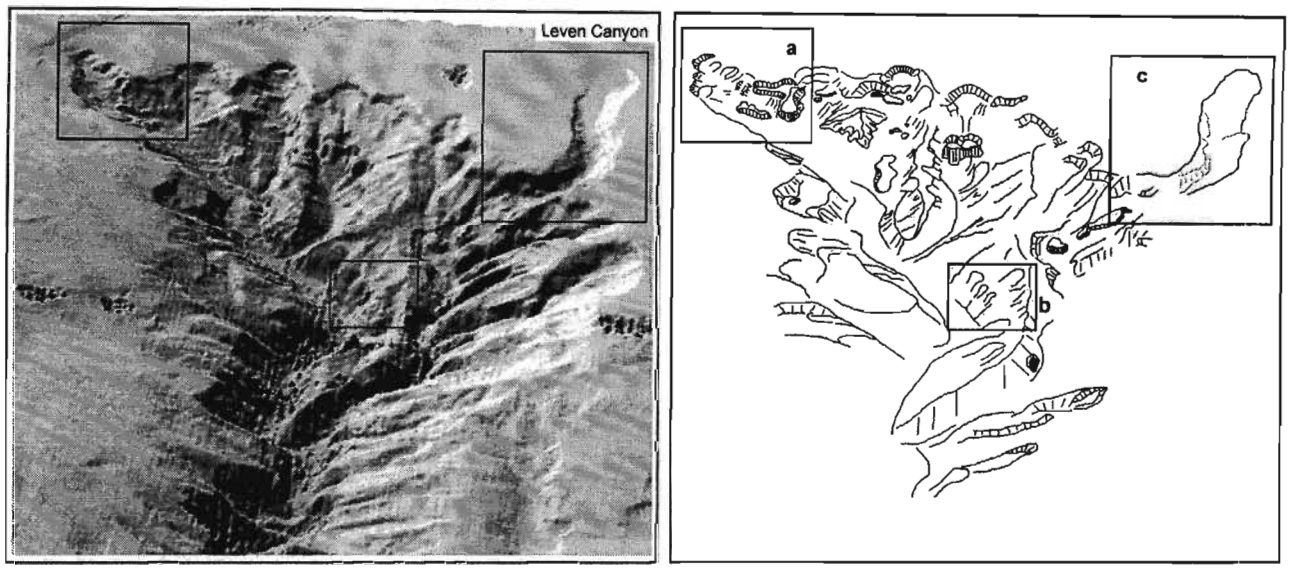

Fig. 9. Three dimensional view, and interpretative sketch of the head of Leven Canyon, exhibiting several landslide morphologies. View is from the south–south east, V.E ~ 2×. Inset a depicts an incised inner gorge at the base of a slide on the southern portion of Leven Canyon head. Inset b indicates a series of stranded hanging slides on a small interfluve. Inset c depicts a fluidised landslide extending onto the mid continental shelf. Note the sinuous morphology and lack of appreciable headscarp of this landslide.

Table 1
Summary of the statistical comparison between various landslide attributes for each survey block

	Area	Volume	Runout	Runout slope	HS slope	HS height	Scar slope	LUS	HS depth	D/L
a)										
Leven Point (n=31)										
Area	1.00									
Volume	**0.95**	1.00								
Runout	**0.88**	**0.55**	1.00							
Runout slope	−0.15	−0.04	−0.38	1.00						
HS slope	−0.16	0.00	−0.45	0.16	1.00					
HS height	0.07	0.29	−0.05	−0.02	**0.52**	1.00				
Scar slope	−0.24	−0.09	−0.37	0.15	**0.61**	0.36	1.00			
LUS	−0.42	−0.33	**−0.55**	0.10	0.36	0.01	0.28	1.00		
HS depth	−0.44	−0.30	**−0.52**	−0.20	**0.56**	0.22	0.31	**0.67**	1.00	
D/L	**−0.51**	−0.36	**−0.64**	0.13	**0.60**	**0.53**	0.36	0.38	**0.64**	1.00
b)										
Leadsman (n=20)										
Area	1.00									
Volume	**0.94**	1.00								
Runout	**0.86**	**0.93**	1.00							
Runout slope	0.05	0.08	0.10	1.00						
HS slope	**−0.62**	**−0.62**	**−0.54**	−0.23	1.00					
HS height	0.17	0.34	0.29	0.12	0.11	1.00				
Scar slope	**−0.50**	**−0.54**	**−0.53**	−0.16	**0.80**	0.16	1.00			
LUS	**−0.54**	**−0.57**	**−0.57**	−0.04	0.31	−0.26	0.23	1.00		
HS depth	**−0.59**	**−0.68**	**−0.70**	−0.29	**0.71**	−0.31	**0.67**	**0.50**	1.00	
D/L	**−0.61**	**−0.61**	**−0.67**	−0.41	**0.68**	0.10	**0.59**	0.41	**0.76**	1.00
c)										
Diepgat (n=26)										
Area	1.00									
Volume	**0.88**	1.00								
Runout	**0.80**	**0.77**	1.00							
Runout slope	−0.29	−0.32	−0.47	1.00						
HS slope	0.10	0.04	0.13	−0.26	1.00					
HS height	0.44	**0.69**	**0.67**	**−0.50**	0.18	1.00				
Scar slope	−0.03	−0.13	0.02	−0.09	**0.70**	0.01	1.00			
LUS	−0.33	−0.30	−0.29	0.30	0.08	0.29	0.20	1.00		
HS depth	0.06	0.06	−0.21	−0.08	−0.13	−0.12	−0.14	−0.38	1.00	
D/L	−0.49	−0.30	**−0.60**	0.48	−0.06	−0.14	−0.07	−0.49	−0.12	1.00
d)										
Wright Canyon (n=16)										
Area	1.00									
Volume	**0.93**	1.00								
Runout	−0.01	0.16	1.00							
Runout slope	−0.03	−0.09	−0.20	1.00						
HS slope	0.04	−0.04	−0.19	0.17	1.00					
HS height	−0.02	0.32	0.42	−0.17	0.09	1.00				
Scar slope	−0.04	−0.18	**−0.65**	0.10	**0.58**	−0.25	1.00			
LUS	−0.35	−0.35	0.10	−0.04	**0.70**	0.21	0.42	1.00		
HS depth	0.12	0.09	−0.02	−0.15	**0.78**	0.21	0.41	**0.69**	1.00	
D/L	−0.01	0.20	−0.23	0.06	0.33	**0.73**	0.17	0.23	0.24	1.00
e)										
White Sands (n=16)										
Area	1.00									
Volume	**0.85**	1.00								
Runout	**0.74**	**0.86**	1.00							
Runout slope	**0.57**	**−0.57**	**−0.73**	1.00						
HS slope	**−0.6**	−0.19	−0.18	0.16	1.00					
HS height	−0.09	0.30	0.28	0.04	0.48	1.00				
Scar slope	**−0.61**	−0.45	−0.39	**0.63**	0.39	0.35	1.00			
LUS	−0.45	−0.36	−0.33	0.24	0.48	−0.02	0.23	1.00		
HS depth	0.03	0.18	0.01	0.01	0.14	−0.34	−0.06	−0.12	1.00	
D/L	**−0.59**	−0.47	**−0.65**	**0.67**	0.47	0.42	**0.64**	0.32	−0.19	1.00
f)										
Mabibi (n=7)										
Area	1.00									
Volume	**0.72**	1.00								
Runout	−0.05	**0.63**	1.00							
Runout slope	**0.68**	0.10	**−0.63**	1.00						
HS slope	−0.43	0.18	**0.74**	**−0.68**	1.00					
HS height	0.03	**0.65**	**0.87**	**−0.55**	**0.83**	1.00				
Scar slope	0.35	−0.12	**−0.6**	0.29	**−0.61**	−0.36	1.00			

Table 1 (*continued*)

	Area	Volume	Runout	Runout slope	HS slope	HS height	Scar slope	LUS	HS depth	D/L
f)										
Mabibi (n=7)										
LUS	0.48	0.09	**0.50**	**0.79**	−0.19	−0.17	0.21	1.00		
HS depth	**−0.52**	−0.44	−0.20	−0.44	−0.21	−0.22	0.39	**−0.50**	1.00	
D/L	0.07	0.45	0.49	−0.34	**0.71**	**0.86**	−0.04	0.19	−0.19	1.00
g)										
All areas (n=116)										
Area	1.00									
Volume	**0.91**	1.00								
Runout	**0.68**	**0.60**	1.00							
Runout slope	−0.07	−0.09	−0.25	1.00						
HS slope	−0.01	0.04	−0.22	0.05	1.00					
HS height	0.29	**0.50**	0.36	−0.08	0.39	1.00				
Scar slope	0.17	0.14	−0.09	0.16	**0.57**	0.17	1.00			
LUS	−0.37	−0.31	−0.4	0.04	0.32	−0.03	0.08	1.00		
HS depth	0.11	0.14	−0.18	−0.06	0.38	0.05	0.39	0.17	1.00	
D/L	−0.32	−0.15	**−0.50**	0.15	**0.50**	0.31	0.24	0.38	0.26	1.00
h)										
Cohesive (n=116)										
Area	1.00									
Volume	**0.91**	1.00								
Runout	**0.68**	**0.60**	1.00							
Runout slope	−0.07	−0.09	−0.25	1.00						
HS slope	−0.01	0.04	−0.22	0.05	1.00					
HS height	0.29	**0.50**	0.36	−0.08	0.39	1.00				
Scar slope	0.17	0.14	−0.09	0.16	**0.57**	0.17	1.00			
LUS	−0.37	−0.31	−0.4	0.04	0.32	−0.03	0.08	1.00		
HS depth	0.11	0.14	−0.18	−0.06	0.38	0.05	0.39	0.17	1.00	
D/L	−0.32	−0.15	**−0.50**	0.15	**0.50**	0.31	0.24	0.38	0.26	1.00
i)										
Disintegrative (n=116)										
Area	1.00									
Volume	**0.91**	1.00								
Runout	**0.68**	**0.60**	1.00							
Runout slope	−0.07	−0.09	−0.25	1.00						
HS slope	−0.01	0.04	−0.22	0.05	1.00					
HS height	0.29	**0.50**	0.36	−0.08	0.39	1.00				
Scar slope	0.17	0.14	−0.09	0.16	**0.57**	0.17	1.00			
LUS	−0.37	−0.31	−0.4	0.04	0.32	−0.03	0.08	1.00		
HS depth	0.11	0.14	−0.18	−0.06	0.38	0.05	0.39	0.17	1.00	
D/L	−0.32	−0.15	**−0.50**	0.15	**0.50**	0.31	0.24	0.38	0.26	1.00

HS = headscarp, LUS = local unfailed slope, D/L = ratio between runout distance and head scarp height. Correlation co-efficients greater than 0.5 are highlighted in bold.

Landslide volume is calculated based on the thickness ($T = h \cos \alpha$, where h is the headscarp height, and α the scar slope angle). A basic wedge geometry is used where:

Slide volume $(V) = 1/2(A)(T)$

A is the area derived from the sunshaded bathymetry GIS, corrected for dip aberration based on an average slope angle for the landslide feature.

Limitations to these methods exist. Firstly, by using bathymetric data without the aid of seismic reflection data, the results are biased towards more recent failures that have stronger topographic expressions. As such, features that may be older and lack the consequent bathymetric signature used in this methodology are ignored altogether. Secondly, it is unclear to which stratigraphic depth these failures extend, and the exact volumes of the failed mass accumulating at the base of each slide. This method is useful in that it allows a comparative view of certain "type" landslides that are occurring based on the various features described, and allows a preliminary interpretation of the mechanism (either rheological or mechanical) responsible for canyon enlargement and proliferation.

3. Results

3.1. Landslide location, depth, regional gradient

The majority of landslides from the study area occur in Leven ($n=30$) and Diepgat Canyons ($n=27$), with the other significant locations occurring in the White Sands ($n=14$), Wright ($n=16$) and Leadsman Canyons ($n=19$) (Figs. 2–6). The Mabibi Block, despite having numerous small canyons, has significantly fewer landslides in comparison, with only six recognisable features being measurable based on this study's requisites for failure identification. The remainder of the landslides in the study area occur in the heads of smaller shelf indenting or slope confined canyons that reside between the larger shelf indenting canyons. These are typically narrow, shallow features with linear thalwegs and subdued downslope topography (Fig. 6). Canyons with heads that occur deeper than 120 m below sea level (mbsl) have typically fewer than three failures per canyon, compared to no failures found in the small inter-canyon rills (Fig. 6). Studies by Green et al. (2007) indicate that the Mabibi shelf, despite having fewer failures, has the steepest average gradient of 6° before the shelf edge wedge, followed by Leadsman (5°), Diepgat (5°), Sodwana Bay (4°) and Leven Point (4°) respectively. Average gradients of the shelf edge and upper slope are highest at Mabibi (11.5°), proceeded by Leadsman (9°), Diepgat (8°), Sodwana (6.5°) and Leven (5°).

Landsliding occurs most frequently in the southern flanks of Diepgat, South Leadsman and White Sands Canyons compared to the northern flanks (Figs. 2–6). Conversely, landsliding is most prominent in the northern flanks of Wright, Leven and North Leadsman Canyons (Figs. 2–6). Landslides occur most commonly in the canyon heads of the study area, apart from Diepgat, where a series of semi-circular collapse structures, ~1.5 km across, dominate the upper portions and obscure any older failures (Fig. 4). The headscarps of landslides in the

canyon heads occur parallel to sub-parallel to the canyon axis, whereas those along the canyon walls are orientated parallel to the thalweg. Failures in the lower portions of Leven Canyon occur at strongly sinuous meanders in the thalweg.

3.2. Landslide geomorphology

Landslides occur as cohesive slides with smaller runout distances compared to disintegrative slides (debris or turbiditic flows) where little or no failure rubble is discernible at the base of the failure. Several landslide associated morphologies are common (Fig. 9). These include: 1) incised inner gorges; 2) hanging or perched slides in the canyon headwalls; 3) terraced slides; and 4) benches in the slide material. These occur prominently in several slope failures of Diepgat, Leven, Wright and White Sands Canyons, with exceptions in Leadsman Canyon and the Mabibi canyons. Inner gorges form where the slide terminates close to the thalweg or is truncated by a gully or larger axis-oblique slide leaving a steeply cliffed section at the base of the failure deposit (c.f. Densmore et al., 1997; McAdoo et al., 2000). Several failures, particularly in Leven Canyon have sinuously channelled features, synonymous with fluidised slope failures (Fig. 9, box c).

3.3. Landslide statistics

Table 1a–f summarises the landslide morphometry from each individual survey block and presents the correlation coefficients for the various attributes. A statistical comparison is made of all landslides encountered in the study area (Table 1g), and the morphometric differences between cohesional and non-cohesional failures are also provided (Table 1h–i). These are referred to as cohesive and disintegrative slides respectively. Landslide area, volume, headscarp height, local unfailed slope and headscarp slope are presented as histograms for the various survey blocks (Figs. 10–14).

3.4. Area, volume, runout

The largest failures occur in Diepgat Canyon. The aerial extents of 13 of the 27 failures exceed 80000 m^2 (Fig. 10). The largest failure (so large as to not fit to the scale of Fig. 10) in Diepgat Canyon covers an area of sea floor 928024 m^2 in extent. Leven Canyon and Wright Canyon are the only other canyons to possess failures exceeding 80000 m^2, the largest failures disturbing 105519 m^2, 90577 m^2 (Leven) and 199129 m^2 (Wright) of sea floor respectively (Fig. 10). The mean areas encompassed by landslides are calculated at 107703 m^2 (Diepgat), 23023 m^2 (Leven), 19457 m^2 (Sodwana), 10666 m^2 (Mabibi) and 10467 m^2 (Leadsman).

Fig. 15 is a plot depicting landslide area vs. headscarp depth for the study area. Landslide area correlates poorly with headscarp depth for all canyons except Mabibi and Leadsman Canyons, which have a moderate negative correlation indicating a reduction in slide area with depth. The largest failures are distributed at random depths throughout the study area. Conversely, the smaller isolated landslides in the heads of the Mabibi Canyons tend to occur at ~100 mbsl.

Volume relationships exhibit similar trends across each canyon (Fig. 11). Volume correlates well with landslide runout for all canyons, excluding Wright Canyon (Table 1). Landslide area similarly has a poor correlation with runout in both Wright Canyon, and the Mabibi area, yet has a strong correlation with runout for the other survey blocks. The mean runout values of 413±48 m (Diepgat), 165±28 m (Leadsman), 404±66 m (Leven), 157±14 m (Mabibi), 168±19 m (White Sands) and 229±25 m (Wright) show a strong variability in runout within the study area. Overall, cohesive slides have significantly lower runout values of 190 m, compared to 439 m of disintegrative slides and turbidity flows. Leven Canyon, and to a lesser extent, Leadsman Canyon, tend to have landslides with larger runouts at shallower depths, whereas Diepgat, the Sodwana Bay, and Mabibi Canyons have a random spread of runout distance with depth (Fig. 16, Table 1).

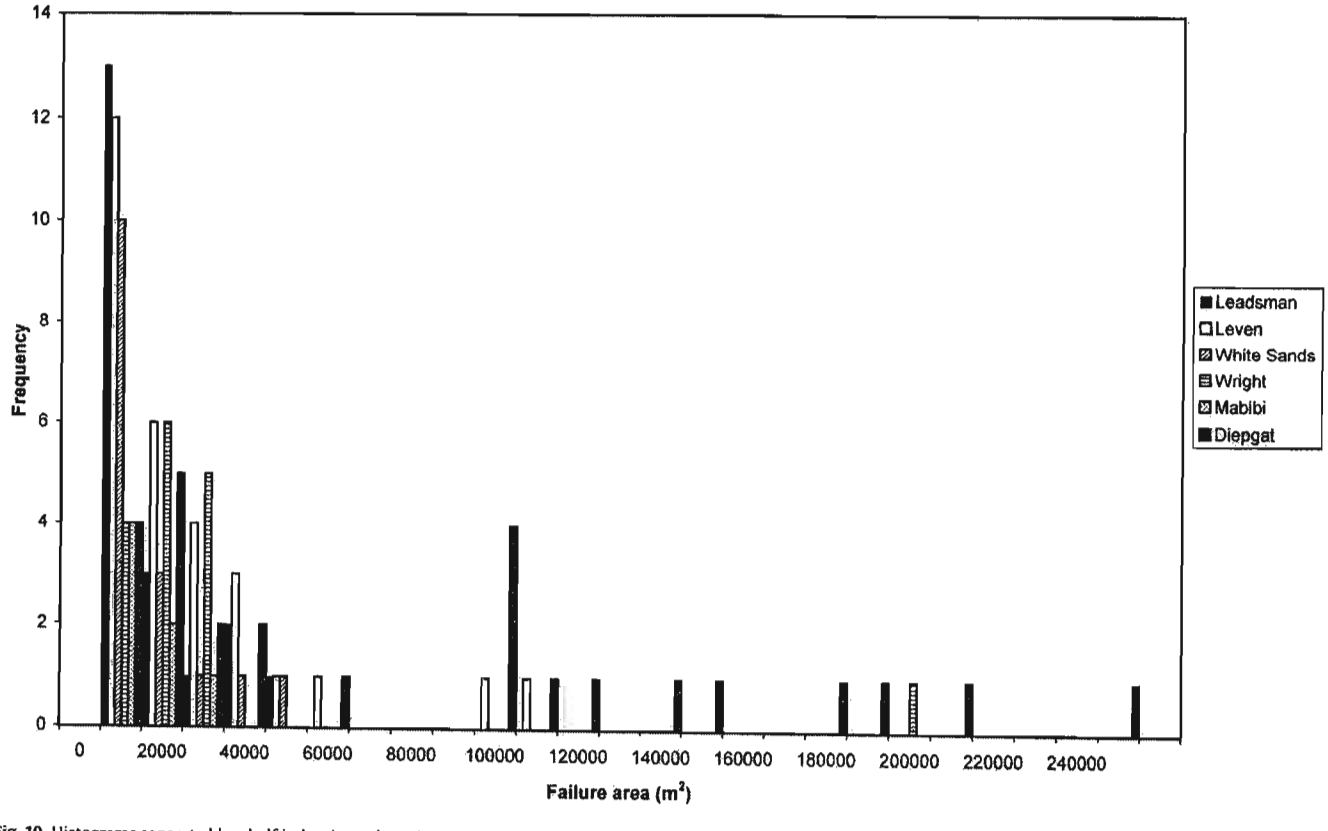

Fig. 10. Histograms separated by shelf indenting submarine canyon/survey block. This depicts area. The submarine canyons of Mabibi are included as a single entry owing to their uniform size and morphology. North and South Leadsman canyons are similarly included as a single entity (Leadsman).

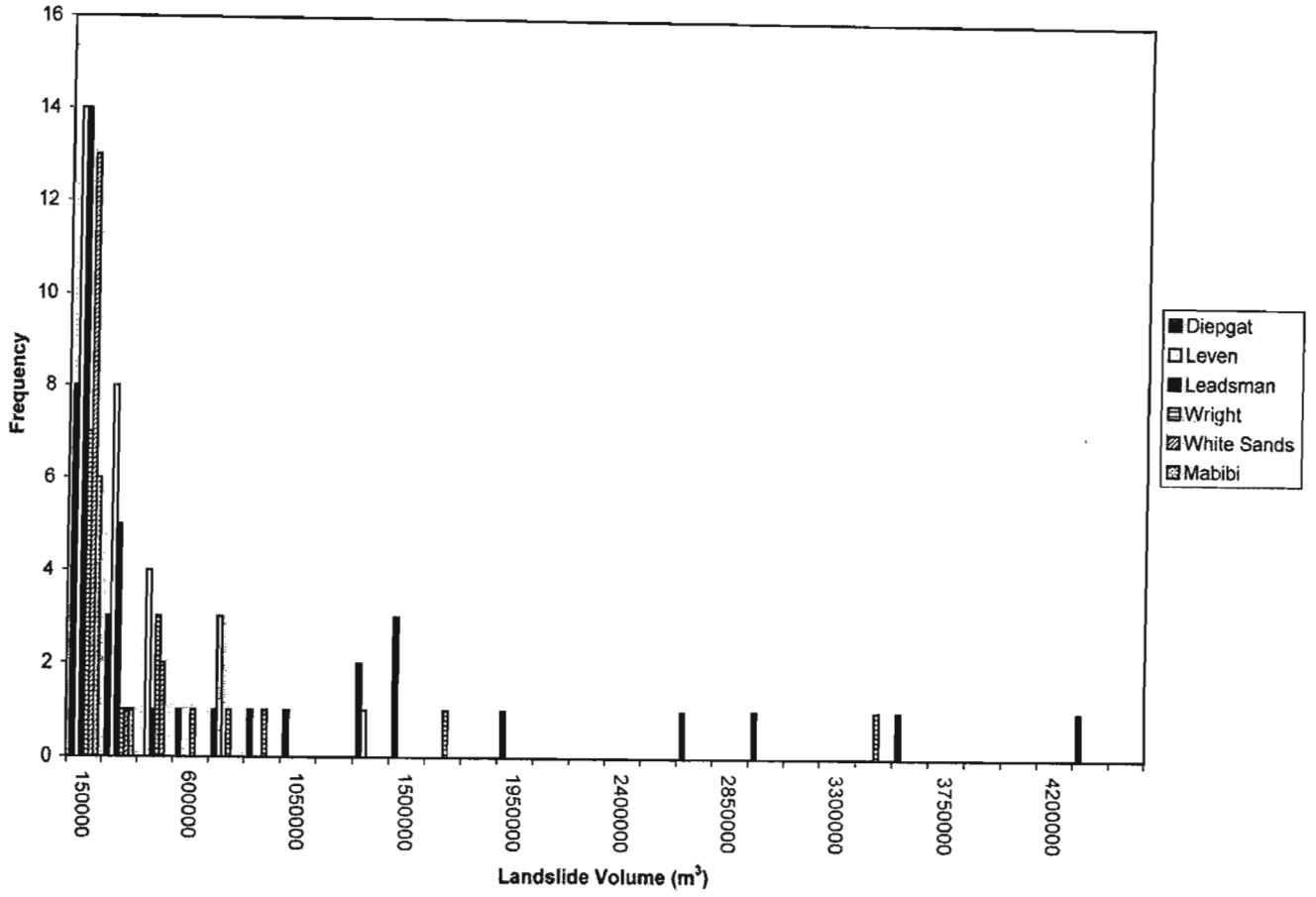

Fig. 11. Histograms separated by shelf indenting submarine canyon/survey block. This depicts volume. The submarine canyons of Mabibi are included as a single entry owing to their uniform size and morphology. North and South Leadsman canyons are similarly included as a single entity (Leadsman).

3.5. Slope gradients

The highest mean local unfailed slope (LUS) gradients occur in Mabibi at 15.6°±2.6°, compared to Leadsman's 14.7°±1.8°, Wright Canyon's 13.5°±1.9°, White Sands Canyon's 12.4°±1.3° and 11.81°±1° for Leven Canyon (Fig. 14). Despite having the largest failure areas, Diepgat Canyon has the lowest mean LUS gradients at 9°±0.7°. The adjacent unfailed slope gradient increases with depth in Wright, Leven and Leadsman Canyons. Conversely, the LUS gradient decreases with depth in Diepgat canyon, and remains variable in White Sands Canyon and the canyons of Mabibi. Mean scar slope gradients are steepest in the landslides of Diepgat Canyon (40.7°±1.2°), followed by those of Wright (33.3°±2°), Leadsman (33.2°±1.9°), Leven (32°±1.8°), and White Sands (27.5°±1.9°) Canyons. Mabibi Block has the gentlest mean scar slopes at 26°±1°. Scar slopes in all cases are steeper than the LUS; however, those areas with the highest LUS do not necessarily have the steepest scar slopes as confirmed by the Mabibi area (Table 1f). Scar slope is unaffected by depth, the values fluctuating randomly across depth profiles for all the canyons, apart from the Leadsman Canyon system, which has a good correlation between increasing depth and increasing scar angle (Fig. 17; Table 1b).

3.6. Headscarps

Headscarp heights and angle vary considerably throughout the study area, the tallest and steepest headscarps occur in Wright Canyon (50.9±7.3 m; 63.6±3.3) (Figs. 12 and 13). The mean headscarp height of failures in Diepgat Canyon is 35±3.8 m, with a mean slope of 50.7°±1.6°. The headscarps of Leven (27.6±3.9 m; 49.6°±2.4°), White Sands (21.8±1.7 m; 46.3°±2°), Leadsman (19.6±1.7 m; 49.8°±2.7°) and Mabibi (17.6±2.7 m; 45.6°±2.5°) are comparatively smaller and gentler. Diepgat and Wright Canyons have the largest degree of variability in headscarps, compared to the comparative uniformity in height of the headscarps of the Mabibi, Leadsman and White Sands Canyons (Fig. 13).

4. Discussion

The five areas presented here have a marked degree of spatial variation in their morphometric characteristics, which suggests that different controls are being exerted on the submarine canyon evolution. Here the correlative relationships of the variables measured (Table 1) are discussed and an attempt to define the possible mechanical or rheological influences imposed on the geomorphology of the study area, in relation to each canyon system is made.

The strongest correlations exist between headscarp slope and headscarp depth (Table 1) indicating that for Leven, Leadsman, and White Sands Canyons, headscarp slope increases with depth. McAdoo et al. (2000) show that headscarp height and slope may be used as a proxy for sediment strength, steeper scarps indicating sediment overconsolidation and higher dynamic strengths, in comparison to gentler scarp slopes that indicate normally consolidated and weaker material. Similar trends are evident from the scar slope vs. depth relationships. This suggests that sediment strength increases with depth within these three canyons, a trend observed from borehole data (Du Toit and Leith, 1974) and seismic data (Sydow, 1988; Shaw, 1998) which indicate that canyons most likely incise loosely consolidated (inferred by Sydow (1988) as Palaeocene age) silty sandstones, as observed from

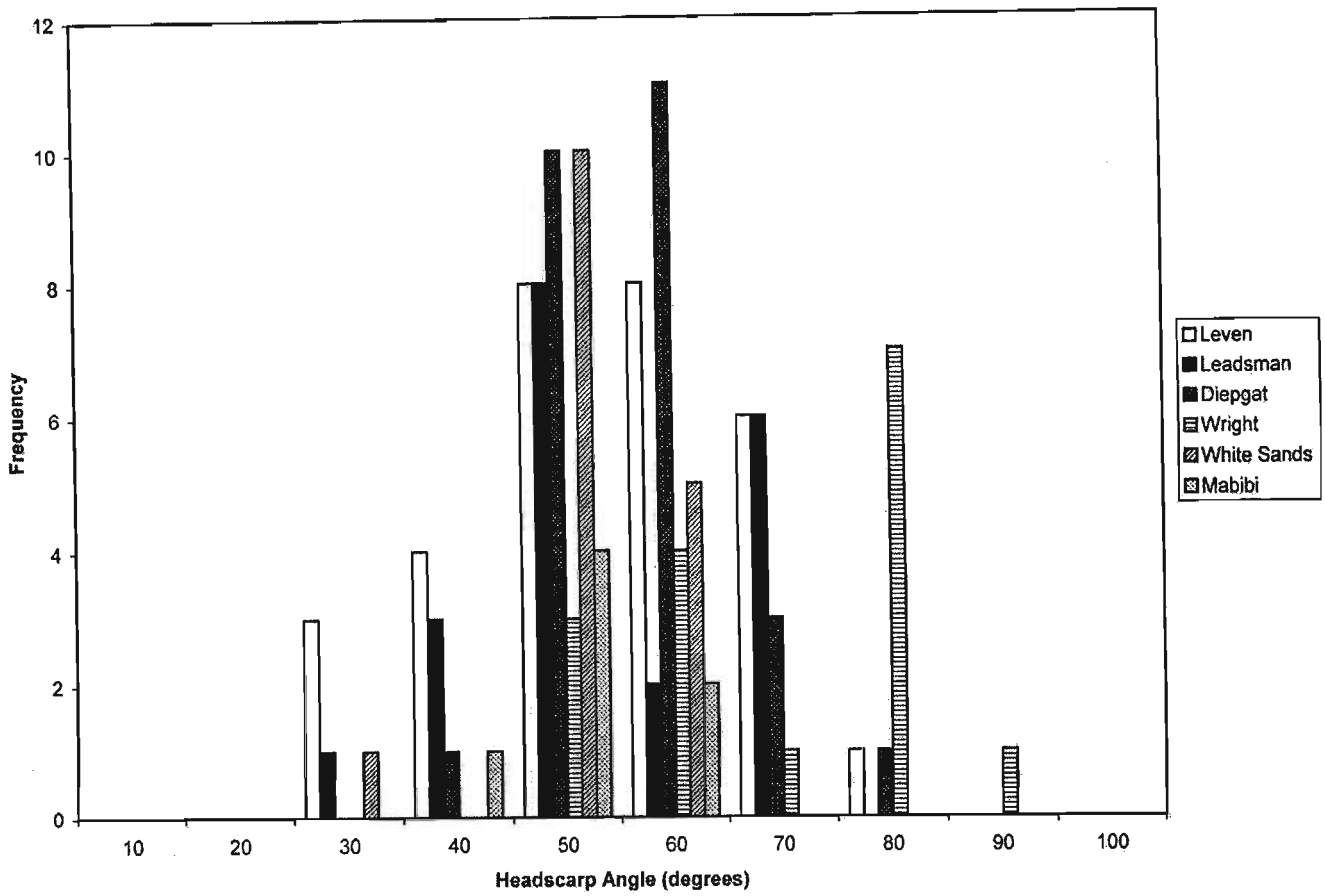

Fig. 12. Histograms separated by shelf indenting submarine canyon/survey block. This depicts headscarp slope. The submarine canyons of Mabibi are included as a single entry owing to their uniform size and morphology. North and South Leadsman canyons are similarly included as a single entity (Leadsman).

submersible dive observations (Green, 2004) before meeting more consolidated silty sandstones (Green, 2004). These are aged by virtue of their microfossil assemblages from gravity cores (Siesser, 1977) which sampled the acoustic basement of the area, assigning it a late Cretaceous (Maastrichtian) age. These rocks are typically of higher strength than the Palaeocene silty sandstones of the area (R. Maud pers. comm). Puzzlingly, this trend is not reflected in any of the depth-headscarp height relationships (Table 1) and suggests that the headscarp height may be significantly altered by subsequent re-failure along the scarp, reducing its height, but maintaining the angle of repose of the failing sediment. The coalescence of headscarps confirms that these failures are subject to re-failure, which would influence the headscarp height to some extent.

Crozier (1973) and McAdoo et al. (2000) consider runout a good prediction of rheology during failure (i.e. rotational slides, viscous or fluid flows etc.). Increasing runout values indicate increasingly higher mobility within the failure mass (Norem et al., 1990). Runout values compared to depth of failure indicate that 1) sediment in the upper portions of Leadsman and Leven Canyons is weaker or fluidised during failure and 2) sediment strength in Diepgat, Wright, White Sands and the Mabibi Canyons does not vary with depth (Fig. 16). Submersible dives indicate that the upper portions of Leadsman and Leven Canyons comprise carbonate cemented beachrock and aeolianite, which mantle partially consolidated Tertiary mud-rich silts and sands. A reduction in strength in the overlying materials is thus unlikely. Rather, the large runouts and small headscarps may be the result of the partial fluidisation of the failed mass (Mohrig et al., 1998) due to fluid sapping in the canyon heads. Subduction derived fluid seeps from convergent margins produce similar canyon slope failure via seepage (Orange and Breen, 1992; Orange et al., 1994, 1997; McAdoo et al., 1997), though the fluid source is incompatible with a passive margin such as that of Northern KwaZulu-Natal. Fluid escape and slope failure via slope overburdening, is recognised from passive margin settings (Robb, 1984; Dugan and Flemings, 2000), but is irreconcilable with the absence of an offshore aquifer along the KwaZulu-Natal margin (c.f Martin, 1984). Fresh water seeps in the northern KwaZulu-Natal region appear to be driven rather by an established hydraulic head from the fringing groundwater table (Meyer et al., 2001) than by any means of overpressuring on an underlying offshore acquirer.

Artesian conditions on the Florida Escarpment are documented by Paull et al. (1990) who consider this to be the dominant driving force in canyon formation and slope failure. A similar system of headless canyons is produced, but differs in that dissolution is the dominant process in comparison to the KwaZulu-Natal canyons where few dissolution features are evident (Green, 2004). Fluid introduction is most likely the product of fresh water exchange between the perched water Table of the fringing coastal waterbodies and the lower continental shelf along the unconformity between Cretaceous and Tertiary sediments (Meyer et al., 2001; Ramsay and Miller, 2006). In the case of Wright Canyon, despite the moderately large mean runout distance of the landslides, the poor correlation between area and runout indicates that the failed material is particularly cohesive, precluding the dissipation of the slide masses over wider areas. In the case of Leven Canyon's sinuous upper tributary (Fig. 9, box c), this landslide morphology could possibly be the result of alongshelf-transported sediments being intercepted by this canyon limb, forming fluid turbidity currents (e.g. Boyd et al., 2008) which exploit a pre-existing scar (e.g. Pratson and Coakley, 1996). This appears unlikely as

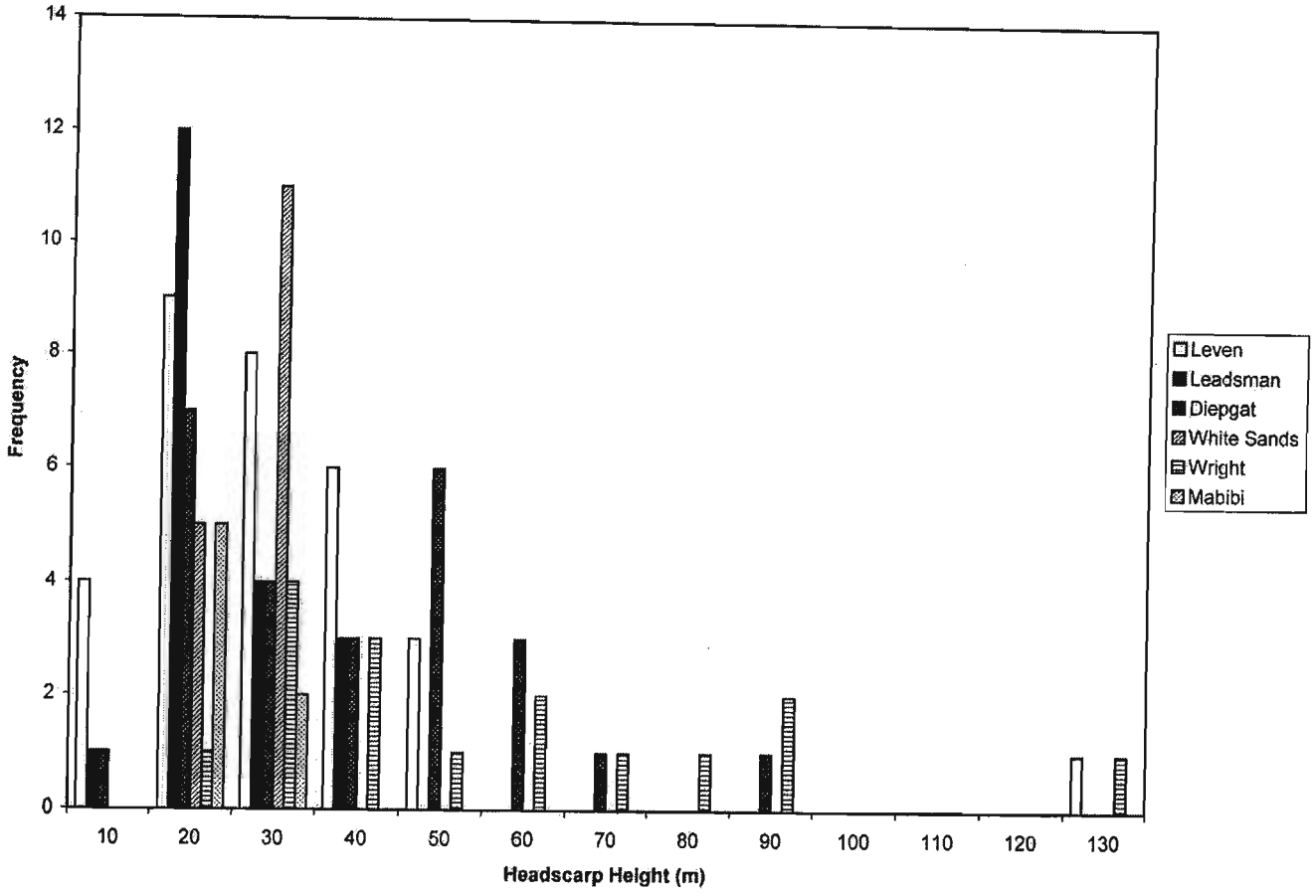

Fig. 13. Histograms separated by shelf indenting submarine canyon/survey block. This depicts headscarp height. The submarine canyons of Mabibi are included as a single entry owing to their uniform size and morphology. North and South Leadsman canyons are similarly included as a single entity (Leadsman).

along-shelf sediment transport in this region is limited by the sediment starved nature of the region (Cooper, 1994; Ramsay et al., 2006). We thus consider this morphology, again, a product of fluid exchange with the coastal aquifer and the continental shelf.

Hampton et al. (1996) provide a review of several submarine landslide studies and indicate that a range of headscarp height to runout ratios (*D/L*) occurs, varying from 0.1 for slumps, to 0.002 for flows. This is several times lower than the average *D/L* values for sub-aerial landslides as described by Ritter et al. (1995). McAdoo et al. (2000) indicate that for the both the eastern and western U.S continental slope, slumps have a *D/L* ratio of 0.02, compared to 0.015 for blocky slides and 0.002 for disintegrative slides. In the case of the northern KwaZulu-Natal continental margin, cohesive slides such as slumps have average *D/L* ratios of 0.14, compared to a ratio of 0.05 for disintegrative slides (including fluid flows which have *D/L* ratios <0.01). This indicates that slide masses are moving seven to twenty five times the distance in open slope settings, such as those measured from the U.S continental slope, compared to intra-canyon slides. Failure runout within a canyon setting is thus constrained by: 1) proximity of the thalweg to the failure, particularly if the failure is occurring perpendicular to the thalweg; 2) the thalweg width, narrower thalwegs will cause a damming effect of sediment against the facing canyon wall; and 3) the efficiency of catastrophic along-thalweg sediment flows to remove slide deposits.

The canyons of Mabibi are the least incised of the area (Green et al., 2007), yet occur on the steepest section of continental slope and shelf and have the least and smallest landslides. Those landslides measured are retrogressive slumps in the heads of shelf indenting canyons. The nature of these landslides is related to the relative shallowness of the canyon thalwegs, which are under-incised, compared to the larger shelf indenting canyons studied (Green et al., 2007). Studies by Pratson and Coakley (1996) indicate that failures will only occur in the flanking walls of the thalweg once critical oversteepening of the walls is achieved via downcutting of the thalweg. Prior to this, failures will be restricted to headward retrogressive slumping as the canyon excavates towards the shelf before capturing the shelf sediments and incising to the point of wall failure and widening of the system. This explains the rill-like appearance of the strongly linear, slope confined and shelf indenting canyons, which have failures restricted to the upper canyon limits. The Mabibi regional slope gradient (as described by Green et al., 2007) is the steepest studied as a result of this relative under-incision.

The largest landslides (e.g. 928 024 m^2) occurring on relatively shallow average slope gradients (~4°) of the Diepgat outer shelf (Fig. 4), are cohesive, and have headscarp heights and slopes (e.g. 62 m; 36°) in the lower range of distribution. This indicates that the material is unlikely to have a fluid rheology during failure, despite the failure size. It appears that these failures could be deep seated landslide features initiated by earthquake activity, which would account for the size of the failure and the intact slide mass. Landslide pre-conditioning factors such as underlying weak layers (Kvalstad et al., 2005) along which progressive deformation may occur provide an equally plausible hypothesis for landslide generation, causing failure in a bedding plane parallel style (Masson et al., 2006). However, it seems most likely on the basis of work by Bryn et al. (2005) and Kvalstad et al. (2005) that pre-conditioning factors such as high sediment availability during lowstand and underlying weak layers (in the partially consolidated Tertiary strata) must be met with an accompanying trigger, in this case

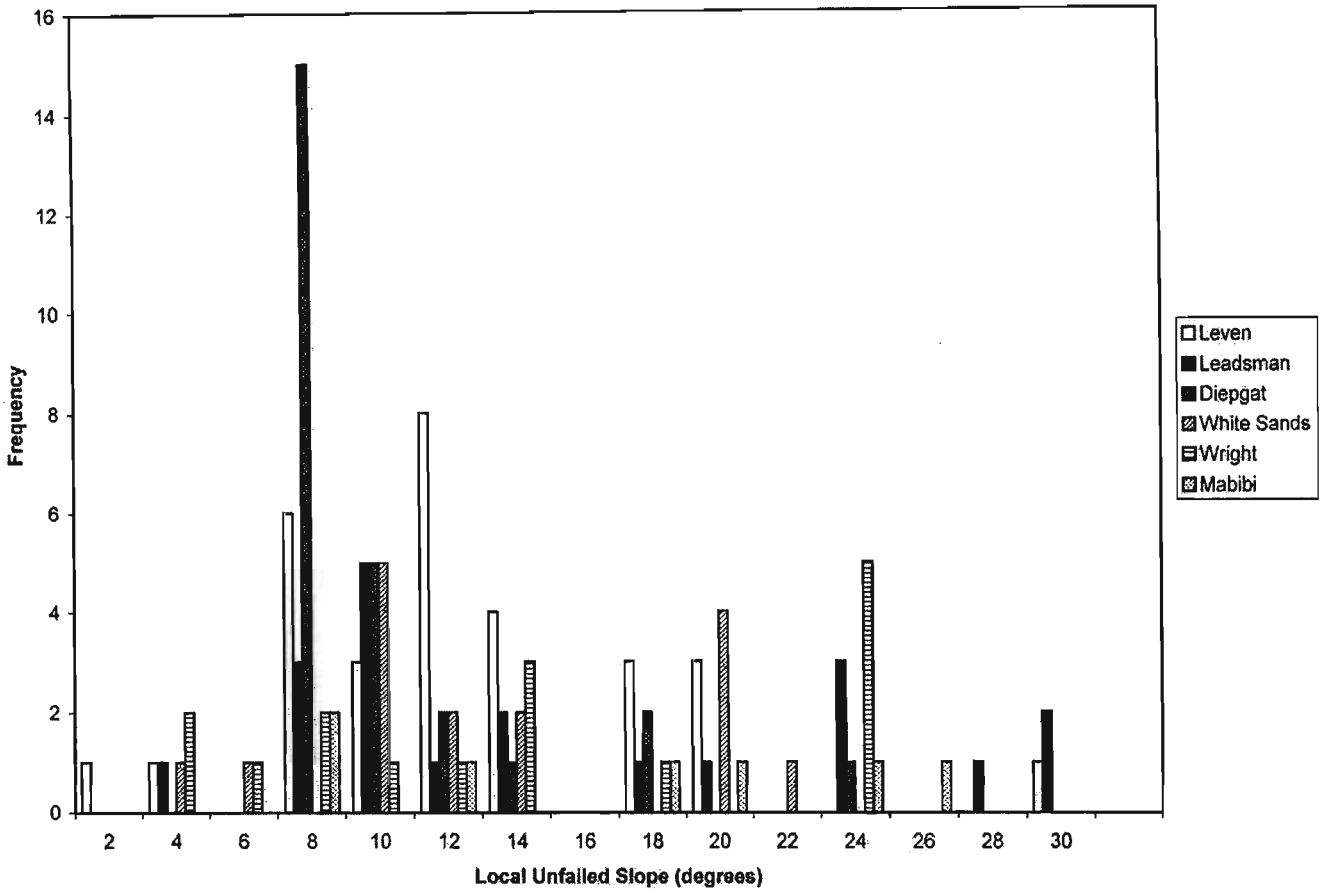

Fig. 14. Histograms separated by shelf indenting submarine canyon/survey block. This depicts local unfailed slope. The submarine canyons of Mabibi are included as a single entry owing to their uniform size and morphology. North and South Leadsman canyons are similarly included as a single entity (Leadsman).

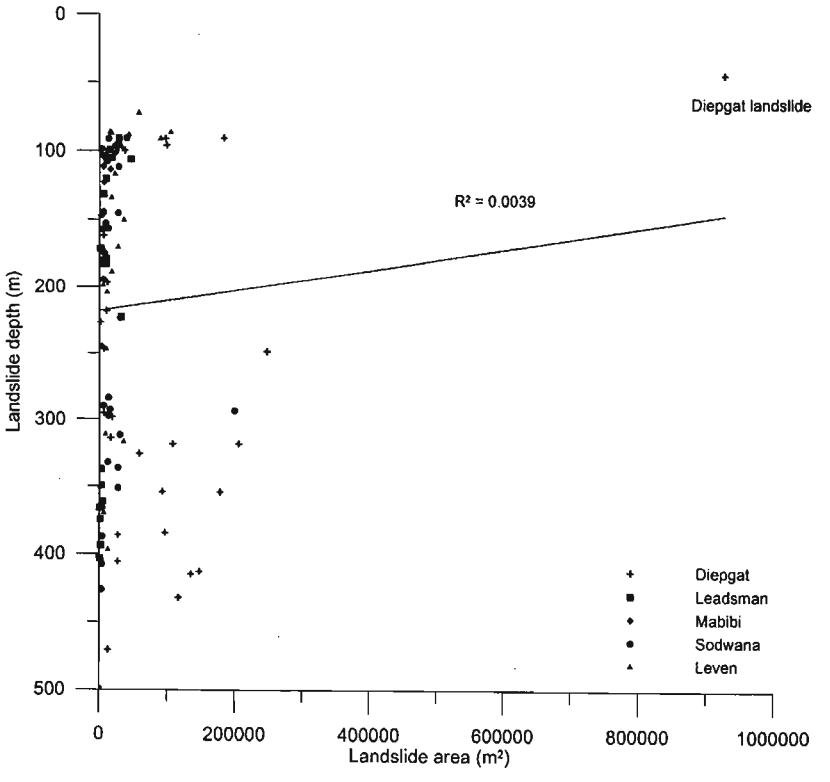

Fig. 15. Plot of landslide depth against landslide area. Area correlates poorly with depth (R^2=0.0039).

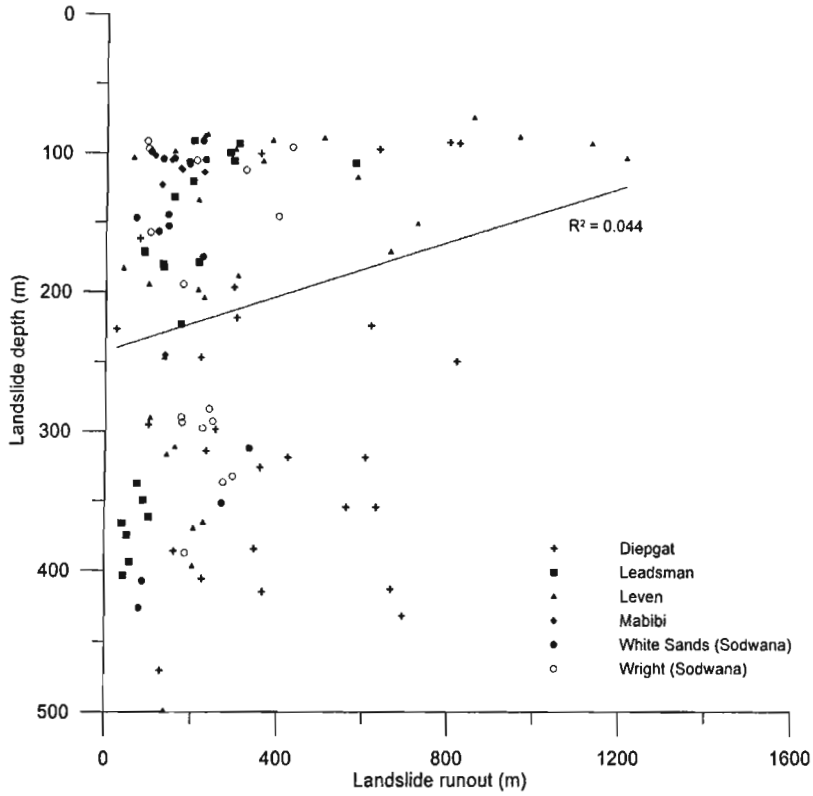

Fig. 16. Plot of landslide depth against runout distance. Note that Leadsman and Leven Canyons have comparatively larger runout distances at ~100 m depth compared to those of deeper landslides, both in Leven/Leadsman Canyons and other canyons studied throughout the depth range of landslide occurrences.

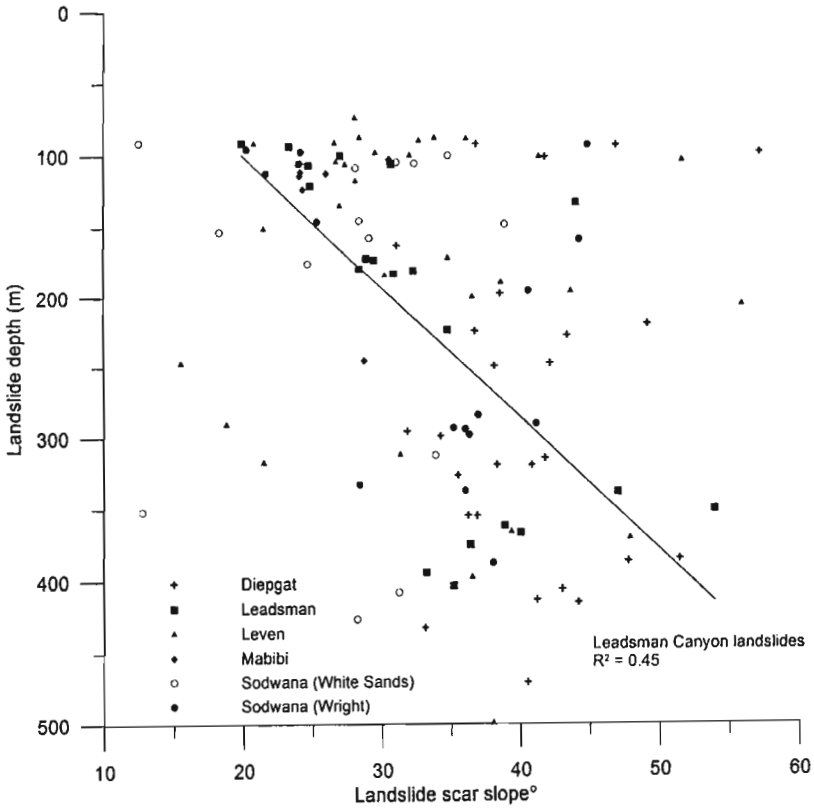

Fig. 17. Plot of landslide depth against scar slope. A very poor correlation between depth and scar slope is evident (R^2=0.139). Note that the regression line is for the Leadsman Canyon system, showing a moderate correlation between the two variables (R^2=0.446).

possibly an earthquake. The most recent seismic activity to have occurred in the area is the 1932 Zululand Earthquake of a surface wave magnitude of 6.8 (Hartnady, 2002). This may have been the possible trigger for the largest landslide in Diepgat Canyon head.

The deep seated nature of this type of failure would expose more consolidated material that would be less likely to fail, steepening the continental shelf (McAdoo et al., 2000). A similar type of failure occurs in the mid-slope portions of Wright Canyon; however the failure area is significantly smaller. The next largest failures, apart from those of Diepgat Canyon, occur in the mid continental slope regions of Leven Canyon (Fig. 3), on the shallowest regional slope, with low headscarp angles and small head scarp height modes. These are disintegrative, and indicate that rheology was significantly weaker during failure compared to the failures of Diepgat and Wright Canyons of comparative size.

Overall, the most well defined landslides occur in the heads of the large shelf indenting canyons, which reside in the Mio/Pliocene shelf edge wedge (Green et al., 2007). The presence of hanging slides, benches, and incised gorges attest to periods of thalweg downcutting, where the slide extended to a palaeo-thalweg floor, and was subsequently stranded once downcutting of the canyon continued. Incised gorges would be preserved when material at the toe of the slide was removed by this incision (Densmore et al., 1997), which would also leave pronounced erosional benches in the slide material. Periods of periodic slope clearing thus occurred, interspersed with periods of thalweg excavation. Benches possibly represent periods of increased thalweg erosion at the base of the failure (Nelson et al., 1970). Similar examples are documented by McAdoo et al. (2000) for the New Jersey continental slope and Arzola et al. (2008) for the western Iberian continental slope. Models presented by Pratson et al. (1994) and Pratson and Coakley (1996) for the continental margin of the US Atlantic, indicate that canyon incision by sediment flow is followed by several episodes of along-thalweg retrogressive failure, interspersed with side wall failure. Arzola et al. (2008) ascribe this type of canyon response to instability processes preconditioned by the resultant steep topography. These models also explain the complex failure morphology of the canyons of northern KwaZulu-Natal. The smaller narrow canyons with failures restricted to the canyon heads represent a change in erosional regime from a downward eroding sediment flow phase responsible for the formation of inter-canyon rills with no failures (Fig. 18) such as those commonly seen in the Mabibi Block, to a headward eroding phase once oversteepening relative to the downslope portions of the inter-canyon rill is sufficient to cause headward slumping (Fig. 19), such as Diepgat Canyon. The larger canyons exhibit evidence for catastrophic headwall failure due to oversteepening by downward eroding sediment flow, periodic catastrophic slope clearances and active canyon enlargement by retrogressive failure, as envisioned by these modelling attempts. The role of axial incision is similarly documented by both Baztan et al. (2005) and Arzola et al. (2008), where stages of axial incision and oversteepening are shown to be the key pre-conditioning factor in the establishment of mass wasting processes that affect the canyon head and flanks. The fact that hanging slides, benches and incised gorges are preserved, suggests that the canyons of northern KwaZulu-Natal are currently in a period of quiescence following a period of axial incision, where the walls are not currently subject to catastrophic slope clearances. The low sediment availability of the area (Cooper, 1994), particularly during highstand of the Holocene, has reduced the impetus for sediment loading of the shelf and the means to incise the thalweg, which has resulted in canyon quiescence (Green et al., 2007).

The random distribution of failures with depth in all canyons implies that there is no dominating influence on the depth zonation of failure. In particular, the largest failures are spread at random and are not restricted to depths of the previous lowstand of ~18 000 BP at −125 m (Green and Uken, 2005) or the penultimate lowstand of ~180 000 BP at −130 m (Ramsay and Cooper, 2002; Green and Uken, 2005). Posamentier and Vail (1988) and Posamentier et al. (1988) indicate that the maximum degree of erosion will occur during the maximum rate of sea-level fall (i.e. towards the lowstand systems tract). Thus, despite lowstand conditions (which provide favourable pre-conditioning factors) having prevailed, failures appear to be unrelated to the sea levels of the last and penultimate glacial periods, suggesting that sediment starved conditions were operating since at least these times. The presence of sea-level notches throughout the failures of the heads of the canyons at the LGM level indicates that these failures pre-date this time period (Green and Uken, 2005). The notable exception is Diepgat Canyon head, the landslides within which post-date the LGM (Green and Uken, 2005).

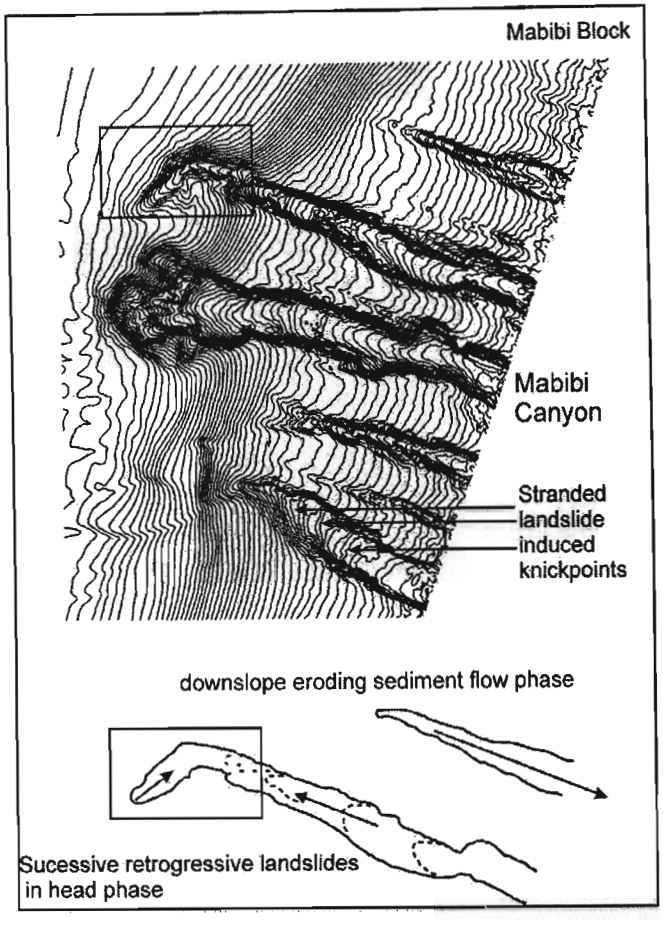

Fig. 18. Bathymetric contours and interpretative schematic from Mabibi Block (highlighted in Fig. 6) depicting the evolution from slope rills, commonly observed between larger erosive features, to narrow shelf indenting canyons with a single retrogressive failure in the head portions. Note the evidence in the contour data for older scar morphology preserved successively downslope in the small canyon as the head advances landwards, stranding older landslide scarps.

5. Conclusions

Data are presented, derived form the morphometric analysis of 117 mass wasting features found within a series of submarine canyons from the northern KwaZulu-Natal continental margin. It is postulated that the various relationships between the measured characteristics of area, volume, depth, headscarp height, headscarp slope, runout distance, runout slope, scar slope and local unfailed slope may give a reasonable indication of dynamic rheology in the absence of core and seismic data for the area. Furthermore, particular differences in these relationships between the various canyons are apparent, and indicate different processes responsible for the growth and evolution of these systems. Diepgat, and to a lesser extent Wright Canyon have

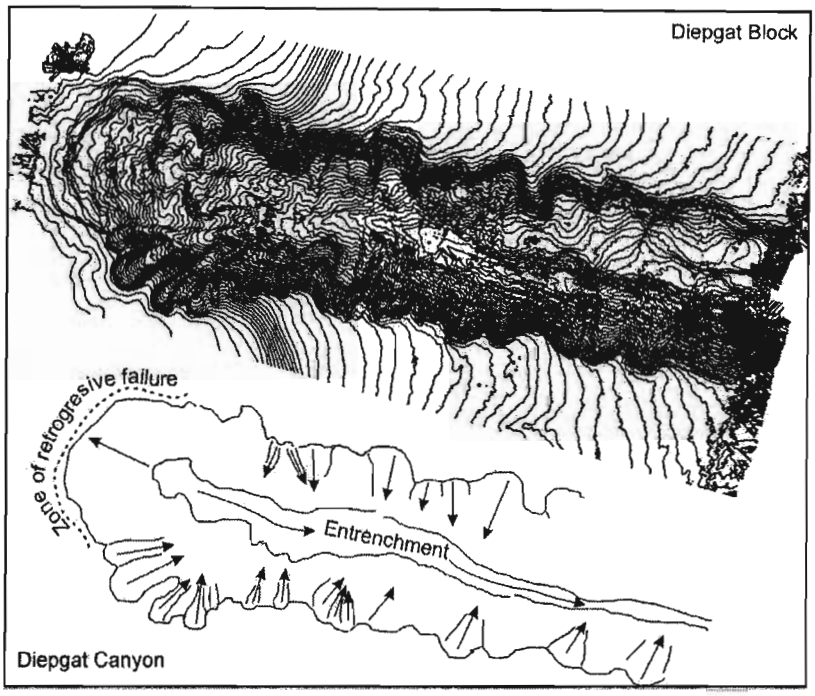

Fig. 19. Bathymetric contours and interpretative schematic of the large shelf indenting Diepgat Canyon. Retrogressive failure, coupled with the entrenchment of the axis by failure derived sediment flows, oversteepen the canyon form relative to the flanks. This prompts lateral extension by retrogressive, axis perpendicular landsliding which further entrench the canyon axis.

relatively large failures (compared to the others measured) despite indications that the failure rheology was competent. Conversely, Leven and Leadsman Canyons have failures with large areas and fluid rheologies. A possible seismic trigger, accompanied by favourable pre-conditioning factors is considered for the Diepgat and Wright landslides, whereas the failures, particularly those in the head, of Leven Canyon may be a product of fresh water sapping on the mid shelf alluded to in the morphometric analysis.

The presence of particular failure morphologies indicates the importance of both upslope and downslope erosion in canyon evolution. These two processes are emphasized by the change in landslide type, size and number as the system evolves from an initial downslope eroding sediment flow phase to the headward eroding excavation phase. Early growth in the canyon form conforms to landslide free rills, followed by simple retrogressive slumping in the canyon head, culminating in the widening of the canyon by numerous axis-normal wall failures.

The preservation of erosional benchmarks, hanging slumps and inner gorges attests to periods of catastrophic slope clearance during the excavation phase. The random pattern of landslide depth relative to the sea-level expressions of the previous two lowstands suggests a period of quiescence since at least the last glaciation. Canyon systems are thus unlikely to be actively enlarging, barring: 1) the pre-conditioning factors which future lowstand episodes can provide i.e. sufficient sediment to the outer shelf to increase overburdening, cyclic loading or downward incision by axially constrained sediment flows; and 2) a suitable trigger.

Acknowledgements

This research was funded by the African Coelacanth Ecosystem Programme through the National Research Foundation, the Department of Environmental Affairs and Tourism, the Department of Science and Technology and the German Government. John Goff is acknowledged for various discussions concerning headward eroding submarine canyons. Peter Ramsay and Warwick Miller of Marine GeoSolutions are thanked for the collection and processing of multibeam bathymetry, on which this study is based. We wish to thank Russel Wynn, an anonymous reviewer and David Piper for their constructive reviews from which this paper benefitted. This study comprises part of A.G.'s PhD thesis at the University of KwaZulu-Natal.

References

Arzola, R.G., Wynn, R.B., Lastras, G., Masson, D.G., Weaver, P.P.E., 2008. Sedimentary features and processes in submarine canyons: a case study from the Nazaré and Setúbal Canyons, west Iberian margin. Mar. Geol. 250, 64–88.

Bang, N.D., 1968. Submarine canyons off the Natal coast. S. Afr. Geogr. J. 50, 45–54.

Baztan, J., Berné, S., Olivet, J-L., Rabineau, M., Aslanian, D., Gaudin, M., Réhault, J-P., Canals, M., 2005. Axial incision: the key to understand submarine canyon evolution (in the western Gulf of Lion). Mar. Petr. Geol. 22, 805–826.

Boyd, R., Ruming, K., Goodwin, I., Sandstrom, M., Schröder-Adams, C., 2008. Highstand transport of coastal sand to the deep ocean: a case study from Fraser Island, southeast Australia. Geology 36, 15–18.

Bryn, P., Berg, K., Lien, R., Forsberg, C.F., Solheim, A., Kvalstad, T.J., 2005. Explaining the Storegga slide. Mar. Petr. Geol. 22, 11–19.

Canals, M., Lastras, G., Urgeles, R., Casamor, J.L., Minert, J., Cattaneo, A., De Batist, M., Halfidason, H., Imbo, Y., Laberg, J.S., Locat, J., Long, D., Longva, O., Masson, D.G., Sultan, N., Trincardi, F., Bryn, P., 2004. Slope failure dynamics and impacts from sea floor and shallow sub-sea floor geophysical data: case studies from the COSTA project. Mar. Geol. 213, 9–72.

Coleman, J.M., Prior, D.B., 1988. Mass wasting on continental margins. Annu. Rev. Earth Planet. Sci. 16, 101–119.

Cooper, J.A.G., 1994. Lagoons and Microtidal coasts. In: Carter, R.W.G., Woodruffe, C.D. (Eds.), Coastal Evolution: Late Quaternary Shoreline Morphodynamics. Cambridge Univ. Press, Cambridge, pp. 219–265.

Crozier, M.J., 1973. Techniques for the morphometric analysis of landslips. Z. Geomorphol. 17, 78–101.

Densmore, A.L., Anderson, R.S., McAdoo, B.G., Ellis, M.A., 1997. Hillslope evolution by bedrock landslides. Science 275, 369–372.

Dingle, R.V., 1977. The anatomy of a large submarine slump on a sheared continental margin (SE Africa). J. Geol. Soc. London 134 (3), 293–310.

Dingle, R.V., 1980. Large allochthonous sediment masses and their role in the construction of the continental slope and rise of southwestern Africa. Mar. Geol. 37, 33–354.

Dingle, R.V., Robson, S., 1985. Slumps, canyons and related features on the continental margin off East London, SE Africa (SW Indian Ocean). Mar. Geol. 67, 37–54.

Dingle, R.V., Siesser, W.G., Newton, A.R., 1983. Mesozoic and Tertiary geology of southern Africa. A.A. Balkema, Rotterdam. 375 pp.

Du Toit, S.R., Leith, M.J., 1974. The J(c)-1 bore-hole on the continental shelf near Stanger, Natal. Trans. Geol. Soc. S. Afr. 77, 247–252.

Dugan, B., Flemings, P.B., 2000. Overpressure and fluid flow in the New Jersey continental slope: implications for slope failure and cold seeps. Science 289, 288–292.

Emery, K.O., Uchupi, E., Bowin, C.O., Phillips, J., Simpson, E.S.W., 1975. Continental margin off western Africa: Cape St Francis (South Africa) to Walvis Ridge (South West Africa). Am. Assoc. Pet. Geol. Bull. 59, 3–59.
Farre, J.A., McGregor, B.A., Ryan, W.B.F., Robb, J.M., 1983. Breaching the shelfbreak; Passage from youthful to mature phase in submarine canyon evolution In: Stanley, D.J., Moore, G.T. (Eds.), The Shelfbreak: Critical Interface on Continental Margins. Soc. Econ. Palaeontogr. Mineral. Spec. Pub., vol. 33, pp. 25–39.
Flemming, B.W., 1978. Underwater sand dunes along the southeast African continental margin-observations and implications. Mar. Geol. 26, 177–198.
Flemming, B.W., 1981. Factors controlling shelf sediment dispersal along the southeast African continental margin. Mar. Geol. 42, 259–277.
Goodlad, S.W., 1986. Tectonic and sedimentary history of the mid-Natal Valley (SW Indian Ocean). Bulletin of the Joint Geological Survey/University of Cape Town, Marine Geosci. Unit 15, 415 pp.
Green, A.N., 2004. Cruise report FRS Algoa cruise, Marine Geoscience programme. African Coelacanth Ecosystem Programme report, 2004-1, 10pp.
Green, A.N., Uken, R., 2005. First observations of sea level indicators related to glacial maxima at Sodwana Bay, Northern KwaZulu-Natal. S. Afr. J. Sci 101, 236–238.
Green, A.N., Goff, J.A., Uken, R., 2007. Geomorphological evidence for upslope canyon-forming processes on the northern KwaZulu-Natal shelf, South Africa. GeoMar. Lett. doi:10.1007/s00367-007-0082-2.
Greene, G., Maher, N.M., Paull, C.K., 2002. Physiography of the Monterey Bay National Marine Sanctuary and implications about continental margin development. Mar. Geol. 181, 55–82.
Hampton, M.A., Lee, H.J., Locat, J., 1996. Submarine landslides. Rev. Geophys 34, 33–59.
Hartnady, C.J.H., 2002. Earthquake hazard in Africa: perspectives on the Nubia-Somalia plate boundary. S. Afr. J. Sci 98, 425–428.
Hünerbach, V., Masson, D.G., Partners, C.P., 2004. Landslides in the North Atlantic and its adjacent seas: an analysis of their morphology, setting and behaviour. Mar. Geol. 213, 343–362.
Kvalstad, T.J., Andresen, L., Forsberg, C.F., Berg, K., Bryn, P., Wangen, M., 2005. The Storegga slide: evaluation of triggering sources and slide mechanics. Mar. Petr. Geol. 22, 245–256.
Lutjeharms, J.R.E., 2006. The ocean environment off south-eastern Africa: a review. S. Afr. J. Sci 102, 419–425.
Martin, A.K., 1984. Plate tectonic status and sedimentary basin in-fill of the Natal Valley (SW Indian Ocean). Bulletin of the Joint Geological Survey/University of Cape Town, Marine Geoscience Unit 14, 209 pp.
Martin, A.K., Flemming, B.W., 1986. The Holocene shelf sediment wedge off the south and east coast of South Africa. Canadian Society of Petroleum Geologists Memoir 2, 27–44.
Masson, D.G., Harbitz, C.B., Wynn, R.B., Pederson, G., Løvholt, F., 2006. Submarine landslides—process, triggers and hazard prediction. Phil. Trans. Royal Soc. A 364, 2009–2039.
McAdoo, B.G., Orange, D.L., Screaton, E., Lee, H., Kayen, R., 1997. Slope basins, headless canyons, and submarine palaeoseismology of the Cascadia accretionary complex. Basin Res. 9, 313–324.
McAdoo, B.M., Pratson, L.F., Orange, D.L., 2000. Submarine landslide geomorphology, US continental slope. Mar. Geol. 169, 103–136.
Meyer, R., Talma, A.S., Duvenhage, A.W.A., Eglington, B.M., Taljaard, J., Botha, J.F., Verwey, J., Van der Voort, I., 2001. Geohydrological investigation and evaluation of the Zululand coastal aquifer. Water Research Commission Report 221/1/01. Pretoria: Water Research Commission, 51 pp.
Miller, W.R., 2001. The bathymetry, sedimentology and seismic stratigraphy of Lake Sibaya—northern KwaZulu-Natal. Council for Geoscience Bulletin 131, 94 pp.
Mohrig, D., Whipple, K.X., Hondzo, M., Ellis, C., Parker, G., 1998. Hydroplaning of subaqueous debris flows. GSA Bull 110 (3), 387–394.
Nelson, C.H., Carlson, P.R., Byrne, J.V., Alpha, T.R., 1970. Development of the Astoria Canyon-Fan physiography and comparison with similar systems. Mar. Geol. 8, 259–291.
Norem, H., Locat, J., Schieldrop, B., 1990. An approach to the physics and the modelling of submarine flowslides. Mar. Geotechnol. 9, 93–111.
Orange, D.L., Breen, N.A., 1992. The effects of fluid escape on accretionary wedges 2. Seepage force, slope failure, headless submarine canyons and vents. J. Geophys. Res. 97, 9277–9295.
Orange, D.L., Anderson, R.S., Breen, N.A., 1994. Regular canyon spacing in the submarine environment: the link between hydrology and geomorphology. GSA Today 4, 29–39.
Orange, D.L., McAdoo, B., Moore, C.J., Tobin, H., Screaton, E., Chezar, H., Lee, H., Reid, M., Vail, R., 1997. Headless submarine canyons and fluid flow on the toe of the Cascadia accretionary complex. Basin Res. 9, 303–312.
Partridge, T.C., Maud, R.R., 1987. Geomorphic evolution of southern Africa since the Mesozoic. S. Afr. J. Geol. 90, 179–208.
Paull, C.K., Spiess, F.N., Curray, J.R., Twichell, D.C., 1990. Origin of Florida Canyon and the role of spring sapping on the formation of submarine box canyons. GSA Bull. 102, 502–515.
Piper, D.J.W., Cochonat, P., Morrison, M.L., 1999. The sequence of events around the epicenter of the Grand Banks earthquake: initiation of debris flow and turbidity current inferred from sidescan sonar. Sedimentology 46, 79–97.
Posamentier, H.W., Jervey, M.T., Vail, P.R., 1988. Eustatic controls on clastic deposition, I. Conceptual framework. In: Wilgus, C.K., Hastings, B.S., Kendall, C.G.St.C., Posamentier, H.W., Ross, C.A., Van Wagoner, J.C. (Eds.), Sea-level Changes: An Integrated Approach. Spec. Publ. SEPM., vol. 42, pp. 125–154.
Posamentier, H.W., Vail, P.R., 1988. Eustatic controls on clastic deposition, II. Sequence and systems tracts models. In: Wilgus, C.K., Hastings, B.S., Kendall, C.G.S.C., Posamentier, H.W., Ross, C.A., Van Wagoner, J.C. (Eds.), Sea-level Changes: An Integrated Approach. Spec. Publ. SEPM., 42, pp. 125–154.
Pratson, L.F., Coakley, B.J., 1996. A model for the headward erosion of submarine canyons induced by downslope eroding sediment flows. Geol. Soc. Am. Bull. 108, 225–234.
Pratson, L.F., Ryan, W.B.F., Mountain, G.S., Twitchell, D.C., 1994. Submarine canyon initiation by downslope-eroding sediment flows: evidence in late Cenozoic strata on the New Jersey continental slope. Geol. Soc. Am. Bull. 106, 395–412.
Ramsay, P.J., 1994. Marine geology of the Sodwana Bay shelf, Southeast Africa. Mar. Geol. 120, 225–247.
Ramsay, P.J., 1996. Quaternary marine geology of the Sodwana Bay shelf, northern KwaZulu-Natal. Bulletin of the Geological Survey of South Africa 117, 86pp.
Ramsay, P.J., Cooper, J.A.G., 2002. Late Quaternary sea-level change in South Africa. Quat. Res. 57, 82–90.
Ramsay, P.J., Miller, W.R., 2006. Marine geophysical technology used to define coelacanth habitats. S. Afr. J. Sci. 102, 427–434.
Ramsay, P.J., Schleyer, M.H., Leuci, R., Muller, G.A., Celliers, L., Harris, J.M., Green, A.N., 2006. The development of an expert marine geographic information system tp provide an environmental and economic decision support system for proposed tourism developments within and around the Greater St Lucia Wetland Park world heritage site. Report Innovation Fund Project 24401, 92 pp.
Ritter, D.F., Kochel, R.C., Miller, J.R., 1995. Process Geomorphology, 3rd ed. W.C. Brown Publishers, Boston. 576 pp.
Robb, J.M., 1984. Spring sapping on the lower continental slope, offshore New Jersey. Geol. 12, 278–282.
Shaw, M.J., 1998. Seismic stratigraphy of the northern KwaZulu-Natal upper continental margin. Unpublished MSc thesis, Department of Geology and Applied Geology, University of Natal, Durban, 190 pp.
Siesser, W.G., 1977. Biostratigraphy and micropalaeontology of continental margin samples. Technical report, Joint Geological Survey/University of Cape Town Marine Geoscience Unit, 9, 108–117.
Sydow, C.J., 1988. Stratigraphic control of slumping and canyon development on the continental margin, east coast, South Africa. Unpublished BSc Hons thesis, Department of Geological Sciences, University of Cape Town, 55 pp.
Tripsanas, E.K., Piper, D.J.W., Jenner, K.A., Bryant, W.R., 2008. Submarine mass-transport facies: new perspectives on flow processes from cores on the eastern North American margin. Sedimentology 55, 97–136.
Twichell, D.C., Roberts, D.G., 1982. Morphology, distribution and development of submarine canyons on the United States Atlantic continental slope between Hudson and Baltimore Canyons. Geol 10, 408–412.
Van Heerden, I.L., 1987. Sedimentation in the greater St Lucia complex as elated to palaeo-sea levels. Abstract, 6th National Oceanographic Symposium, Stellenbosch. Paper 157, 00B-106.
Wright, C.I., Miller, W.R., Cooper, J.A.G., 2000. The late Cenozoic evolution of coastal water bodies in Northern KwaZulu-Natal, South Africa. Mar. Geol. 167, 207–229.

Geo-Mar Lett
DOI 10.1007/s00367-007-0082-2

ORIGINAL

Geomorphological evidence for upslope canyon-forming processes on the northern KwaZulu-Natal shelf, SW Indian Ocean, South Africa

Andrew N. Green · John A. Goff · Ron Uken

Received: 30 May 2006 / Accepted: 30 March 2007

Abstract A geomorphological and statistical analysis of slope canyons from the northern KwaZulu-Natal continental margin is documented and compared with submarine canyons from the Atlantic margin of the USA. The northern KwaZulu-Natal margin is characterized by increasing upslope relief, concave slope-gradient profiles and features related to upslope growth of the canyon forms. Discounting slope-gradient profile, this morphology is strikingly similar to canyon systems of the New Jersey slope. Several phases of canyon incision indicate that downslope erosion is also an important factor in the evolution of the northern KwaZulu-Natal canyon systems. Despite the strong similarities between the northern KwaZulu-Natal and New Jersey slope-canyon systems, key differences are evident: (1) the concavity of the northern KwaZulu-Natal slope, contrasting with the ~linear New Jersey slope; (2) the relative isolation of the northern KwaZulu-Natal canyons, rather than the dense clustering of the New Jersey canyons; and (3) the absence of strongly shelf-breaching canyons along the northern KwaZulu-Natal margin. In comparison with the New Jersey margin, we surmise a more youthful stage of canyon evolution, a result of either the canyons themselves being younger or the formative processes being less active. Less complicated patterns of erosion resulting from reduced sediment availability have developed in northern KwaZulu-Natal. The reduction in slope concavity on the New Jersey margin may be the result of grading of the upper slope by intensive headward erosion, a process more subdued—or less evident—on the KwaZulu-Natal margin.

A. N. Green (✉) · R. Uken
Joint Council for Geoscience—University of KwaZulu-Natal,
Marine Geoscience Unit, School of Geological Sciences,
University of KwaZulu-Natal,
Westville,
Durban 4000, South Africa
e-mail: Greena1@ukzn.ac.za

J. A. Goff
Institute for Geophysics, Jackson School of Geoscience,
University of Texas at Austin,
4412 Spicewood Springs Road, Building 600,
Austin, TX 78759, USA

Introduction

Recent acquisition of high-resolution multibeam bathymetric data from the upper slope and continental shelf of northern KwaZulu-Natal, South Africa (Fig. 1) has provided the basis for a detailed investigation of the geomorphology of continental slope canyons in this region. These data were collected for the African Coelacanth Ecosystem Programme, as part of an initiative to map the south-eastern Indian Ocean coelacanth habitat. Submarine canyons which impinge the continental shelf break in this region satisfy the morphological and bathymetric constraints of this "fossil fish" habitat (Fricke and Plante 1988; Fricke and Hissmann 1994), i.e. shelter requirements, in the form of caves and overhangs, associated with lower than present-day sea levels of between 100 and 130 m depth (Green et al. 2007).

To date, bathymetric studies from this area have either concentrated on small portions of the continental shelf (Ramsay 1994) or have favoured regional interpretations of the lower rise and abyssal plain, making use of low-resolution bathymetric data (Dingle et al. 1978; Goodlad 1986). Our survey, employing a 100-kHz Reson Seabat 8111 ER multibeam echosounder, covered 392 km^2 over depths ranging from ~30 to 850 m, with a spatial resolution of ~10 m^2. Submarine canyons and gullies are prevalent throughout this area, indicating that periods of erosion have occurred, or are still actively operating as major morpho-

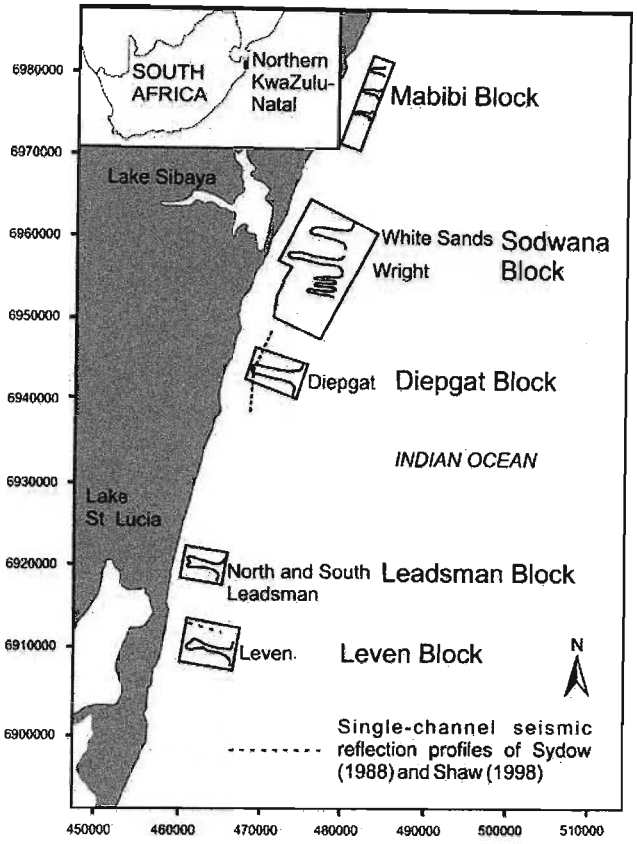

Fig. 1 Location map of the northern KwaZulu-Natal continental margin, with multibeam survey blocks, available seismic data, and major canyons indicated. Northing and easting coordinates are in meters, Universal Trans-Mercator (UTM) projection zone 36

logic influences on the upper continental margin. Studies by Goodlad (1986), Sydow (1988), Ramsay (1996) and Shaw (1998) have attempted to address the origins of these systems; however, a comprehensive geomorphological study has previously been impossible due to the non-availability of high-resolution bathymetric mapping systems.

Work by Adams and Schlager (2000), O'Grady et al. (2000) and Goff (2001) has aimed to quantitatively classify the shape of continental slopes as a means of inferring depositional and erosional processes. Goff (2001) focused in particular on the downslope progression of canyon relief in relation to the slope profile, and inferred from these quantities either "upslope" or "downslope" physical processes (e.g. Pratson and Coakley 1996) of canyon growth. We applied this methodology to the northern KwaZulu-Natal upper continental margin canyon systems, comparing these with previous analyses on the Atlantic margin of the USA, to provide a first tentative model for the formation of these canyons.

Theories of canyon formation

The earliest hypotheses for the formation of slope-canyon systems considered these to be the products of downslope eroding turbidity flows (Daly 1936). Later evidence gathered by more comprehensive echosounding surveys (Chamberlain 1964), dives (Shepard et al. 1964) and oceanographic surveys (Drake et al. 1978) indicated that processes such as creep, slumping and internal waves (Carlson and Karl 1988) were also important factors. Since the early 1980s, substantial improvements in sonar technology has resulted in a better understanding of the morphology of canyon systems. Twichell and Roberts (1982), using side scan sonar images of the New Jersey continental slope, documented canyons and gullies existing which were evidently in several different stages of evolution. Canyons and gullies which had not yet breached the shelf break ("headless canyons") provided evidence of canyon-forming processes which were not necessarily related to river systems and the supply of sands to the shelf edge. Farre et al. (1983) associated the presence of slump deposits with headless canyons, and proposed a model of canyon formation based on retrogressive headward slumping of the canyon head and walls. Once these canyon heads had breached the shelf break by progressive upslope slumping, a constant supply of sediment from the shelf would be entrained within the canyon, and the system would then erode downwards via turbidity currents. Slope-confined canyons are thus considered by Farre et al. (1983) as immature stages in canyon development, which eventually evolve headwards into mature canyons which breach the shelf break. This "upslope" erosion theory of canyon formation has been supported by a number of authors investigating southern African slope canyons (e.g. Dingle and Robson 1985; Sydow 1988; Ramsay 1996; Shaw 1998).

More recently, evidence for a combined upslope and downslope eroding model of canyon formation was provided by Pratson et al. (1994) and Pratson and Coakley (1996), based on multibeam bathymetry, single-channel seismic reflection profiles and computer modelling of the New Jersey continental slope. These studies revealed a cyclic process of canyon cut-and-fill as shelf-edge depocentres shift and bury areas of active canyon incision. The subdued topography of filled canyons is then exploited during subsequent depocentre shifts where buried channels have created bathymetric lows in the middle portions of the slope, thereby constraining sediment flows which are ignited from a theoretically oversteepened upper slope. This downslope sediment flow is today considered to be the major impetus of modern canyon initiation. As these flows erode the floor of the older canyon, they oversteepen the walls and head, causing a series of large retrogressive slumps which advance headwards along this chute, and excavate much of the canyon profile (Pratson and Coakley 1996). Where canyons have not existed previously, rilling induced by the downward flow of sediment acts as the topographic constraint from which the canyon develops.

Canyons are thus viewed as erosional systems evolving from slope-confined, through shelf-breaching to defunct existence, driven primarily by sediment flows and relative sediment supply.

In his quantitative analysis of slope-canyon systems on the USA Atlantic margin, Goff (2001) examined variations in slope gradient and canyon relief with depth. He identified what he considered to be two canonical ways in which canyon relief progresses along the slope. Along the New Jersey margin, canyon relief increases upslope, terminating in large, amphitheatre-shaped indentations in the shelf edge. Further south, along the Virginia margin, canyons are narrow and small at the top but increase in relief and breadth while converging downslope to the slope/rise break. Goff (2001) hypothesized that these two patterns correspond to a predominance of "upslope" and "downslope" processes respectively, the former exhibiting similarities to spring-sapping systems, the latter to subaerial fluvial systems.

The slope gradients documented by Goff (2001) also revealed important differences between the two sites, with the New Jersey slope exhibiting a nearly constant gradient from shelf break to rise, and the Virginia slope a general decrease in gradient with depth (i.e. concave). Goff (2001) attributed the lack of steepening towards the top of the New Jersey slope to the extensive grading of the upper slope by the headward-growing canyons. This could explain the lack of oversteepening which would otherwise have been predicted by the Pratson and Coakley (1996) model. Goff (2001) argued that the concave profiles on the Virginia slope are also consistent with a downslope, fluvial-style erosion process which might be caused by turbidity flows.

Study area

Seismic investigations by Sydow (1988) and Shaw (1998) provide a basic stratigraphic framework for the region, and demonstrate that the northern KwaZulu-Natal continental shelf is typically underlain by thick sedimentary sequences of upper Cretaceous and Tertiary age (Du Toit and Leith 1974). A shelf-edge wedge of Miocene/Pliocene age is prominent (Fig. 2), having been deposited as a series of rapidly prograding clinoforms (Sydow 1988) which formed as a result of increased terrigenous sediment influx promoted by rapid uplift of the hinterland during this time period (Partridge and Maud 1987). Depocentre shifting as resulting from tectonic instability and basin warping would have been common during this time period. Unfortunately, a lack of reliable borehole data precludes a confident interpretation of the sub-surface geology of the study area, and this stratigraphic interpretation therefore remains speculative.

Early to mid-Pleistocene sediments are uncommon on this shelf, with only thin exposures of late Pleistocene sediments persisting along the east coast of southern Africa (Dingle et al. 1983; Ramsay 1994; Miller 2001). These

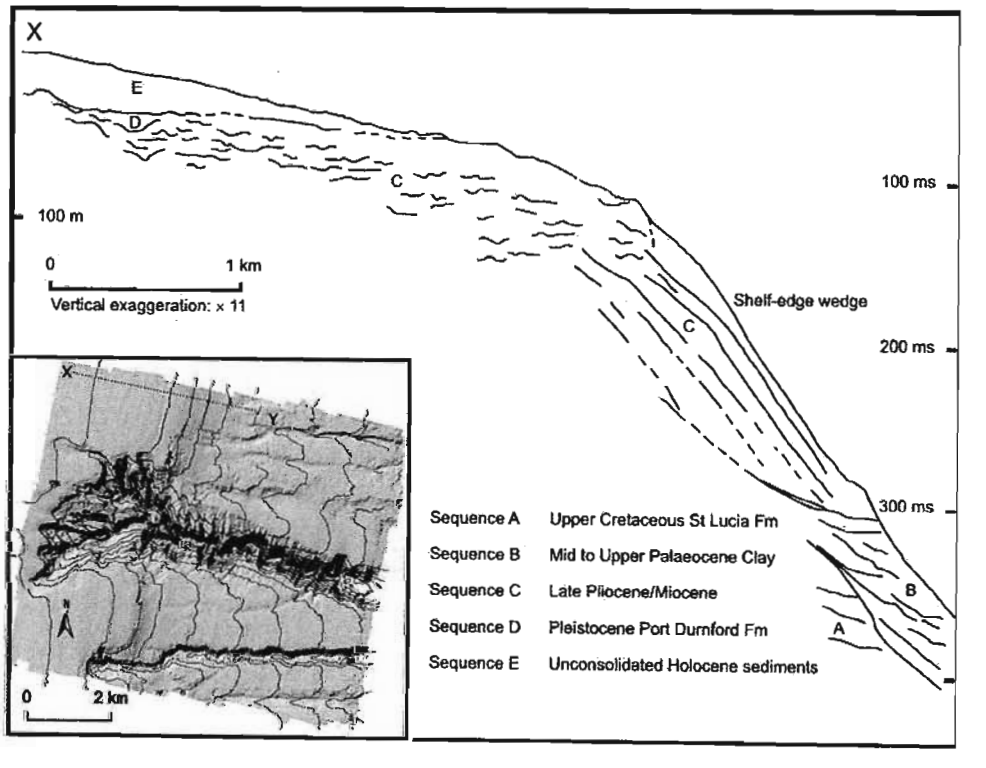

Fig. 2 Interpretative line drawing of the seismic stratigraphy of the continental shelf and upper slope of northern KwaZulu-Natal (after Sydow 1988). A strongly prograding shelf-edge wedge, of possible Miocene/Pliocene age, defines the steepest part of the upper slope, immediately below the shelf edge. Inset depicts the location of the seismic track (*dotted line*) in the Leven survey block

sediments comprise thin aeolianite/beachrock reef complexes which occur as discrete lineaments on the shelf, at the shelf edge and in canyon heads (Ramsay 1994). These are associated with sea-level lowstands during the Pleistocene, and comprise carbonate-cemented beach or dune sands. Holocene sediments occur as a thin veneer of unconsolidated shelf sand which is readily mobilized by bottom currents, taking the form of large subaqueous dune fields which mantle older relict gravels (Ramsay 1994, 1996). These are driven by the southward-flowing Agulhas Current, which may attain velocities of up to 3 m s^{-1} in this region.

Materials and methods

Submarine canyon systems are geomorphically complex, often with narrow and steep features. Adequate characterization of such canyons requires the dense coverage of high-quality bathymetry which is available only with multibeam technology. We surveyed the continental shelf and rise between depths of ~30 and 850 m within five survey blocks (Fig. 1), using a 100-kHz Reson Seabat 8111 ER multibeam echosounder (cf. Ramsay and Miller 2006). These data resolve vertically to within 30 cm, with the final sounding data output as a 10 m matrix.

The survey area comprised five regions, identified here as the Leven, Leadsman, Diepgat, Sodwana and Mabibi blocks (Fig. 1). Six large canyons were surveyed in the study area: the Leven canyon (Leven block); Leadsman South and Leadsman North canyons (Leadsman block); Diepgat canyon (Diepgat block); and Wright and White Sands canyons (Sodwana block), as well as a number of smaller canyons (Fig. 1).

The quantitative analysis presented here follows the statistical characterization techniques developed by Goff (2001). From a stochastic viewpoint, canyon systems are considered as ensembles, rather than discrete morphological features. As such, canyons are included within a bulk assemblage of features which comprise the upper slope and continental shelf. A series of shelf-parallel profiles were initially extracted from the bathymetric datasets along a series of slope-parallel, low-order (degree four or less) polynomial curves fitted to selected isobaths. Isobath intervals of 50 m were chosen. However, in areas of particular interest, these were increased to 25-m intervals. Each profile was then analyzed based on the parameters outlined by Goff (2001). The slope gradient for each profile

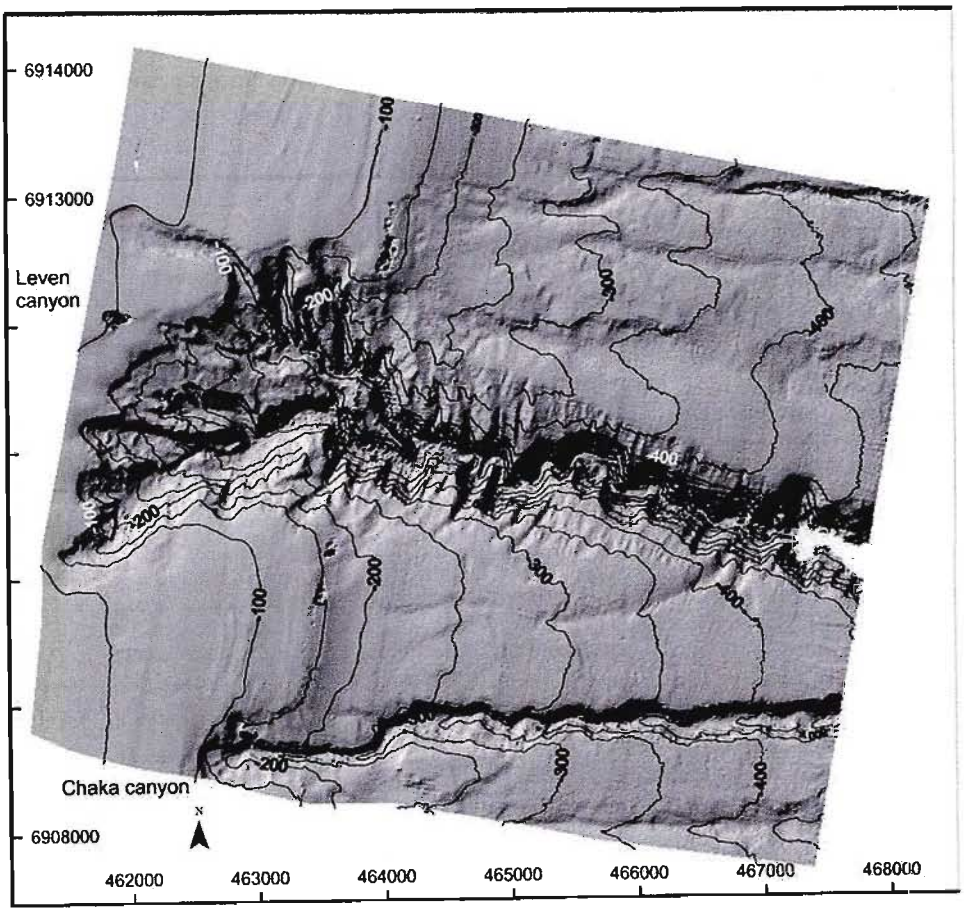

Fig. 3 Bathymetric data in the Leven survey block, artificially illuminated from the northeast. Contours are in meters. Northing and easting coordinates are in meters, UTM projection zone 36. Highly subdued, and thus presumably older rill-like canyon morphologies are present both north and south of the large, shelf-indenting Leven canyon. Chaka canyon, further to the south, also indents the shelf edge, but with a much smaller headwall area

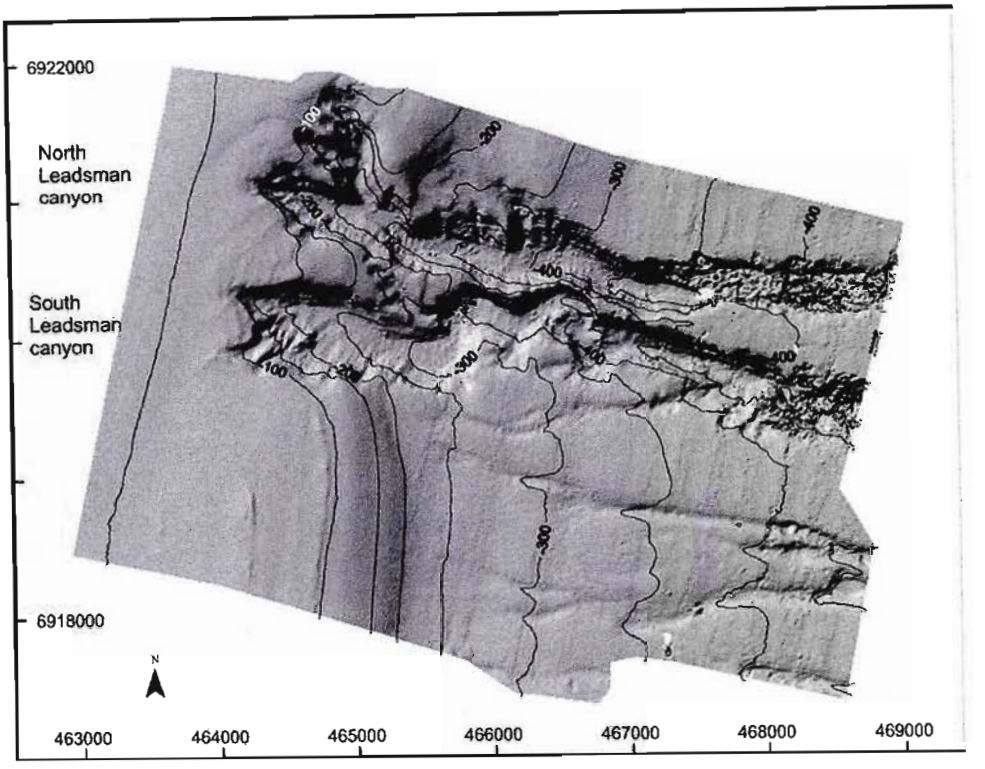

Fig. 4 Bathymetric data from the Leadsman survey block, artificially illuminated from the northeast. Contours in meters. Northing and easting coordinates are in meters, UTM projection zone 36. As with the Leven block (Fig. 2), subdued/older rill-like morphologies are seen in proximity to the larger North and South Leadsman canyons

depth is calculated from the downslope spacing between adjacent profiles, and the difference in mean depth between these profiles. The root mean square (RMS) relief is a measure of the departure from the mean depth, and is calculated by taking the square root of the profile variance. Profiles typically extend for 3–4 km alongslope, and were extracted to water depths up to 550 m.

In addition, several slope-perpendicular cross sections were constructed for each canyon thalweg and the adjacent uneroded slope, in order to give a better visualization of the downslope progression in canyon incision, compared to unaffected slope profiles.

Results

Morphologic observations

Throughout the study area, the largest canyons terminate in amphitheatre-shaped indentations at, or immediately past the shelf edge. Some canyons, such as Leven (Fig. 3), North and South Leadsman (Fig. 4) and Diepgat (Fig. 5), possess large arcuate slumps which extend into the outer shelf regions. Aside from Wright and White Sands canyons of the Sodwana block (Fig. 6), the largest canyons are relatively isolated, interspersed by smaller, shelf-indenting, subdued or slope-confined canyons. Mabibi block (Fig. 7) comprises smaller, narrow and straight shelf-indenting features, some of which coalesce into apron-shaped indentations.

In all survey blocks, we observe a contrasting morphology; some canyons are sharply defined in their relief whereas others are more subdued (Figs. 3, 4, 5, 6 and 7). In accordance with the interpretations of Pratson et al. (1994) for similarly contrasting canyon morphology on the New Jersey slope, we identify these findings as evidence of recently active and moribund canyons respectively.

Quantitative classification

Our plot of slope gradient as a function of water depth in the five survey blocks (Fig. 8) reflects a consistent behaviour: (1) a sharp increase in average slope gradient, denoting the shelf break, (2) a strong peak in gradient, with a maximum slope in the ~150–200 m depth range, corresponding to the shelf-edge wedge, and (3) a gradual decrease in gradient with depth below the shelf-edge wedge. The generally concave trend of decreasing gradient with depth is similar to that of the Virginia slope examined by Goff (2001); however, the Virginia slope does not exhibit a sharp peak in slope gradient on the upper slope, rather maintaining slopes of 7–8° from the shelf edge to ~750 m water depth before substantially declining. Peak slope gradients are highest in the Mabibi, Leadsman and Diepgat areas, reaching values of ~8–12°. The Sodwana Bay and Leven blocks are more subdued, with peak gradients of ~5–7°. Apart from Mabibi, survey areas attain a minimum slope gradient of 2–3° near depths of approx. 400 m. Diepgat has the shallowest slope gradient of 2° at a depth of 425 m.

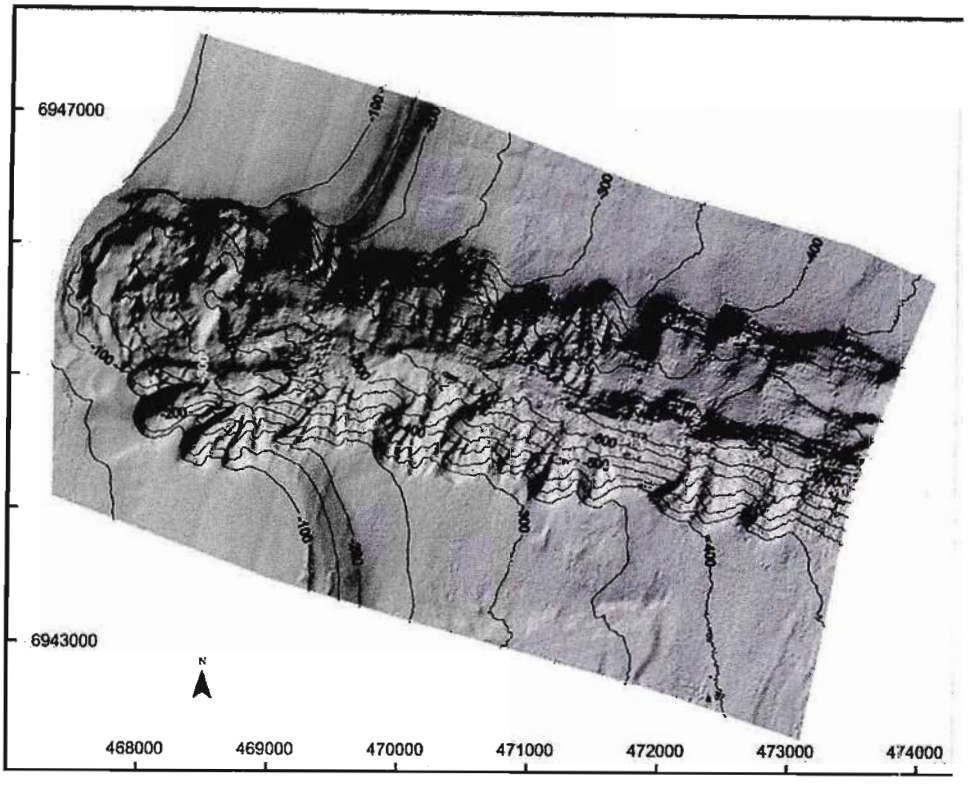

Fig. 5 Bathymetric data from the Diepgat survey block, artificially illuminated from the northeast. Contours in meters. Northing and easting coordinates are in meters, UTM projection zone 36. Diepgat canyon exhibits a deeply excavated thalweg and prominent semicircular landslides in the head. These features are characteristic of headward growth in the upper canyon regions, by retrogressive failure

Although the overall relief varies by as much as a factor of 4 among the five blocks, the plot of RMS relief (Fig. 9) indicates a general pattern (with minor exceptions) of decreasing relief with water depth below the shelf break. Peak RMS values are at depths slightly shallower than for the peak slope values, i.e. where the canyon heads indent into the shelf edge.

The statistical analysis of these canyon systems is complemented visually by dip-direction bathymetric profiles (Fig. 10). Here, the convex nature of the continental slope and the oversteepened shelf edge are readily apparent in all survey blocks. Diepgat has the widest continental shelf of the study area, with Sodwana and Mabibi having the narrowest widths. These profiles also demonstrate the decreasing progression of canyon relief with water depth: the difference between thalweg and interfluve is largest at, or near the shelf edge and then decreases steadily with depth.

Discussion

With the possible exception of Wright canyon (Fig. 6), none of the canyons we mapped are morphologically similar to the mature, shelf-breaching canyons characterized by Farre et al. (1983) on the US Atlantic margin. Rather than terminating in amphitheatre-shaped heads, shelf-breaching canyons extend landwards across the shelf in a narrowing valley. Wright canyon does exhibit a small narrowing valley protruding landwards from a semicircular shelf indentation, and may thus be indicative of evolving towards a shelf-breaching system. Its thalweg exhibits a pronounced sinuosity, which was cited by Farre et al. (1983) as evidence of maturity. The remaining shelf-indenting canyons appear to conform to the "immature" phase described by Farre et al. (1983), with amphitheatre-shaped heads and generally straight thalwegs. Some of these channels show evidence of retrogressive failure, semicircular collapse structures occurring most notably in the Diepgat (Fig. 5) and, to a lesser extent, Mabibi block canyons (Fig. 7). Farre et al. (1983) and Pratson and Coakley (1996) suggest these as the primary mechanisms of youthful canyon formation. Unpublished seismic data discussed by Shaw (1998) indicate that these features are the result of large retrogressive slumping on the outer continental shelf. In the case of Diepgat, slope-parallel seismic profiles reveal preserved glide-plain scars of buried landslides within the canyon walls, suggesting that processes of canyon growth must have been active prior to a stage of burial, followed by later canyon re-excavation.

Dominance of upslope processes

The five areas presented here exhibit similar trends in slope gradient and relief with increasing depth, despite variation in the size and depth of incision of the various canyons

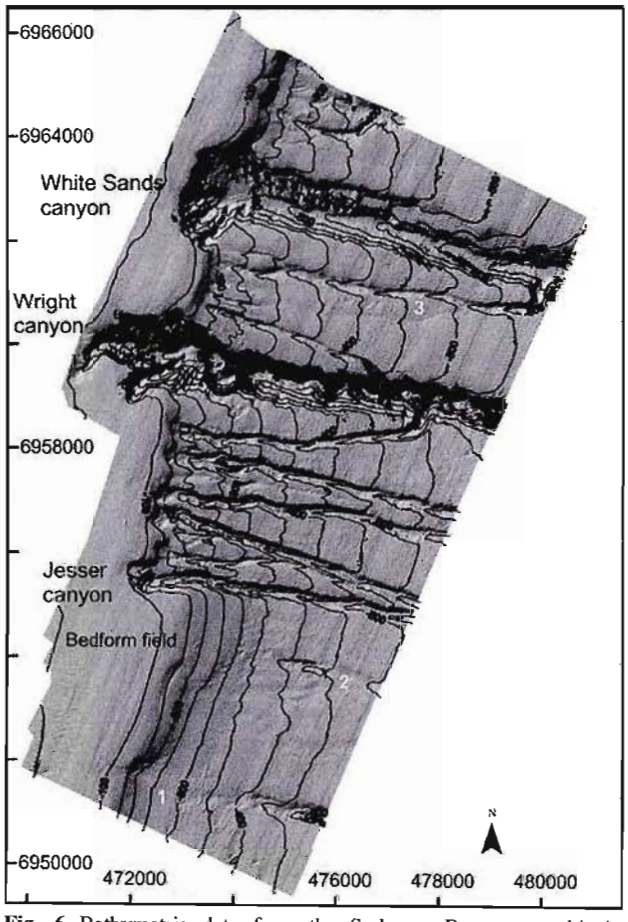

Fig. 6 Bathymetric data from the Sodwana Bay survey block, artificially illuminated from the northeast. Contours in meters. Northing and easting coordinates are in meters, UTM projection zone 36. Two large shelf-indenting canyons are present (White Sands and Wright canyons), with smaller shelf-indenting canyons to the south. As with the Leven and Leadsman blocks (Figs. 2 and 3), subdued-relief rill-like features are present (denoted by white numerals *1–3*). The southernmost of these (*1*) appears to be almost completely filled by sediment in the middle portions

encountered. The gradient profiles (Fig. 8) indicate a concave shape relative to the continental slope, similarly to Goff's (2001) observations for the Virginia slope. Mitchell (2005) identifies concave gradients as evidence of downslope eroding processes such as turbidity flows. However, the decreasing canyon relief with depth observed in our region (Fig. 9) is the reverse of the trend for the Virginia canyons. Rather, it exhibits strong similarities to the New Jersey canyons, which are inferred by Goff (2001) to be formed primarily by "upslope" (e.g. retrograde failures, sapping) processes. Goff (2001) also raised the possibility that the outcropping of more resistant strata on the lower New Jersey slope could be inhibiting erosion, but our observations are confined to the upper slope, and borehole data of Du Toit and Leith (1974) as well as previous seismic studies (cf. Sydow 1988; Shaw 1998) suggest that the KwaZulu-Natal canyons have largely eroded into uniform, late Cretaceous mudstones, siltstones and sandstones exceeding 1 km in thickness. Neither the New Jersey nor Virginia continental slopes of the eastern United States exhibit the characteristic upper-slope gradient peak observed in our profiles, which is created by a preserved Miocene/Pliocene outer shelf wedge which is only partly dissected by the canyons. This part of the upper continental

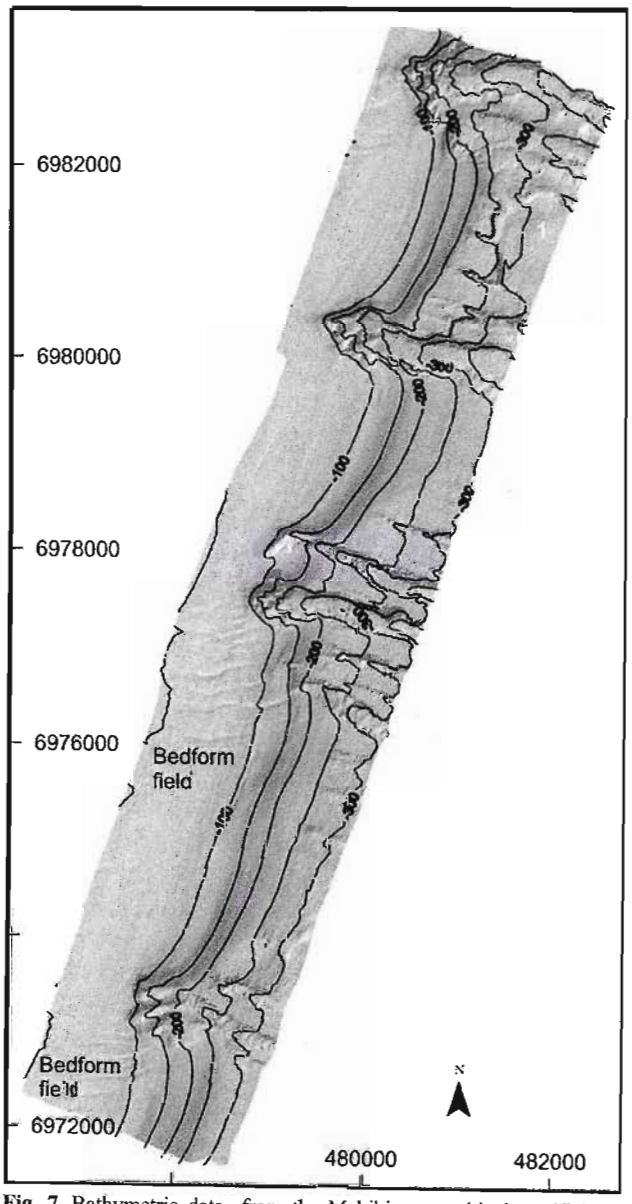

Fig. 7 Bathymetric data from the Mabibi survey block, artificially illuminated from the northeast. Contours in meters. Northing and easting coordinates are in meters, UTM projection zone 36. Five shelf-indenting canyons are mapped, many with semicircular collapse morphologies at their heads, along with numerous smaller canyons which head below ~200 m water depth. In the northern part of the survey area, we mapped what appears to be the headwall (denoted by *1*) of a large slide which removed the lower portions of at least two small canyons

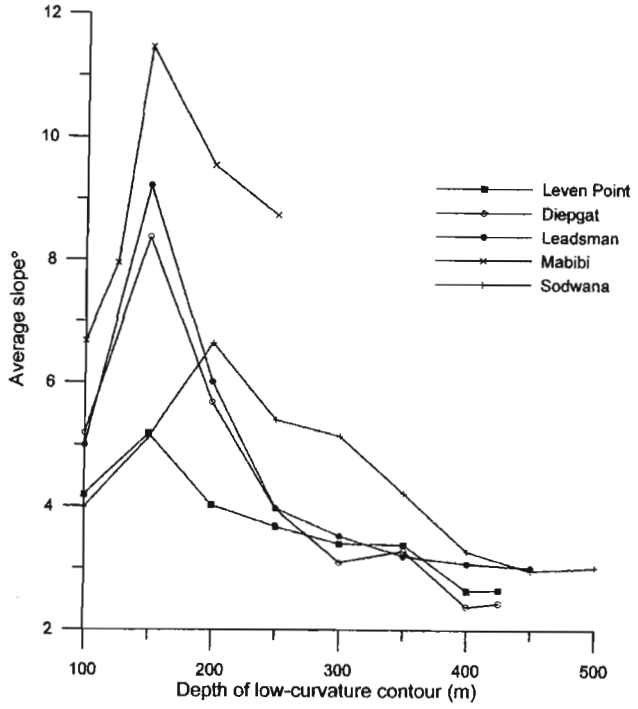

Fig. 8 Average downslope gradient derived from slope-parallel, low-curvature bathymetric profiles for the five survey blocks, plotted versus profile depth. Peaks correspond to steepening of the Miocene/ Pliocene shelf-edge wedge

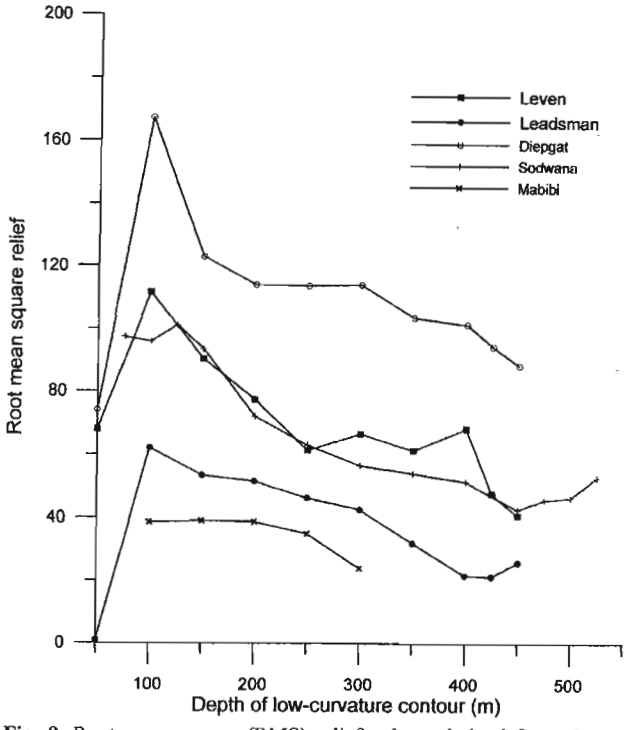

Fig. 9 Root mean square (RMS) relief values, derived from slope-parallel, low-curvature bathymetric profiles for the five survey blocks plotted versus profile depth. RMS values typically decrease downslope of the shelf-edge wedge (of approx. 100-150 m depth)

slope may be oversteepened and may thus represent a potential source of retrogressive failure, as envisioned by the modelling work of Pratson and Coakley (1996).

Additional similarities between the KwaZulu-Natal and New Jersey slope-canyon systems include the shared presence of inter-canyon rills, interspersed with larger shelf-indenting canyons, the amphitheatre-shaped heads of the larger canyons, and the presence of multiple generations of canyon formation. Additional differences are likewise notable. These include (1) the relative isolation of the northern KwaZulu-Natal canyons from each other, compared to the densely eroded nature of the New Jersey margin, and (2) the absence of strongly shelf-breaching canyons, such as the Hudson canyon, on the KwaZulu-Natal shelf. Of the largest canyons in the study area, only Wright canyon exhibits the beginnings of a landward-narrowing valley (Fig. 6), characteristic of shelf-breaching canyons (Farre et al. 1983).

To explain this mixture of morphological similarities and differences, we hypothesize that the KwaZulu-Natal canyon systems are essentially similar to the New Jersey canyons in their upslope formative processes, but are in a far more youthful stage of evolution, either because they are younger or because the canyon-forming processes have not been as active as on the New Jersey margin. The morphology of these canyons is strikingly similar to that predicted by the numerical model of Pratson and Coakley (1996), even more so than the New Jersey slope canyons which formed the basis for this model. Their model hypothesizes that preferential sedimentation on the upper slope leads to oversteepening. As a result, retrogressive failures develop, which work upslope and eventually broaden into amphitheatre-shaped heads at the shelf-edge. Failures also lead to turbidity flows, and thus a combination of upslope- and downslope-forming processes. The Pratson and Coakley (1996) modelling effort was limited in the number of canyons considered, and the time span of the run, and so never reached a point where the resulting synthetic morphology was as dissected by canyons as was the New Jersey slope. We also suggest that the greater extent of retrograde failure on the New Jersey shelf has substantially graded the upper slope there, and is the principal reason that the slope-gradient profiles differ substantially between the two regions.

As noted above, the Virginia canyon systems differ from the New Jersey and KwaZulu-Natal canyon systems primarily in that the Virginia canyons increase, rather than decrease in relief and breadth downslope. Gradient analysis by Mitchell (2005) suggests that the canyons of the Virginia slope have been eroded by many small sedimentary flows, analogous to that of tributary flows in a subaerial fluvial setting of which the frequency increases with the up-stream/canyon-contributing area. The similarities in steepness of the upper slope of the Virginia and northern KwaZulu-Natal margins, and thus

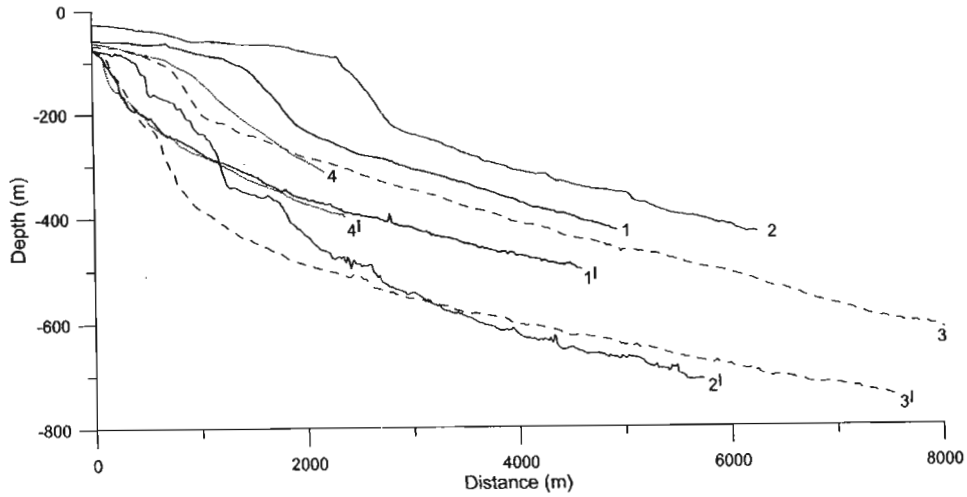

Fig. 10 Representative dip profiles for canyon thalwegs (*primed numbers*) and adjacent, uneroded slopes (*unprimed numbers*) for South Leadsman (*1*), Diepgat (*2*), White Sands (*3*) and South Island Rock canyons (*4*). The upper slope is steepest at ~150 m depth, corresponding to the shelf-edge wedge. These shelf-indenting canyons have maximum relief (seen here as the difference between the two profiles) typically at, or immediately landwards of the shelf edge

dissimilarity in canyon morphology suggest that, although steep, the KwaZulu-Natal slope is not oversteepened to the extent that slope overburdening is the sole driving force behind headward canyon growth. Fluid sapping in the mid- to outer shelf may be partly responsible for the formation of a headward-eroding headless canyon system (Robb 1984; Orange and Breen 1992; Orange et al. 1994), which might emulate the predicted headward pattern in the Pratson and Coakley (1996) model. Diver (Ramsay, personal communication) and submersible observations, in addition to geohydrological studies (Meyer et al. 2001), indicate that artesian conditions do exist in the heads of some of the canyons of northern KwaZulu-Natal. However, the extent to which artesian conditions on the shelf may influence the geomorphology of this area is unclear. Alternatively, the KwaZulu-Natal upper slope may be oversteepened if the sediments of the outer shelf wedge are more readily mobilized than those of the upper Virginia slope, in which case the Pratson and Coakley (1996) model would be fully applicable for our region.

Downslope capture of canyons

Three generations of canyon cutting are evident in Fig. 11. The shelf-indenting White Sands canyon, for example, is a sharply defined feature, and is therefore inferred to be of the most recent generation (third generation). It truncates a canyon with a more subdued morphology immediately to its south (second generation) which, in turn, truncates an even more subdued canyon to its south (first generation). Slumping is noted at the base of the second-generation canyon, near where it enters the White Sands canyon (Figs. 6 and 11). This is the result of entrenchment of the third-generation canyon thalweg, undercutting the fill of the second generation.

In explaining the contrasting morphology of recently active and moribund canyons, Pratson et al. (1994) and Pratson and Coakley (1996) describe the evolution of submarine canyons as resulting from the exploitation of the downslope reaches of older, buried or defunct canyons by downslope-eroding sediment flows. The prevalence of multiple generations of canyon incision throughout the study area, particularly in White Sands canyon (Fig. 6), supports their hypothesis. As envisioned by Pratson et al. (1994), each subsequent canyon generation has shared the downslope reaches of a common bathymetric low, and then diverged towards the shelf break where upper-slope sedimentation has reduced the constraining effect of older canyon incision. The first-generation canyon is then sheltered from the prevailing sediment input by the Agulhas Current on the shelf by the larger second-generation canyon, thus precluding the further growth or reestablishment of the older canyon by sediment starvation. It appears that the more subdued canyons occupying the lee side of each larger, second-generation or third-generation slope-indenting canyon have ceased eroding towards the shelf break as a result of this up-current sediment capture.

The straight, narrow, slope-confined canyons with no discernible retrogressive failures present throughout the study area are analogous to the slope rills of Pratson and Coakley (1996). Whether these are relicts of larger systems which have been buried, choked by a shift in depocentre, or are modern features actively forming on the upper slope is debatable without the interpretative aid of seismic reflection data. The presence of localized subdued downslope relief in some cases suggests that these features may be older buried systems which have not been reactivated by further exploitative sediment flows which would have been constrained to these topographic lows.

Recent quiescence

Prevalent notching within the canyon heads of the northern KwaZulu-Natal canyons, associated with the previous lowstand at ~18,000 years B.P. (Green and Uken 2005),

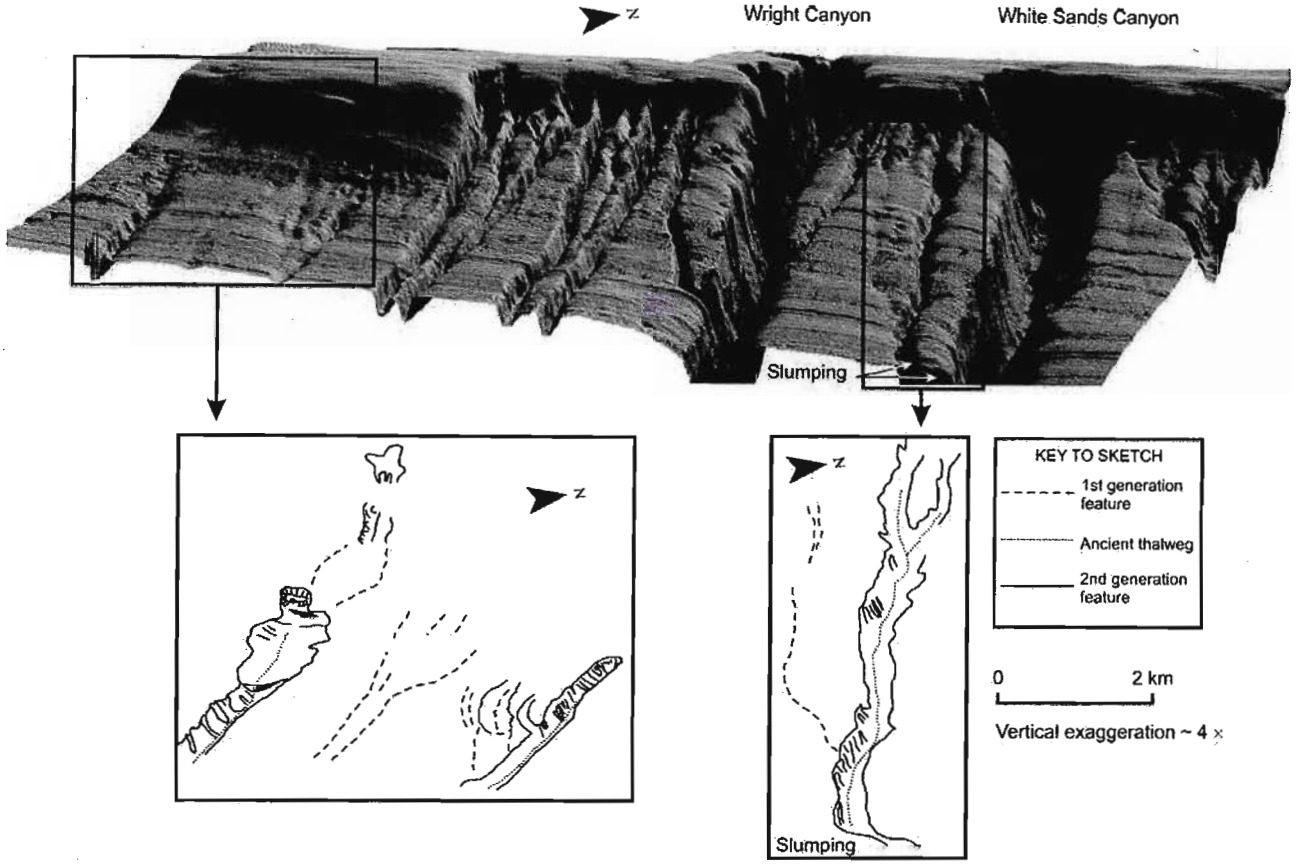

Fig. 11 Three-dimensional view (*top*) of the Sodwana Bay survey block. The older-generation rill-like features are highlighted by blocks, and illustrated by interpretative sketch diagrams (*bottom*) depicting the different stages of erosion (see text for discussion)

suggests that head slumping, and the consequent headward growth of these canyons, has been inactive since at least that time. The lack of fluvial sedimentary inputs, in conjunction with the denudation of slope sediments by the Agulhas Current core, has resulted in the sediment starvation of the shelf and upper slope (Cooper 1994; Ramsay 1996). We envision this starvation as a major limiting factor in the initiation of further upslope erosion by retrogressive failure, and downslope erosion by turbidity flows. Quiescent conditions during high sea-level stands such as that currently being experienced, and the prevailing sediment starvation have resulted in the preservation of both the shelf-edge wedge and the canyon morphology before more complex processes of burial and erosion would take place.

Conclusions

Our study of the geomorphology of the northern KwaZulu-Natal continental slope-canyon systems indicates the dominance of upslope erosional processes in the formation of canyons from this region. Discounting the slope-gradient profile, canyon morphology is strikingly similar to that of the features predicted for a primarily upslope-eroding paradigm by the numerical modelling of Pratson and Coakley (1996). The presence of a steepened shelf-edge wedge could be a potential source for such retrogressive failure, despite being of similar steepness to that found in areas where downslope-eroding canyon systems have developed. If the northern KwaZulu-Natal upper slopes cannot be considered oversteepened, we suggest that freshwater sapping may be the fundamental factor differentiating the two styles of canyon formation. Several generations of canyon incision in the study area indicate that downslope turbidity erosion is also an important factor in the evolution of the KwaZulu-Natal canyons.

Despite the strong similarities between the northern KwaZulu-Natal and New Jersey slope-canyon systems noted above, important differences are documented: (1) the northern KwaZulu-Natal slope is concave whereas the New Jersey slope is essentially linear; (2) the larger northern KwaZulu-Natal canyons are relatively isolated from each other whereas the New Jersey canyons are clustered; and (3) strongly shelf-breaching canyons are absent from the northern KwaZulu-Natal margin. We hypothesize that these differences indicate that the northern KwaZulu-Natal slope canyons are geomorphologically in a more youthful stage of evolution than is the New Jersey

margin, a result either of the canyons themselves being younger or of the formative processes being less active. Recent quiescence of the KwaZulu-Natal margin, coupled with sediment-starved conditions, has resulted in less complicated patterns of erosion having developed, compared to the New Jersey and Virginia continental margins. We postulate that the intensive headward erosion on the New Jersey margin strongly graded the upper slope, reducing any concavity which might have existed.

Acknowledgements This study comprises part of A. Green's PhD thesis at the University of KwaZulu-Natal. This work was made possible by funding received from the African Coelacanth Ecosystem Programme via the National Research Foundation, the Department of Science and Technology, and the Department of Environmental Affairs and Tourism. Multibeam data were collected by Marine GeoSolutions (Pty) Ltd, who we gratefully acknowledge. P.J. Ramsay, an anonymous reviewer and the editor, B.W. Flemming are thanked for their various comments regarding this manuscript. UTIG contribution #1870.

References

Adams EW, Schlager W (2000) Basic types of submarine slope curvature. J Sediment Res 70:814–828

Carlson PR, Karl HA (1988) Development of large submarine canyons in the Bering Sea, indicated by morphologic, seismic and sedimentologic characteristics. Geol Soc Amer Bull 100:1594–1615

Chamberlain TK (1964) Mass transport of sediment in the heads of Scripps Submarine Canyon, California. In: Miller R (ed) Papers in marine geology, Shepard commemorative volume. MacMillan, New York, pp 42–64

Cooper JAG (1994) Lagoons and microtidal coasts. In: Carter RWG, Woodruffe CD (eds) Coastal evolution: late Quaternary shoreline morphodynamics. Cambridge University Press, Cambridge, pp 219–265

Daly RA (1936) The origin of submarine canyons. Am J Sci 5 31:401–420

Dingle RV, Robson S (1985) Slumps, canyons and related features on the continental margin off East London, SE Africa (southwest Indian Ocean). Mar Geol 67:37–54

Dingle RV, Goodlad SW, Martin AK (1978) Bathymetry and stratigraphy of the northern Natal Valley (SW Indian Ocean). A preliminary report. Mar Geol 28:89–106

Dingle RV, Siesser WG, Newton AR (1983) Mesozoic and Tertiary geology of southern Africa. Balkema, Rotterdam

Drake DE, Hatcher PG, Keller Gm (1978) Suspended particulate matter and mud deposition in upper Hudson Submarine Canyon. In: Stanley DJ, Kelling GE (eds) Sedimentation in submarine canyons, fans and trenches. Dowden Hutchinson Ross, Stroudsburg, PA, pp 33–41

Du Toit SR, Leith MJ (1974) The J(c)-1 bore-hole on the continental shelf near Stanger, Natal. Trans Geol Soc S Afr 77:247–252

Farre JA, McGregor BA, Ryan WBF, Robb JM (1983) Breaching the shelfbreak; Passage from youthful to mature phase in submarine canyon evolution. In: Stanley DJ, Moore GT (eds) The shelfbreak: critical interface on continental margins. Soc Econ Palaeontol Mineral Spec Publ 33:25–39

Fricke H, Hissmann K (1994) Home range and migrations of the living coelacanth *Latimeria chalumnae*. Mar Biol 120:171–180

Fricke H, Plante R (1988) Habitat requirements of the living coelacanth *Latimeria chalumnae* at Grande Comore, Indian Ocean. Naturwissenschaften 15:149–151

Goff JA (2001) Quantitative classification of canyon systems on continental slopes and a possible relationship to slope curvature. Geophys Res Lett 28:4359–4362

Goodlad SW (1986) Tectonic and sedimentary history of the mid-Natal Valley (SW Indian Ocean). Joint Geological Survey/ University of Cape Town, Marine Geoscience Unit Bull 15

Green AN, Uken R (2005) First observations of sea level indicators related to glacial maxima at Sodwana Bay, Northern KwaZulu-Natal. S African J Sci 101:236–238

Green AN, Perritt SH, Leuci R, Uken R, Ramsay PJ (2007) Potential sites for coelacanth habitat using bathymetric data from the western Indian Ocean. S African J Sci (in press)

Meyer R, Talma AS, Duvenhage AWA, Eglington BM, Taljaard J, Botha JF, Verwey J, Van der Voort I (2001) Geohydrological investigation and evaluation of the Zululand coastal aquifer. Pretoria, Water Research Commission Rep 221/1/01

Miller WR (2001) The bathymetry, sedimentology and seismic stratigraphy of Lake Sibaya—Northern KwaZulu-Natal. Council Geosci Bull 131

Mitchell MC (2005) Interpreting long-profiles of canyons in the USA Atlantic continental slope. Mar Geol 214:75–99

O'Grady DB, Syvitski JPM, Pratson LF, Sarg JF (2000) Categorizing the morphologic variability of siliciclastic passive continental margins. Geology 28:207–210

Orange DL, Breen NA (1992) The effects of fluid escape on accretionary wedges. 2. Seepage force, slope failure, headless submarine canyons and vents. J Geophys Res 97:9277–9295

Orange DL, Anderson RS, Breen NA (1994) Regular canyon spacing in the submarine environment: the link between hydrology and geomorphology. GSA Today 4:29–39

Partridge TC, Maud RR (1987) Geomorphic evolution of southern Africa since the Mesozoic. S African J Geol 90:179–208

Pratson LF, Coakley BJ (1996) A model for the headward erosion of submarine canyons induced by downslope eroding sediment flows. Geol Soc Am Bull 108:225–234

Pratson LF, Ryan WBF, Mountain GS, Twitchell DC (1994) Submarine canyon initiation by downslope-eroding sediment flows: evidence in late Cenozoic strata on the New Jersey continental slope. Geol Soc Am Bull 106:395–412

Ramsay PJ (1994) Marine geology of the Sodwana Bay shelf, Southeast Africa. Mar Geol 120:225–247

Ramsay PJ (1996) Quaternary marine geology of the Sodwana Bay shelf, northern KwaZulu-Natal. Bull Geol Surv S Afr 117

Ramsay PJ, Miller WR (2006) Marine geophysical technology used to define coelacanth habitats on the KwaZulu-Natal shelf, South Africa. S African J Sci 102:427–434

Robb JM (1984) Spring sapping on the lower continental slope, offshore New Jersey. Geology 12:278–282

Shaw MJ (1998) Seismic stratigraphy of the northern KwaZulu-Natal upper continental margin. M Sc Thesis, University of Natal, Durban

Shepard FP, Curray JR, Innan DL, Murray EA, Winterer EL, Dill RF (1964) Submarine geology by diving saucer: bottom currents and precipitous submarine canyon walls continue to a depth of at least 300 meters. Science 145:1042

Sydow CJ (1988) Stratigraphic control of slumping and canyon development on the continental margin, east coast, South Africa. BSc Honours Thesis, University of Cape Town, Cape Town

Twichell DC, Roberts DG (1982) Morphology, distribution and development of submarine canyons on the United States Atlantic continental slope between Hudson and Baltimore Canyons. Geology 10:408–412

APPENDIX 4

Whilst every care has been taken in presenting raw data in this thesis from which interpretations have been made, often times the scale and resolution of the data does not lend itself well to depiction within a thesis (owing to the space constraints). Raw seismic data in the form of SEG-Y data has not been included digitally for fears of misuse by others. Sedimentological data (mean, sorting, skewness and contour maps thereof) derived from shipek grab samples have not been included in this thesis for fear of adding additional and unnecessary bulk, superfluous to the main arguments presented herein. These data are earmarked for publication at a later date.